



N76 24145

**STUDY OF THE APPLICATION OF ADVANCED
TECHNOLOGIES TO LAMINAR-FLOW CONTROL
SYSTEMS FOR SUBSONIC TRANSPORTS VOLUME
II: ANALYSIS**

**LANGLEY RESEARCH CENTER
HAMPTON, VA**

MAY 76

**STUDY OF THE APPLICATION OF
ADVANCED TECHNOLOGIES TO
LAMINAR-FLOW CONTROL SYSTEMS
FOR SUBSONIC TRANSPORTS**

May, 1976

VOLUME II: ANALYSES

By: *R. F. Sturgeon*
J. A. Bennett
F. R. Etchberger
R. S. Ferrill
L. E. Meade



Prepared under Contract No. NAS1-13694

by

The Lockheed-Georgia Company
A Division of Lockheed Aircraft Corporation
Marietta, Georgia
for

NATIONAL AERONAUTICS AND SPACE ADMINISTRATION

(NASA-CR-144949) STUDY OF THE APPLICATION
OF ADVANCED TECHNOLOGIES TO LAMINAR-FLOW
CONTROL SYSTEMS FOR SUBSONIC TRANSPORTS.
VOLUME 2: ANALYSES Final Report
(Lockheed-Georgia Co.) 471 p HC \$12.00

N76-24145

Unclass

G3/02 26915

1. Report No. NASA CR-144949		2. Government Accession No.		3. Recipient's Catalog No.	
4. Title and Subtitle Study of the Application of Advanced Technologies to Laminar-Flow Control Systems for Subsonic Transports Volume II: Analyses				5. Report Date May 1976	
				6. Performing Organization Code	
7. Author(s) R. F. Sturgeon, J. A. Bennett, F. R. Etchberger, R. S. Ferrill, L. E. Meade				8. Performing Organization Report No. LG76ER0076	
9. Performing Organization Name and Address Lockheed-Georgia Company 86 South Cobb Drive Marietta, Georgia 30060				10. Work Unit No.	
				11. Contract or Grant No. NAS 1-13694	
12. Sponsoring Agency Name and Address Langley Research Center National Aeronautics and Space Administration Hampton, Virginia				13. Type of Report and Period Covered Contractor Report - Final	
				14. Sponsoring Agency Code	
15. Supplementary Notes This document supercedes preliminary issue dated, January 15, 1976.					
16. Abstract <p>A study was conducted to evaluate the technical and economic feasibility of applying laminar flow control to the wings and empennage of long-range subsonic transport aircraft compatible with initial operation in 1985. For a design mission range of 10,186 km (5500 n mi), advanced technology laminar-flow-control (LFC) and turbulent-flow (TF) aircraft were developed for both 200- and 400-passenger payloads, and compared on the basis of production costs, direct operating costs, and fuel efficiency.</p> <p>As a part of the study, parametric analyses were conducted to establish the optimum geometry for LFC and TF aircraft, advanced LFC system concepts and arrangements were evaluated, and configuration variations maximizing the effectiveness of LFC were developed. For the final LFC aircraft, analyses were conducted to define maintenance costs and procedures, manufacturing costs and procedures, and operational considerations peculiar to LFC aircraft.</p> <p>Compared to the corresponding advanced technology TF transports, the 200- and 400-passenger LFC aircraft realized reductions in fuel consumption up to 28.2%, reductions in direct operating costs up to 8.4%, and improvements in fuel efficiency, in ssm/lb of fuel, up to 39.4%. Compared to current commercial transports at the design range, the LFC study aircraft demonstrate improvements in fuel efficiency up to 131%.</p> <p>Research and technology requirements requisite to the development of LFC transport aircraft were identified.</p>					
17. Key Words (Suggested by Author(s)) Fuel Conservation Laminar-Flow Control Boundary-Layer Control			18. Distribution Statement		
19. Security Classif (of this report) Unclassified		20. Security Classif. (of this page) Unclassified		21. No. of Pages 441	
				22. Price*	

*For sale by the National Technical Information Service, Springfield, Virginia 22151

FOREWORD

Contract NAS1-13694 between the National Aeronautics and Space Administration and the Lockheed-Georgia Company, effective November 25, 1974, provided for the study of the application of advanced technologies to laminar-flow-control systems for subsonic transport aircraft. The contract was sponsored by the Aeronautical Systems Division of the Langley Research Center and jointly managed by *R. D. Wagner* and *J. B. Peterson, Jr.*

At the Lockheed-Georgia Company, the study was performed under the cognizance of *R. H. Lange*, Manager of the Transport Design Department, with *R. F. Sturgeon* serving as study manager. Principal contributors to the study include the following:

<i>J. A. Bennett</i>	Aerodynamics
<i>H. V. Davis</i>	Production Costs
<i>F. R. Etchberger</i>	Design
<i>R. S. Ferrill</i>	Thermodynamics/Propulsion
<i>H. D. Hall</i>	Maintenance
<i>L. B. Lineberger</i>	Structures
<i>L. E. Meade</i>	Materials/Manufacturing
<i>E. Stephens</i>	Weights
<i>G. Swift</i>	Acoustics
<i>S. G. Thompson</i>	Operating Costs

This document, which comprises Volume I: Summary, and Volume II: Analyses, is the final technical report summarizing the studies performed and is submitted in fulfillment of the terms of the above contract.

CONTENTS

Section	Page
FOREWORD	iii
FIGURES	xiii
TABLES	xxv
ABBREVIATIONS	xxix
SYMBOLS	xxxi
SUMMARY	xxxv
1.0 INTRODUCTION	1
2.0 STUDY APPROACH	3
2.1 Study Objectives	3
2.2 Scope	3
2.3 Study Plan	6
3.0 BASIC STUDY DATA AND METHODOLOGY	9
3.1 Introduction	9
3.2 Configuration Nomenclature	9
3.3 Generalized Aircraft Sizing Program	10
3.3.1 Basic Flow of Program Calculations	10
3.3.2 Input of LFC System Characteristics	10
3.3.3 Major LFC Calculations in GASP	12
3.4 Economic Analyses	12
3.4.1 Methodology	12
3.4.2 Assumptions	18
3.4.3 LFC System Costs	18
3.5 Reference Technology Level	20

Section		Page
	3.5.1 Aerodynamics	20
	3.5.2 Propulsion Systems	25
	3.5.3 Structures and Materials	31
4.0	AERODYNAMIC DESIGN AND LAMINAR BOUNDARY-LAYER ANALYSIS	35
4.1	Introduction	35
4.2	General Aerodynamic Design Requirements	36
	4.2.1 Implications of Wing/Body Aerodynamic Design	36
	4.2.2 Aerodynamic Design as a Part of Overall Aircraft Design	38
	4.2.3 Aerodynamic Design Concepts	39
4.3	Airfoil Development	44
	4.3.1 Airfoil Variations	44
	4.3.2 Airfoil Selection and Definition	46
	4.3.3 Summary of Airfoil Design Studies	53
4.4	Laminar Boundary-Layer Analysis	53
	4.4.1 Quasi-Three-Dimensional Laminar Boundary-Layer Program	54
	4.4.2 LFC Suction Requirements	58
5.0	PARAMETRIC CONFIGURATION ANALYSES	63
5.1	Introduction	63
5.2	LFC Configuration Analyses	63
	5.2.1 Parametric Procedures	63
	5.2.2 Parametric Data: LFC-200-S	67
	5.2.3 Parametric Data: LFC-200-R	81
	5.2.4 Parametric Data: LFC-400-S	86
	5.2.5 Parametric Data: LFC-400-R	94
5.3	TF Configurations	100
	5.3.1 Parametric Procedures	100
	5.3.2 Parametric Data: TF-200	101
	5.3.3 Parametric Data: TF-400	106

Section		Page
6.0	LFC SYSTEM CONCEPT EVALUATIONS	111
6.1	Introduction	111
6.2	Surfaces	111
	6.2.1 Criteria	111
	6.2.2 Materials	114
	6.2.3 Design Concepts	115
	6.2.4 Manufacturing Concepts	126
6.3	Ducting and Distribution System	127
	6.3.1 Criteria	127
	6.3.2 Materials	128
	6.3.3 Design Concepts	130
	6.3.4 Manufacturing Concepts	131
6.4	Suction Units	131
	6.4.1 Criteria	131
	6.4.2 Design Considerations	132
	6.4.3 Independent Suction Power Systems	135
	6.4.4 Integrated Suction Power Systems	137
	6.4.5 Suction Unit Configuration Summary	143
7.0	LFC CONFIGURATION DEVELOPMENT	145
7.1	Introduction	145
7.2	Initial LFC Baseline Configuration	145
7.3	Chordwise Extent of Laminarization	148
	7.3.1 General Considerations	148
	7.3.2 Configurations	151
	7.3.3 Results and Analysis	151
7.4	Configuration Variations	158
	7.4.1 Fuselage-Mounted Suction Units	160

Section		Page
	7.4.2 External Landing-Gear Pods	162
	7.4.3 External Landing-Gear/Fuel-Tank Pods	162
	7.4.4 External Fuel Tanks	162
	7.4.5 Fuselage Slot Injection	165
	7.4.6 Relaxed Static Stability	166
7.5	Configuration Evaluations	167
	7.5.1 Evaluation Procedure	167
	7.5.2 Design Constraints	168
	7.5.3 Configuration Summary	171
	7.5.4 Evaluation Results	188
7.6	Configuration Selection	189
	7.6.1 Selection Procedure	189
	7.6.2 Selected Configurations	190
8.0	LFC CONFIGURATION DESCRIPTIONS	197
8.1	Introduction	197
8.2	Configuration LFC-200-S	197
	8.2.1 General Arrangement	197
	8.2.2 Aircraft Systems	200
	8.2.3 LFC Systems	202
8.3	Configuration LFC-200-R	258
	8.3.1 General Arrangement	258
	8.3.2 Aircraft Systems	258
	8.3.3 LFC Systems	258
8.4	Configuration LFC-400-S	277
	8.4.1 General Arrangement	277
	8.4.2 Aircraft Systems	280
	8.4.3 LFC Systems	280

Sec

Section

Page

8.5	Configuration LFC-400-R	293
8.5.1	General Arrangement	293
8.5.2	Aircraft Systems	293
8.5.3	LFC Systems	296
8.6	Acoustics	305
8.6.1	Acoustic Design Criteria	307
8.6.2	Aircraft Configuration Considerations	308
8.6.3	LFC Surface Acoustic Environment	308
8.6.4	Regions Subject to Acoustically Induced Transition	315
8.6.5	Minimization of Acoustically Induced Transition	315
9.0	LFC MANUFACTURING, MAINTENANCE, AND OPERATION	321
9.1	Introduction	321
9.2	LFC Manufacturing Concepts	321
9.2.1	Manufacturing Procedures	321
9.2.2	Manufacturing Costs	336
9.3	LFC System Maintenance	337
9.3.1	Maintenance Requirements	339
9.3.2	Scheduled Maintenance Concept	342
9.3.3	Ground Support Equipment	343
9.3.4	Maintenance Costs	344
9.4	LFC Operational Considerations	350
9.4.1	Permissible Roughness Height	350
9.4.2	Surface Contamination	353
9.4.3	Effect of In-Flight LFC System Loss	368
10.0	TF CONFIGURATION DEVELOPMENT	373
10.1	Introduction	373

Section	Page
10.2 Configuration TF-200	373
10.2.1 Configuration Variations	373
10.2.2 Configuration Description	375
10.3 Configuration TF-400	375
10.3.1 Configuration Variations	375
10.3.2 Configuration Description	378
11.0 COMPARISON OF LFC AND TF AIRCRAFT	383
11.1 Introduction	383
11.2 Comparison of 200-Passenger Aircraft	383
11.2.1 Weight	385
11.2.2 Drag	385
11.2.3 Costs	385
11.3 Comparison of 400-Passenger Aircraft	391
11.3.1 Weight	391
11.3.2 Drag	391
11.3.3 Costs	394
11.4 Evaluation of DOC Sensitivity	398
11.4.1 Fuel Price, Maintenance Costs, and Production Costs	398
11.4.2 Stage Length	407
11.5 Summary Comparisons	407
11.5.1 Configuration Variations	407
11.5.2 Fuel Efficiency	411
11.5.3 Direct Operating Cost	412
11.5.4 Comparison with Current Transports	412

Section	Page
12.0 RESEARCH AND TECHNOLOGY REQUIREMENTS	415
12.1 Introduction	415
12.2 LFC Airfoil development	416
12.2.1 Laminar Boundary-Layer Stability Criteria	416
12.2.2 Airfoil Design Data Bank	419
12.2.3 Trailing-Edge Trimming Devices	421
12.3 LFC System Development	422
12.3.1 Suction Tolerances	423
12.3.2 Surface Design	424
12.3.3 Ducting Design	426
12.3.4 Suction Units	426
12.4 Materials	427
12.4.1 Analysis and Laboratory Testing	428
12.4.2 Flight Testing	429
12.5 Design	430
12.5.1 High-Aspect-Ratio Wings	430
12.5.2 LFC Wing Design	431
12.6 Manufacturing and Quality Control Procedures	433
12.7 Operational Evaluations	434
REFERENCES	437

FIGURES

No.		Page
1	Aircraft Life Cycle and Mission Profile	1
2	Study Plan	7
3	Generalized Aircraft Sizing Program	11
4	Generalized Aircraft Sizing Program, LFC Subroutine	13
5	Parametric Description of Airfoil Pressures and Suction	14
6	Parametric Drag Calculations with Part-Chord Laminar Flow Control	15
7	Airfoil Design Concepts	21
8	LFC Aerodynamics Criteria	22
9	Wing Section Design Curves for Supercritical LFC Airfoil	23
10	Wing Section Design Curves for Supercritical TF Airfoil	23
11	Wing Section Design Curves for X-21 Rooftop 6-Series Type Airfoil	24
12	Wing Section Design Curves for High-Aft-Loaded Rooftop Airfoil	24
13	Engine Performance Computer Input	27
14	Aerodynamic Design Procedure for LFC and TF Wings	35
15	Advantage of Increased Speed	37
16	Refinement of Wing/Body Design	40
17	Determination of Wing/Body Geometry	41
18	Wing Isobar Patterns	42
19	Simple Sweep Relationships	42
20	Velocity Increments	43
21	Pressure Distribution of Baseline LFC Wing	47
22	Viscous Transonic Airfoil Program Results	49
23	Baseline Airfoil Section with 0.070 rad (4 deg) Flap Deflection	53

Figures (Continued)

No.		Page
24	Extent of Laminarization for Parametric Configurations	64
25	Baseline Selection Procedure, LFC-200-S	65
26	Baseline Selection Procedure, LFC-200-R, LFC-400-S, and LFC-400-R	66
27	Block Fuel vs. Wing Loading and Aspect Ratio, LFC-200-S, $\Lambda = 0$	68
28	Block Fuel vs. Wing Loading and Aspect Ratio, LFC-200-S $\Lambda = 0.174$ rad (10 deg)	69
29	Block Fuel vs. Wing Loading and Aspect Ratio, LFC-200-S, $\Lambda = 0.349$ rad (20 deg)	70
30	Block Fuel vs. Wing Loading and Aspect Ratio, LFC-200-S, $\Lambda = 0.524$ rad (30 deg)	71
31	Block Fuel and Wing Loading vs. Wing Sweep, LFC-200-S	72
32	Wing t/c Ratio vs. Cruise Mach Number, LFC-200-S	73
33	Wing t/c Ratio vs. Wing Sweep, LFC-200-S	73
34	Effect of Wing Sweep and Cruise Mach Number on Block Fuel and Relative DOC, LFC-200-S	75
35	Effect of Cruise Altitude and cruise Mach Number on Block Fuel and Relative DOC, LFC-200-S, $\Lambda = 0$	76
36	Effect of Cruise Altitude and Cruise Mach Number on Block Fuel and Relative DOC, LFC-200-S $\Lambda = 0.349$ rad (deg)	77
37	Engine Bypass Ratio Variations, LFC-200-S	78
38	Variation of Block Fuel with FAR Field Length, LFC-200-S	79
39	Block Fuel vs. Wing Loading and Aspect Ratio, LFC-200-R, $\Lambda = 0$ and $\Lambda = 0.174$ rad (10 deg)	83
40	Block Fuel vs. Wing Loading and Aspect Ratio, LFC-200-R, $\Lambda = 0.349$ rad (20 deg) and $\Lambda = 0.524$ rad (30 deg)	84
41	Block Fuel and Wing Loading vs. Wing Sweep, LFC-200-R	85

Figures (Continued)

No.		Page
42	Block Fuel vs. Wing Loading and Aspect Ratio, LFC-400-S, $\Lambda = 0$ and $\Lambda = 0.174$ rad (10 deg)	87
43	Block Fuel vs. Wing Loading and Aspect Ratio, LFC-400-S, $\Lambda = 0.349$ rad (20 deg) and $\Lambda = 0.524$ rad (30 deg)	88
44	Block Fuel and Wing Loading vs. Wing Sweep, LFC-400-S	89
45	Engine Bypass Ratio Variations, LFC-400-S	91
46	Airport Performance vs. Wing Loading and Cruise Power Ratio, LFC-400-S	92
47	Block Fuel vs. Wing Loading and Cruise Power Ratio, LFC-400-S	93
48	Block Fuel vs. Wing Loading and Aspect Ratio, LFC-400-R, $\Lambda = 0$ and $\Lambda = 0.174$ rad (10 deg)	95
49	Block Fuel vs. Wing Loading and Aspect Ratio, LFC-400-R, $\Lambda = 0.349$ rad (20 deg) and $\Lambda = 0.524$ rad (30 deg)	96
50	Block Fuel and Wing Loading vs. Wing Sweep, LFC-400-R	97
51	Airport Performance vs. Wing Loading and Cruise Power Ratio, LFC-400-R	98
52	Block Fuel vs. Wing Loading and Cruise Power Ratio, LFC-400-R	99
53	Baseline Selection Procedure, TF-200 and TF-400	101
54	Block Fuel vs. Wing Loading and Aspect Ratio, TF-200	103
55	Relative DOC vs. Wing Loading and Aspect Ratio, TF-200	104
56	Engine Bypass Ratio Variations, TF-200	105
57	Block Fuel vs. Wing Loading and Aspect Ratio, TF-400	107
58	Airport Performance vs. Wing Loading and Cruise Power Ratio, TF-400	108

Figures (Continued)

No.		Page
59	Block Fuel vs. Wing Loading and Cruise Power Ratio, TF-400	110
60	LFC Surface Panel, Configuration 1	119
61	LFC Surface Panel, Configuration 2	119
62	LFC Surface Panel, Configuration 3	120
63	LFC Surface Panel, Configuration 4	120
64	LFC Surface Panel, Configuration 5	122
65	LFC Surface Panel, Configuration 6	122
66	LFC Surface Panel, Configuration 7	123
67	LFC Surface Panel, Configuration 8	123
68	LFC Surface Panel, Configuration 9	125
69	LFC Surface Panel, Configuration 10	125
70	Effect of Duct Area on Suction Unit Characteristics	129
71	Candidate Suction Unit Configurations	133
72	Fuel Consumption of Suction Power Unit Operating on Suction Pump Discharge Airflow	138
73	General Arrangement, Initial LFC-200-S Baseline Configuration	146
74	Laminarization Efficiency vs. Chordwise Extent of Laminarization	150
75	Weight Parameters vs. Chordwise Extent of Laminarization	152
76	Wing Parameters vs. Chordwise Extent of Laminarization	153
77	Fuel and Cost Parameters vs. Chordwise Extent of Laminarization	154
78	Aircraft Drag Coefficients, C_D , vs. Chordwise Extent of Laminarization	155
79	$C_D S$ vs. Chordwise Extent of Laminarization	156
80	Aircraft Drag Coefficients, C_D , vs. Chordwise Extent of Laminarization from 0 to 1.0	157
81	Schematic of Fuselage-Mounted LFC Suction Units	161
82	Schematic of External Landing-Gear Pod	163

Figures (Continued)

No.		Page
83	Schematic of External Landing-Gear/Fuel Pod	164
84	Schematic of Wing-Tip Fuel Tank	165
85	Schematic of Flap-Fairing/Fuel Pod	166
86	Schematic of LFC Suction Pump Installation for Fuselage Slot Injection	167
87	Schematic of Fuselage Slot	168
88	Variation of Duct Area and Fuel Volume with Wing Box Length	169
89	Variation of Wing Weight with Wing Box Length	170
90	Sequence of Configuration Variations LFC-200	172
91	Configuration Summary, LFC-200-S-1	173
92	Configuration Summary, LFC-200-S-2	174
93	Configuration Summary, LFC-200-S-3	175
94	Configuration Summary, LFC-200-S-4	176
95	Configuration Summary, LFC-200-S-5	177
96	Configuration Summary, LFC-200-S-6	178
97	Configuration Summary, LFC-200-S-7	179
98	Configuration Summary, LFC-200-S-8	180
99	Configuration Summary, LFC-200-S-9	181
100	Configuration Summary, LFC-200-S-10	182
101	Configuration Summary, LFC-200-S-11	183
102	Configuration Summary, LFC-200-S-12	184
103	Configuration Summary, LFC-200-S-13	185
104	Configuration Summary, LFC-200-S-14	186

Figures (Continued)

No.		Page
105	General Arrangement LFC-200-S	198
106	Schematic of Aircraft Fuel System	203
107	Distributed Suction Velocity Profile for Wing, LFC-200-S	205
108	Distributed Suction Velocity Profile for Horizontal Tail, LFC-200-S	206
109	Distributed Suction Velocity Profile for Vertical Tail, LFC-200-S	207
110	Pressure Coefficients for Wing, LFC-200-S	208
111	Pressure Coefficients for Horizontal Tail, LFC-200-S	209
112	Pressure Coefficients for Vertical Tail, LFC-200-S	210
113	Boundary Layer Velocity Gradient, LFC-200-S	212
114	Suction Slot Design Chart	213
115	Slot Design Limit Parameters, Upper Wing Surface, LFC-200-S	215
116	Slot Spacing and Pressure Loss vs. Slot Width, Upper WS 370, LFC-200-S	217
117	Slot Spacing and Pressure Loss vs. Chord Location Upper WS 370, LFC-200-S	218
118	Effect of Slot Size on Required Suction Pump Pressure Ratio, Upper WS 370, LFC-200-S	219
119	Slot Spacing and Pressure Loss vs. Slot Width, Upper WS 1150, LFC-200-S	220
120	Slot Spacing and Pressure Loss vs. Chord Location, Upper WS 1150, LFC-200-S	221
121	Slot Spacing and Pressure Loss vs. Slot Width, Upper WS 100, LFC-200-S	223
122	Slot Sizing and Pressure Loss vs. Chord Location, Upper WS 100, LFC-200-S	224

Figures (Continued)

No.		Page
123	Wing Upper Surface Planform, LFC-200-S	225
124	Slot Spacing Planform, Wing Upper Surface, LFC-200-S	227
125	Slot Width, w_s , Upper Wing Surface, LFC-200-S	228
126	Slot Flowpath Length, t_s , Upper Wing Surface, LFC-200-S	229
127	Surface Panel Configuration, LFC-200-S	231
128	Typical LFC Surface Panel	232
129	Typical LFC Wing Section	233
130	Laminar Wing Regions, LFC-200-S	235
131	Schematic of Ducting and Distribution System	237
132	Collector Duct Local Characteristics, 1.016 cm (0.40 in) Collector Height, Upper Wing, LFC-200-S	238
133	Wing Root Collector Duct Characteristics, Upper Wing, LFC-200-S	240
134	Collector Exit to Trunk Duct Pressure Matching, Upper Wing, LFC-200-S	241
135	Collector Exit and Trunk Duct Flow Mach Number Characteristics, Upper Wing, LFC-200-S	242
136	LFC Surface Panel Transfer Ducting	245
137	Ducting Arrangement for Wing-Mounted LFC Suction Units	246
138	Trailing-edge Trunk Duct, Flap, and Spoiler Arrangement	247
139	Trailing-edge Trunk Duct and Aileron Arrangement	248
140	Horizontal-to-vertical Fin Transfer Ducting	249
141	Ducting Arrangement for Fin-Mounted Suction Unit	249

Figures (Continued)

No.		Page
142	Normalized Wing Suction Characteristics, LFC-200-S	251
143	Comparison of Normalized Wing and Empennage Suction Characteristics, LFC-200-S	252
144	Normalized Empennage Suction Characteristics, LFC-200-S	254
145	Independently Powered Wing Suction Unit, LFC-200-S	255
146	Independently Powered Empennage Suction Unit, LFC-200-S	256
147	General Arrangement, LFC-200-R	259
148	LFC Suction Unit Installation, LFC-200-R	260
149	Boundary Layer Velocity Gradient, LFC-200-R	262
150	Slot Spacing and Pressure Loss vs. Slot Width, Upper WS 370, LFC-200-R	263
151	Slot Spacing and Pressure Loss vs. Chord Location, Upper WS 370, LFC-200-R	265
152	Wing Section, LFC-200-R	267
153	Wing Root Collector Duct Characteristics, Upper Wing, LFC-200-R	268
154	Collector Duct Local Characteristics, 0.635 cm (0.25 in) Collector Height, LFC-200-R	269
155	Collector Exit to Trunk Duct Pressure Matching, Upper Wing, LFC-200-R	270
156	Collector Exit and Trunk Duct Flow Mach Number Characteristics, Upper Wing, LFC-200-R	271
157	Normalized Airplane Suction Characteristics, LFC-200-R	274
158	Bleed-Burn Powered Suction Unit, LFC-200-R	275
159	General Arrangement, LFC-400-S	278
160	Slot Spacing and Pressure Loss vs. Slot Width, Upper WS 480, LFC-400-S	281

Figures (Continued)

No.		Page
161	Wing Upper Surface Planform, LFC-400-S	282
162	Slot Spacing and Pressure Loss vs. Chord Location, Upper WS 480, LFC-400-S	283
163	Wing Root Collector Duct Characteristics, Upper Wing, LFC-400-S	287
164	Collector Duct Local Characteristics, 1.778 cm (0.70 in) Collector Height, Upper Wing, LFC-400-S	288
165	Collector Exit to Trunk Duct Pressure Matching, Upper Wing, LFC-400-S	289
166	Collector Exit and Trunk Duct Flow Mach Number Characteristics, Upper Wing, LFC-400-S	290
167	Normalized Airplane Suction Characteristics, LFC-400-S	292
168	Bleed-Burn Powered Suction Unit, LFC-400-S	293
169	General Arrangement, LFC-400-R	294
170	Slot Spacing and Pressure Loss vs. Slot Width, Upper WS 480, LFC-400-R	297
171	Slot Spacing and Pressure Loss vs. Chord Location, Upper WS 480, LFC-400-R	298
172	Wing Root Collector Duct Characteristics, Upper Wing, LFC-400-R	300
173	Collector Duct Local Characteristics, 1.016 cm (0.40 in) Collector Height, Upper Wing, LFC-400-R	302
174	Collector to Trunk Duct Pressure Matching, Upper Wing, LFC-400-R	303
175	Collector Exit and Trunk Duct Flow Mach Number Characteristics, Upper Wing, LFC-400-R	304
176	Normalized Airplane Suction Characteristics, LFC-400-R	306

Figures (Continued)

No.		Page
177	Bleed-Burn Powered Suction Unit, LFC-400-R	307
178	Acoustically Induced Transition Criteria	309
179	Nacelle Acoustic Design for FAR 36 -10 EPNdB	310
180	Noise Level Contours, LFC-200-S and LFC-200-R	313
181	Noise Level Contours, LFC-400-S and LFC-400-R	314
182	Acoustically Induced Transition Sensitivity	316
183	LFC Surfaces Subject to Acoustically Induced Transition, LFC-200-S and LFC-200-R	317
184	LFC Surfaces Subject to Acoustically Induced Transition, LFC-400-S and LFC-400-R	318
185	Control of Acoustically Induced Transition by Increased Suction	320
186	Surface Panel Fabrication	322
187	Surface Panel Assembly	327
188	Leading Edge Fabrication	330
189	Leading Edge Assembly	331
190	Primary Duct Fabrication and Assembly	333
191	Secondary Duct Fabrication and Assembly	334
192	Surface Panel Installation	335
193	Permissible Roughness Height	352
194	Histogram of Insect Size in the Aerial Population Near the Ground	354
195	Effect of Air Temperature on Density of Insect Aerial Population	356

Figures (Continued)

No.		Page
196	Effect of Wind Velocity on Density of Insect Aerial Population	357
197	Vertical Distribution of Insect Aerial Population Density	358
198	Calculated Chordwise Variation of Contamination Over the Normal Range of Incidence Occurring in Flight	359
199	Effect of Incidence on Lower Surface Roughness Envelope	361
200	Effect of Wing Profile on the Lower Surface Roughness Envelope	362
201	Comparison of Permissible and Estimated Roughness Heights	364
202	Mechanical Leading-Edge Devices for Removal of Insect Contamination	366
203	Effect of Ice Crystals on LFC Operation	369
204	Aircraft Visible-Cloud Time	370
205	Effect of LFC System Loss on Range Capability, LFC-200-R	371
206	General Arrangement, TF-200	376
207	General Arrangement, TF-400	380
208	Sensitivity of DOC to Fuel Price and LFC Maintenance Cost, TF-200 and LFC-200-S	399
209	Sensitivity of DOC to Fuel Price and LFC Maintenance Cost, TF-200 and LFC-200-R	400
210	Sensitivity of DOC to Fuel Price and LFC Maintenance Cost, TF-400 and LFC-400-R	401
211	Sensitivity of DOC to Fuel Price and LFC Maintenance Cost, TF-400 and LFC-400-R	402
212	Sensitivity of DOC to Fuel Price and LFC Production Cost, TF-200 and LFC-200-S	403

Figures (Continued)

No.		Page
213	Sensitivity of DOC to Fuel Price and LFC Production Cost, TF-200 and LFC-200-R	404
214	Sensitivity of DOC to Fuel Price and LFC Production Cost, TF-400 and LFC-400-S	405
215	Sensitivity of DOC to Fuel Price and LFC Production Cost, TF-400 and LFC-400-R	406
216	Variation of Aircraft and Mission Parameters with Stage Length, TF-200	408
217	Variation of Aircraft and Mission Parameters with Stage Length, LFC-200-R	409
218	Sensitivity of DOC to Stage Length, TF-200 and LFC-200-R	410
219	Fuel Efficiency Comparisons	414

TABLES

No.		Page
1	Aircraft Pricing Elements	17
2	Weight Technology Factors	33
3	Configuration Matrix: LFC-200-S	65
4	Configuration Matrix: LFC-200-R, LFC-200-S, and LFC-400-R	67
5	Configuration Matrix: TF-200	100
6	Sources of Porous Materials	114
7	Candidate Porous LFC Surface Materials	116
8	Required Property Improvements for Porous LFC Surface Materials	117
9	LFC Surface Panel Comparison	124
10	Summary Comparison of Suction Power Units	144
11	Weight Statement: Initial LFC-200-S Baseline Configuration	147
12	Configuration Variations: Chordwise Extent of Laminarization	151
13	Criteria for Normal and Relaxed Static Stability	166
14	Summary of Configuration Evaluation Results: LFC-200-S	189
15	Comparison of LFC-200-S Configuration Variations	191
16	Comparison of LFC-200-R Configuration Variations	192
17	Comparison of LFC-400-S Configuration Variations	193
18	Comparison of LFC-400-R Configuration Variations	194
19	Reductions in Fuel Consumption for LFC Configuration Variations	195
20	Weight Statement: LFC-200-S	199
21	LFC Surface Panel Weight Summary: LFC-200-S	234

Tables (Continued)

No.		Page
22	Weight Statement: LFC-200-R	261
23	LFC Surface Panel Weight Summary: LFC-200-R	264
24	Weight Statement: LFC-400-S	279
25	LFC Surface Panel Weight Summary: LFC-400-S	285
26	Weight Statement: LFC-400-R	295
27	External Noise Source Characteristics	311
28	Internal Noise Source Characteristics	312
29	Maximum Sound Pressure Levels on LFC Surfaces	315
30	Standard Hours per Panel for LFC Surfaces	338
31	Material Cost per Panel for LFC Surfaces	339
32	Standard Hours per Section for LFC Leading Edges	340
33	Material Cost per Section for LFC Leading Edges	341
34	Maintenance Labor Requirements for LFC Systems, LFC-200-S	345
35	Maintenance Labor Requirements for LFC Systems, LFC-200-R	346
36	Maintenance Labor Requirements for LFC Systems, LFC-400-S	347
37	Maintenance Labor Requirements for LFC Systems, LFC-400-R	348
38	Maintenance Material Requirements for LFC Systems	349
39	Mean Insect Separation Distances	355
40	Comparison of TF-200 Configuration Variations	374
41	Reductions in Fuel Consumption for TF-200 Configuration Variations	375
42	Weight Statement: TF-200	377
43	Comparison of TF-400 Configuration Variations	379
44	Weight Statement: TF-400	381

Tables (Continued)

No.		Page
45	Summary Comparison of 200-Passenger TF and LFC Aircraft	384
46	Comparison of Weight Elements for 200-Passenger TF and LFC Aircraft	386
47	Comparison of C_D Components for 200-Passenger TF and LFC Aircraft	387
48	Comparison of Production Costs for 200-Passenger TF and LFC Aircraft	388
49	Comparison of R&D Costs for 200-Passenger TF and LFC Aircraft	389
50	Comparison of DOC Elements for 200-Passenger TF and LFC Aircraft	390
51	Summary Comparison of 400-Passenger TF and LFC Aircraft	392
52	Comparison of Weight Elements for 400-Passenger TF and LFC Aircraft	393
53	Comparison of C_D Components for 400-Passenger TF and LFC Aircraft	394
54	Comparison of Production Costs for 400-Passenger TF and LFC Aircraft	395
55	Comparison of R&D Costs for 400-Passenger TF and LFC Aircraft	396
56	Comparison of DOC Elements for 400-Passenger TF and LFC Aircraft	397
57	Reductions in Fuel Consumption for LFC and TF Configuration Variations	411
58	Summary Comparison of Fuel Efficiency	412
59	Summary Comparison of DOC	413
60	Summary Comparison of DOC Variations	413

ABBREVIATIONS

APU	auxiliary power unit
AR	aspect ratio
ATA	Air Transport Association
ATC	air traffic control
ATT	advanced technology transport
BPR	bypass ratio
DOC	direct operating cost, c/skm (c/ssm)
ECS	environmental control system
EPNdB	effective perceived noise level, decibels
FPR	fan pressure ratio
FS	wing front spar, fuselage station
LE	leading edge
L/D	lift to drag ratio
LFC	laminar flow control
LFC-200-S	LFC aircraft for the 200-passenger mission based on criteria for a stable laminar boundary layer.
LFC-200-R	LFC aircraft for the 200-passenger mission based on relaxed boundary-layer stability criteria.
LFC-400-S	LFC aircraft for the 400-passenger mission based on criteria for a stable laminar boundary layer.
LFC-400-R	LFC aircraft for the 400-passenger mission based on relaxed boundary-layer stability criteria.
M	Mach number
MAC	mean aerodynamic chord, m (ft)
MLG	main landing gear
OEW	operating empty weight, kg (lb)
OPR	overall pressure ratio
PL	payload, kg (lb)
P&WA	Pratt & Whitney Aircraft
R&T	research and technology
RS	wing rear spar
RSS	relaxed static stability
SAS	stability augmentation system

SFC	specific fuel consumption, $\frac{\text{mg/s}}{\text{N}}$ $\left(\frac{\text{lb/hr}}{\text{lb}}\right)$
SLS	sea level standard
SSM	seat statute mile
TE	trailing edge
TF	turbulent flow
TF-200	Conventional turbulent-flow aircraft for the 200-passenger mission.
TF-400	Conventional turbulent-flow aircraft for the 400-passenger mission.
TIT	turbine inlet temperature, $^{\circ}\text{K}$ ($^{\circ}\text{F}$)
TOGW	takeoff gross weight, kg (lb)
T/W	thrust-to-weight ratio
VPF	variable pitch fan
W/S	aircraft wing loading, kg/m^2 (lb/ft^2)
WS	wing station

SYMBOLS

a	speed of sound, m/s (ft/s)
b	wing span, m (ft)
c	local wing chord, m (ft)
C_D	drag coefficient
c_f	skin friction coefficient
C_L	lift coefficient
C_p	pressure coefficient
c_s	slot spacing, cm (in)
e	span efficiency factor
F_n	net thrust, N (lb)
H	cruise altitude, m (ft)
H	shape factor, δ^*/θ
k	height of three-dimensional surface roughness, m (ft)
m	mass, kg (lb)
n	crossflow velocity, m/s (ft/s)
P	absolute pressure, N/m ² (lb/in ²)
R	Reynolds number
R_c	wing chord Reynolds number
R_e	boundary-layer tangential-flow Reynolds number
R_k	roughness Reynolds number
R_s	length Reynolds number
R_n	boundary layer crossflow Reynolds number

R_θ	boundary layer momentum thickness Reynolds number
S	area, m^2 (ft^2)
s	surface distance, m (ft)
t/c	wing thickness-to-chord ratio, measured streamwise
T	absolute temperature, $^{\circ}K$ ($^{\circ}F$)
U	potential flow velocity, m/s (ft/s)
U_o	free stream velocity, m/s (ft/s)
U_e	velocity at edge of boundary layer, m/s (ft/s)
v_s	area suction velocity, m/s (ft/s)
W_A	engine airflow, kg/s (lb/s)
w_n	boundary layer crossflow velocity component in the direction normal to the potential flow streamline, m/s (ft/s)
w_s	slot width, mm (in)
x/c	chord location
$(x/c)_L$	chordwise extent of laminarization
x	streamwise coordinate, m (ft)
y	coordinate normal to surface, m (ft)
z	spanwise coordinate, m (ft)
α	angle of attack, rad (deg)
β	crossflow angle, rad (deg)
β	slot design parameter
γ	ratio of specific heats
δ	boundary-layer thickness, m (ft)
δ^*	boundary-layer displacement thickness, m (ft)

η	cruise power ratio, wing semispan location
η_F	Froude efficiency
η_L	laminarization efficiency = effective chordwise extent of laminarization/chordwise extent of laminar surfaces
θ	boundary-layer momentum loss thickness, m (ft)
Λ	wing sweep angle, rad (deg)
λ	ratio of thrust horsepower lost to shaft horsepower extracted
μ	absolute viscosity, Ns/m^2 (lb s/ft ²)
ν	kinematic viscosity, M^2/s (ft ² /s)
ρ	density, kg/m^3 (lb/ft ³)
σ	slot design parameter
τ	slot design parameter

Subscripts

o	free-stream
s	slot
L	laminar
k	roughness
e	edge of boundary layer

SUMMARY

A study was conducted to evaluate the technical and economic feasibility of applying laminar flow control to the wings and empennage of long-range subsonic transport aircraft compatible with initial operation in 1985. For a design mission range of 10,186 km (5500 n mi), advanced technology laminar-flow-control (LFC) and turbulent-flow (TF) aircraft were developed for both 200- and 400-passenger payloads, and compared on the basis of production costs, direct operating costs, and fuel efficiency.

As a part of the study, parametric analyses were conducted to establish the optimum geometry for LFC and TF aircraft, advanced LFC system concepts and arrangements were evaluated, and configuration variations maximizing the effectiveness of LFC were developed. For the final LFC aircraft, analyses were conducted to define maintenance costs and procedures, manufacturing costs and procedures, and operational considerations peculiar to LFC aircraft.

Major conclusions of the study, categorized according to study phase, are summarized below. It should be observed that both aircraft and LFC system configurations are extremely sensitive to the requirements of the design mission. Therefore, the conclusions of this study are of limited applicability for LFC aircraft with varying mission requirements.

Parametric Configuration Analyses

- (1) On the basis of minimum fuel consumption, the optimum cruise speed for LFC aircraft is $M \leq 0.75$.
- (2) On the basis of minimum DOC for a fuel price of \$0.93/l (\$0.35/gal), the optimum cruise speed for LFC aircraft is $M = 0.76 - 0.79$.
- (3) Fuel consumption of LFC aircraft is minimized by selecting the maximum wing loading and aspect ratio consistent with design and performance constraints.
- (4) For 200-passenger transport aircraft, fuel efficiency is limited by wing volume constraints.
- (5) For 400-passenger transport aircraft, fuel efficiency is limited by airport performance constraints.

LFC System Concepts

- (1) No porous materials are currently available which are compatible with the requirements of LFC surfaces.
- (2) The laser may be adapted to slotting or perforating LFC surfaces with a resultant decrease in both manufacturing cost and time.
- (3) For the time frame considered in this study, non-structural slotted LFC surfaces are most compatible with the requirements of a commercial transport aircraft.
- (4) If independently-powered suction units are used, operation on ram air is more efficient than operation on suction air.
- (5) If adequate volume is available for ducting, bleed-burn suction power units are more efficient than independent units or other integrated unit configurations.
- (6) No performance improvement is achieved through integration of the suction pumps with the aircraft ECS, APU, or high-lift systems.
- (7) If it is determined that an insect contamination problem exists, several in-flight cleaning methods are sufficiently promising to justify further development.

Aircraft Configurations

- (1) The addition of external fuel tanks to aircraft with a wing volume constraint improves fuel efficiency.
- (2) The incorporation of relaxed static stability improves the fuel efficiency of all study aircraft
- (3) Both external fuel and relaxed static stability provide a greater improvement in fuel efficiency for the TF aircraft than for the LFC aircraft.

Configuration Comparisons

- (1) Compared to advanced technology TF aircraft of equal productivity, the LFC study aircraft achieve reductions in fuel consumption ranging up to 28.2%.

- (2) Compared to advanced technology TF aircraft of equal productivity, the LFC study aircraft achieve reductions in DOC up to 8.4% at a fuel price of \$0.093/l (\$0.35/gal).
- (3) Compared to current commercial transport aircraft, LFC study aircraft demonstrate fuel efficiency improvements up to 131% at the design range.

Research and Technology Requirements

- (1) Technology development is required in several areas, including LFC airfoil and system development, materials, design, and manufacturing.
- (2) The development of an LFC demonstrator vehicle is of primary importance.

A comprehensive summary of study objectives, procedures, and results is included in Volume I of this report.

1.0 INTRODUCTION

The recognition of potential long-term shortages of petroleum-based fuel, evidenced by increasing costs and limited availability since 1973, has emphasized the need for improving the efficiency of long-range transport aircraft. This requirement forms a common theme in the recent literature devoted to the analysis of future transport aircraft systems (ref. 1-5). All of these analyses recognize the contribution of aerodynamic drag reduction to aircraft efficiency and that, of the variety of drag reduction concepts which have been subjected to critical analysis, laminar flow control offers the greatest improvement.

Both the theoretical methods and the engineering and design techniques requisite to the application of laminar flow control have been reasonably well-known since the mid-1940's. The validity of this background and the potential of laminar flow control were partially evaluated in the 1960-1966 period by the X-21A Laminar Flow Control Demonstration Program conducted by Northrop (ref. 6-9). This program, which included analysis, design, fabrication, and flight test investigations, realized significant decreases in aircraft drag and fuel consumption and demonstrated technical feasibility by achieving predictable and repeatable system performance at chord Reynolds numbers up to 40×10^6 . However, the program was terminated before full operational practicability in a realistic environment was established. Since essentially no development has been undertaken since the termination of the X-21A program, questions related to the economic and operational feasibility of laminar flow control have remained unanswered.

The current and projected influence of fuel costs and availability on airline operations, combined with the technological innovations of the past decade, provide a reasonable justification for the further development of laminar flow control as applied to long-range transport aircraft. This report summarizes the results of studies conducted to evaluate the technical and economic feasibility of applying laminar flow control to long-range subsonic transport aircraft for initial operation in 1985. In performing the evaluation, parametric analyses are conducted to define optimum advanced technology configurations for laminar-flow-control and turbulent-flow transports designed for the same mission. For selected configurations, conceptual designs, manufacturing costs and procedures, and maintenance costs and procedures are developed. The relative benefits are evaluated through comparisons of the selected laminar flow control transports with similarly optimized turbulent-flow transports. Advances in technology necessary for the development of practical laminar flow control transports are identified and the research and development programs requisite to such advances are outlined.

2.0 STUDY APPROACH

This section outlines the basic assumptions and criteria which are fundamental to all aspects of the study. Included is a definition of study objectives, assumed technology levels, mission requirements, design criteria, and the overall study plan employed to achieve study objectives.

2.1 STUDY OBJECTIVES

The study described in this report has two primary objectives:

- (1) The evaluation of the technical and economic feasibility of applying laminar flow control to the wings and empennage of long-range transport aircraft.
- (2) The identification of advances in specific technology areas requisite to such application.

2.2 SCOPE

All analyses conducted as a part of this study are consistent with the guidelines and requirements outlined below.

(1) Basic Study Missions

o 200-Passenger Mission

Design Payload –

23,769 kg (52,400 lb), consisting of 200 passengers and 4536 kg (10,000 lb) of belly cargo

Design Range –

10,186 km (5500 n mi)

FAR Field Length (SLS) –

3353 m (11,000 ft)

o 400-Passenger Mission

Design Payload –

47,538 kg (104,800 lb), consisting of 400 passengers and 9072 kg (20,000 lb) of belly cargo

Design Range –
10,186 km (5500 n mi)

FAR Field Length (SLS) –
3353 m (11,000 ft)

(2) Aircraft Life Cycle

- o The assumed life cycle of the aircraft evaluated in this study is shown in figure 1(a). For initial passenger operation in 1985, the following technology levels are appropriate:

Airframe technology level – 1980
Engine technology level – 1979

- o Based on the assumed life cycle, the following guidelines are used for the economic analyses of study aircraft:

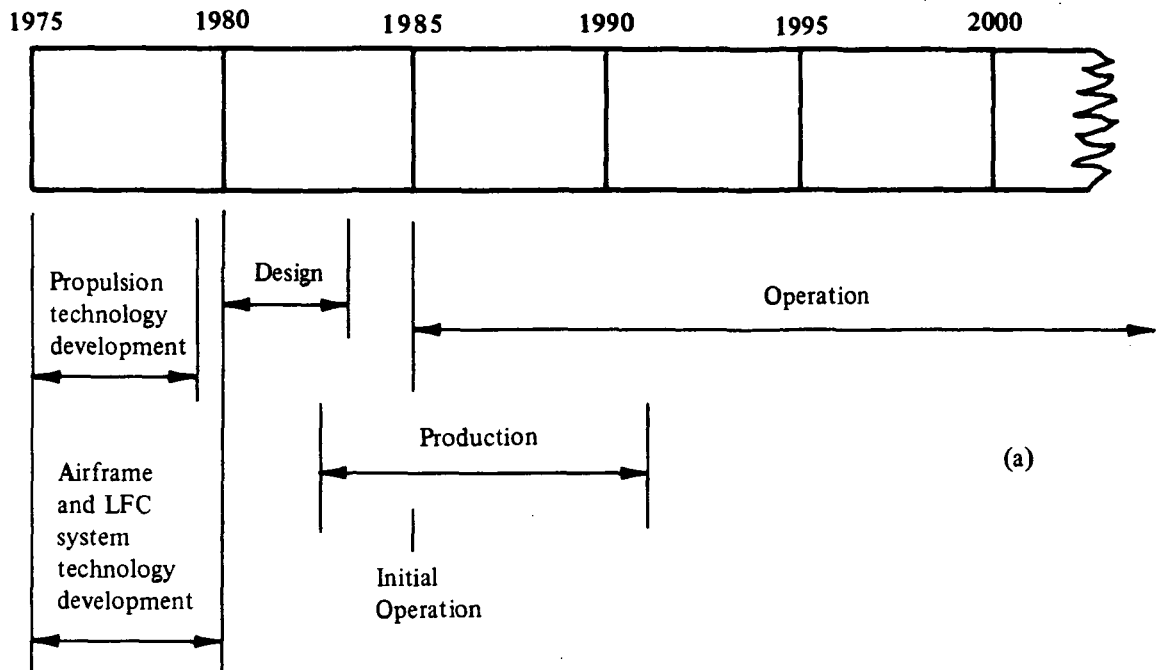
All costs are expressed in January 1, 1975 dollars
Total aircraft production – 350
Aircraft production rate – 3/mo
Fuel prices –
 \$0.066/l (\$0.25/gal)
 \$0.132/l (\$0.50/gal)
 \$0.264/l (\$1.00/gal)

(3) Mission Profile

- o The mission profile for all study aircraft is defined by figure 1(b).
- o All aircraft evaluated are compatible with the Air Traffic Control Systems and the general operating environment envisioned for the post-1985 time period.

(4) Design Criteria

- o The aircraft studied satisfy the requirements for type certification in the transport category under Federal Aviation Regulations – Part 25, and are capable of operating under pertinent FAA rules.
- o All aircraft satisfy the noise requirements of Federal Aviation Regulations – Part 36 minus 10 EPNdB.



Segment

- 1 Taxi to begin take-off position
 - 2 Take-off ground roll
 - 3 Take-off air distance and initial climb with flaps down
 - 4 Climb to 10,000 feet with speed limit of 250 knots
 - 5 Climb to altitude with prescribed speed schedule with no LFC
 - 6 Cruise with LFC (at constant altitude)
 - 7 Descend to approach pattern
 - 8 Landing approach with flaps down
 - 9 Landing air distance
 - 10 Landing ground roll
 - 11 Taxi to ramp
- (b)

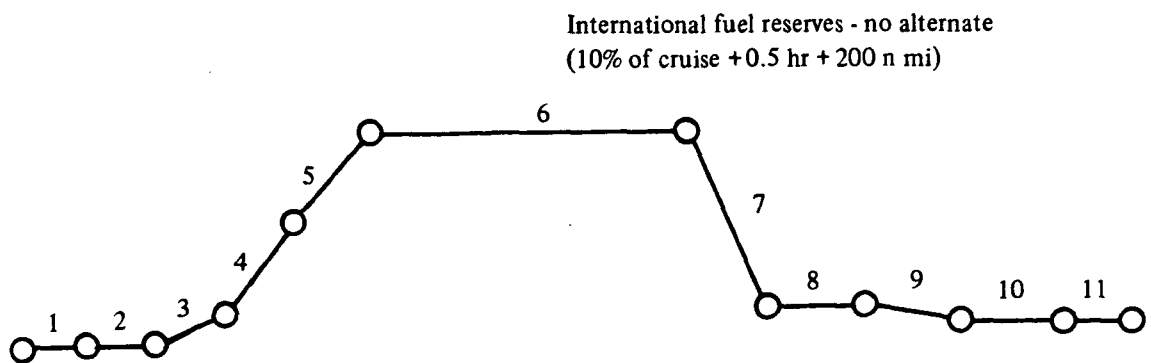


Figure 1. — Aircraft life cycle and mission profile

(5) Laminar Boundary-Layer Stability Criteria

- o Neutral stability – Values of both the boundary-layer crossflow Reynolds number, R_n , and the boundary-layer tangential flow Reynolds number, R_e , are limited to values lower than the minimum critical values for stability.
- o Relaxed stability – The value of the boundary-layer crossflow Reynolds number, R_n , is increased by a factor of 1.8 above the minimum critical value for stability. The value of the boundary-layer tangential flow Reynolds number R_e , is increased by 200 above the minimum critical value for stability.

(6) Configuration Constraints

- o This study is directed toward a practical commercial transport aircraft for initial operation in 1985. Therefore, only conventional aircraft configurations are evaluated. Variations which maximize the effectiveness of laminar flow control, such as flying wings or aircraft with aspect ratios sufficiently high to require external struts, are not considered.
- o The configurations of this study recognize the preference of commercial airlines for low-wing passenger aircraft.
- o The configurations of this study do not use the fuselage for fuel storage. The fuel volume available in the wing, the wing carry-through structure, and external fuel tanks is employed as required.

2.3 STUDY PLAN

The general approach used in conducting the total study is illustrated by figure 2. Section numbers of this report which correspond to the activities outlined in the study plan are included in this figure.

Starting with a common data base, parametric configuration analyses are conducted to evaluate the effect of aircraft geometry, operational, and performance parameters on the fuel efficiency of both laminar-flow-control (LFC) and turbulent-flow (TF) transport aircraft for 200- and 400-passenger payloads at the design range. In this phase of the study, the characteristics of LFC system elements are represented parametrically to permit the investigation of a large number of configuration variations. Based on these parametric investigations, preliminary baseline configurations are selected for both LFC and TF aircraft on the basis of minimum fuel consumption for the design mission.

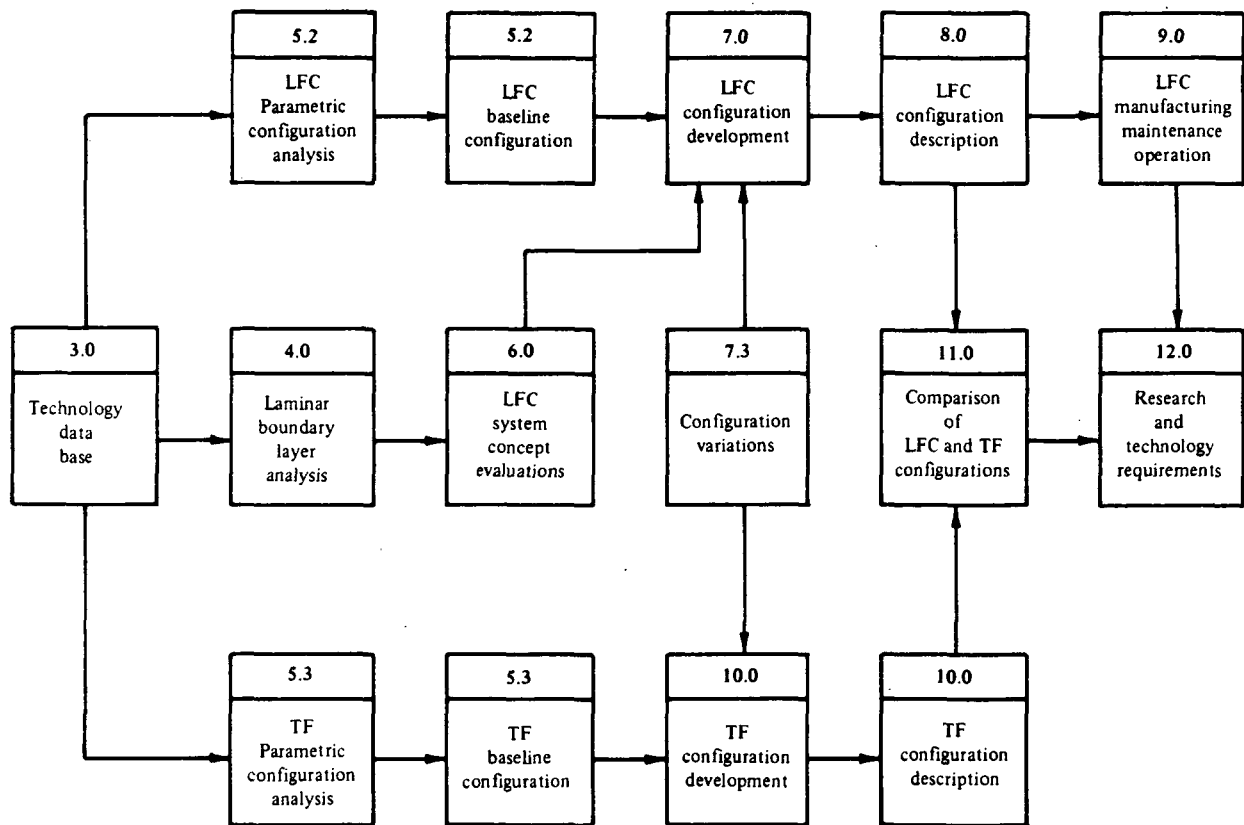


Figure 2. – Study plan

In the LFC concept evaluation phase, potential improvements in LFC system performance through the application of technology advances are investigated. Included are evaluations of advanced concepts for

- (1) LFC surfaces
- (2) Ducting and distribution systems
- (3) LFC suction units

- (4) Fuselage slot blowing
- (5) Advanced materials for LFC surfaces and internal components
- (6) Advanced manufacturing procedures for LFC system elements.

To the extent possible, evaluations are conducted as independent trade studies. For elements which are configuration sensitive, as for example, LFC suction units, the LFC baseline configuration is used as a vehicle for concept evaluation.

For advanced LFC concepts determined to be technically feasible and offer significant performance improvements, conceptual designs are developed and the LFC baseline configuration is modified as required to accommodate the concept. The performance of each configuration variation is evaluated on the basis of fuel consumption for the design mission. The LFC system elements comprising the most fuel-efficient configurations are combined to form preferred LFC configurations for both design payloads and both sets of boundary-layer stability criteria.

For the selected LFC configurations, design details, manufacturing costs and procedures, and maintenance costs and procedures are developed to permit realistic comparisons with the TF configurations modified to reflect all technology advantages incorporated into the LFC configurations.

In the evaluation and comparison phase, the relative benefits of LFC are evaluated through comparisons of the selected LFC configurations with the selected TF configurations. As a part of this evaluation, all pertinent performance, operational, and cost parameters are compared, including a definition of relative direct operating costs as a function of assumed fuel prices, LFC system maintenance costs, and LFC system production costs.

The identification of Research and Technology Requirements necessary to permit development of practical LFC commercial transports is a direct output of investigations conducted in the concept evaluation phase and the evaluation and comparison phase of the study.

3.0 BASIC STUDY DATA AND METHODOLOGY

3.1 INTRODUCTION

The complexities inherent in the completion of a systems study, involving analyses at the aircraft, system, and subsystem levels, dictate that study data and analytical procedures be considered in two separate categories. In the first category are the data which are fundamental to all aspects of the study and the analytical procedures which are used repeatedly throughout the study. The second category includes data and methodology which are used for a single specific analysis. This section is devoted to a description of the study data and methodology in the first category. For specific applications, study data and procedures are described as they are used.

Included in the discussions which follow are definitions of study aircraft configurations, a description of parametric computer programs, an outline of costing assumptions and procedures, and a definition of the reference technology level applicable to all study aircraft.

3.2 CONFIGURATION NOMENCLATURE

As outlined in section 2.2, the scope of the study requires the development of laminar-flow-control aircraft for two sets of stability criteria and two different design payloads. For comparative purposes, advanced technology turbulent-flow aircraft are required for each payload. Consequently, a total of six aircraft are developed during the course of the study. The following nomenclature is used in subsequent discussions of study aircraft configurations:

TF-200	Conventional turbulent-flow aircraft for the 200-passenger mission.
LFC-200-S	LFC aircraft for the 200-passenger mission based on criteria for a stable laminar boundary layer.
LFC-200-R	LFC aircraft for the 200-passenger mission based on relaxed boundary-layer stability criteria.
TF-400	Conventional turbulent-flow aircraft for the 400-passenger mission.

LFC-400-S	LFC aircraft for the 400-passenger mission based on criteria for a stable laminar boundary layer.
LFC-400-R	LFC aircraft for the 400-passenger mission based on relaxed boundary-layer stability criteria.

3.3 GENERALIZED AIRCRAFT SIZING PROGRAM

3.3.1 BASIC FLOW OF PROGRAM CALCULATIONS

The basic parametric sizing methodology used in this study has been employed with specialized modifications for a variety of in-house and contractual studies. The Generalized Aircraft Sizing Program (GASP) was recently used in the Advanced Transport Technology Study, and is described in detail in reference 10. The basic flow of program calculations is illustrated by figure 3. Dotted blocks indicate specialized changes to the program to accommodate LFC configurations. The parametric methodology for the effects of the LFC system are discussed in subsequent sections.

3.3.2 INPUT OF LFC SYSTEM CHARACTERISTICS

The LFC system is characterized by and sizing results are sensitive to the following inputs to the parametric sizing program:

- (1) Type of LFC suction power
 - Option 1:
Independently-powered suction units
 - Option 2:
Suction units integrated with primary propulsion system
 - Option 3:
Suction units integrated with other aircraft systems
- (2) Number and location of LFC suction units
- (3) Parametric geometric description of LFC glove and suction ducts
- (4) Parametric suction surface external pressures and suction distributions

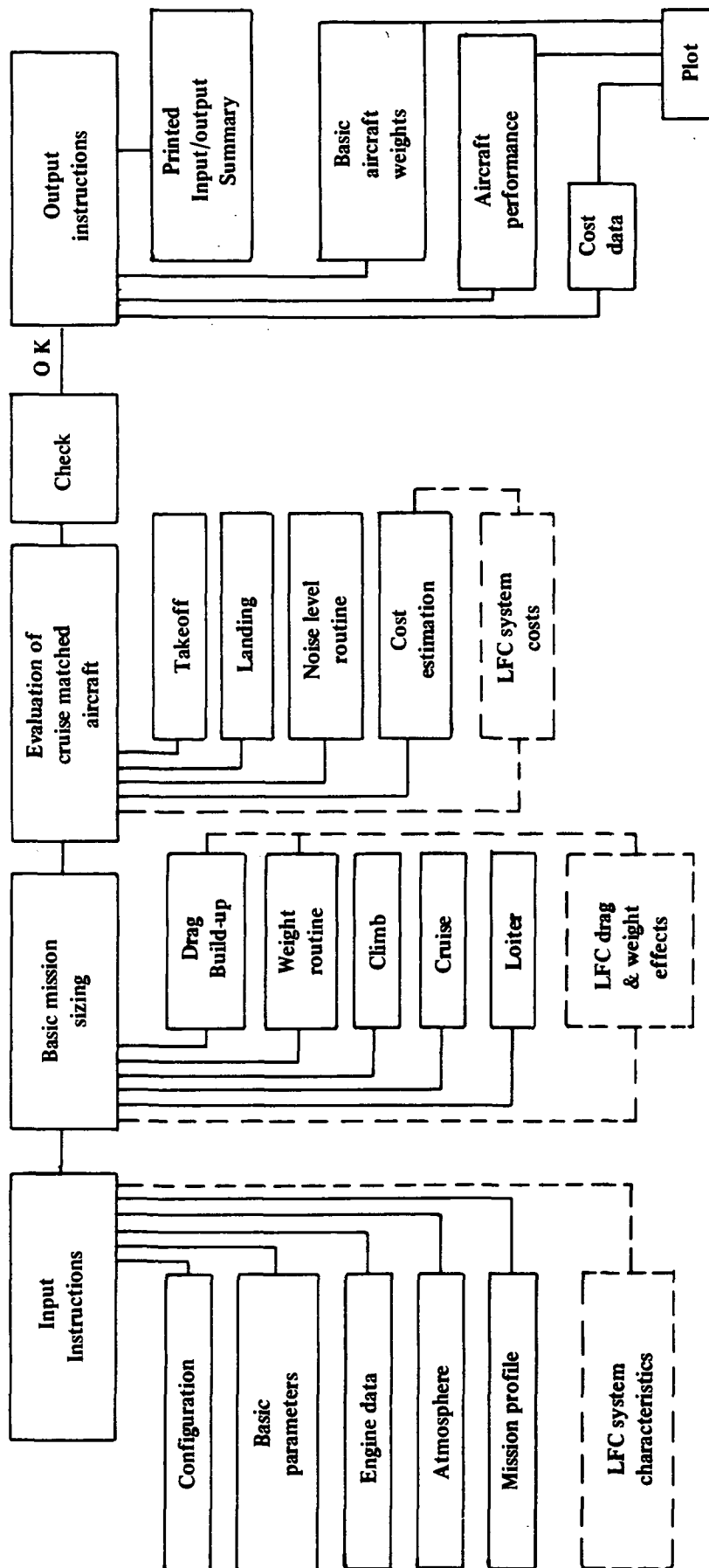


Figure 3. – Generalized aircraft sizing program

- (5) Extent of laminar flow provided by extent of LFC suction described in (3)
- (6) Parametric incremental costs of LFC systems

3.3.3 MAJOR LFC CALCULATIONS IN GASP

The flow of major LFC calculations in GASP is illustrated by figure 4. The LFC Aerodynamics Module allows examination of varying airfoil concepts through use of the detailed input description illustrated in figure 5. The method for evaluating drag with LFC operating is illustrated in figure 6. Turbulent flow is assumed for climb performance calculations by setting the value of (x/c) for transition equal to zero for drag calculations in this phase of the mission.

3.4 ECONOMIC ANALYSES

To ensure a valid comparison of the relative economics of LFC and TF aircraft configurations, identical costing procedures and assumptions were employed for both types of aircraft. Cost increments resulting from the incorporation of the LFC system were calculated as additions to the basic aircraft cost.

3.4.1 METHODOLOGY

3.4.1.1 Aircraft Pricing

The Airplane Cost Estimating Model used for pricing the aircraft of the subject study is a subroutine of GASP developed to estimate the cost to the manufacturer and the price to the airlines of conceptual transport aircraft. The maximum benefit of this program is realized in parametric cost analyses in which a large number of designs are to be considered. This program is also adaptable to economic sensitivity studies.

This model differs appreciably from former models which utilize a parametric method based on relationships between physical and performance characteristics of previously costed aircraft. Production labor and material costs in the current model are developed from anticipated hour per pound and dollar per pound values for each subsystem. These values are developed from an analysis of the specific design being studied utilizing historical cost for existing conventional subsystems, and predicted cost for conceptual system designs.

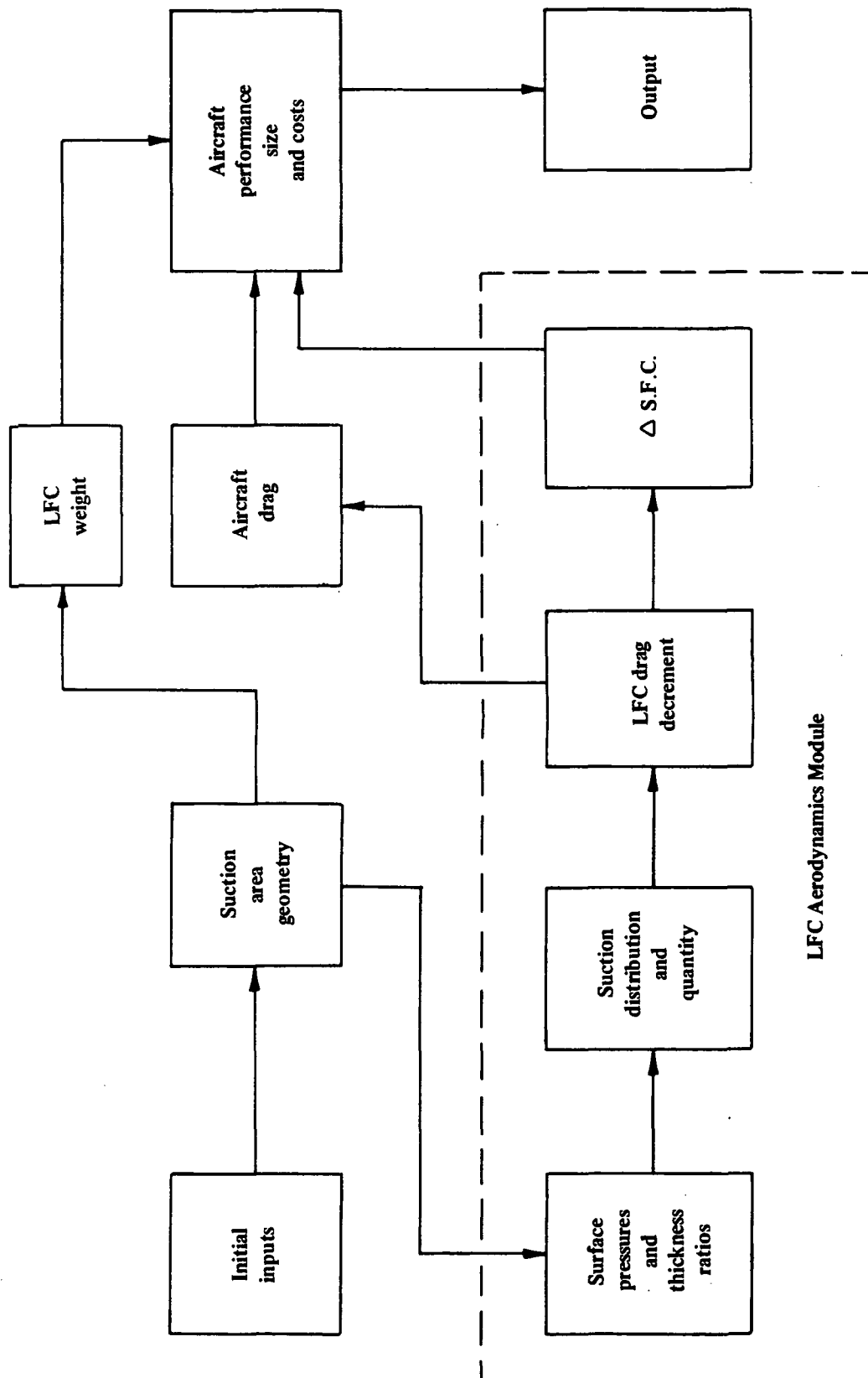


Figure 4. — Generalized aircraft sizing program, LFC subroutine

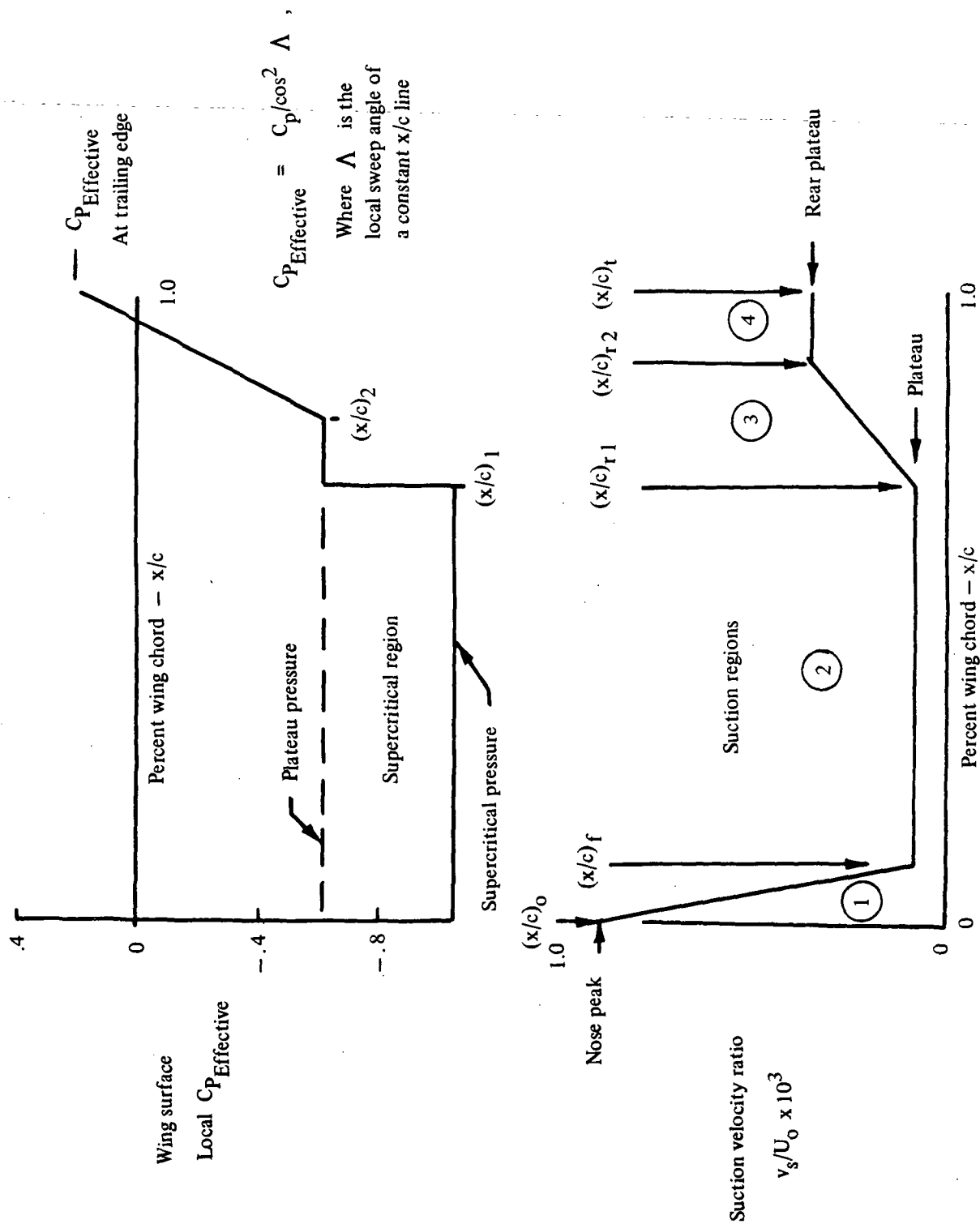


Figure 5. — Parametric description of airfoil pressures and suction

$$C_D = K \cdot \left\{ C_{F_{Total}} \cdot \frac{S_{Laminarized}}{S_{Reference}} + C_{F_{No suction}} \cdot \frac{S_{No suction}}{S_{Reference}} \right\} + \Delta C_{D_{Correlation}}$$

Where: $K = 1 + 2(t/c) + 60(t/c)^4$

$$C_{F_{Total}} = C_{F_{Laminar}} \cdot (x/c)_{Transition} + C_{F_{Turbulent}} \cdot [1 - (x/c)_{Transition}]$$

$$C_{F_{Laminar}} = \left\{ \frac{1.328}{\left(\frac{\rho_{\infty} V_{\infty}}{\mu_{\infty}} X_{Transition} \right)^{\frac{1}{2}}} \right\} / (1 + 0.72 M_{\infty}^2)^{0.12}$$

$$C_{F_{Turbulent}} = (C_{F_{Turbulent}})_{M=0} / (1 + 0.18 M_{\infty}^2)^{0.5}$$

From the correlated Karman-Schoenherr Laws, for $M = 0$

$$\log_{10} \left\{ \frac{\rho_{\infty} V_{\infty}}{\mu_{\infty}} C \left[1 - (x/c)_{Transition} \right] C_{F_{Turbulent}} \right\} = 0.242 \sqrt{C_{F_{Turbulent}}}$$

To correlate parametric method with detailed drag method

$$\Delta C_{D_{Correlation}} = -0.0005$$

Figure 6. — Parametric drag calculations with part-chord laminar flow control

This concept is necessary for the aircraft currently being studied since takeoff gross weight decreases with increased composite application and the use of LFC. If the parametric method were used to cost such aircraft, the cost would be lower than conventional aircraft since takeoff gross weight is such a significant factor.

The research and development costs utilize the Rand equations (ref. 11), historical Company data, and factors for modification of each element. The factors are developed from individual analysis of the design and cost data pertinent to the subject design.

The cost elements in the model are divided into two major categories: Production, which includes the cost elements associated with production of the aircraft; and development, which includes elements charged to the airplane program development. The element breakdown of each of these categories is shown in table 1. Categories exist for any element needed to generate the "flyaway" cost. As requirements dictate, additional elements beyond those shown may be added. To permit costing of LFC system elements, LFC surface, ducting, and suction unit costs were added and R&D cost factors were added to the appropriate cost elements. If conventional airplanes are costed in this model, the LFC system costs are zeroed out, and the R&D cost factors are reduced to one, negating the tooling and engineering increases provided for LFC cost increments.

A model with this degree of sophistication obviously requires more input data than former cost models, but several advantages are realized. The cost is more accurate in that each subsystem is separately costed and costs are based on the weight of each subsystem, thereby eliminating the use of takeoff gross weight as a costing parameter.

3.4.1.2 Direct Operating Costs

For years the 1967 Air Transportation Association methodology for calculating direct operating cost has been employed. Recently, the airlines have justifiably criticized the methodology as being outdated and not representative of direct cost in the current environment. The two primary jet aircraft of the 1967 fleet were the Douglas DC-8 and the Boeing 707. Current airline fleets are interspersed with numerous jet aircraft from turboprop to turbojet and from small jet passenger transport aircraft to the jumbo jets or wide body transports. There is no question of the need for cost data which more nearly typifies today's airline fleet environment.

Several steps have been made to correct this discrepancy. Boeing developed a set of equations based on updated fleet operations and associated costs and American Airlines developed a set of equations for propulsion subsystem maintenance costing (ref. 12). Calculation of direct operating costs in this study utilized a combination of these methodologies. A computerized model was developed as a subroutine of GASP to permit rapid calculation of DOC.

TABLE 1. AIRCRAFT PRICING ELEMENTS

Production	
Wing	Sustaining engineering
Tail	Technical data
Body	Production tooling maintenance
Landing gear	Miscellaneous
Flight controls	Engineering change order
Nacelles	Quality assurance
Propulsion	Airframe warranty
Engine	Airframe fee
Air induction	Airframe cost
Fuel system	Engine warranty
Start system	Engine fee
Engine controls	Engine cost
Fire extinguishing	Avionics cost
Exhaust/thrust reverser	Research and development
Lube system	Total flyaway cost
Propellers	
Total propulsion	
Instruments	
Hydraulics	
Electrical	
Electronics racks	
Furnishings	
Air conditioning	
Anti icing	
APU	
Final assembly	
Production flight	
LFC surfaces	
LFC ducting	
LFC suction system	
System integration	
Total empty manufacturing cost	
Research and Development	
	Development technical data
	Design engineering
	Development tooling
	Development test article
	Flight test
	Special support equipment
	Development spares
	Engine development
	Avionics development
	Total research and development
	LFC research and development

The elements that comprise the total direct operating cost are essentially the same as those in the 1967 ATA equations, and include crew cost, fuel and oil, insurance, airframe maintenance labor and material, engine maintenance labor and material, maintenance burden, and depreciation. As in the case of the aircraft pricing program, operating costs peculiar to the LFC system elements are added to the DOC of the basic airplane to obtain the DOC for the LFC aircraft configurations.

3.4.2 ASSUMPTIONS

The following assumptions were employed for the generation of aircraft price and direct operating cost data for both the LFC and TF study aircraft:

- (1) All costs are expressed in January 1, 1975, dollars
- (2) Total production: 350 units
- (3) Production rate: 3 units/month
- (4) Learning curve
 - o Labor: 75%
 - o Materials: 89%
- (5) Spares
 - o Airframe: 6%
 - o Engine: 30%
- (6) Utilization: 4200 hr/year
- (7) Depreciation: 14 years to 10%
- (8) Fuel price
 - o \$0.066/l (\$0.25/gal)
 - o \$0.132/l (\$0.50/gal)
 - o \$0.263/l (\$1.00/gal)

3.4.3 LFC SYSTEM COSTS

The economics of LFC transport aircraft are distinguished from those of comparable TF transports by the production, development, and operating cost increments attending the incorporation of the LFC system elements. The system elements peculiar to the LFC aircraft include the LFC surfaces, ducting, and suction units.

3.4.3.1 Pricing of LFC Systems

In the generation of production cost data for LFC system elements, it is assumed that LFC surfaces, ducting, and structural components required for installation are fabricated by an airframe manufacturer. The engines, compressors, and controls which form the LFC suction pumps are procured as a unit from an appropriate engine manufacturer.

LFC Surfaces and Ducting – A detailed analysis of production labor and material costs was completed for each of the selected LFC surface and ducting configurations. A complete description of both labor and material requirements for the final LFC configurations is presented in section 9.2.

LFC Suction Units – The costs of suction units and controls for the LFC aircraft are based on estimates for each specific unit provided by an engine manufacturer. Following is the cost per kilogram (pound), including development costs, of the suction units used on the final LFC aircraft:

LFC-200-S	\$1124/kg	(\$510/lb)
LFC-200-R	\$1045/kg	(\$474/lb)
LFC-400-S	\$1299/kg	(\$589/lb)
LFC-400-R	\$1199/kg	(\$544/lb)

These estimates are in close agreement with the data of references 11 and 13 for turboshaft engines of comparable characteristics.

Development – Development costs for LFC aircraft were modified as follows relative to the TF aircraft:

- (1) Design engineering – Increased by 15%, based on the data of reference 14.
- (2) Development tooling – Increased by 8%, based on the data of reference 14.
- (3) Development test articles – No specific cost increment was included. This element is a function of production cost, which reflects the additional cost of LFC system components.
- (4) Flight test – Increased by 25% to reflect the test requirements attending the addition of LFC system components.
- (5) Special support equipment – No specific cost increment was included. This element is a function of design engineering cost, which includes the 15% increment specified in (1).
- (6) Development spares – No specific cost increment was included. This element is a function of the production cost and spares factor and therefore reflects the additional cost of LFC system components.

- (7) Engine development — All costs for engine development are included in engine production costs.

3.4.3.2 Operating Costs for LFC Systems

A comprehensive maintenance analysis, discussed in section 9.3, was performed for each component of the LFC systems incorporated in the final study aircraft. Maintenance labor and material costs for each component were summed to obtain the total maintenance cost peculiar to the LFC aircraft. These costs were input into the costing subroutine of the GASP to include the influence of LFC system maintenance requirements on the DOC of LFC transports.

3.5 REFERENCE TECHNOLOGY LEVEL

3.5.1 AERODYNAMICS

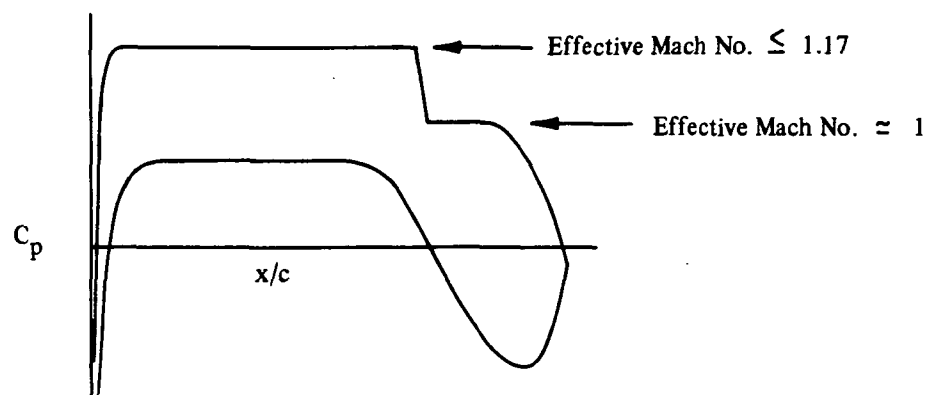
The level of aerodynamics technology considered in this study includes the use of advanced airfoil sections, as reflected in the supercritical airfoil concept. Other aerodynamics technology, involving the degree of suction necessary to maintain laminar flow and other LFC aerodynamics were taken at the X-21 state of the art defined in references 15 and 16. Figure 7 illustrates airfoil types considered and figure 8 gives a summary of the LFC aerodynamics criteria utilized.

3.5.1.1 Baseline Supercritical Airfoil

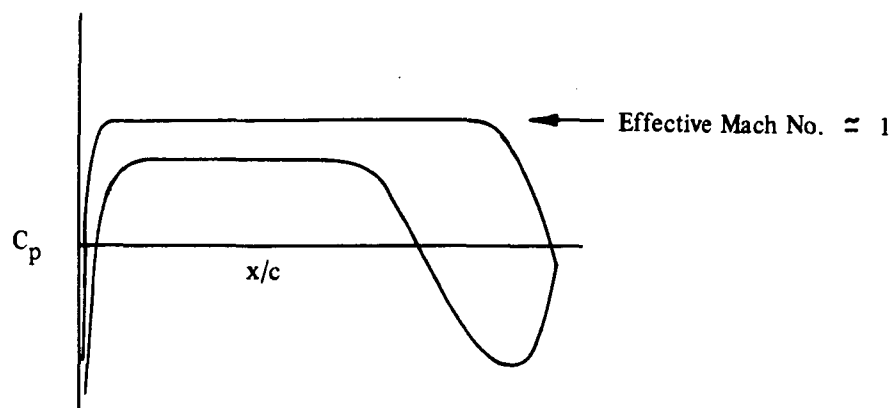
Favorable supercritical flow permits design of wings with low sweep and greater thicknesses than used for X-21 LFC wings. For LFC configurations, the design curves summarized in figure 9 are typical of those used for establishing the relation among Mach number, lift coefficient, sweep angle, and thickness ratio. For turbulent configurations the design curves given in figure 10 were used. The turbulent wings have slightly less capability than the LFC wings since viscosity destroys more aft-loading lift for the fully turbulent airfoils.

3.5.1.2 X-21 Rooftop 6-Series Type Airfoil

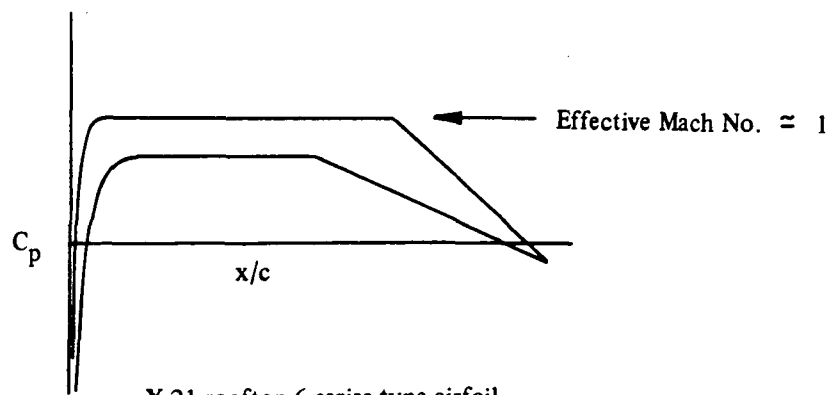
During the X-21 LFC program, use of 6-series type airfoils required a comparatively large wing sweep angle. In this study, LFC configurations with wings of this type were compared to configurations with baseline supercritical wings. Wing section design curves used for these comparisons are presented in figure 11.



Baseline supercritical airfoil



High aft loaded rooftop airfoil



X-21 rooftop 6-series type airfoil

Figure 7. — Airfoil design concepts

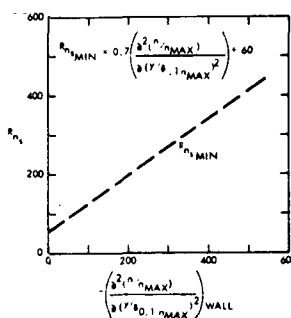
BOUNDARY LAYER CRITERIA WITH NO SOUND DISTURBANCE

TANGENTIAL FLOW REYNOLDS NO.

$$\log_{10} RN = 1.371 + 5.528H - 1.944H^2 \quad \text{IF } H \leq 2.6$$

$$\log_{10} RN = 1/[(.346H - .515)] \quad \text{IF } H > 2.6$$

- STAGNATION ZONE MOMENTUM THICKNESS REYNOLDS NO. ≤ 100
- LOW UNIT REYNOLDS NO. AND/OR CHORD REYNOLDS NO.
- MINIMUM CROSSFLOW STABILITY LIMIT REYNOLDS NO. AS INDICATED BELOW



R_{n_s} CROSSFLOW STABILITY LIMIT REYNOLDS NUMBER, BASED ON n_{MAX} AND δ 0.1 n_{MAX}

n CROSSFLOW VELOCITY IN THE BOUNDARY LAYER OF THE DISTANCE y FROM THE WALL

n_{MAX} MAXIMUM CROSSFLOW VELOCITY

y NORMAL DISTANCE FROM THE WALL

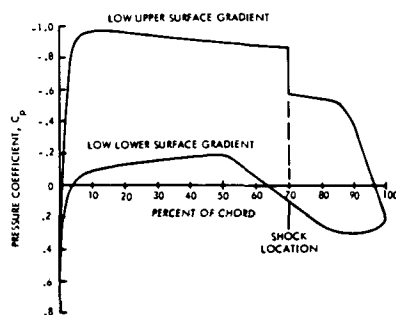
δ 0.1 n_{MAX} BOUNDARY LAYER THICKNESS WHERE CROSSFLOW VELOCITY IS 0.1 n_{MAX}

LAYOUT REQUIREMENTS

- SMALL SIZED NACELLE AND SUCTION PUMP PODS
- HIGH WING LOCATION PREFERENCE
- LOCAL CONTOURING OF NACELLES, PODS, AND FUSELAGE INTERSECTIONS WITH FLYING SURFACES TO MAXIMIZE EXTENT OF STRAIGHT ISOBARS
- AFT LOCATION OF WING-MOUNTED PODS OR NACELLES TO MINIMIZE PRESSURE INTERFERENCE AND ACOUSTIC DISTURBANCES
- MINIMUM SWEEP AND MAXIMUM ASPECT RATIO

POTENTIAL FLOW PRESSURES

- STRAIGHT ISOBARS BOTH UPPER AND LOWER SURFACES (IMPLIES SIMILAR CHORDWISE PRESSURES AT ALL SPAN STATIONS)
- LARGE EXTENT OF LOW PRESSURE GRADIENT IN CHORD DIRECTION AND INITIAL RAPID ACCELERATION OF VELOCITY AT LEADING EDGE AS INDICATED IN ILLUSTRATION
- PRESSURES COMPATIBLE WITH LOCAL EFFECTIVE MACH NO. ≤ 1.17
- TRAILING EDGE PRESSURE COEFFICIENT ~ 0.20 MINIMUM



SMOOTHNESS CRITERIA

CHORD REYNOLDS NO. $= 80 \times 10^6$
CHORD $= 45$ FT.

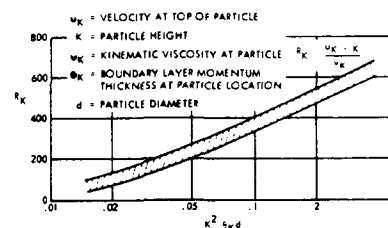
- FOR TWO-DIMENSIONAL SURFACE WAVES (SINGLE WAVES), THE ALLOWABLE WAVE AMPLITUDE RATIO IS GIVEN BY THE FORMULA

$$\frac{a}{\lambda} \approx \left(\frac{59000 C \cos^2 \Lambda}{\lambda (Re)^{1.5}} \right)^{1/2}$$

WHERE a = DOUBLE WAVE AMPLITUDE λ = WAVE-LENGTH
 C = CHORD AND Λ = SWEEP-BACK ANGLE. MULTIPLE WAVES, ONE-THIRD OF THE VALUE SHOULD BE USED.

- FOR FORWARD-FACING STEPS, THE ALLOWABLE STEP HEIGHT IS GIVEN BY $(Re/h) \cdot (h) \approx 1800$, h = STEP HEIGHT, AND REPRESENTATIVE VALUE $h = 0.010$ IN. FOR AFT-FACING STEPS, ONE-HALF OF THIS VALUE IS ALLOWED.
- FOR GAPS, THE ALLOWABLE GAP WIDTH IS EXPRESSED BY $(Re/h) \cdot (g) \approx 15000$, WHERE g IS THE GAP WIDTH. REPRESENTATIVE VALUE $g = 0.09$ IN.

ALLOWABLE THREE-DIMENSIONAL ROUGHNESS FOR LAMINAR FLOW



ACOUSTIC DISTURBANCE

- ADD 20% TO TOTAL SUCTION REQUIREMENT TO AVOID CROSSFLOW DESTABILIZATION OF STRONG SOUND ENVIRONMENT
- USE LOW NOISE LEVEL ENGINE CYCLES
- QUANTITATIVE X-21A RESULTS AS ILLUSTRATED BELOW

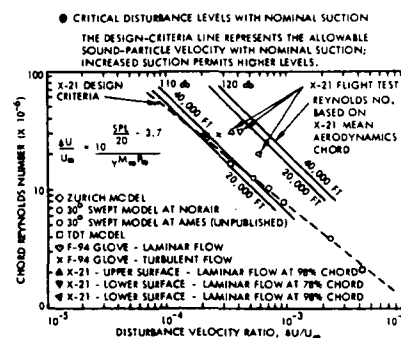


Figure 8. — LFC aerodynamics criteria

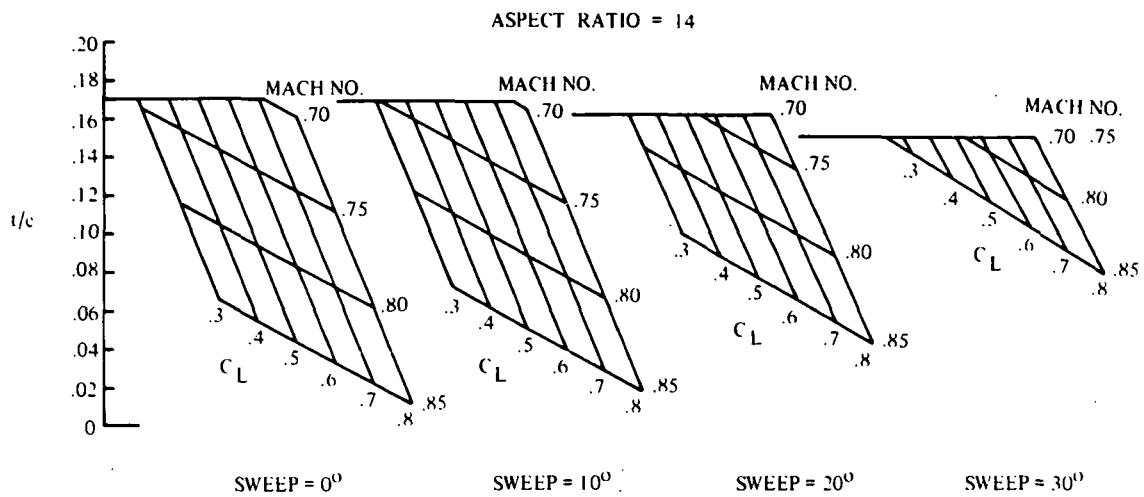


Figure 9. — Wing section design curves for supercritical LFC airfoil

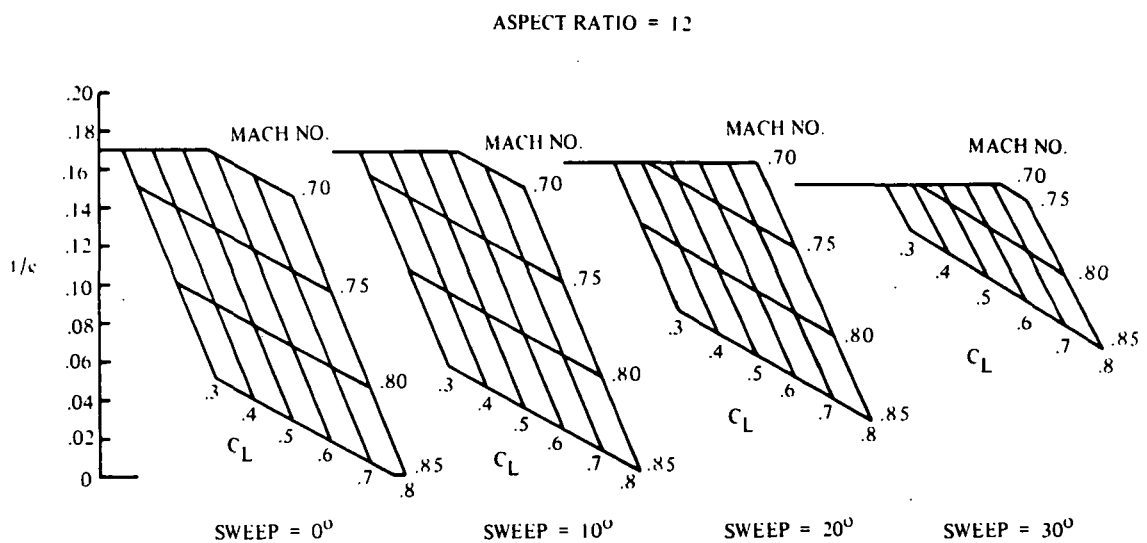


Figure 10. — Wing section design curves for supercritical TF airfoil

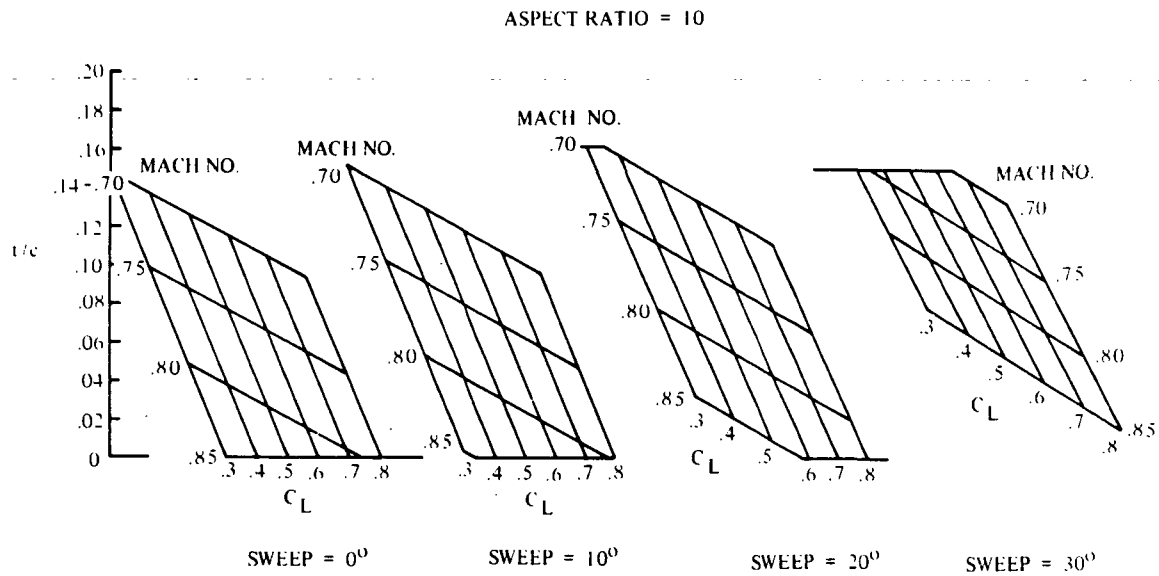


Figure 11. — Wing section design curves for X-21 rooftop 6-series type airfoil

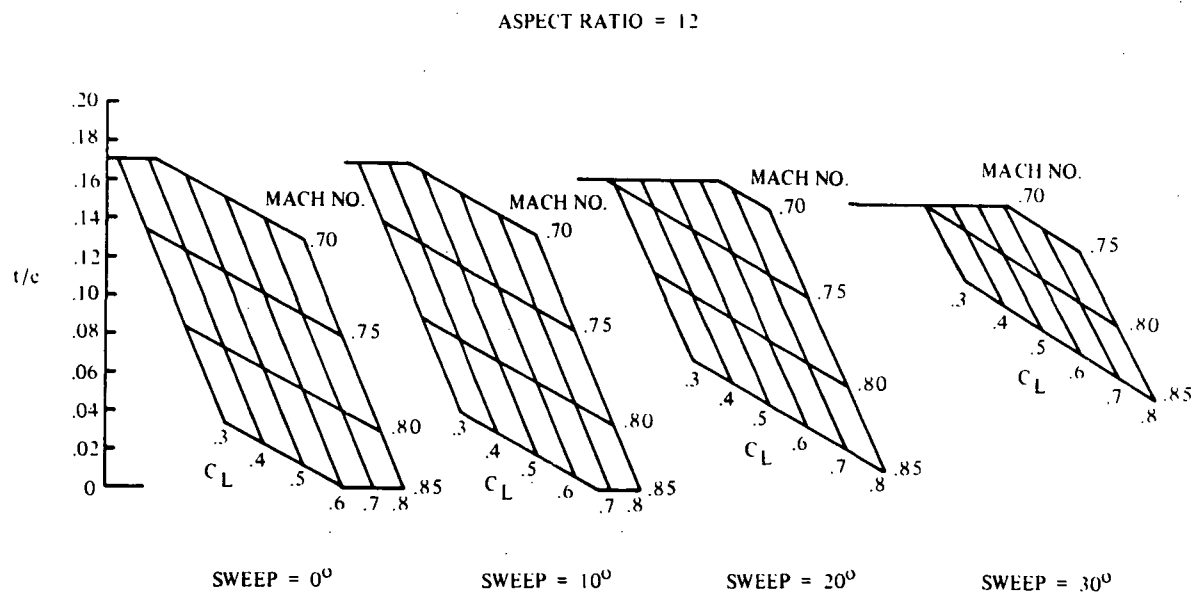


Figure 12. — Wing section design curves for high-aft-loaded rooftop airfoil

3.5.1.3 High Aft-Loaded Rooftop Airfoil

Adding high aft loading to the X-21 type rooftop airfoil produces an airfoil with performance between that of the X-21 rooftop and the supercritical airfoil. LFC wing section design curves used in the study for this concept are presented in figure 12.

3.5.1.4 LFC Suction Requirements

Using X-21 suction data from reference 15 and recent calculations from a quasi-three-dimensional laminar boundary layer program, parametric suction requirements were developed for use in the majority of the study. For initial stages of the study a conservative level of suction was chosen to give sufficient suction to account for large system inefficiencies and acoustic disturbances and still maintain a fully stable laminar boundary layer. Later boundary-layer calculations and airfoil optimization indicated that suction could be reduced approximately 30% and still give a stable laminar boundary layer. This level of suction was used for the final LFC-200-S and LFC-400-S configurations. The minimum suction level which can be used is one which results in an unstable boundary layer in which disturbances do not amplify sufficiently to cause transition to turbulent flow. This suction level offers another 35% reduction in suction level and was used for the final LFC-200-R and LFC-400-R configurations.

3.5.2 PROPULSION SYSTEMS

The propulsion aspects of the LFC airplane fall naturally into two basic categories: the primary propulsion system and the LFC suction system. These systems may be independent or related, depending on whether the LFC suction system is independently powered or derives all or part of its power from the primary system. The initial parametric studies were oriented toward a rapid evaluation of the system variables and convergence on the more promising airplane configurations. Toward this end, it was concluded that the initial effort would be best served by the choice of a completely independent LFC suction system. It was further observed that the multitude of variables and system configurations possible for the LFC suction system demanded the bulk of the propulsion study effort. It was therefore concluded that parametric primary propulsion system data would be selected from readily available sources and applied to this study with the minimum effort consistent with valid results and comparisons. This approach is admissible since the basis of comparison in this study is a turbulent-flow airplane generated to the same technology levels and utilizing the same parametric primary propulsion system data.

3.5.2.1 Primary Propulsion System

Engine Selection – The choices of existing parametric data for the primary propulsion system were determined to lie between study data generated by Detroit Diesel Allison Division of GMC (DDA) and data generated by Pratt & Whitney Aircraft (P&WA). The DDA data were generated under

Contract NAS 3-16727 to NASA Lewis for the QCSEE Study Program and are reported in reference 17. The P&WA data were generated under Contract NAS 3-15550 to NASA Lewis in support of the ATT System Study and are reported in reference 18. Both of these data incorporated advanced engine technologies for the 1975 to 1985 time period and embodied quiet engine features consistent with noise levels below the FAR 36 level.

The DDA data were oriented to short haul STOL applications with cruise speeds in the 0.6 to 0.8 Mach range with particular emphasis on high takeoff thrust and low sideline noise. As a consequence, this engine family covered a fan pressure ratio range from 1.15 to 1.5 with the primary emphasis on the lower fan pressure ratios. To meet the stringent sideline noise limitations of 95 EPNdB at 152 m (500 ft), most of the energy was extracted from the core exhaust flow in order to reduce the core exhaust velocity and thereby core noise generation. This resulted in slightly non-optimum cruise performance.

The P&WA engines were generated for the 10,186 km (5500 n mi) ATT mission (ref. 10) in which the field lengths were less important. The engines were oriented to FAR 36-10 EPNdB noise levels and were optimized for minimum specific fuel consumption (SFC) at 0.95 Mach cruise speed. As a consequence of these objectives, the engines were in the fan pressure ratio range from about 1.5 to 1.9.

Comparison of these parametric engine data with each other and with the LFC mission requirements led to the conclusion that the P&WA data corresponded closely with the study requirements and were therefore selected. This conclusion was confirmed by the initial trade studies that resulted in selection of engines that fell in the pressure ratio range near 1.5 and where the P&WA ATT engines showed superior cruise SFC characteristics.

The selected P&WA data were based on a regression analysis of 19 cycles with selected combinations of bypass ratio, overall pressure ratio and TIT. Each cycle was matched for $M = 0.95$ cruise at 12,192 m (40,000 ft) and all were sized to produce equal thrust at cruise. Rated thrust, fuel flow, weight, fan pressure ratio, and noise data were provided for each. In the ATT study, these data were corrected for inlet losses, exhaust system characteristics, nacelle drag, acoustic treatment, power extraction, and bleed extraction and put in a form readily usable in the GASP. The primary variable in the P&WA data was bypass ratio (BPR) which was retained for use in the computer program. The format of the computer input data is shown in figure 13. The P&WA parametric data provided a family of engines similar to the example having different core engine cycles with overall pressure ratio (OPR) and turbine inlet temperature (TIT) as the primary core variables. As a simplification to the current study, the OPR was chosen at 25 and the TIT at 2300 based on the experience gained in the ATT study. While this selection may not be optimum for the current study, evidence from the ATT study indicates that the effort involved in further refining the selection would not be warranted by the minor performance improvements. It will be noted that the basic parametric data of figure 13 includes scaling factors such that the computer can match the engine to the airplane appropriately and provide input data to the weight and cost routines in the computer program.

Example — not to scale

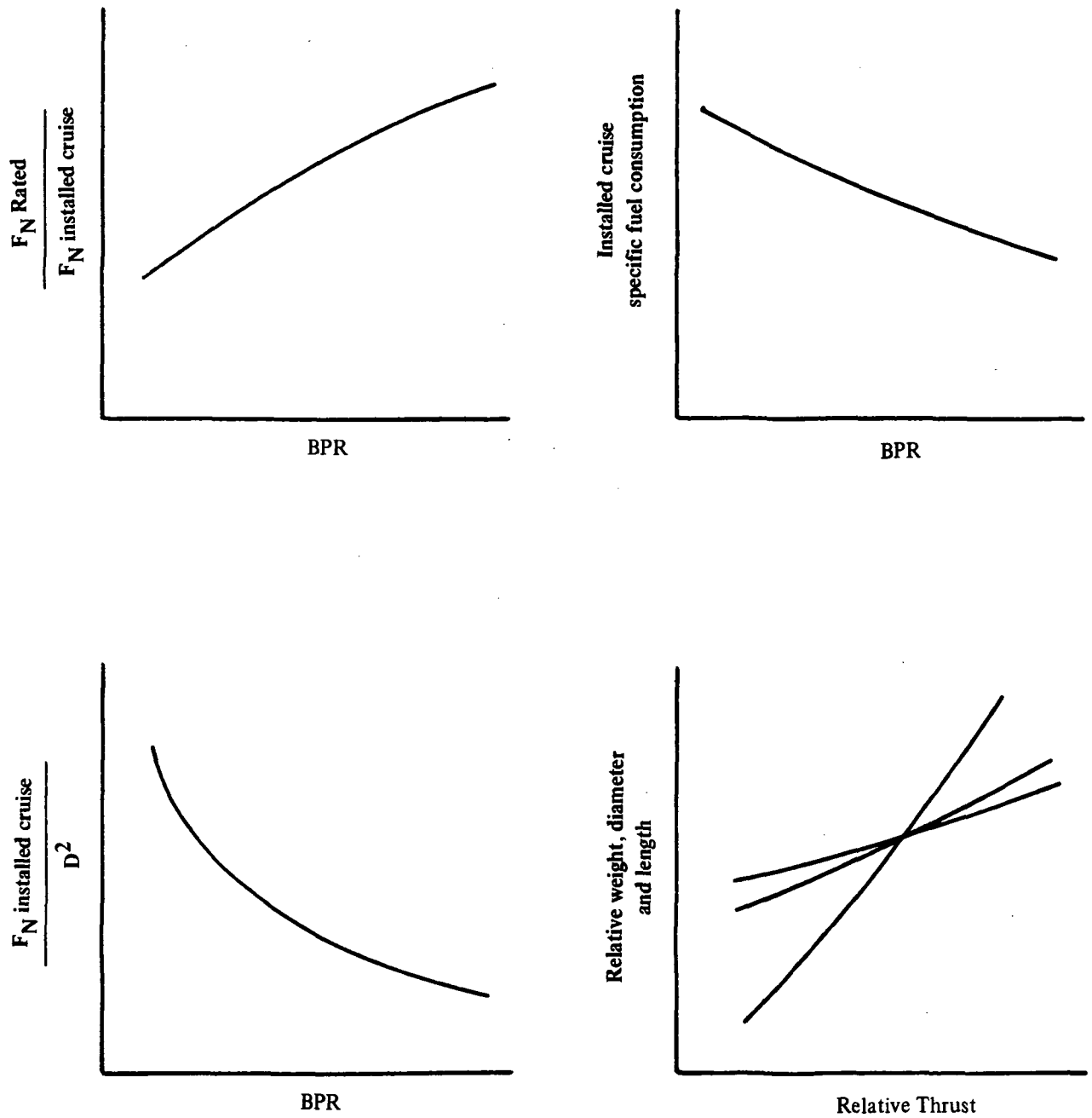


Figure 13. — Engine performance computer input

Engine Installation — The nacelle configuration and installation losses applied to the ATT engine data in reference 10 are generally consistent with those required for the LFC and TF airplanes of this study. The ATT inlet, although swept to accommodate the higher Mach cruise and for acoustic and flow field reasons, yields performance characteristics that are compatible with the requirements of the current study. The inlet recovery losses are primarily the result of the inlet acoustic treatment to meet the FAR 36-10 EPNdB noise criteria which is also compatible with the current study. Similarly, the exhaust system configuration of the ATT installations is also compatible with the current study and again the pressure losses are primarily the result of fan and primary exhaust duct acoustic treatment. The nacelle drag is scalable with engine thrust since it constitutes an essentially constant percentage of the engine gross thrust at a given Mach.

The engine bleed and power extraction are largely a function of the airplane size and number of passengers, and therefore are not precisely a function of the scaled engine thrust. Scaling these losses with engine size introduces a 0.2 to 0.4% error in the engine data for the current study. This discrepancy is optimistic in the case of the LFC airplane since the engines are smaller for the LFC airplane than for a TF airplane of essentially the same size. This discrepancy in the data is deemed acceptable.

Engine Noise — The study of reference 10 evaluated airplanes to meet FAR 36. FAR 36-10 and FAR 36-20 EPNdB noise goals. The engine performance and cycle data were therefore evaluated for acoustic treatment to meet each of these three noise levels. The current study includes the assumption of a FAR 36-10 noise limitation so only those data from the ATT study were used. The ATT study also explored variations in the number of fan stages along with bypass ratio and corresponding fan pressure ratio as they relate to the noise limits. This evaluation showed that the best DOC resulted from selection of a single stage fan at the lowest bypass ratio possible consistent with the noise limitation. A bypass ratio of 4 was found to be the minimum that would meet the noise criteria. Early parametric evaluations of the LFC airplane showed that bypass ratios in the order of 5 to 6.5 were dictated for minimum fuel consumption. This is consistent with the ATT findings and indicates that the LFC airplane should be readily capable of meeting the FAR 36-10 noise criteria without the necessity of iterating the fan pressure ratio against the noise criteria. As a consequence, the noise subroutine of the ATT study was not employed in the parametric engine selection of the LFC study.

The FAR 36 noise limits are a function of the airplane TOGW and the number of engines. These functions are such that reduction of the TOGW by 50 percent (which is the order of magnitude for the LFC airplane compared to the ATT airplane) reduces the takeoff flyover noise limit by 5 EPNdB while it reduces takeoff-sideline and landing-approach-flyover limits by 2 EPNdB. This same 50% reduction in engine thrust would reduce the engine noise distribution by about 3 EPNdB assuming that acoustic treatment was scaled linearly with engine dimensions. This indicates that scaling effects exist in meeting the requirements of FAR 36 -10 but tradeoffs are involved that tend to balance out any performance effects resulting from these modified relative noise limits. Acoustic tradeoff studies to meet the scaled limits were judged to be beyond the scope of this study. Consequently the acoustic treatment was assumed to be scalable to meet the scaled FAR 36-10

limits. In any case, the discrepancies that may exist in the absolute performance data are present in both the LFC and non-laminar airplane data to approximately the same degree, thereby eliminating these discrepancies from the comparative data.

The ATT study assumed specific technological improvements in acoustic design, material and operational techniques as delineated in reference 10. In the light of more recent developments, some of these assumed improvements appear to be somewhat optimistic; also the presence of airframe noise on approach provides a noise floor on approach at a level of about FAR 36-5. In the same period, there appears to be a shift in the target noise levels for the 1980 time frame from FAR 36-10 to FAR 36-5.

Re-examination of the technology improvement assumptions is somewhat beyond the scope of this study also and in the light of apparent trends toward higher allowable noise levels, it was concluded that the assumptions of the ATT study would be retained without alternation. Further, the ATT nacelle acoustic designs did not include any tolerance. A 3 EPNdB tolerance to allow for new aircraft and engine design to provide a reasonable business risk for noise certification would give the aircraft levels consistent with the new goals. Recognizing the above considerations and limitations, the parametric installed engine performance data with acoustic treatment for FAR 36-10 EPNdB was adopted from the ATT study without alternation.

3.5.2.2 LFC Suction System

Three distinct methods of mathematically simulating the suction units were employed in the course of the parametric studies. In the initial parametric analysis, the equivalent suction-pump-drag (D_p) method was used to assess LFC system penalties. Subsequent analyses were based on a detailed definition of independently powered suction units and such units integrated with the primary propulsion system.

Equivalent Suction Pump Drag – The initial parametric analysis was oriented toward the generation of rough-order-of-magnitude characteristics and configuration data to serve as a starting point to all disciplines for basic analysis and mathematical modelling. For this purpose, the classical equivalent suction-pump-drag (D_p) method was selected and applied, with minor revision, from the equations presented in reference 19.

Examination of this method revealed several limitations to its application in the current study. The method is based on the assumption that shaft power to drive the suction pump is extracted directly from the exhaust of the primary propulsion unit. This method of integrating the propulsion systems is the most efficient method of integration and invalidates its direct application to other suction unit power extraction methods. The installation problems associated with geared units proves to be a severe restriction on the airplane configuration and is discussed elsewhere in this report. The basic equation presented in the reference allows for but does not recognize primary propulsion FPR, indicative of cruise exhaust velocity, as a variable. In actuality, the referenced equations were derived for turbojet propulsion systems wherein the cruise exhaust pressure ratios

velocities varied over a relatively narrow band and operated with relatively low Froude efficiencies (η_F). In this study, the FPR of the basic engine was allowed to vary over a considerably broader range with further variations for a particular engine as a consequence of variations in part power cruise operation. The engine core exhaust pressure ratio was also allowed to vary with fan pressure ratio with the result that the λ ratio (thrust horsepower lost)/(shaft horsepower extracted) varied significantly. This variation is such that, as the core exhaust is reduced toward free stream velocity U_∞ , as in the case of very high bypass engines, λ approaches infinity thus yielding values of D_p that approach infinity.

The classical equivalent D_p method inherently assumes that the weight and fuel flow increments of the suction pump accrue at the level of primary engine T/W and SFC respectively for the equivalent suction pump drag.

This is not acceptable since the T/W and SFC of fan engines vary significantly with FPR, BPR, and part power conditions. In the event that a direct-drive suction pump unit is employed, the primary propulsion unit must be redesigned to achieve an optimum match for the fan, core, and suction unit drive turbines. This design approach invalidates the above assumption of weight and fuel flow increments even for the direct drive pump. Additionally, the approach does not recognize various levels of C_p and v_s/U_∞ over the upper and lower airfoil surfaces and assumes that the Froude propulsive efficiency of the primary propulsors will improve with power extraction.

Many of the above shortcomings of the classical equivalent suction drag approach to LFC evaluation may be easily overcome by minor modifications and innovations to the basic procedure, while some of the limitations are very cumbersome to eliminate. It was therefore concluded that the equivalent suction drag method would only be used in the initial parametric evaluations and alternative methods were employed for subsequent parametric evaluations. For the initial parametric evaluations, the equivalent suction drag method was adjusted to allow for upper and lower surface C_p values and equation constants were evaluated for a primary propulsion fan engine representative of the FPR range anticipated for the LFC airplane.

Independently Powered Suction Units – The second level of parametric evaluations incorporated an independently powered suction unit devised to satisfy the airplane configuration and suction requirements determined in the initial parametric. The approach used in defining this basic parametric suction unit is discussed more fully in section 6.4. The characteristics of this basic suction unit were incorporated in the GASP program together with conventional procedures for scaling the weight and fuel flow for wing surface area. This procedure was restricted to independently powered suction units and assumed a fixed wing loading but permitted evaluations with any primary propulsion system and airplane size.

At the time of the final parametric evaluations, the foregoing assumptions relative to the suction units had been found consistent with the parametric airplanes. The use of independently powered units was dictated by the limitations on fuel volume and duct space, which restricted the design to the use of four suction units distributed along the wing. The independently powered suction

was therefore reduced to simplified equation form and incorporated in GASP. The wing suction parameter v_s/U_o , together with sucked wing areas and air densities were integrated within the computer to define the suction flow requirements. Wing surface C_p values were used to define the pressure ratio requirements. The suction pump weight and power requirements were derived from these suction flow and pressure ratio requirements.

Since the power generator for the suction unit matches the power requirements of the suction pumps, the power generator weight and fuel flow were evaluated in terms of the same parameters. Thus the complete suction unit weight and fuel consumption were defined in terms of C_p , wing sucked area, and the integration of v_s/U_o . Relatively minor changes to constants appearing in these equations were sufficient to adapt the equations to the empennage unit with its different suction requirements.

Integrated Suction Units – Subsequent to the parametric studies a study was made of alternatives to the independently powered LFC suction system. These studies, described in section 6.4, showed that significantly lower suction unit weight and fuel flow resulted from employment of a bleed-burn system to power the suction pumps. In this system, high pressure air is bled from the primary propulsion engines and ducted to the suction pump. This air is fed through a burner and turbine to produce the power required to drive the suction pump. Since the primary propulsion units operate at part power at cruise where the LFC suction is required, there is little penalty to primary propulsion unit weight to provide this bleed, which results in a significant reduction in suction unit power generator weights. Since the suction unit power generator can utilize the full pressure ratio and TIT of the slave burner for generation of suction pump power, cycle improvements accrue that also result in suction power fuel savings with a relatively smaller penalty to the primary propulsion system fuel consumption. A generalized equation was produced similar to that for the independently powered suction units that represents the bleed-burn system weights and fuel flows as a function of wing C_p values, wing sucked areas, and the integration of v_s/U_o . This equation included the weight and fuel flow penalties of the primary propulsion units as well as the weight of ducting and insulation for the bleed air.

To minimize the number of suction units, the wing and empennage suction systems were combined in the case of the bleed-burn system. An additional modification to the bleed-burn equation was derived based on wing and empennage C_p values, sucked area and v_s/U_o integration. These equations were also incorporated in the GASP program.

3.5.3 STRUCTURES AND MATERIALS

3.5.3.1 Materials

The definition of the reference materials technology level for both the LFC and TF configurations of this study is based on the following criteria:

- (1) A materials technology that is technically achievable for design commitment in 1980.
- (2) A materials technology that offers a significant improvement to structural weight and integrity.

The selection of materials for the major structural components of the study configurations was based on the results reported in the NASA ATT studies of reference 10.

In selecting materials for application in the ATT studies, candidate materials were compared on the basis of weight and cost for specific applications to the airframe structure. Selections were made for several levels of application of advanced materials on the basis of cost per pound of weight saved. Technology factors, computed for the three levels of application, were applied to the analytical weight equations used in the parametric airplane sizing program. The weight or technology factors were developed for a constant-size airplane by substituting different materials and structural concepts and computing the weights of structural elements for identical structural requirements. The full benefits of advanced materials were realized by resizing the total airplane, including the power plant and other systems, to take advantage of the lower structural weights.

In computing the technology factors, candidate materials and structural concepts were examined for each element of the structure. A weight factor of 1.00 was assigned to the conventional aluminum structure. Each of the other concepts was sized to identical structural requirements. The ratio of the weight of the advanced material and concept to that of aluminum was defined as the weight factor.

As a result of the relatively slow progress in the application of advanced materials since the completion of the ATT studies and the early design commitment date, a moderate use of advanced materials was assumed for the study aircraft. For both the LFC and TF aircraft, advanced materials were used in aircraft secondary structure to the extent that 21% of the total airframe weight is composite material.

Table 2 describes the distribution of advanced materials among the airframe components and lists the corresponding weight technology factors.

As indicated by this table, utilization of composites for 21% of the airframe weight results in study aircraft which weight about 90% of that of comparable current transports.

TABLE 2. WEIGHT TECHNOLOGY FACTORS

Component	Composite Weight (%)	Weight Technology Factor
Wing	24	0.91
Fuselage	16	0.89
Horizontal tail	26	0.92
Vertical tail	17	0.94
Nacelles	32	0.90
Landing gear	0	1.00
Weighted average	21	0.90

The weight technology factors of table 2 were used in the GASP for both LFC AND TF aircraft configurations.

3.5.3.2 Structures

Structural criteria for both conventional and LFC configurations are to the level of current passenger airplane technology. There are no structural technology advancements assumed in the design of either the primary or secondary structure. All primary structure is designed with current-usage aluminum alloys. Special consideration is given to fatigue and fracture toughness properties of the structure. Most secondary structure is designed with composite materials to reduce weight.

3.5.3.3 Weight and Balance

The basic airplane weights are predicted from a group of typical preliminary design parametric equations based on current transport aircraft. Some modifications for particular configuration variations such as light-weight passenger accommodations were made. Other adjustments include weight reductions for composite secondary structure and necessary allowances for the LFC system based on detailed analyses of representative design layouts. The wing is located to provide optimum balanced configurations with a forward limit of 20% MAC and an aft limit of 40% MAC.

4.0 AERODYNAMIC DESIGN AND LAMINAR BOUNDARY LAYER ANALYSIS

4.1 INTRODUCTION

Aerodynamic design of TF configurations followed established methods for design of efficient high-subsonic aircraft. The potential-flow portions of these methods are equally applicable to design of LFC aircraft and require only minor modification. Figure 14 summarizes the overall wing design sequence which was utilized for both TF and LFC configurations. In this figure, elements 1, 3, and 10 are the only items in the design sequence with considerations peculiar to LFC. Due to the similarity of basic design requirements for TF and LFC, only typical LFC baseline designs are discussed in detail in this section. To establish a background for these discussions, the general requirements and methods common to TF and LFC designs are outlined.

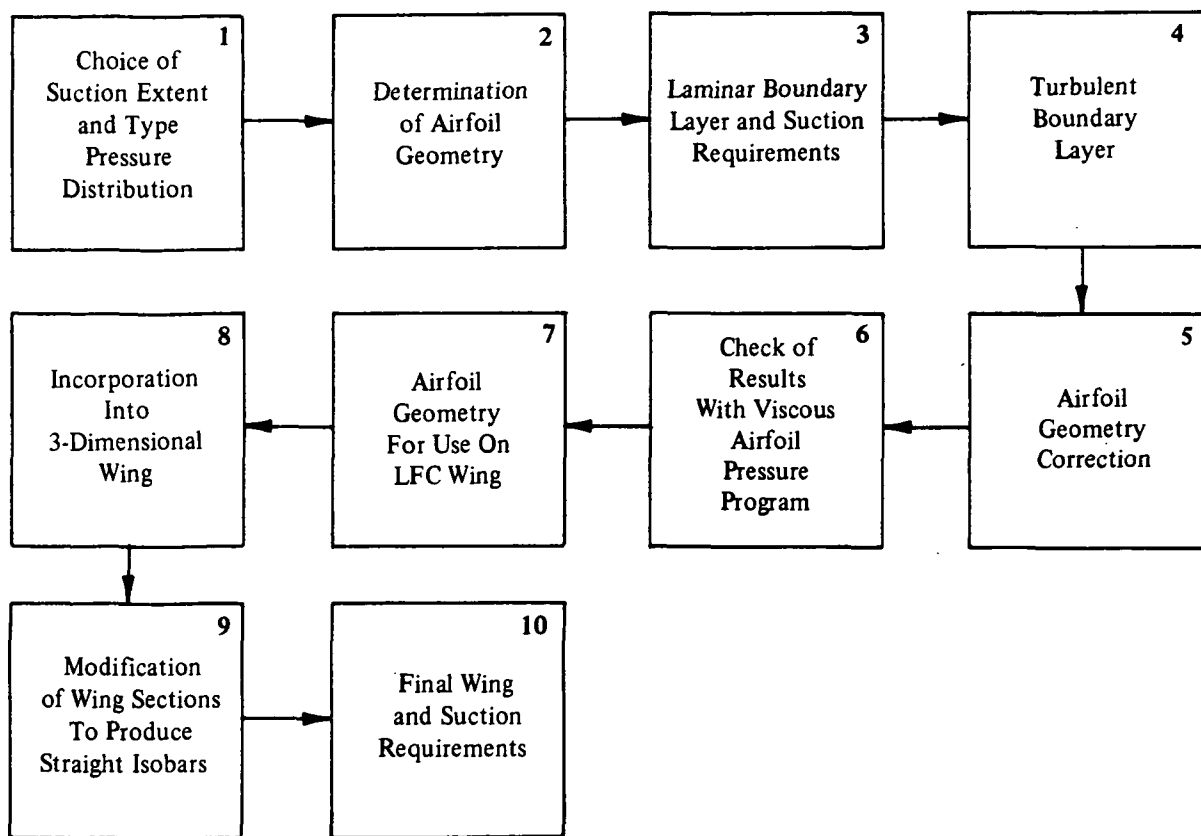


Figure 14. — Aerodynamic design procedure for LFC and TF wings

4.2 GENERAL AERODYNAMIC DESIGN REQUIREMENTS

The requirements for a good aerodynamic configuration are primarily related to the wing/body configuration. Wing/body design and analysis methods have been developed based on combining an interacting set of partial solutions to approximate very complex non-linear total solutions. The resulting unified set of approximate solutions has proved to be adequate for engineering design and analysis purposes. These methods were thus chosen as the basis of the design methodology used in this systems study.

In this sub-section, the importance of the proper wing/body design to overall configuration results is outlined and the aerodynamic design sequence and requirements used in the study are discussed.

4.2.1 IMPLICATIONS OF WING/BODY AERODYNAMIC DESIGN

It is necessary to consider the importance of the wing design as an individual component since a small improvement in the wing can make a significant difference in the overall effectiveness of the aircraft. The elements of the range equation which are influenced directly by the wing design are shown by the following simple Breguet formula:

$$\text{Range} = M \cdot \frac{L}{D} \cdot \frac{a}{\text{SFC}} \cdot \ln \left[\frac{W_e + \text{Payload} + \text{Fuel}}{W_e + \text{Payload}} \right]$$

where:

M	=	Mach number
L/D	=	cruise lift/drag ratio
a	=	speed of sound
SFC	=	specific fuel consumption
W_e	=	OEW

The cruise Mach number is obviously influenced by the wing drag rise characteristics; the aircraft lift/drag ratio is heavily influenced by the wing aerodynamic efficiency; the wing may weigh 25% of the total empty weight of the long-range aircraft considered; and the wing must carry most of the fuel. For these reasons it is of prime importance to devote particular attention to the wing design. This is true of the TF configuration, but is absolutely crucial to the success of the LFC configuration.

The advantages of speed are fairly apparent since a faster aircraft obviously permits more rapid delivery of passengers and/or cargo and enhances the operational utility of the aircraft. However, there is also a significant increase in cruise efficiency which can be derived from an increased drag divergence Mach number if increased speed can be achieved without penalizing the weight and

lift/drag ratio of the aircraft. Figure 15 demonstrates this efficiency increase in terms of the familiar parameter $M(L/D)$. Since range is proportional to this factor at a fixed altitude, $M(L/D)$ is maximized to provide maximum range. In the case of LFC configurations, the desire for an increased Mach number must be weighed against the requirement for additional sweep as M is increased. In this study a cruise Mach number of 0.80 resulted from this desire to minimize sweep.

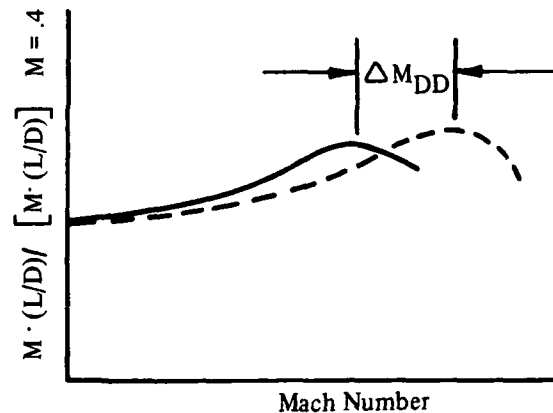


Figure 15. — Advantage of increased speed

It is also necessary to consider the substantial influence of the body on the overall effectiveness of an aircraft. The significance of an effective body design in the total vehicle configuration concept can be demonstrated by reviewing Breguet's range equation. The fuselage affects the airplane lift-to-drag ratio, the weight empty of the vehicle, and the capability of transporting payload. A reconciliation of those three factors must be accomplished in order to optimize fuselage design. The fuselage and its protuberances contribute approximately 16 percent of the total cruise drag for typical TF configurations examined in this study. In the case of LFC configurations, the fuselage becomes a serious limiting factor in achieving higher lift/drag ratios. This characteristic is pointed out in more detail by Lachmann in reference 20. For LFC configurations in this study, the fuselage typically contributes 21 percent of the total cruise drag. Thus, there must be a clear understanding of the significance of design decisions associated with the fuselage and the impact that these may have on the aerodynamics of the aircraft. The fuselage also comprises approximately 19 percent of the aircraft basic structural weight.

The separate design processes for the wing and body are complicated by the necessity for their effective combination. Such a combination can be accomplished through use of design and analysis methods for determining practical high speed wing/body aerodynamic designs.

4.2.2 AERODYNAMIC DESIGN AS A PART OF OVERALL AIRCRAFT DESIGN

Aerodynamic design and analysis methodology has evolved on the basis of certain general requirements for wing/body aerodynamic design within the context of the overall aircraft design process. This process can be thought of in terms of a preliminary design stage and a detailed design stage.

From the aerodynamics viewpoint, the preliminary design phase consists of a series of increasingly detailed studies of the configuration geometry and the associated aerodynamic performance implications. The first of these studies is a broad parametric design study which establishes a gross geometric definition. Section 5.0 of this report is devoted to this phase of the analysis. The purposes of these parametric studies are:

- (1) Selection of a preferred near-optimum design from alternative candidate systems.
- (2) Determination of performance/cost goal sensitivity to aerodynamics, weight, power plant, and suction system characteristics.

The configuration which emerges from the broad parametric analysis has certain geometric parameters defined. These primary parameters include:

- (1) Wing aspect ratio
- (2) Wing sweep
- (3) Wing average thickness ratio
- (4) Wing taper ratio
- (5) Wing planform shape
- (6) Empennage geometry
- (7) Cruise Mach number
- (8) Cruise lift coefficient

In the case of LFC aircraft, the following parameters are also defined:

- (1) LFC system suction requirements
- (2) LFC system geometry
- (3) Number of LFC suction units

Following this stage of the design process in this study, the parametric configuration geometry is examined and an initial detailed baseline wing/body shape is established to satisfy all performance requirements. A discussion of the aerodynamic concepts involved in this stage is presented in the following section.

4.2.3 AERODYNAMIC DESIGN CONCEPTS

All wing/body design procedures are based on the premises that (1) surface pressure distribution is the determinant of the characteristics of an aircraft configuration, and therefore, (2) design of a satisfactory configuration depends on specifying surface pressure criteria which produce the desired characteristics and derivation of the geometry which produces the appropriate surface pressures. Surface pressure is the independent variable, and all other parameters are developed from specified surface pressures and are dependent variables. In order to provide a better understanding of the effects of the various parameters involved in wing/body design, procedures are based on relatively simple separate wing theories, body theories, and superposition theory in a way which permits following an iterative design process. In this way an increasingly detailed design and analysis of the wing/body can be accomplished by successively adding detail in each iterative step. Emphasis is placed on proper tailoring of the wing, and the body is considered mainly in relation to its influence on the wing. The process consists of the general levels of detail illustrated by figure 16.

In the first level of detail shown in step 1 of figure 16, a wing planform, basic body geometry, and design cruise point(s) of Mach number and lift coefficient are specified by the broad parametric baseline definition. The body geometry is then transformed to an equivalent body of revolution and the body overpressures in the remote field are calculated. Utilizing the wing planform, a spanwise distribution of twist, θ , is determined in step 2 which results in a spanwise loading closely approximating desired loading. The chosen loading may be subject to constraints such as linear lofted twist distribution and necessary structural requirements.

When the approximate spanwise variation of lift is known, reference is made to a library of two-dimensional design upper surface pressure distributions which have demonstrated satisfactory performance. The airfoils are developed in step 3, using two-dimensional simple sweep theory with only body overpressure effects on the wing being taken into account. With this definition of the airfoil sections, the wing is lofted and the camber distribution is calculated at sufficient stations to permit accurate lifting surface calculations.

The twist distribution for a cambered lifting surface which approximates the desired loading is determined in step 4. This twist distribution can be considered as being composed of the planar wing twist distribution and an incremental twist distribution as is indicated in figure 16 in the second level of detail. The control station sections remain unchanged in the second level of detail, and the spanwise variation of lift coefficient are only slightly different from that calculated previously.

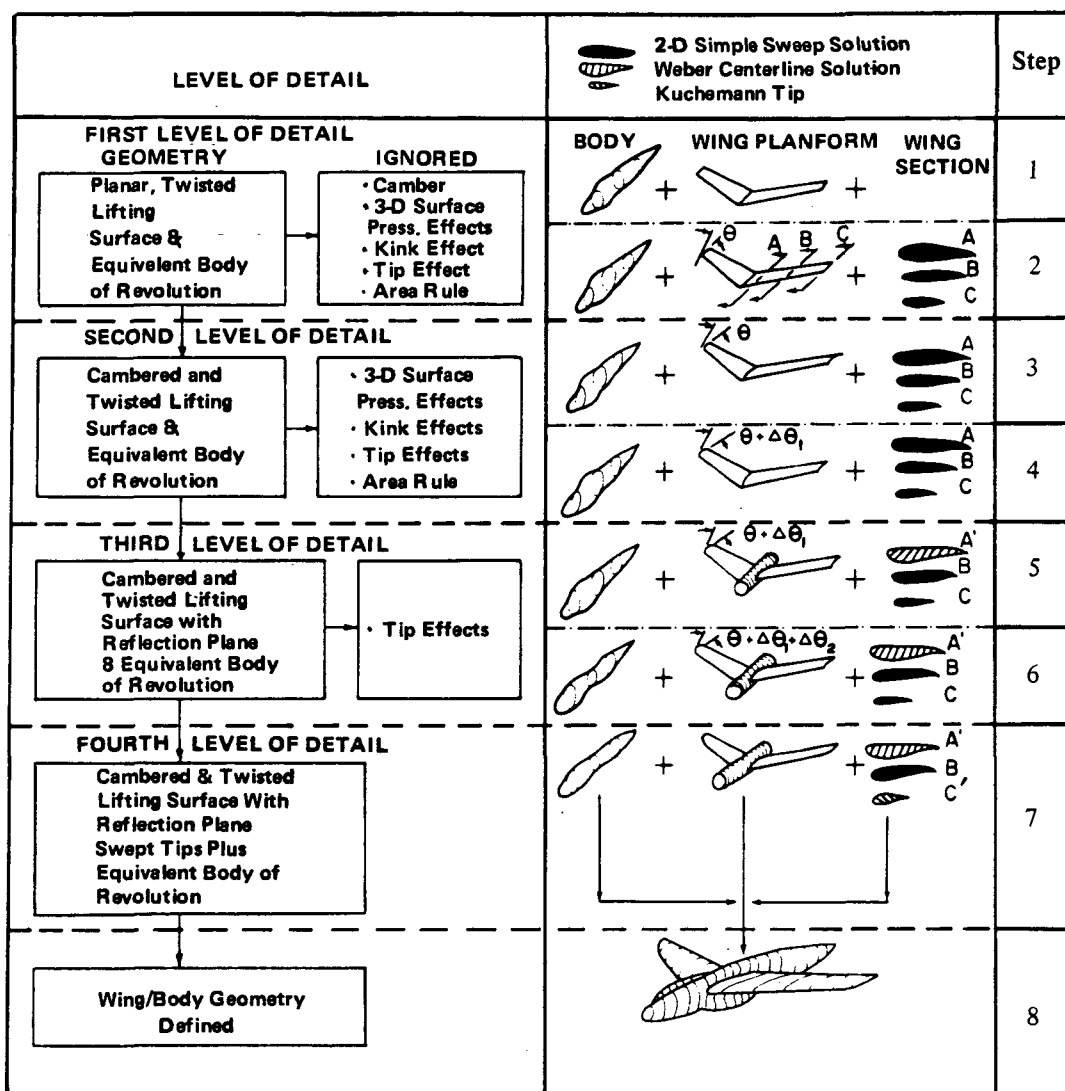


Figure 16. — Refinement of wing/body design

In step 5, an approximate centerline solution based on two-dimensional theory for the inboard control station, which should be at or near the fuselage side, is determined. Utilizing this solution, a modified inboard control station is developed permitting the wing isobars to lie along straight line elements, usually constant x/c stations, in the spanwise direction. A simple method to determine the spanwise location at which the centerline section shape changes to a two-dimensional shape based on simple sweep theory is employed. This station is usually chosen as a new control station. At this point the wing/body area distribution is inspected so that any required and acceptable body waisting can be accomplished. If properly executed, the body waisting can also help alleviate the unsweeping of the wing isobars near the fuselage; although this can normally be accomplished without body waisting, working only with the wing. With this definition of the section shapes, the wing is lofted and the optimum spanwise variation of wing twist is determined for the cambered planform with hollow cylindrical reflection boundaries approximating the body effect on the wing

Since specification of surface pressure distribution is the basic criterion for wing design, the characteristics of three-dimensional wing isobars will be briefly discussed. In figure 18(a), two sample cases are shown in which the isobars, or lines of constant pressure, are mapped from experimental data for a swept wing at two different angles of attack. Note that the isobars are not swept in a uniform fashion over the entire span of the wing, and are distorted by tip effects, inboard effects, viscosity, and other flow phenomena not accounted for by two-dimensional theory.

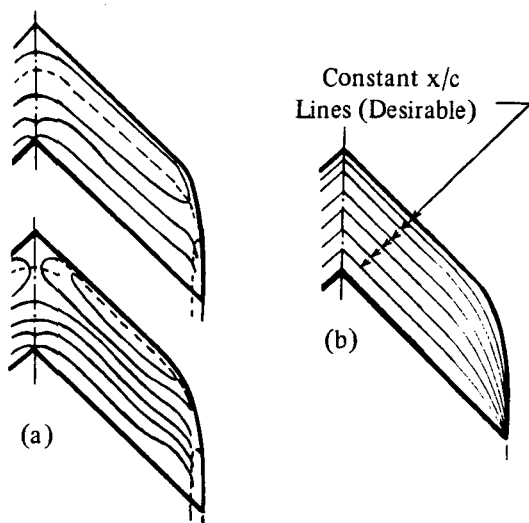


Figure 18. — Wing isobar patterns

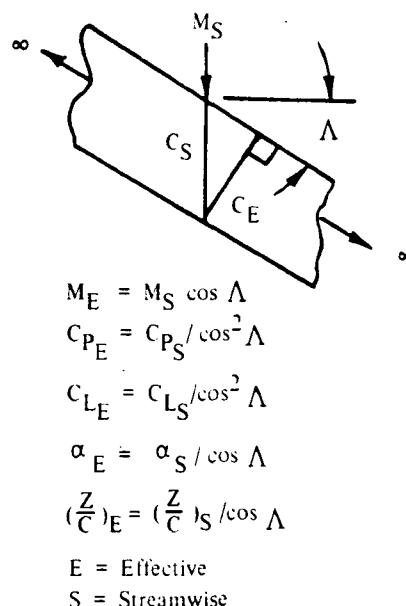


Figure 19. — Simple sweep relationships

A more desirable pressure distribution, particularly for LFC wings, is shown in figure 18(b), in which the isobars are distributed along constant x/c lines. Therefore, at high Mach number all portions of the wing become drag divergent simultaneously, avoiding drag creep and premature drag rise. Straight isobars also improve the compatibility of calculated results with basic assumptions of the theoretical models, and provide the small spanwise pressure gradients which are required for an efficient LFC system as outlined in reference 15. The spacing of the isobars determines pressure gradient, while the sweep and the magnitude of the pressure associated with each isobar determine the local effective Mach number spanwise variation along the isobar. The Mach number at which the sections become critical can be determined by examination of wing isobars as subsonic flow conditions approaching mixed flow conditions. A favorable wing isobar pattern can be established for penetration of the mixed flow region and efficient cruise with regions of local supersonic flow on the wing.

Use of surface pressure distribution as the primary criterion for both the TF and LFC wing designs facilitated use of two-dimensional knowledge and its extension to three-dimensional cases. The ability to use two-dimensional information for three-dimensional design is, however, a controversial subject and deserves some discussion. Based on experience, specification of surface pressure distribution is an excellent criterion for both two-dimensional and three-dimensional design and can

be a primary input in the wing design process. Surface pressure distribution criteria are reasonably well established by economical two-dimensional analytical and experimental work. The applicability of such two-dimensional work to three-dimensional design has been demonstrated by reference 22.

The two-dimensional methods used are based on simple sweep theory relationships which are available in any text; however, the basic definitions are summarized here for clarity. The effective direction in simple sweep theory is that direction which is normal to the wing leading edge. The effective two-dimensional pressure coefficient, angle of attack, and thickness are then defined by the relationships to the sweep angle, Λ , noted in figure 19.

If a tapered wing is considered, an extension of simple sweep theory may be made by considering the effective direction as the normal to constant percent chord element lines. The sweep angle used in defining the pressure coefficient, lift coefficient, angle of attack, and airfoil ordinates then becomes a function of chordwise position.

In deriving airfoil section shapes for prescribed surface pressures at various spanwise stations on the three-dimensional wing, the first step is to select a satisfactory effective upper design surface pressure distribution and a type of basic thickness shape which produces satisfactory lower surface pressures. Initial incremental velocity components can then be defined by linear superposition theory as functions of non-dimensional chordwise distance. These velocity components are those due to the angle of attack, camber, and thickness as illustrated by figure 20.

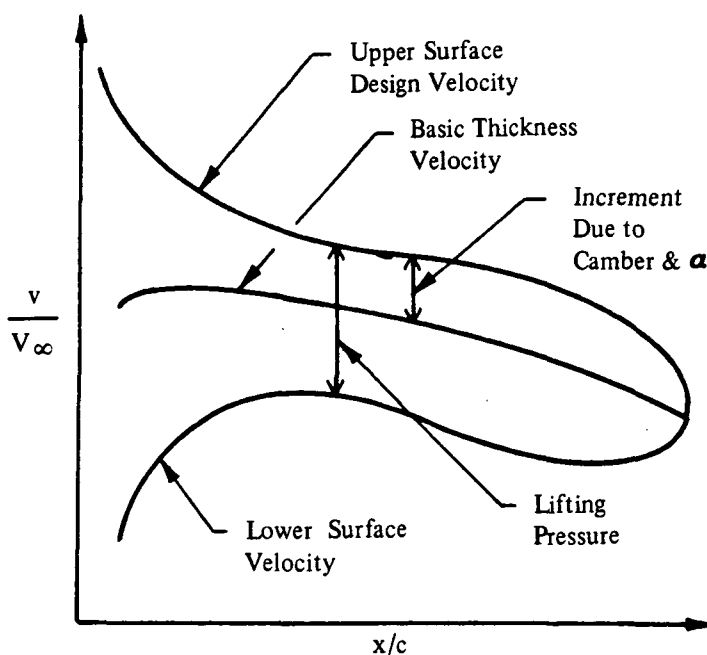


Figure 20. — Velocity increments

4.2.3.2 Scope of Study Design and Analysis

All elements of the design and analysis methodology outlined previously were not conducted during this study for all TF and LFC configurations. Only the design and analysis necessary to validate overall system results and sensitivities and permit definition of research and technology requirements was performed. The level of detail for the TF configurations extended to step 2 of figure 16, since performance of these configurations can be predicted on the basis of numerous design exercises previously conducted. For LFC configurations, some additional detail design was performed because of the criticality of efficient LFC system operation to the achievement of relatively uniform pressures on the wing surfaces. Adequate analysis was conducted to achieve such pressure distributions, but refinement of the LFC configuration was not completed through step 8. This is considered to be necessary only when a decision is made to conduct wind tunnel tests on a specific LFC configuration concept.

With the scope of design and analysis thus defined, subsequent sections discuss airfoil development and laminar boundary layer analysis, the two principle elements of the LFC configuration design exercises.

4.3 AIRFOIL DEVELOPMENT

As previously outlined, airfoil sections can be developed for swept wings using simple sweep concepts and the wing/body design refined to ensure the surface pressures and flow pattern necessary for either good TF or LFC performance. There are, however, several airfoil concepts which can be used on either TF or LFC configurations. The concepts considered in this study are discussed in section 4.3.1. Geometry definition of the selected airfoil concept is discussed in section 4.3.2.

4.3.1 AIRFOIL VARIATIONS

As discussed in section 3.5, three distinct types of airfoil section were considered in the course of this study:

- (1) X-21 rooftop 6-series type airfoil
- (2) Baseline supercritical airfoil
- (3) High aft-loaded rooftop airfoil

The X-21 rooftop airfoil was considered primarily for correlation purposes with previous design data on the X-21. Parametric methodology describing the requirements for LFC suction and allowable airfoil thickness were developed with the aid of this correlation.

After the basic methodology synthesizing X-21 results was satisfactorily completed, extensions were made to permit analysis of the supercritical airfoil, and this section was chosen for use on baseline LFC configurations. The advantages of this section, which are evident in comparing the various wing design curves presented in section 3.5, include greater values of combined allowable thickness, Mach number, and lift.

To ensure that other concepts do not produce superior overall results due to low suction requirements and attendant reductions in weight and LFC, the high aft-loaded rooftop airfoil was compared to the baseline supercritical airfoil.

Discussion is omitted on studies of X-21 type airfoils, since these are simply the high aft-loaded rooftop airfoils with the high aft-loading removed. Subsequent sections discuss the pertinent characteristics of the other two concepts, and present additional details on design of the baseline supercritical airfoil sections.

4.3.1.1 Supercritical Airfoil

The supercritical airfoil chosen as a baseline in this study is typical of the Whitcomb family of airfoils, and is characterized by an extensive upper surface region of supercritical flow terminated by a shock of moderate strength at approximately 0.72 chord. This shock is probably too strong to permit economical maintenance of laminar flow downstream. Shock position on the airfoil thus has a prime effect on suction requirements as evidenced in figure 5, where normally $(x/c)_1$, the shock position, also corresponds to $(x/c)_2$, the position at which increased suction is required to maintain laminar flow on the upper surface. Downstream of the shock, a region of flat pressure gradient is maintained to approximately 0.85 chord to permit adjustment of the flow from a supersonic to a subsonic level of velocity before the rear pressure rise is encountered. The end of the flat gradient region is indicated by $(x/c)_2$ in figure 5. A high suction velocity ratio region exists near the airfoil leading edge due to adverse effects of sweep. Reduction of sweep reduces this requirement. For no leading edge sweep, region 2 extends essentially to the leading edge.

LFC supercritical airfoils have slightly better performance than TF supercritical airfoils since the turbulent boundary layer in the rear pressure rise region has lost less of its initial energy for the LFC case. Also, on the final LFC concept, a trailing edge flap was developed to aid in adjusting aft gradients to levels which do not cause trailing edge separation. This difference between TF and LFC sections is evident when comparing the wing design curves of figure 9 with those of figure 10.

A problem area with the supercritical airfoil is the drag associated with termination of the supercritical region by a moderately strong shock. Some modification of the baseline section developed would thus probably be necessary to reduce this drag to an acceptably low level. In addition, the shock may move forward on the airfoil as lift is decreased from the design level, thus causing transition prematurely, unless a trailing edge flap is used to dump unneeded lift. This condition occurs as fuel burns off during a constant Mach number, constant altitude cruise.

4.3.1.2 Rooftop Airfoil

The shock location stability and shock loss problems outlined in section 4.3.1.1 can both be eliminated by restricting Mach numbers on the upper surface to subsonic effective values. The resultant airfoil, however, loses potential performance, as evidenced by comparison of figure 12 with figure 9. Overall study results show that optimum aircraft with this airfoil require greater sweep and a larger extent of laminarization to achieve fuel consumption levels comparable to the supercritical concept, as long as the supercritical airfoil suffers no undue shock loss penalty. A low technical risk requirement might dictate use of the high aft-loaded rooftop section, however. In this case, the larger loss of fuel consumption efficiency would occur for the 200-passenger aircraft, as compared to 400-passenger aircraft, due to the less critical fuel and internal volume requirements of the larger aircraft.

A particularly interesting possibility for a rooftop section is to operate the supercritical airfoil at a lift coefficient of 0.15 to 0.20 below the lift for which a full supercritical flow region is evident. At this condition, the shock disappears and the upper surface pressures take on the character illustrated by the dotted line pressure plateau in figure 5 or the initial-design-requirement line in figure 21. The only restriction on this approach is that the initial supercritical airfoil be thin enough so that lower surface Mach numbers do not become supercritical at the lower lift coefficients. The case illustrated in figure 21 is such a case.

4.3.2 AIRFOIL SELECTION AND DEFINITION

After consideration of all factors influencing choice of a baseline airfoil, the supercritical section was selected for study aircraft because this airfoil:

- (1) Offers potential aerodynamic performance advantages.
- (2) Is most compatible with practical suction gloves and ducting.
- (3) Provides better matches of cruise/airport-performance thrust requirements.
- (4) Can include the basic rooftop section as an off-design case.
- (5) Perhaps most importantly, presents the fuller range of cruise aerodynamics problems which have to be resolved for successful LFC operation.

Sections 4.3.2.1 and 4.3.2.2 discuss the manner in which the baseline LFC airfoil section was initially designed and later modified.

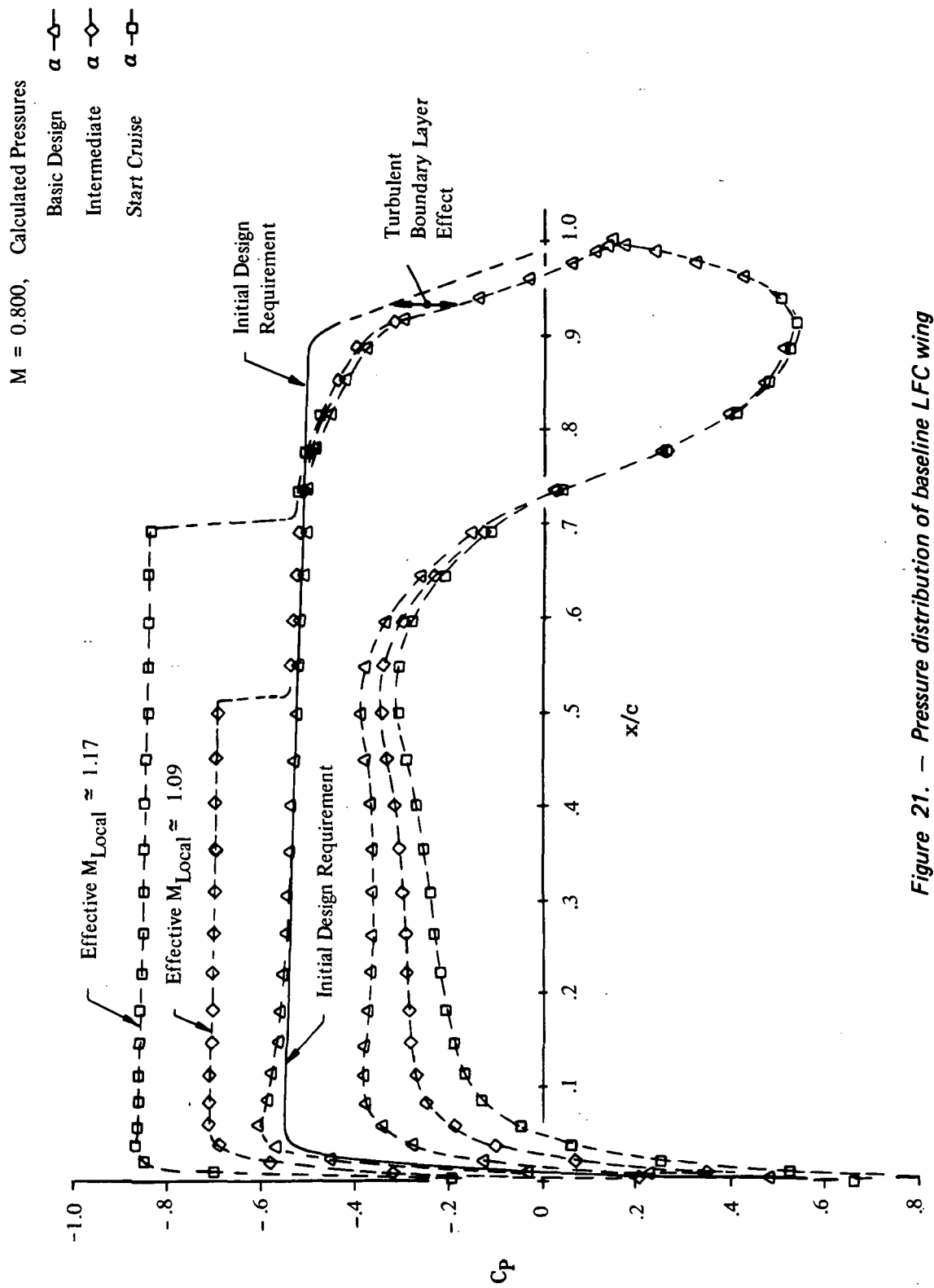


Figure 21. — Pressure distribution of baseline LFC wing

4.3.2.1 Basic Airfoil Design

The basic airfoil design was initiated by selecting a baseline lift coefficient, Mach number, and leading and trailing edge sweep angle from parametric study results. The design pressure distribution for the upper surface was then chosen as that indicated in figure 21. This corresponds to a sonic rooftop distribution operating at a C_L decrement of 0.16 below the C_L for which a full supercritical flow is obtained. Choice of this C_L for airfoil definition in lieu of the higher required lift level permits entirely subsonic theory to be used in initializing airfoil geometry and also permits use of the well-established design methodology outlined earlier in this section. The design sequence then follows the outline of figure 14.

In order to economically check transonic characteristics of the resulting initial section, the three-dimensional airfoil section was converted to a two-dimensional section, and several cases were run on the Garabedian and Korn transonic airfoil program. During these runs, transition was generally held fixed, simulating LFC over the forward portion of the section.

Basic Section Results – The basic results for the section at its effective Mach number of 0.738 and effective lift coefficient of 0.670 are presented in figure 22(a). Note that the shock is both stronger and farther forward than desirable, indicating the requirement for airfoil revisions. Such a shock position would probably cause boundary layer transition at approximately $x/c = 0.55$. A computation for this transition location was made for comparison to the base case. This case, shown in figure 22(b), shows a slight forward movement and increase in strength of the shock with a slight decrease of aft loading, as would be expected. Approximately 16 counts of drag penalty would be suffered, however, because of the transition movement.

Effects of Changes in Lift – Ignoring temporarily the potential undersirable forward movement of transition, the effect of C_L variation at constant Mach number was considered. To check higher lift coefficients more compatible with higher wing loadings in the parametric studies, a C_L of 0.797 was run with the Transonic Airfoil Program (TAP). Results for this case are given in figure 22(c), and show an increase in shock strength and rearward movement with increase of lift. The drag increases approximately 18 counts. If transition were to move to the shock location, approximately 10 additional counts of drag increase would result compared to transition at 0.72 x/c . Figure 22(d) gives TAP results for a lift which is lower than basic design lift. For this case compared to design conditions, there is essentially no drag change. The shock moves slightly forward and becomes weaker, exhibiting expected behavior. At this stage, it was evident that more rear loading and a more aft shock location was desirable for improved performance of the airfoil section. Before undertaking changes of shape, however, a study of Mach number effects on the airfoil pressures was conducted.

Mach Number Effects – Study of Mach number effects has the extra benefit of defining section performance as wing sweep is changed slightly. Figure 22(e) shows results applicable to decreasing the wing sweep from the baseline sweep of 0.396 rad (22.7 deg) to approximately 0.323 rad (18.5 deg) while slightly lowering lift coefficient and increasing thickness ratio. In this case, there is a

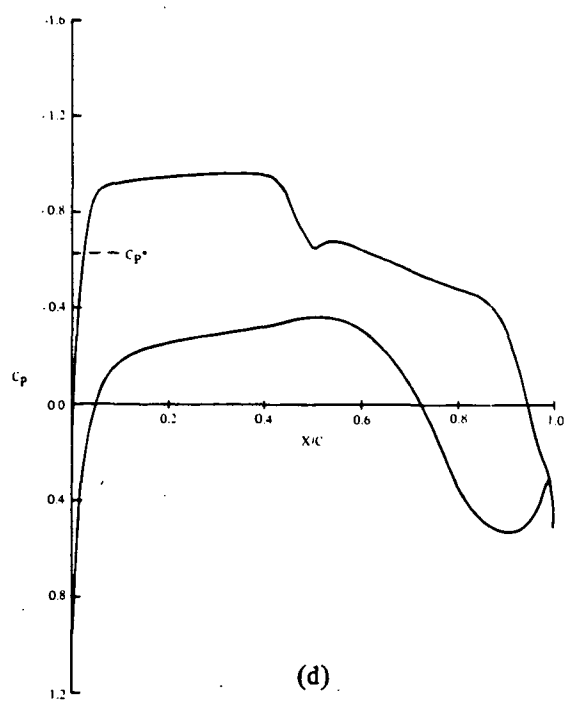
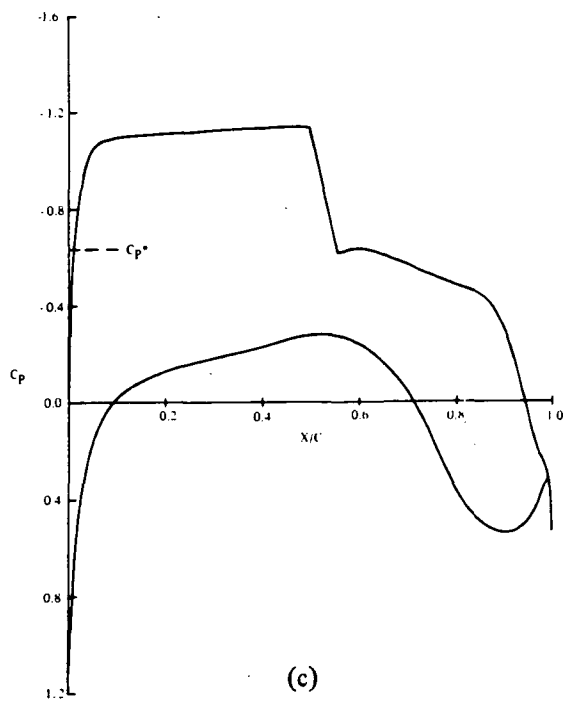
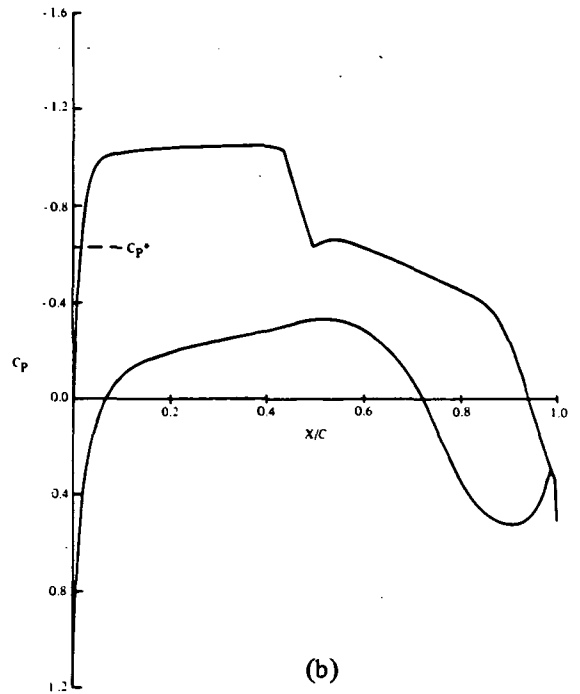
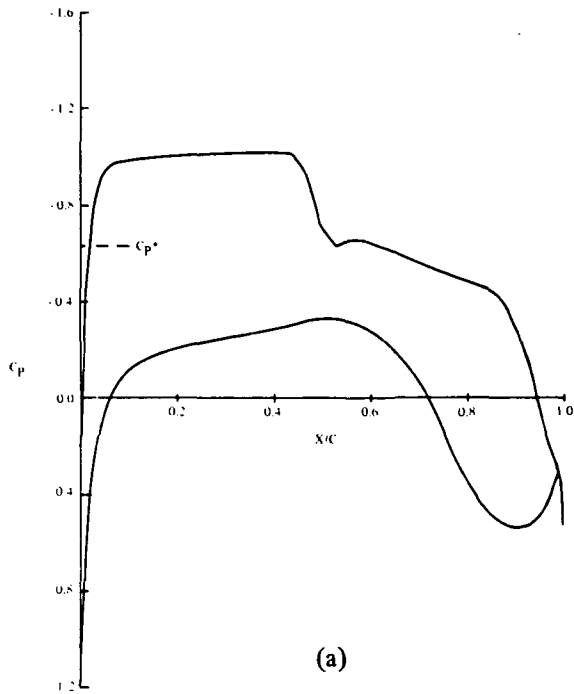


Figure 22. — Viscous transonic airfoil program results

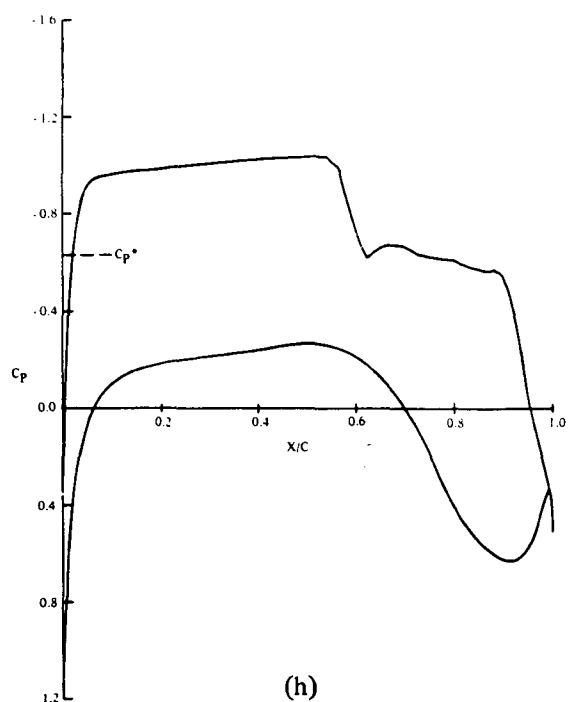
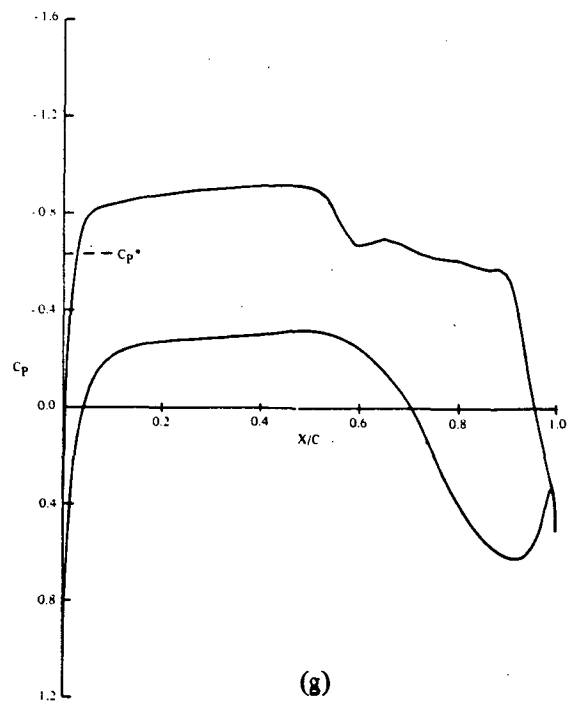
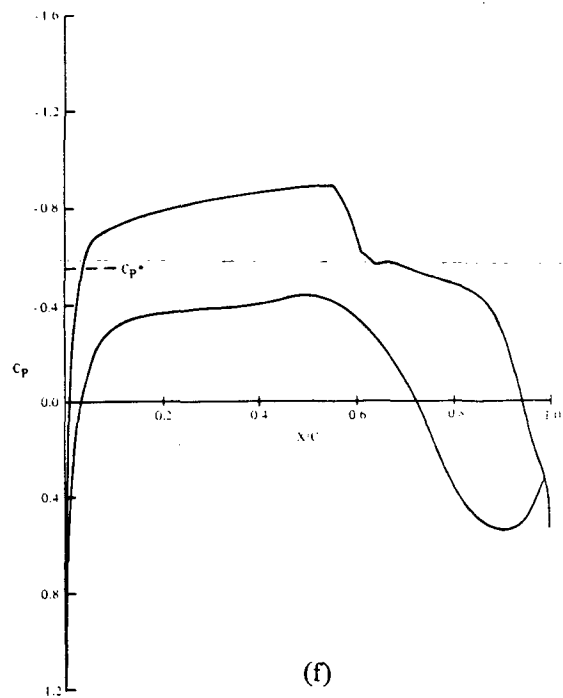
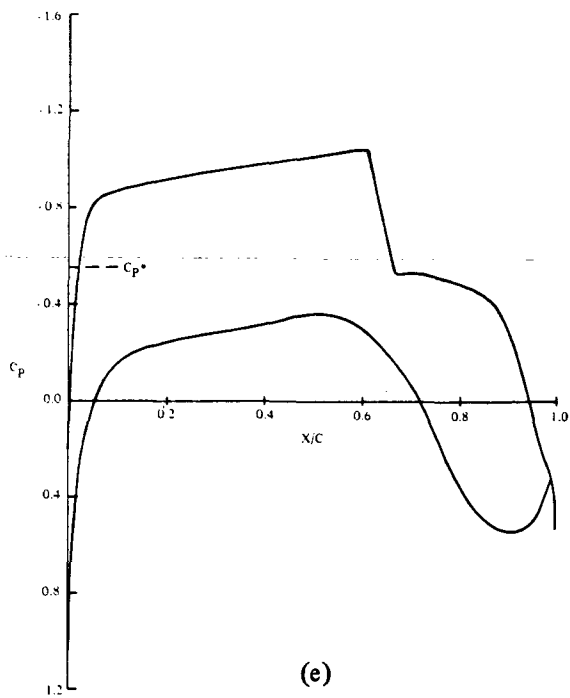


Figure 22. — Continued

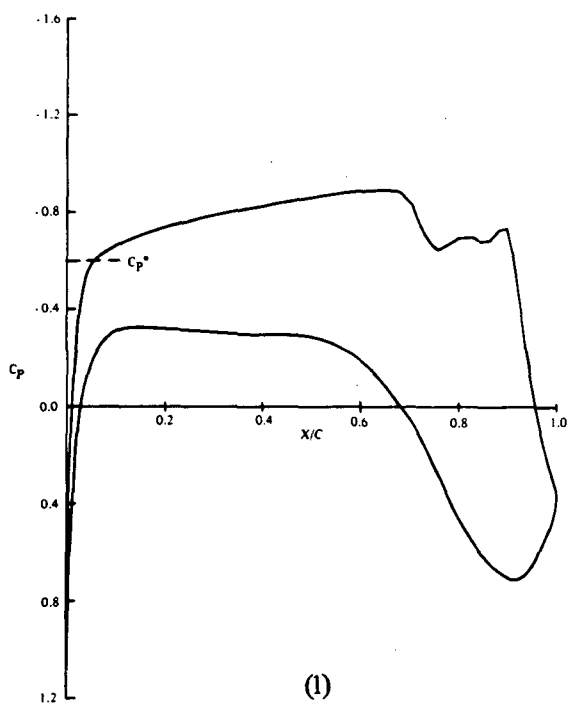
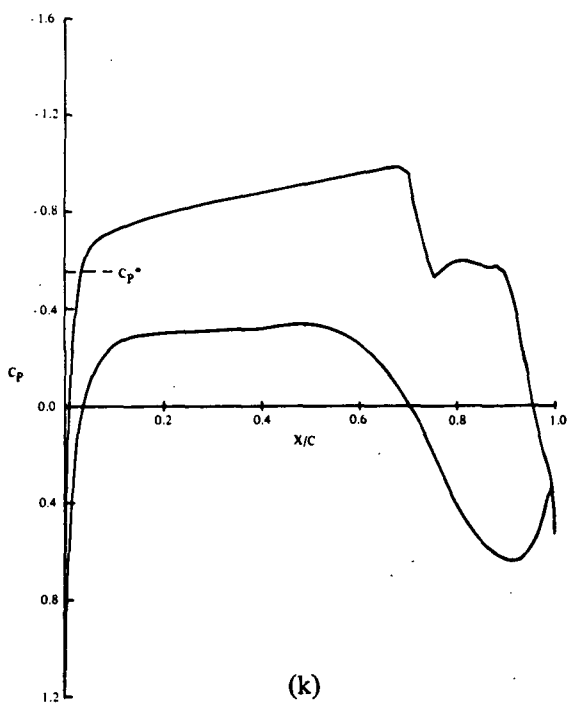
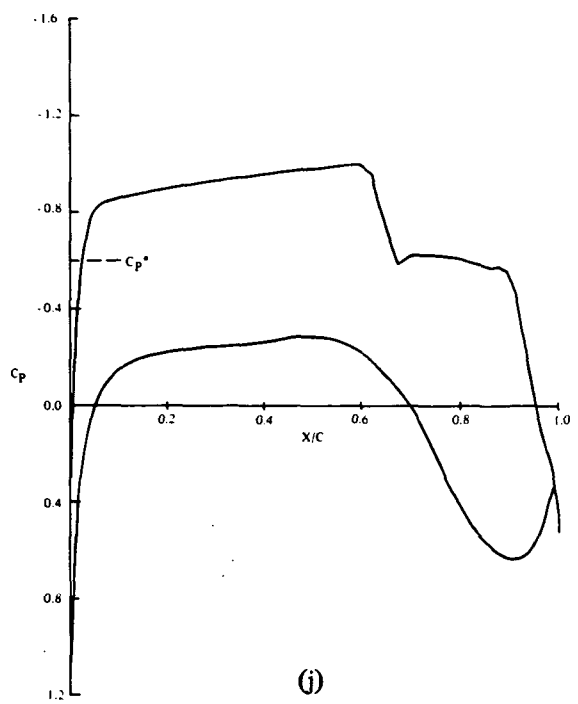
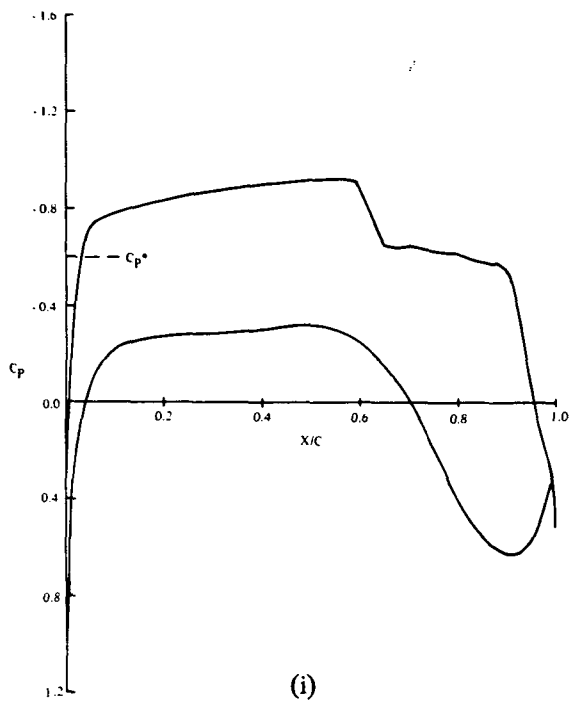


Figure 22. — Continued

significant aft shift of the shock and increase of shock strength compared to the case of figure 22(d), but the shock location is much more compatible with the suction extent of 0.75 chord. For this case, there is a drag increase of only approximately 11 counts. This case can also be considered a fixed geometry with a Mach number increase at constant C_L and indicates, when compared with figure 22(d), that $dC_D/dM \approx 0.055$, which is a reasonable definition for drag divergence Mach number. To examine the effects of reduced C_L at the higher Mach number of 0.76, the case presented in figure 22(f) shows a more favorable aft position of the shock and a reduction in shock strength. A drag decrease of approximately 5 counts would be expected for this case. Note the closer proximity, however, of lower surface C_p values to the critical C_p^* value denoting occurrence of effective supersonic flow.

4.3.2.2 Modifications to the Basic LFC Airfoil

Based on the preceding observations of the initial baseline airfoil behavior, some simple modifications were formulated to improve the performance and versatility of the basic airfoil design. The most significant of these was the addition of a 0.12 chord trailing edge flap to increase aft loading and promote a weaker shock strength. Figure 22(g) presents data for this modification with a flap-down deflection of 0.070 rad (4 deg). Note the lower average supersonic region velocities and weaker shock compared to figure 22(a). Surprisingly, however, the drag benefits of the lower shock losses are apparently offset by a higher aft pressure drag, so that drag is approximately the same for the two cases.

At a higher lift coefficient of 0.80, shown in figure 22(h), the forward supercritical region development is almost identical with the baseline case of figure 22(a). The drag level is approximately 12 counts higher due to higher aft pressure drag.

Increased Mach Number Effects — The effect of increased Mach number is illustrated in figure 22(i). As in the case of the basic airfoil, the shock is farther aft and of about the same strength, at $M = 0.747$ as compared to $M = 0.738$. The drag level is increased approximately 4 counts for the 0.009 change in Mach number.

Increased Lift Effects — The final versions of the baseline LFC configurations operated at higher wing loadings than the initial baseline W/S of 537 kg/m^2 (110 lb/ft^2). The modified section was checked at higher C_L values corresponding to W/S values greater than 586 kg/m^2 (120 lb/ft^2). Figure 22(j) shows the result of this check. Note that the shock location has approached the design location of 0.70 to 0.75 chord, and further refinement should guarantee the proper location. The drag of this configuration compared to the original section at a lower design lift and Mach number is 10 counts higher. A sweep of 0.366 rad (21.0 deg) corresponds to the effective design Mach number of 0.747. For an effective Mach number of 0.76, Figure 22(k) corresponds to a sweep of approximately 0.323 rad (18.5 deg) and produces practically the same drag as the lower sweep and higher C_L of figure 22(j).

Effect of Additional Flap Deflection – At the effective Mach number of 0.747, the deflection of the flap was also increased from 0.070 rad (4 deg) to 0.140 rad (8 deg). Figure 22(1) presents this result and shows that the shock is well positioned at 0.70 to 0.75 chord, and there is a supersonic reacceleration behind the main shock. Due to the exceptionally high aft pressure gradient imposed by the 0.140 rad (8 deg) deflection, these results must be viewed with some reservations, pending experimental verification. Taken literally, however, there is only a 5 count drag increment for this case, when compared to the basic airfoil, and a 3 count increment compared to the basic 0.070 rad (4 deg) flap modification.

4.3.3 SUMMARY OF AIRFOIL DESIGN STUDIES

The airfoil design studies showed that the use of a small trailing edge flap can minimize the unfavorable effects of large movements of the upper surface shock on supercritical airfoils. When incorporated into a three-dimensional wing, there should be at least six trailing edge trimming devices per semispan to ensure that a controlled shock location, lift level, and relatively uniform upper and lower surface pressures are simultaneously achievable. The final airfoil section shape is illustrated in figure 23. Only small additional geometry modifications should be required on this basic shape to produce an acceptable section for use on a three-dimensional wing. It is quite possible that shock losses and aft pressure drag on this airfoil may be higher than on some other optimized airfoil. However, to provide a more accurate evaluation of the supercritical airfoil and a shock-free supercritical or sonic rooftop airfoil section, formulation of a family of LFC airfoils and verification of this family through experiment is required. This requirement is discussed in section 12.

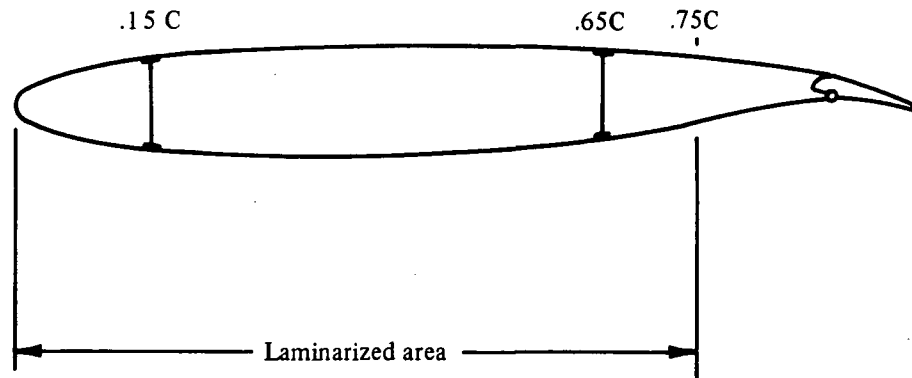


Figure 23. – Baseline airfoil section with 0.070 rad (4 deg) flap deflection

4.4 LAMINAR BOUNDARY LAYER ANALYSIS

Discussion of airfoil development to this point was based on the assumption that sufficient suction with the appropriate distribution was applied to produce the desired extent of laminar flow. In

order to establish credible suction levels and distributions, suction quantities used for the X-21 were examined and related to requirements for the different supercritical sections, using data from reference 15. A quasi-three-dimensional laminar boundary layer program was used to predict required suction quantities. It was found that X-21 levels of suction were close to those required to satisfy the criteria for a completely stable laminar boundary layer. This may have been partly due to allowance for design margin and other contingencies on the experimental aircraft.

After initial parametric studies and the airfoil design studies outlined in section 4.3.2, a more optimistic stable boundary layer cross-flow criterion was assumed, largely due to the flexibility provided by the trailing edge trimming device in adjusting the pressure distribution at different off-design conditions. For the more optimistic stable boundary layer, a decrease of approximately 30 percent in suction was estimated. As discussed in section 3.0, this level was used for LFC-200-S and LFC-400-S configurations during final study stages.

Based on the results of reference 23, the possibility exists for permitting the laminar boundary layer to become unstable, while preventing amplification of the instability into transition through judicious application of suction. In using these criteria, as recommended by reference 24, the allowable cross-flow stability limit Reynolds number is increased by 80 percent to achieve a reduction of 35 percent in required suction. As demonstrated by the LFC-200-R and LFC-400-R study aircraft, the reduction of suction to an unstable level can produce as much as a 4 percent reduction in fuel consumption if the details can be satisfactorily resolved. This area of investigation, therefore, should receive considerable attention in future development plans.

4.4.1 QUASI-THREE-DIMENSIONAL LAMINAR BOUNDARY LAYER PROGRAM

Following are the salient features of the laminar boundary layer program:

- (1) Implicit finite difference scheme to solve partial differential equations of motion.
- (2) Stability criteria built into method are:
 - o 2-dimensional criterion relating local boundary layer Reynolds number to local velocity profile shape factor.
 - o Cross-flow Reynolds number criterion.
 - o Attachment line criterion based on leading edge spanwise flow Reynolds number.
- (3) On option, automated iteration for minimum suction for stability.
- (4) Inputs required are wing section geometry, chordwise pressures and suction, sweep, and chord Reynolds number.

- (5) Output includes calculated velocity profiles, skin friction data, integral parameters, stability criteria.
- (6) Does not account for spanwise pressure gradient and large Mach number effects.

For the cases considered in this study, the basic methodology gives reasonably accurate boundary layer profiles for all regions of suction with the exceptions of the tips of the flying surfaces and the wing/body and empennage intersections. In these regions, laminar flow was assumed to transition as depicted in figures 91 through 104 of section 7. It appears that, in such intersection regions, the penalties necessary to laminarize the junctions are greater than the benefits accruing from the lower external drag.

4.4.1.1 General Program Description

The basic method solves the steady, incompressible laminar boundary layer equations for flow over an infinite yawed wing with distributed suction in a way which is reliable, accurate and computationally efficient. In order to facilitate use in engineering studies involving the specification of suction quantities for maintaining laminar flow, semi-empirical transition criteria are built into the method. The program has the additional capability of searching for the optimum distribution of suction quantity compatible with the preservation of laminar flow to a specified point on the chord.

The requirements for reliability, accuracy, and computational efficiency are met by employing an implicit finite-difference scheme to solve the partial differential equations of motion. Specifically, the extended Choleski method is used. This method has been used in earlier viscous flow calculations and is also being used widely in the solution of other parabolic, initial-value problems.

Three semi-empirical stability criteria are built into the method to test for incipient transition. One is the conventional two-dimensional criterion relating the local boundary layer Reynolds number to the local velocity-profile shape factor. This criterion is applied to the flow components normal to the leading edge. The second is a three-dimensional criterion applied to the crossflow; i.e., the flow components perpendicular to the local streamlines at the edge of the boundary layer. The third is an attachment-line criterion applied to the spanwise flow along the leading edge. Stability of the laminar boundary layer is assumed to be preserved when the appropriate criteria indicate stability. Instability is assumed to exist when any one of them so indicates. The search for the optimal suction distribution is provided by successively increasing the suction quantity, at each chordwise station in turn, until the appropriate criteria indicates stability.

4.4.1.2 Boundary Layer Stability Criteria

Three separate criteria are used to judge the stability of the laminar flow against incipient transition.

Stability of the Chordwise Flow – The flow normal to the leading edge is assumed to behave

two-dimensionally and to conform to a two-dimensional stability criterion. An appropriate one, based on Tollmien-Schlichting stability theory, is presented in figure IX-15 of reference 25. A critical Reynolds number, $R_{e_{crit}}$ where

$$R_{e_{crit}} = \frac{U_e \delta^*}{\nu}$$

is given as a function of the chordwise shape factor $H = \delta^* / \theta$, where

$$\delta^* = \int_0^\infty (1 - U/U_e) dy$$

$$\theta = \int_0^\infty (1 - U/U_e) (U/U_e) dy$$

the function can be approximated by

$$R_{e_{crit}} = 1.371 + 5.528 H - 1.944 H^2,$$

for $H \leq 2.6$, and

$$R_{e_{crit}} = 1/(0.346 H - 0.515)$$

for $H > 2.6$.

In order to permit evaluation of suction quantities producing an unstable laminar boundary layer, a tangential flow instability Reynolds number increment, $\Delta R_{e_{crit}}$, was introduced such that the tangential transition

Reynolds number, $R_{e_{tran}}$, is defined by

$$R_{e_{tran}} = R_{e_{crit}} + \Delta R_{e_{crit}}$$

where

$$\Delta R_{e_{crit}} = K_t H$$

where

$$K_t = \Delta R \theta$$

and is taken as +200 for cases using relaxed boundary layer stability criteria.

If the actual value of $U_e \delta^* / \nu$ exceeds the value of $R_{e_{tran}}$, the boundary layer is judged to be unstable.

Stability of the Crossflow – The crossflow is defined as the flow component normal to the external streamlines, and the crossflow velocity, w_n , is given by

$$w_n = -U \sin \beta + w \cos \beta$$

where

$$\tan \beta = W_e / U_e.$$

Reference 3-6 provides a criterion for judging the stability of the crossflow, which takes the form

$$R_{n_{crit}} = -0.7 \frac{\delta^2(0.1)}{w_{n_{max}}} \frac{\partial^2 w_n}{\partial y^2} + 60$$

where $w_{n_{max}}$ is the maximum local crossflow velocity, and $\delta(0.1)$ is a thickness defined as the (larger of the two) value(s) of y where

$$w_n = 0.1 w_{n_{max}} \quad R_{n_{crit}} \text{ is defined as}$$

$$R_{n_{crit}} = \frac{w_{n_{max}} \delta(0.1)}{\nu}$$

In order to permit evaluation of an unstable laminar boundary layer, a cross-flow instability Reynolds number increment, $\Delta R_{e_{crit}}$, was introduced such that the cross-flow transition Reynolds number, $R_{n_{tran}}$, is defined by

$$R_{n_{tran}} = R_{n_{crit}} + K_c R_{n_{crit}}$$

where K_c is a correlation constant and is normally taken as +0.800 for cases based on relaxed boundary layer stability criteria.

If the actual value of $w_{n_{\max}} \delta (0.1)/\nu$ exceeds the value of $R_{n_{\text{crit}}}$, the boundary layer is judged to be unstable.

Stability of the Attachment Line Flow – At the attachment line $U = 0$, and the flow is all in the Z-direction. A common stability criterion for this region requires that, for stability,

$$R_{\theta} \leq 100$$

where

$$R_{\theta} = \frac{\theta_a W_e}{\nu}$$

and

$$\theta_a = \int_0^{\infty} (1 - W/W_e) (W/W_e) dy$$

At the attachment line, this third criterion is the only applicable one. Elsewhere, if either of the first two criteria indicate instability the flow is judged to be unstable.

4.4.2 LFC SUCTION REQUIREMENTS

Three distinct levels of suction were used during the course of the study. The suction levels and distributions were defined by parametric equations for the suction regions specified in figure 5.

4.4.2.1 Preliminary Suction Requirements for Stable Boundary Layer Stability Criteria

During early study stages, suction requirements for a stable laminar boundary were correlated with the data of reference 15 to establish empirical constants for the parametric equations.

For suction region 2 on the wing upper surface:

$$\left(\frac{v_s}{U_{0U-2}} \right) = C_1 \left(\frac{1.0 + 0.2 M_{sc}^2}{1.0 + 0.2 M_0^2 \cos^2 \Lambda_f} \right)^{\frac{y}{y-1}} \cos \Lambda_f$$

$$C_1 = \text{a constant} = \frac{.759}{4000}$$

$$M_{sc} = \text{the effective supercritical Mach number corresponding to the effective supercritical pressure coefficient illustrated in figure 5.}$$

- M_o = free stream Mach number.
 Λ_ρ = the sweep angle of the given x/c station at which v_s is being evaluated
 v_s = the incompressible suction velocity required
 U_o = the free stream velocity
 γ = the ratio of specific heats = 7/5

At the beginning of suction region 1 on the upper surface of the wing:

$$\left(\frac{v_s}{U_o}\right)_{U-1} = (1.0 + C_2 \sin^2 \Lambda_\rho)^2 \left(\frac{v_s}{U_o}\right)_{U-2}$$

where C_2 = a constant = 13.333

At the end of suction region 3 and for suction region 4 on the upper surface of the wing:

$$\left(\frac{v_s}{U_o}\right)_{U-3} = \left[1.0 + C_3 \left| C_{P_{\text{Grad}}} - C_{P_{\text{TE}}} \right| \left(\frac{(x/c)_{r2} - (x/c)_1}{1.0 - (x/c)_1} \right) \right] \left(\frac{v_s}{U_o}\right)_{U-2}$$

where C_3 = a constant = 6.0

$C_{P_{\text{Grad}}}$ = (plateau effective pressure coefficient + supercritical effective pressure coefficient) / 2

$C_{P_{\text{TE}}}$ = effective trailing edge pressure coefficient

$(x/c)_1$ = shock location

$(x/c)_{r2}$ = location of the end of suction region 3, usually at $x/c = 0.90$

Similarly for the lower surface of the wing in suction region 2:

$$\left(\frac{v_s}{U_o}\right)_{L-2} = C_4 \left(\frac{1.0 + 0.2M_{\text{Plat}}^2}{1.0 + 0.2M_o^2 \cos^2 \Lambda_\rho} \right)^{\frac{\gamma}{\gamma-1}} \cos \Lambda_\rho$$

where L denotes lower surface

$$C_4 = \text{a constant} = \frac{1.138}{4000}.$$

M_{Plat} = the effective Mach number corresponding to the effective plateau pressure coefficient illustrated in figure 5.

At the beginning of suction region 1 on the lower surface of the wing:

$$\left(\frac{v_s}{U_o} \right)_{L-1} = (1.0 + C_5 \sin^2 \Lambda_\ell) \left(\frac{v_s}{U_o} \right)_{L-2}$$

where $C_5 = \text{a constant} = 5.333$

At the end of suction region 3 and for suction region 4 on the lower surface of the wing:

$$\frac{v_s}{U_o}_{L-3} = \left[1.0 + C_6 \left| C_{P_{\text{Plat}}} - C_{P_{\text{TE}}} \right| \left(\frac{(x/c)_{r2} - (x/c)_2}{1.0 - (x/c)_2} \right) \right] \left(\frac{v_s}{U_o} \right)_{L-2}$$

where $C_6 = \text{a constant} = 2.5$

$C_{P_{\text{Plat}}}$ = effective plateau pressure coefficient

Similar equations were used for both sides of the vertical tail and horizontal tail for estimating suction requirements.

4.4.2.2 Final Suction Requirements for Stable Boundary Layer Stability Criteria

During later stages of the study, suction requirements were revised downward due to the addition of trailing edge trimming devices. These flaps limit pressure distribution variations to minimize the requirement for additional suction necessary for off-design pressures.

The form of parametric equations for the final suction is identical to that for the preliminary suction. Only the values for the constants C_1 , C_2 , C_e , C_4 , C_5 , and C_6 are changed. Following is a comparison of these constants for preliminary and final suction levels.

	Final	Preliminary
C_1	.5005/4000.	.759/4000.
C_2	14.00	13.333
C_3	6.00	6.00
C_4	.5005/4000.	1.1385/4000.
C_5	7.00	5.333
C_6	3.50	2.50

Note that the changes to lower surface suction (constants C_4 , C_5 , C_6) are greater than changes to upper surface suction. The above revised constants were used in computing suction flow requirements for LFC-200-S and LFC-400-S configurations. Sections 8.2.3 and 8.4.3 discuss the use of these flows in final configuration analysis. Similar constants were used for calculation of horizontal and vertical tail requirements. Figures 107 through 112 in section 8 present design pressure and suction distribution curves for the final LFC-200-S configuration.

4.4.2.3 Suction Requirements for Relaxed Boundary Layer Stability Criteria

The final LFC configurations studies are based on a suction level and distribution intended to prevent transition, but to permit an unstable laminar flow; i.e., a flow in which predicted instability Reynolds numbers are exceeded in the laminar boundary layer calculations. The form of equations introduced in section 4.4.2.1 remained the same with the following values for constants C_1 through C_6 .

	Relaxed	Final	Preliminary
C_1	.3337/4000.	.5005/4000.	.759/4000.
C_2	9.333	14.00	13.333
C_3	4.00	6.00	6.00
C_4	.3337/4000.	.5005/4000.	1.1385/4000.
C_5	4.667	7.00	5.333
C_6	2.333	3.50	2.50

The relaxed constants were used in computing suction flow requirements for wings of LFC-200-R and LFC-400-R configurations. Similar constants were used for calculation of horizontal and vertical tail requirements.

5.0 PARAMETRIC CONFIGURATION ANALYSES

5.1 INTRODUCTION

As the initial task in the selection of baseline configurations for subsequent detailed investigations, a comprehensive analysis was conducted to evaluate the influence of aircraft performance and geometry parameters on the fuel efficiency of commercial transport aircraft compatible with mission requirements. These analyses were conducted for both 200- and 400- passenger TF aircraft, and for 200- and 400-passenger LFC aircraft for two sets of boundary layer stability criteria. Included in this section is a description of the basic parametric configuration, the parametric procedures employed, a summary of parametric results, and a definition of the parameters selected for baseline LFC and TF configurations.

5.2 LFC CONFIGURATION ANALYSES

5.2.1 PARAMETRIC PROCEDURES

A conventional wide-body fuselage configuration, sized for the required passenger and cargo payload with associated accommodations, was used for all parametric analyses. The parametric configurations use five LFC suction units with two pylon-mounted units per wing semi-span and one tail-mounted unit. A non-structural LFC surface configuration is assumed, with a weight of 7.323 kg/m^2 (1.5 lb/ft^2) above that of the basic wing structure. Suction requirements for the parametric studies are consistent with those outlined in section 4.0. Laminar areas of the wings and empennage for parametric aircraft are illustrated by figure 24.

In view of the large number of variables considered in the parametric studies and the requirement for analyzing four distinct LFC configurations, values of variables which are relatively insensitive to configuration variations were selected as a part of the analysis of the first configuration and considered as constants in subsequent analyses. Thus, the parametric studies conducted for Configuration LFC-200-S are somewhat more extensive than those conducted for LFC-200-R, LFC-400-S, and LFC-400-R. The values of cruise Mach number, cruise altitude, engine bypass ratio, and the number and location of primary engines selected as a result of LFC-200-S analyses were used for all subsequent configuration evaluations.

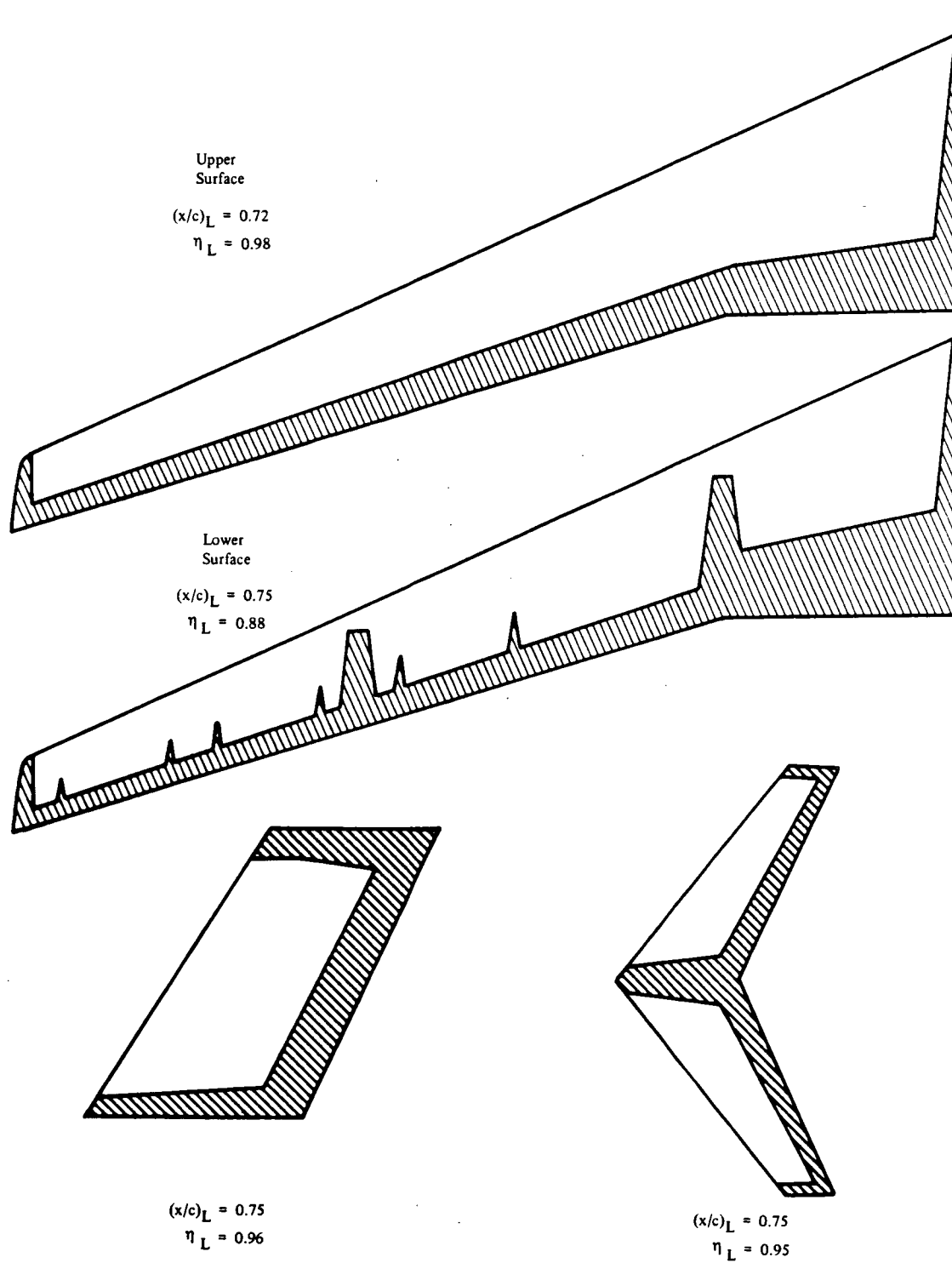


Figure 24. — Extent of laminarization for parametric configurations

The procedure used in the selection of the LFC-200-S baseline configuration is illustrated by figure 25. As outlined in this figure, an initial matrix of LFC aircraft was exercised in the GASP with fuselage geometry, main propulsion engine characteristics, and the chordwise extent of laminarization held constant. These initial parametric investigations assumed three primary propulsion engines, with two engines mounted on the aft fuselage and one mounted in the tail using an S-duct arrangement. An engine bypass ratio of 7.50 and a cruise power ratio of 0.80 were used. For fixed values of these parameters, the influence of the variables shown in table 3 was evaluated by allowing aircraft size to vary as required to perform the specified mission. All combinations of the variables listed in table 3 were considered, resulting in the evaluation of a matrix of 768 aircraft configurations.

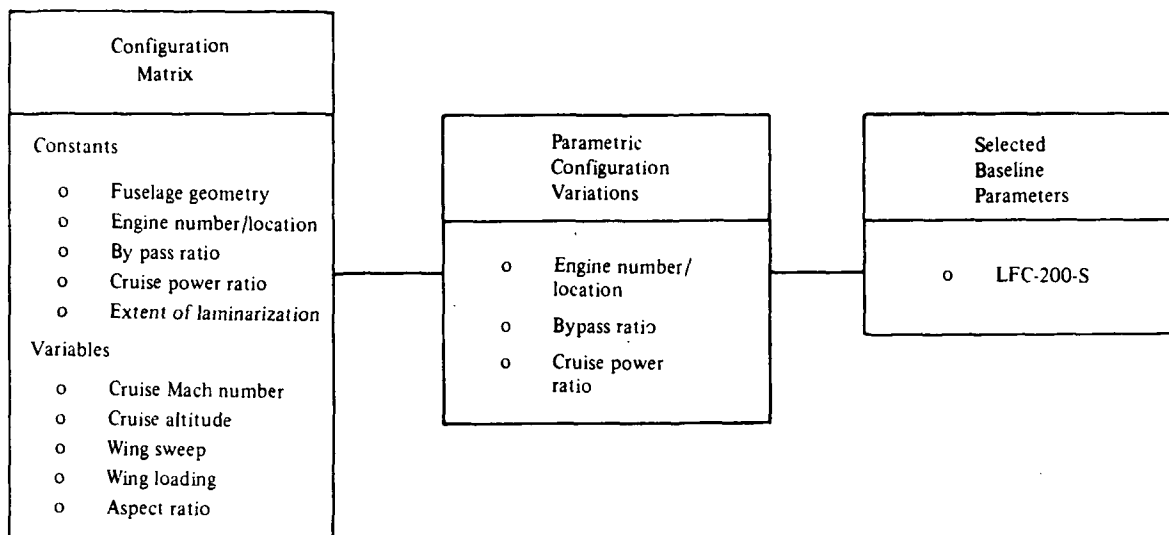


Figure 25. — Baseline selection procedure, LFC-200-S

TABLE 3. CONFIGURATION MATRIX: LFC-200-S

M	0.70	0.75	0.775	0.80
H,m, (ft)	10,973 (36,000)	12,192 (40,000)	13,411 (44,000)	
Λ , rad (deg)	0	0.175 (10)	0.349 (20)	0.524 (30)
W/S, kg/m ² (lb/ft ²)	391 (80)	488 (100)	586 (120)	683 (140)
AR	8	10	12	14

In general, the parametric configurations defined by the first phase of the analysis do not satisfy takeoff distance and second-segment climb gradient requirements. For parametric configurations which minimize fuel consumption, as determined from the configuration matrix, engine number and location, cruise power ratio, and bypass ratio were varied to define point-design configurations compatible with takeoff distance and second-segment climb requirements. The LFC-200-S baseline configuration was selected from these point-design configurations on the basis of fuel efficiency and compatibility with projected airline traffic.

Figure 26 outlines the procedure followed in the selection of baseline configuration parameters for Configurations LFC-200-R, LFC-400-S, and LFC-400-R. The procedure is similar to that employed in the LFC-200-S analysis with the exception of the definition of constant values for cruise Mach number, cruise altitude, primary engine configuration, and engine bypass ratio. Table 4 lists the matrix of variables considered in the parametric evaluation of Configurations LFC-200-R, LFC-400-S, and LFC-400-R.

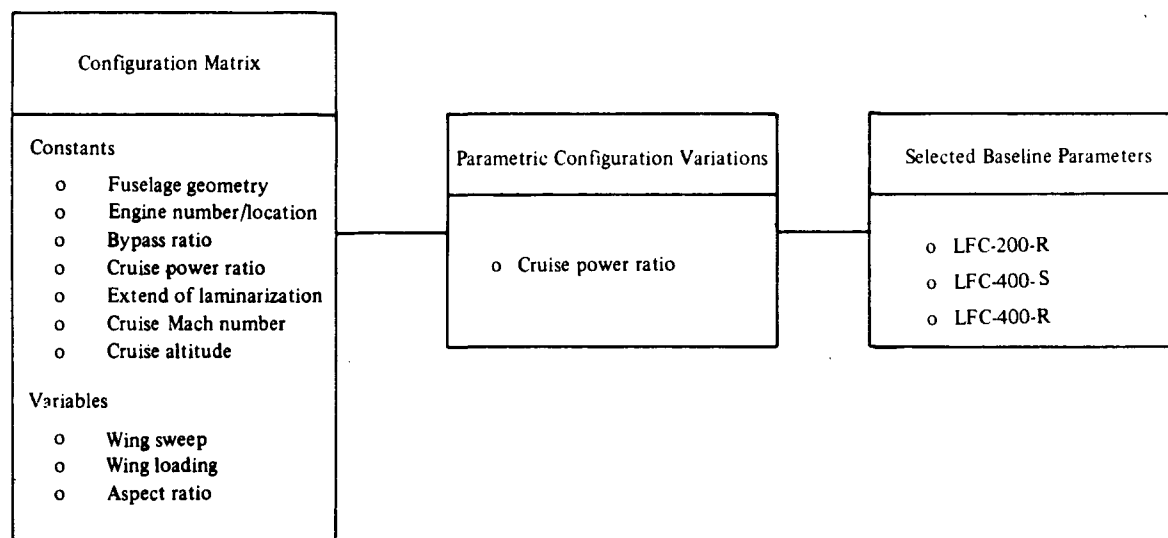


Figure 26. — Baseline selection procedure, LFC-200-R, LFC-400-S, and LFC-400-R

**TABLE 4. CONFIGURATION MATRIX: LFC-200-R,
LFC-400-S, AND LFC-400-R**

M	0.80			
H, M (ft)	11,582 (38,000)			
Λ , rad (deg)	0	0.175 (10)	0.349 (20)	0.524 (30)
W/S, kg/m ² (lb/ft ²)	391 (80)	488 (100)	586 (120)	683 (140)
AR	8	10	12	14

5.2.2 PARAMETRIC DATA: LFC-200-S

5.2.2.1 Wing Geometry

Figures 27 through 30 illustrate representative results of the parametric study. For a cruise altitude of 10,973 m (36,000 ft), these figures show the effect of variations in wing loading, aspect ratio, and cruise Mach number on block fuel for wing sweep angles of 0, 0.174 rad (10 deg), 0.349 rad (20 deg), and 0.524 rad (30 deg). For all cruise speeds, fuel consumption is minimized by configurations with unswept wings, high wing loading, and high aspect ratio.

Of particular significance in the selection of LFC configuration parameters is the fuel volume limit, shown as a dashed line in figures 27-30. The combination of a relatively small payload, a long mission range, and the wing volume required for ducting and distribution of LFC suction air, places a severe constraint on the selection of wing parameters. In these figures, only the values of wing loading and aspect ratio which lie above the fuel volume limit line represent aircraft configurations with adequate fuel volume to satisfy the design mission requirements.

Figure 31 summarizes the block fuel and wing loading of $M = 0.75$ and $M = 0.80$ LFC configurations as a function of wing sweep angle for an aspect ratio of 14. All of the configurations represented by the curves of this figure have the minimum fuel volume required for the design mission and thus represent the optimum LFC configurations compatible with realistic design constraints. It is significant, and not unexpected, that cruise at $M = 0.75$ results in a lower block fuel requirement than cruise at $M = 0.80$ for all wing sweep angles. The minimum block fuel for $M = 0.75$ aircraft is realized by an unswept wing, while a wing sweep of about 0.384 rad (22 deg) minimizes block fuel for $M = 0.80$ aircraft. Insight into the nature of the fuel volume constraint is provided by figures 32 and 33, which show wing thickness-to-chord ratios as a function of cruise M and wing sweep for selected values of wing loading and aspect ratio.

$H, m (ft) = 10.973 (36.000)$
 $BPR = 7.50$
 $\eta = 0.80$
 --- Internal fuel volume limit

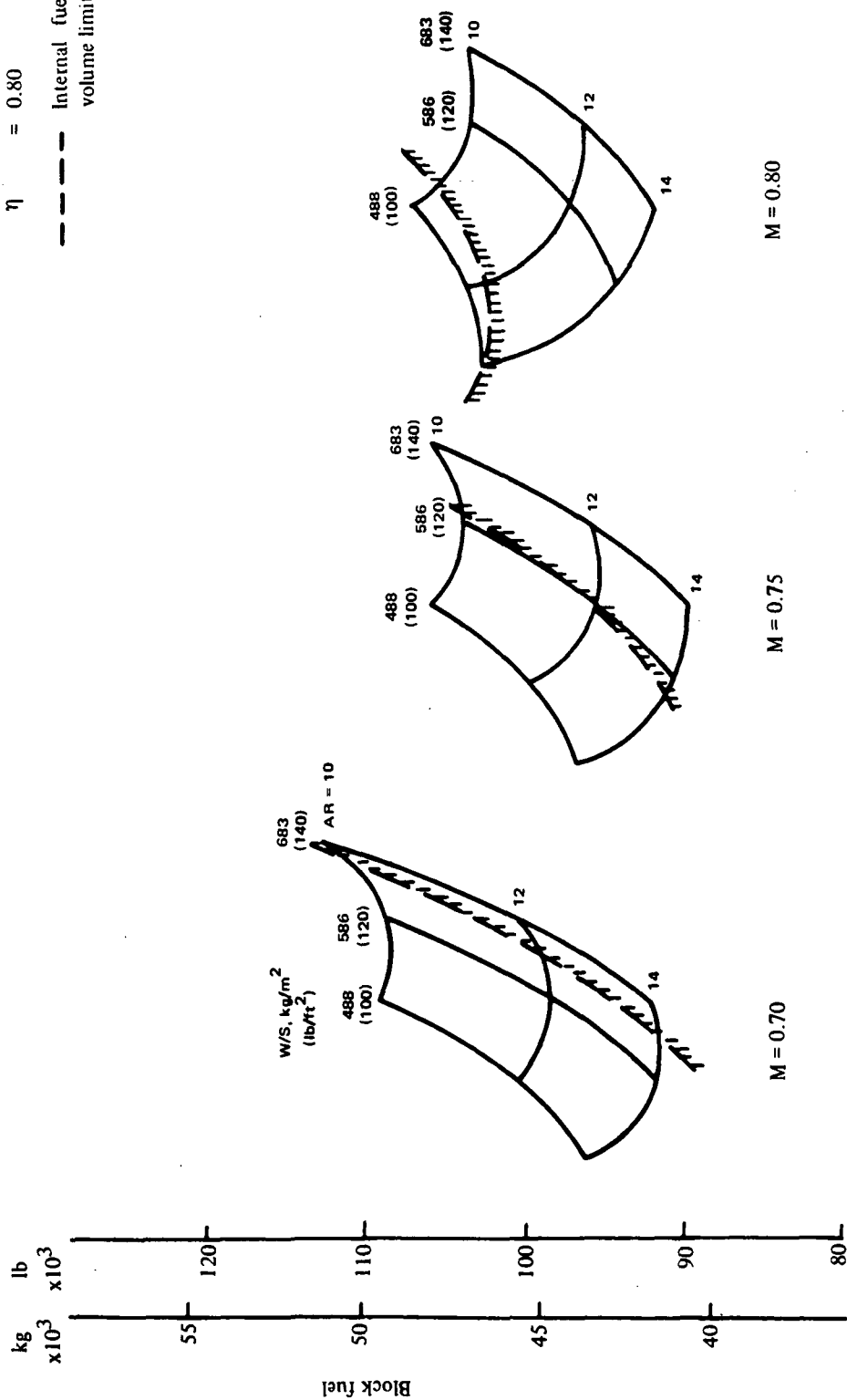


Figure 27. -- Block fuel vs. wing loading and aspect ratio, LFC-200-S, $\Lambda = 0$

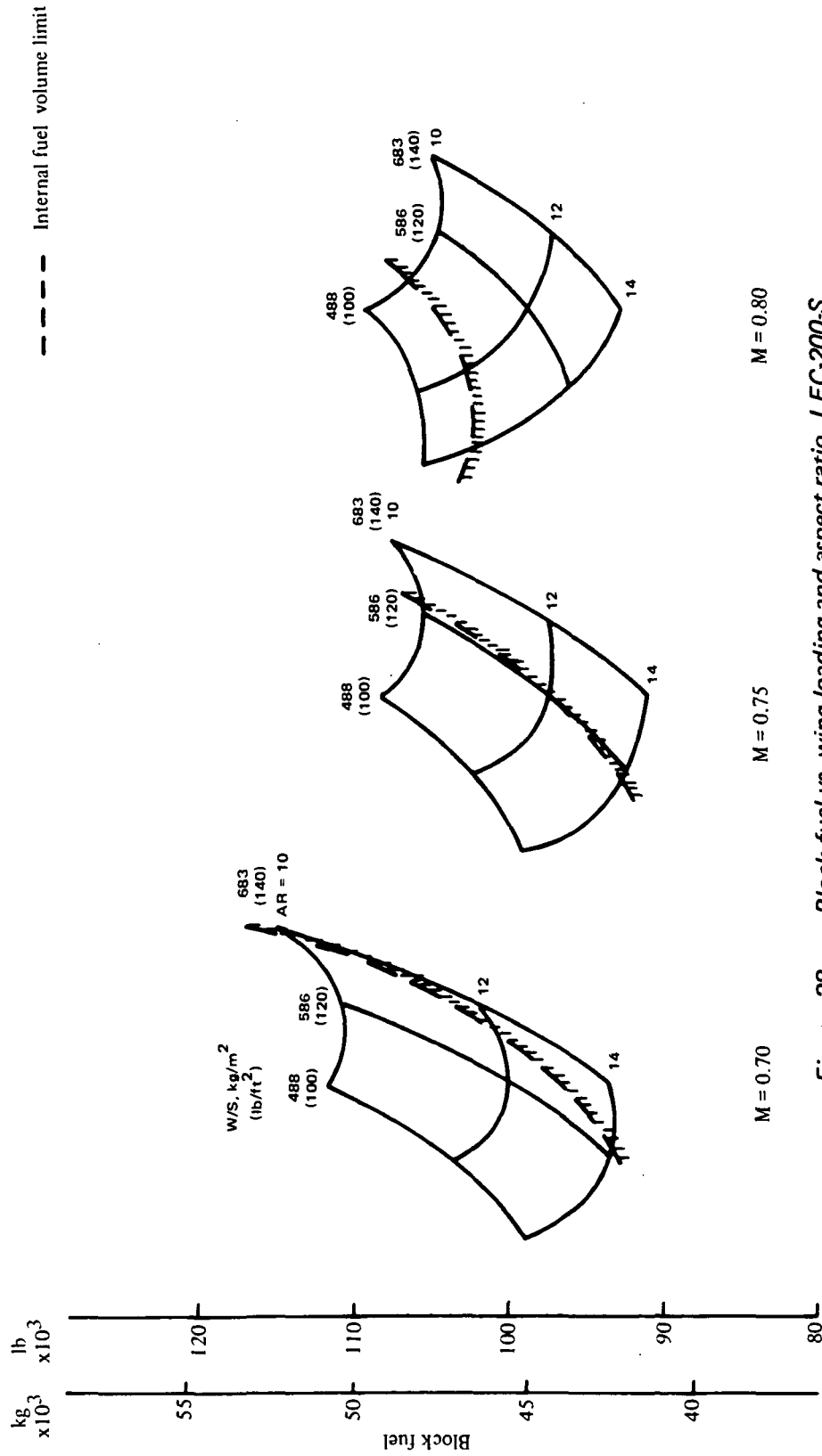


Figure 28. — Block fuel vs. wing loading and aspect ratio, LFC-200-S
 $\Lambda = 0.174$ rad (10 deg)

H_m (ft) = 10,973 (36 000)
 BPR = 7.50
 η = 0.80
 --- Internal fuel

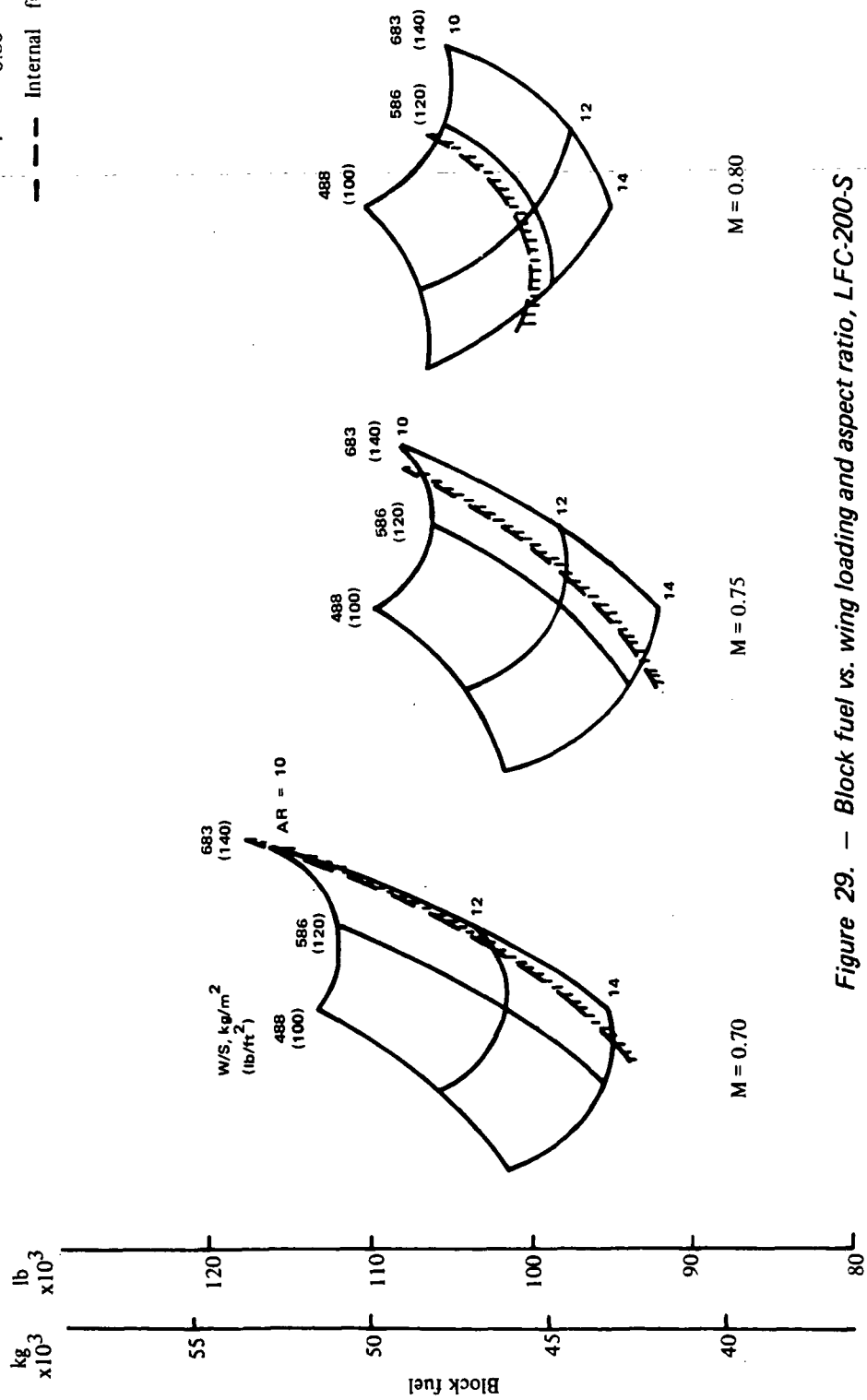


Figure 29. — Block fuel vs. wing loading and aspect ratio, LFC-200-S
 $\Lambda = 0.349$ rad (20 deg)

Figure 1 consists of three graphs showing Block fuel (kg and lb) versus W/S (kg/m² and lb/ft²) for Mach numbers 0.70, 0.75, and 0.80. The graphs are arranged horizontally. The y-axis for all graphs is Block fuel, with scales in kg (0 to 55) and lb (90 to 120). The x-axis for all graphs is W/S, with scales in kg/m² (0 to 140) and lb/ft² (0 to 100). Each graph contains three curves representing internal fuel volume limits: 488 (100), 586 (120), and 683 (140). A dashed line represents the internal fuel volume limit. The graphs are labeled M = 0.70, M = 0.75, and M = 0.80.

Figure 30. — Block fuel vs. wing loading and aspect ratio, LFC-200-S,
 $\Lambda = 0.524 \text{ rad (30 deg)}$

H, m (ft) = 10,973 (36,000)
 AR = 14
 BPR = 7.50
 η = 0.80

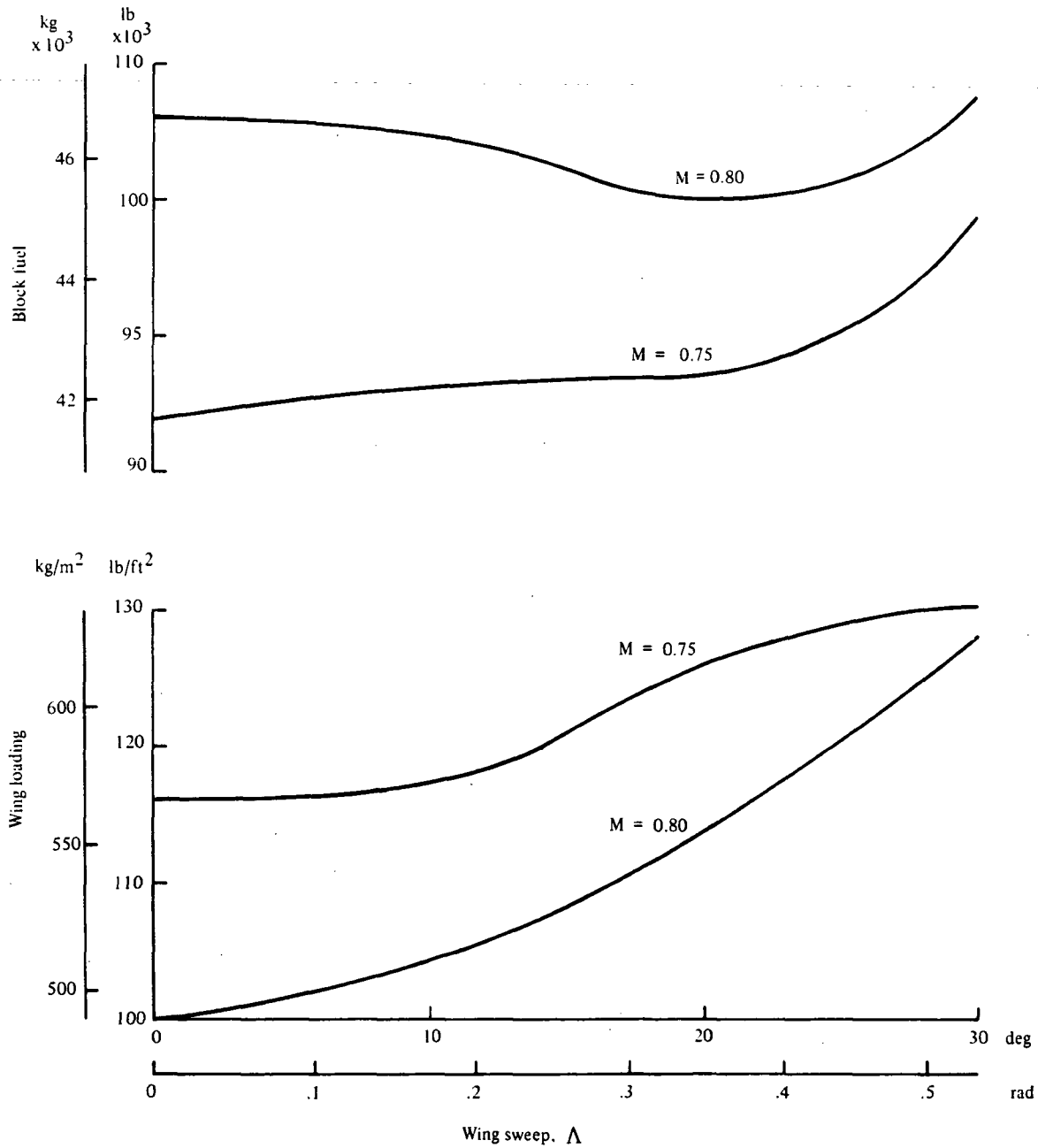


Figure 31. — Block fuel and wing loading vs. wing sweep, LFC-200-S

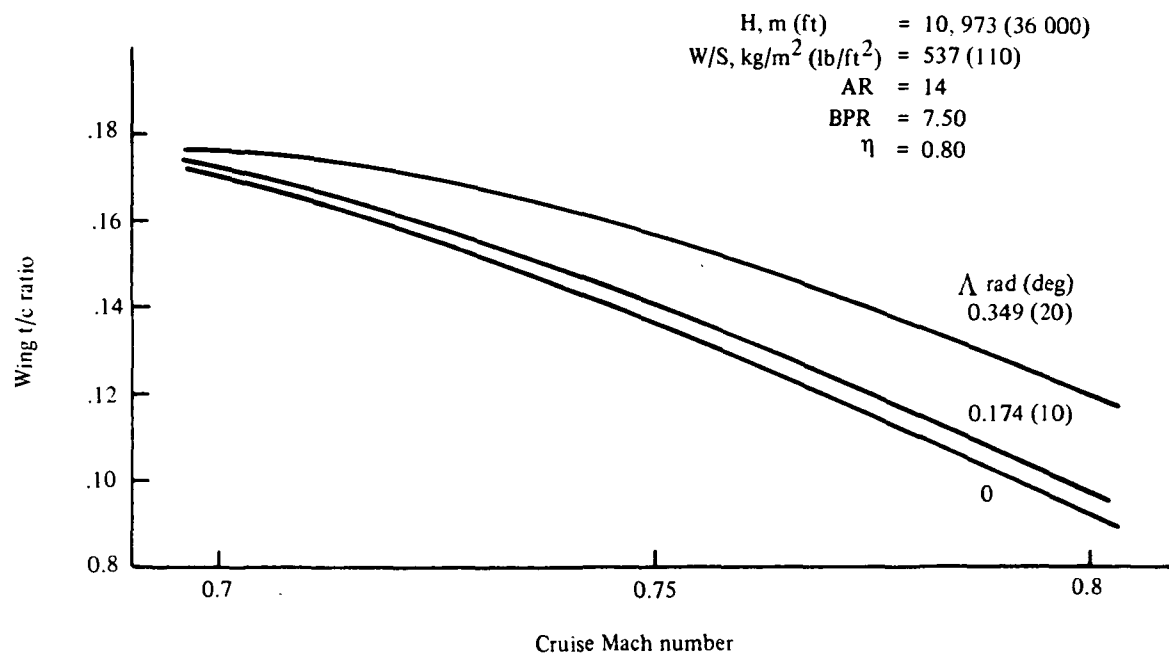


Figure 32. — Wing t/c ratio vs. cruise Mach number, LFC-200-S

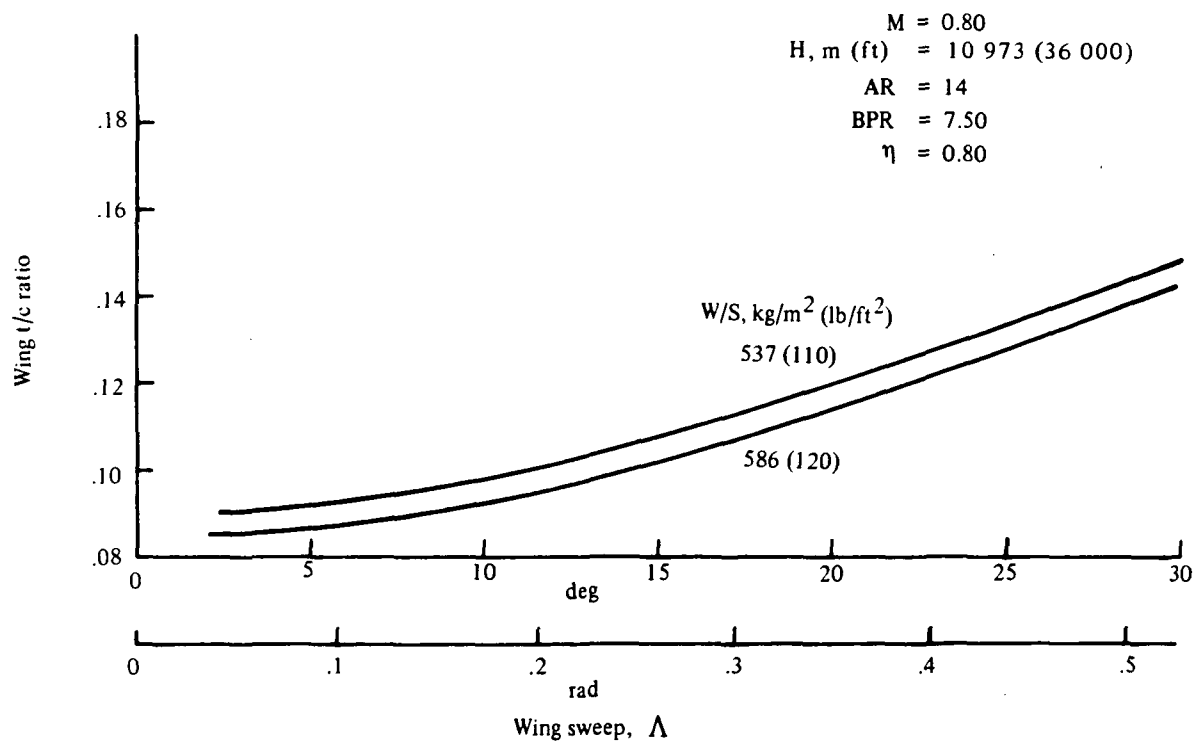


Figure 33. — Wing t/c ratio vs. wing sweep, LFC-200-S

5.2.2.2 Cruise Parameters

The influence of cruise M and wing sweep on block fuel and DOC is shown in figure 34 for configurations with a wing loading of 537 kg/m^2 (110 lb/ft^2) and aspect ratio of 14. It will be observed that fuel consumption is minimized by selecting a cruise M of 0.75 or less, but that minimum DOC occurs for a cruise M of about 0.78.

Figures 35 and 36 illustrate the effect of cruise altitude and cruise M on block fuel and DOC for configurations with the same wing loading and aspect ratio for wing sweep angles of 0 and 0.349 rad (20 deg). For either wing sweep, minimum block fuel is obtained at the lowest altitude considered at a cruise M of 0.75 or less. Minimum DOC is also realized by cruising at the lowest altitude, but optimum cruise M is from 0.75 to 0.79, depending on altitude and wing sweep.

5.2.2.3 Engine Parameters

As noted in section 5.2.1, the parametric configurations defined in the configuration matrix were based on a constant cruise power ratio of 0.80, and do not recognize a field length constraint. For a representative configuration geometry, bypass ratio and cruise power ratio variations were conducted as required to satisfy the specified FAR field length requirement of 3353 m (11,000 ft). In conducting these variations, it was determined that a cruise altitude of 11,582 m (38,000 ft) allowed a better match of cruise and takeoff thrust requirements than cruise at 10,973 m (36,000 ft).

The variation of FAR field length, block fuel, and DOC with aspect ratio and engine bypass ratio is shown in figure 37 for $M = 0.75$ aircraft with fixed wing sweep and wing loading. Configurations with the lower aspect ratio demonstrate better takeoff performance, but block fuel and DOC are minimized by the high-aspect-ratio configurations. Fuel consumption is minimized by selecting a bypass ratio of about 6.0. This value also represents a reasonable compromise relative to takeoff performance and DOC.

Analyses were conducted for configurations employing 3 and 4 aft-mounted main propulsion engines. Figure 38 shows that the 4-engine configuration results in a lower relative fuel consumption and illustrates the fuel penalty incurred by LFC aircraft as a result of aircraft performance requirements. It is characteristic of LFC aircraft, which exhibit low drag during cruise conditions, that the main engines are sized by takeoff requirements and are thus appreciably larger than required for cruise. Following are the cruise power ratios corresponding to the FAR field lengths shown in figure 38 for the 4-engine configurations;

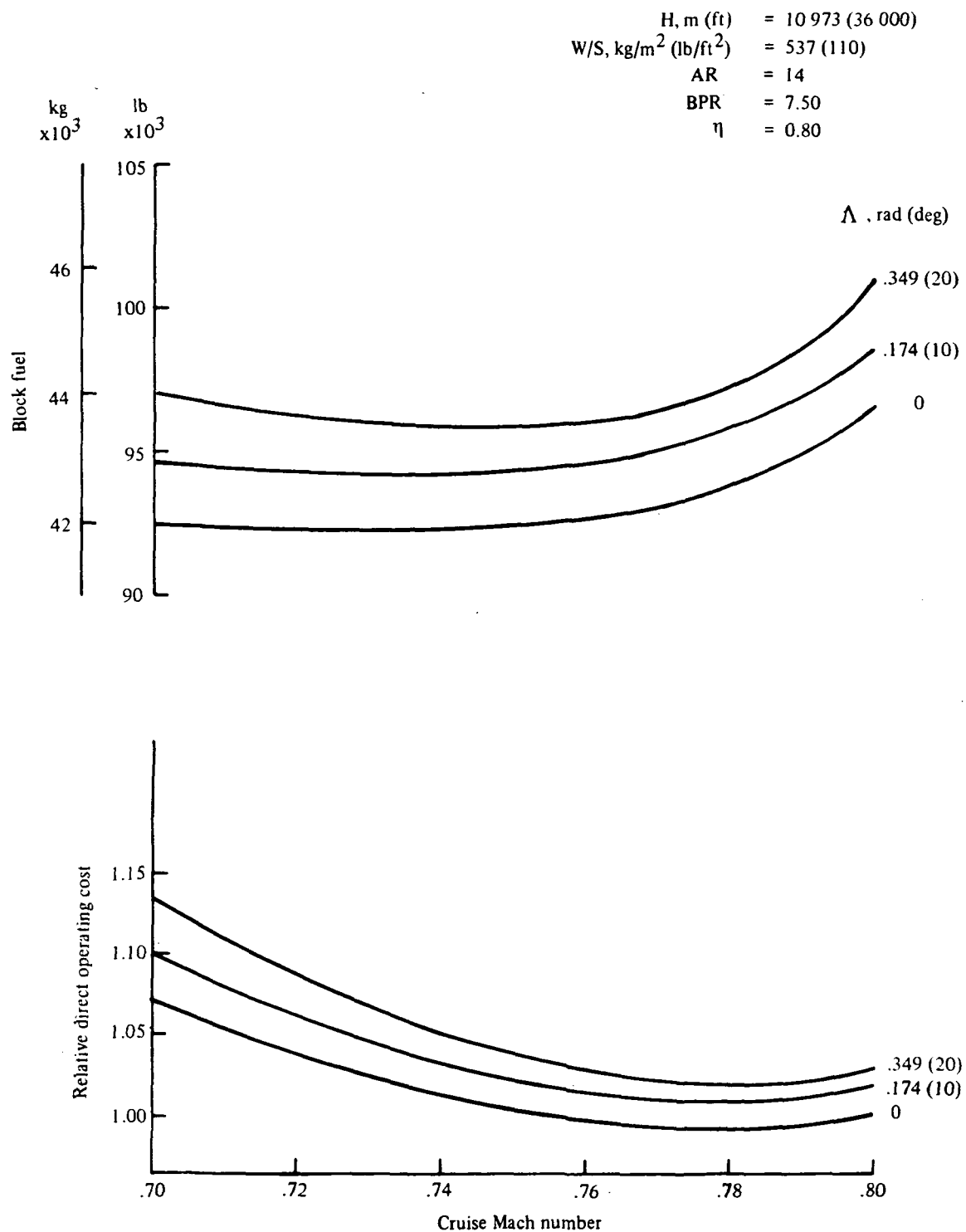


Figure 34. — Effect of wing sweep and cruise Mach number on block fuel and relative DOC, LFC-200-S

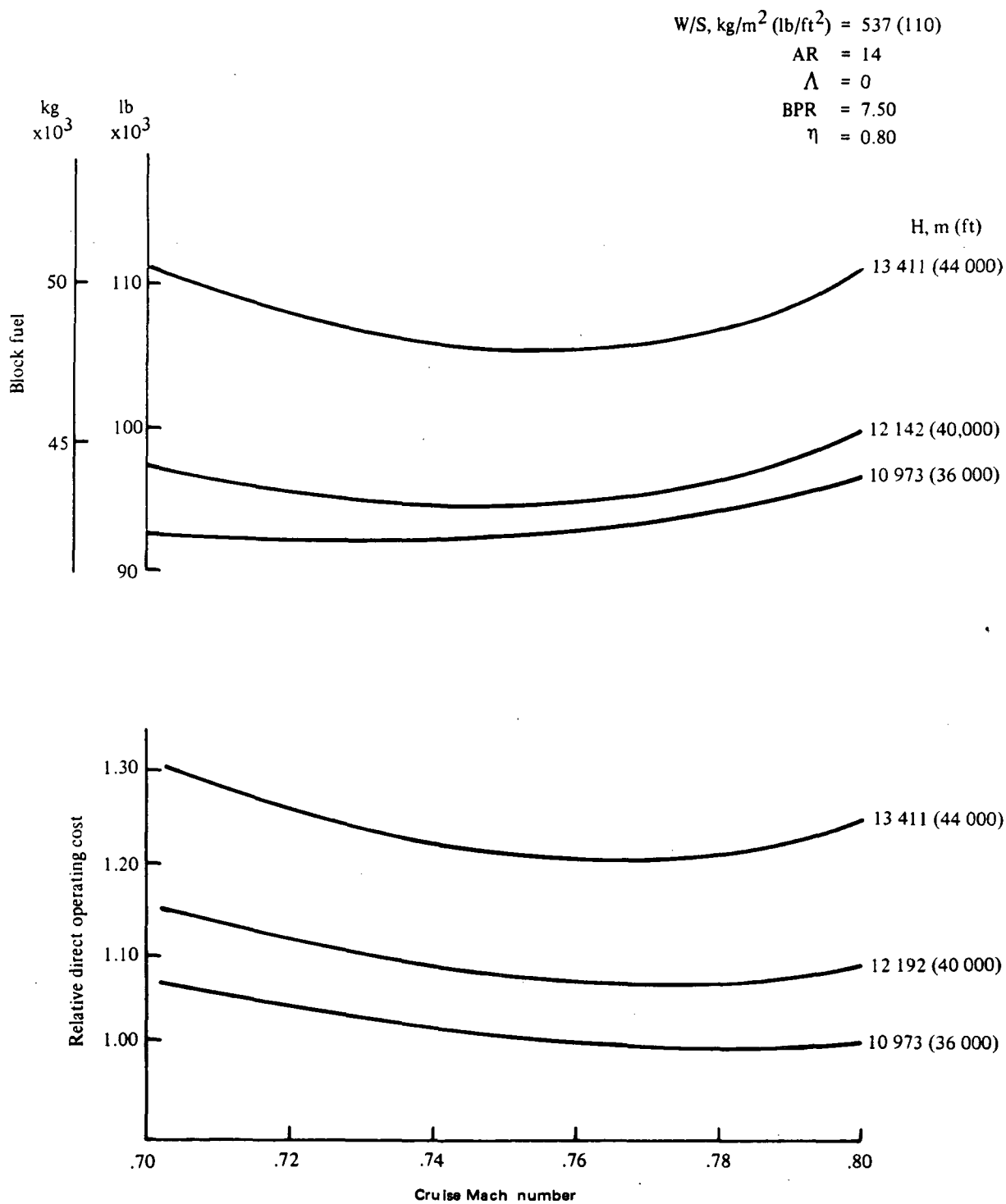


Figure 35. — Effect of cruise altitude and cruise Mach number on block fuel and relative DOC, LFC-200-S, $\Lambda = 0$

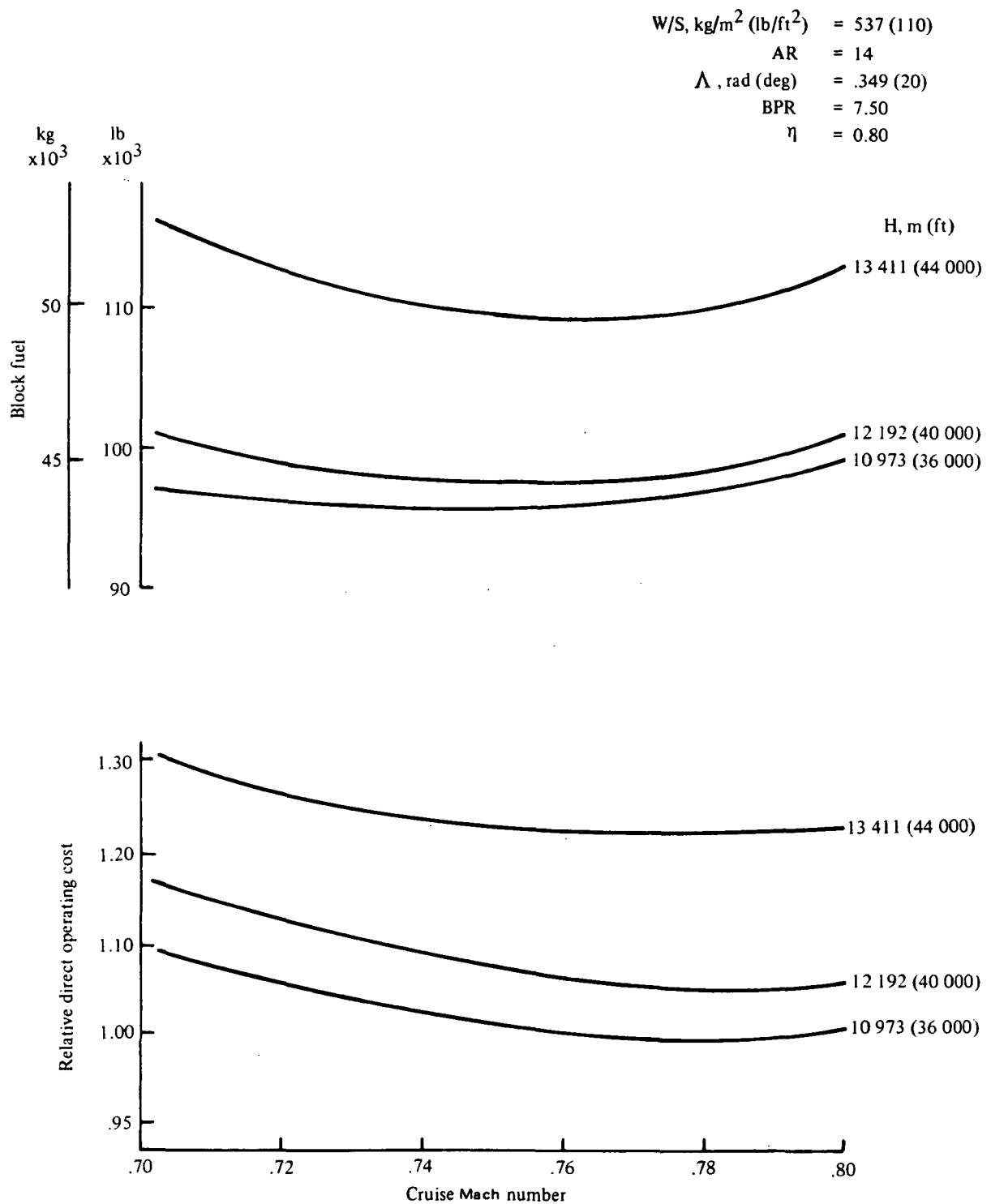


Figure 36. — Effect of cruise altitude and cruise Mach number on block fuel and relative DOC, LFC-200-S, $\Lambda = 0.349$ rad (20 deg)

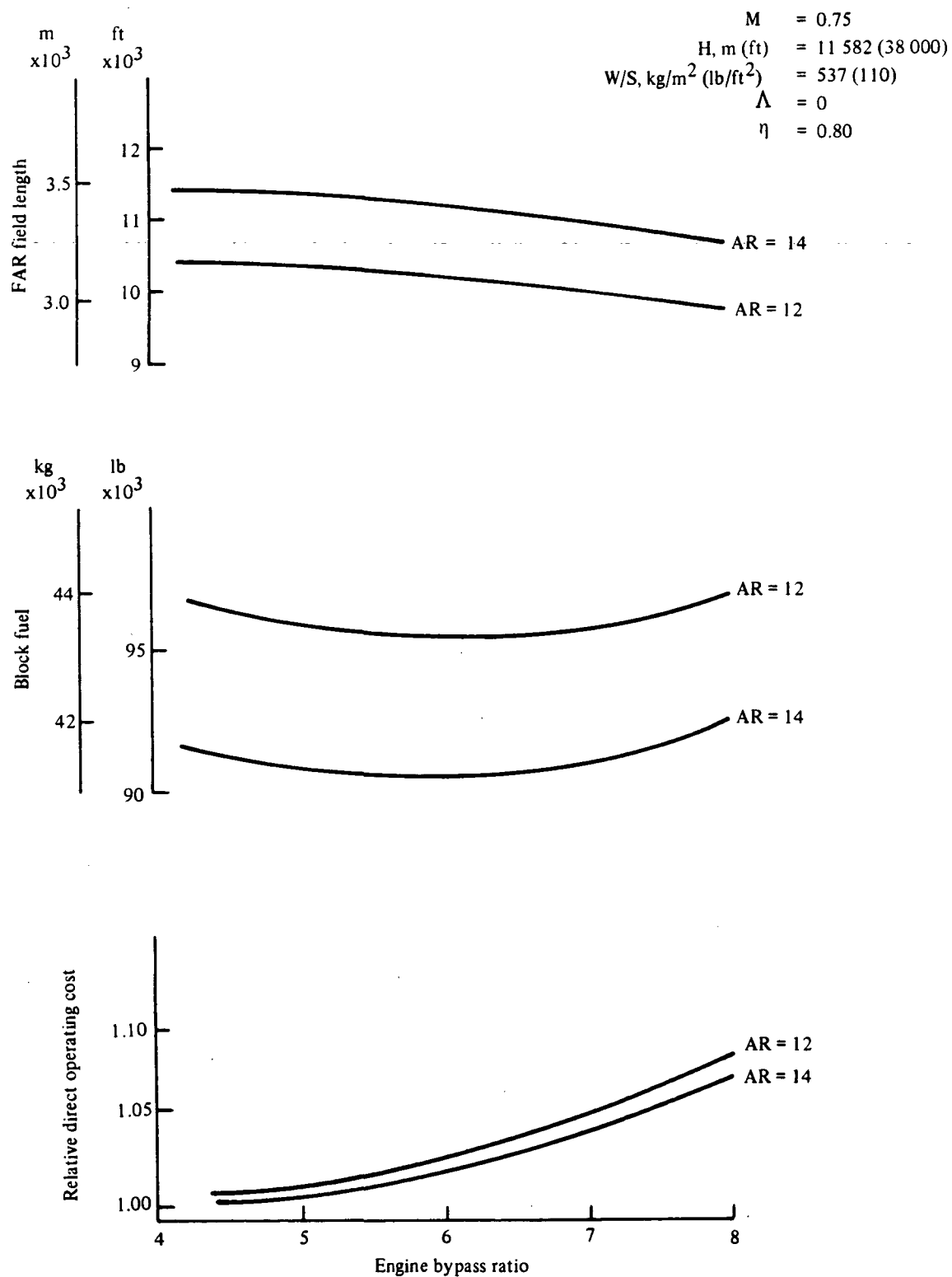


Figure 37. — Engine bypass ratio variations, LFC-200-S

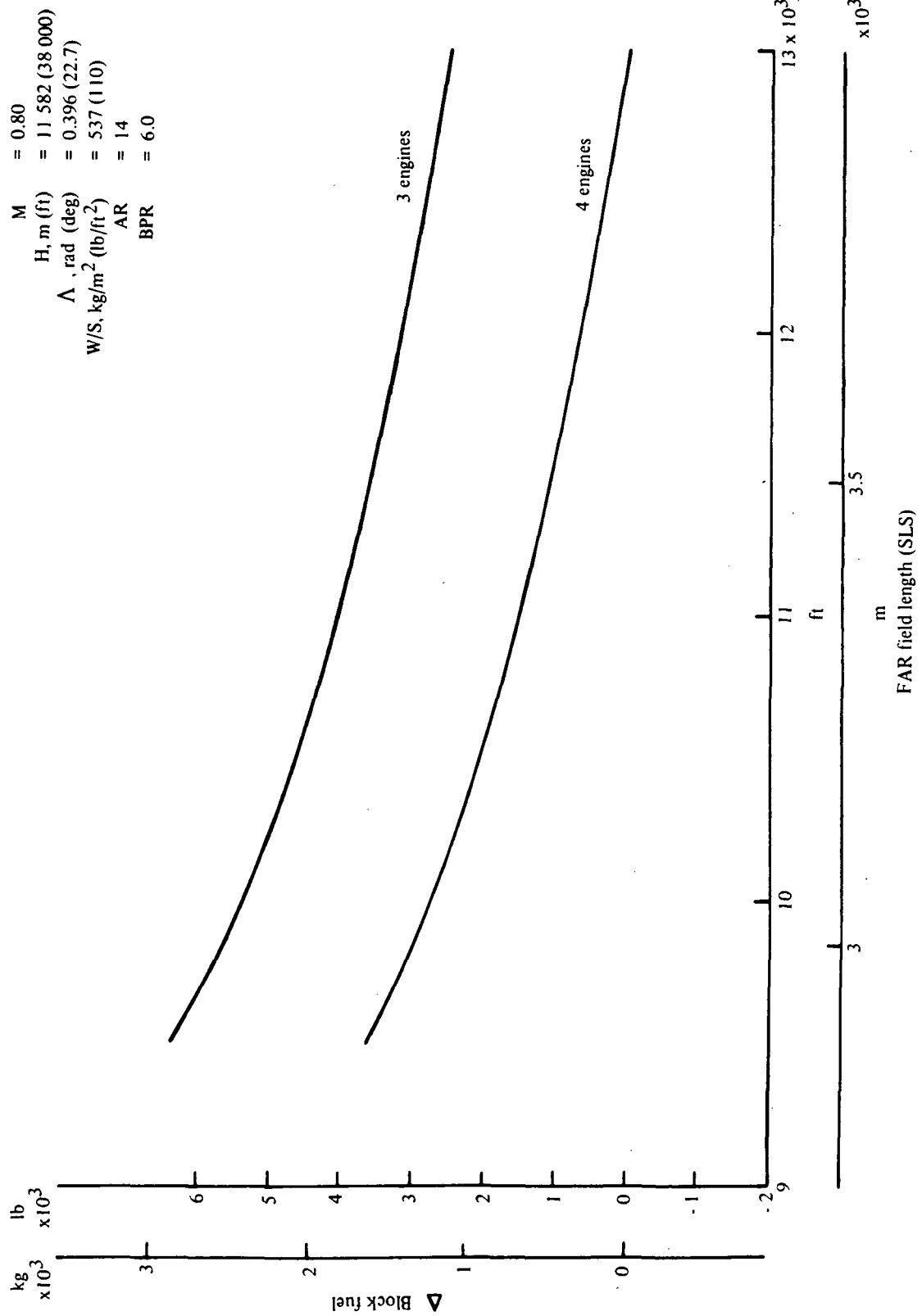


Figure 38. — Variation of block fuel with FAR field length, LFC-200-S

FAR field length, m (ft)	Cruise power ratio
3048 (10,000)	0.76
3353 (11,000)	0.80
3658 (12,000)	0.85
3962 (13,000)	0.89

For the 3353 m (11,000 ft) FAR field length requirement of this study, an LFC aircraft requires only 80% of available engine thrust at cruise conditions. This compares to a value ranging from 88% to 98% for TF transports.

5.2.2.4 Baseline Configuration Parameters

The following summarizes the implications of the data generated in the parametric analysis of LFC-200-S:

- (1) *Cruise Mach number* – Fuel consumption of LFC aircraft is minimized by selecting a cruise M of 0.75 or less. On the basis of DOC, the optimum cruise M is between 0.76 and 0.79, depending on aircraft configuration.
- (2) *Cruise Altitude* – Both fuel consumption and DOC are minimized for LFC aircraft by selecting the lowest cruise altitude which permits a reasonable match of cruise and takeoff thrust requirements.
- (3) *Wing Geometry* – Within the constraints imposed by considering only conventional aircraft configurations, fuel consumption of LFC aircraft is minimized by selecting the highest wing loading and aspect ratio and lowest wing sweep compatible with fuel volume requirements for the design mission.
- (4) *Engine Bypass Ratio* – An engine bypass ratio of 6.0 minimizes fuel consumption, provides reasonable airport performance, and does not incur a significant penalty in DOC.
- (5) *Number and Location of Primary Engines* – To minimize both the influence of engine noise on the laminar boundary layer and the loss of laminar area due to pylon/wing interference, it is desirable to employ fuselage-mounted engines on LFC aircraft. The use of four fuselage-mounted engines provides better takeoff and second-segment climb performance and minimizes block fuel.

If selection of the baseline configuration is based entirely on the minimization of fuel consumption, the parametric analyses of the preceding section dictate the selection of an LFC baseline with the following characteristics:

Cruise M:	0.75
Cruise altitude:	11,582 m (38,000 ft)
Wing sweep:	0
Wing loading:	537 kg/m ² (110 lb/ft ²)
Aspect ratio:	14
Bypass ratio:	6.0

In addition to minimizing fuel consumption for the design mission, the resultant configuration eliminates potential spanwise contamination problems attending the crossflow inherent in the boundary layer of swept-wing aircraft.

However, in view of the more favorable direct operating costs at higher cruise speeds and the current and projected flow of airline traffic at speeds of $M = 0.80$ or greater, a cruise M of 0.80 was determined to be appropriate for the aircraft of this study. Consequently, the LFC baseline configuration and all subsequent configurations developed during the course of the study are designed for cruise at $M = 0.80$.

Based on the parametric data of the preceding section, the optimum wing geometry for cruise at $M = 0.80$ is defined by a quarter-chord wing sweep of 0.396 rad (22.7 deg), a wing loading of 537 kg/m² (110 lb/ft²), and an aspect ratio of 14.

In summary, consistent with both specified mission requirements and a cruise M of 0.80, the following parameters define the selected 200-passenger baseline LFC configuration:

Cruise M:	0.80
Cruise altitude:	11,582 m (38,000 ft)
Wing sweep:	0.396 rad (22.7 deg)
Wing loading:	556 kg/m ² (114 lb/ft ²)
Aspect ratio:	14
Bypass ratio:	6.00
Cruise power ratio:	0.80

The detailed development of Configuration LFC-200-S is described in sections 7.0 and 8.2.

5.2.3 PARAMETRIC DATA: LFC-200-R

Based on the results of analyses conducted for LFC-200-S, the following constants were selected for the initial parametric studies of LFC-200-R:

Cruise M:	0.80
Cruise altitude, m (ft):	11,582 (38,000)
Bypass ratio:	6.00
Cruise power ratio:	0.80

5.2.3.1 Wing Geometry

Figures 39 and 40 illustrate the effect of variations in wing loading, aspect ratio, and wing sweep on fuel consumption for LFC-200-R at the design range. The internal fuel volume limit identified on these figures defines the limiting values of wing loading and aspect ratio for each wing sweep angle and thereby establishes the minimum block fuel for practical aircraft designs.

Figure 41 summarizes the minimum block fuel points from figures 39 and 40 as a function of wing sweep angle and shows the wing loading associated with each value of wing sweep. For the specified cruise conditions, a wing sweep of 0.349 rad (22.7 deg) minimizes fuel consumption. The wing loading corresponding to this wing sweep is 590 kg/m^2 (121 lb/ft^2).

5.2.3.2 Engine Parameters

The airport performance of LFC-200-R is sufficiently similar to that of LFC-200-S that the previously selected bypass ratio of 6.00 and cruise power ratio of 0.80 are appropriate for the baseline configuration.

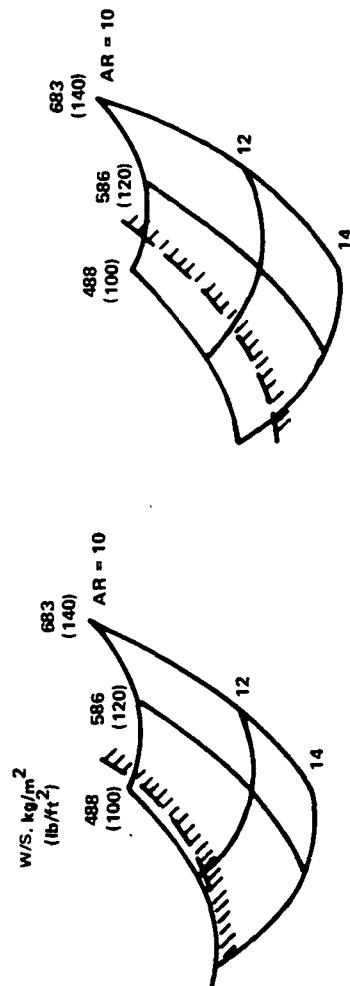
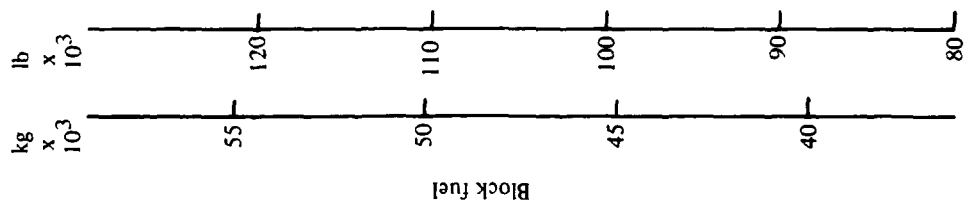
5.2.3.3 Baseline Configuration Parameters

The general trends of the parametric data describing LFC-200-R are observed to be similar to those exhibited by LFC-200-S. The primary difference in the results is the lower level of fuel consumption demonstrated by the LFC-200-R configurations. This results from the reduced suction requirements and the attendant reduction in LFC system weight, fuel flow, and wing volume requirements. The reduction in both fuel volume and ducting required for this configuration permits an increase in wing loading of about 34 kg/m^2 (7 lb/ft^2) which provides an additional improvement in fuel efficiency.

Following is a summary of the selected baseline configuration parameters for LFC-200-R:

$M = 0.80$
 $H, m (ft) = 11,582 (38,000)$
 $BPR = 6.00$
 $\eta = 0.80$

--- Internal fuel volume limit



$\Lambda = 0$

$\Lambda = 0.174 \text{ rad (10 deg)}$

Figure 39. — Block fuel vs. wing loading and aspect ratio, LFC-200-R,
 $\Lambda = 0$ and $\Lambda = 0.174 \text{ rad (10 deg)}$

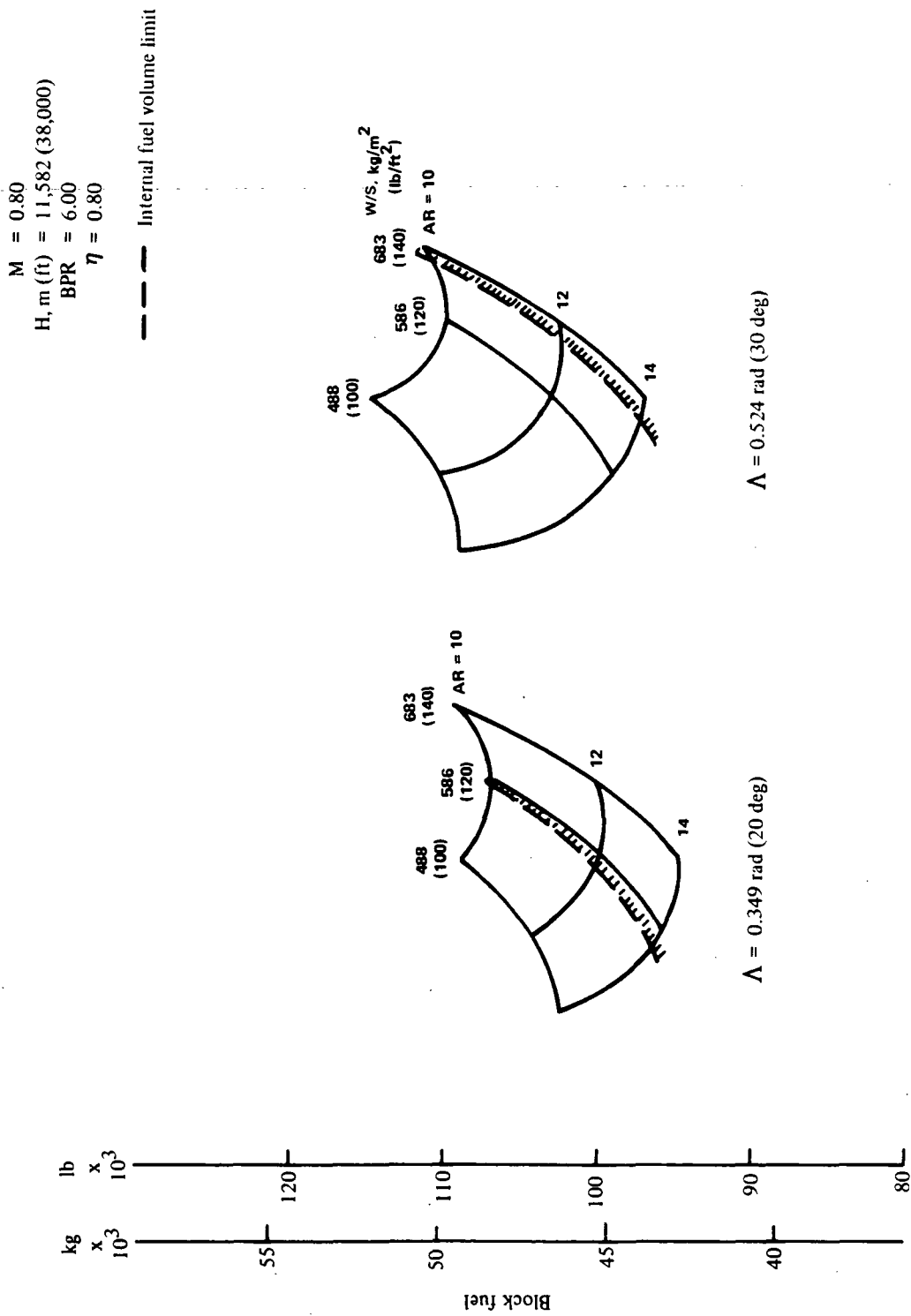


Figure 40. — Block fuel vs. wing loading and aspect ratio, LFC-200-R,
 $\Lambda = 0.349$ rad (20 deg) and $\Lambda = 0.524$ rad (30 deg)

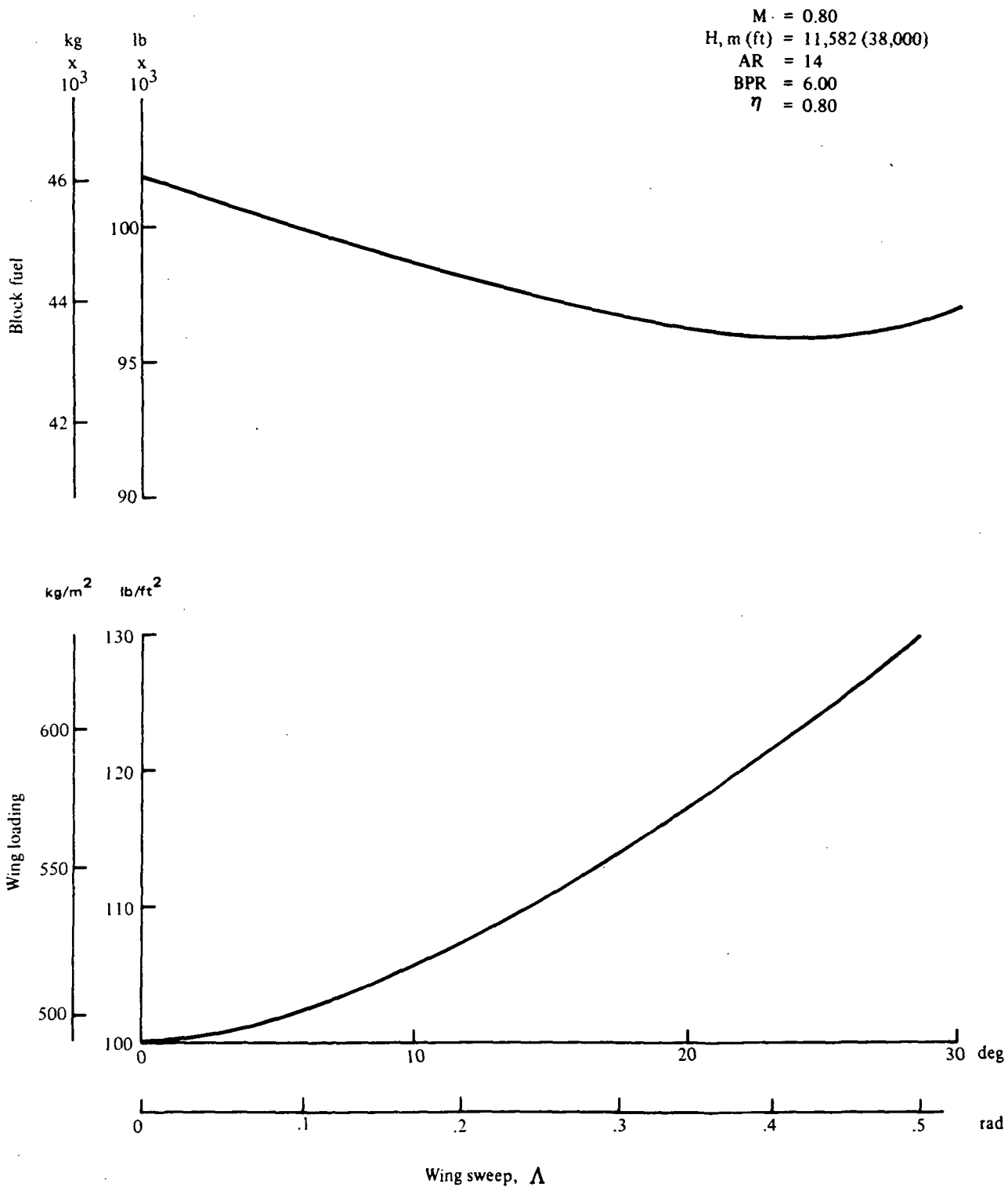


Figure 41. — Block fuel and wing loading vs. wing sweep, LFC-200-R

Cruise M:	0.80
Cruise altitude:	11,582 m (38,000 ft)
Wing sweep:	0.396 rad (22.7 deg)
Wing loading:	590 kg/m ² (121 lb/ft ²)
Aspect ratio:	14
Bypass ratio:	6.00
Cruise power ratio:	0.80

The detailed development of Configuration LFC-200-R is described in section 8.3.

5.2.4 PARAMETRIC DATA: LFC-400-S

The following constants were used in the initial parametric studies of LFC-400-S:

Cruise M:	0.80
Cruise altitude, m (ft):	11,582 (38,000)
Bypass ratio:	6.00
Cruise power ratio:	0.75

With the exception of the cruise power ratio, which was decreased from 0.80 to 0.75 in anticipation of higher wing loadings and an attendant degradation of airport performance, these constants are identical to those used in the analysis of 200-passenger aircraft.

5.2.4.1 Wing Geometry

The effect of variations in wing loading, aspect ratio, and wing sweep on fuel consumption for LFC-400-S is illustrated by figures 42 and 43. As in the case of the analyses conducted for the 200-passenger LFC aircraft, these data show that fuel consumption is minimized by selecting the highest aspect ratio and wing loading compatible with the wing volume available for fuel and LFC system ducting.

The minimum values of block fuel, as established by the internal fuel volume limit, are plotted in figure 44 as a function of wing sweep. This figure shows that wing sweep angle of about 0.396 rad (22.7 deg) minimizes fuel consumption. The wing volume at this wing sweep angle permits a wing loading of 678 kg/m² (139 lb/ft²).

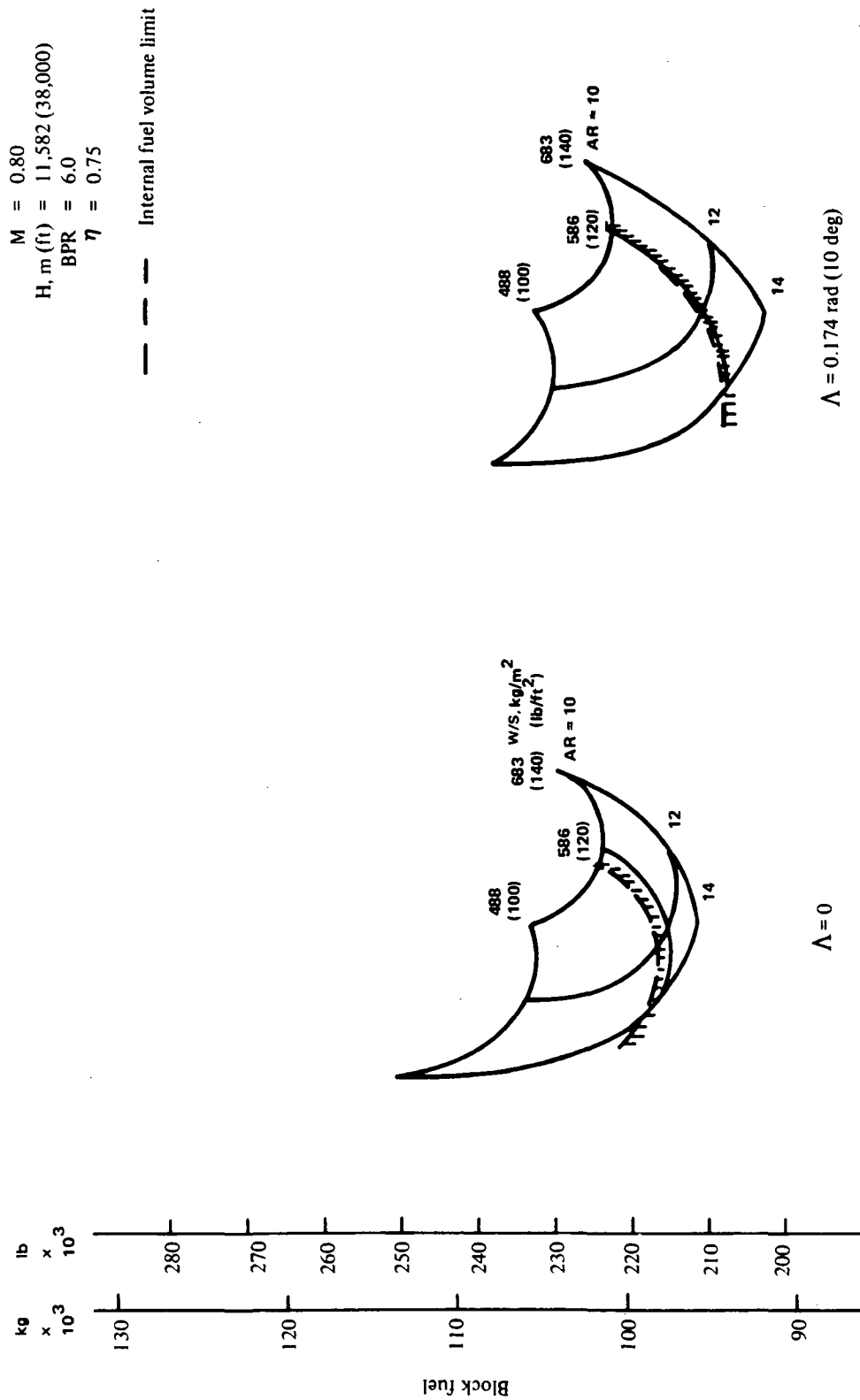
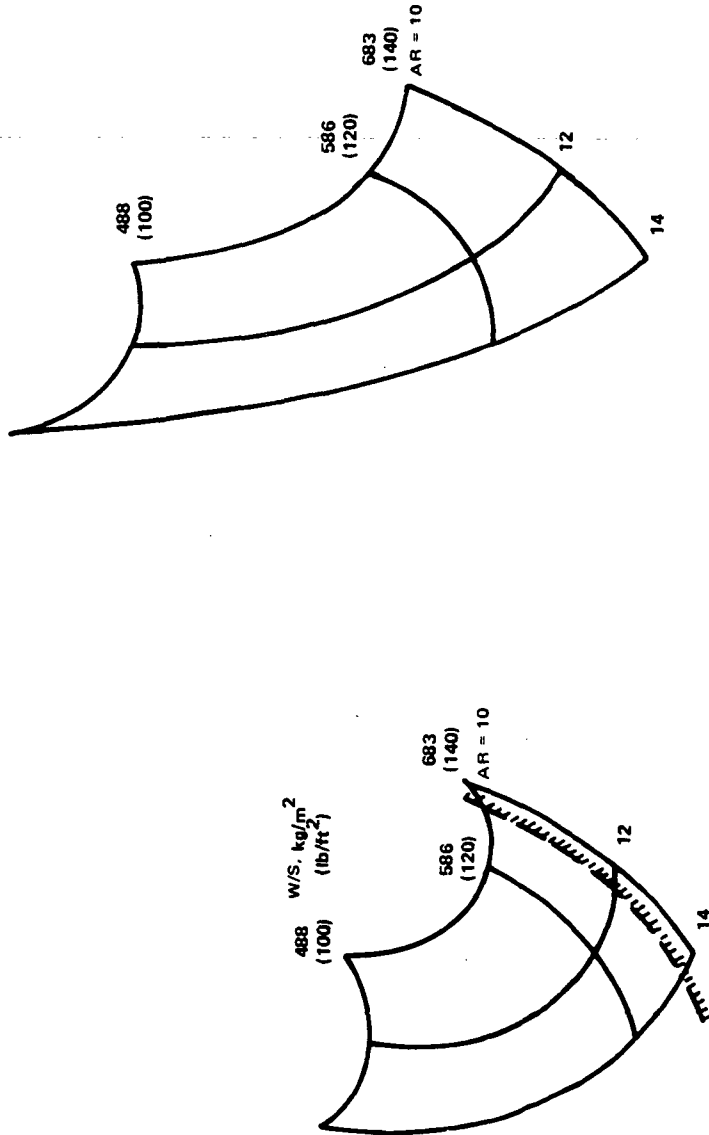
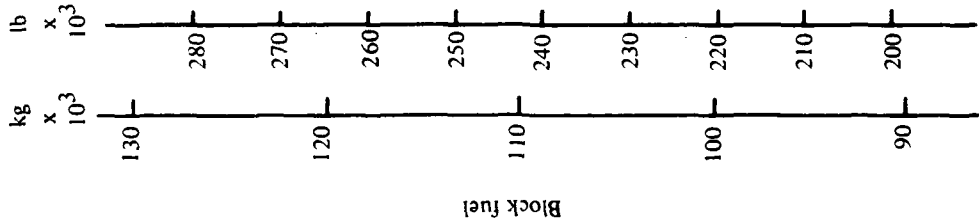


Figure 42. — Block fuel vs. wing loading and aspect ratio, LFC-400-S,
 $\Lambda = 0$ and $\Lambda = 0.174 \text{ rad (10 deg)}$

$M = 0.80$
 $H_{lm}(ft) = 11,582 (38,000)$
 $BPR = 6.0$
 $\eta = 0.75$
--- Internal fuel volume limit



$\Lambda = 0.349$ rad (20 deg) $\Lambda = 0.524$ rad (30 deg)

Figure 43. — Block fuel vs. wing loading and aspect ratio, LFC-400-S,
 $\Lambda = 0.349$ rad (20 deg) and $\Lambda = 0.524$ rad (30 deg)

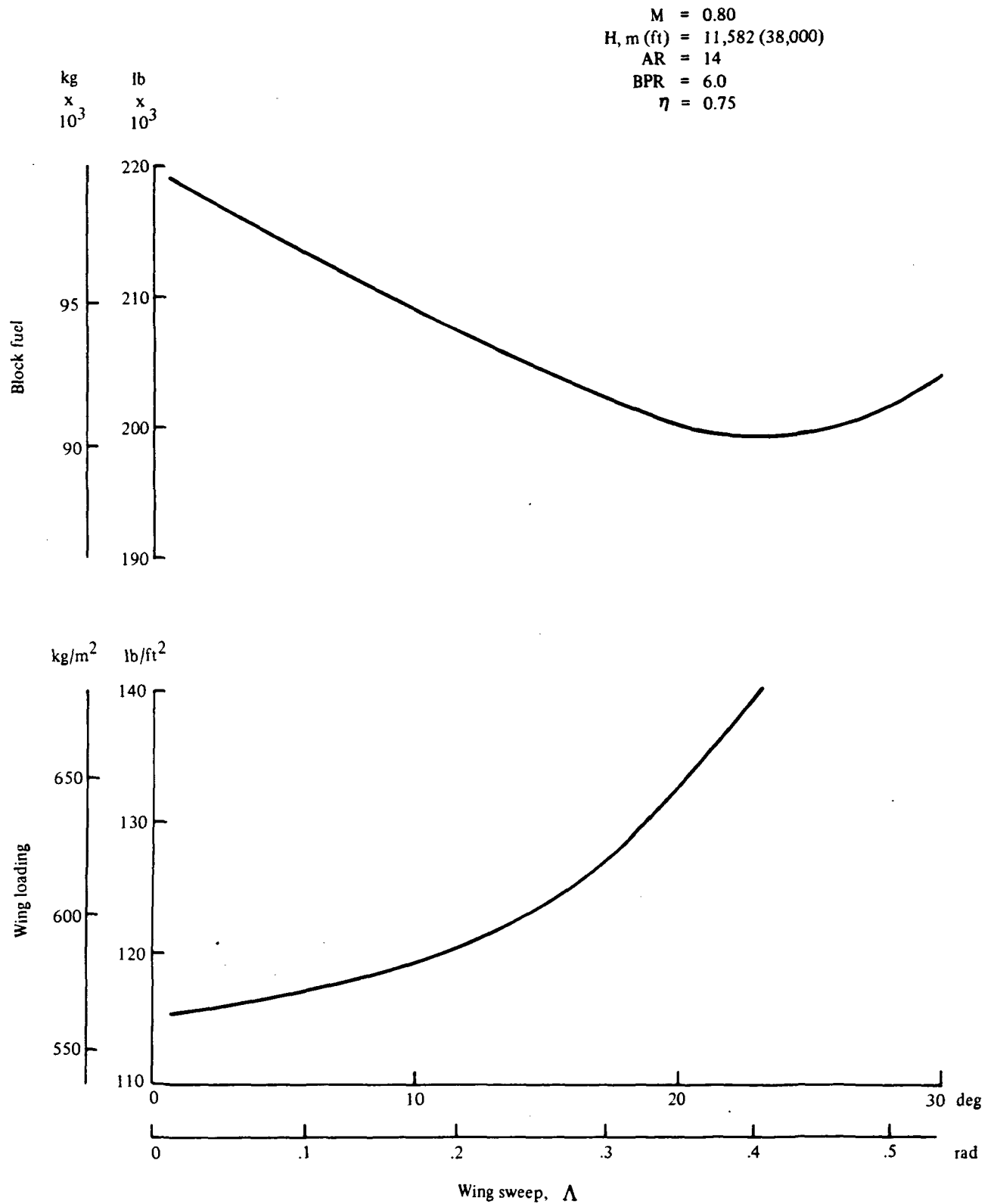


Figure 44. — Block fuel and wing loading vs. wing sweep, LFC-400-S

5.2.4.2 Engine Parameters

The results of engine bypass ratio variations conducted for the LFC-400-S configuration are presented in figure 45. For this analysis, a constant aspect ratio and wing sweep were maintained and wing loading and cruise power ratio were allowed to vary as required to satisfy the FAR field length requirement of 3353 m (11,000 ft). As shown by figure 45, the value of 6.00 selected for the initial parametric investigations provides a reasonable compromise between minimum fuel consumption and direct operating costs. The relaxation of the fuel volume constraint permits the use of much higher wing loadings for 400-passenger aircraft than were achievable for the 200-passenger configurations. Selection of wing loading and cruise power ratio combinations which satisfy airport performance requirements while minimizing fuel consumption thus becomes more critical for the 400-passenger mission. Figure 46 illustrates the influence of wing loading and cruise power ratio on FAR field length and includes the limitation imposed by the second-segment climb gradient requirement. This figure shows that second-segment climb requirements are critical only up to a wing loading 527 kg/m^2 (108 lb/ft^2). Above that wing loading, the FAR field length requirement establishes the limiting values of wing loading and cruise power ratio.

In figure 47, the data of the previous figure are cross plotted to show the combined limits imposed by airport performance requirements and internal fuel volume limits on the minimization of fuel consumption. The minimum value of block fuel is achieved at the intersection of the FAR field length limit and the internal fuel volume limit lines. Thus, minimum fuel consumption is obtained at a wing loading of 673 kg/m^2 (138 lb/ft^2) and cruise power ratio of 0.72.

5.2.4.3 Baseline Configuration Parameters

The major differences in the parametric results for 200- and 400-passenger LFC configurations are the higher wing loadings and lower cruise power ratios required to minimize fuel consumption in the 400-passenger aircraft. Following is a summary of the selected baseline configuration parameters for LFC-400-S:

Cruise M:	0.80
Cruise altitude:	11,582 m (38,000 ft)
Wing sweep:	0.396 rad (22.7 deg)
Wing loading:	673 kg/m^2 (138 lb/ft^2)
Aspect ratio:	14
Bypass ratio:	6.00
Cruise power ratio:	0.72

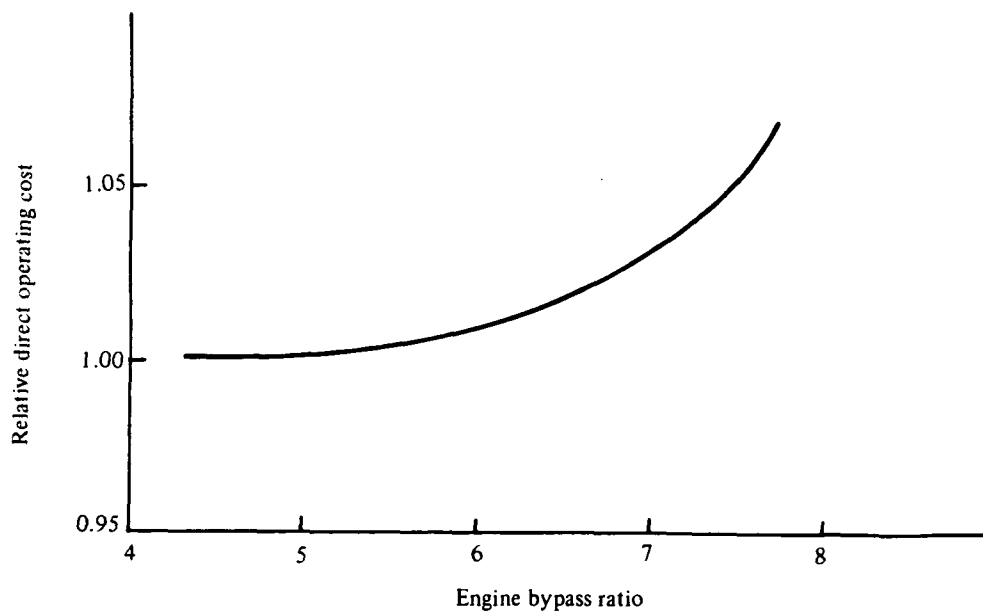
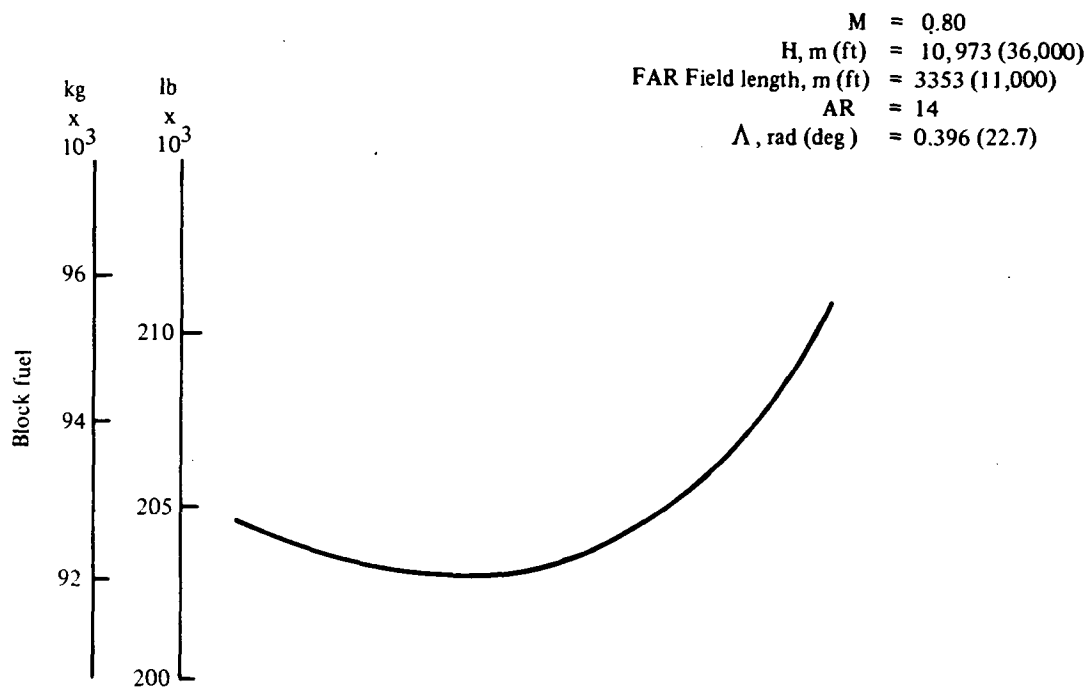


Figure 45. — Engine bypass ratio variations, LFC-400-S

$M = 0.80$
 $H, m (ft) = 11,582 (38,000)$
 $\Lambda, rad (deg) = 0.396 (22.7)$
 $AR = 14$
 $BPR = 6.00$

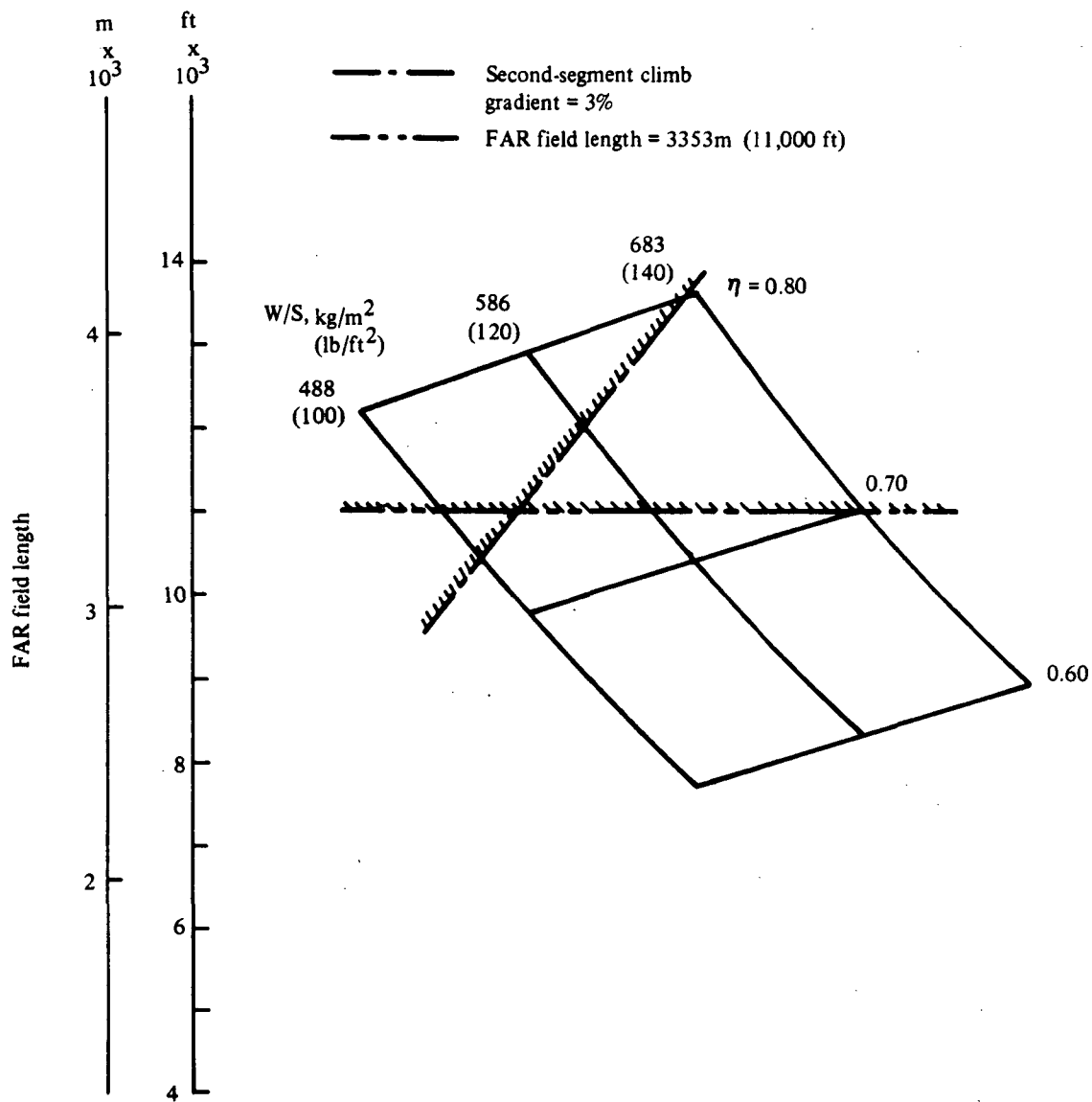


Figure 46. — Airport performance vs. wing loading and cruise power ratio, LFC-400-S

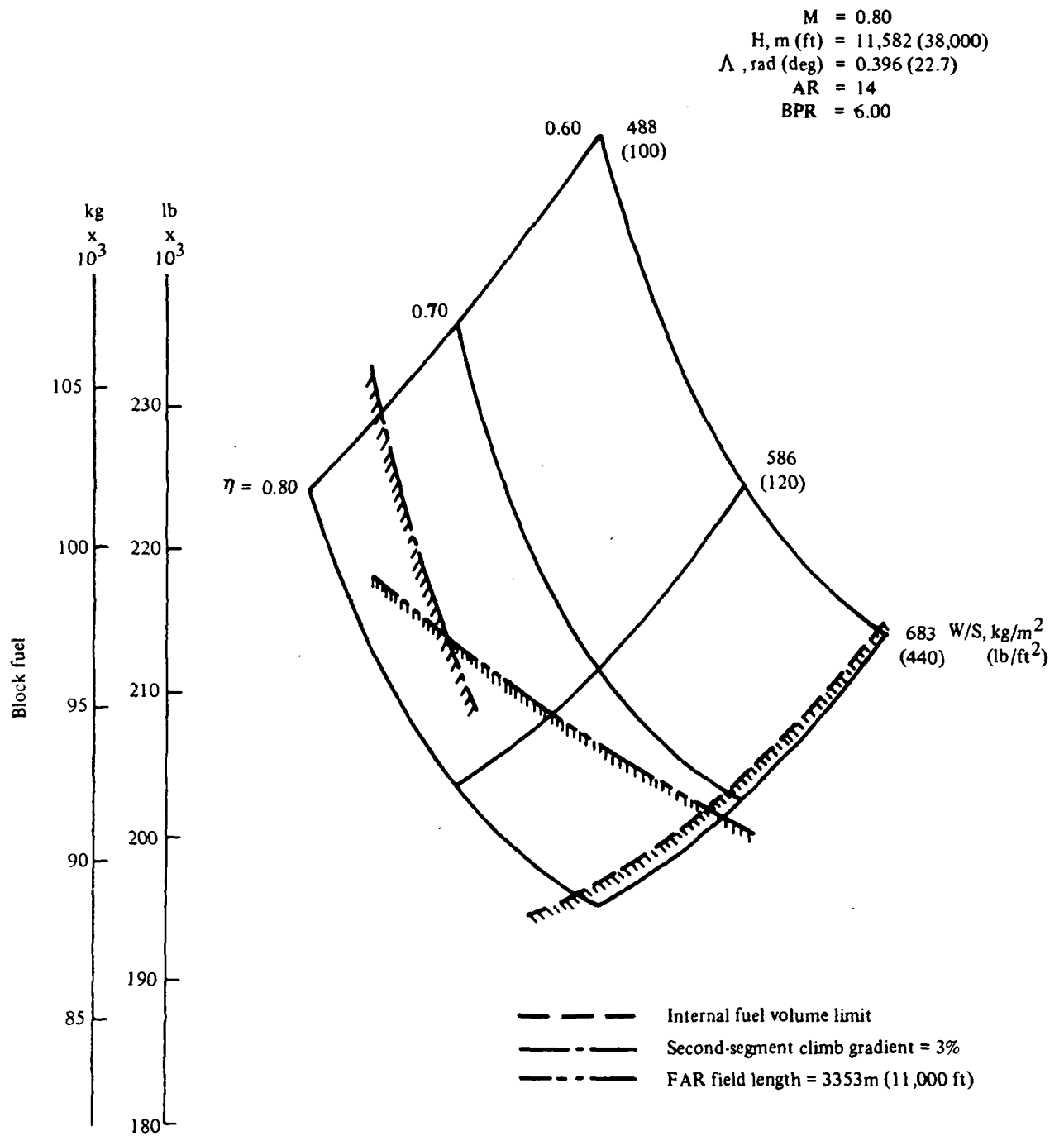


Figure 47. — Block fuel vs. wing loading and cruise power ratio, LFC-400-S

The detailed development of Configuration LFC-400-S is described in section 8.4.

5.2.5 PARAMETRIC DATA: LFC-400-R

The following constants were assumed in the initial parametric studies of LFC-400-R:

Cruise M:	0.80
Cruise altitude, m (ft):	11,582 (38,000)
Bypass ratio:	6.00
Cruise power ratio:	0.70

The selection of a cruise power ratio of 0.70, rather than the value of 0.75 used in the analysis of LFC-400-S, is dictated by the parametric results of the previous section.

5.2.5.1 Wing Geometry

Figures 48 and 49 show the effect of variations in wing loading, aspect ratio, and wing sweep on fuel consumption for LFC-400-R. Minimum values of block fuel and the associated wing loadings are plotted as a function of wing sweep angle in figure 50. Block fuel is minimized by selecting a wing sweep of about 0.396 rad (22.7 deg). The wing loading achievable at this wing sweep is greater than the value of 683 kg/m² (140 lb/ft²) established as a maximum for acceptable airport performance.

5.2.5.2 Engine Parameters

Figures 51 and 52 illustrate the influence of wing loading and cruise power ratio on airport performance and fuel consumption. Since there is no fuel volume constraint at the wing sweep and aspect ratio selected for the LFC-400-R configuration, the minimum fuel consumption achievable is established by the FAR field length limit. As shown by figure 52, minimum block fuel is obtained at a wing loading of 683 kg/m² (140 lb/ft²) and a cruise power ratio of 0.705.

5.2.5.3 Baseline Configuration Parameters

Following is a summary of the selected baseline configuration parameters for LFC-400-R:

$M = 0.80$
 $H, m (ft) = 11,582 (38,000)$
 $BPR = 6.00$
 $\eta = 0.70$
 --- Internal fuel volume limit

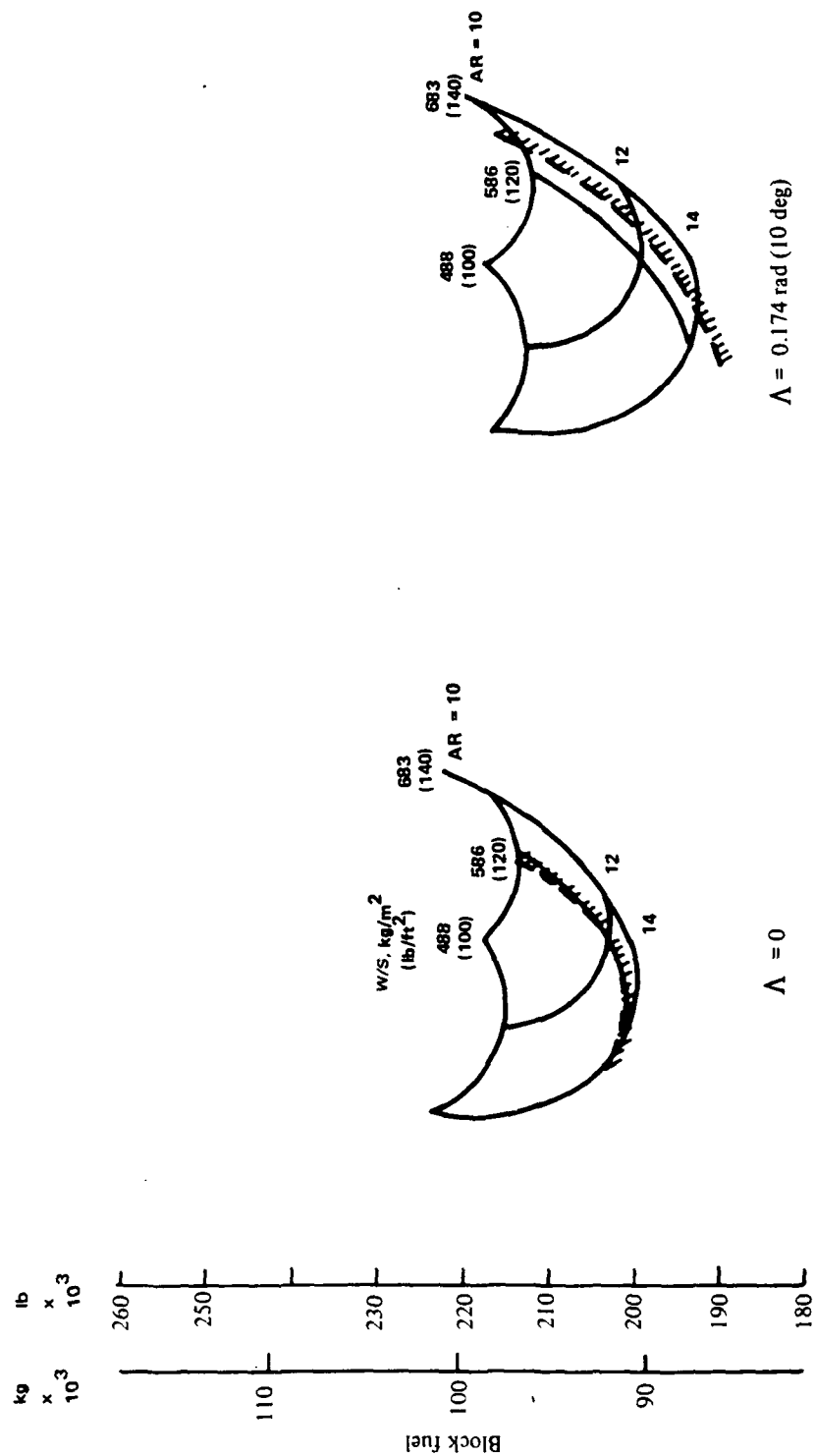
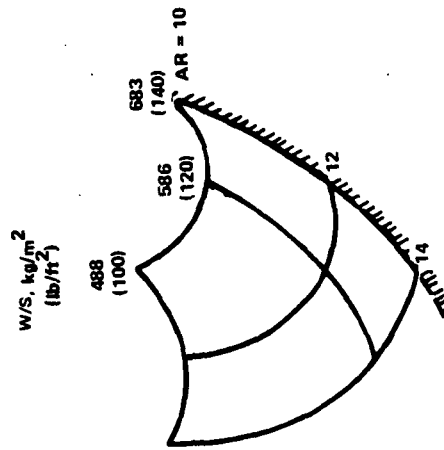
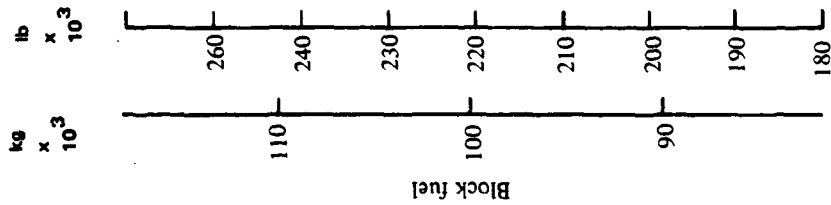


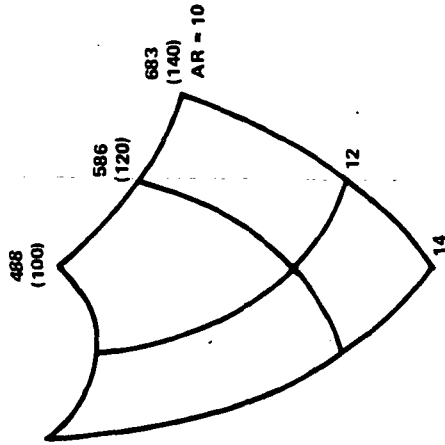
Figure 48. — Block fuel vs. wing loading and aspect ratio, LFC-400-R,
 $\Lambda = 0$ and $\Lambda = 0.174$ rad (10 deg)

$M = 0.80$
 $H, m (ft) = 11,582 (38,000)$
 $BPR = 6.00$
 $\eta = 0.70$

--- Internal fuel volume limit



$\Lambda = 0.349$ rad (20 deg)



$\Lambda = 0.524$ rad (30 deg)

Figure 49. — Block fuel vs. wing loading and aspect ratio, LFC-400-R,
 $\Lambda = 0.349$ rad (20 deg) and $\Lambda = 0.524$ rad (30 deg)

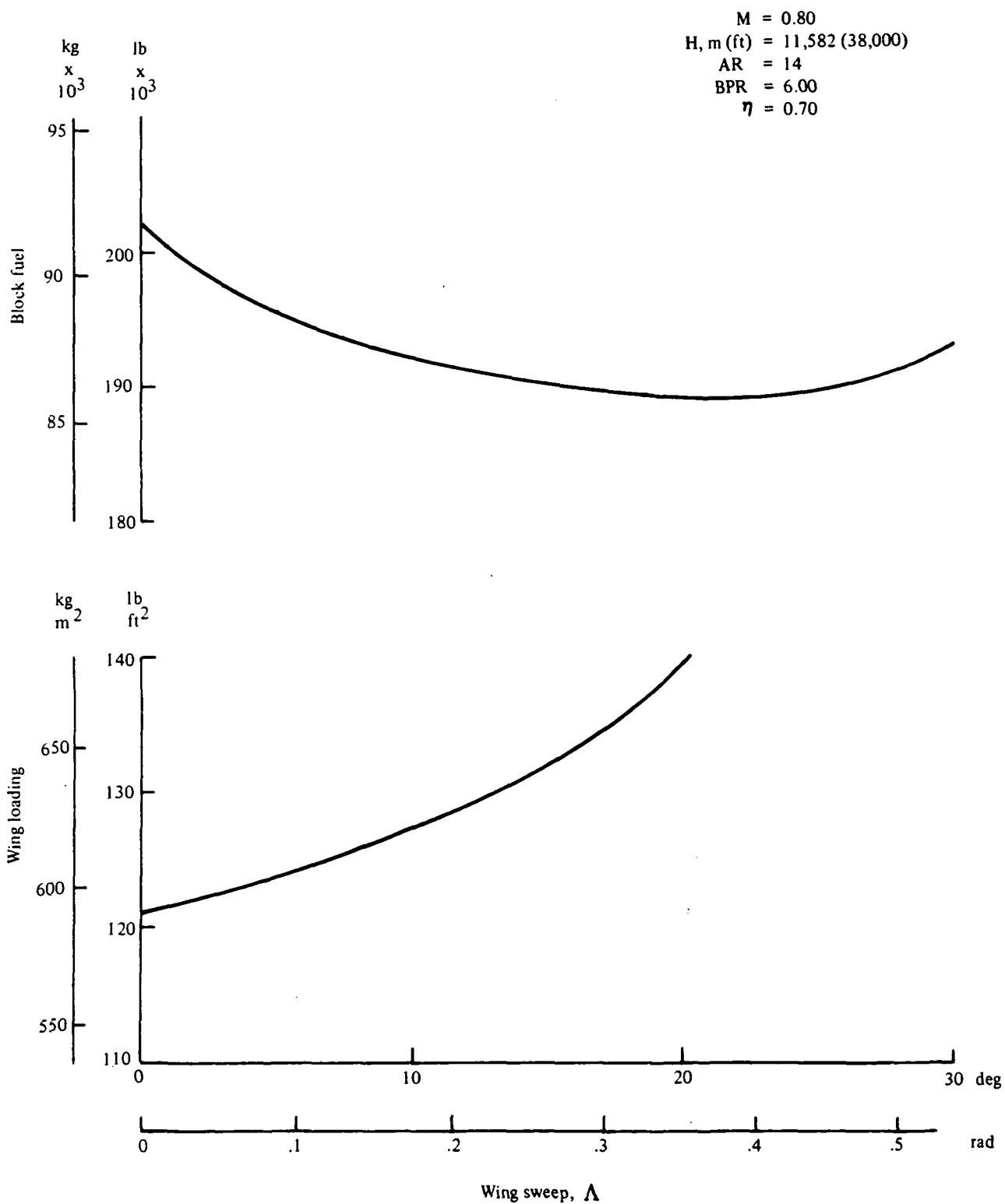


Figure 50. — Block fuel and wing loading vs. wing sweep, LFC-400-R

$M = 0.80$
 $H, m (ft) = 11,582 (38,000)$
 $\Lambda, rad (deg) = 0.396 (22.7)$
 $AR = 14$
 $BPR = 6.00$

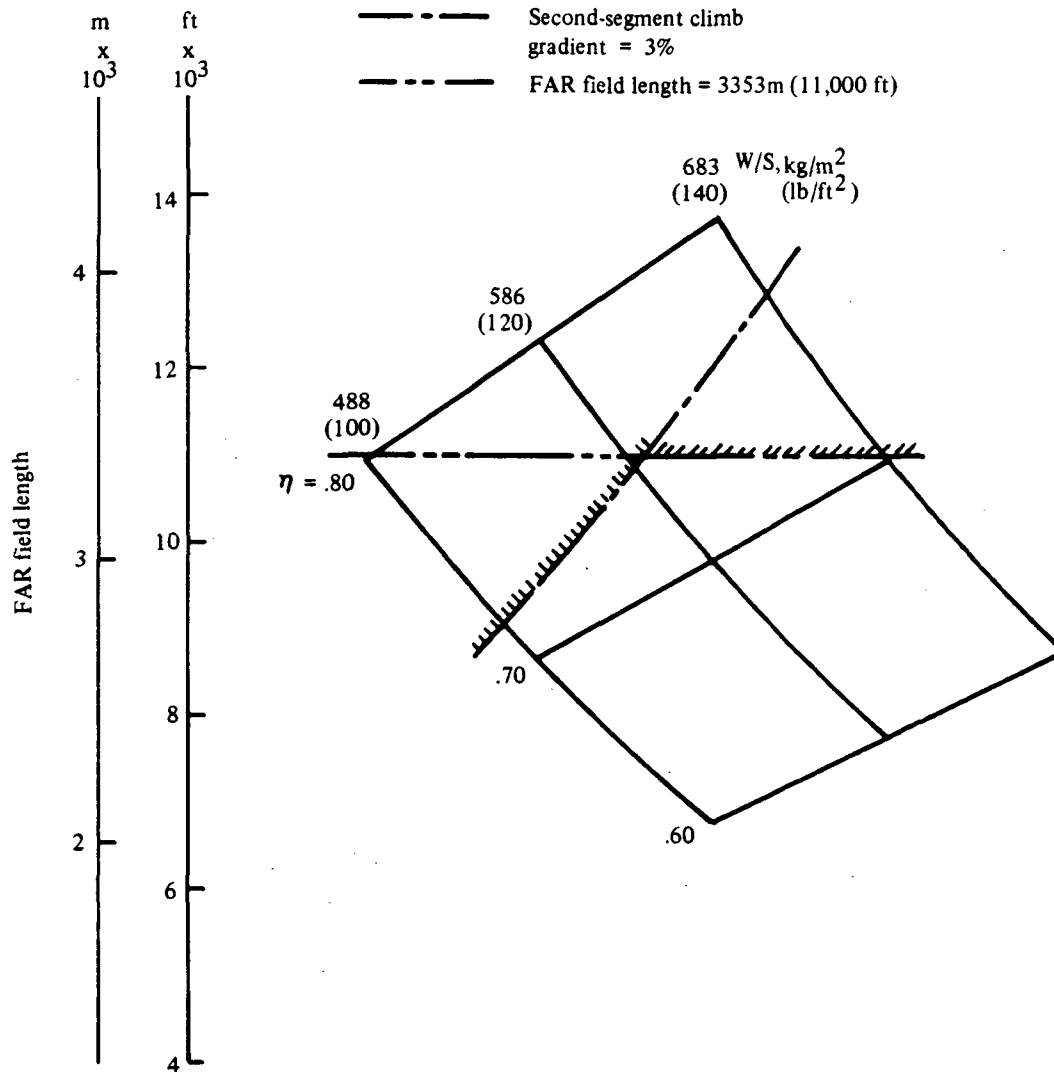


Figure 51. — Airport performance vs. wing loading and cruise power ratio,
 LFC-400-R

$M = 0.80$
 $H, m (ft) = 11,582 (38,000)$
 $\Lambda, rad (deg) = 0.396 (22.7)$
 $AR = 14$
 $BPR = 6.00$

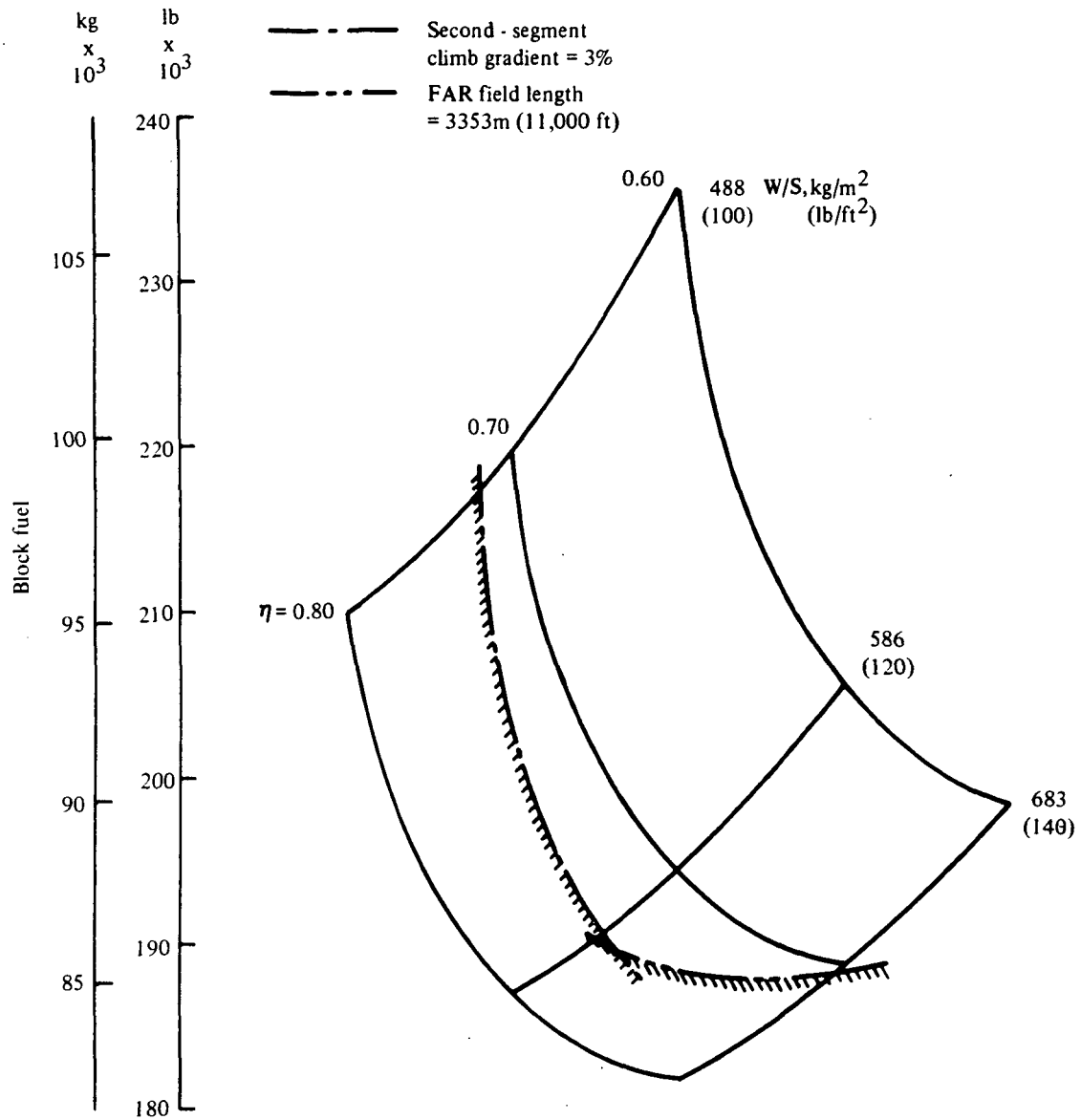


Figure 52. — Block fuel vs. wing loading and cruise power ratio, LFC-400-R

Cruise M:	0.80
Cruise altitude:	11,582 m (38,000 ft)
Wing sweep:	0.396 rad (22.7 deg)
Wing loading:	683 kg/m ² (140 lb/ft ²)
Aspect ratio:	14
Bypass ratio:	6.00
Cruise power ratio:	0.705

The detailed development of Configuration LFC-400-R is described in section 8.5.

5.3 TF CONFIGURATION ANALYSES

5.3.1 PARAMETRIC PROCEDURES

The analysis conducted to permit selection of optimum parameters for the turbulent-flow configurations followed essentially the same sequence used for the LFC investigations of the previous section. As shown by figure 53, the primary difference in the procedure used for selecting baseline parameters was the definition of constants and variables in the configuration matrix. As a result of applicable background data for similar aircraft (ref. 10), it was possible to select near-optimum values of cruise M, cruise altitude, and wing sweep, and thereby consider a smaller number of variables in the TF configuration matrix than was necessary in the LFC configuration matrix.

The fuselage configuration employed for the TF configuration analysis was identical to that of the corresponding LFC configurations. Based on the results of reference 10, a cruise M of 0.80, a cruise altitude of 10,973 m (36,000 ft), and a wing sweep of 0.476 rad (25 deg) were used in all of the analyses.

The variables considered in the TF-200 configuration matrix are listed in table 5.

TABLE 5. CONFIGURATION MATRIX: TF-200

Engine number/location	3/fuselage	4/fuselage	4/wing
W/S, kg/m ² (lb/ft ²)	488 (100)	586 (120)	683 (140)
AR	8	12	14

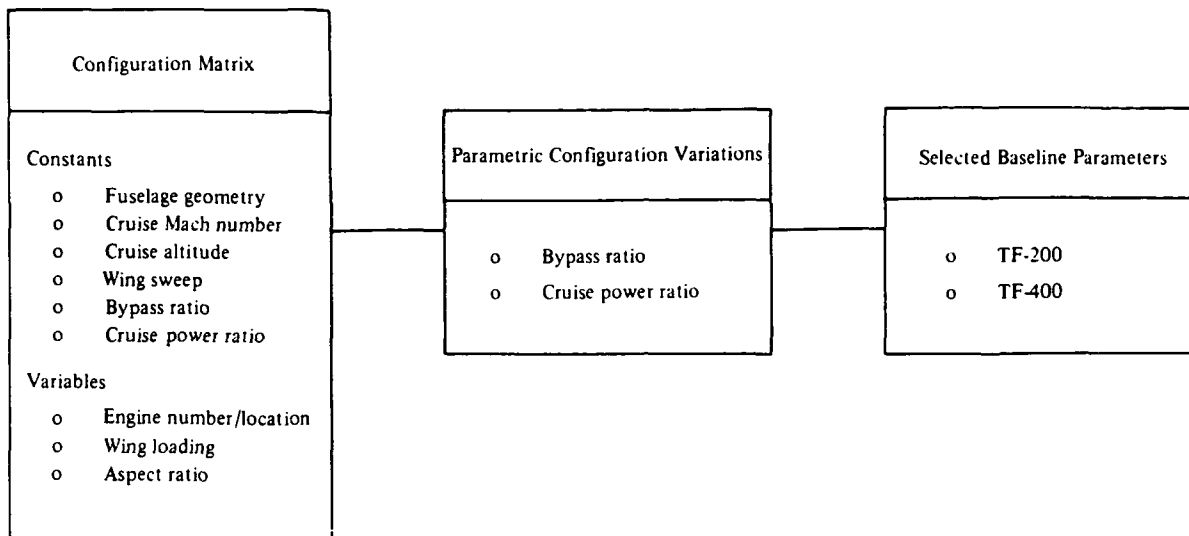


Figure 53. — Baseline selection procedure, TF-200 and TF-400

Consideration of all combinations of the variables in table 5 required the evaluation of 36 aircraft configurations.

It will be observed from table 5 that greater latitude is available in locating main propulsion engines on the TF configurations than was assumed in the LFC analyses. The potential aerodynamic and acoustic interference resulting from employing wing-mounted engines for LFC aircraft is not a consideration on TF transports.

With the exception of the number and location of the primary propulsion engines, which were selected on the basis of TF-200 analyses, the TF-400 configuration matrix was identical to the TF-200 matrix.

5.3.2 PARAMETRIC DATA: TF-200

An engine bypass ratio of 4.5 and a cruise power ratio of 0.90 were used in exercising the initial matrix of TF-200 configurations.

5.3.2.1 Wing Geometry

Fuel consumption for the design mission is shown as a function of wing loading and aspect ratio in figure 54. Data are presented for TF-200 configurations with 3 fuselage-mounted, 4 fuselage-mounted, and 4 wing-mounted main propulsion engine arrangements. The trends illustrated by these data are similar to those of figures 27-30 for the LFC aircraft in that minimization of fuel consumption requires the selection of both a high wing loading and a high aspect ratio. It will be observed, however, that an aspect ratio greater than 14 is required to minimize fuel consumption for the LFC aircraft while the optimum value for TF aircraft is between 12 and 13.

The fuel volume limits shown in figure 54 indicate that somewhat greater wing loading can be realized in the configurations with fuselage-mounted engines, with the result that these configurations demonstrate greater fuel efficiency than the configuration with wing-mounted engines. This is a result of the loss of fuel volume due to the dry-bay areas required in the wing for the wing-mounted engines.

Minimum block fuel values for the 3 and 4 fuselage-mounted engine configurations are approximately the same. Figure 55 indicates that, on the basis of direct operating cost, the 4-engine arrangement is significantly better than the 3-engine arrangement. This figure also shows that an aspect ratio of 10.0 is required to minimize DOC, compared to a value of 12.50 for minimization of fuel consumption.

On the basis of the data presented in figures 54 and 55, a conventional configuration with 4 fuselage-mounted engines, as aspect ratio of 12.50, and a wing loading of 120.5 was selected for further optimization.

5.3.2.2 Engine Parameters

Figure 56 shows the influence of variations in engine bypass ratio on the selected configuration. Considering the minimization of fuel consumption and the compromise required between takeoff performance and DOC, a bypass ratio of 6.0 is near optimum for the design mission.

5.3.2.3 Baseline Configuration Parameters

Optimization of wing loading and cruise power ratio as required to satisfy FAR field length and second-segment climb gradient requirements results in the selection of the following parameters for the baseline TF-200 configuration:

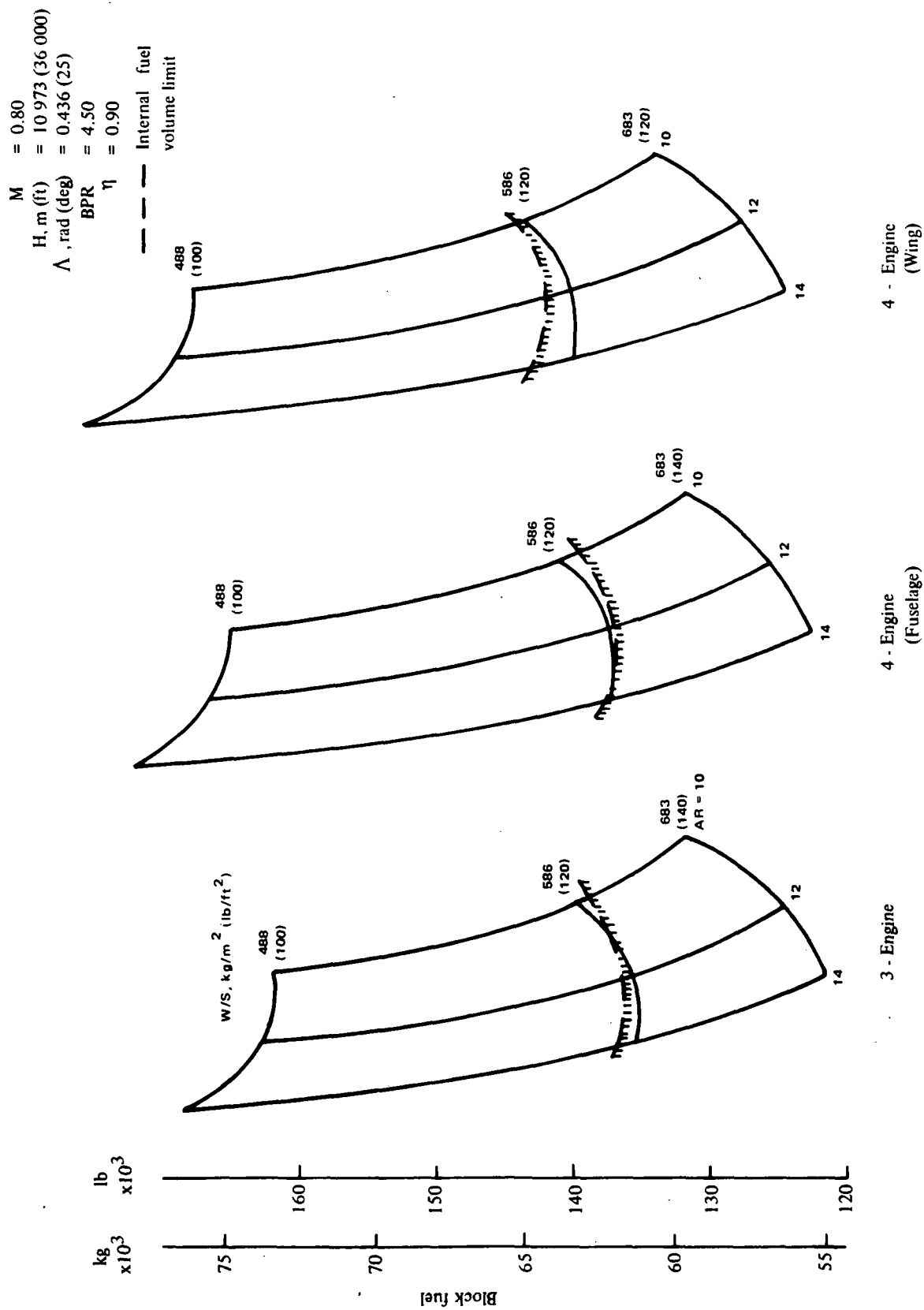


Figure 54. — Block fuel vs. wing loading and aspect ratio, TF-200

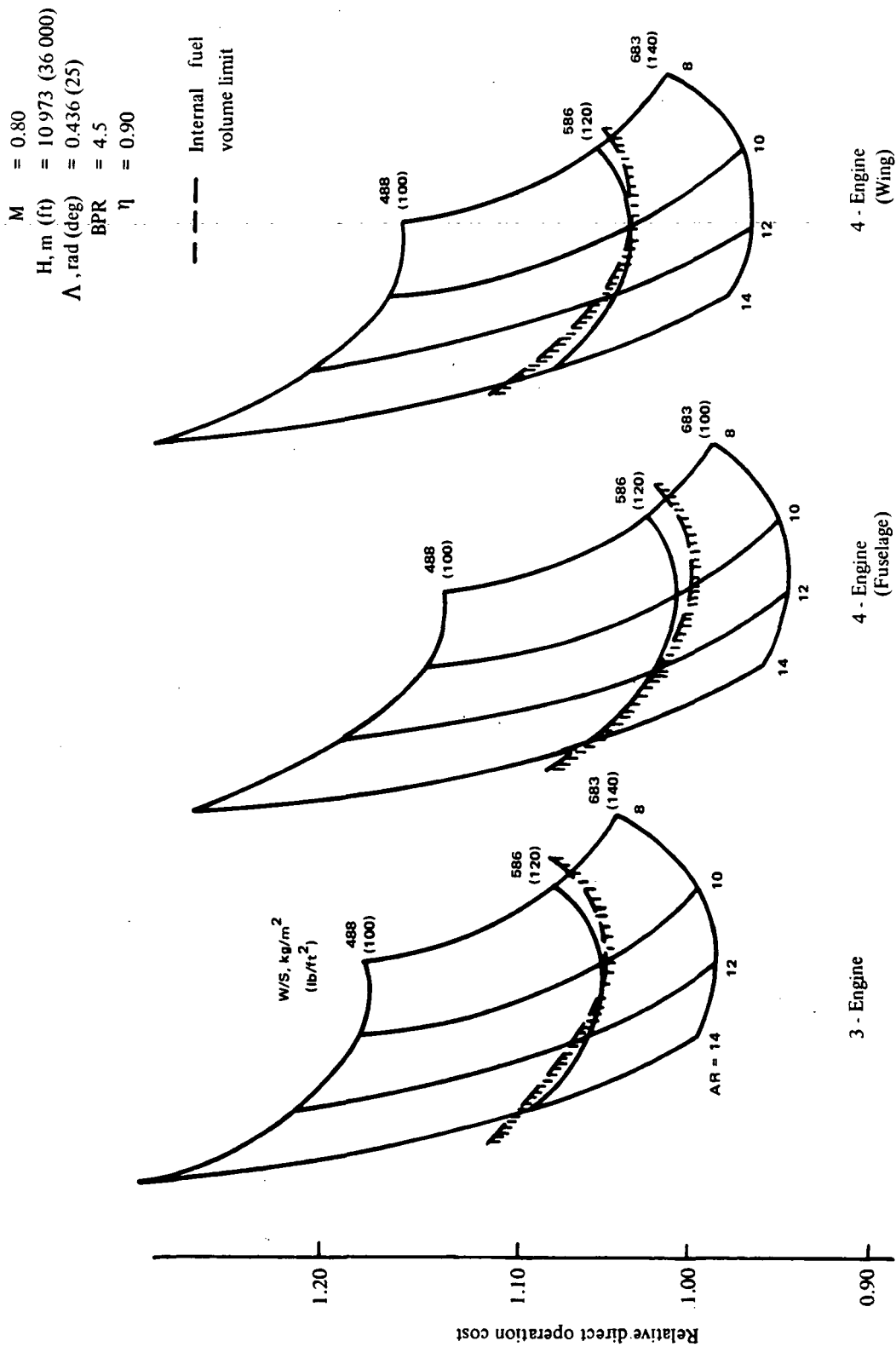


Figure 55. — Relative DOC vs. wing loading and aspect ratio, TF-200

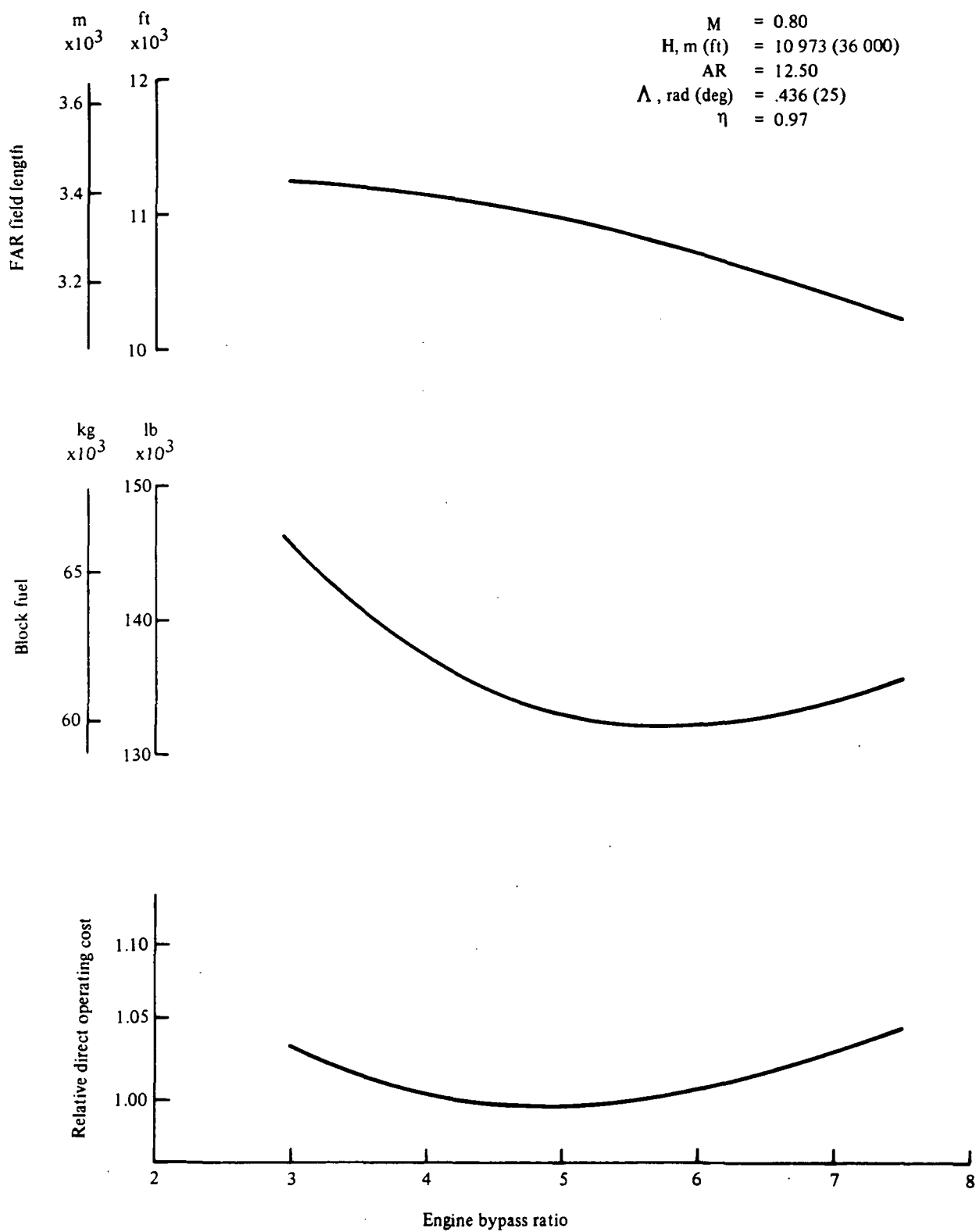


Figure 56. — Engine bypass ratio variations, TF-200

Cruise M:	0.80
Cruise altitude:	10,973 m (36,000 ft)
Wing sweep:	0.436 rad (25.0 deg)
Wing loading:	595 kg/m ² (122.0 lb/ft ²)
Aspect ratio:	12.50
Bypass ratio:	6.0
Cruise power ratio:	0.92

The detailed development of Configuration TF-200 is described in section 10.2.

5.3.3 PARAMETRIC DATA: TF-400

Based on the results of the previous section, the configuration matrix for TF-400 assumed the use of four fuselage-mounted engines and a bypass ratio of 6.0. In anticipation of higher wing loadings and the associated impact on airport performance, a cruise power ratio of 0.80 was used.

5.3.3.1 Wing Geometry

The influence of wing loading and aspect ratio on fuel consumption for Configuration TF-400 is shown in figure 57. These data follow the general trends established by previous parametric investigations in that minimization of block fuel requires selection of the highest wing loading and aspect ratio considered to be feasible. It should be observed that wing volume in the TF-400 configuration satisfies fuel volume requirements for wing loadings greater than the maximum W/S of 683 kg/m² (140 lb/ft²) considered in the investigation. Since no internal fuel volume limit exists for this configuration, limiting values of wing loading and aspect ratio are established by airport performance requirements.

5.3.3.2 Engine Parameters

Figure 58 illustrates the influence of wing loading and cruise power ratio on airport performance for aspect ratios of 10, 12, and 14, including the limits imposed by FAR field length and second-segment climb gradient requirements. At all wing loadings above 586 kg/m² (120 lb/ft²), the FAR field length requirement establishes the limiting values for wing loading and cruise power ratio.

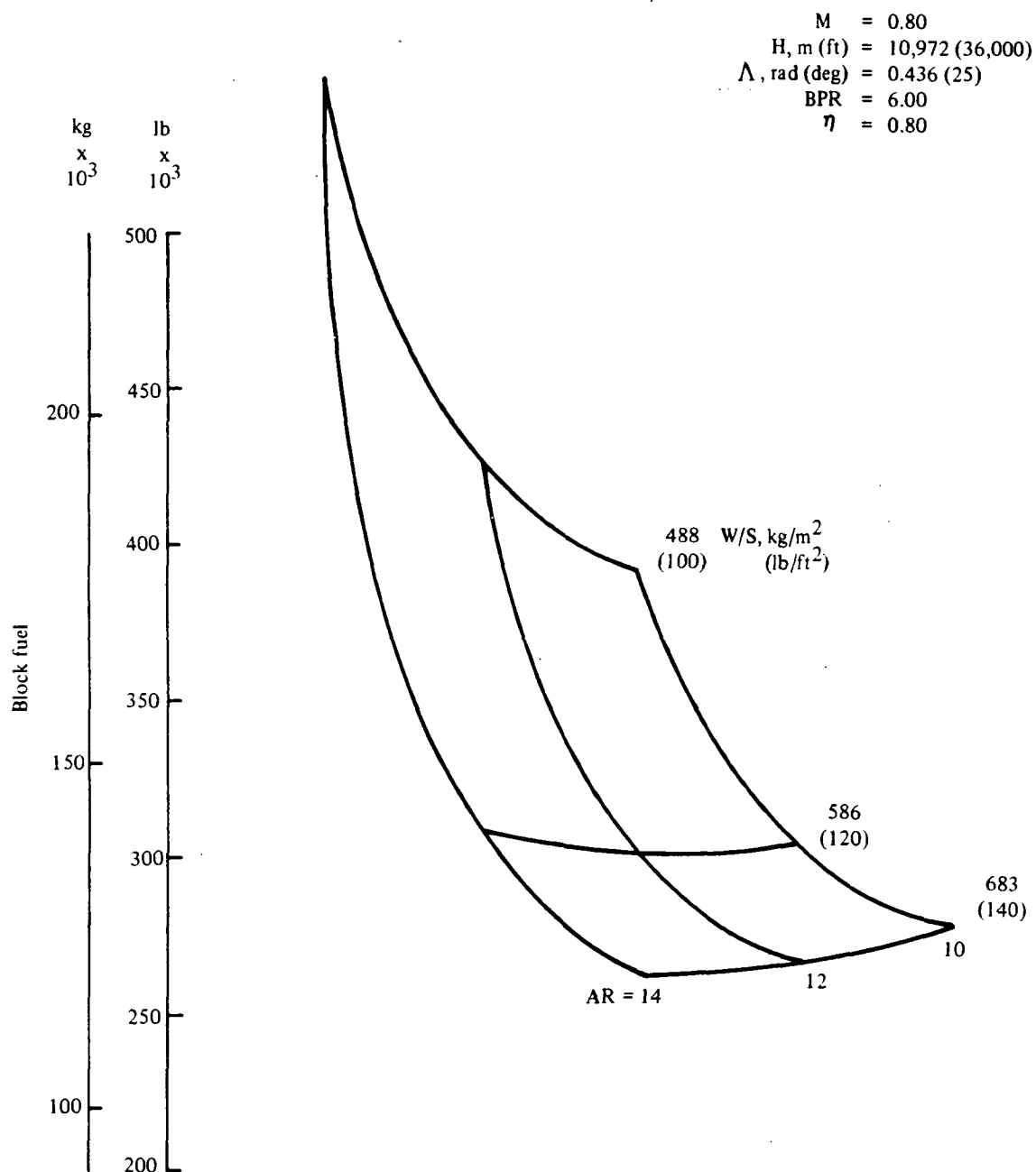


Figure 57. — Block fuel vs. wing loading and aspect ratio, TF-400

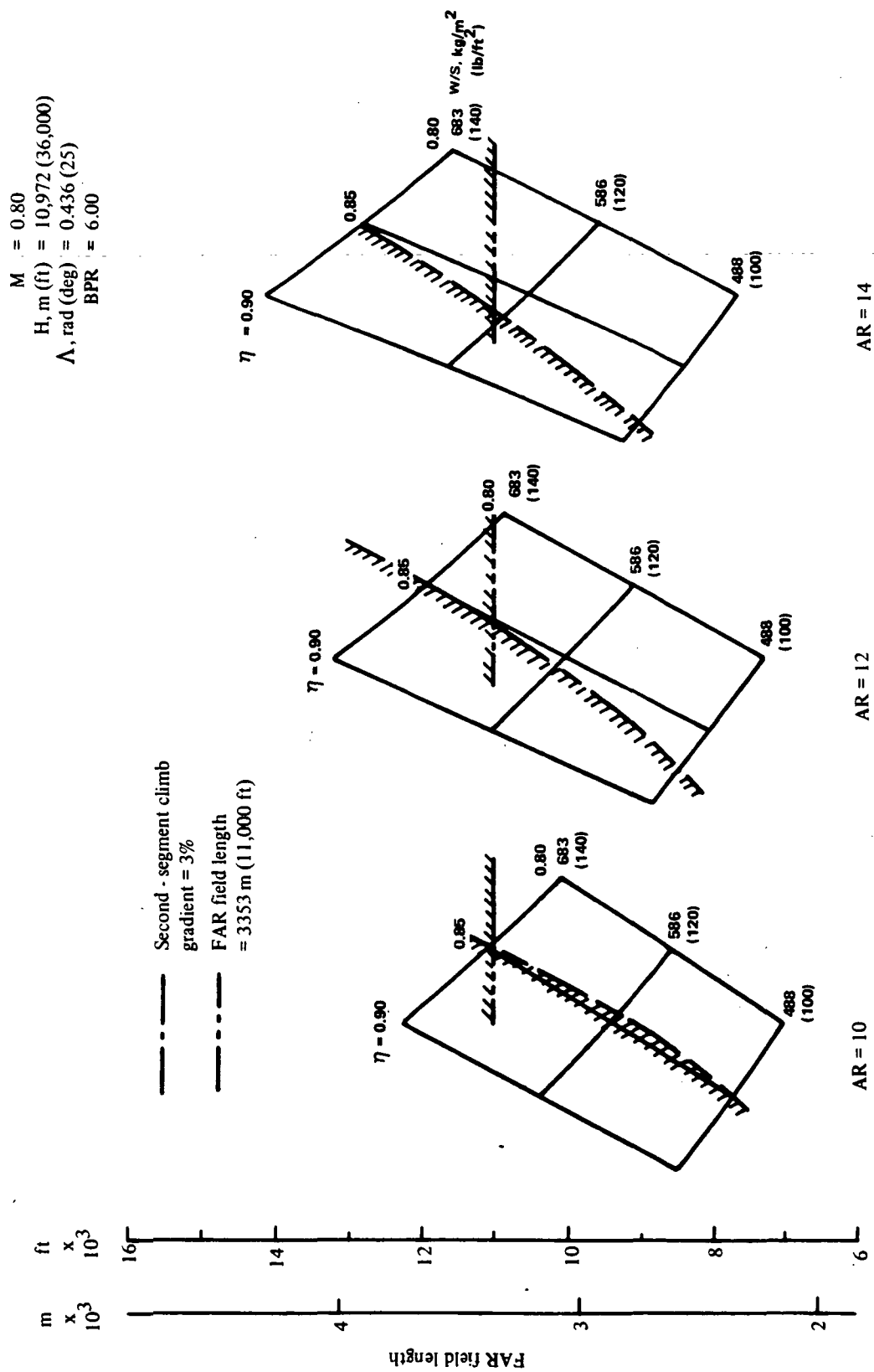


Figure 58. — Airport performance vs. wing loading and cruise power ratio, TF-400

Figure 59 shows the effect of airport performance constraints on fuel consumption. As defined by the FAR field length requirement, the minimum value of block fuel is achieved for an aspect ratio of 12.2 at a wing loading of 683 kg/m^2 (140 lb/ft^2) and a cruise power ratio of 0.81.

5.3.3.3 Baseline Configuration Parameters

Following is a summary of the selected baseline configuration parameters for TF-400:

Cruise M:	0.80
Cruise altitude:	10,973 m (36,000 ft)
Wing sweep:	0.436 rad (25.0 deg)
Wing loading:	683 kg/m^2 (140 lb/ft^2)
Aspect ratio:	12.20
Bypass ratio:	6.00
Cruise power ratio:	0.81

The detailed development of Configuration TF-400 is described in section 10.3

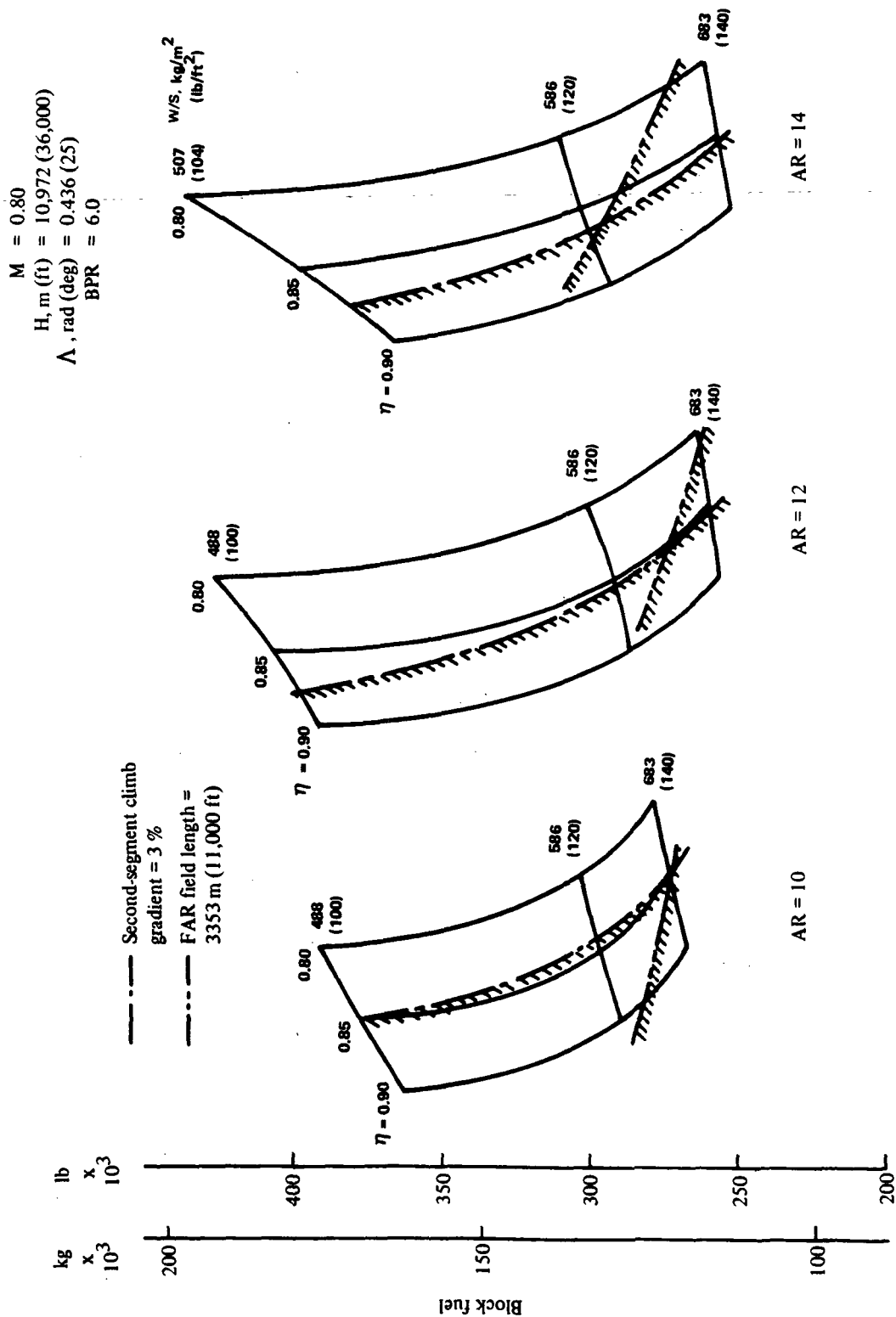


Figure 59. — Block fuel vs. wing loading and cruise power ratio, TF-400

6.0 LFC SYSTEM CONCEPT EVALUATIONS

6.1 INTRODUCTION

Laminar-flow-control aircraft are distinguished from conventional turbulent-flow aircraft by the incorporation of a suitable surface for removing a portion of the boundary layer, ducting to collect the accumulated flow, and suction units to create the pressure differentials requisite to system operation. The benefits obtained through the application of LFC, in the form of reduced drag and fuel consumption, are reduced by the weight and fuel flow of the systems peculiar to the LFC aircraft. The desirability of minimizing LFC system penalties is obvious. Consequently, this section is devoted to an evaluation of alternative concepts for LFC surfaces, ducting and distribution systems, and suction units. Consistent with the technology level assumed for the study aircraft, advanced materials, design concepts, and manufacturing procedures are evaluated to permit the selection of LFC system elements which minimize the weight, cost, and complexity of LFC aircraft.

6.2 SURFACES

6.2.1 CRITERIA

6.2.1.1 Aerodynamic

The aerodynamic requirements for the suction surface are interrelated with those of the internal ducting system configuration in such a manner that neither can be considered independently. General considerations of this interrelation are discussed in section 4.3. The aerodynamic considerations for the suction surface are primarily related to the requirement for smoothly distributed flow induction conforming to a prescribed pattern. The surface must be such that the inflow occurs in relatively small increments to prevent creation of disturbances in the laminar flow over the surface. Once the flow passes through the surface, it enters the internal ducting system at discrete points that tend to produce local variations in the suction pressures immediately under the surface. While the internal ducting is designed to minimize such internal pressure variations, they still exist to a level requiring sufficient pressure drop through the surface.

Slotted Surfaces – Two criteria are established for slotted surfaces in reference 15, relating to the design limitations of the slot. A term is defined for use with sharp-edged slots to provide a limitation to slot design that prevents separation of the boundary flow turning into the slot. Separation of this flow results in unstable and uncontrollable flow through the slot. This term, β is defined as τ / R_w , where τ is $2t_s/w_s$, w_s is the width of the slot, and t_s is the thickness of the material through which the slot is cut and represents the length of the streamwise passage through the slot. R_w is the slot Reynolds number defined by the slot width. If the slot width is too large

relative to the slot passage length, the flow will separate on the upstream sharp edge and will not re-attach. A lower limit criteria for β was established as 0.03. If this cannot be maintained for the given thickness of the surface material, two alternatives exist for meeting the β limit. The leading edge of the slot may be rounded or the slot path may be built up in some manner to attain a greater slot passage length. The latter alternative appears to be more compatible with production and operational requirements.

The second criteria for slotted surfaces requires a minimum ΔC_p level of 0.03 based on free stream q_0 . This results in a minimum pressure drop across the surface in the order of 1% relative to free stream total pressure or 2.5% of the local surface static pressure.

Porous or Perforated Surfaces – Similar surface pressure drop criteria are assumed to be adequate for porous or perforated surfaces used in conjunction with the same internal ducting configuration concepts as employed for the slotted surface. In the assumption of this criteria for porous surfaces it is assumed that the porous suction is applied in spanwise bands similar to the spacing of a slotted surface. This selection is based on a recognition that the means for adjusting the suction inflow to match the laminarization and local surface pressure requirements for a porous surface dictates either an extremely careful tailoring of the surface porosity or an internal ducting system that can provide the requisite tailoring. The manufacturing quality control required to maintain a tailored porosity appears prohibitive. Further, localized contamination of the porous material would tend to perturb the tailoring excessively. Some surface tailoring of the porous surface may be readily accomplished by variations in widths of porous spanwise strips or the spacing of the strips. The strips may be controlled by internally blocking off the porosity of selected segments of the porous surface material. It is probable that, in contrast to the slot configurations wherein maximum permissible slot spacing is desired to reduce manufacturing cost and decrease sensitivity to production tolerances, a maximum number of porous strips would be desirable to provide a more continuous suction inflow and reduce sensitivity to localized contamination.

A perforated surface may be tailored in a manner similar to that of the porous material. Additional tailoring may be accomplished by variation of hole size and spacing. No firm criteria exist for perforated surfaces. However, it is known that if hole size and spacing are too large, disturbances occur in the wake of each perforation that may produce transition to turbulent flow even if sufficient suction inflow is maintained. A reasonable criteria for perforation hole size appears to be on the order of 0.076 mm (.003 in) with spacings sufficient to produce surface pressure losses similar to those of the slotted surface. This results in perforation densities in the order of 0.6 – 2.3 per mm² (400 – 1500 per in²). Application of the criteria defined for slotted configurations appears to be appropriate for perforated surfaces.

6.2.1.2 Surface Smoothness

Smoothness criteria for LFC surfaces established by reference 15 include the following maximum values for steps, gaps, and surface waviness:

- (1) Steps
- | | | mm | in |
|---|--------------------------|------|------|
| o | Forward-facing chordwise | .330 | .013 |
| o | Aft-facing chordwise | .178 | .007 |
| o | Spanwise | .330 | .013 |
- (2) Gaps
- | | | | |
|---|-----------------------|-------|------|
| o | Chordwise or spanwise | 2.692 | .106 |
|---|-----------------------|-------|------|
- (3) Surface waviness
- | | | | |
|---|-----------|--|--|
| o | Chordwise | | |
|---|-----------|--|--|

Wavelength		Double wave amplitude			
		Single		Multiple	
m	ft	mm	in	mm	in
.152	0.5	.254	0.010	.076	0.003
.305	1.0	.356	0.014	.127	0.005
.610	2.0	.483	0.019	.152	0.006
.914	3.0	.584	0.023	.203	0.008

- o Spanwise

Double chordwise values

6.2.1.3 Structural

Subsequent discussions in this section outline the advantages of utilizing non-structural LFC surfaces which are attached to the wing primary structure in a way that allows deflection of the wing without the imposition of loads on the LFC surface. For this application, LFC surface materials are required to have tensile and compressive strengths in the $3.4 \times 10^7 - 6.9 \times 10^7 \text{ N/m}^2$ ($5000 - 10000 \text{ lb/in}^2$) range and in-plane shear strength approximately 15 to 30% of the tensile strength. To achieve an acceptable LFC surface weight, the density of surface materials should be in the range of 692 kg/m^3 (0.025 lb/in^3) to 2768 kg/m^3 (0.10 lb/in^3).

6.2.2 MATERIALS

Candidate LFC surface materials were evaluated for application to both slotted and porous surface configurations. Materials were evaluated relative to the following criteria:

- o Strength
- o Flight environmental resistance
- o Resistance to impact
- o Micro-surface smoothness
- o Weight
- o Cost

Throughout the evaluations, consideration was given to the fabrication, installation, and maintenance requirements peculiar to LFC surfaces.

6.2.2.1 Slotted Surfaces

Materials compatible with the requirements of slotted LFC surfaces include aluminum and titanium. Considering the requirement for cutting numerous slots with widths of 0.076 mm (.003 in) to 0.254 mm (0.10 in), the fabrication characteristics of aluminum are advantageous. The slot edges of an aluminum surface can be chemically or anodically treated for corrosion protection.

Fiber reinforced composite materials are generally not suitable for use in a slotted LFC surface. Exposure of the slot edges to the environment results in material degradation due to the entry of moisture into the laminate. In the specific case of Kevlar fiber trimmed in laminate form, the cut fiber ends result in an unacceptable fuzz along the cut edge that is very difficult to remove.

6.2.2.2 Porous Surfaces

A variety of materials are available within the industry in porous or perforated form. The most common sources of such materials are listed in table 6.

TABLE 6. SOURCES OF POROUS MATERIALS

Acoustic Suppression

- o FRP/Polyimide
- o Perforated Aluminum
- o Screen
- o Sintered Metals

Filtration

- o Thermoplastics
- o Sintered Stainless Steels

Leather-like Materials

However, the relatively low volume air flow requirement of LFC surfaces, ranging from 0.015 to 0.15 m³/sec/m² (0.05 to 0.5 ft³/sec/ft²), requires a porosity appreciably below that of commonly available materials. The uniformity of porosity and the maximum size of each porous opening is critical in obtaining uniform LFC over the wing surface. The available porous materials, used for sound suppression in engine nacelles, generally exhibit openings far in excess of the maximum size acceptable for LFC surfaces.

The existing technology for producing micro-porosity in plastics is currently available in non-reinforced plastics having inadequate strength for this application. However, a combination of a reinforced composite having excessive porosity, laminated to a 3-5 mil thickness of micro-porous plastic film such as Tedlar (Dupont tradename), a polyvinylfluoride film, or Celgard (Celanese tradename), with minute perforations of the required size and spacings, may provide a porous LFC surface having suitable local surface micro-smoothness.

A listing of candidate porous materials for application to LFC surfaces is presented in table 7. Property improvements requisite to utilization of the most promising materials for LFC surfaces are outlined in table 8.

6.2.3 DESIGN CONCEPTS

The technology level on which study aircraft are based limits the use of composite materials to fairings and secondary aircraft structure. Primary structure is primarily aluminum and is designed to currently accepted industry standards. The early operational date of study aircraft precludes the use of bonded composite materials for primary structure such as the wing and tail components.

Since this study is directed toward the application of LFC to a production, commercial passenger transport, the systems to be considered for use must lend themselves to attaining repeatability in mass production and test, and exhibit operational repeatability in day-to-day airline operations with the application of economically acceptable airline-industry methods of maintenance and overhaul.

TABLE 7. CANDIDATE POROUS LFC SURFACE MATERIALS

Material	Porosity	Strength	Flight environment	Impact	Surface smoothness	Weight $\text{kg/m}^3 \times 10^4$	lb/in^3	Cost $\$/\text{m}^2$	Cost $\$/\text{ft}^2$
Hi density polyethylene-porex	Yes	No	Yes	Yes	Yes	0.060	0.022	6.4-21.5	.6-2
Porous acoustic glass fabric PI	No	Yes	Unknown	Yes	No	.193	.07	21.5	2
Sintered stainless steel wire mesh	Yes	Yes	No	Yes	Yes	.415	.15	538	50
Sintered stainless steel powder	Yes	No	Yes	Yes	Yes	.415	.15	645	60
Molded graphite epoxy	No	Yes	Yes	Unknown	No	.138	.05	645	60
Perforated aluminum	No	Yes	Yes	Yes	No	.277	.10	108	10
Woven composite structure	No	Yes	No	Yes	No	23.9-71.8* (kg/m^2)	.5-1.5* (lb/ft^2)	483-1075	45-100

* Entire sandwich panel structure

TABLE 8. REQUIRED PROPERTY IMPROVEMENTS FOR POROUS LFC SURFACE MATERIALS

Porex – Porous Thermoplastic With Reinforcement	Strength, apply porous plastic technology to reinforced plastics
Glass Fabric – Epoxy or PI	Improve porosity, surface smoothness, and long time resistance to flight environment
Advanced Composite	Improve porosity, surface smoothness, and long time resistance to flight environment
Woven Composite Structure	Improve resistance to flight environment and surface smoothness

To satisfy these requirements, LFC systems must be designed, manufactured, installed, and tested in an extensive prototype program so that a production run of airplanes can be expected to meet specification standards with little or no individual tuning. In addition it must be possible to maintain the LFC systems with a minimum of abnormal maintenance procedures while meeting the stringent airline requirements for vehicle dispatch in an intercontinental operational environment.

Based on these considerations and a recognition of the sensitivity of laminar flow to surface smoothness, it was decided to utilize non-structural LFC surface panels. Thus, damaged panels became expendable, at least to the extent that they are line-replaceable, and minimize dispatch delay in normal operations. The replaced panel can be repaired or scrapped depending on the type and extent of damage. Another important feature of bolt-on panels is that they may be removed to gain access to the wing box for fuel system inspection and maintenance. Since these panels cover rather large areas of a surface, normal wing access panel closures can be employed, and the wing areas available for laminarization are independent of the number, size, and shape of openings required in the basic wing.

The LFC surface panels also permit the use of minimum instrumentation to evaluate LFC system operation. Replacement of a single panel may correct system degradation without the extensive instrumentation required for a built-in, total coverage system. The faulty panel can be replaced quickly, and then cleaned, repaired, or scrapped as indicated by inspection.

6.2.3.1 LFC Surface Panel Configurations

Early analyses indicated the importance of minimizing the thickness of LFC surface panels in order to maximize the thickness of the structural wing box. This approach saves weight in both the box structure and in the LFC surface panels. The approach also allows for maximizing the space available in leading and trailing edges for installing necessary ducting plus the normal flap, spoiler, and aileron systems.

A number of LFC surface configurations were studied. All configurations were of non-structural, add-on type construction, fastened to basic wing structure with a mechanical fastener system consisting of net diameter holes in the surface panel and over-size holes in basic structure with floating, sealed, dome-type plate nuts attached to basic structure. This floating panel concept facilitates maintenance and repair and avoids transmitting structural loads to the comparatively fragile LFC panels.

LFC Surface Panel – Configuration 1 – The LFC surface panel shown in figure 60 has a slotted outer skin, a solid inner skin and a drilled, corrugated intermediate skin. The holes drilled in the intermediate skin serve as throttling holes to control suction as required at different wing surface locations. The spanwise throttling ducts formed by the corrugated intermediate skin carry LFC air spanwise to LFC pumps. Intermittent flanged bulkheads oriented chordwise support the slotted outer skin as required. The LFC panel configuration will accommodate either slotted or porous outer skin.

LFC Surface Panel – Configuration 2 – The LFC panel configuration shown in figure 61 considers the use of a corrugated skin on the basic wing box in order to minimize the loss of basic box thickness. Either porous or slotted outer skins are accommodated by this construction. In the event that the outer skin requires additional support between corrugations of the inner skin, a truss-core honeycomb would be used in the voids beneath the outer skin. The inner layer of the LFC panel could be porous material rather than a drilled solid sheet. Boundary layer air is sucked through the outer skin slots or pores, through the throttling holes in the inner skin into the ducts formed by the corrugations in the basic wing skins, thence spanwise to the LFC pumps.

LFC Surface Panel – Configuration 3 – The panel configuration shown in figure 62 attempts to relieve the design and manufacturing complications imposed by the corrugated basic wing skin used in Configuration 2. The spanwise ducts formed by the corrugations in Configuration 2 are replaced by “Z” section spanwise members and another layer of solid skin. Either porous or slotted outer skin and porous or slotted intermediate skin supported as required by truss-core honeycomb can be used.

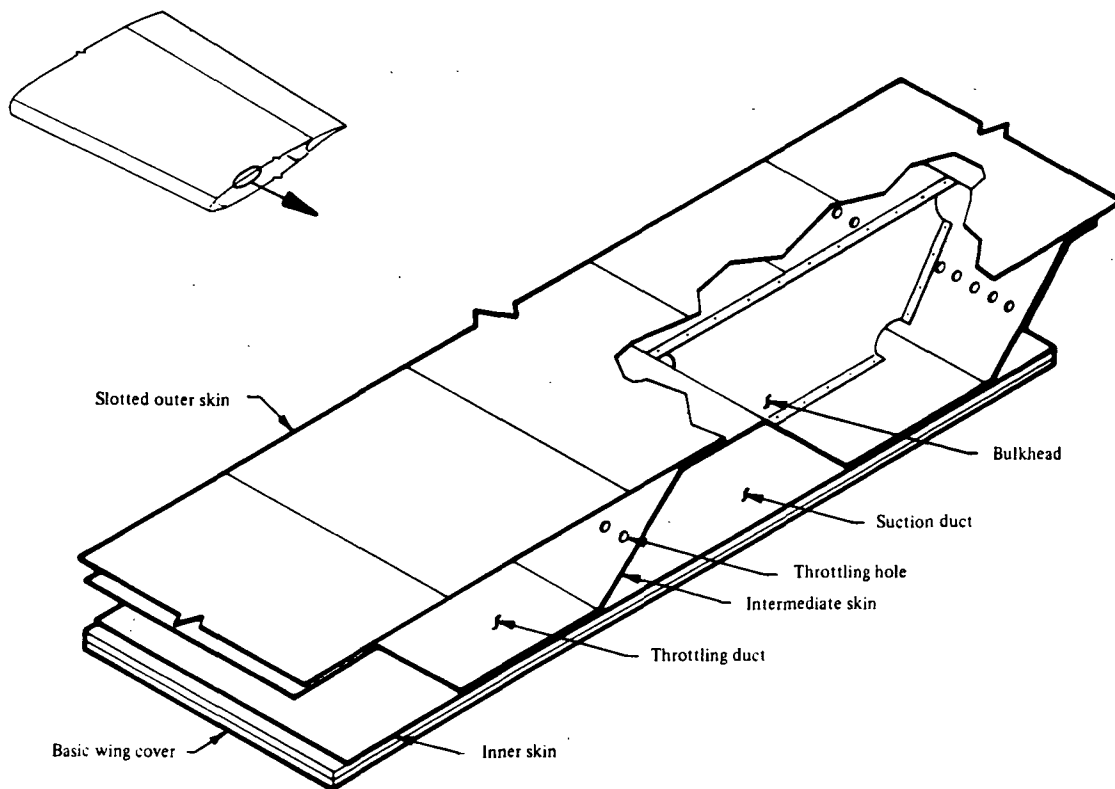


Figure 60. — LFC surface panel, configuration 1

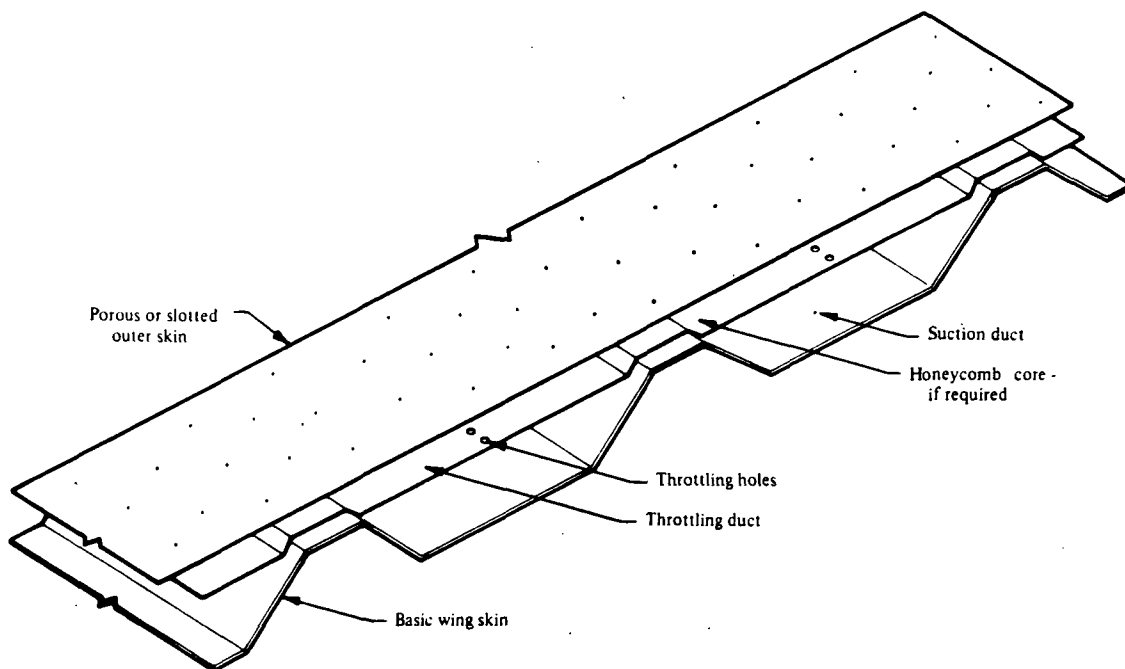


Figure 61. — LFC surface panel, configuration 2

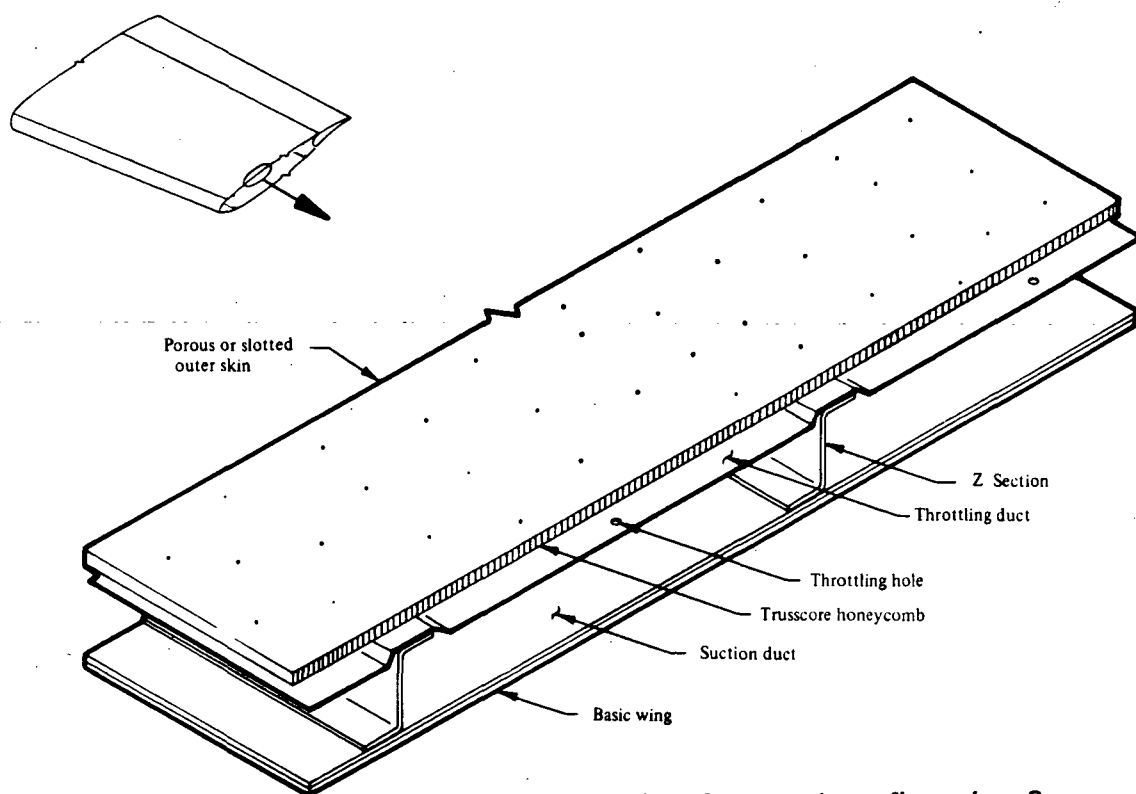


Figure 62. — LFC surface panel, configuration 3

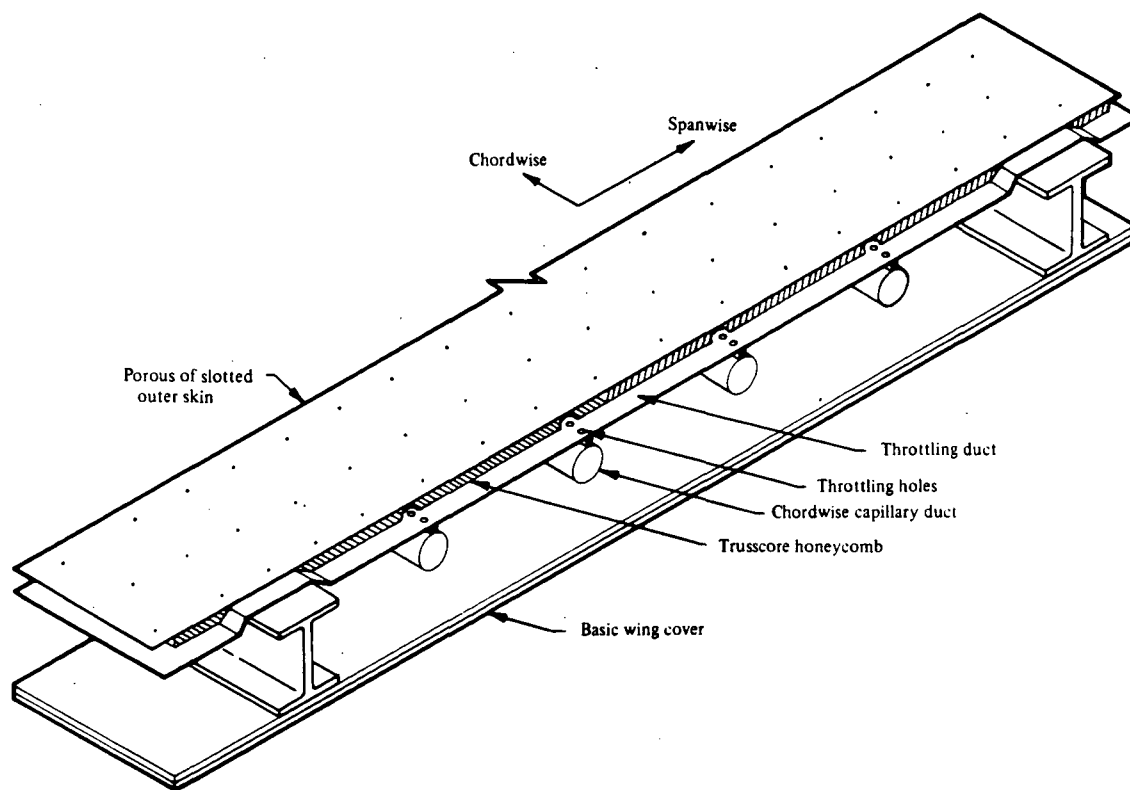


Figure 63. — LFC surface panel, configuration 4

LFC Surface Panel – Configuration 4 – In order to minimize the thickness of the LFC panel and thus maximize the basic wing structure it is beneficial to take the boundary layer air chordwise. This is true since the duct size depends on the area sucked. Therefore, taking the air chordwise allows each duct to carry air from a smaller surface area. Configuration 4, shown in figure 63, pulls boundary layer air from the surface through either slots or pores, through trusscore honeycomb, through throttling holes into closely spaced capillary ducts oriented chordwise, which dump into spanwise trunk ducts located in the wing leading and trailing edges. The chordwise capillaries are supported on the intermediate skin and protrude into a cavity formed by chordwise “I” stiffeners and an inner skin which rests on the basic wing box structural skin.

LFC Surface Panel – Configuration 5 – Another version of chordwise capillary ducting is shown in figure 64. A corrugated inner skin with drilled throttling holes dumps the boundary layer air into chordwise ducts formed by external “I” section spaces fastened to the basic wing structural skin. This configuration will accommodate only slotted outer skins.

LFC Surface Panel – Configuration 6 – Previous panel configuration studies were based on the data of reference 15. When preliminary suction requirements data became available for a finite baseline airplane developed in this study, it was possible to reduce LFC surface panel thickness. Figure 65 depicts a panel using slotted outer skin. This panel concept employs a bonded five-ply panel comprised of three layers of aluminum sheet separated by two plies of honeycomb core. Slots are machined in the upper honeycomb layer to correspond to the slot spacing in the outer skin. The intermediate skin contains drilled throttling holes, spaced in a pattern to match chordwise capillary ducts slotted into the lower layer of honeycomb core. Prior to machining the slots in both layers of honeycomb, a filler material is introduced in the honeycomb in the areas to be slotted so that a smooth-walled duct exists after machining.

LFC Surface Panel – Configuration 7 – The concept shown in figure 66 provides less complication in manufacture than does Configuration 6. A 5-ply slotted panel concept is used in which composite strips are laid in spanwise or chordwise directions as required, replacing the honeycomb layers used in Configuration 6. By careful selection of the aspect ratio of both chordwise and spanwise slots, it is possible to reduce the overall panel thickness, thus increasing basic wing box thickness resulting in a small overall weight saving. This configuration was selected for use in the baseline LFC aircraft described in section 7.2.

A further improvement, identified as Configuration 7A, is envisioned by the simple expedient of substituting polyurethane foam in place of Kevlar for use as the filler strips forming spanwise and chordwise capillary ducts.

LFC Surface Panel – Configuration 8 – This panel, shown in figure 67, comprises three layers of fibrous sheet (Kevlar) panels separated by two layers of corrugated sheet oriented spanwise in the upper layer and chordwise in the lower to form the capillary ducting.

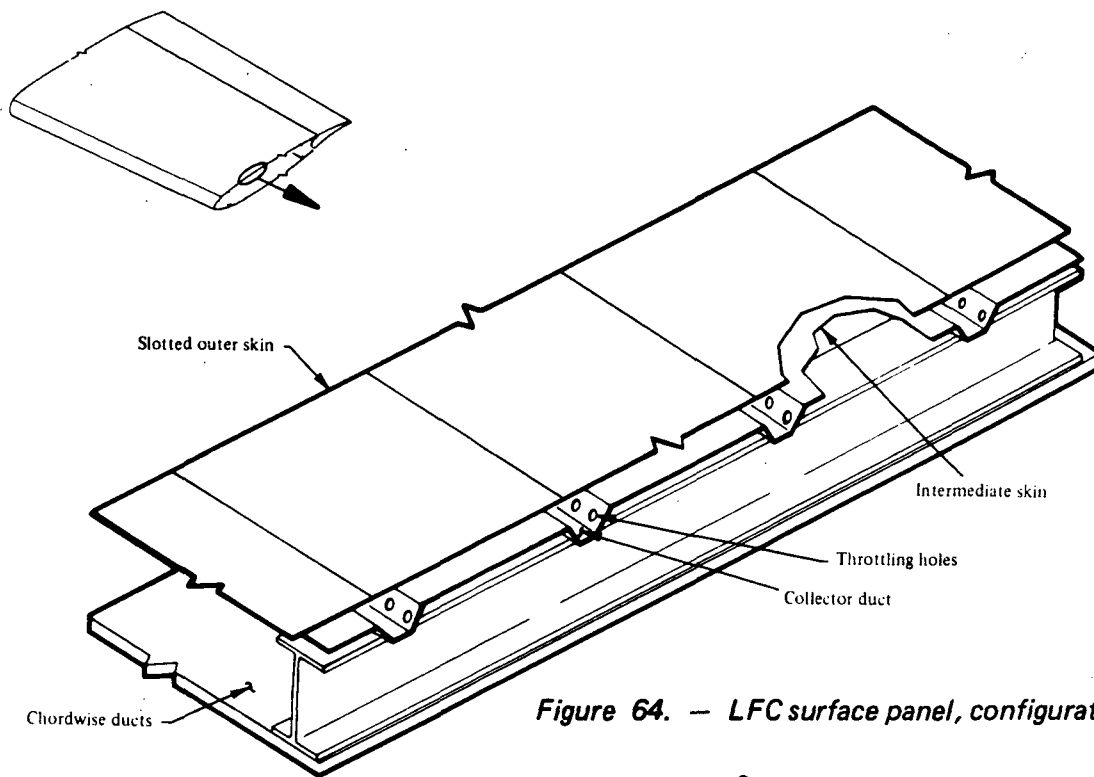


Figure 64. — LFC surface panel, configuration 5

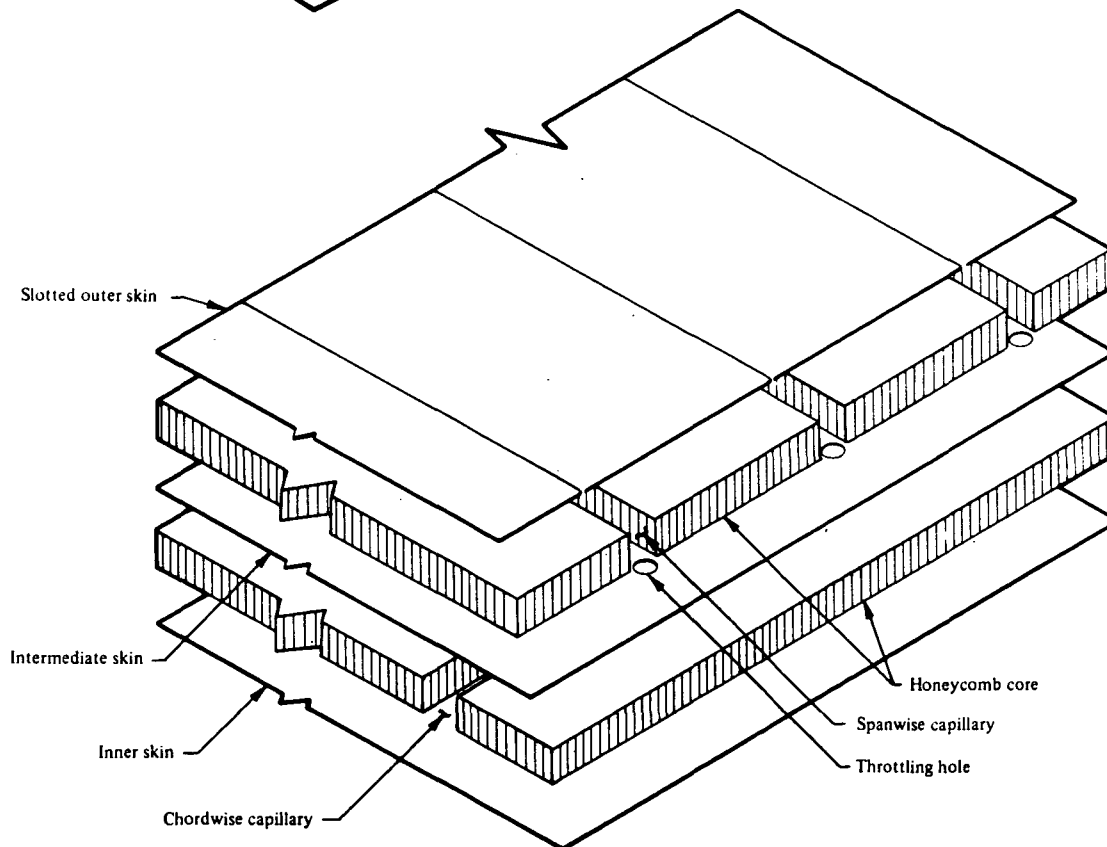


Figure 65. — LFC surface panel, configuration 6

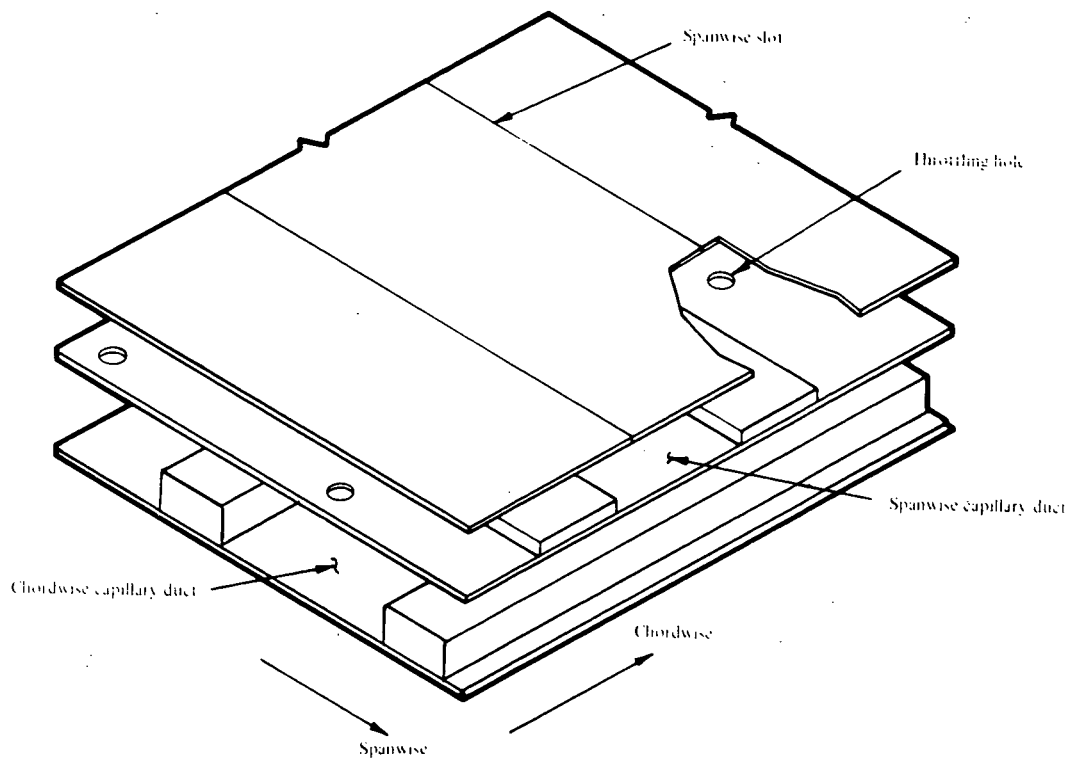


Figure 66. — LFC surface panel, configuration 7

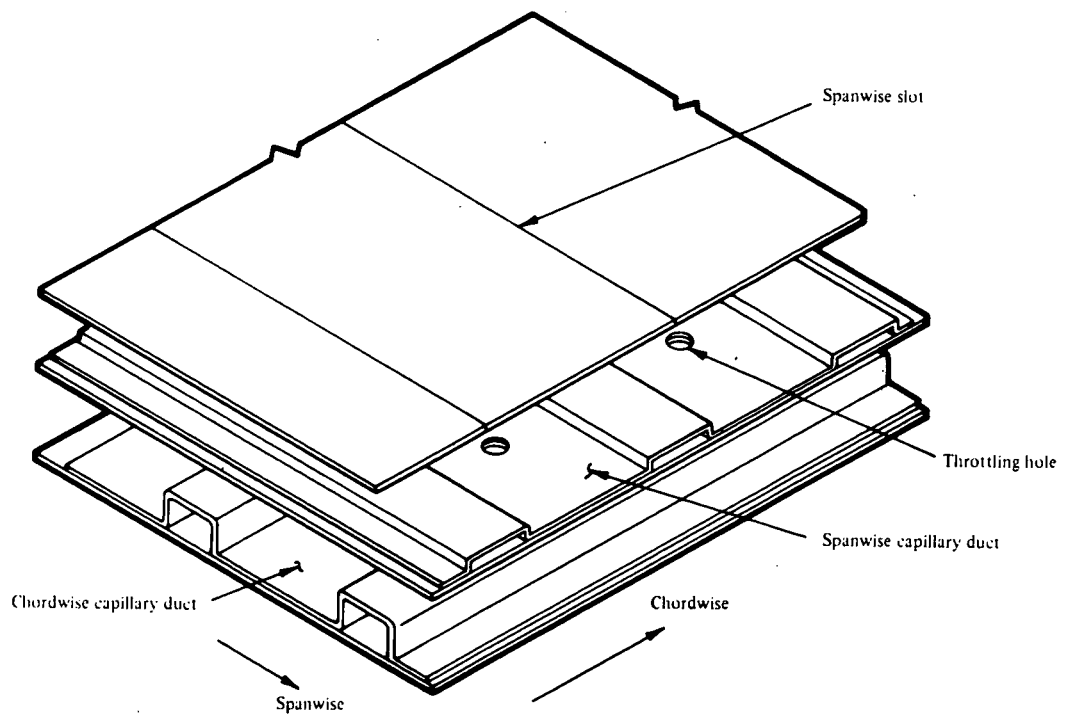


Figure 67. — LFC surface panel, configuration 8

LFC Surface Panel – Configuration 9 – This panel, shown in figure 68, uses two separate continuously woven fiber panels bonded together to form the spanwise and chordwise ducting required for the LFC surface.

LFC Surface Panel – Configuration 10 – The surface panel shown in figure 69, is constructed of a slotted aluminum outer sheet, an intermediate sheet of Kevlar containing drilled throttling holes, and a solid inner sheet of Kevlar. The outer sheet is separated from the intermediate sheet and supported by light-weight Kevlar filler strips oriented spanwise to form ducts to carry the air sucked through the surface to the throttling holes located in the intermediate sheet.

The inner sheet is separated from the intermediate sheet by light-weight Kevlar corrugations oriented chordwise forming capillary ducting to carry air forward or aft as required to the trunk ducts in the wing leading and trailing edges.

6.2.3.2 LFC Surface Panel Selection

Table 9 tabulates the characteristics of the 11 LFC surface panels studied. Panel thickness, weight per unit area, and the relative cost per unit area of each panel are shown. As indicated by table 9, the surface panel designated as Configuration 10 offers both cost and weight advantages, and was therefore selected as the configuration for use on the final LFC aircraft.

TABLE 9. LFC SURFACE PANEL COMPARISON

Configuration	Thickness		Weight		Relative cost	Remarks
	cm	in	kg/m ²	lb/ft ²		
1	4.45	1.75	10.84	2.22	.70	Seal problems
2	2.95	1.16	5.47	1.12	Not compared	Complicates basic wing design
3	4.45	1.75	11.77	2.41	1.2	Too heavy
4	4.45	1.75	6.30	1.29	1.5	Complicates manufacture
5	4.45	1.75	7.81	1.60	0.6	Complicates manufacture
6	2.18	0.86	5.47	1.12	1.15	Complicates manufacture
7	1.12	0.44	6.30	1.29	1.0	Selected as baseline at mid-term
7A	1.12	0.44	2.34	0.48	0.95	Polyurethane foam - unsound in vibration environment
8	1.17	0.46	4.93	1.01	1.4	Too expensive
9	1.12	0.44	4.49	0.92	1.02	Manufacturing technology not in hand
10	1.12	0.44	3.91	0.80	1.05	Selected for final aircraft

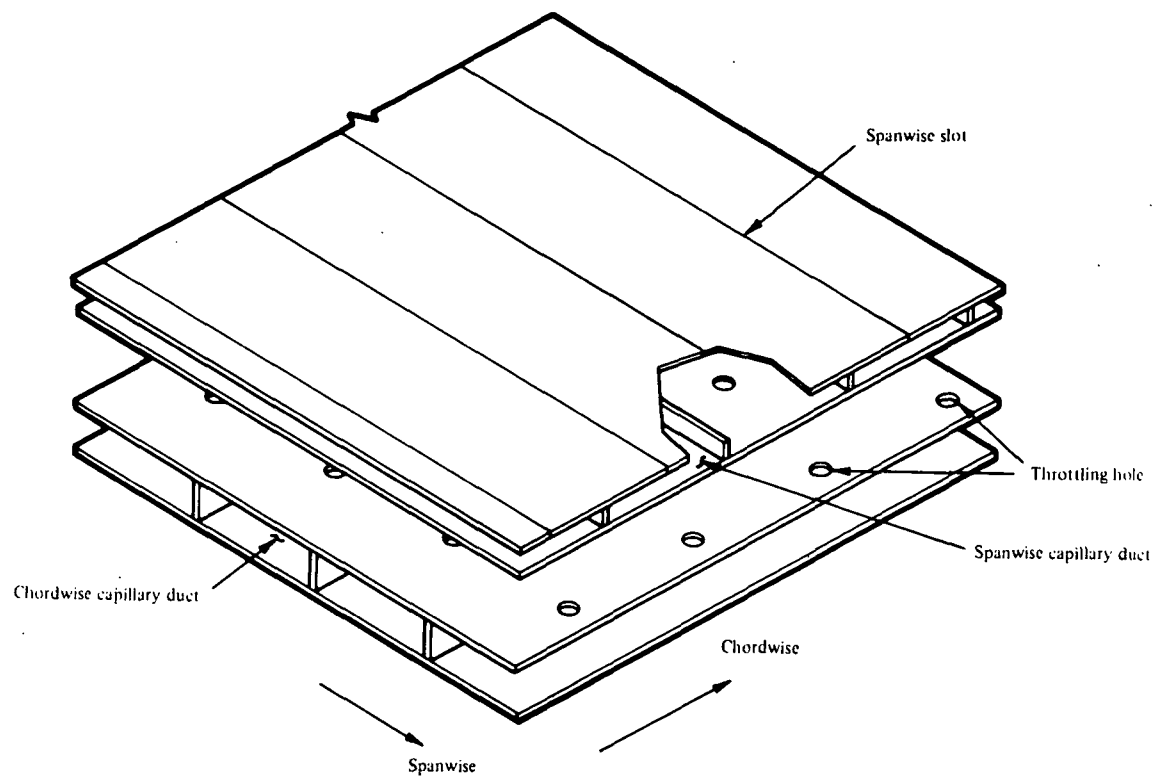


Figure 68. — LFC surface panel, configuration 9

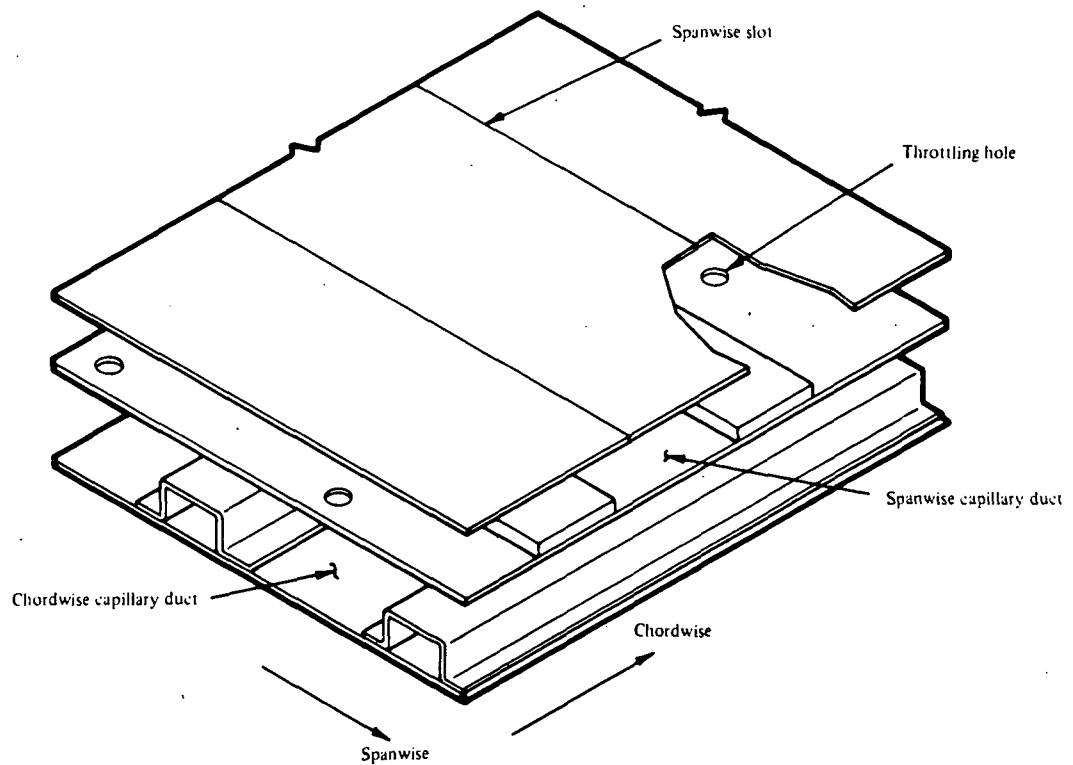


Figure 69. — LFC surface panel, configuration 10

6.2.4 MANUFACTURING CONCEPTS

Applicable manufacturing techniques were identified and evaluated for creating suction slots or perforations in LFC surfaces. As discussed in section 6.2.2, slots are only compatible with metal faces. The edges of the slots in metal faces can be chemically treated for corrosion resistance. Slots in reinforced plastics leave fiber ends exposed to the environment, which results in the entry of moisture into the plastic laminate with subsequent environmental degradation. For creating slots, three manufacturing techniques were considered:

- (1) *Saw* – It was found in reference 26 that a jewelers saw may be used to cut slots as narrow as 0.051 mm (.002 in). The saw slot width tolerance is .013 mm (.0005 in). Therefore, the minimum practical size is 0.076 mm (.003 in). With a potential of sawing slots up to 0.38 m/min (15 in/min), industry experience has only achieved rates on the order of 0.18 m/min (7 in/min).
- (2) *Electron Beam* – The electron beam can cut clean slots, but the minimum width that can be controlled to reasonable accuracy is on the order of .127 mm (0.005 in). The electron beam is slower than the laser by a factor of two.
- (3) *Laser* – The laser can cut slots as narrow as 0.051 mm (.002 in) at rates of 7.62 m/min (300 in/min) and can be fully automated. This appears to be the most promising method for the fabrication of slotted LFC surfaces.

The following summarizes the results of investigations conducted to evaluate manufacturing concepts for perforated and porous LFC surfaces:

- (1) *Laser and Electron Beam* – These methods for perforating composite facings burn the plastic matrix around the holes and are therefore unsatisfactory for this application.
- (2) *Drill* – The method, which is easily automated, provides exact placement of perforations. However, the practical minimum hole size is much larger than the 0.254 mm (.010 in) diameter maximum considered usable for LFC. Drill life due to the plastic resin abrasiveness is very low. While drilling rates of 90 holes/min are possible in aluminum, rates on the order of 32 holes/min are more common in practice. Drilling holes in cured composites leaves fibers exposed to the environment that are impractical to seal.
- (3) *Inherent Porosity* – Micro porosity created during the processing of the reinforced plastic composite facings appears to be the best method for fabricating porous LFC surfaces. Current technology abounds in processes for non-reinforced porous plastics. Many processes also exist for leather-like materials having fibrous reinforced porous construction. Efforts underway in current programs are resulting in

reinforced composites that are suitable for LFC surfaces. The major remaining task is a determination of the porosity required to produce the mass air flow and pressure drop required for reliable laminar flow. Manufacturing composite surfaces with inherent porosity, either by controlled resin content or foaming, or by inclusion of fugitive materials, produces a porous composite with the fibers coated with resin and sealed from the environment.

6.3 DUCTING AND DISTRIBUTION SYSTEMS

6.3.1 CRITERIA

The primary function of the suction surface and internal ducting system is to remove the low-energy boundary-layer air from the airfoil surfaces as required to maintain laminar flow over the surface. Accomplishment of this function is dependent on removal of this boundary layer air in a selective manner such that the boundary layer is prevented from building up at any point on the surface sufficient to cause the occurrence of transition to turbulence. It is apparent, therefore, that the suction inflow of air is not uniform over the surface. It is also apparent that the variation in local pressure over the airfoil surface necessitates various levels of suction pressure differentials in order to achieve the requisite level of air inflow.

While it is necessary to maintain the required minimum level of inflow, excessive inflow of air has a deleterious effect on airplane performance. Excessive inflow of the boundary layer air has a tendency to make the flow over the surface more sensitive to minute surface irregularities or suction inflow disturbances such as might occur behind discrete perforations and slots. This sensitivity can cause transition to turbulent flow even though sufficient suction levels are maintained. There appears to be some evidence that excessive inflow through a slot can cause transition because of the effective aerodynamic negative step behind the inflowing air. Secondly, the induction of excessive boundary layer air implies that some of the higher energy level air in the outer layers of the boundary layer is ingested. Induction of this air results in a ram drag on the airplane which must be counteracted by the suction pumps in re-accelerating this air to free stream velocity or higher. The result is a direct loss in overall airplane performance. Thirdly, the induction of excessive air into the internal ducting system results in higher duct velocities and higher pressure losses in the internal ducting system. This loss must be made up by larger pumps operating through a greater pressure ratio, which is reflected in the airplane as suction unit weight and fuel flow increases. These constraints dictate that the suction surface and internal ducting be the subject of a very careful design analysis in order to match the local suction requirements over the laminarized surface.

The internal ducting of the system must be sized and configured to provide a low level of pressure loss while matching the suction flow requirements for all points on the laminarized surface. Large ducting obviously satisfies this requirement but wing structure and fuel tanks in the wing impose

restrictions on the volume available for ducting. From the examination of a number of possibilities discussed in section 6.3.3, it was concluded that the internal ducting system adopted for the study airplanes provided the greatest relief to these conflicting requirements. In this system, surface covers are employed that include the suction surface with sub-surface spanwise ducts to preclude any abrupt spanwise changes in the suction inflow at a wing chord location. Below these spanwise ducts are chordwise collector ducts that collect the flow from the spanwise ducts and pass the suction air forward on the upper surfaces or aft on the lower surfaces to trunk ducts located forward and aft of the wing box structure. The transition of the airflow from the spanwise sub-surface ducts to the collector ducts is controlled through metering orifices that are sized to achieve the required chordwise suction flow distribution while matching the local external surface pressures. These metering orifices are also influenced by the local internal pressures within the collector duct.

The potential for loss of laminarization due to acoustic feedback through the aerodynamic flowpath of the suction surface is recognized but no criteria are known to exist. Sources of such noise are the compressor noise of the suction pumps and the noise generated by the air flowing through the internal ducting. No significant problem is anticipated from the suction pump compressor due to the attenuation of the myriad of small ducts and orifices of the internal ducting system. However, if a problem from this source should be encountered, it can be overcome with minor penalty by applying acoustic linings to the ducting in the immediate vicinity of the suction unit inlets.

The noise generated by the flow within the ducting is not considered to present a problem so long as the internal duct Mach number is maintained at a low value. Relatively low duct Mach numbers are also dictated by the requirement to maintain low duct pressure losses. A cursory evaluation of the effect of duct size on the suction unit is shown in figure 70 which shows the variation of suction unit weight and fuel flow with variations in duct area. The curve indicates that 15% duct loss is a reasonable compromise, since the penalties for a decrease in duct area rise rapidly, while increasing the duct area to reduce duct losses results in only modest gains. The 15% duct loss level results in peak collector duct Mach numbers on the order of 0.2 to 0.3 at the wing root while the trunk duct Mach number may reach as high as 0.5, depending on the configuration. No criteria have been established for limiting duct Mach number from the standpoint of noise generation, but 0.2 Mach appears to be a desirable target with an upper limit of 0.3. Thus, either pressure losses or duct Mach number may be a determining factor in duct sizing, but for the reasons cited previously, it is desirable to maintain the duct sizes as low as practical. The final selection of the ducting system is configuration oriented and is discussed in section 8.0.

6.3.2 MATERIALS

Materials evaluated for ducting included aluminum, thermoplastics (polycarbonates), fiberglass reinforced plastic, graphite reinforced plastics, and Kevlar-49 reinforced plastics. Aluminum, having a density of approximately $0.277 \times 10^4 \text{ kg/m}^3$ (0.10 lb/in^3) and thermoplastics, having a sensitivity to chlorinated solvents commonly used as a safety cleaning solvent, were eliminated from

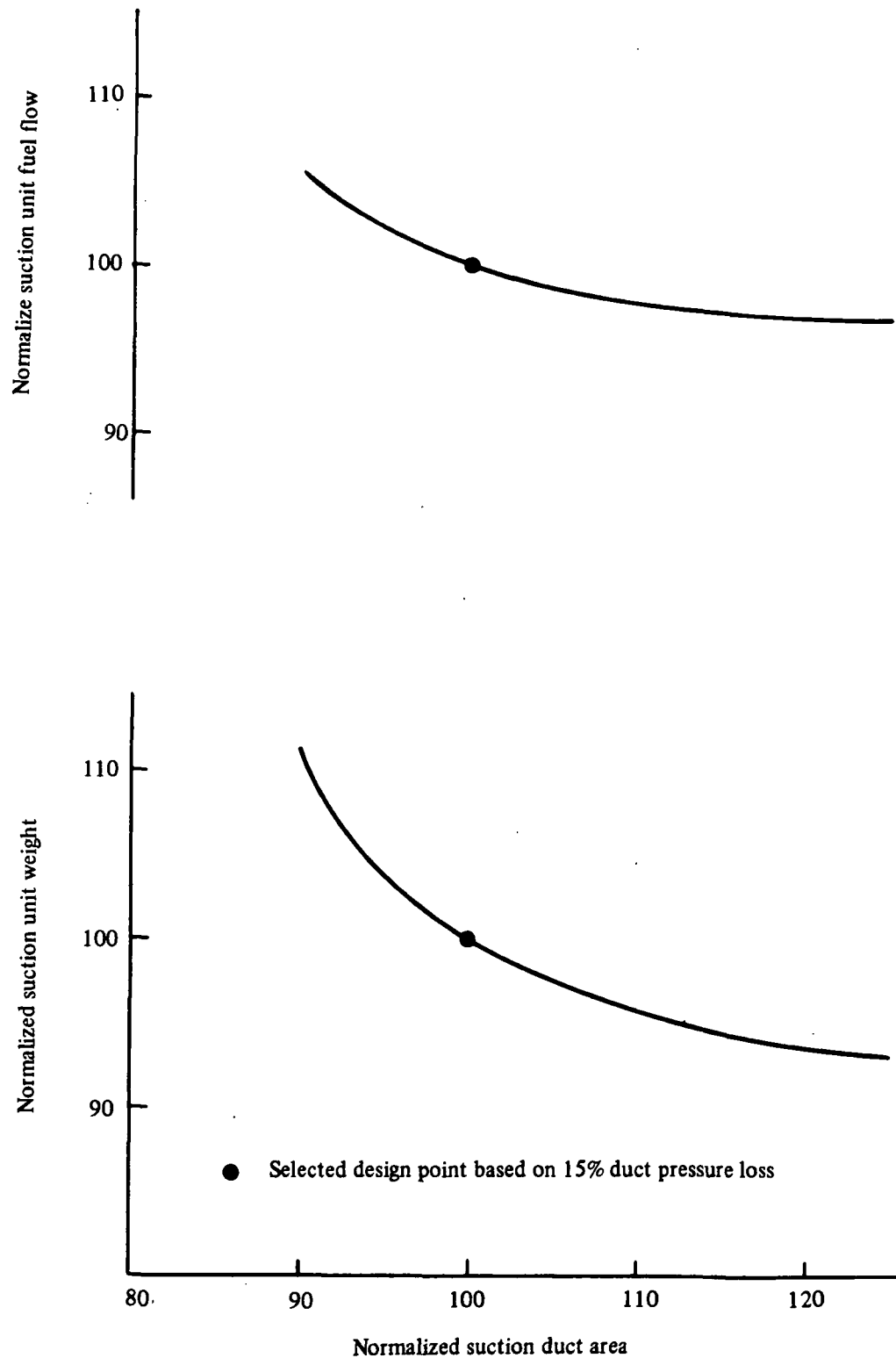


Figure 70. — Effect of duct area on suction unit characteristics

consideration. Simple manufacturing techniques involving the use of washout mandrels, overwrapped with fiber reinforced plastic, and subsequently with heat-shrinkable tape, are applicable to any of the reinforcements such as glass, graphite, or Kevlar-49. Glass having a density in laminate form generally above $0.193 \times 10^4 \text{ kg/m}^3$ (0.072 lb/in^3) was eliminated, leaving graphite with a laminate density of $.155 \times 10^4 \text{ kg/m}^3$ (0.056 lb/in^3) and Kevlar-49 with a laminate density of $.139 \times 10^4 \text{ kg/m}^3$ (0.050 lb/in^3). Kevlar-49 was selected on the basis of lower density and a cost which is less than half that of graphite at current prices. In the future, if pitch fiber graphite comes on the market at current projected prices, it could replace Kevlar-49 with graphite at competitive prices.

6.3.3 DESIGN CONCEPTS

Every effort must be expended to design the optimum ducting system within the constraints imposed by the LFC surface design selected and the volume available within the wing for structure, fuel tanks, plumbing, wiring, control surfaces, and actuators. Design of the ducting system requires consideration of the fuel volume required, the wing spar locations, the wing aspect ratio, wing taper ratio, airfoil thickness, flap and spoiler configuration, actuators and controls, and the percent chord over which LFC treatment is to be applied.

Two basic ducting schemes of the wing were considered during the study, both dictated by the various LFC surface panel schemes presented in section 6.2.3. The ducting system begins at the inner surface of the outer slotted or porous skin panel, and thus ducting near the surface is described as part of the discussions of various surface panel concepts. As a result of duct volume limitations, the baseline LFC-200-S configuration used for preliminary design studies required a total of five LFC suction units — two on each wing, and one in the vertical fin. Each wing was divided into two parts of approximately equal surface area. The LFC suction unit was located so that it laminarized approximately equal areas inboard and outboard of its location on the wing.

The first of the basic ducting systems considered for use was dictated by LFC panel Configurations 1, 2 and 3. This ducting system consists of spanwise ducting within the surface panel to the point at which an LFC suction unit is located. At this site within the wing, a sealed double-rib plenum chamber is installed through which the air is carried chordwise into the LFC pump inlet. Since the aerodynamic shape and thickness of the wing is fixed, such spanwise ducting at any local wing location requires more depth beneath the aerodynamic contour than a chordwise system. Thus, it is more expensive in terms of both basic wing box thickness and surface panel thickness.

The second ducting system considered was dictated by the basic concept of LFC panel Configurations 4 through 10. The ducting system consists of spanwise and chordwise ducts within the LFC surface panel as shown in figures 60-69. The boundary layer air is sucked through these ducts to the aft chordwise extremity of the wing lower surface panel and the forward chordwise

extremity of the wing upper surface panel. At this point the air is sucked through transfer ducts. These transfer ducts carry the air from the chordwise capillaries into the spanwise trunk ducts in the wing leading or trailing edges to the LFC suction units. The ducts are routed through dry bays in the wing into the inlet of the LFC suction units.

6.3.4 MANUFACTURING CONCEPTS

Three concepts for manufacturing the LFC ducting were considered. The common concept of fabricating duct halves with flanges and subsequent joining of the outward facing flanges was eliminated because of the weight required for extra material in flanges and fasteners and the volume required in the wing for installation. Another commonly used concept of thermoforming of ducts from thermoplastics also involves the forming of duct halves with subsequent joining of flanges. This concept was eliminated due to material sensitivity to cleaning solvents and wing volume requirements. The concept of using washout mandrels which are overwrapped with epoxy-impregnated Kevlar-49 fabric and subsequently with heat-shrinkable tape followed by curing in an oven has proven to be a repeatable, low cost, manufacturing method for making cylindrical shapes with tool surface smoothness on the inner wall surfaces. This concept was selected on the basis of weight, wing volume requirements, and low manufacturing cost.

6.4 SUCTION UNITS

6.4.1 CRITERIA

The suction units for LFC aircraft are comprised of a suction pump, or compressor, and a power unit. The basic design requirements for the compressor are dictated by the aircraft characteristics which define the quantity of airflow and the pressure ratio through which the compressor must pump the air. The varied airplane requirements for takeoff, climb, cruise, approach and landing impose broad bands to these requirements. However, the scope of the current study requires operation of the LFC system only during cruise at constant altitude. Therefore, the requirements placed on the LFC suction units are minimal, as compared to units required to operate under all flight conditions. This approach also has the benefit of reducing the contamination of the system by the dirt, corrosive pollutants and insects present at the lower altitudes and in the terminal area.

The power unit must provide sufficient power to drive the compressor at the design conditions with a minimum impact on total airplane fuel consumption and weight, and without presenting unacceptable installation complications or compromising the airplane configuration. The suction unit must be amenable to a compact installation compatible with practical locations on the airplane

dictated by the suction requirements. Maintenance, logistics, and initial cost dictate that all suction units on the airplane be of the same configuration, and be compatible with the varied suction requirements of both wing and empennage.

In view of the multitude of airplane oriented options to be evaluated in the parametric matrices, it was concluded that many of the suction unit options would be eliminated from consideration by independent evaluations and only those that showed the most promise would be incorporated in the GASP.

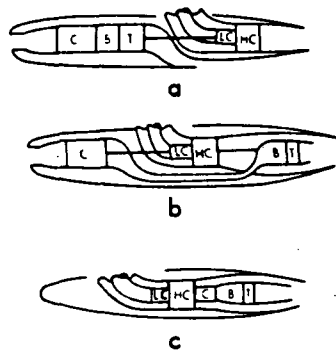
The initial parametric evaluation produced basic airplane configuration data and identified general levels and characteristics of the required suction system. The evaluation also identified the attainment of sufficient fuel volume and suction duct space in the wing as a significant constraints in aircraft design which have a direct influence on the selection of the suction units. Figure 71 presents the various candidate suction unit configurations to be considered. All of these systems were evaluated against the parametric suction system requirements and are discussed in the following sections.

6.4.2 DESIGN CONSIDERATIONS

6.4.2.1 Number and Location of Suction Units

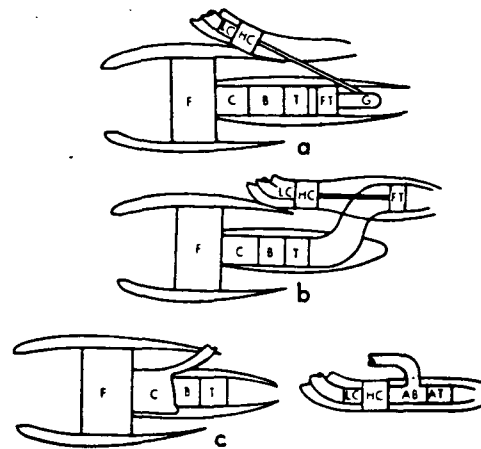
Experience has proven that numerous advantages accrue from utilizing the minimum number of propulsive power units on an airplane consistent with performance constraints. These advantages include higher reliability, lower initial installation and maintenance costs, lower installation weight, and less flight crew fatigue. Although the suction units are not propulsive power units in the conventional sense, they are subject to the same considerations. Theoretically, it might be possible to accomplish the total suction requirements of the airplane by a single suction unit. However, such a unit would be quite large and locating the unit in a symmetrical airplane configuration would become difficult without impacting other required features or systems in the fuselage. Further, a failure of the suction unit in a single-unit configuration would have as much or more impact on airplane performance as the failure of a primary propulsion unit.

A reasonable compromise is provided by utilizing two suction units to provide the entire suction requirements of the airplane. The choice of two units does entail an involved suction ducting system to collect the suction flow at the inlets to the two units. In some airplane configurations, it was found that sufficient space for the required ducting was not available in the wing without severely impacting the wing structure and fuel volume. In these cases it was necessary to adopt a more localized suction unit system in which the wing was segmented with multiple independent ducting and suction unit systems. In these configurations, a portion of the wing suction flow was ducted to a wing-mounted suction unit located at approximately the centroid of the sucked area. Commonality of the wing-mounted units with the empennage suction unit dictated that four wing



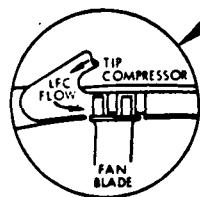
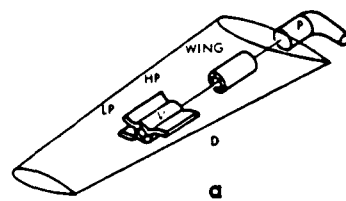
C POWER TURBINE COMPRESSOR
B POWER TURBINE BURNER
T POWER TURBINE
LC LOW PRESSURE LFC COMPRESSOR
HC HIGH PRESSURE LFC COMPRESSOR

Part 1. — Independently powered suction pump concepts

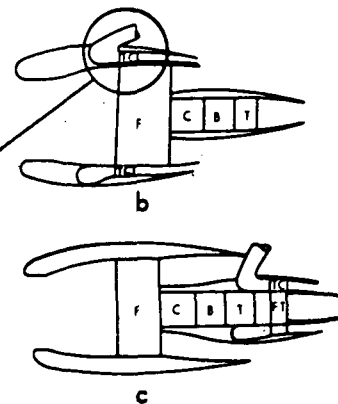


F FAN
C GAS GENERATOR COMPRESSOR
B GAS GENERATOR BURNER
T PROPULSION ENGINE TURBINE
FT FREE TURBINE
G GEARBOX
AB AUXILIARY BURNER
AT AUXILIARY TURBINE
LC LOW PRESSURE LFC COMPRESSOR
HC HIGH PRESSURE LFC COMPRESSOR

Part 2. — Integrated suction pump concepts



V VANED COMPRESSOR
P POWER UNIT
LP LOW PRESSURE SUCTION
HP HIGH PRESSURE SUCTION
D DISCHARGE AIR
F FAN
C GAS GENERATOR COMPRESSOR
B GAS GENERATOR BURNER
T PROPULSION ENGINE TURBINE
TC TIP LFC COMPRESSOR
FT FREE TURBINE



Part 3. — Advanced technology suction pump concepts

Figure 71. — Candidate suction unit configurations

units were marginally compatible with empennage suction unit requirements. A choice of three wing segments required wing suction units that were grossly incompatible with the empennage requirements, thus precluding commonality of all suction units. Therefore if ducting restrictions prevented the use of two suction units, the alternative was four wing-mounted units with a fifth unit located in the aft fuselage to provide empennage suction.

6.4.2.2 Suction Unit Compressors

Axial-flow suction pump compressors are most compatible with system requirements, as a result of their high volume flow, light weight and compactness. The only apparent contender is a vane pump that can be located along the span of the wing to pump the flow in a highly localized manner, thus conserving ducting. This type of unit is illustrated in part 3-a of figure 71. Such a system entails a common spanwise shaft powering all the vane pumps along a semispan. An evaluation of such a system shows that, aside from the basic seal, lubrication and wear problems associated with a vane pump, the poor compressible volume flow characteristics of a vane pump require comparatively large units. The thickness of the wing dictates a limitation to the outer diameter of these units. The basic independent variables available for achieving the required volume flow are length and rotational speed. The speed is restricted by limitations of the long drive shaft subjected to wing flexure and the tip velocities of the vanes. With these restrictions, the units are relatively long and a weight analysis indicates that the units are not competitive with the axial flow compressor and the associated ducting. This type of unit was given no further consideration.

The conventional axial flow compressor requires relatively homogenous inlet pressure and velocity field and cannot tolerate large radial or circumferential distortions in these parameters without encountering severe structural and stall problems. Obviously, the suction flows from the various aerodynamic surfaces are not at a single source pressure. In addition, different losses in the ducting system flow paths result in the components of suction air reaching the suction unit inlet at discretely different pressure levels. To achieve the requisite homogeneity at the compressor inlet, it is necessary to either throttle the air at higher pressures to produce pressure losses adequate to match the lower pressure airflows, or the airflow must be segmented into various pressure levels. Examination of the combinations of flow and pressure at the suction unit inlet indicates that the performance penalties associated with throttling to achieve homogenous pressures for a single entry compressor are prohibitive. In most cases, the basic pressure level differences between the upper and lower wing are such that throttling to achieve a single entry suction pump imposes a weight and fuel-flow penalty on the suction units on the order of twenty-five percent or greater. The alternative is to maintain separate inlets for two or more inlet pressure levels. In all cases examined, all the flow can be brought to one of two discrete pressure levels by throttling a relatively small portion of the flow. Thus, two suction unit inlets were used for all configurations.

To meet the requirement for dual suction unit inlets, two separate compressors operating through different pressure levels are employed in order to achieve common discharge pressure. It is advantageous, however, to employ a single suction compressor with a main component to pump all

of the suction flow from the higher pressure inlet condition to the desired discharge pressure condition with a boost (or pre-compression) component located coaxially in front of the main component inlet to pump the low-pressure air up to the pressure level of the high-pressure air.

The distortions likely to still exist in the inlets of both pump components resulting from the mixing of the various components of suction airflow a short distance upstream of the inlets dictates rather conservative compressor design techniques. This precludes use of the high compressor average stage loadings prevalent in current compressor design. The number of stages required for the main compressor component is therefore based on modest stage loadings and the pressure ratio required to pump the higher inlet pressure air to the desired discharge pressure level. The required pre-compression component stages are similarly based on the pressure ratio required to pump the low-pressure suction flow to the pressure level of the high suction pressure air so that all of the unit suction air enters the main compressor at essentially the same pressure level. The actual number of stages required for the suction compressor components is best illustrated by the discussions of the specific units for the LFC-200-S and LFC-200-R configurations in sections 8.2.3.3 and 8.3.3.3, respectively.

6.4.2.3 Suction Unit Discharge Velocity

The discharge velocity from the suction pump must be at least equal to the free stream velocity in order to completely nullify the aerodynamic surface drag that the LFC system is intended to overcome. Discharging the suction air at free stream velocity produces a gross thrust that is exactly equal to the friction and ram drags and duct losses associated with the suction airflow. The propulsive efficiency of discharging the suction airflow at free stream velocity is greatly superior to that of the primary propulsion units. Also, all of the penalties associated with ingesting this air have been overcome. It is therefore apparent that increasing the exit velocity of the suction airflow produces additional thrust at better propulsive efficiency than the primary unit. In addition, to produce the same thrust increment, the primary unit is required to ingest more air, thus entailing an increase in ram drag which the unit must overcome. Theoretically, performance improvements accrue from discharging the suction flow at exhaust velocities up to that of the primary propulsion engines. In some cases, it appears that the trade-offs involved preclude the selection of primary propulsion unit exhaust velocities as the discharge velocity for the suction air. An example of this is discussed in section 8.3.3.3 for the LFC-200-R configuration.

6.4.3 INDEPENDENT SUCTION POWER SYSTEMS

The large number of airplane configurations investigated in the parametric study required the use of an independent power system for the suction units in order to expedite the study. Subsequently, an independent investigation of alternative systems was conducted and the more promising power systems were incorporated in the parametric evaluations. The units investigated are illustrated in part 1 of figure 71.

6.4.3.1 Operation on Ram Air

In order to achieve the maximum simplification and flexibility in the early parametric studies, a conventional shaft engine of advanced 1980-85 technology was selected to power the suction compressors. This unit includes a conventional core engine of high-pressure ratio with a highly loaded aircooled turbine as illustrated in part 1-a of figure 71. The shaft power is derived from a free power turbine sized to extract power from the core engine leaving only sufficient energy in the exhaust gases to provide an exhaust velocity equal to free stream velocity. This choice was made in order to match the gross thrust of the power unit with the ram drag, thus resulting in a zero net thrust and drag. The unit is configured for a conventional ram inlet with pressure recoveries of 99.8 percent at cruise without any compromise for off-cruise conditions. The ram inlet requires that the power unit be located forward of the suction compressor. Since it is desirable to have a direct coaxial drive between the power unit and compressor, the power unit turbine exhaust must discharge through a scroll, downward and aft, with the drive shaft passing through the center of the scroll. This necessitated a front drive for the suction compressor with the suction discharge air directed axially aft. The spacing between the power and the suction compressor is dictated by the power unit exhaust scroll and the dual coaxial suction compressor inlet ducts with the connecting shaft sized accordingly. The power unit and suction compressor are connected by a simple truss so the entire assembly can be handled as a unit.

This unit served as a baseline for both technology level and performance for all subsequent comparisons.

A derivative of this configuration, illustrated as part 1-b of figure 71, separated the power turbine compressor from the burner and power turbine to provide ram inlet for the power turbine compressor while providing coaxial exhaust of both the power turbine and suction compressor. The problems with alignment and flexure of the shafting at high rotational speeds, as well as unit weight and performance penalties, are prohibitive. Therefore this configuration was deleted from further consideration.

6.4.3.2 Operation on Suction Air

An obvious alternative to operation of the power unit on ram air is operation on air discharged from the suction compressor since compensation for the penalties associated with taking this air aboard the airplane has already been provided. This unit is illustrated as part 1-c of figure 71 and comparative summary data are presented in section 6.4.5. For this evaluation, the suction compressor configured to discharge the air at free stream velocity was assumed, since this provides essentially the same inlet pressure to the power unit available from the ram inlet. Unfortunately, the suction compressor elevates the temperature of this air about 200°F in pumping it back to a pressure equivalent to that of ram air. As would be expected, this elevated temperature imposes severe penalties on the power unit. The turbine inlet temperature limits and turbine cooling requirements of the ram air system of section 6.4.3.1 were assumed as the technology and mechanical limits for this unit. Recognizing these constraints, two limiting cycles emerge as the

outer boundaries for the present unit. One of these has the same power unit compressor discharge pressure as the baseline unit of section 6.4.3.1 but an appreciably higher compressor discharge temperature. This higher compressor discharge temperature restricts the combustion fuel/air ratio below that of the baseline in order to maintain the same TIT, thus reducing the efficiency of the cycle. The elevated compressor discharge temperature necessitates an increase in the percentage of airflow used for turbine cooling because of the reduced cooling effectiveness. This also reduces the cycle efficiency. The other boundary for the present unit is the assumption of the same fuel/air ratio as the baseline unit with an adjustment of compressor discharge pressure and temperature to maintain the same turbine inlet temperature and effective turbine cooling as the baseline. These limitations also reduce the cycle efficiency.

Since the most efficient configuration is between these boundaries, intermediate cycles were evaluated. Figure 72 presents a ratio of the SFC of the unit operating on suction air to the SFC of the baseline ram air unit of section 6.4.3.1 plotted against core compressor pressure ratio. It will be observed that, at best, the fuel consumption of the unit operating on suction air is nearly 40 percent higher than that of the baseline unit of section 6.4.3.1 operating on ram air.

Section 6.4.5 presents a summary comparison of the most promising candidate power systems and outlines comparative fuel flow, weight, and other parameters. As shown in section 6.4.5, no appreciable advantages are demonstrated by the suction power unit operating on suction air other than some simplification of the installation. However, there are significant performance and weight penalties. Therefore no further consideration was given to operation of the suction power unit on suction air.

6.4.4 INTEGRATED SUCTION POWER SYSTEMS

Attending the incorporation of an LFC suction system is both a potential supply of air aboard the airplane and a requirement for drive power. There are a variety of potential applications for such a supply of air, including the numerous pneumatic aircraft systems. Additionally, there are power systems aboard the airplane from which the LFC suction system may be powered. Integration of these systems appears to offer attractive possibilities for decreasing weight and improving performance by designing the LFC airflow to perform additional functions or designing a power system already aboard the airplane to supply all or part of the LFC suction system power requirements.

6.4.4.1 Integration with Primary Propulsion Engines

The primary propulsion engines are basically selected to meet the takeoff thrust requirements and provide good specific fuel consumption at cruise thrust levels. These requirements, must be satisfied while providing adequate reserves for climb and failed-engine conditions. These criteria result in the selection of engines that operate at part-power cruise conditions on a conventional

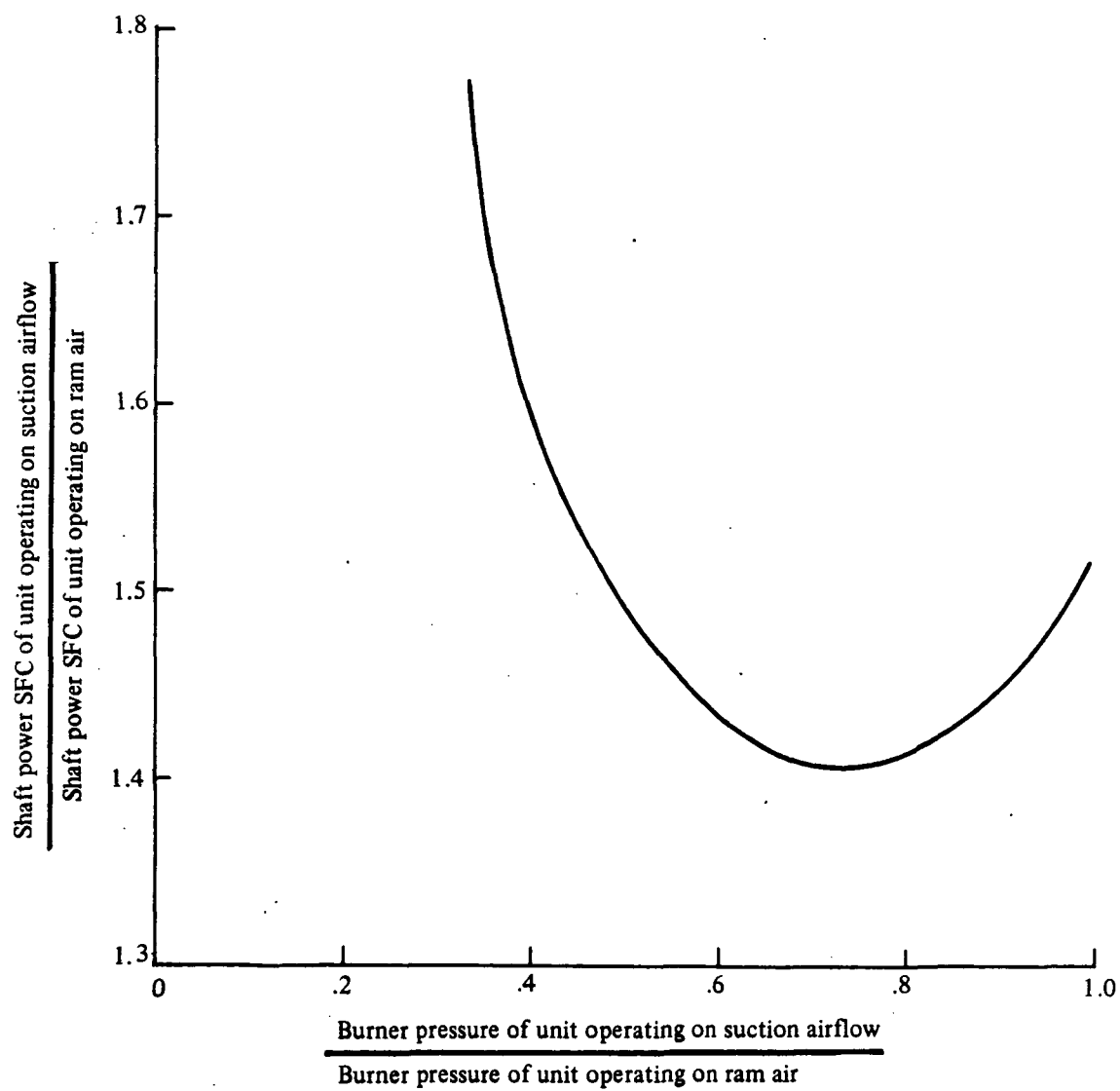


Figure 72. — Fuel consumption of suction power unit operating on suction pump discharge airflow

subsonic transport airplane. The takeoff thrust level is largely dictated by the requirement for rapid acceleration of the airplane mass while airplane drag has a relatively minor influence. In the cruise mode, the required thrust level is dictated entirely by the airplane drag.

It is therefore apparent that the LFC airplane takeoff thrust levels are similar to those of a conventional airplane. However, the cruise thrust requirement is drastically reduced for the LFC airplane compared to the conventional airplane. The primary propulsion engines are selected with recognition of this change in takeoff to cruise thrust relationship but the end result still tends toward a lower part-power cruise condition for the LFC engines. As a result, the primary propulsion engines are capable of providing extra power at cruise which may be employed to drive the suction units.

Integral Primary/LFC Engines – The most obvious possibility is to design the primary propulsion engines to provide the LFC suction directly in one completely integrated unit. Such a unit is illustrated in parts 3-b and 3-c of figure 71. These units are included as advanced technology concepts because considerable analysis and development is required to eliminate an otherwise high risk. Such an integration can be accomplished by locating the suction portion of the composite unit at the fan tip as extensions to the fan blading of the primary engine. The difference in pressure between the ram inlet of the primary and suction inlet for the LFC required independent inlets and flow paths through the compression cycle. The LFC discharge can be mixed with the fan discharge. The annular height of the suction inlet, located at the fan tip diameter, is relatively small and the performance of the suction unit suffers dramatically from any leakage from the higher pressure fan flow path into the suction flow path. Adequate sealing of these flow paths from each other at the large diameter of the fan tip does not appear to be possible within the assumed technological time frame.

Numerous other problems such as independent control of suction regardless of primary engine thrust, suction shut-off in the terminal area, ducting suction flow to the primary engine location, and distributing the flow around the fan case into the suction inlet, resulted in deletion of this concept from further consideration. Although the diameter of the turbine tip configuration illustrated as part 3-c of figure 71 relieves some of the sealing problems, the seal problem is complicated by the high temperatures of the turbine discharge. In addition, other considerations of the fan tip configuration apply. Consequently, the turbine tip configuration was deleted from further consideration.

Primary Direct-Drive Systems – The second choice for integration of the suction system with the primary propulsion system is a geared system illustrated as part 2-a in figure 71 in which power is extracted from the primary propulsion system through a series of gears and shafts to provide a direct drive to the suction pump compressor. To satisfactorily accomplish this, the suction compressor must be located in close proximity to the primary propulsion engines. Various primary propulsion engine locations were investigated, but no completely satisfactory location was found for this configuration. Location of primary propulsion engines in a conventional under-wing location creates a flow disturbance in the vicinity of the engines such that the resulting local de-laminarization on the wing more than offsets any advantages that integration might have. The

unconventional location of the engines below and behind the aft wing spar introduce torsional forces on the wing box structure with an attendant structural weight penalty that more than offsets the potential benefits. Gear drives from aft-fuselage-mounted engines are not possible unless the suction compressor is mounted in the nacelle with the primary propulsion engine. In this case, complexities in ducting the LFC suction air to the suction pump compressor become prohibitive. An alternative direct drive is illustrated at part 2-b of figure 71 in which the primary propulsion engine core exhaust is diverted through an auxiliary turbine which powers the suction pump compressor. While this configuration offers some advantages, it suffers from all the disadvantages of the geared system. Both configurations were therefore deleted from further consideration.

Bleed and Burn Systems – The third choice for integration of the suction system with the primary propulsion engines is the bleed and burn system in which air is bled from the high-pressure compressor discharge of the primary propulsion engines, ducted to the suction unit location, introduced to a burner where fuel is also introduced, and the combustion products pass through a power turbine which drives the suction pump compressor. A specific system of this type is illustrated as part 2-c of figure 71 and is discussed in section 8.3.3.3 wherein it was applied to the LFC-200-R airplane configuration. Such a system lacks the high theoretical efficiency of the integrated systems discussed previously but does show performance advantages over the baseline independently powered suction systems discussed in section 6.4.3 and has numerous advantages over the previously discussed integrated systems. By manifolding the bleed air from the primary propulsion engines, the location and number of suction units can be completely independent of the number and location of primary propulsion engines. The ducting for the high-pressure bleed air, even with the required insulation, is much smaller and lighter than the ducting for the suction air. It is therefore preferable to duct this air to the suction unit rather than duct the suction air to the vicinity of the primary propulsion engines. The system performance does suffer from pressure losses in the high-pressure air ducting but still shows performance advantages over the independently powered systems in both weight and fuel flow. Comparative data are provided in section 6.4.5.

There are additional penalties associated with the bleed-burn system accrued by the primary propulsion engine. Bleeding the required air from the compressor discharge of a conventional high-bypass core engine has the effect of significantly increasing the SFC and turbine inlet temperature of the engine. These effects are largely a result of a mismatch between the core airflow and power requirements of the compressor and the reduced gas flow and power output of the turbine. The undesirability of the increased SFC is obvious, while the elevated TIT has a more subtle effect on turbine life. Although the turbine operates well under the limiting temperatures while cruising with this bleed, the long-cruise periods during which the turbine is subjected to this condition effects turbine blade creep and seal wear, which impact turbine life and maintenance/overhaul costs.

These effects may be minimized by designing the engine cycle to provide for continuous bleed. In this study, this was accomplished by defining the same core-power match with bleed that the conventional engine has without bleed. The bleed airflow requirement was established and the compressor power required to produce this high-pressure flow was determined. The power

employed to drive the fan was reduced by this amount and the fan airflow was reduced accordingly. The effect of this manipulation is to maintain the same engine fuel flow and TIT while reducing fan flow by an amount equivalent to the power employed to produce the bleed airflow. This results in a decrease in fan thrust and consequently a modest increase in engine SFC.

In applying bleed-burn systems to the aircraft of this study, weight allowances were included for the reduction in fan size and the increase in core compressor size. Since the primary propulsion engines are scalable, the thrust decrease was counteracted by scaling the engine up slightly. In the actual study analysis procedures, these adjustments to the primary propulsion engines were applied through adjustment to the allocated suction system parametric weight and fuel flow equations, since they are a direct function of suction requirements. This method eliminated the need to alter the parametric primary propulsion engines for various suction requirements or systems. The above effects accrued by the primary propulsion engine are reflected in the comparative data presented in section 6.4.5. The bleed-burn system offers advantages over all other systems and was used for several specific final configurations discussed in section 8.

6.4.4.2 Integrated Pneumatic/Power Systems

The possibilities of integrating the LFC suction system with airplane pneumatic and auxiliary power systems were investigated with the result that there is little potential benefit from such integrations. The Environmental Control System (ECS) requires only approximately 47 percent of the airflow available from one suction unit of a five-unit system or 19 percent of the flow available from one unit of a two-unit suction system. Simultaneously, the ECS system requires an air pressure nearly four times that available from the suction unit. Any performance gains from such an integration would be modest at best and would be far out-weighted by the added weight and complexity required to overcome these gross incompatibilities.

Integration of the suction system power unit with the Auxiliary Power Unit (APU) presents similar gross incompatibilities. The power capability of the suction power unit far exceeds the requirements for an APU. The requirement for operation of an APU under static airplane conditions while parked at the terminal is contrary to the concept of avoiding any operation of the suction system at low altitude and particularly at the terminal because of contamination. Avoiding this incompatibility requires de-clutching of the suction compressor from the suction power unit and either bleeding the power unit or driving a separate compressor to provide the ground air normally provided by an APU for primary engine starting and ground ECS. This arrangement could be provided but the adverse impact on suction system interchangeability, weight, cost, complexity, and reliability outweigh the penalties of a separate APU.

For these reasons, no further consideration was given to integration of the suction units with the APU or any normal airplane pneumatic system.

6.4.4.3 Integration with Aircraft Performance Augmentation Systems

The potential for utilizing the suction airflow exhaust to provide further aircraft performance improvements is attractive, although feasible applications are few.

Integration with High-Lift Systems — The possibility of using the suction airflow discharge to blow the wing surfaces for takeoff performance improvement is obvious. Examination of this possibility reveals, however, that a wing leading edge or flap blowing system requires a complicated ducting and distribution system as well as complex valving system in the vicinity of the suction compressor. There is little likelihood of achieving commonality with LFC system ducting. Since wing volume available for LFC system ducting represents a serious design constraint there is no possibility of satisfying additional ducting requirements. Operation of the suction system in the terminal area is objectionable from the standpoint of contamination. Venting the suction compressor inlet to ambient results in excessive noise levels for a blowing system unless the units are severely throttled.

The airplane terminal area performance is generally quite satisfactory and any performance improvements from this type of system integration are more than overbalanced by the associated complexities and problems.

Integration with Fuselage Slot System — Integration of the suction system with a fuselage slot blowing system is feasible and offers some potential performance improvements. The suction airflow is reasonably compatible with the flow requirements of a forward fuselage slot. The fuselage slot flow is required to exit the slot at approximately 0.3 Mach number. This requires a significantly lower pressure ratio for the main suction compressor units. A baseline suction unit was modified for the required discharge pressure by deletion of stages with the consequent reduction in independent power unit size, weight, and fuel flow. Allowance was made for a 10 percent pressure loss in the ducting from the suction pump exit to the slot. This unit was reduced to a parametric form for use in the GASP. Design concepts for this configuration and results of the configuration evaluation are included in sections 7.4.5 and 7.5.3, respectively.

It is of interest to note that, by discharging the suction airflow at $M = 0.3$ rather than at free stream velocity, the net thrust of the suction system is negative and represents about 60 percent of the drag accrued by the wing boundary layer and suction system airflow removed by the LFC system. This indicates that a major portion of the advantages of LFC have been nullified by the low discharge velocity of the fuselage slot. Unless the improvements in fuselage drag from the slot blowing exceed the penalties to the LFC system, there can be no net gain in airplane performance. It may be possible to overcome this cancelling effect by utilizing the suction airflow at a much higher discharge velocity as the primary flow in an ejector system which removes low velocity air from the fuselage surface and discharges it at approximately $M = 0.3$. The characteristics of such a system are unknown and the analysis of a system of this type is beyond the scope of this study.

6.4.5 SUCTION UNIT CONFIGURATION SUMMARY

In the foregoing sections, investigations were described for each of the suction unit concepts illustrated in figure 71 including consideration of integrating the LFC suction system with airplane pneumatic and auxiliary power systems. With the exception of fuselage slot blowing, integration of the LFC system and aircraft systems proved to be infeasible. The advantages of fuselage slot blowing can only be determined from an airplane analysis, since reduction of fuselage drag is a determining influence. This system was therefore reduced to parametric form and exercised in the GASP computer program for the evaluations discussed in section 7.5.

In the foregoing discussions, an axial flow suction pump compressor of semi-conventional design was selected for all suction units and all but three suction unit power systems were eliminated. The three power unit concepts include an independent unit of conventional shaft engine design operating on ram air, a similar unit operating on air discharged from the suction pump compressor, and an integrated unit powered by a burner and turbine unit supplied with high-pressure bleed air from the primary propulsion units. These concepts are illustrated as part 1-a, part 1-c, and part 2-c of figure 71.

A direct comparison of these units is presented in table 10 where parameters are normalized to the independently powered unit operating on ram air. In this comparison, identical suction pump compressors were assumed for all units with the suction pump airflow discharged at free stream velocity. Power units were also assumed to discharge at free stream velocity. All parameters shown were not applicable to all concepts since the bleed-burn system does not have a power unit compressor as such, nor do the other concepts have any involvement with the primary propulsion units or bleed air ducting. Where applicable, the bleed-burn peculiar parameters are normalized to the basic value of the parameter for the independent ram air unit. It should be noted that the primary propulsion unit experiences a decrease in net thrust at constant fuel flow when air is bled from the compressor. The engine experiences the ram drag associated with the bleed airflow but is not credited with the thrust which is discharged from the bleed-burn turbine at free stream velocity. The bleed-burn turbine is conversely credited with the thrust from this airflow but is not charged with the ram drag. The primary propulsion Δw_f evaluation was therefore evaluated for only the increment in fuel flow required to restore the airplane to the level of total airplane net thrust that exists without the bleed system.

It is readily apparent from this tabulation that the independently powered unit operating on suction compressor discharge air suffers appreciably in both total weight and fuel flow at all burner pressures. The only advantage offered by this unit is its compactness, which does not compensate for the performance and weight penalties.

The comparison of weight and fuel consumption parameters between the independent unit operating on ram air and the bleed-burn unit indicate a distinct and significant advantage for the integrated bleed-burn unit. As discussed earlier in this section and described relative to specific airplane configurations in section 8, ducting the bleed airflow to the burner presents problems in some airplane configurations. For this reason, both concepts were reduced to a parametric

evaluation and were incorporated in GASP for use in parametric airplane evaluations and final airplane configuration definitions.

TABLE 10. SUMMARY COMPARISON OF SUCTION POWER UNITS

Normalized performance parameters	Independent power units				Integrated bleed-burn power units
	Ram inlet	Suction pump discharge inlet			
Power unit compressor inlet temperature	1.0	1.356	1.356	1.356	-
Power unit compressor inlet pressure	1.0	0.891	0.891	0.891	-
Burner pressure duct loss (%)	-	-	-	-	10.0
Burner pressure	1.0	1.0	0.676	0.335	0.900
Burner inlet temperature	1.0	1.356	1.226	1.0	1.0
Turbine inlet temperature	1.0	1.0	1.0	1.0	1.0
Turbine cooling air (% of total power unit airflow)	16.3	22.1	19.5	16.3	16.3
Power turbine ΔT	1.0	.425	.551	.659	2.61
Power unit total airflow	1.0	2.381	1.811	1.476	0.442
Power unit fuel flow	1.0	1.517	1.401	1.763	0.442
Shaft power SFC	1.0	1.517	1.401	1.763	-
Primary propulsion ΔW_f^*	-	-	-	-	0.497
Total chargeable W_f	-	-	-	-	0.939
Total fuel flow	1.0	1.517	1.401	1.763	.939
Normalized weight parameters					
Suction pump weight	1.0	1.0	1.0	1.0	1.0
Power unit weight	1.0	2.545	2.00	1.491	0.373
Primary propulsion Δ weight **	-	-	-	-	0.725
Duct weight ***	-	-	-	-	0.155
Installation weight	1.0	1.540	1.283	1.042	0.708
Suction unit total chargeable weight	1.0	1.666	1.388	1.128	0.862
<p>* Increased from fuel flow for primary propulsion engine at same total airplane net thrust as with zero bleed.</p> <p>** Scaled to provide same installed takeoff thrust.</p> <p>*** Weight of insulated primary propulsion engine compressor discharge bleed air ducting from aft engine location to wing-root suction unit location.</p>					

7.0 LFC CONFIGURATION DEVELOPMENT

7.1 INTRODUCTION

As observed in the previous section, many of the LFC system concepts impact overall aircraft design to an extent which requires the definition of a specific aircraft configuration for concept evaluation. In addition, there are feasible airframe configuration variations which offer the potential of greater compatibility with LFC system requirements and a resultant improvement in fuel efficiency. This section is devoted to the evaluation of such LFC system concepts and aircraft configuration variations and the selection of final LFC aircraft for subsequent comparison with the corresponding TF transports.

The parametric results of section 5.2 and design layouts of representative LFC system installations for the four LFC aircraft configurations under consideration show that the combination of LFC suction requirements and fuel volume limitations placed the most severe design constraints on the LFC-200-S configuration. Consequently, this configuration was selected as the initial baseline for the evaluation of LFC system concepts and configuration variations. The results of these investigations were applied to the LFC-200-R, LFC-400-S, and LFC-400-R configurations as dictated by the design constraints peculiar to each configuration.

The procedure followed in conducting these evaluations included the development of an initial LFC baseline configuration, definition of LFC system concepts and aircraft variations, modification of the baseline configuration to accommodate the concept or variation, optimization of the modified configuration, and comparison of this configuration with the baseline. From these comparisons, the LFC system concepts and aircraft variations which minimized fuel consumption were combined into final LFC configurations.

7.2 INITIAL LFC BASELINE CONFIGURATION

The configuration parameters selected in section 5.2.2 form the basis for the development of the initial LFC-200-S baseline aircraft. A summary of these parameters and the characteristics of the resultant point-design configuration is shown on the general arrangement drawing of figure 73. A detailed weight statement for this configuration is included in table 11.

The initial LFC baseline airplane is a wide-body configuration designed to carry 200 passengers, their baggage, and 4536 kg (10,000 lb) of cargo over an intercontinental range of 10,186 km (5500 n mi) at Mach 0.80. A typical cabin arrangement accommodates 40 first-class and 160 tourist-class passengers in a two-aisle configuration with underfloor galley provisions.

$M = 0.80$
 $H, m \text{ (ft)} = 11,582 \text{ (38,000)}$
 $\Lambda, \text{rad (deg)} = 0.396 \text{ (22.7)}$
 $AR = 14.00$
 $S, m^2 \text{ (ft}^2\text{)} = 270.8 \text{ (2915)}$

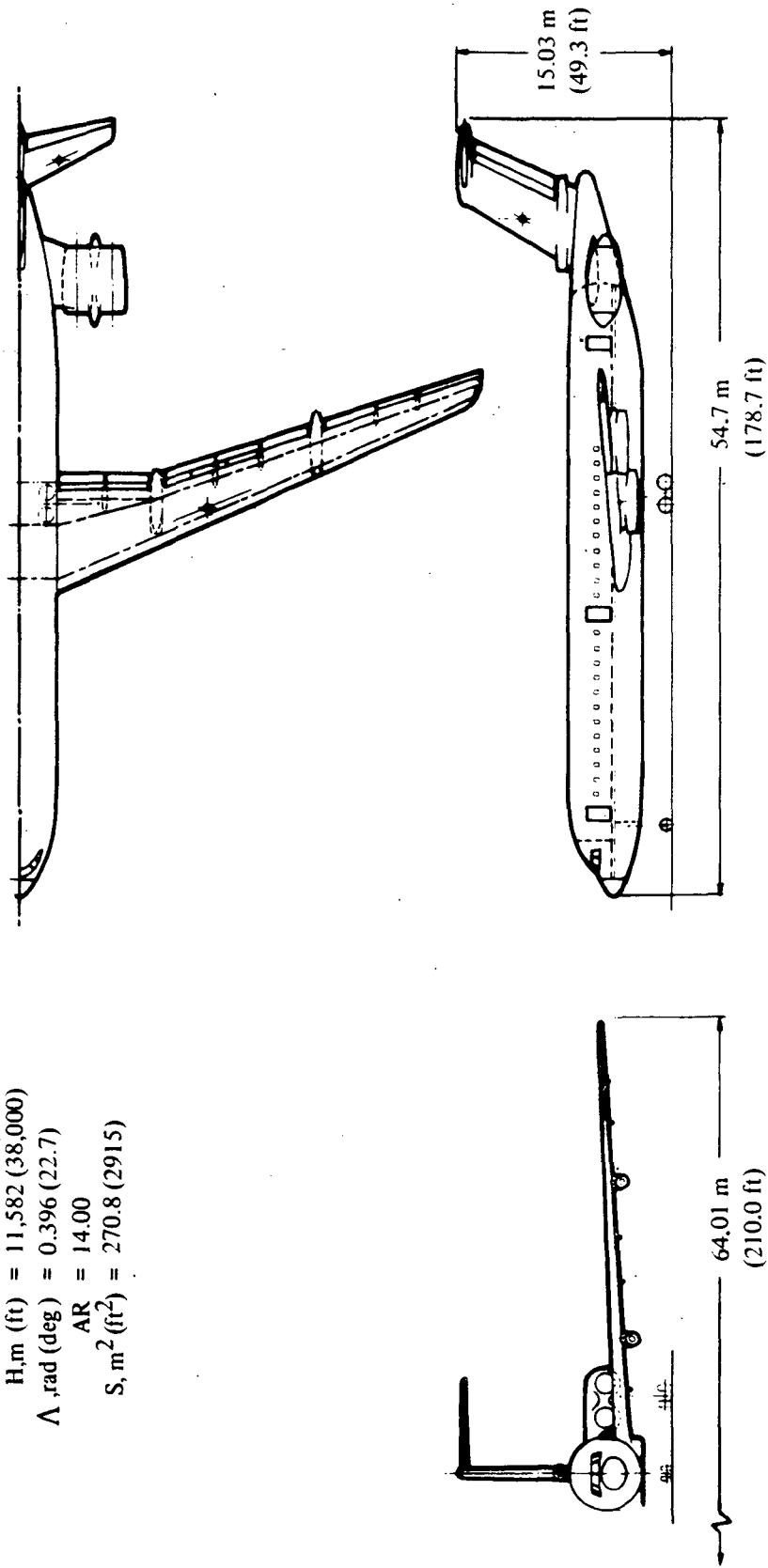


Figure 73. — General arrangement, initial LFC-200-S baseline configuration

TABLE 11. WEIGHT STATEMENT: INITIAL LFC-200-S BASELINE CONFIGURATION

Item	kg	lb
Structure	(57,734)	(127,279)
Wing	27,594	60,833
Wing LFC glove	2,635	5,809
Empennage	(4,149)	(9,147)
Horizontal tail	1,381	3,044
Horizontal LFC glove	440	970
Vertical tail	1,653	3,644
Vertical LFC glove	675	1,489
Fuselage	13,634	30,058
Landing gear	(7,562)	(16,671)
Nose	983	2,167
Main	6,579	14,504
Nacelle and pylon	(2,159)	(4,761)
Nacelle	903	1,991
Pylon	289	637
Noise treatment	967	2,133
Propulsion system	(11,756)	(25,918)
Engines	5,733	12,640
Fuel system	1,252	2,760
Thrust reversers	963	2,124
LFC engines	1,155	2,546
LFC installation	1,432	3,156
LFC ducts	313	691
Miscellaneous	907	2,000
Systems and equipment	(17,355)	(38,261)
Auxiliary power system	295	650
Surface controls	1,466	3,233
Instruments	611	1,347
Hydraulics and pneumatic	683	1,506
Electrical	2,314	5,101
Avionics	1,089	2,400
Furnishings	8,611	18,983
Airconditioning and AI	2,254	4,971
Auxiliary gear - equipment	32	70
Weight empty	(86,845)	(191,457)
Operating equipment	6,570	14,485
Operating weight	(93,415)	(205,942)
Payload - passenger	19,233	42,400
Cargo	4,536	10,000
Zero fuel weight	(117,184)	(258,342)
Fuel	54,034	119,122
Gross weight	(171,218)	(377,464)
AMPR weight	75,949	167,436

As shown on figure 73, the LFC baseline airplane is a low-wing, "T"-tail monoplane with four aft-fuselage-mounted propulsion engines. Two LFC suction units are installed under each wing and one is installed in the base of the vertical tail. The airplane and power plants are designed to meet community noise level requirements of FAR Part 36 minus 10 EPNdB. Fuel stowage is in the wing and includes the volume of the wing center section.

The wing is a moderately swept, high aspect ratio structure with mid-span ailerons mounted on either side of the outboard LFC pump. Full-span flaps are provided, including drooped ailerons, to provide the specified airport performance. Spoilers are located over the inboard flaps. The wing surfaces are covered with slotted LFC panels from 3% to 72% chord on the upper and 3% to 75% chord on the lower surface. Empennage surfaces are provided with similar panels from 3% to 75% chord.

Associated aircraft systems are assumed to reflect a technology level compatible with initial aircraft operation in 1985.

7.3 CHORDWISE EXTENT OF LAMINARIZATION

The reduction of profile drag by increasing the chordwise extent of the laminar boundary layer on the wings and empennage is an obvious method of improving the fuel efficiency of LFC aircraft. The penalties which accompany greater laminarization, in terms of LFC system weight, cost, and complexity are less obvious. However, for a practical aircraft design, they are of such significance as to limit the optimum chordwise extent of laminarization to values well below the theoretical ideal of full-chord laminarization.

It should be observed that the optimum chordwise extent of laminarization is a function of the design mission. Each variation in design mission requirements changes the design constraints which ultimately define the optimum aircraft geometry. Both laminarization efficiency and the suction schedule required to laminarize the boundary layer are strongly influenced by aircraft geometry. Therefore, the optimum chordwise extent of laminarization, as established by the interaction of these variables, can be expected to vary with changes in the design mission. However, while the specific results of this section are applicable only to the configuration evaluated, the general trends are representative of those for all configurations.

7.3.1 GENERAL CONSIDERATIONS

The parametric analyses of section 5.0 and the concept evaluations of section 6.0 were conducted for configurations with laminar surfaces extending to chordwise locations of 0.72 on the wing upper surface, 0.75 on the wing lower surface, and 0.75 on the empennage. The assumed chordwise extent of laminar flow was limited to these values by the shock location on the wing upper surface and trailing-edge devices on the wing lower surface and empennage.

While these limitations are necessary in analyses involving a large number of parametric configurations, it is reasonable to consider specific configuration arrangements which are compatible with greater chordwise laminarization. General considerations relevant to the configuration changes necessary to permit laminarization behind the locations used on the baseline configuration include the following:

- (1) *Shock Location* – Laminarization to a greater value of x/c requires the use of an airfoil section without a standing shock or one for which the shock is sufficiently weak that laminar flow can be maintained through the shock by employing greater suction. While such sections are well known, as described in section 4.0, the attendant t/c ratios are appreciably lower than those of the modified supercritical section employed on the baseline aircraft. As a result, overall configuration performance is constrained by wing volume available for fuel and ducting.
- (2) *Trailing-Edge Devices* – If it is assumed to be technically feasible to maintain laminar flow across movable surfaces, the additional weight and cost associated with laminarizing flaps and ailerons may prove to be economically infeasible. However, for appropriate airfoil sections, it is possible to design control and high-lift devices which require as little as $0.15 c$. Thus it is possible to consider laminarization to $x/c = 0.85$.
- (3) *Wing Spar Location* – For laminarization behind the locations assumed for the baseline configuration, it is necessary to relocate the wing spars to provide the increased duct volume required. This change decreases the wing box size with an attendant reduction in fuel volume and an unfavorable impact on performance.
- (4) *Laminarization Efficiency* – As illustrated by figure 74, the regions of the wing which cannot be laminarized become a greater fraction of total wing area as the chordwise extent of laminarization is increased. For the upper wing surface, the losses due to fuselage and wing tip interference are relatively small, with a laminarization efficiency of 0.97 available at $(x/c)_L = 0.85$. However, for the lower surface, the flap-track fairings at $x/c = 0.50$ and the landing-gear doors at $x/c = 0.65$ eliminate much of the potential laminar area in this region. At $(x/c)_L = 0.85$, the laminarization efficiency for the lower wing surface is 0.83.
- (5) *Cruise Power Ratio* – As aircraft drag is decreased, the ratio of cruise-to-takeoff power must also decrease in order to maintain the specified takeoff performance. Thus, the condition of having engines appreciably larger than required for cruise, which is common to all LFC aircraft, is aggravated by increasing the chordwise extent of laminarization.
- (6) *LFC System Weight* – For regions of the wing forward of $x/c = 0.65$, the total weight of LFC system components is very nearly a linear function of total laminarized area. On the aft portion of the wing, suction requirements increase rapidly in the region of the shock on the upper surface and in the pressure recovery region on the lower surface, with a corresponding increase in LFC system weight per unit laminarized area.

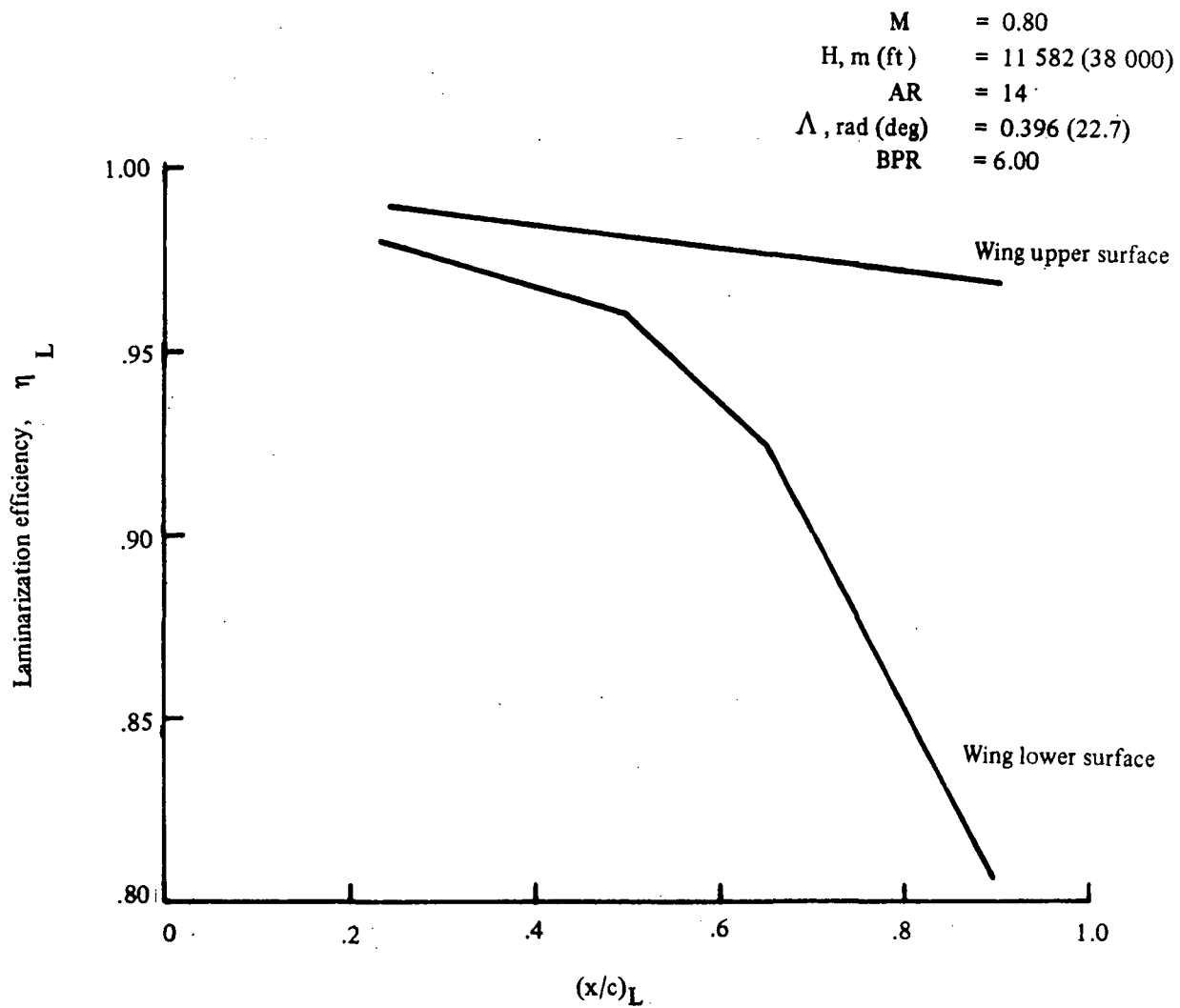


Figure 74. — Laminarization efficiency vs. chordwise extent of laminarization

7.3.2 CONFIGURATIONS

The interaction of the considerations outlined above is sufficiently complex that evaluation of the optimum chordwise extent of laminarization requires the development of a specific point-design configuration for each variation in laminar area. The analyses of this study were conducted through the development of configuration variations based on the baseline LFC configuration described in section 7.2. All configurations are identical to the baseline with the exception of variations required in wing spar location, laminarization efficiency, wing loading, and cruise power ratio necessary to define a practical aircraft compatible with mission requirements.

For each configuration, appropriate values of spar location and laminarization efficiency were determined and the configuration was exercised through the GASP to establish the maximum wing loading consistent with fuel volume requirements and the maximum cruise power ratio consistent with required airport performance. The resultant configuration represents the optimum variation of the baseline for the selected chordwise extent of laminarization. Table 12 lists the values of appropriate parameters for each of the four configurations evaluated.

TABLE 12. CONFIGURATION VARIATIONS:
CHORDWISE EXTENT OF LAMINARIZATION

$(x/c)_L$.30	.60	.72	.85
Front spar x/c	.08	.08	.15	.18
Rear spar x/c	.62	.62	.65	.63
Cruise power ratio	.92	.82	.80	.81
W/S, kg/m^2	581	559	537	510
(lb/ft^2)	(119.0)	(114.5)	(110.0)	(104.5)

7.3.3 RESULTS AND ANALYSIS

In figures 75 through 80, the variation of pertinent aircraft geometry, weight, and performance parameters is shown as a function of the chordwise extent of laminarization, $(x/c)_L$.

Figure 75 illustrates the increase in LFC system weight with increasing $(x/c)_L$. Aircraft gross weight is observed to decrease up to a value of $(x/c)_L = 0.60$ and increase rapidly as laminarization is extended behind this location. This is consistent with the trend of wing area and wing loading shown in figure 76, and is a direct result of the smaller wing box volume available for fuel at values of $(x/c)_L$ greater than 0.60.

The variation of LFC fuel, block fuel, and DOC with $(x/c)_L$ is shown in figure 77. As would be expected, the fuel consumed by the LFC engines approximates a linear increase with increasing $(x/c)_L$. However, this figure shows that both aircraft block fuel and DOC are minimized by values

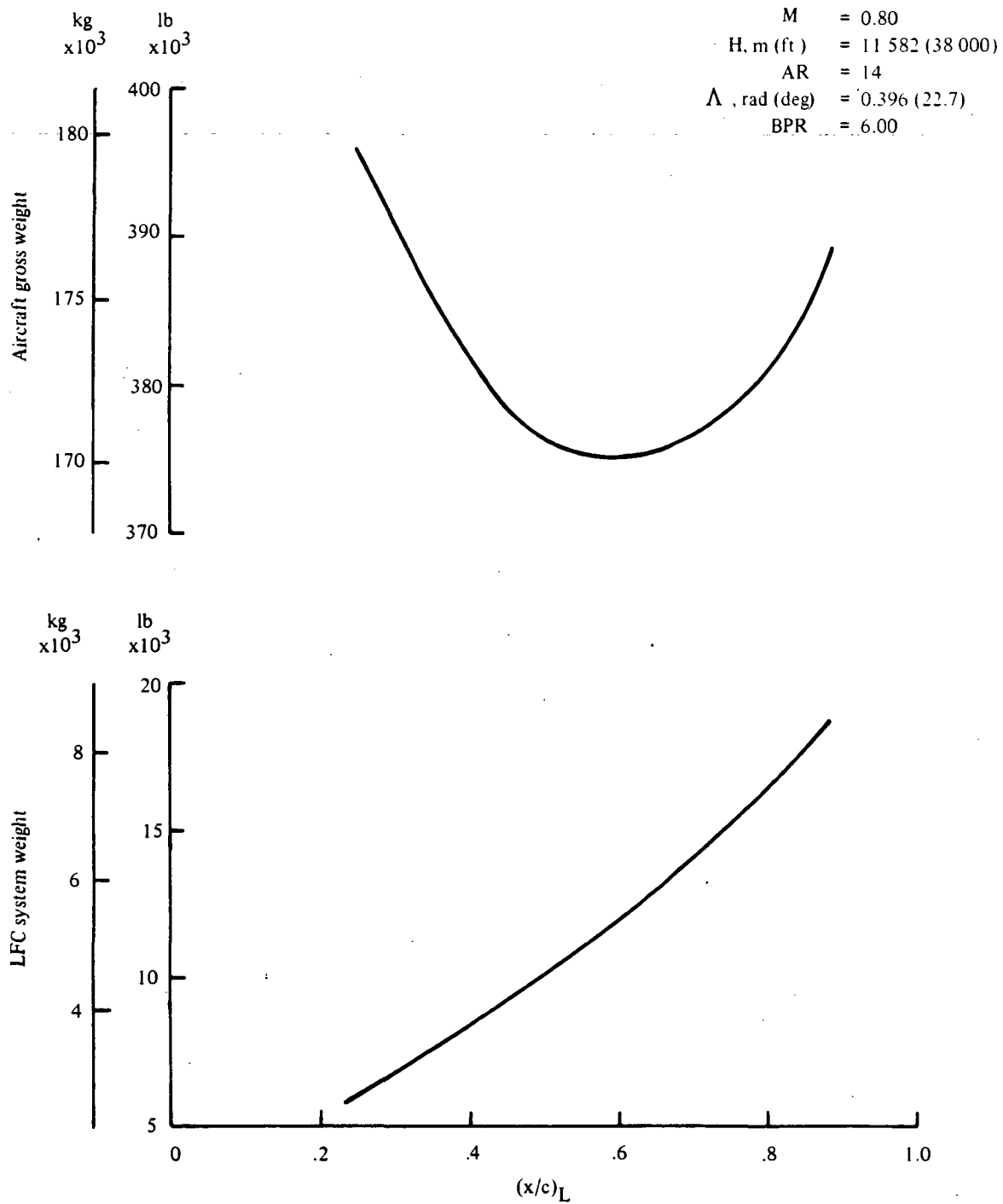


Figure 75. — Weight parameters vs. chordwise extent of laminarization

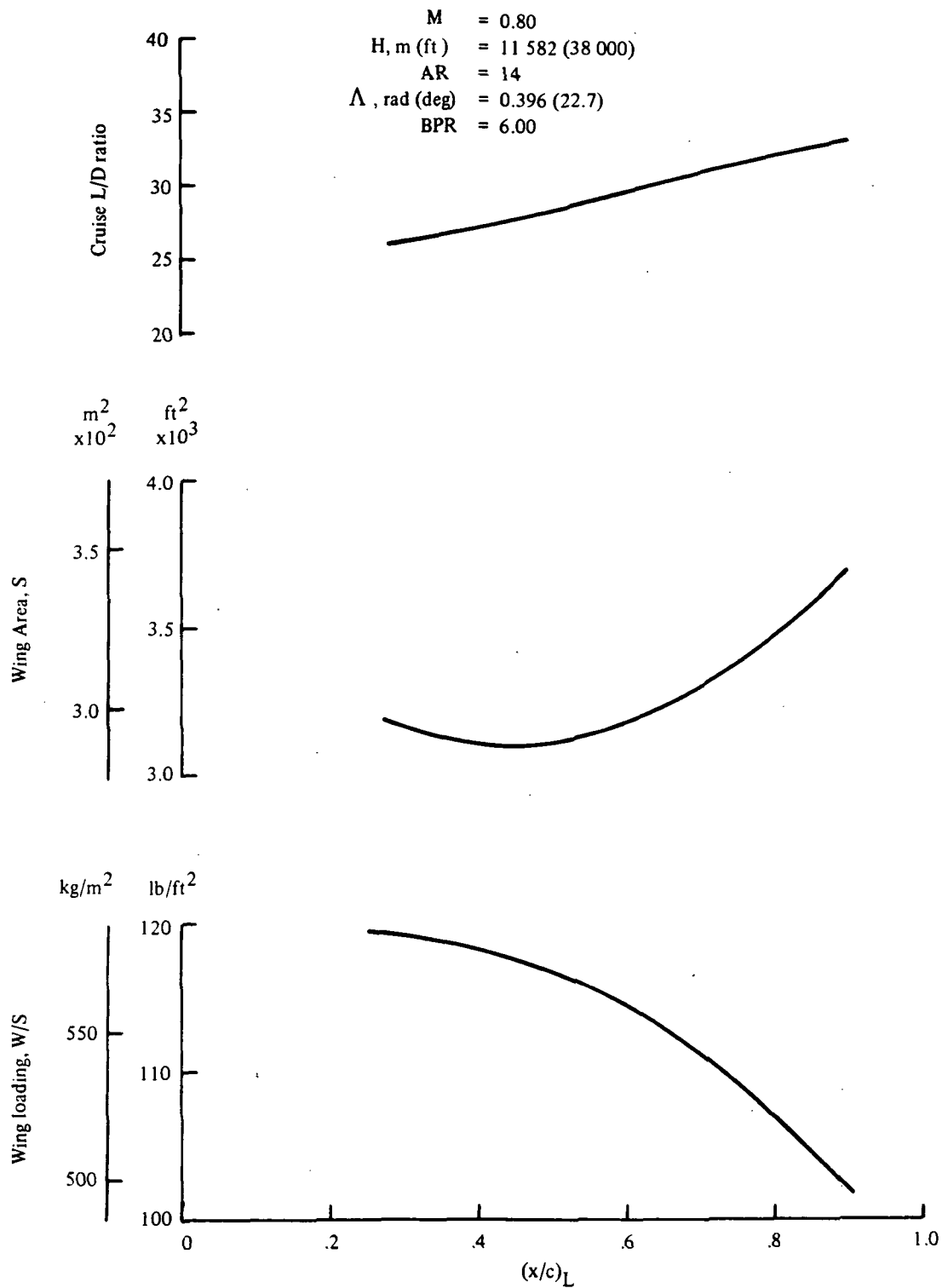


Figure 76. — Wing parameters vs. chordwise extent of laminarization

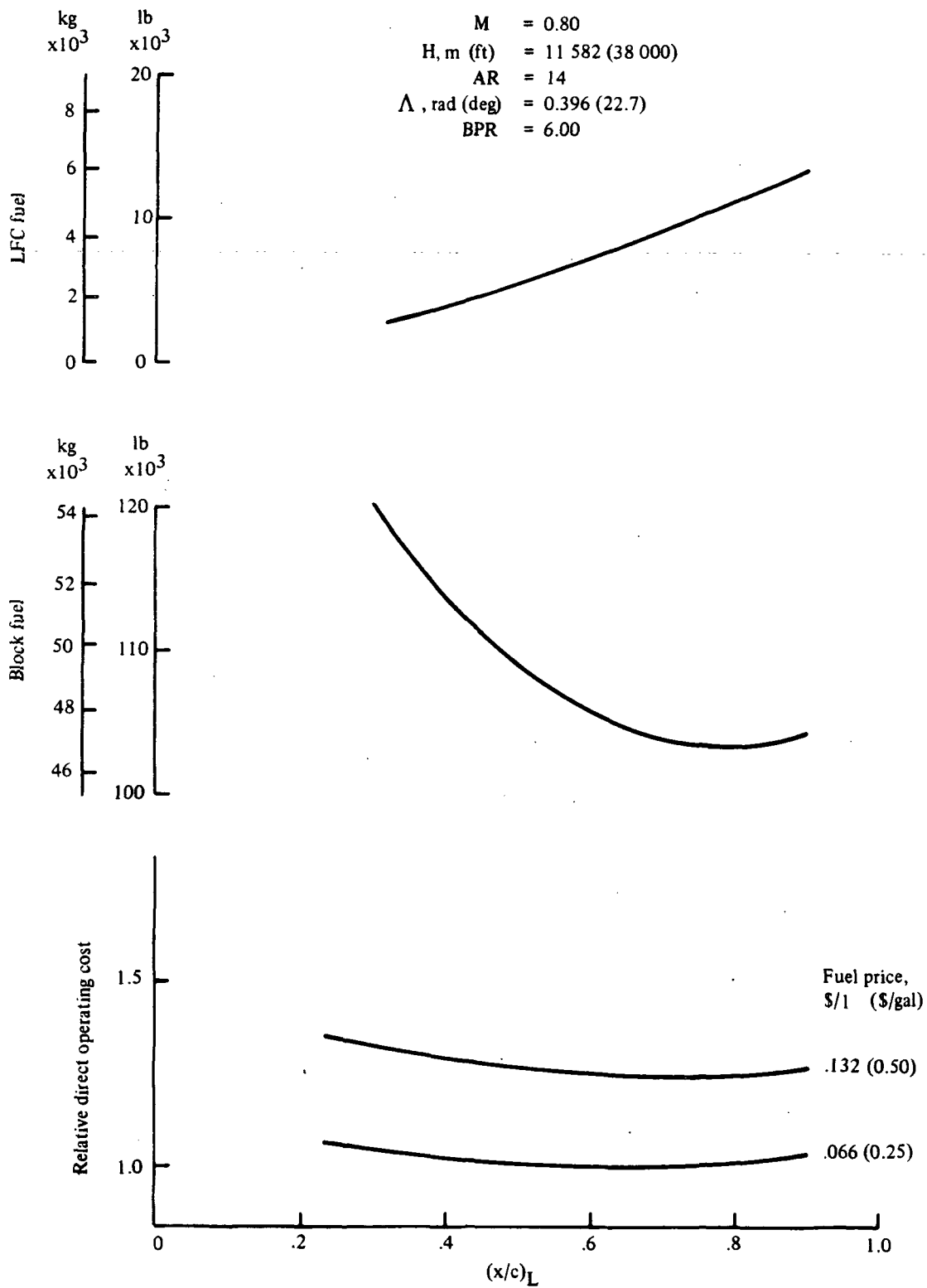


Figure 77. — Fuel and cost parameters vs. chordwise extent of laminarization

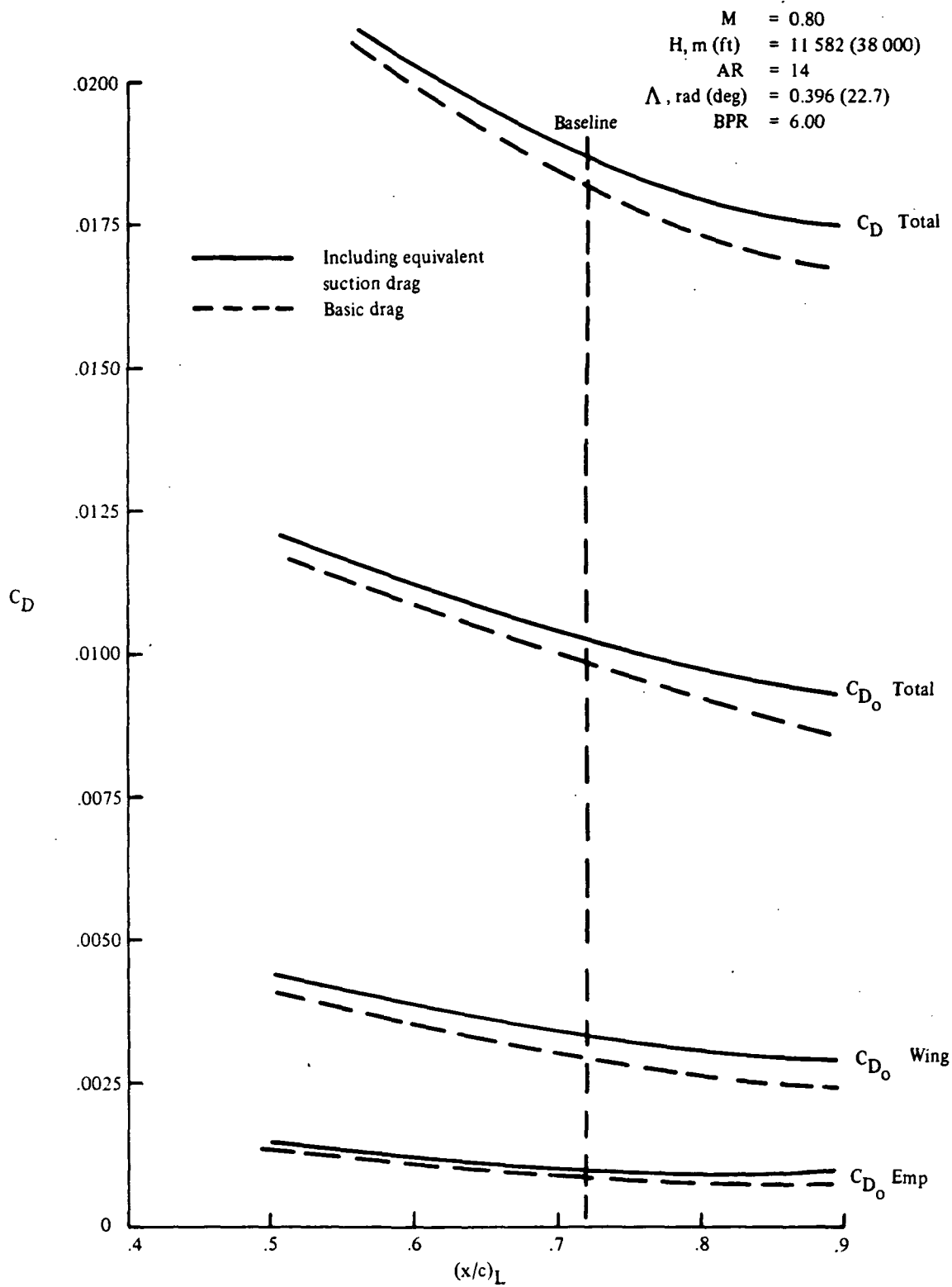


Figure 78. — Aircraft drag coefficients, C_D , vs. chordwise extent of laminarization

$M = 0.80$
 $H, m (ft) = 11\ 582 (38\ 000)$
 $AR = 14$
 $\Lambda, rad (deg) = 0.396 (22.7)$
 $BPR = 6.00$

Includes equivalent suction drag

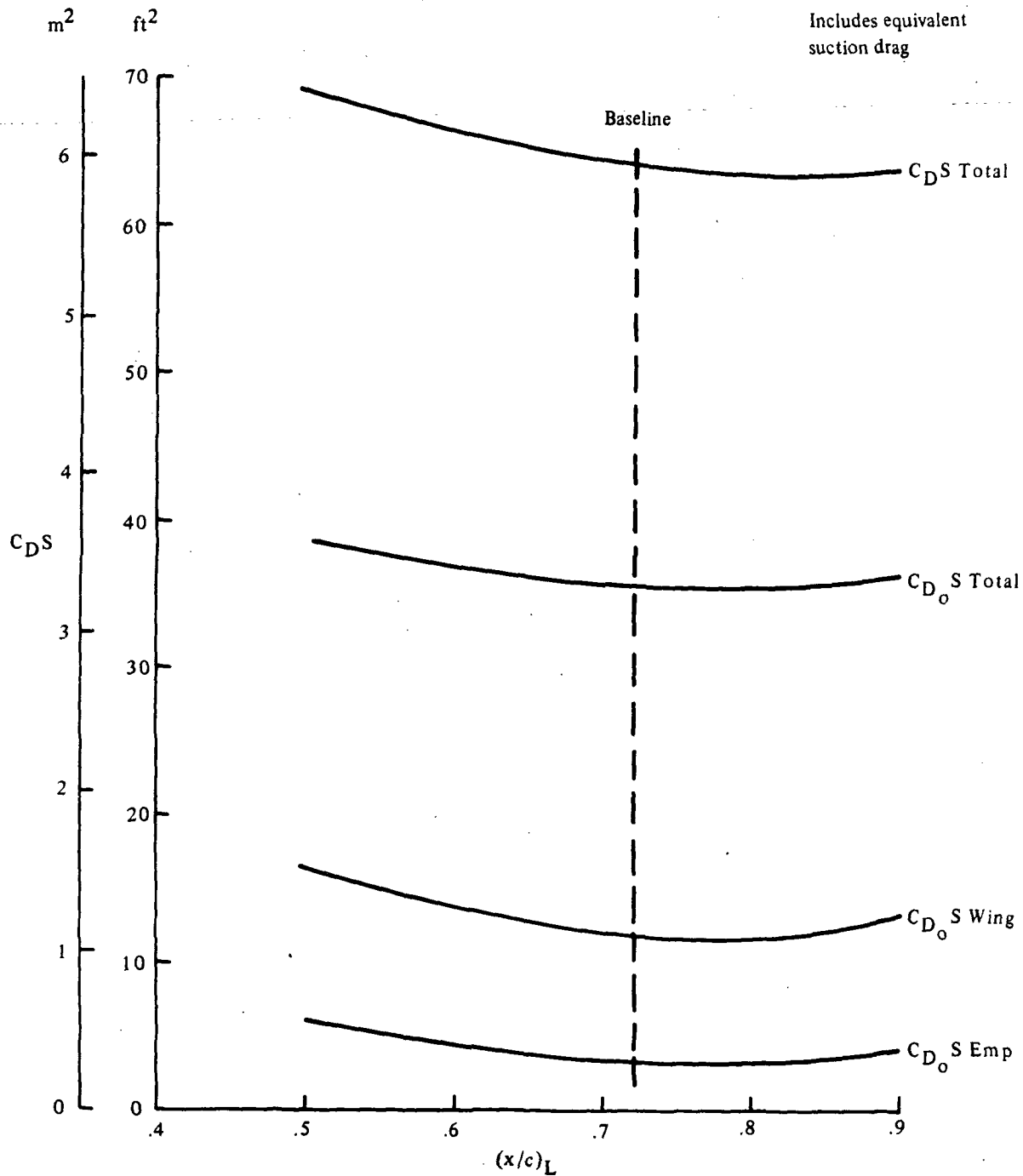


Figure 79. — $C_D S$ vs. chordwise extent of laminarization

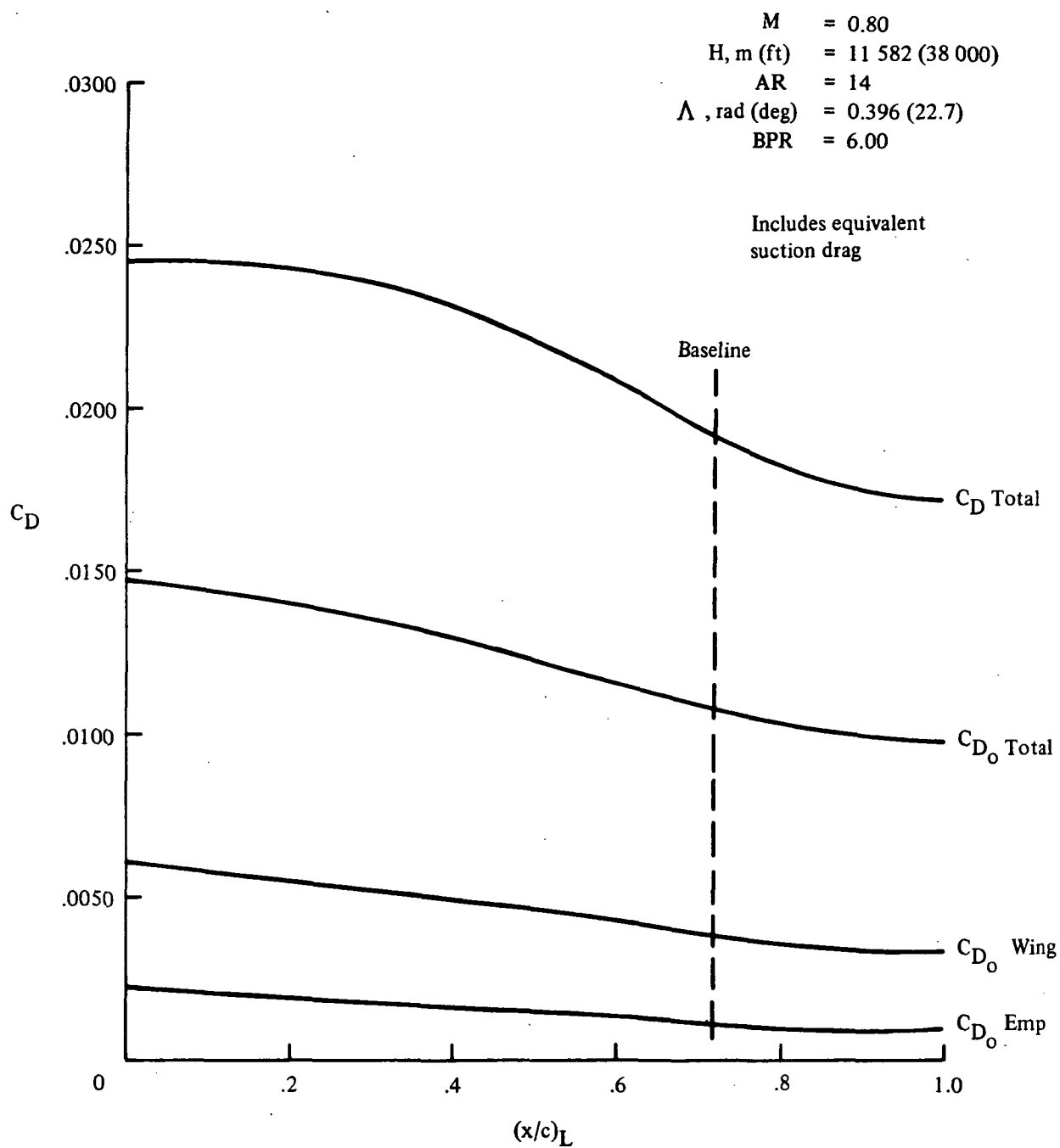


Figure 80. — Aircraft drag coefficients, C_D , vs. chordwise extent of laminarization from 0 to 1.0

of $(x/c)_L$ which are well below the maximum values evaluated. The minimum block fuel is achieved at $(x/c)_L = 0.78$ and minimum DOC occurs at values of $(x/c)_L$ ranging from 0.62 to 0.74, depending on the assumed fuel price.

Reference to the aircraft gross weight curve in figure 75 and the drag data presented in figures 78 and 79 explains this behavior of both block fuel and DOC. As shown in figure 78, drag coefficients for all aircraft elements decrease as $(x/c)_L$ is increased, although the rate of decrease slows as laminarization is extended behind $(x/c)_L = 0.75$. However, since the reference wing area must increase as $(x/c)_L$ is increased, aircraft drag decreases at an even lower rate. In figure 79, the product $C_D S$ is shown as a function of $(x/c)_L$. This figure shows that, although C_D continues to decrease with increasing $(x/c)_L$, aircraft drag increases for $(x/c)_L$ greater than 0.78.

Thus, in view of the very small decrease in block fuel achieved by extending laminarization from 0.72 to 0.78, the minimization of DOC at $(x/c)_L$ of 0.62 to 0.74, and the uncertainty of laminarizing through the shock, it appears that the nominal value of $(x/c)_L = 0.72$ selected for the baseline configuration is near optimum.

For purposes of comparison, figure 80 shows the decrease in C_D realized by the baseline LFC aircraft as compared to a turbulent configuration of the same geometry.

7.4 CONFIGURATION VARIATIONS

The parametric configuration analyses of section 5.2 indicated that the fuel efficiency of LFC aircraft may be improved by the following configuration changes:

- (1) Higher aspect ratio
- (2) Higher wing loading
- (3) Greater laminarized area
- (4) More efficient LFC system components

Design constraints which define limiting values for each of these factors and approaches to relaxing such constraints are discussed in the narrative which follows.

Aspect Ratio – Parametric study results indicate the potential for improved aircraft fuel efficiency by selecting an aspect ratio greater than the value of 14 used for the LFC baseline configuration defined in section 7.2. However, in addition to the structural uncertainties involved in postulating higher aspect ratios for conventional aircraft configurations, wing volume available for ducting and fuel places a practical limit of 14 on wing aspect ratio. Since this aspect ratio dictates the use of

multiple wing-mounted LFC engines and severely constrains design variations in the ducting and distribution system, it may be advantageous to select a lower aspect ratio to gain flexibility in the location of LFC engines and compressors and improved ducting efficiency.

Wing Loading — As a result of fuel volume limitations, wing loading for the LFC baseline configuration was limited to a maximum value of 537 kg/m^2 (110 lb/ft^2). The parametric analyses of section 5.2 indicate the potential for improved fuel efficiency with increases in wing loading to values greater than 683 kg/m^2 (140 lb/ft^2).

Fuel volume for a given configuration may be increased by selecting an airfoil permitting greater thickness-to-chord ratio, increasing wing sweep, or using external fuel. The modified supercritical airfoil employed on the LFC baseline provides the greatest thickness-to-chord ratio available for the design cruise speed. Increasing wing sweep is undesirable from the standpoint of LFC system requirements. Therefore, the use of external fuel offers the greatest promise in this area. Consequently, three concepts for augmenting wing fuel capacity are considered:

- (1) Wing tip tanks
- (2) Faired anti-drag body tanks
- (3) External pods with adequate volume for both landing gear stowage and fuel.

Laminar Area — The extent of effective laminarization on the LFC baseline configuration was limited by the following:

- (1) Wing upper surface
 - o Shock location at $x/c = 0.72$
 - o Surface discontinuities at $x/c = 0.75$ resulting from control surfaces and high-lift devices
- (2) Wing lower surface
 - o Surface discontinuities at $x/c = 0.75$ chord resulting from control surfaces and high-lift devices
 - o Laminar area lost due to flap-track fairings
 - o Laminar area lost due to LFC engines and compressors
 - o Laminar area lost due to landing gear doors.

Approaches to extending the limits outlined above include the following:

- (1) Alternative airfoil sections to eliminate shock

- (2) Laminarization behind shock
- (3) The use of 15%-chord trailing-edge devices rather than the 25%-chord devices employed on the LFC baseline configuration
- (4) Location of LFC engines and compressors in the fuselage to minimize laminar area lost on the wing lower surface
- (5) Stowage of landing gear in wing-mounted pods to minimize laminar area lost on the wing lower surface.

LFC System Components – The characteristics and locations of LFC system elements on the LFC baseline were dictated by the limited wing volume available for fuel and ducting. The use of external fuel, along with a possible decrease in aspect ratio, permits consideration of alternative LFC system arrangements which may provide both weight reduction and improvement of system efficiency.

Variations in LFC system configurations include the following:

- (1) Fuselage-mounted LFC engines and compressors
- (2) Integration of LFC engines and compressors with a fuselage slot injection system
- (3) Integration of LFC engines with the primary propulsion system
- (4) Improvement of duct efficiency
- (5) Lower wing sweep
- (6) Application of lightweight LFC surfaces.

Detailed descriptions of LFC system concepts are presented in section 6.0. The remainder of this section is devoted to a discussion of potential aircraft configuration variations.

7.4.1 FUSELAGE-MOUNTED SUCTION UNITS

Available laminar area is increased and overall LFC system complexity is reduced through the use of two fuselage-mounted LFC suction units rather than the five wing/empennage mounted units required on the baseline configuration. A representative installation of such units is shown schematically in figure 81.

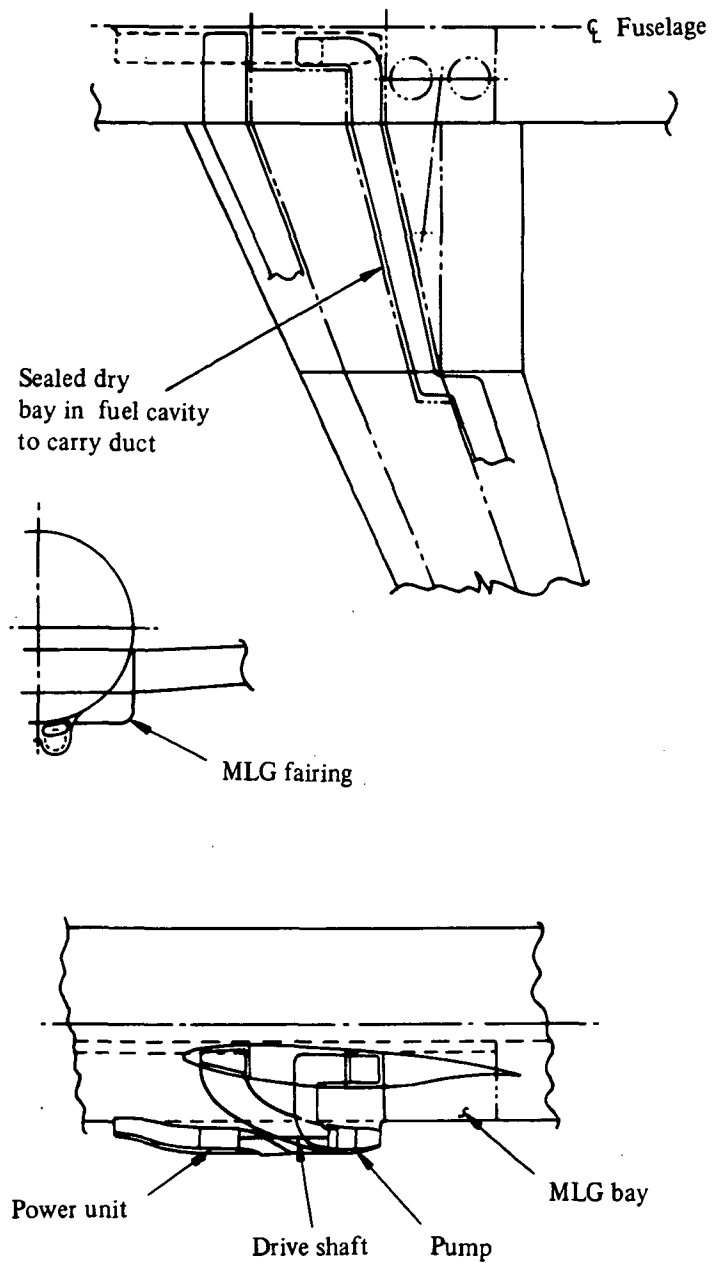


Figure 81. — Schematic of fuselage-mounted LFC suction units

Two properly sized units are installed beneath the fuselage, one either side of the vertical centerline, in pods providing the generator ram-air inlets, and the required exhaust ducts. Suction air is carried through the trunk ducts in the wing leading and trailing edges to the pump low- and high-pressure inlets. The trailing-edge trunk duct must be jogged through the rear spar into spanwise and chordwise dry-bays in the inboard fuel cells in order to retain the space necessary for installing the main landing gear in a normal mounting position.

7.4.2 EXTERNAL LANDING-GEAR PODS

In order to avoid taking the trailing edge trunk duct into the inboard fuel tank, the use of a pod-mounted main landing gear was explored. As shown in figure 82, the main landing gear is installed beneath the rear spar in a pivot joint with a drag link connected to a fitting beneath the front spar.

The gear retracts aft into a faired pod as shown. To minimize the gear profile when retracted, it is expedient to hinge the strut piston in the stowed position, thus introducing additional complication in the gear design in the form of an additional piston and locks. A minimum profile pod is faired into the wing as shown in figure 82.

7.4.3 EXTERNAL LANDING-GEAR/FUEL-TANK PODS

The external landing-gear pod provides another method of storing external fuel. As shown in figure 83, the landing gear pod is extended in length to provide volume for approximately 4536 kg (10,000 lb) of fuel. The fuel is carried in cantilevered cells above and aft of the stowed main landing gear.

This main landing-gear pod/external-tank configuration allows the trailing edge suction duct to be carried into the wing center section to the pump pod without piercing the rear spar and lower wing skin as shown in figure 81 for the two-pump configuration described in section 7.4.1.

7.4.4 EXTERNAL FUEL TANKS

Several configurations for external fuel tankage were explored to determine the most feasible method of supplementing internal wing tankage.

7.4.4.1 Tip Tank

A conventional tip tank is shown in figure 84. This tank is installed to a closure rib and the wing spars at the wing tip. The tank is sized to accommodate approximately 4536 kg (10,000 lb) of fuel, with the necessary fuel lines, valves, and fuel quantity probes required for filling and fuel transfer.

Length = 10.4 m (34.2 ft)
Width = 1.7 m (5.7 ft)
Height = 2.5 m (8.3 ft)
 $A_{wet} = 54.8 \text{ m}^2 (590 \text{ ft}^2)$

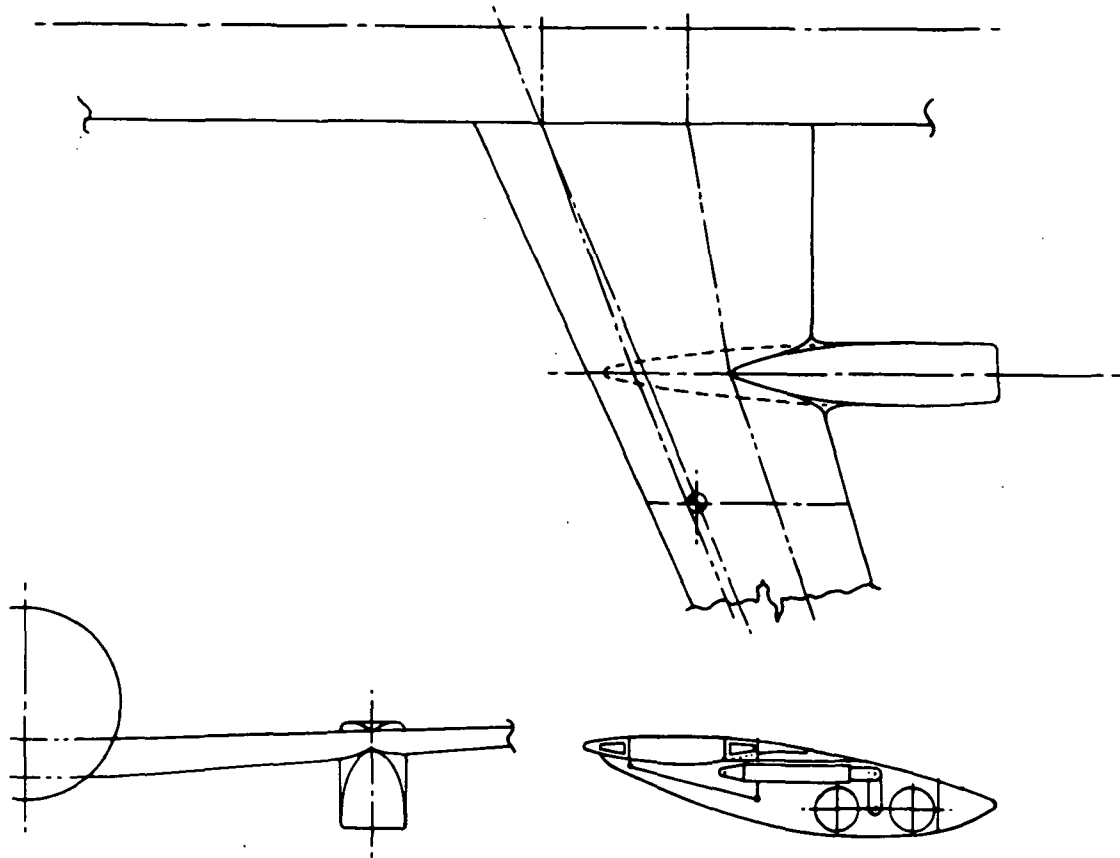


Figure 82. — Schematic of external landing-gear pod

7.4.4.2 Faired Anti-Drag Body Tank

Since the basic LFC wing design requires externally-mounted hinges and actuators for flaps and ailerons, their fairings afford space for storing external fuel. The size of the flap hinge/actuator fairing is increased in length, as shown in figure 85, to carry approximately 476 kg (1050 lb) of fuel. Five such pods are required per wing, thus providing 4760 kg (10,500 lb) external fuel capacity.

Length = 12.1 m (39.8 ft)
Width = 1.7 m (5.7 ft)
Height = 2.8 m (9.3 ft)
Awet = 74.3 m² (800 ft²)

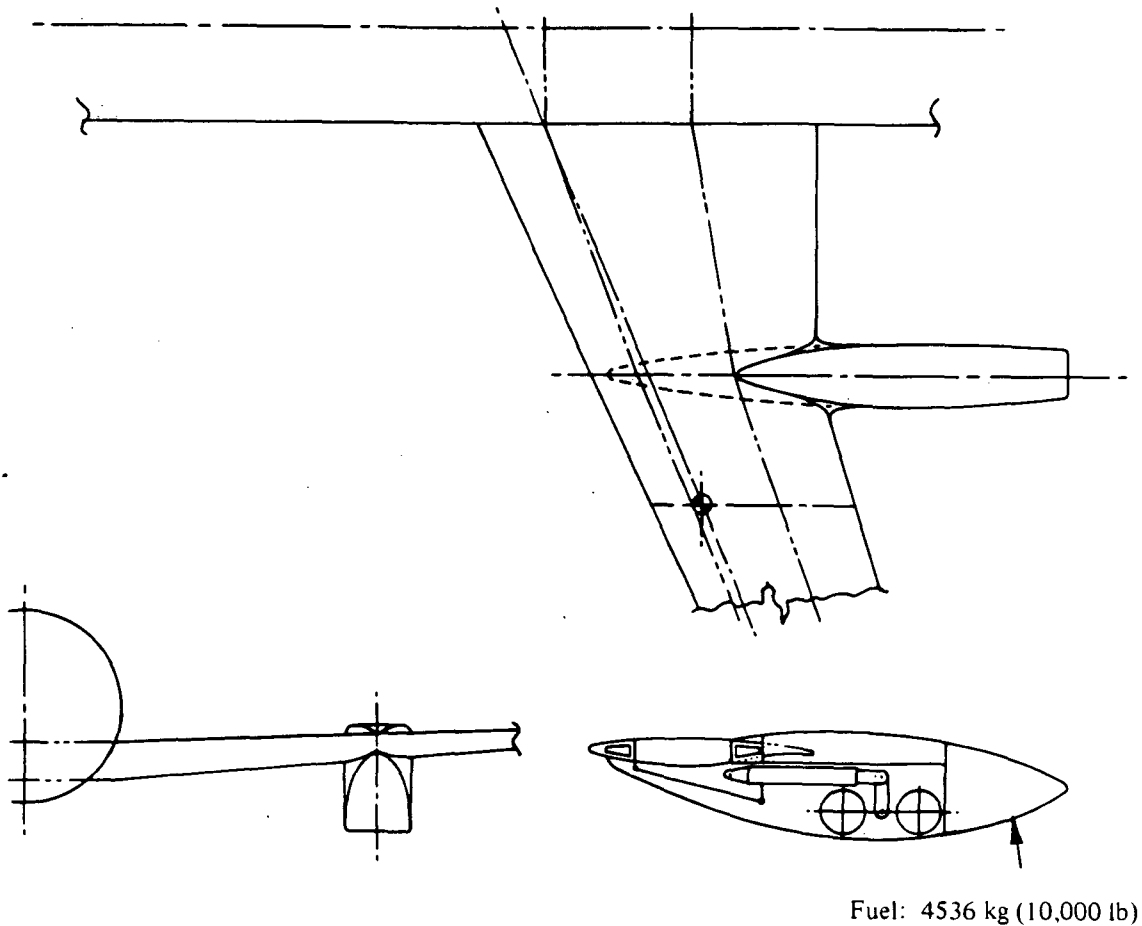


Figure 83. — Schematic of external landing-gear/fuel pod

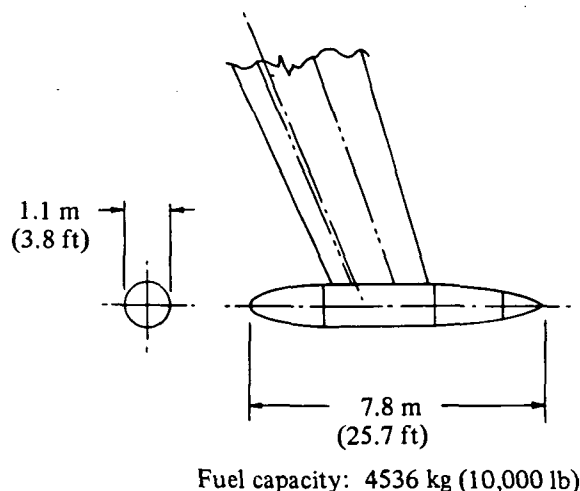


Figure 84. — Schematic of wing-tip fuel tank

7.4.5 FUSELAGE SLOT INJECTION

To provide for forward fuselage slot injection, it is necessary for the suction pump/power generator unit to be installed in the fuselage and wing root areas as shown in figure 86. The power generator unit is slung beneath the fuselage belly and mounted under the front spar. The generator is provided with pod enclosed ram inlet and exhaust ducts as shown. A forward extending shaft drives the suction pump through a series of right-angle gear boxes so that the pump and its ducting is within the fuselage pressure shell, thus minimizing structural penalties for the installation.

Suction pump exhaust air is ducted through the fuselage belly into a sealed plenum at the proper forward fuselage location. This sealed plenum is formed by two heavy fuselage frames with a plate on the interior flanges and the fuselage pressure skin on the exterior side, as shown in figure 87. To minimize structural penalties incurred by piercing the pressure vessel, stringers are carried through the plenum, and sealed at the cutouts in the fuselage frames.

To provide continuous blowing into the boundary layer, a series of sixty-three coalescing nozzles are installed on the fuselage skin and supported by stringer and frame caps. Exhaust air from the pumps pressurizes the plenum and then is injected into the boundary layer through these nozzles. A complete fuselage ring fairing is installed over the nozzles as shown.

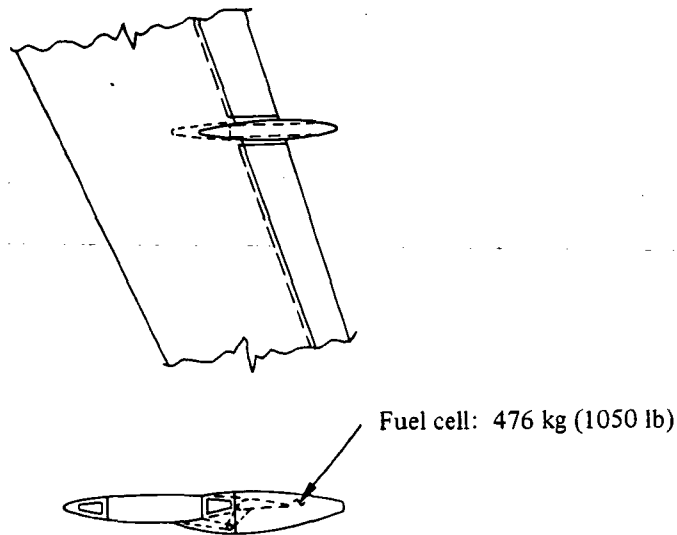


Figure 85. — Schematic of flap-fairing/fuel pod

7.4.6 RELAXED STATIC STABILITY

In sizing the vertical and horizontal tails of configurations employing relaxed static stability, adequate requirements for engine-out control, pitch acceleration capability, and yaw acceleration capability were imposed. Criteria used for sizing the empennage of both normal and RSS configurations are summarized in table 13.

TABLE 13. CRITERIA FOR NORMAL AND RELAXED STATIC STABILITY

Type stability	Aft C.G. (x/c) MAC	Approximate forward C.G. (x/c) MAC	Yaw acceleration control (rad/sec ²)	Pitch acceleration control (rad/sec ²)	Type rudder
Normal	.40	.11	.116	.265	Single - Hinged
Relaxed	.50	.19	.116	.265	Double - Hinged

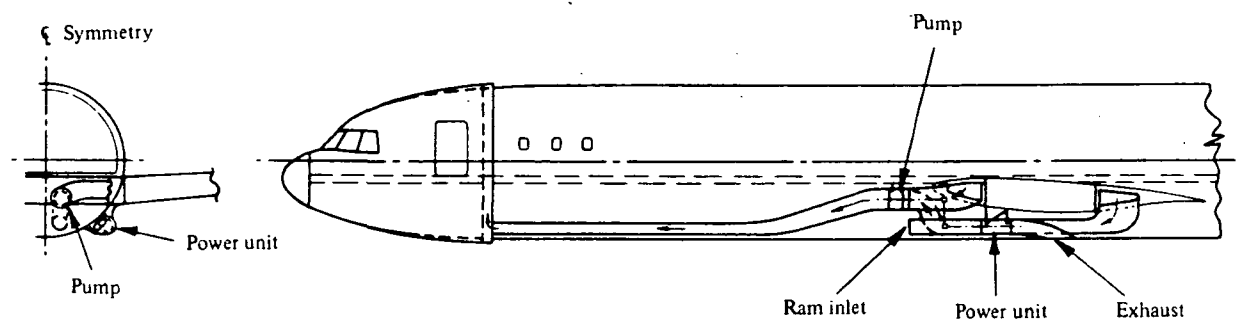


Figure 86. — Schematic of LFC suction pump installation for fuselage slot injection

For all RSS configurations, a 0.3 c double-hinged rudder was used to ensure sufficient control to trim engine-out yawing moment. For configurations with all primary propulsion engines mounted on the fuselage, engine-out control was non-critical. All RSS configurations use a 0.25 c single-hinged elevator with variable incidence for trim.

7.5 CONFIGURATION EVALUATIONS

7.5.1 EVALUATION PROCEDURE

The LFC system concepts described in section 6.0 and the aircraft configuration variations of section 7.3 were evaluated through variations of the LFC-200-S baseline configuration. The following procedure was used in the evaluation of each concept:

- (1) Development of design layouts to define concept geometry and interfaces with other configuration elements.
- (2) Calculation of weight increments
- (3) Calculation of variations in laminar area
- (4) Calculation of drag increments
- (5) Definition of LFC system components
- (6) Modification of the LFC baseline configuration as required to accommodate the concept.

Upon completion of these steps, the resulting configuration was exercised in the GASP to define the optimum point-design configuration compatible with mission requirements.

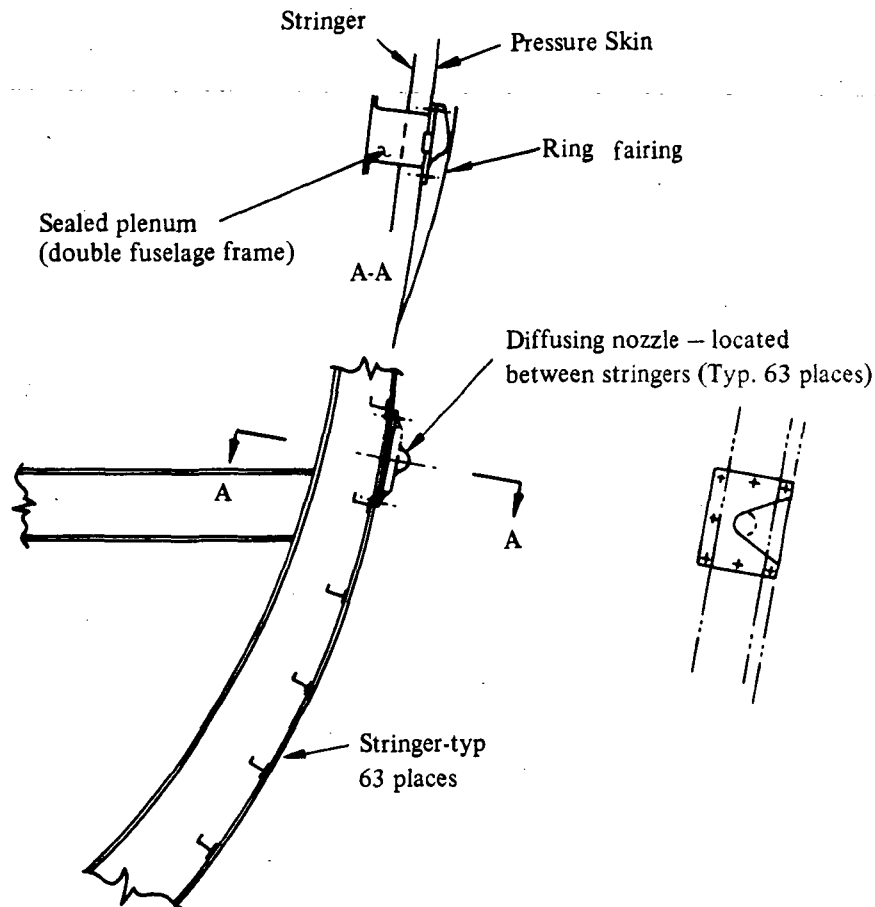


Figure 87. — Schematic of fuselage slot

7.5.2 DESIGN CONSTRAINTS

The parametric results of section 5.2 indicate that maximum fuel efficiency in LFC aircraft is achieved by selecting the highest practical aspect ratio. However, the selection of a lower aspect ratio is required to gain flexibility in the location of LFC system components. Wing volume constraints of the LFC baseline configuration are such that neither the number or location of the LFC engine/compressor units may be changed without incurring a significant decrease in fuel efficiency.

$W/S, \text{ kg/m}^2 (\text{lb/ft}^2) = 537 (110)$
 $\Lambda, \text{ rad (deg)} = 0.396 (22.7)$
 $t/c = 0.1216$

LFC surface 3%-75% c
 two fuselage-mounted
 LFC engines

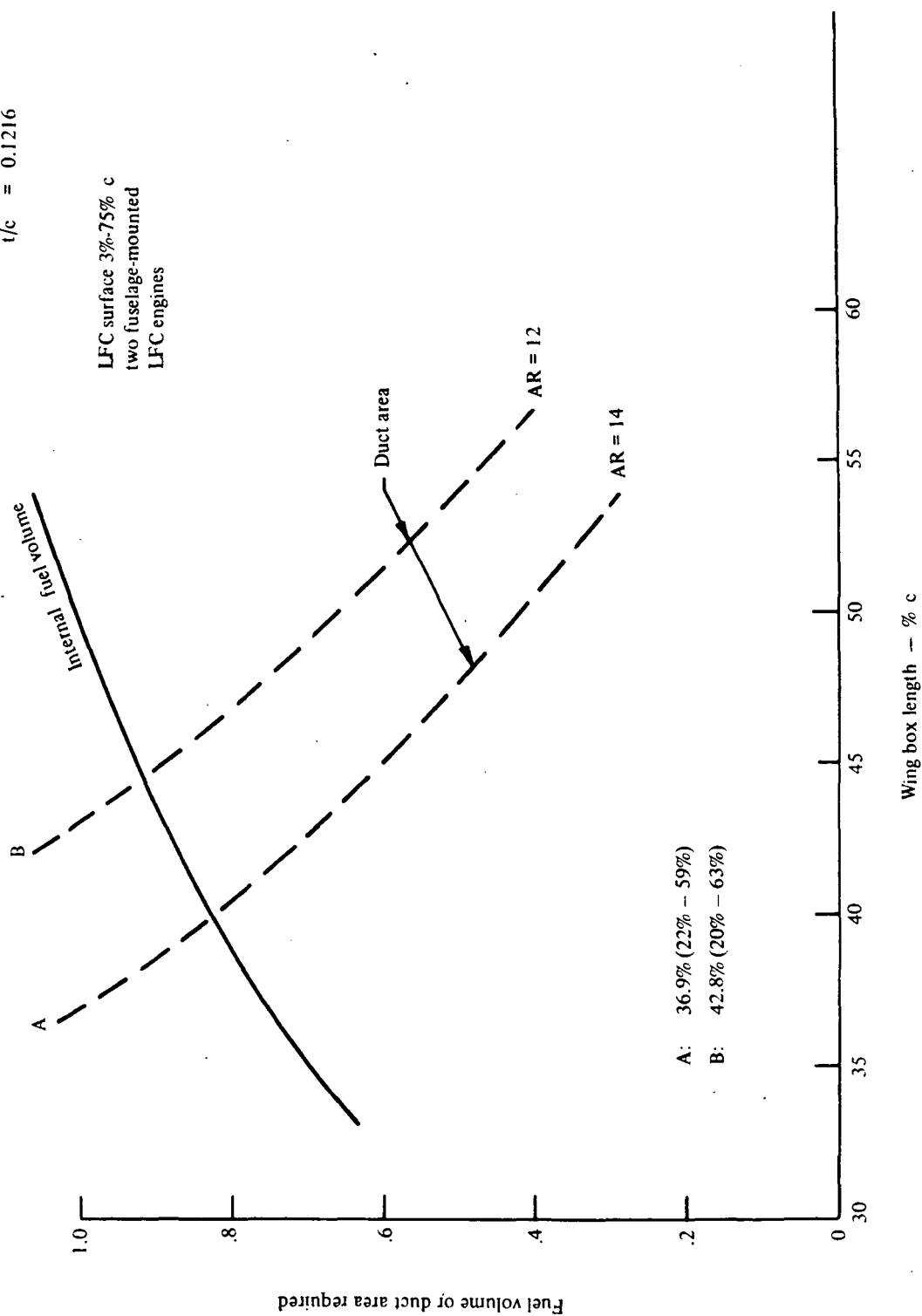


Figure 88. — Variation of duct area and fuel volume with wing box length

Since several of the LFC concepts of section 6.0 require integration of the LFC engines with other aircraft systems, greater access to the LFC engines must be provided than is available in the baseline configuration. Except for very low aspect ratio wings, which incur prohibitive penalties in fuel efficiency, adequate access to the LFC engines is achieved only by locating the engines in the wing-root region or the fuselage. Figure 88 shows the relation of fuel volume requirements, duct volume requirements, and wing spar locations for aspect ratios of 12 and 14. As shown by this figure, the duct volume necessary for location of the LFC engines in the fuselage requires a decrease in the wing box size and the use of external fuel to compensate for the attendant reduction in fuel volume. The relative penalty in wing weight which results from the reduction in spar separation is shown in figure 89.

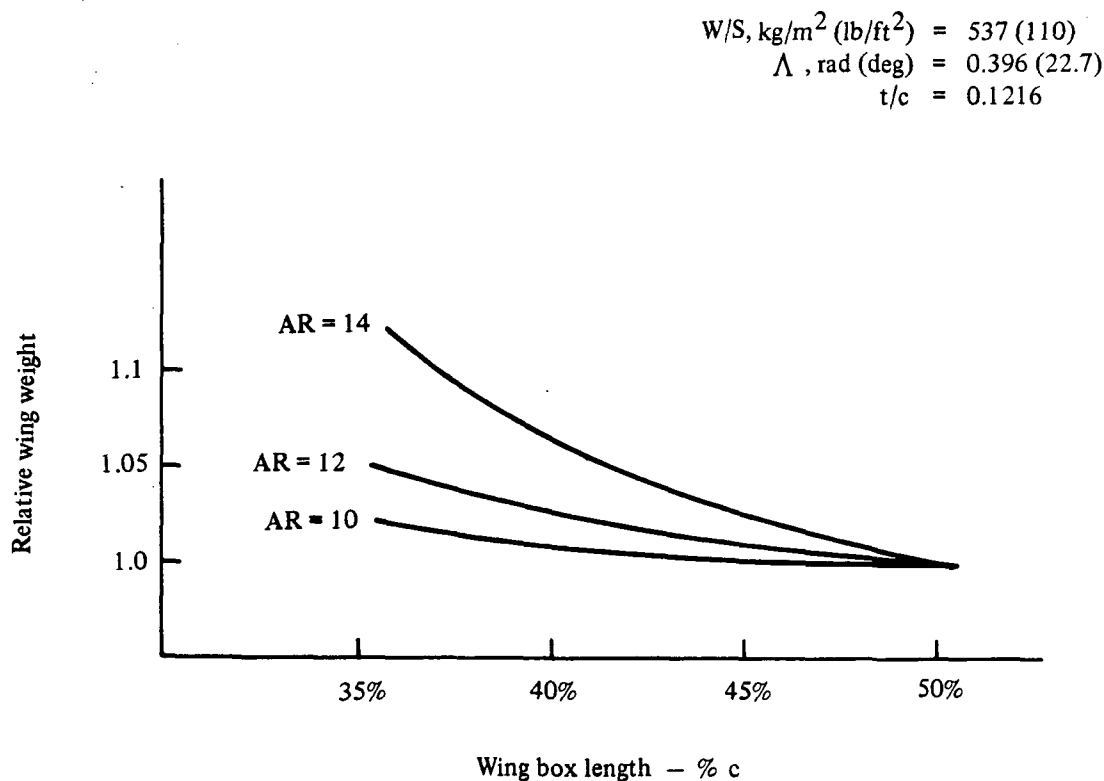


Figure 89. — Variation of wing weight with wing box length

7.5.3 CONFIGURATION SUMMARY

Figure 90 summarizes the characteristics of the configurations evaluated and outlines the sequence in which the variations were conducted. It should be observed that configurations LFC-200-S-2 through LFC-200-S-7 have an aspect ratio of 12, while all other configurations have an aspect ratio of 14. Summaries of configuration characteristics are presented in figures 91 through 104. Pertinent observations for each configuration follow.

LFC-200-S-1 – For the purposes of this evaluation, the LFC baseline configuration developed in section 7.2 is designated as LFC-200-S-1. Figure 91 summarizes configuration characteristics.

LFC-200-S-2 – Other than a reduction in aspect ratio from 14 to 12, this configuration is identical to the baseline. Figure 92 shows that this change results in a reduction of 4000 kg (8819 lb) in aircraft gross weight but increases fuel consumption by 901 kg (1986 lb).

LFC-200-S-3 – This configuration, described in figure 93, employs two fuselage-mounted LFC engines, rather than the five wing/tail mounted LFC engines used on the baseline configuration. As discussed in section 7.3, provision of adequate volume for the full-span trunk ducts requires relocation of the wing spars from $x/c = 0.15$ and 0.65 to $x/c = 0.20$ and 0.63 . The landing gear of this configuration is stowed in the wing root and fuselage. Volume behind the rear spar is inadequate for both landing gear and the aft trunk duct. The aft trunk duct penetrates the rear spar at 0.31 semispan and runs through the wing box inboard of this point to the LFC engines. The additional reduction in fuel volume negates the benefits of the external tanks with the result that wing loading is reduced to 513 kg/m^2 (105 lb/ft^2). This increases fuel consumption by 1181 kg (2604 lb) over that of the baseline configuration.

LFC-200-S-4 – With the goal of using two fuselage-mounted engines without penetrating the rear spar and running a trunk duct through the wing box, this configuration uses underwing pods for landing gear stowage and additional fuel volume. This allows an increase in wing loading to 559 kg/m^2 (114.5 lb/ft^2). However, performance is penalized by the weight and drag of the external pods to the extent that this configuration requires 2738 kg (6037 lb) more fuel than the baseline. A configuration summary is presented in figure 94.

LFC-200-S-5 – Rather than the 9072 kg (20,000 lb) of external fuel provided by the underwing pods of the previous configuration, this variation employs both pods and tip tanks for a total of 18,144 kg (40,000 lb) of external fuel. While this additional fuel volume permits an increase in wing loading to 614 kg/m^2 (125.8 lb/ft^2) with an attendant decrease in wing area and LFC system weight, the weight and drag penalties of the pods and tanks results in an increase of 2263 kg (4990 lb) of block fuel. Figure 95 summarizes configuration characteristics.

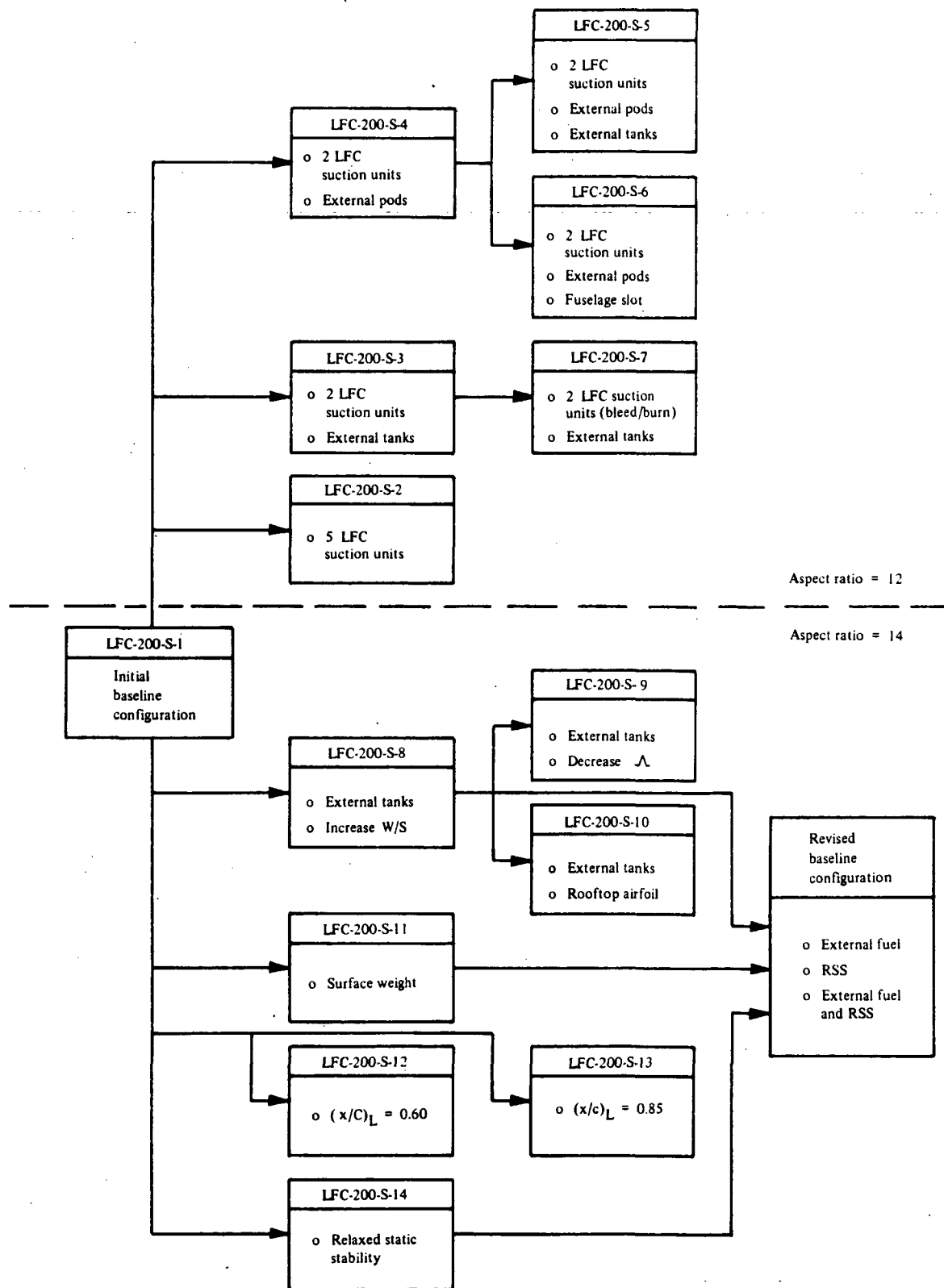


Figure 90. — Sequence of configuration variations LFC-200

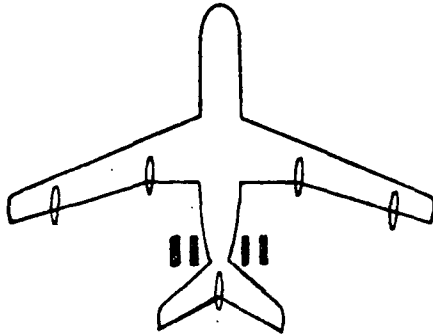
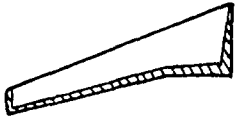
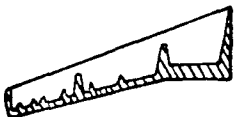


LFC-200-S-1		
Configuration Variations	External Fuel, kg (lb)	0
Initial baseline		
CONFIGURATION		CONFIGURATION SUMMARY
		<u>AIRCRAFT</u>
		Aspect ratio 14
		Wing loading, kg/m ² 537
		(lb/ft ²) 110
		Wing area, m ² (ft ²) 309 3327
		Wing sweep, rad (deg) 0.396 22.7
		Wing t/c 0.1216
		Front spar x/c 0.15
		Rear spar x/c 0.65
		Gross weight, kg (lb) 171,218 377,464
		Empty weight, kg (lb) 86,845 191,457
		<u>FLIGHT</u>
		Cruise power ratio 0.80
		Cruise L/D 31.16
LAMINARIZATION		<u>LFC SYSTEM</u>
	(x/c) _L η _L	Engines 5
	0.72 0.97	Surface weight, kg/m ² 7.323
	0.75 0.87	(lb/ft ²) 1.50
	0.75 0.95	Weights, kg (lb)
	0.75 0.96	Engines 1155 2546
		Installation 1432 3156
		Surfaces 3750 8 268
		Ducting 313 691
		Total 6650 14,661
		<u>BLOCK FUEL</u>
		Primary engines, kg (lb) 42,356 93,377
		LFC engines, kg (lb) 4,546 10,022
		Total, kg (lb) 46,902 103,399

Figure 91. — Configuration summary, LFC-200-S-1

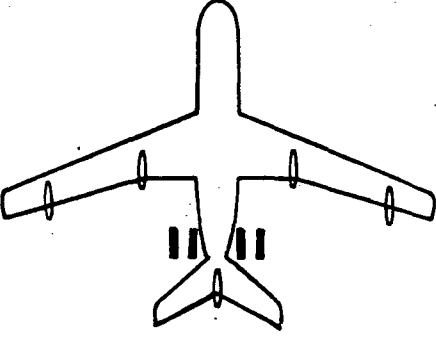

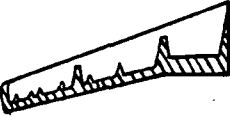


LFC-200-S-2		
Configuration Variations	External Fuel, kg (lb)	0
(1) Aspect ratio		
CONFIGURATION		CONFIGURATION SUMMARY
		<u>AIRCRAFT</u>
		Aspect ratio 12
		Wing loading, kg/m ² 537
		(lb/ft ²) 110
		Wing area, m ² (ft ²) 302 3252
		Wing sweep, rad (deg) 0.396 22.7
		Wing t/c 0.1208
		Front spar x/c 0.15
		Rear spar x/c 0.65
		Gross weight, kg (lb) 167,217 368,645
		Empty weight, kg (lb) 81,909 180,576
		<u>FLIGHT</u>
		Cruise power ratio 0.83
		Cruise L/D 29.07
LAMINARIZATION		<u>LFC SYSTEM</u>
	(x/c) _L η_L	Engines 5
	0.72 0.97	Surface weight, kg/m ² 7.323
		(lb/ft ²) 1.50
	0.75 0.85	Weights, kg (lb)
	0.75 0.95	Engines 1119 2468
	0.75 0.96	Installation 1388 3059
		Surfaces 3590 7915
		Ducting 287 632
		Total 6384 14,074
		<u>BLOCK FUEL</u>
		Primary engines, kg (lb) 43,440 95,766
		LFC engines, kg (lb) 4,362 9,619
		Total, kg (lb) 47,802 105,385

Figure 92. — Configuration summary, LFC-200-S-2

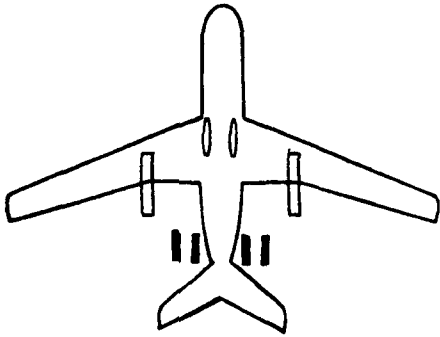
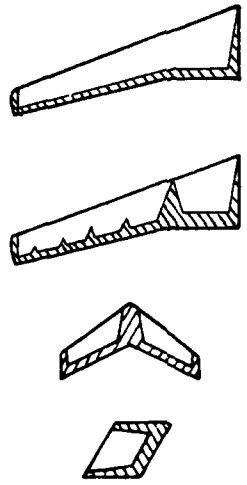
LFC-200-S-4		
Configuration Variations	External Fuel, kg (lb)	9072 (20,000)
(1) Aspect ratio		
(2) External gear/fuel pods		
(3) Two LFC engines		
CONFIGURATION 	CONFIGURATION SUMMARY	
	<u>AIRCRAFT</u>	
	Aspect ratio	12
	Wing loading, kg/m ² (lb/ft ²)	559 114.5
	Wing area, m ² (ft ²)	300 3224
	Wing sweep, rad (deg)	0.396 22.7
	Wing t/c	0.1180
	Front spar x/c	0.20
	Rear spar x/c	0.63
	Gross weight, kg (lb)	172,514 380,322
	Empty weight, kg (lb)	85,170 187,765
	<u>FLIGHT</u>	
	Cruise power ratio	0.84
	Cruise L/D	28.31
LAMINARIZATION <div> <div>(x/c)_L</div> <div>η_L</div> </div> 		
	0.72	0.97
	0.75	0.95
	0.75	0.95
	0.75	0.96
	<u>LFC SYSTEM</u>	
	Engines	2
	Surface weight, kg/m ² (lb/ft ²)	7.323 1.50
	Weights, kg (lb)	
	Engines	788 1737
	Installation	977 2153
	Surfaces	3688 8130
	Ducting	535 1180
	Total	5988 13,200
	<u>BLOCK FUEL</u>	
	Primary engines, kg (lb)	46,453 102,409
	LFC engines, kg (lb)	3,187 7,027
	Total, kg (lb)	49,640 109,436

Figure 94. — Configuration summary, LFC-200-S-4

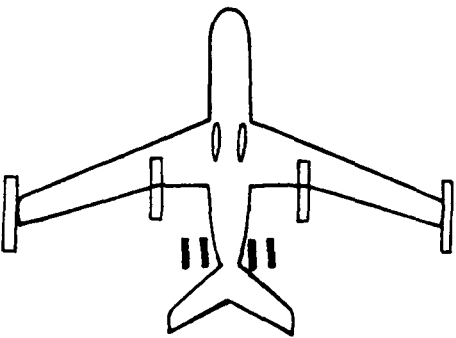

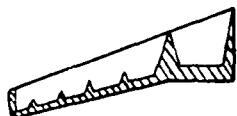


LFC-200-S-5			
Configuration Variations		External Fuel, kg (lb)	18,144 (40,000)
(1) Aspect ratio	(3) External gear/fuel pods		
(2) Wing tip tanks	(4) Two LFC engines		
CONFIGURATION		CONFIGURATION SUMMARY	
		<u>AIRCRAFT</u>	
		Aspect ratio	12
		Wing loading, kg/m ² (lb/ft ²)	614 125.8
		Wing area, m ² (ft ²)	268 2888
		Wing sweep, rad (deg)	0.396 22.7
		Wing t/c	0.1111
		Front spar x/c	0.20
		Rear spar x/c	0.63
		Gross weight, kg (lb)	169,727 374,177
		Empty weight, kg (lb)	33,061 183,115
<div>LAMINARIZATION</div> <div> <div>  </div> <div>  </div> <div>  </div> <div>  </div> </div> <div> <div>(x/c)_L</div> <div>0.72</div> <div>0.75</div> <div>0.75</div> <div>0.75</div> </div> <div> <div>η_L</div> <div>0.97</div> <div>0.95</div> <div>0.95</div> <div>0.96</div> </div>		<u>FLIGHT</u>	
		Cruise power ratio	0.81
		Cruise L/D	27.67
		<u>LFC SYSTEM</u>	
		Engines	2
		Surface weight, kg/m ² (lb/ft ²)	7.323 1.50
		Weights, kg (lb)	
		Engines	685 1511
		Installation	850 1873
		Surfaces	3236 7133
		Ducting	507 1117
		Total	5278 11,634
		<u>BLOCK FUEL</u>	
		Primary engines, kg (lb)	46,459 102,422
		LFC engines, kg (lb)	2 706 5967
		Total, kg (lb)	49,165 108,389

Figure 95. — Configuration summary, LFC-200-S-5

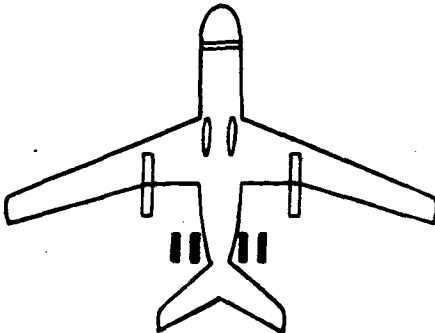
LFC-200-S-6				
Configuration Variations		External Fuel, kg (lb)	9072	(20,000)
(1) Aspect ratio	(3) Two LFC engines			
(2) External gear/fuel pods	(4) Fuselage slot			
CONFIGURATION		CONFIGURATION SUMMARY		
		<u>AIRCRAFT</u>		
		Aspect ratio	12	
		Wing loading, kg/m ² (lb/ft ²)	561 115	
		Wing area, m ² (ft ²)	302	3246
		Wing sweep, rad (deg)	0.396	22.7
		Wing t/c	0.1177	
		Front spar x/c	0.20	
		Rear spar x/c	0.63	
		Gross weight, kg (lb)	174,511	384,724
		Empty weight, kg (lb)	86,432	190,546
		<u>FLIGHT</u>		
		Cruise power ratio	0.82	
		Cruise L/D	28.84	
LAMINARIZATION		<u>LFC SYSTEM</u>		
		Engines	2	
		Surface weight, kg/m ² (lb/ft ²)	7.323 1.50	
		Weights, kg (lb)		
		Engines	623	1374
		Installation	973	2145
		Surfaces	3674	3100
		Ducting	568	1253
		Total	5838	12,873
		<u>BLOCK FUEL</u>		
		Primary engines, kg (lb)	47,990	105,799
		LFC engines, kg (lb)	2,289	5,046
		Total, kg (lb)	50,279	110,845

Figure 96. — Configuration summary, LFC-200-S-6

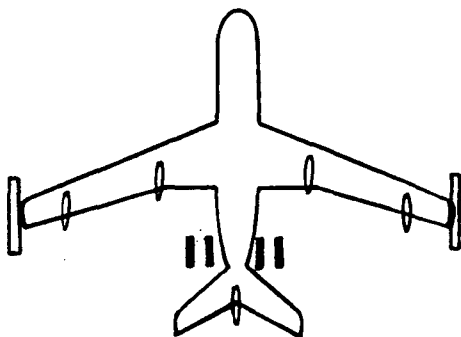




LFC-200-S-8		
Configuration Variations	External Fuel, kg (lb)	9072 (20,000)
(1) Wing tip tanks		
CONFIGURATION		CONFIGURATION SUMMARY
		<u>AIRCRAFT</u>
		Aspect ratio 14
		Wing loading, kg/m ² (lb/ft ²) 581 119
		Wing area, m ² (ft ²) 278 2995
		Wing sweep, rad (deg) 0.396 22.7
		Wing t/c 0.1156
		Front spar x/c 0.15
		Rear spar x/c 0.65
		Gross weight, kg (lb) 167,924 370,202
		Empty weight, kg (lb) 84,512 186,315
		<u>FLIGHT</u>
		Cruise power ratio 0.78
		Cruise L/D 30.57
LAMINARIZATION		<u>LFC SYSTEM</u>
(x/c) _L η _L		Engines 5
 0.72 0.97		Surface weight, kg/m ² (lb/ft ²) 7.323 1.50
 0.75 0.87		Weights, kg (lb)
 0.75 0.95		Engines 1041 2295
 0.75 0.96		Installation 1290 2844
		Surfaces 3309 7294
		Ducting 297 655
		Total 5937 13,088
		<u>BLOCK FUEL</u>
		Primary engines, kg (lb) 42,220 93,078
		LFC engines, kg (lb) 3,946 8,698
		Total, kg (lb) 46,166 101,776

Figure 98. — Configuration summary, LFC-200-S-8.

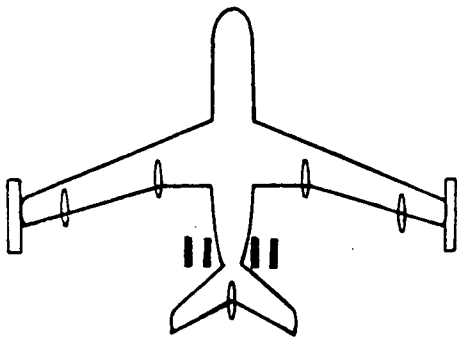

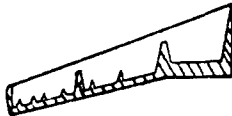



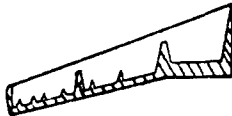



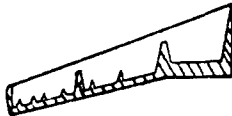


LFC-200-S-9																																																																										
Configuration Variations	External Fuel, kg (lb)	9072 (20,000)																																																																								
(1) Wing tip tanks																																																																										
<p>CONFIGURATION</p> 	<p>CONFIGURATION SUMMARY</p> <p><u>AIRCRAFT</u></p> <table> <tr> <td>Aspect ratio</td><td colspan="2">14</td></tr> <tr> <td>Wing loading, kg/m²</td><td colspan="2">537</td></tr> <tr> <td>(lb/ft²)</td><td colspan="2">110</td></tr> <tr> <td>Wing area, m² (ft²)</td><td>314</td><td>3382</td></tr> <tr> <td>Wing sweep, rad (deg)</td><td>0.274</td><td>15.7</td></tr> <tr> <td>Wing t/c</td><td colspan="2">0.1024</td></tr> <tr> <td>Front spar x/c</td><td colspan="2">0.15</td></tr> <tr> <td>Rear spar x/c</td><td colspan="2">0.65</td></tr> <tr> <td>Gross weight, kg (lb)</td><td>174,030</td><td>383,665</td></tr> <tr> <td>Empty weight, kg (lb)</td><td>89,342</td><td>196,963</td></tr> </table> <p><u>FLIGHT</u></p> <table> <tr> <td>Cruise power ratio</td><td colspan="2">0.79</td></tr> <tr> <td>Cruise L/D</td><td colspan="2">31.43</td></tr> </table> <p><u>LFC SYSTEM</u></p> <table> <tr> <td>Engines</td><td colspan="2">5</td></tr> <tr> <td>Surface weight, kg/m²</td><td colspan="2">7.323</td></tr> <tr> <td>(lb/ft²)</td><td colspan="2">1.50</td></tr> <tr> <td>Weights, kg (lb)</td><td colspan="2"></td></tr> <tr> <td>Engines</td><td>1084</td><td>2390</td></tr> <tr> <td>Installation</td><td>1344</td><td>2962</td></tr> <tr> <td>Surfaces</td><td>3824</td><td>8430</td></tr> <tr> <td>Ducting</td><td>316</td><td>696</td></tr> <tr> <td>Total</td><td>6568</td><td>14,478</td></tr> </table> <p><u>BLOCK FUEL</u></p> <table> <tr> <td>Primary engines, kg (lb)</td><td>42,668</td><td>94,066</td></tr> <tr> <td>LFC engines, kg (lb)</td><td>4,546</td><td>10,022</td></tr> <tr> <td>Total, kg (lb)</td><td>47,214</td><td>104,088</td></tr> </table>		Aspect ratio	14		Wing loading, kg/m ²	537		(lb/ft ²)	110		Wing area, m ² (ft ²)	314	3382	Wing sweep, rad (deg)	0.274	15.7	Wing t/c	0.1024		Front spar x/c	0.15		Rear spar x/c	0.65		Gross weight, kg (lb)	174,030	383,665	Empty weight, kg (lb)	89,342	196,963	Cruise power ratio	0.79		Cruise L/D	31.43		Engines	5		Surface weight, kg/m ²	7.323		(lb/ft ²)	1.50		Weights, kg (lb)			Engines	1084	2390	Installation	1344	2962	Surfaces	3824	8430	Ducting	316	696	Total	6568	14,478	Primary engines, kg (lb)	42,668	94,066	LFC engines, kg (lb)	4,546	10,022	Total, kg (lb)	47,214	104,088
Aspect ratio	14																																																																									
Wing loading, kg/m ²	537																																																																									
(lb/ft ²)	110																																																																									
Wing area, m ² (ft ²)	314	3382																																																																								
Wing sweep, rad (deg)	0.274	15.7																																																																								
Wing t/c	0.1024																																																																									
Front spar x/c	0.15																																																																									
Rear spar x/c	0.65																																																																									
Gross weight, kg (lb)	174,030	383,665																																																																								
Empty weight, kg (lb)	89,342	196,963																																																																								
Cruise power ratio	0.79																																																																									
Cruise L/D	31.43																																																																									
Engines	5																																																																									
Surface weight, kg/m ²	7.323																																																																									
(lb/ft ²)	1.50																																																																									
Weights, kg (lb)																																																																										
Engines	1084	2390																																																																								
Installation	1344	2962																																																																								
Surfaces	3824	8430																																																																								
Ducting	316	696																																																																								
Total	6568	14,478																																																																								
Primary engines, kg (lb)	42,668	94,066																																																																								
LFC engines, kg (lb)	4,546	10,022																																																																								
Total, kg (lb)	47,214	104,088																																																																								
<p>LAMINARIZATION</p> <table> <tr> <th></th><th>(x/c)_L</th><th>η_L</th></tr> <tr> <td></td><td>0.72</td><td>0.97</td></tr> <tr> <td></td><td>0.75</td><td>0.87</td></tr> <tr> <td></td><td>0.75</td><td>0.95</td></tr> <tr> <td></td><td>0.75</td><td>0.96</td></tr> </table>		(x/c) _L	η_L		0.72	0.97		0.75	0.87		0.75	0.95		0.75	0.96																																																											
	(x/c) _L	η_L																																																																								
	0.72	0.97																																																																								
	0.75	0.87																																																																								
	0.75	0.95																																																																								
	0.75	0.96																																																																								

Figure 99. — Configuration summary, LFC-200-S-9

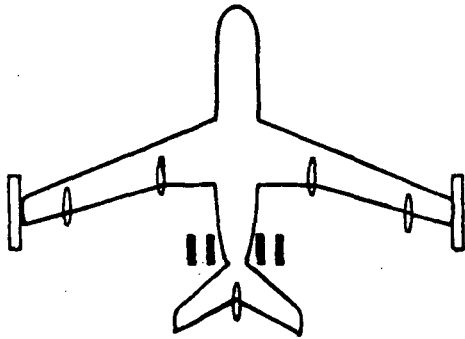

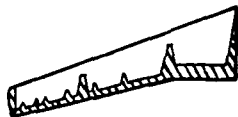


LFC-200-S-10			
Configuration Variations		External Fuel, kg (lb)	9072 (20,000)
(1) Wing tip tanks			
(2) Rooftop airfoil			
(3) Laminar to x/c = 0.85			
CONFIGURATION		CONFIGURATION SUMMARY	
		<u>AIRCRAFT</u>	
		Aspect ratio 14	
		Wing loading, kg/m ² (lb/ft ²) 544 111.5	
		Wing area, m ² (ft ²) 320 3449	
		Wing sweep, rad (deg) 0.524 30.0	
		Wing t/c 0.1162	
		Front spar x/c 0.20	
		Rear spar x/c 0.63	
		Gross weight, kg (lb) 179,947 396,708	
		Empty weight, kg (lb) 94,534 208,409	
<u>FLIGHT</u>			
Cruise power ratio 0.78			
Cruise L/D 32.21			
<u>LAMINARIZATION</u>		<u>LFC SYSTEM</u>	
(x/c) _L η_L		Engines 5	
 0.85 0.97		Surface weight, kg/m ² (lb/ft ²) 7.323 1.50	
 0.80 0.86		Weights, kg (lb)	
 0.85 0.95		Engines 1149 2534	
 0.85 0.96		Installation 1425 3141	
		Surfaces 4445 9800	
		Ducting 319 703	
		Total 7338 16,178	
		<u>BLOCK FUEL</u>	
		Primary engines, kg (lb) 43,483 95,861	
		LFC engines, kg (lb) 4,389 9,677	
		Total, kg (lb) 47,872 105,538	

Figure 100. — Configuration summary, LFC-200-S-10

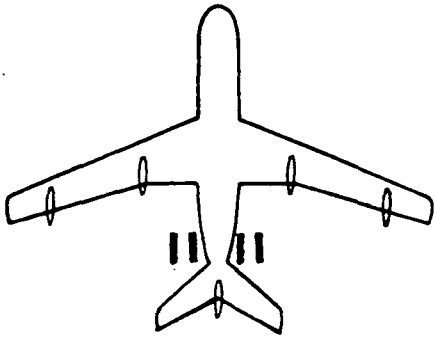

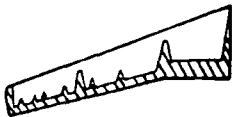



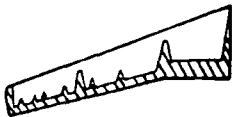



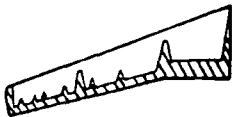


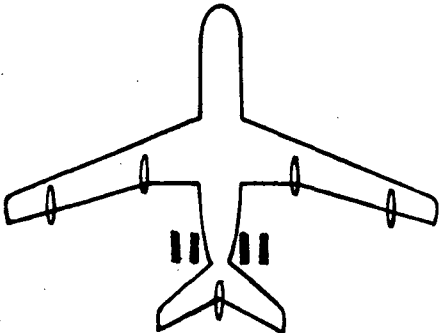
LFC-200-S-11																	
Configuration Variations	External Fuel, kg (lb)	0															
(1) LFC surface weight																	
<p>CONFIGURATION</p> 	CONFIGURATION SUMMARY																
	<p><u>AIRCRAFT</u></p> <p>Aspect ratio 14</p> <p>Wing loading, kg/m² 537 (lb/ft²) 110</p> <p>Wing area, m² (ft²) 298 3213</p> <p>Wing sweep, rad (deg) 0.396 22.7</p> <p>Wing t/c .1216</p> <p>Front spar x/c 0.15</p> <p>Rear spar x/c 0.65</p> <p>Gross weight, kg (lb) 165,281 364,511</p> <p>Empty weight, kg (lb) 82,484 181,910</p> <p><u>FLIGHT</u></p> <p>Cruise power ratio 0.81</p> <p>Cruise L/D 30.94</p> <p><u>LFC SYSTEM</u></p> <p>Engines 5</p> <p>Surface weight, kg/m² 3.348 (lb/ft²) 0.686</p> <p>Weights, kg (lb)</p> <p>Engines 1123 2477</p> <p>Installation 1392 3071</p> <p>Surfaces 1645 3627</p> <p>Ducting 308 679</p> <p>Total 4468 9854</p> <p><u>BLOCK FUEL</u></p> <p>Primary engines, kg (lb) 41,132 90,713</p> <p>LFC engines, kg (lb) 4416 9740</p> <p>Total, kg (lb) 45,548 100,459</p>																
<p>LAMINARIZATION</p> <table> <tr> <th></th><th>(x/c)_L</th><th>η_L</th></tr> <tr> <td></td><td>0.72</td><td>0.97</td></tr> <tr> <td></td><td>0.75</td><td>0.87</td></tr> <tr> <td></td><td>0.75</td><td>0.95</td></tr> <tr> <td></td><td>0.75</td><td>0.96</td></tr> </table>		(x/c) _L	η _L		0.72	0.97		0.75	0.87		0.75	0.95		0.75	0.96		
	(x/c) _L	η _L															
	0.72	0.97															
	0.75	0.87															
	0.75	0.95															
	0.75	0.96															

Figure 101. — Configuration summary, LFC-200-S-11

LFC-200-S-12		
Configuration Variations	External Fuel, kg (lb)	0
(1) Laminar to x/c = 0.60		
CONFIGURATION	CONFIGURATION SUMMARY	
	<u>AIRCRAFT</u>	
	Aspect ratio	14
	Wing loading, kg/m ² (lb/ft ²)	559 114.5
	Wing area, m ² (ft ²)	295 3178
	Wing sweep, rad (deg)	0.396 22.7
	Wing t/c	0.1189
	Front spar x/c	0.08
	Rear spar x/c	0.62
	Gross weight, kg (lb)	170,149 375,109
	Empty weight, kg (lb)	84,655 186,628
<u>FLIGHT</u>		
Cruise power ratio	0.82	
Cruise L/D	29.66	
<u>LFC SYSTEM</u>		
Engines	5	
Surface weight, kg/m ² (lb/ft ²)	7.323 1.50	
Weights, kg (lb)		
Engines	972 2142	
Installation	1205 2656	
Surfaces	2906 6406	
Ducting	306 675	
Total	5389 11,897	
<u>BLOCK FUEL</u>		
Primary engines, kg (lb)	44,282 97,624	
LFC engines, kg (lb)	4,580 7,891	
Total, kg (lb)	47,862 105,515	





LAMINARIZATION		
	(x/c) _L	η_L
	0.60	0.98
	0.60	0.94
	0.60	0.98
	0.60	0.98

Figure 102. — Configuration summary, LFC-200-S-12

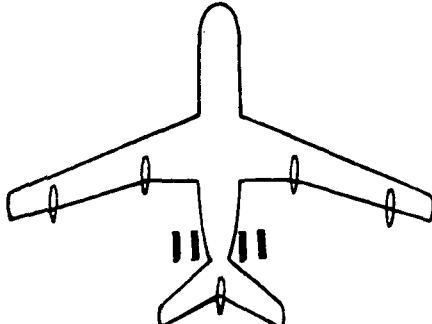

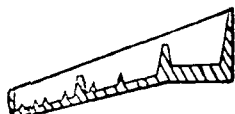


LFC-200-S-13			
Configuration Variations		External Fuel, kg (lb)	0
(1) Laminar to $x/c = 0.85$.			
CONFIGURATION		CONFIGURATION SUMMARY	
		<u>AIRCRAFT</u>	
		Aspect ratio	14
		Wing loading, kg/m^2 (lb/ft^2)	510 104.5
		Wing area, m^2 (ft^2)	332 3570
		Wing sweep, rad (deg)	0.396 22.7
		Wing t/c	0.1250
		Front spar x/c	0.18
		Rear spar x/c	0.63
		Gross weight, kg (lb)	174,591 384,900
		Empty weight, kg (lb)	90,202 198,859
		<u>FLIGHT</u>	
		Cruise power ratio	0.81
		Cruise L/D	32.63
LAMINARIZATION		<u>LFC SYSTEM</u>	
	(x/c) _L η_L	Engines	5
	0.85 0.97	Surface weight, kg/m^2 (lb/ft^2)	7.323 1.50
	0.80 0.86	Weights, kg (lb)	
	0.82 0.95	Engines	1411 3111
	0.82 0.96	Installation	1749 3356
		Surfaces	4555 10,042
		Ducting	324 715
		Total	8039 17,724
		<u>BLOCK FUEL</u>	
		Primary engines, kg (lb)	41,034 90,464
		LFC engines, kg (lb)	5,879 12,960
		Total, kg (lb)	46,913 103,424

Figure 103. — Configuration summary, LFC-200-S-13

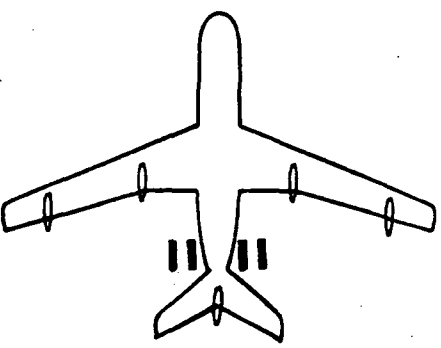
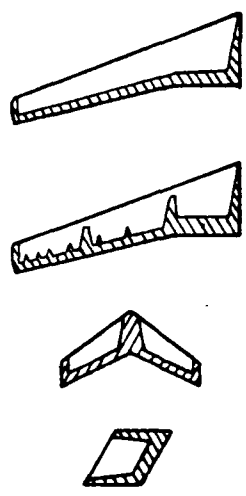
LFC-200-S-14		
Configuration Variations	External Fuel, kg (lb)	0
(1) Relaxed static stability		
CONFIGURATION	CONFIGURATION SUMMARY	
	<u>AIRCRAFT</u>	
	Aspect ratio	14
	Wing loading, kg/m ² (lb/ft ²)	537 110
	Wing area, m ² (ft ²)	304 3273
	Wing sweep, rad (deg)	0.396 22.7
	Wing t/c	0.1216
	Front spar x/c	0.15
	Rear spar x/c	0.65
	Gross weight, kg (lb)	168,409 371,272
	Empty weight, kg (lb)	85,175 187,775
LAMINARIZATION <div> <div>(x/c)_L</div> <div>η_L</div> </div> 	<u>FLIGHT</u>	
	Cruise power ratio	0.80
	Cruise L/D	31.27
	<u>LFC SYSTEM</u>	
	Engines	5
	Surface weight, kg/m ² (lb/ft ²)	7.323 1.50
	Weights, kg (lb)	
	Engines	1140 2514
	Installation	1413 3116
	Surfaces	3498 7711
	Ducting	311 685
	Total	6362 14,026
	<u>BLOCK FUEL</u>	
	Primary engines, kg (lb)	41,451 91,382
	LFC engines, kg (lb)	4,468 9,850
	Total, kg (lb)	45,919 101,232

Figure 104. — Configuration summary, LFC-200-S-14

LFC-200-S-6 – Figure 96 describes the LFC configuration variation adapted to a fuselage slot injection system. Provision of adequate volume for LFC engines and compressors, ducting, and belly cargo in a configuration compatible with the integration of a slot for fuselage blowing requires extension of the fuselage by 1.82 m (6 ft). The weight penalty associated with this variation is 791 kg (1743 lb) and the net drag change is $\Delta C_D = +0.00043$. Compared to LFC-200-S-4, which is identical to this configuration except for the fuselage slot, LFC engine fuel consumption is reduced by 903 kg (1990 lb). However, primary engine fuel consumption is increased by 1542 kg (3399 lb) for a net increase of 639 kg (1409 lb). Compared to the baseline configuration, the increase in fuel consumption is 3378 kg (7446 lb).

LFC-200-S-7 – This configuration, described in figure 97, evaluates the effect of integrating the LFC engine/compressor units with the primary propulsion engines. As discussed in section 6.0, fuel consumption of the LFC engines is reduced but there is an associated increase in weight and fuel consumption of the primary propulsion engines. The aft trunk duct must penetrate the rear spar and run through the wing box as in the case of LFC-200-S-3. The resultant loss of fuel volume limits wing loading to 513 kg/m^2 (105 lb/ft^2). This limitation, combined with the increased weight and fuel consumption of the primary engines, results in a configuration which uses 843 kg (1859 lb) more fuel than the baseline configuration.

LFC-200-S-8 – In configuration LFC-200-S-8, shown in figure 98, the LFC baseline configuration is altered only by the addition of external fuel tanks. The additional fuel volume permits an increase in wing loading from the value of 537 kg/m^2 (110 lb/ft^2) achievable on the baseline to 581 kg/m^2 (119 lb/ft^2). This increase results in a reduction of 736 kg (1623 lb) in fuel consumption.

LFC-200-S-9 – Figure 99 summarizes the characteristics of this variation. In this configuration, the flexibility provided by the addition of external fuel was used to evaluate the impact of reduced LFC suction requirements attending a reduction in wing sweep. While a small reduction in LFC system weight was realized, the increase in wing weight accompanying the lower t/c ratio resulted in a net increase in both aircraft empty weight and fuel consumption. Compared to the baseline, this configuration consumes 312 kg (689 lb) more fuel.

LFC-200-S-10 – This configuration, summarized in figure 100, employs the rooftop airfoil described in section 4.0. As discussed in that section, use of this airfoil section in combination with 15% trailing-edge devices permits laminarization of the wing and empennage to the $x/c = 0.85$ position. The lower t/c ratios provided by this airfoil, as compared to a supercritical section, necessitate an increase in wing sweep to 0.524 rad (30 deg) to achieve an acceptable wing volume. This sweep provides a $t/c = 0.1162$, compared to $t/c = 0.1216$ for the supercritical airfoil at a sweep of 0.396 rad (22.7 deg). Additional fuel volume is lost as a result of the spar relocation required to provide the greater trunk ducting volume necessary for greater laminarization.

The combined effect of these changes is an increase of 970 kg (2139 lb) in fuel consumption compared to the baseline. Relative to LFC-200-S-8, the comparable configuration with external fuel, this variation consumes 1706 kg (3762 lb) more fuel.

LFC-200-S-11 – Figure 101 summarizes the results of decreasing the unit weight of LFC surfaces from 7.32 kg/m^2 (1.50 lb/ft^2) to 3.34 kg/m^2 (0.686 lb/ft^2). This variation results in a reduction of 2180 kg (4807 lb) in LFC system weight, 4330 kg (9547 lb) in aircraft empty weight, and 1334 kg (2940 lb) in fuel consumption relative to the baseline configuration.

LFC-200-S-12 and LFC-200-S-13 – These configurations, described in figure 102 and 103, illustrate the influence of the extent of chordwise laminarization on aircraft characteristics and fuel efficiency. These configurations are the point designs discussed in section 7.3. A thorough analysis of the trends defined by these configurations in combination with the LFC baseline is presented in that section.

LFC-200-S-14 – Figure 104 summarizes the configuration characteristics which result from the application of active controls, in the form of relaxed static stability, to the LFC baseline configuration. The assumptions on which this application is based and a description of the resultant system are discussed in section 7.4.6. As illustrated by figure 104, this variation permits a decrease in the size and weight of both LFC and aircraft components with a resultant fuel savings of 983 kg (2167 lb) compared to the baseline.

7.5.4 EVALUATION RESULTS

Table 14 summarizes the results of the configuration evaluations in terms of increments in fuel consumption relative to the initial LFC-200-S baseline configuration. As illustrated by this table, a net reduction in fuel consumption is achieved through the modification of the baseline configuration to include the following variations:

Configuration	Variation
LFC-200-S-8	External fuel
LFC-200-S-11	LFC surface weight reduction
LFC-200-S-14	Relaxed static stability

In addition, although not providing a reduction in fuel consumption relative to the baseline configuration, the utilization of bleed/burn LFC suction units results in reduced fuel consumption in configurations which are compatible with the use of fuselage-mounted units. Comparison of configuration LFC-200-S-3 and LFC-200-S-7 illustrates this point.

Consequently, to the extent required by internal fuel volume limitations and permitted by design constraints, these features were incorporated into all the final LFC configurations.

TABLE 14. SUMMARY OF CONFIGURATION EVALUATION RESULTS: LFC-200-S

Configuration	Block fuel		Block fuel relative to baseline		Percent variation relative to baseline
	kg	lb	kg	lb	
LFC-200-1	46,902	103,399		0	0
LFC-200-2	47,803	105,385	901	1986	1.9
LFC-200-3	48,083	106,003	1181	2604	2.5
LFC-200-4	49,640	109,436	2738	6037	5.8
LFC-200-5	49,165	108,389	2263	4990	4.8
LFC-200-6	50,279	110,845	3378	7446	7.2
LFC-200-7	47,745	105,258	843	1859	1.8
LFC-200-8	46,165	101,776	-736	-1623	-1.6
LFC-200-9	47,214	104,088	312	689	.7
LFC-200-10	47,872	105,538	970	2139	2.1
LFC-200-11	45,568	100,459	-1334	-2940	-2.8
LFC-200-12	47,862	105,515	960	2116	2.1
LFC-200-13	46,913	103,424	11	25	0
LFC-200-14	45,919	101,232	-983	-2167	-2.1

7.6 CONFIGURATION SELECTION

7.6.1 SELECTION PROCEDURE

The result of the parametric analyses of section 5.2 were used as the basis for the development of baseline configurations for the LFC-200-S, LFC-200-R, LFC-400-S, and LFC-400-R aircraft. For each of these baseline aircraft, the configuration variations dictated by the results of section 7.5 were evaluated and the variation minimizing fuel consumption was selected for comparison with the corresponding TF configuration.

The following procedure was employed in the development and selection of all LFC aircraft configurations:

- (1) Using the baseline parameters selected in section 5.2, initial design layouts were completed. These layouts were used for initial calculation of
 - o Weight and balance
 - o LFC duct area and weight
 - o LFC surface thickness and weight
 - o LFC suction unit weight and fuel flow
 - o Laminar areas
- (2) The values calculated in (1) were used in the GASP to define a first iteration of the baseline configuration.
- (3) The results of the first iteration were compared to the calculations of (1) and the design layouts were revised as required.
- (4) A second iteration of the baseline was conducted if necessary to satisfy weight and balance and LFC system requirements.
- (5) The final design layout was executed.
- (6) Based on the final design layout, manufacturing procedures and costs and maintenance procedures and costs were estimated.
- (7) A final iteration of the GASP was performed to generate final aircraft development, production, and operating cost data.

A similar procedure was followed in the development of variations from the baseline configurations. However, in most cases each variation was sufficiently similar to the baseline that only one iteration was required to develop final performance, sizing, weight, and cost data.

Detailed descriptions of the final LFC aircraft are presented in section 8.0. Manufacturing and maintenance data are included as a part of section 9.0.

7.6.2 SELECTED CONFIGURATIONS

Tables 15 through 18 summarize the characteristics of the baseline configurations and the final configuration variations evaluated for the LFC-200-S, LFC-200-R, LFC-400-S, and LFC-400-R aircraft.

For the 200-passenger aircraft described in tables 15 and 16, the baseline configuration was modified to include the addition of external fuel and relaxed static stability individually and in combination. For both LFC-200-S and LFC-200-R configurations, the combination of external fuel

TABLE 15. COMPARISON OF LFC-200-S CONFIGURATION VARIATIONS

Characteristic	Baseline	Variation		
		External Fuel	RSS	External Fuel RSS
Cruise M	0.80	0.80	0.80	0.80
Cruise altitude, m (ft)	11,582 (38,000)	11,582 (38,000)	11,582 (38,000)	11,582 (38,000)
Wing sweep, rad (deg)	0.396 (22.7)	0.396 (22.7)	0.396 (22.7)	0.396 (22.7)
Aspect ratio	14.00	14.00	14.00	14.00
Wing loading, kg/m ² (lb/ft ²)	573 (117.35)	623 (127.55)	584 (119.70)	636 (130.33)
Wing t/c ratio	.1171	.1109	.1157	.1092
Wing area, m ² (ft ²)	278.9 (3002)	253.5 (2729)	265.2 (2855)	241.4 (2599)
Cruise L/D	30.21	29.65	29.52	29.00
Engine thrust, N (lb)	96,037 (21,591)	100,814 (22,665)	94,974 (21,352)	100,151 (22,516)
Bypass ratio	6.00	6.00	6.00	6.00
Cruise power ratio	0.81	0.78	0.82	0.78
Gross weight, kg (lb)	164,694 (363,082)	162,643 (358,560)	159,712 (352,231)	158,276 (348,934)
Empty weight, kg (lb)	82,474 (181,822)	81,031 (178,639)	78,295 (172,607)	77,271 (170,350)
Block fuel, kg (lb)	45,069 (99,358)	44,662 (98,461)	44,434 (97,958)	44,144 (97,320)
Fuel efficiency, skm/kg fuel (ssm/lb fuel)	42.25 (12.75)	45.58 (12.84)	45.90 (12.93)	46.15 (13.01)
Flyaway cost, \$10 ⁶	25.704	25.322	24.817	24.529
DOC, \$/skm (μ /ssm)				
Fuel price, \$/l (\$/gal)				
0.066 (0.25)	0.839 (1.351)	0.834 (1.342)	0.822 (1.323)	0.819 (1.318)
0.132 (0.50)	1.025 (1.650)	1.018 (1.639)	1.006 (1.619)	1.002 (1.612)
0.264 (1.00)	1.398 (2.250)	1.388 (2.233)	1.373 (2.210)	1.366 (2.199)

TABLE 16. COMPARISON OF LFC-200-R CONFIGURATION VARIATIONS

Characteristic	Baseline	Variation		
		External Fuel	RSS	External Fuel RSS
Cruise M	0.80	0.80	0.80	0.80
Cruise altitude, m (ft)	11,582 (38,000)	11,582 (38,000)	11,582 (38,000)	11,582 (38,000)
Wing sweep, rad (deg)	0.396 (22.7)	0.396 (22.7)	0.396 (22.7)	0.396 (22.7)
Aspect ratio	14.00	14.00	14.00	14.00
Wing loading, kg/m ² (lb/ft ²)	573 (117.35)	626 (128.20)	585 (119.80)	640 (131.00)
Wing t/c ratio	.1171	.1105	.1156	.1088
Wing area, m ² (ft ²)	267.7 (2882)	243.0 (2616)	255.4 (2749)	231.7 (2494)
Cruise L/D	29.92	29.36	29.26	28.76
Engine thrust, N (lb)	92,287 (20,748)	97,531 (21,927)	91,429 (20,555)	96,913 (21,788)
Bypass ratio	6.00	6.00	6.00	6.00
Cruise power ratio	0.82	0.78	0.82	0.78
Gross weight, kg (lb)	158,145 (348,645)	156,703 (345,465)	153,954 (339,405)	152,687 (336,612)
Empty weight, kg (lb)	78,546 (173,162)	77,425 (170,690)	74,844 (165,000)	73,932 (162,990)
Block fuel, kg (lb)	42,799 (94,354)	42,642 (94,009)	42,381 (93,433)	42,198 (93,028)
Fuel efficiency, skm/kg fuel (ssm/lb fuel)	47.65 (13.42)	47.83 (13.47)	48.12 (13.56)	48.29 (13.62)
Flyaway cost, \$10 ⁶	24.547	24.254	23.756	23.503
DOC, ¢/skm (¢/ssm)				
Fuel price, \$/l (\$/gal)				
0.066 (0.25)	0.777 (1.251)	0.775 (1.247)	0.763 (1.228)	0.761 (1.224)
0.132 (0.50)	0.954 (1.536)	0.951 (1.530)	0.938 (1.509)	0.935 (1.505)
0.264 (1.00)	1.308 (2.105)	1.304 (2.098)	1.288 (2.073)	1.284 (2.066)

TABLE 17. COMPARISON OF LFC-400-S CONFIGURATION VARIATIONS

Characteristic	Baseline	RSS
Cruise M		
Cruise altitude, m (ft)	11,582 (38,000)	11,582 (38,000)
Wing sweep, rad (deg)	0.396 (22.7)	0.396 (22.7)
Aspect ratio	14.00	14.00
Wing loading, kg/m ² (lb/ft ²)	684 (140.00)	684 (140.00)
Wing t/c ratio	.1033	.1033
Wing area, m ² (ft ²)	480.2 (5169)	457.5 (4925)
Cruise L/D	30.46	30.05
Engine thrust, N (lb)	228,552 (51,383)	217,881 (48,984)
Bypass ratio	6.00	6.00
Cruise power ratio	0.70	0.70
Gross weight, kg (lb)	377,851 (744,821)	321,895 (709,645)
Empty weight, kg (lb)	174,059 (383,728)	161,895 (356,912)
Block fuel, kg (lb)	88,422 (194,933)	85,123 (187,661)
Fuel efficiency, skm/kg fuel (ssm/lb fuel)	46.11 (12.99)	47.88 (13.50)
Flyaway cost, \$10 ⁶	41.519	39.435
DOC, ¢/skm (¢/ssm)		
Fuel price, \$/1 (\$/gal)		
0.066 (0.25)	0.652 (1.049)	0.627 (1.009)
0.132 (0.50)	0.834 (1.342)	0.803 (1.292)
0.264 (1.00)	1.199 (1.929)	1.154 (1.857)

TABLE 18. COMPARISON OF LFC-400-R CONFIGURATION VARIATIONS

Characteristic	Baseline	RSS
Cruise M	0.80	0.80
Cruise altitude, m (ft)	11,582 (38,000)	11,582 (38,000)
Wing sweep, rad (deg)	0.396 (22.7)	0.396 (22.7)
Aspect ratio	14.00	14.00
Wing loading, kg/m ² (lb/ft ²)	684 (140.00)	684 (140.00)
Wing t/c ratio	.1033	.1033
Wing area, m ² (ft ²)	463.8 (4993)	444.4 (4784)
Cruise L/D	30.28	29.90
Engine thrust, N (lb)	220,523 (49,578)	211,502 (47,550)
Bypass ratio	6.00	6.00
Cruise power ratio	0.70	0.71
Gross weight, kg (lb)	326,374 (719,520)	312,654 (689,273)
Empty weight, kg (lb)	166,116 (366,217)	155,566 (342,959)
Block fuel, kg (lb)	85,357 (188,177)	82,599 (182,096)
Fuel efficiency, skm/kg fuel (ssm/lb fuel)	47.76 (13.46)	49.35 (13.91)
Flyaway cost, \$10 ⁶	40.170	38.344
DOC, ¢/skm (¢/ssm)		
Fuel price, \$/l (\$/gal)		
0.066 (0.25)	0.633 (1.019)	0.612 (0.985)
0.132 (0.50)	0.810 (1.303)	0.782 (1.259)
0.264 (1.00)	1.161 (1.869)	1.123 (1.808)

and RSS provides the lowest fuel consumption and the lowest direct operating costs. Therefore, these configurations were selected for comparison with the 200-passenger TF aircraft.

Tables 17 and 18 outline the characteristics of the final LFC-400-S and LFC-400-R configuration variations. The wing volume available for fuel in the 400-passenger aircraft is sufficient to permit a wing loading of 684 kg/m^2 (140 lb/ft^2) without the addition of external fuel tanks. Therefore, the final configuration variations for these aircraft were limited to the addition of RSS to the baseline configurations.

As indicated by tables 17 and 18, the application of RSS reduces the fuel consumption and direct operating costs of both the LFC-400-S and LFC-400-R aircraft and is therefore included on the configurations selected for comparison with the corresponding TF aircraft.

Table 19 summarizes the reductions in fuel consumption relative to the baseline configurations afforded by the variations evaluated for the final LFC aircraft. Fuel savings are relatively small for the 200-passenger aircraft, ranging from 1.4% for LFC-200-R to 2.1% for LFC-200-S. For the 400-passenger aircraft, in which the empennage represents a larger fraction of total aircraft wetted area and weight, the addition of relaxed stability provides a fuel reduction in the range of 3 to 4%.

TABLE 19. REDUCTIONS IN FUEL CONSUMPTION FOR LFC CONFIGURATION VARIATIONS

Configuration	Variation								
	External fuel			RSS			External fuel RSS		
	<u>kg</u>	<u>lb</u>	<u>%</u>	<u>kg</u>	<u>lb</u>	<u>%</u>	<u>kg</u>	<u>lb</u>	<u>%</u>
LFC-200-S	407	897	0.9	635	1400	1.4	924	2038	2.1
LFC-200-R	156	345	0.4	418	921	0.9	601	1326	1.4
LFC-400-S				3299	7272	3.7			
LFC-400-R				2758	6081	3.2			

8.0 LFC CONFIGURATION DESCRIPTIONS

8.1 INTRODUCTION

The configuration characteristics defined in the preceding section for the four final LFC aircraft established a basis for the detailed development of aircraft and LFC systems. In this section, the final configurations for the LFC-200-S, LFC-200-R, LFC-400-S, and LFC-400-R aircraft are described. Included are descriptions of the aircraft general arrangement and weights, aircraft systems, and LFC systems. An analysis of potential acoustic interference with LFC system operation on the final study aircraft is summarized.

8.2 CONFIGURATION LFC-200-S

8.2.1 GENERAL ARRANGEMENT

Like the baseline airplane described in section 7.2, the LFC-200-S configuration is a wide-body configuration capable of transporting 200 passengers, their baggage, and 4536 kg (10,000 lb) of cargo over the intercontinental range of 10,186 km (5500 n mi) at Mach 0.80. The widebody cabin is designed to accommodate 40 first-class and 160 tourist-class passengers. The cabin is arranged in a spacious two-aisle configuration with the required entry/escape doors, lavatories, and passenger service stations. Galley and baggage provisions are located below the cabin floor. The flight deck, with provisions for a crew of three, provides necessary controls and instrumentation required for long-range commercial operation.

As shown in figure 105, the LFC-200-S is a low-wing T-tail monoplane with four aft-fuselage-mounted propulsion engines. External fuel tanks are located on each wing tip. Two LFC suction units are installed under each wing and one is installed in the base of the vertical tail. The airplane and power plants are designed to meet community noise level requirements specified by FAR Part 36 minus 10 EPNdB.

The LFC-200-S wing is a moderately swept, high-aspect-ratio structure with outboard ailerons. By using aileron deflection, full-span flaps are provided to meet required field performance. Spoilers are located over the inboard flap segments.

Fuel is carried in the total span of the wing, including the cross-fuselage wing box and in the two tip tanks. The upper and lower wing surfaces are provided with LFC suction capability from the leading edge to 75% chord. Empennage LFC surfaces extend from the leading edge to 65% chord. A weight statement for LFC-200-S is presented in table 20.

$M = 0.80$
 $H, \text{ m (ft)} = 11,582 (38,000)$
 $\Lambda, \text{ rad (deg)} = 0.396 (22.7)$
 $AR = 14.00$
 $S, \text{ m}^2 (\text{ft}^2) = 241.4 (2599)$

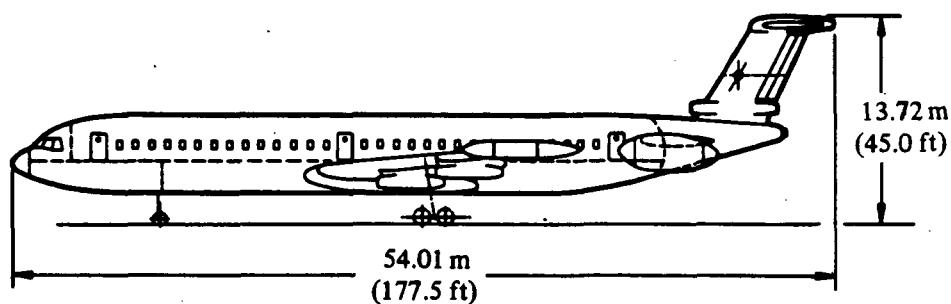
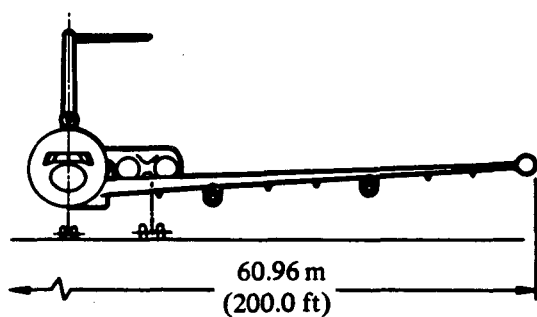
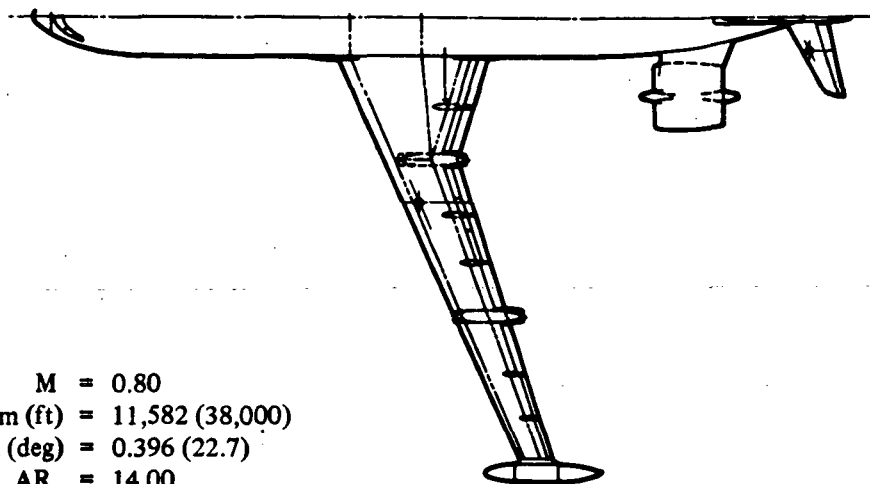


Figure 105. — General arrangement LFC-200-S

TABLE 20. WEIGHT STATEMENT: LFC-200-S

Item	kg	lb
Structure	(49,019)	(108,067)
Wing	21,012	46,323
Wing LFC glove	2,332	5,142
Empennage	(2,166)	(4,775)
Horizontal tail	834	1,838
Horizontal LFC glove	188	414
Vertical tail	899	1,981
Vertical LFC glove	246	542
Fuselage	14,327	31,586
Landing gear	(6,969)	(15,364)
Nose	906	1,997
Main	6,063	13,366
Nacelle and pylon	(2,213)	(4,878)
Nacelle	924	2,037
Pylon	298	656
Noise treatment	991	2,186
Propulsion system	(11,399)	(25,129)
Engines	5,900	13,007
Fuel system	1,736	3,827
Thrust reversers	991	2,185
LFC engines	708	1,560
LFC installation	877	1,933
LFC ducts	277	610
Miscellaneous	907	2,000
Systems and equipment	(16,856)	(37,161)
Auxiliary power system	283	624
Surface controls	1,215	2,679
Instruments	591	1,302
Hydraulics and pneumatic	566	1,248
Electrical	2,244	4,946
Avionics	1,089	2,400
Furnishings	8,611	18,983
Airconditioning and AI	2,229	4,914
Auxiliary gear - equipment	29	65
Weight empty	(77,271)	(170,350)
Operating equipment	6,472	14,267
Operating weight	(83,743)	(184,617)
Payload - passenger	19,233	42,400
Cargo	4,536	10,000
Zero fuel weight	(107,512)	(237,017)
Fuel	50,764	111,916
Gross weight	(158,276)	(348,934)
AMPR weight	66,524	146,658

8.2.2 AIRCRAFT SYSTEMS

8.2.2.1 Structures

The basic aircraft structure for the LFC-200-S conforms to generally accepted aircraft practice. The fuselage is semi-monocoque consisting of aluminum skin, frames, and stringers. The diameter of the cross-section is constant at 5.08 m (200 in) for a major portion of the length. This section tapers down in the forward section to the flight station enclosure. At the aft end the section tapers down to fair with the LFC suction unit exhaust nozzle.

The pressurized portion of the fuselage shell is designed for a cabin altitude of 2438 m (8000 ft) at an altitude of 12,192 m (40,000 ft). Skin thicknesses are established as required to provide satisfactory fatigue life. Bonding is utilized in skin joints for attaching doublers around openings to improve fatigue life of the structure. The skin and stringers are supported by sheet metal frames spaced at intervals of 0.51 m (20 in).

The wing is constructed of built-up sheet metal and machined extrusions. Primary loads are carried in the 2-spar box beam which is designed to accommodate integral fuel tanks. Ribs, spaced 0.76 m (30 in) apart, distribute external loads into the box and support the surface structure. Machine tapered wing skins are employed.

8.2.2.2 Landing Gear System

The landing gear is a conventional tricycle design with four main wheels on each of two main gears and two wheels on the nose gear. The main gears retract inboard while the nose gear retracts forward.

The main gear is a conventional four-wheel bogie. No form of directional steering or swivelling is employed. Hydraulically powered nose gear steering controlled by the captain's handwheel allows a 3.14 rad (180 deg) turn on a runway 45.7 m (150 ft) wide.

8.2.2.3 High Lift System

The high lift system consists of single-slot, hinged, full-span flaps. The flaps on the inboard wing are constant chord, while the outboard flaps are 25% chord. The flaps are hydro-mechanically operated and controlled by a single pilot input. Position indication is provided. A system to prevent asymmetrical flap operation is incorporated.

8.2.2.4 Flight Controls

The primary flight control system consists of controls for horizontal stabilizer and elevators, rudder, ailerons, and spoilers. Geared elevators, driven mechanically by the stabilizer and a double-hinged rudder increase effectiveness in pitch and yaw axes in low-speed flight. An active control system, in the form of relaxed static stability, is incorporated in the empennage controls.

The control system is an irreversible hydro-mechanical system. All controls and instrumentation necessary for the operation of the aircraft in the air and on the ground are located in the flight station compartment.

Several panels of the spoiler system are used in flight to supplement the ailerons for lateral control during low-speed flight. All spoilers are deployed on the ground during landing rollout or rejected takeoff.

8.2.2.5 Propulsion

The propulsion system is comprised of four engines with inlets, cowlings, and associated equipment. Two propulsion units are siamese podded on either side of the aft fuselage. The gear box and accessories are located external to the fan duct. The lower portion of the siamese pod opens for easy access to the engine and accessories for trouble-shooting and adjustment.

The engines are based on Pratt and Whitney STF 429 advanced engine technology.

8.2.2.6 Subsystems

The primary aircraft functional systems are separated into individual localized centers throughout the airframe. There is a separate service center for the hydraulic, environmental, electrical, electronic, and fuel systems. Each of these systems maintain necessary interface with the cockpit through instrumentation and controls.

Hydraulic – The hydraulic system consists of four independent systems, each having multiple independent power sources. An auxiliary system is powered by an auxiliary power unit to provide ground self-sufficiency and emergency in-flight power.

Power transfer units between certain pairs of primary hydraulic systems provide cross-pressurization between systems without any interflow of fluid between the independent systems.

Environmental – The environmental system provides for passenger comfort during ground and in-flight operations. The system consists of air cycle refrigeration packs that condition compressed

air extracted from all four propulsion engines to provide cabin ventilation and control of cabin temperature and pressure. The auxiliary power unit provides compressed air for ground air conditioning and can also provide supplemental air conditioning as required during takeoff, climb, descent, and landing.

The oxygen subsystem comprises the crew oxygen system and the passenger supplemental oxygen system. The systems are independent. The crew system is a low pressure system providing flow to five flight deck stations. Also included in the crew system is a portable cylinder providing free oxygen for emergency or first aid breathing.

The passenger supplemental oxygen system comprises a series of chemical oxygen generators manifolded to drop-out masks at each passenger seat. Portable continuous flow units are also dispersed throughout the cabin to meet emergency conditions.

Electrical — Electrical power required for communications, navigation, passenger comfort, and other functional systems is provided by integrated constant-speed-drive, brushless AC generator units mounted on each engine. An auxiliary integrated-drive generator unit is mounted on the APU to provide ground electrical power. This unit can also be operated in flight.

Electronics — The electronics systems comprise communications, navigation, passenger communications, and avionic flight controls required to operate a commercial passenger airplane over world-wide international routes.

Fuel — The fuel system, illustrated schematically in Figure 106, is comprised of a tip tank, two main tanks, and one auxiliary tank in each wing. An additional auxiliary tank is located in the center wing box within the fuselage. Each main tank feeds one main engine and one LFC suction unit. The aft-fuselage-mounted suction unit and the APU are fed from the center wing auxiliary tank.

Fuel from the tip tanks and outer wing panel auxiliary tanks is fed into the main tanks as required. All fuel system components, including the boost pumps, fuel probes, and fuel level control valves, are removable from outside the wing LFC covers. For access into the fuel cells for inspection, maintenance, or repair, it is necessary to remove LFC surface panels in order to uncover the access panels in the structural wing. Ground pressure fueling is accomplished from the main landing wheel well.

8.2.3 LFC SYSTEMS

The general criteria for the LFC suction system and the complex nature of these criteria are discussed in section 6.2.1 and 6.3.1. Although a complete detailed design analysis of a suction system compatible with these criteria is beyond the scope of this system study, the suction surface,

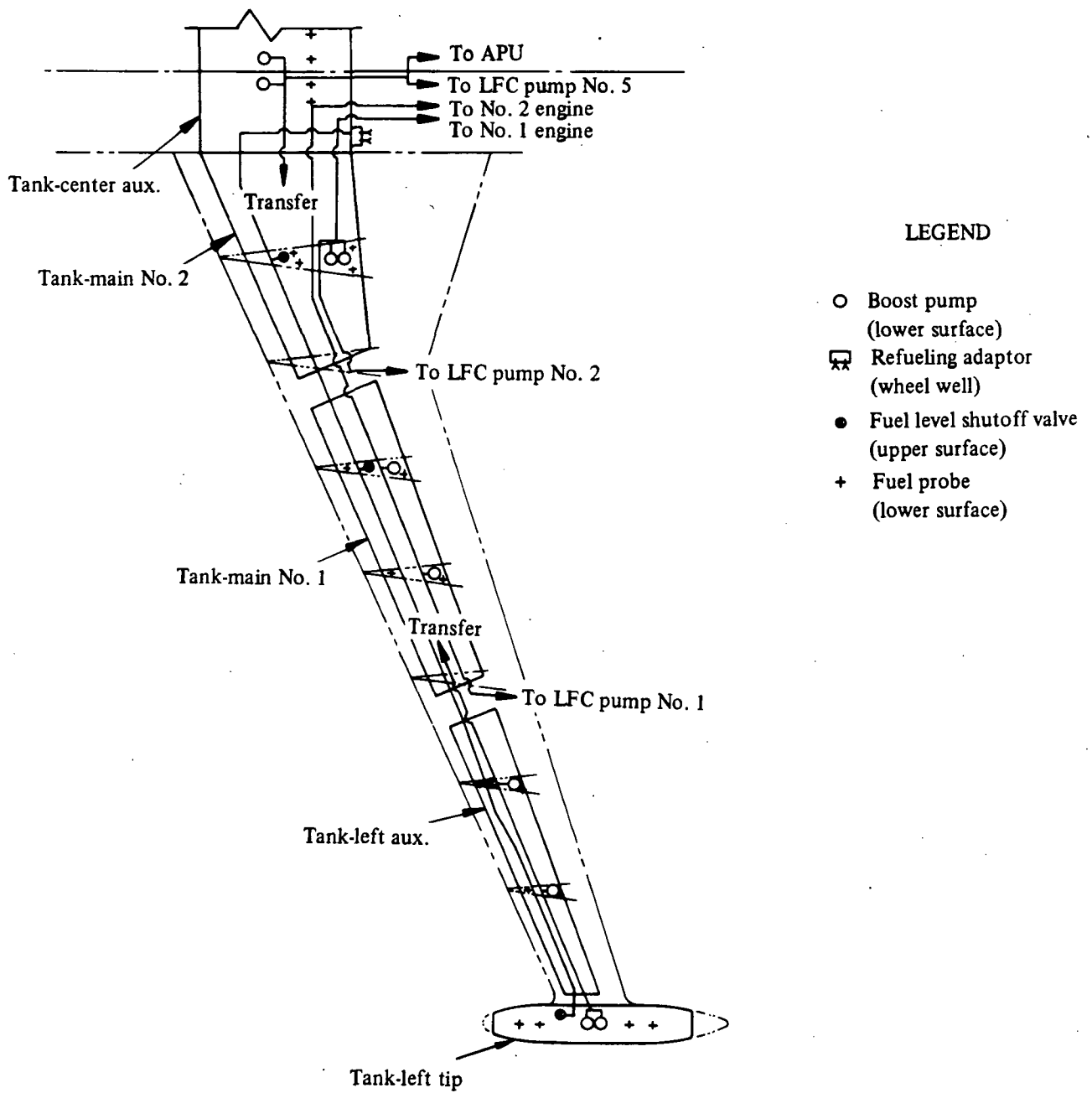


Figure 106. — Schematic of aircraft fuel system

internal ducting, and suction pumps for the point design airplanes are analyzed in sufficient depth to ensure that no insurmountable problems or conceptual fallacies exist. The selected systems are consistent with the requirements of a production LFC transport aircraft.

The suction flow, flow distribution requirements, and surface pressure distribution are delineated for the selected airfoil by the methods discussed in section 4.0. The flow distribution is defined in terms of v_s/U_o in which v_s is the distributed suction velocity, representing the normal velocity of the boundary layer air through the surface, and U_o is the free stream velocity. The distributed suction velocity assumes continuous inflow of air over the entire surface at local levels just sufficient to maintain laminar flow. Integration of $\rho S_L v_s$ over the laminarized portion of the airfoil yields the total flow into the surface. Figures 107, 108, and 109 represent the v_s/U_o distribution as a function of x/c for the wing, horizontal, and vertical empennage surfaces, respectively.

The horizontal tail may be required to produce aerodynamic lift in either the upward or downward direction during cruise. Figure 108 presents common maximum and minimum cruise values applicable to both upper and lower surfaces of the horizontal tail. This requirement necessitates either sucking both surfaces continuously to the maximum level or a valving arrangement in the ducting system to apply the high level of suction to the appropriate surface. This requirement is discussed further in section 8.2.3.4.

Figure 109 presents a single v_s/U_o profile for the vertical empennage surface. Since LFC is maintained only during cruise, the aerodynamic characteristics of the vertical tail surface are assumed to be symmetrical.

The local pressure distribution over the aerodynamic surfaces is defined by C_p , which is based on free stream q_o . These local pressures define the pressure at which the sucked air must be ingested and therefore the local pressures of the internal suction system duct pressures required to achieve the desired suction flow levels. Figures 110, 111, and 112 present the C_p characteristics as a function of x/c for the wing, horizontal tail and vertical tail, respectively. It will be noted that upper and lower surface profiles are shown for the wing, maximum and minimum profiles for the horizontal tail, and a single profile for the vertical tail as in the case of the v_s/U_o profiles. It will be noted that, considering an entire surface, higher C_p values correspond to higher v_s/U_o levels as would be expected.

8.2.3.1 Surfaces

The LFC surface is taken to include only the outermost skin of the airfoil surface through which the suction air must pass. All sub-surface ducting of the suction system contribute to the duct losses which involve interrelationships discussed in section 8.2.3.2.

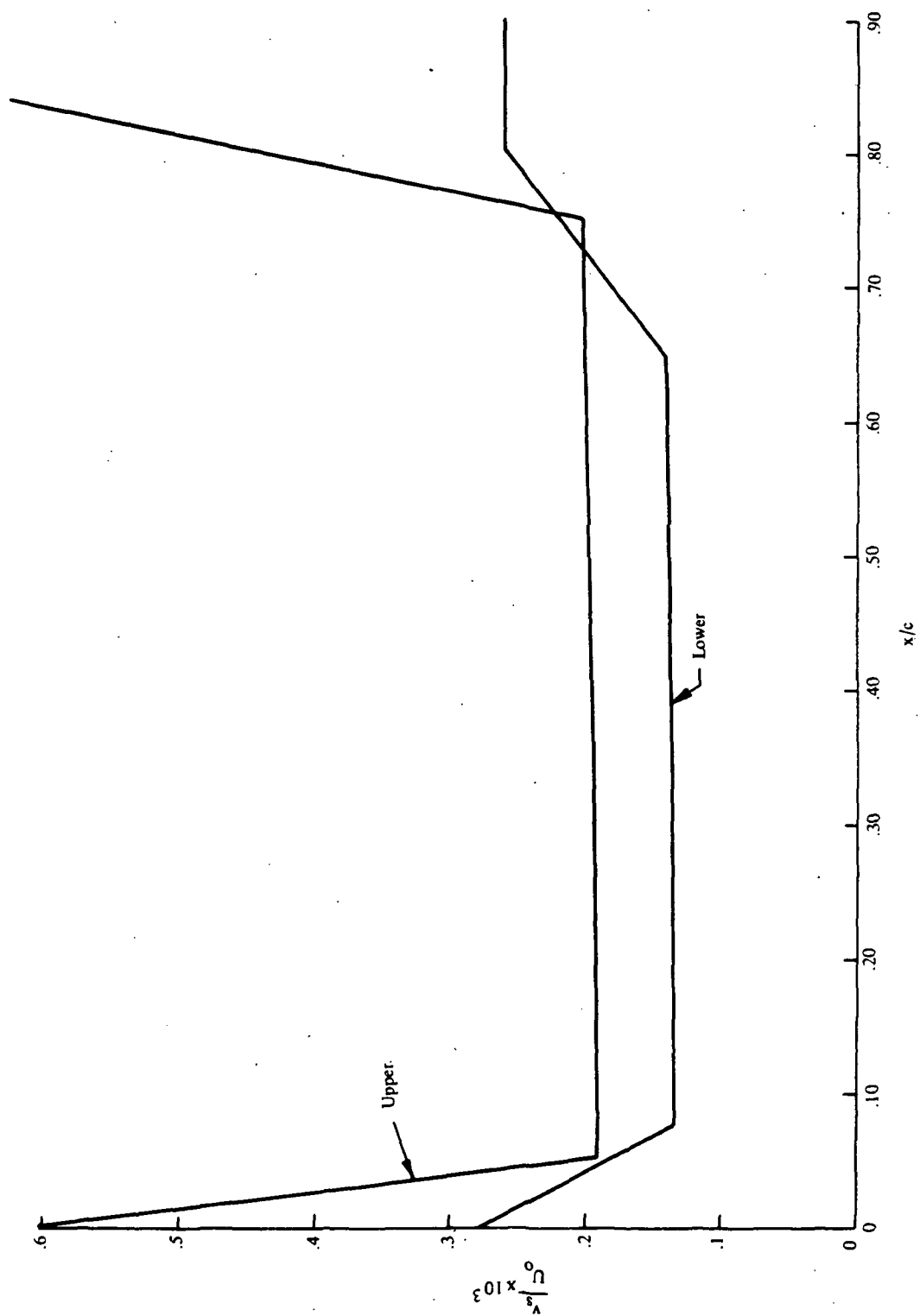


Figure 107. — Distributed suction velocity profile for wing, LFC-200-S

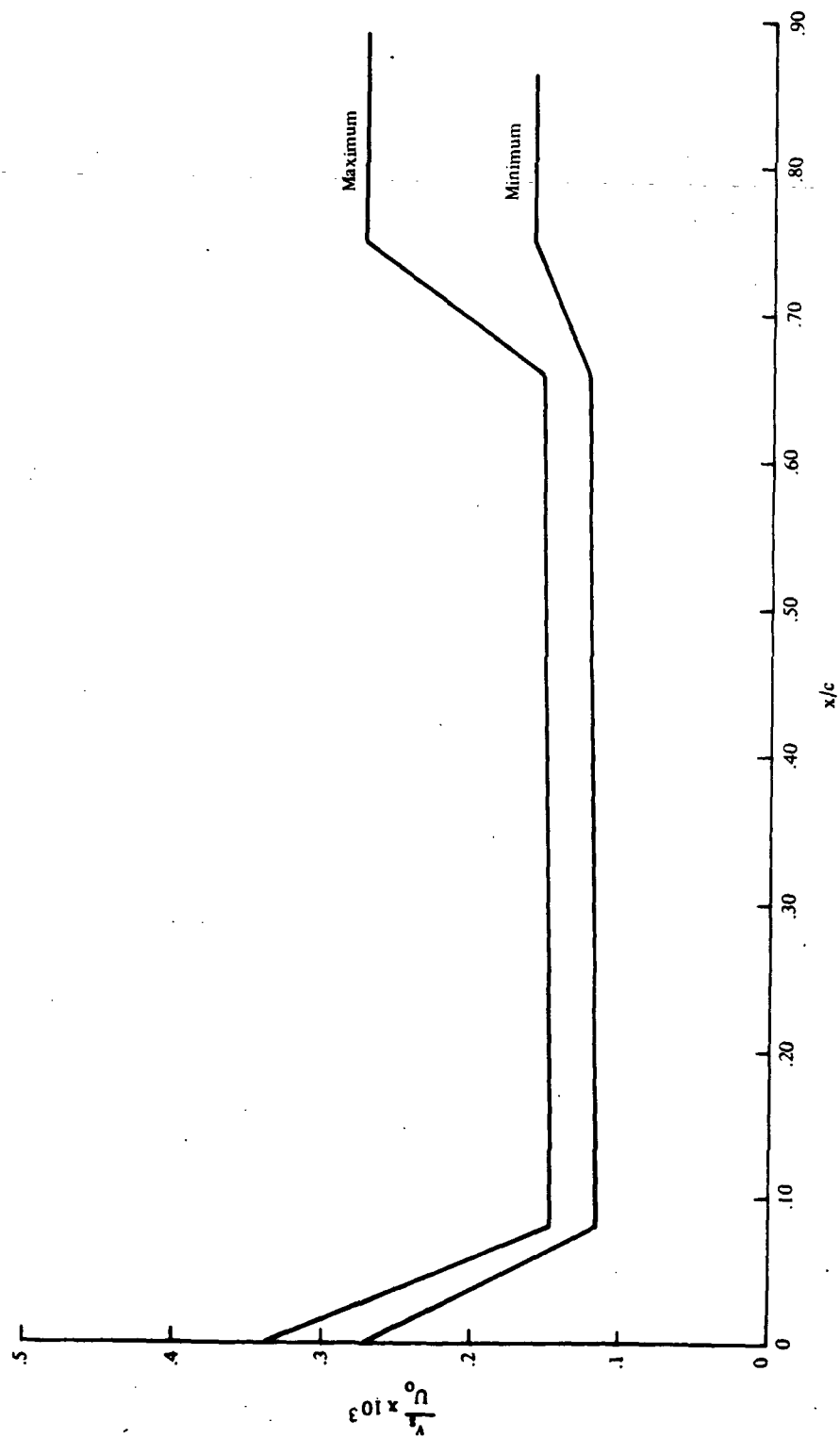


Figure 108. -- Distributed suction velocity profile for horizontal tail, LFC-200-S

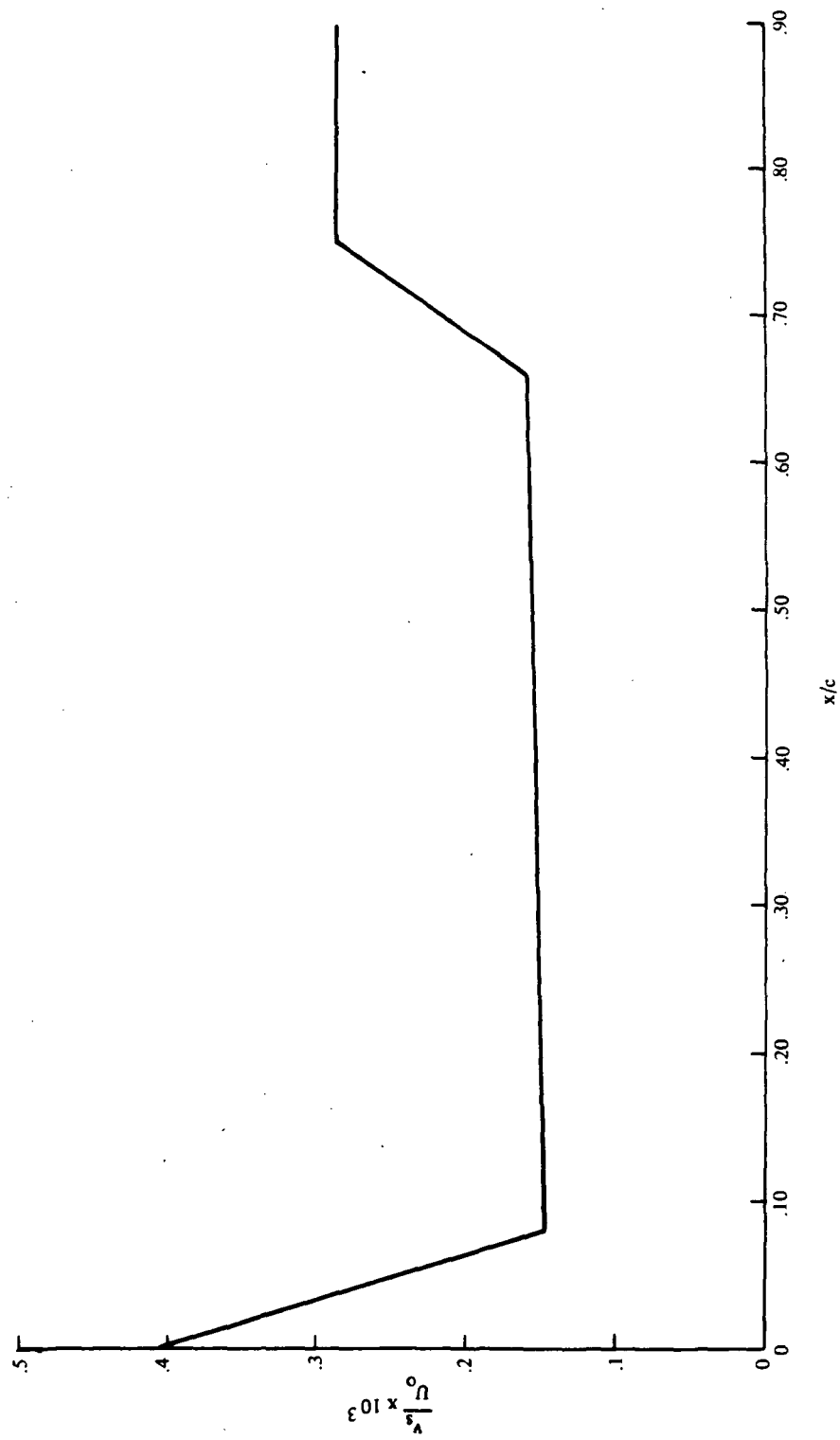


Figure 109. — Distributed suction velocity profile for vertical tail, LFC-200-S

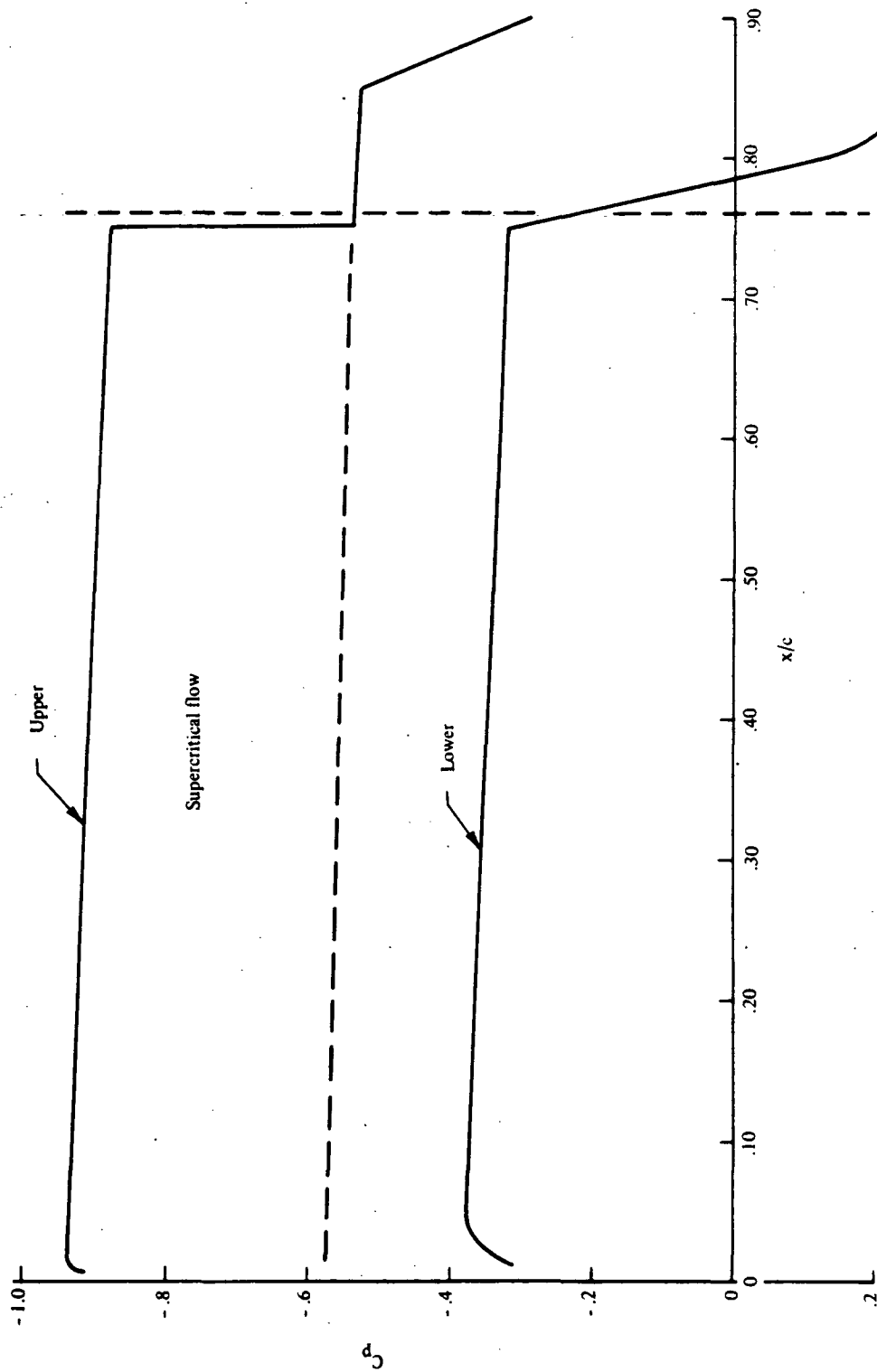


Figure 110. -- Pressure coefficients for wing, LFC-200-S

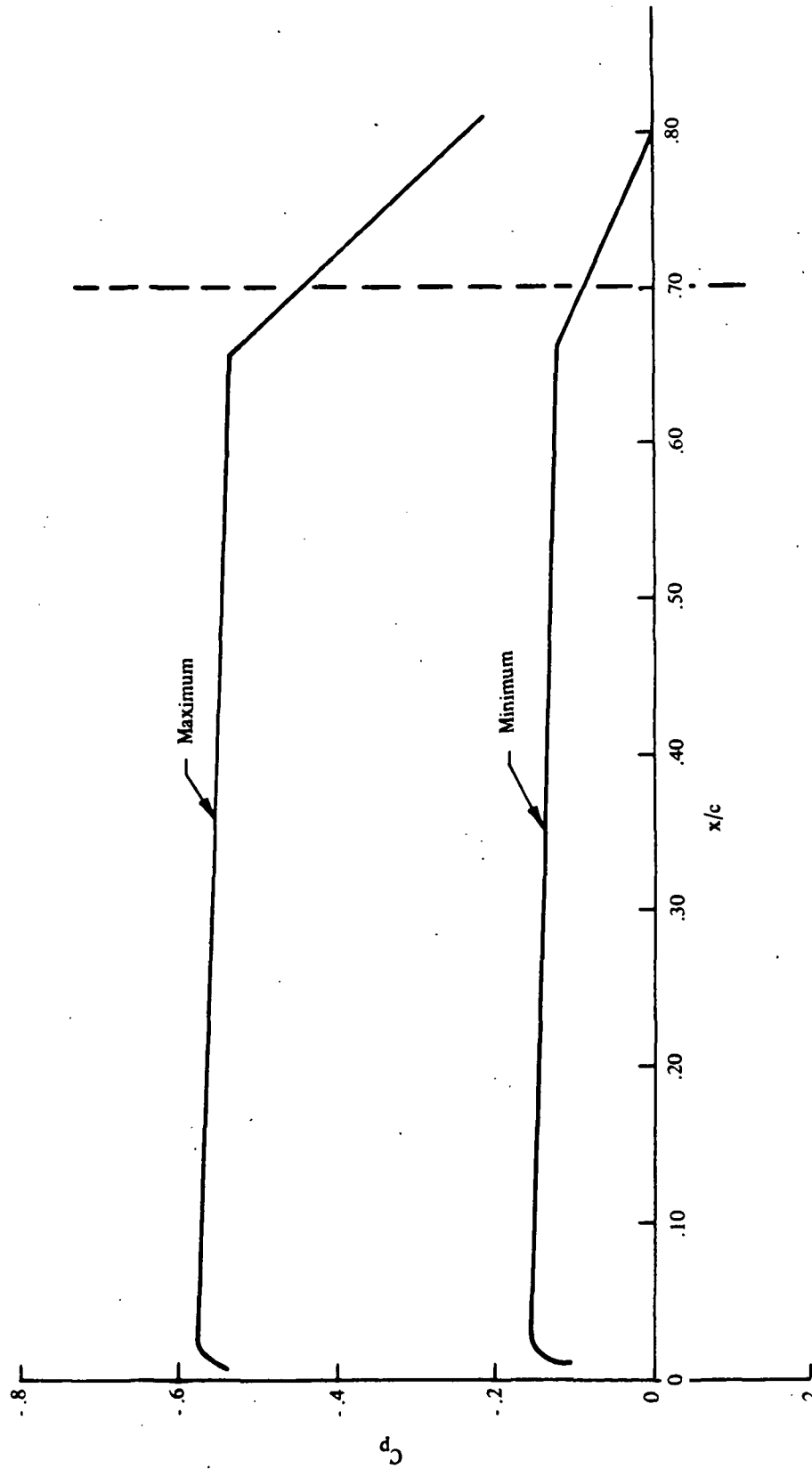


Figure 111. — Pressure coefficients for horizontal tail, LFC-200-S

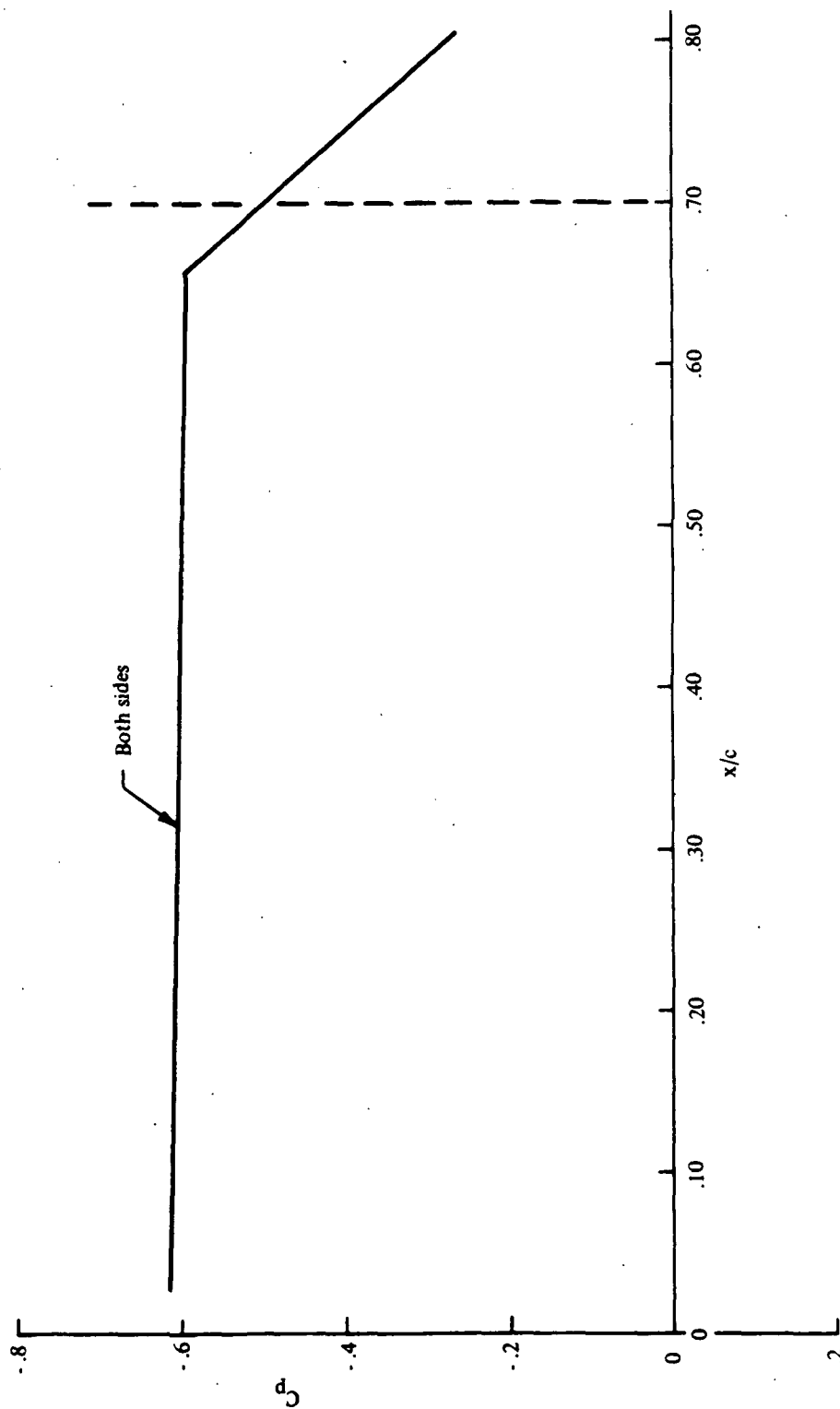


Figure 112. — Pressure coefficients for vertical tail, LFC-200-S

Inspection of the foregoing figures, 107 through 112, reveals that the higher levels of v_s/U_o and lower levels of C_p occur on the upper wing surface. The upper wing, therefore, presents the most stringent suction requirement and determines the higher levels of suction pump pressure ratio. For these reasons, the wing-upper surface was chosen for a more detailed analysis of the suction surface requirements.

A slotted surface was selected for purposes of this analysis because more is known about the criteria and analysis procedures for this type of surface than for the alternative systems. Also, as pointed out in section 6.2.1, similarities exist between the criteria and characteristics of slotted surfaces and those of porous or perforated surfaces.

Methodology — A detailed explanation of the procedures employed for the slotted surface analysis is beyond the scope of this study and would largely duplicate the procedures described in section 3 of reference 15. A requirement for following this analysis procedure is a definition of the laminarized boundary layer velocity gradient. Definition of this gradient was obtained from the Laminar Boundary-Layer Program described in section 4.0. The profile of this characteristic for the upper wing surface is presented on figure 113 as a plot of $\Delta u / \Delta y$ against percent chord. This term is non-dimensionalized against free stream velocity and wing chord in which u represents the ratio of local boundary layer velocity to free stream velocity, and y represents the local normal distance from the wing surface ratioed to the wing chord. Also required is a definition of the local flow sweep angle. This angle was also provided by the boundary layer program.

The nomograph shown in figure 114 was used for definition of slot sizing and spacing. The procedure required an iterative process in which estimated values of surface thickness or slot flow path length, t_s , and slot width, w_s , were selected. The nomograph was entered with slot width and read to the computed value of $\sqrt{\sigma}$ as shown by the dashed line on figure 114. The term σ is defined by the equation:

$$\sigma = \frac{\Delta u}{\Delta y} \frac{\cos \Lambda_s}{R_c \cdot 5} \frac{\rho_s}{\rho_o}$$

in which:

$$\begin{aligned} \Lambda_s &= \text{Local Sweep Angle} \\ R_c &= \text{Chord Reynolds Number} = \frac{\rho_o U_o C}{\mu_o} \\ \rho_s &= \text{Slot Flow Mass Density} \\ \rho_o &= \text{Free Stream Mass Density} \\ U_o &= \text{Free Stream Velocity} \end{aligned}$$

Thence, the nomograph is read down to the computed value of F_o^* and the required spacing (Δc_s) is read to the right. The term F_o^* is defined by the equation:

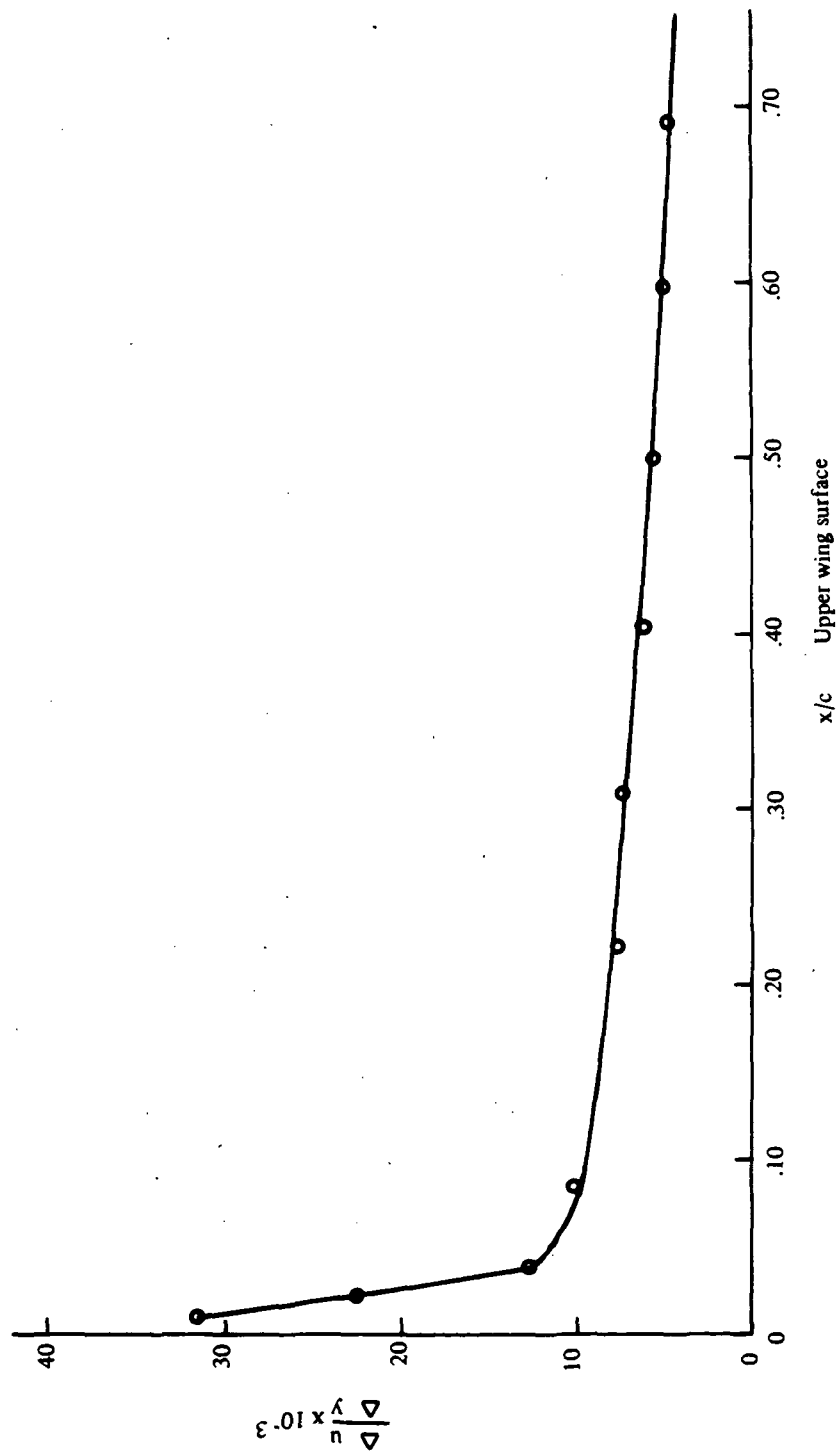


Figure 113. — Boundary layer velocity gradient, LFC-200-S

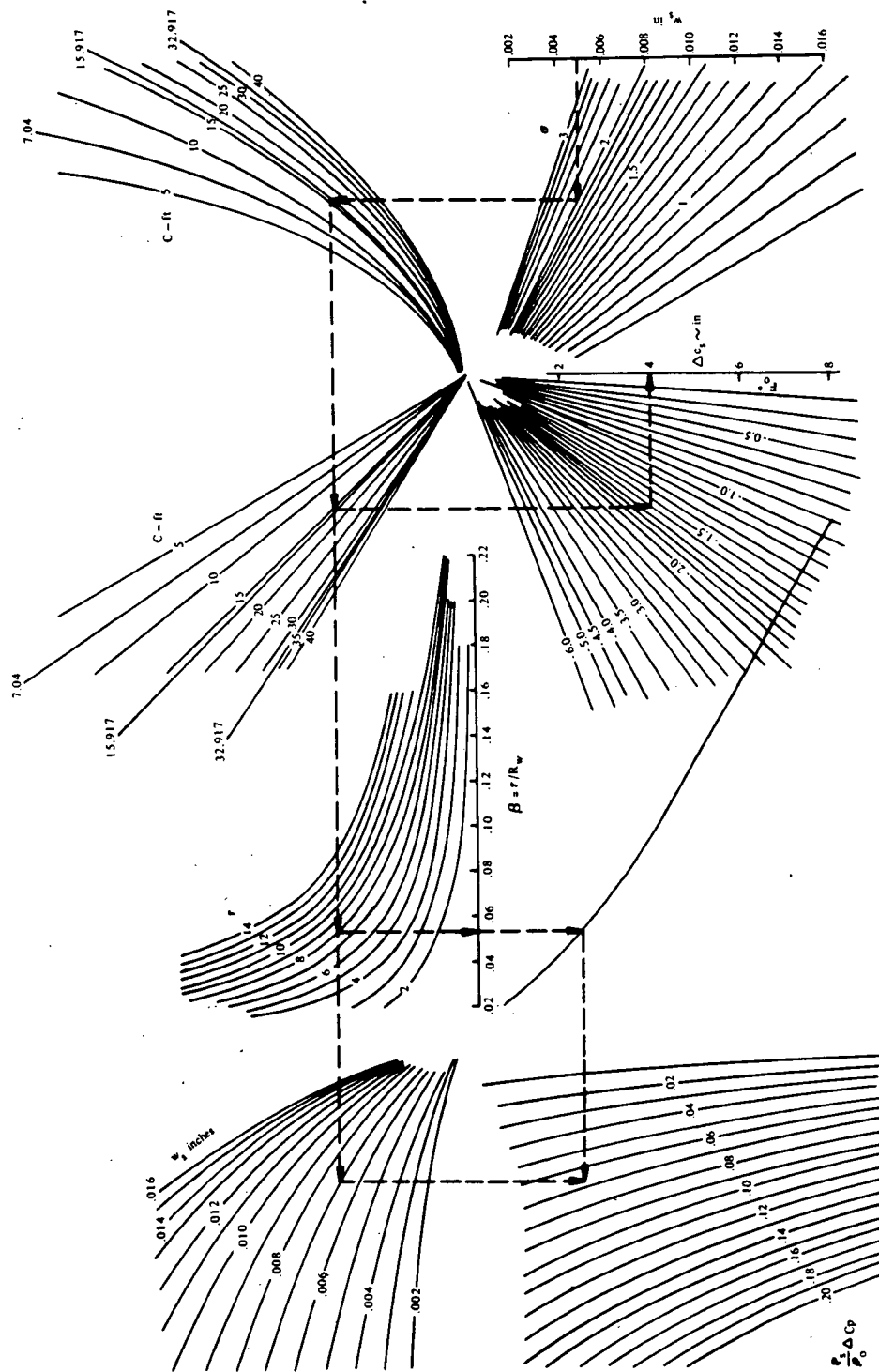


Figure 114. — Suction slot design chart

$$F_o^* = \frac{\rho_s v_s}{\rho_o U_o} R_c^{.5}$$

where v_s = Distributed suction velocity at the surface

From the second family of chord lines, the nomograph is read horizontally to the computed τ and slot width lines. From the τ intersection, the curve is read downward to the β value and on down to the translation line. These terms are defined as:

$$\begin{aligned} \tau &= 2 w_s / t_s \\ \beta &= \tau / R_w \\ \text{where } w_s &= \text{Slot width} \\ t_s &= \text{Slot flowpath length (or material thickness)} \\ R_w &= \text{Slot width Reynolds number} \end{aligned}$$

From the intersection with the appropriate slot width line w_s , the nomograph is read down and the intersection with the translation line is read across to find the intersection at which the point the value of $\frac{\rho_c}{\rho_o} \Delta C_p$ slot is found. From this value the ΔC_p slot, based on q_o , may be computed and the slot pressure drop may be determined.

Comparison of the β and ΔC_p values thus obtained from the nomograph to the lower limit value discussed in section 6.2.1 determines whether the assumed slot width and lost flow path length meet the minimum criteria. If they are found to meet both criteria, the selection then becomes a matter of selecting the best combination from the standpoint of production and/or slot pressure loss. If the β and ΔC_p values do not meet the limiting criteria or the pressure loss through the slot is excessive, new values for w and t must be assumed and the process repeated. The reader is again referred to section 3 of reference 15 for an explanation of the derivation of the above procedure and a more detailed explanation of its application.

Slot Sizing and Spacing – Figure 115 presents a plot of the β and ΔC_p values vs. w_s for a constant t_s of 0.508 mm (0.020 in) for x/c from 0.01 to 0.70. This figure represents upper wing surface characteristics at WS 370, where the break occurs in the wing trailing edge. It will be noted that as w_s is increased, the ΔC_p value increases rapidly while the β value decreases rapidly. Thus, to decrease the slot pressure loss, the slot width should be diminished. This appears contrary to logic, but the associated slot spacing also diminishes such that the slot velocity decreases. It will also be noted that the β and ΔC_p criteria are met over a broad band of t_s values near the

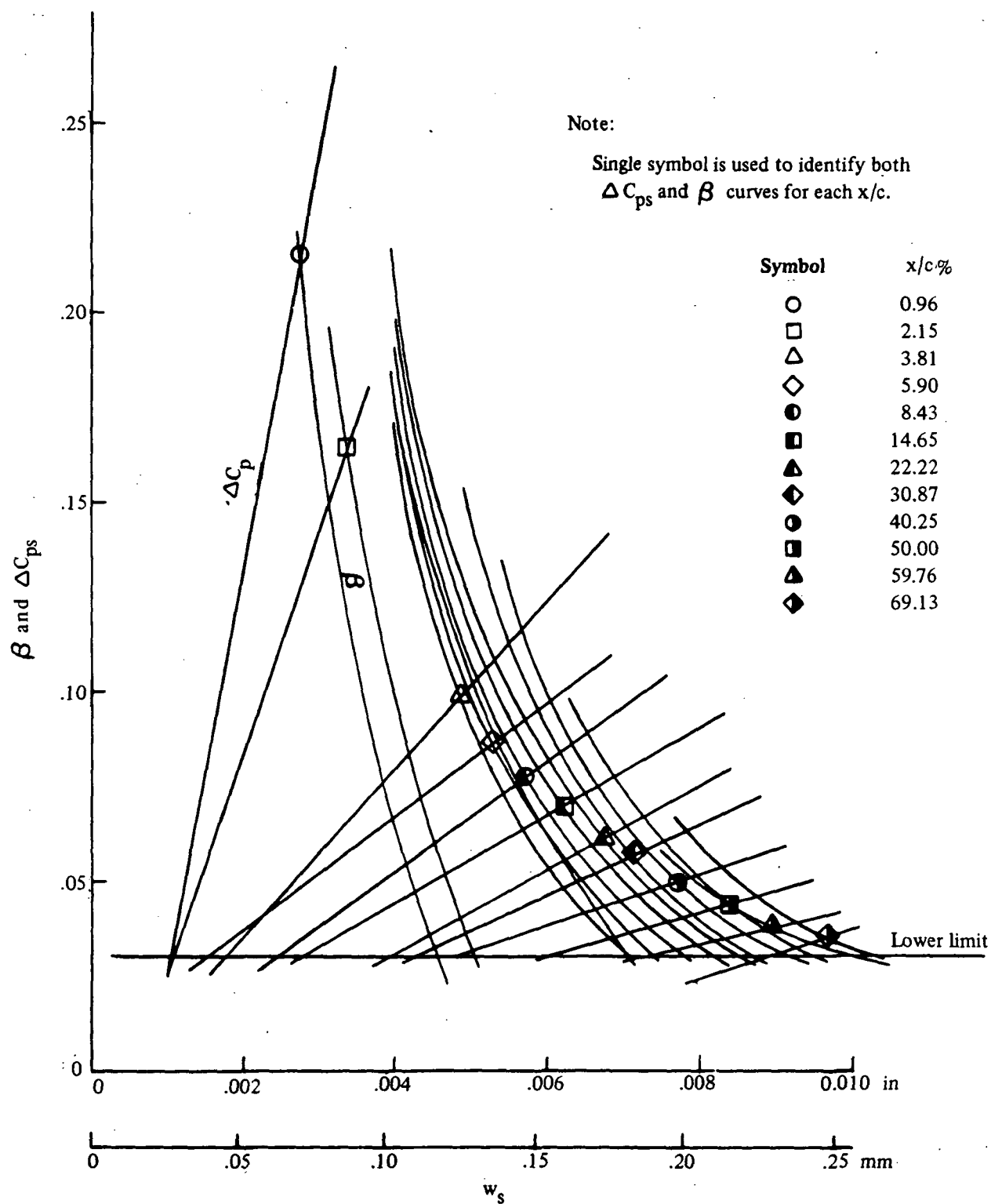


Figure 115. — Slot design limit parameters, upper wing surface, LFC-200-S

leading edge but the ΔC_p values, indicative of slot pressure loss, become quite high at the higher w_s values. Moving back over the airfoil, the band of acceptable w_s values diminishes and translates to progressively higher mean values for w_s . At the same time, the maximum ΔC_p values diminish and the slot spacings increase.

Figure 116 presents companion plots of slot pressure loss, ΔP , expressed as a percent of the free stream total pressure, H_0 and the slot spacing, Δc_s . The limiting values of ΔC_p and β are shown for each chord station. The increase in slot spacing and the attendant increase in slot pressure loss with increasing slot width are readily apparent.

A more physical relation of these characteristics is illustrated by figure 117, which presents limiting values as a function of percent chord. A relatively large spacing may be selected at x/c of approximately 0.05. However, in the forward locations, large spacing results in relatively large pressure losses. Pressure losses of approximately 1% are attainable over virtually the entire surface if sufficiently small slot width and spacing are selected.

The costs of production, quality control, and maintenance are minimized by selecting fewer large, widely spaced, slots. However, the attendant pressure losses may be prohibitive since the suction unit must make up for these losses with a resultant increase in weight and fuel consumption. The basic slot pressure loss may not be too high in itself, but as shown in section 8.2.3.2, there is a considerable cascading effect in duct pressure loss and a small loss at an upstream location is greatly amplified at downstream locations. Figure 118 presents the ratio of H_0 to the pressure immediately inside the slotted suction surface. Neglecting duct losses and the amplifying effects of cascading losses in the ducting, this figure approximates the suction unit pressure ratios required to overcome the slot losses with zero internal duct loss. The impact of these losses is immediately apparent. It indicates, however, that the bulk of the high loss slots are located in the first four percent of the chord at the wing leading edge. The leading edge, extending back to $x/c = 0.04$, requires special and complex fabrication and can be specifically designed and constructed to have relatively closely spaced slots. Since the upper wing surface and leading edge spanwise trunk duct is located in the leading edge, the internal ducting is relatively short. Pressures within the trunk duct are locally at a lower level to overcome the duct losses in the wing cover and a match between the relatively higher pressures in the cover slots with the leading edge requirements can be readily achieved. This is discussed further in section 8.2.3.2.

Similar analyses were performed for the wing tip station and the wing root station. The wing tip station was found to exhibit characteristics similar to those of the previous station. Figure 119 presents the slot loss and spacing characteristics as a function of slot width and figure 120 presents the same parameters as a function of wing chord. Comparison of these figures with figures 116 and 117 for WS 370 shows that slot widths are generally smaller and the slot pressure losses are somewhat higher for the tip station than for WS 370. However, the band of allowable slot spacing is somewhat larger. These differences in characteristics are to be expected from the markedly reduced chord of the tip station. The tip chord is approximately 44% of the chord at station 370.

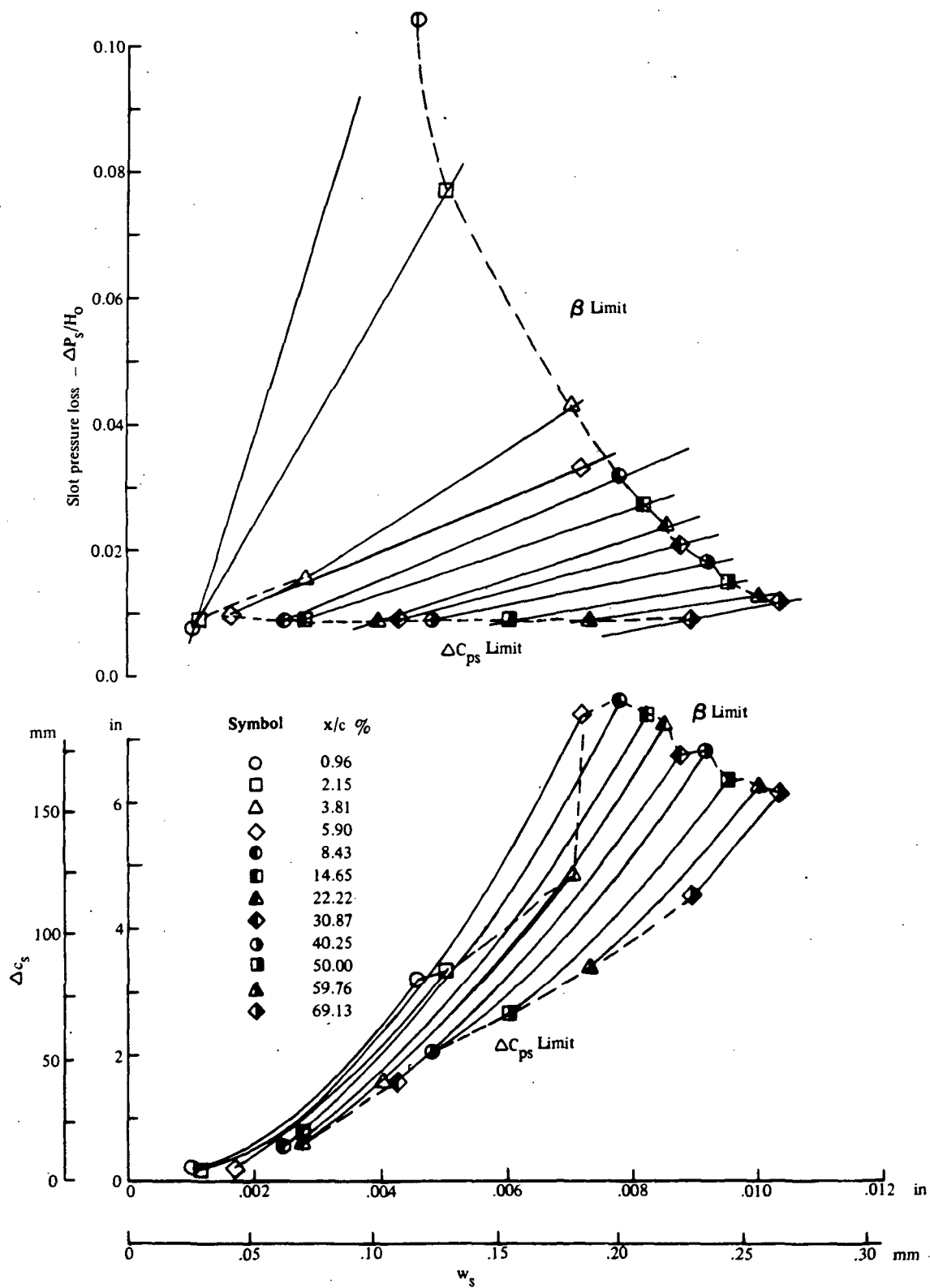


Figure 116. — Slot spacing and pressure loss vs. slot width, upper w_s 370, LFC-200-S

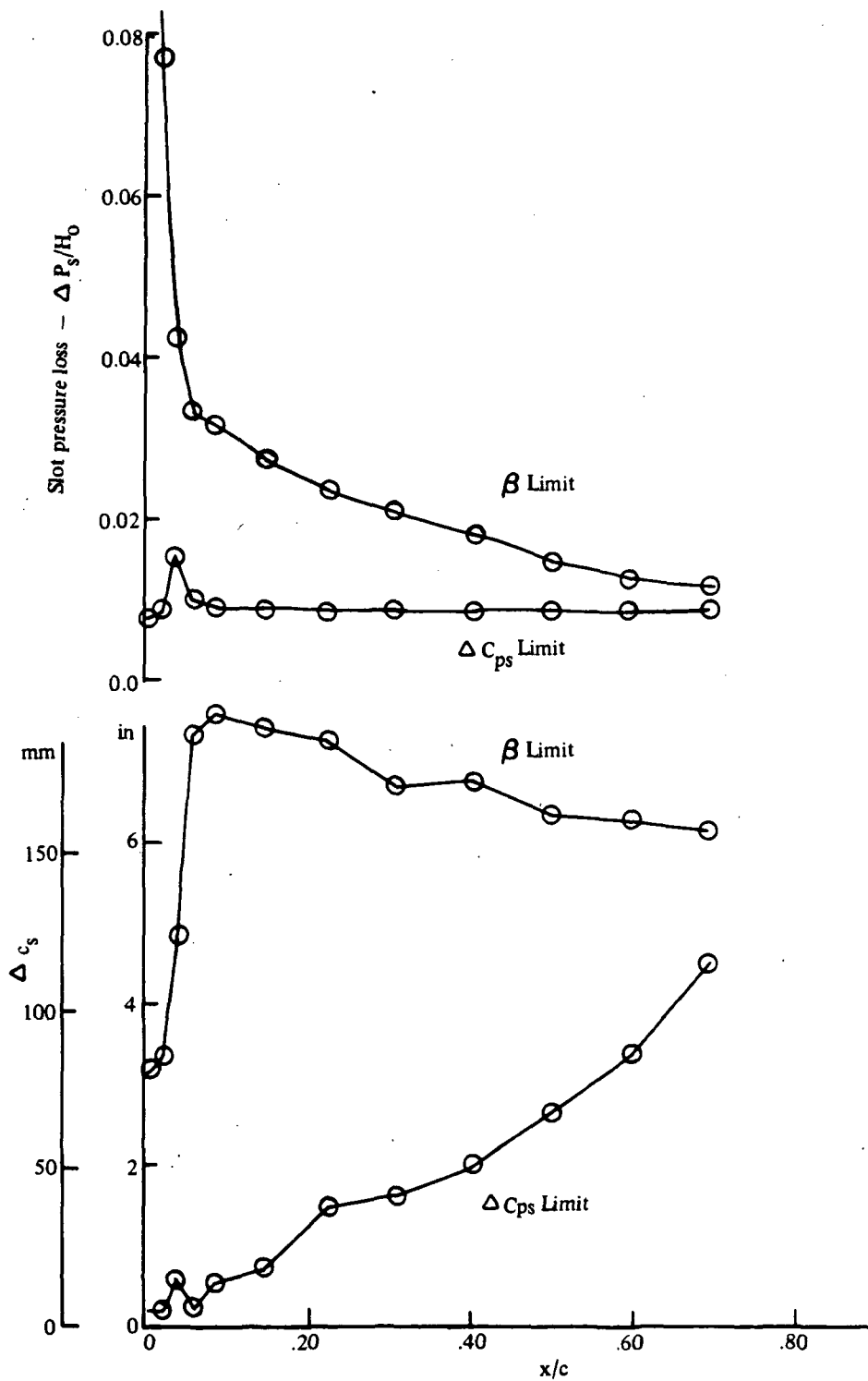


Figure 117. — Slot spacing and pressure loss vs. chord location, upper WS370, LFC-200-S

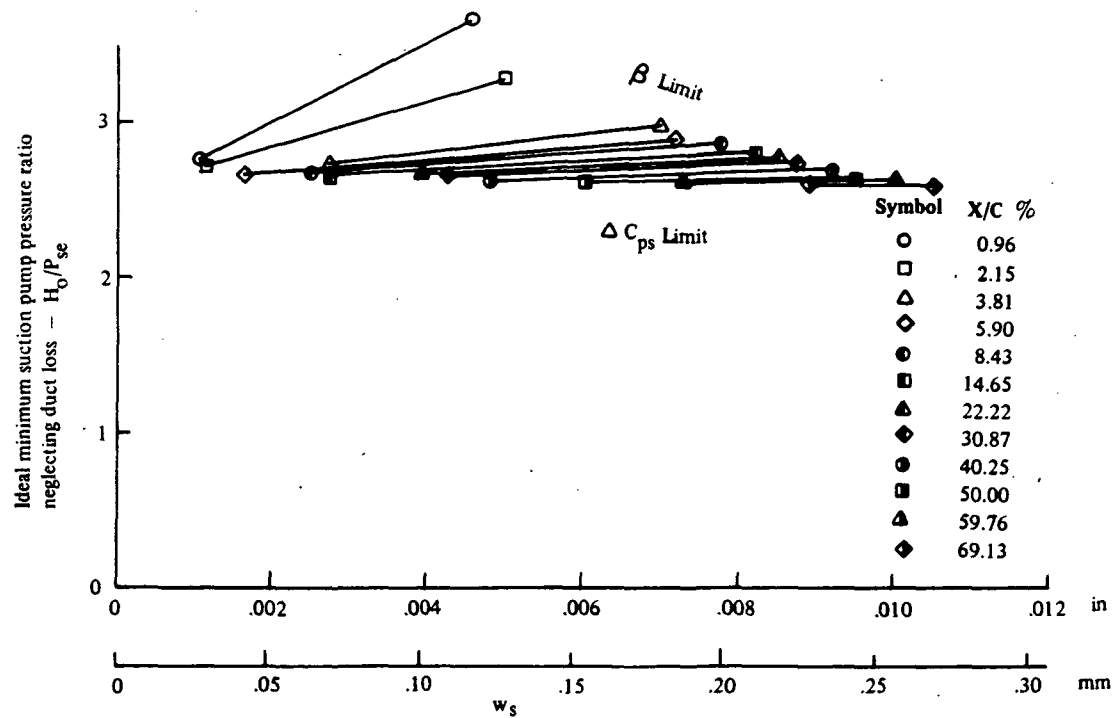
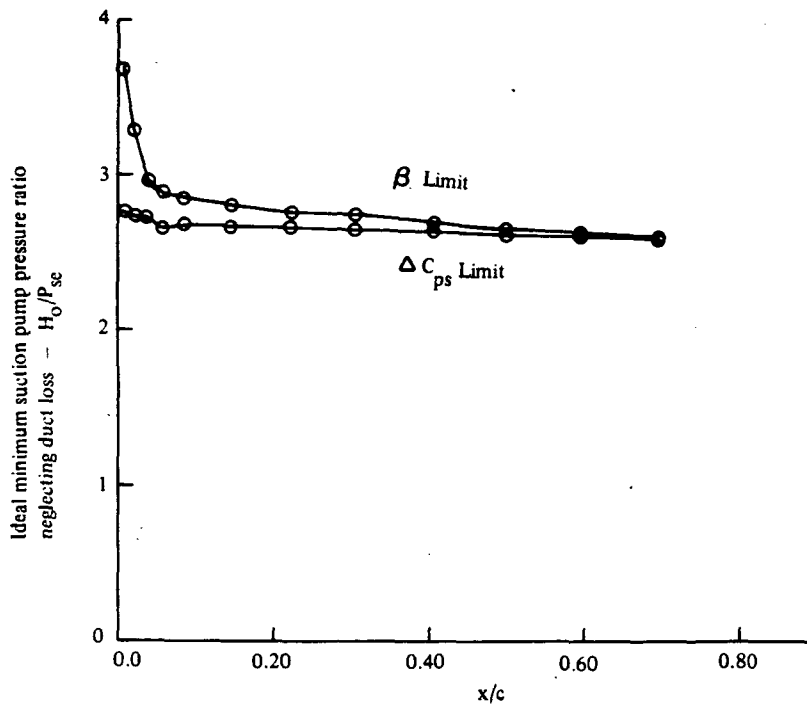


Figure 118. — Effect of slot size on required suction pump pressure ratio, upper WS 370, LFC-200-S

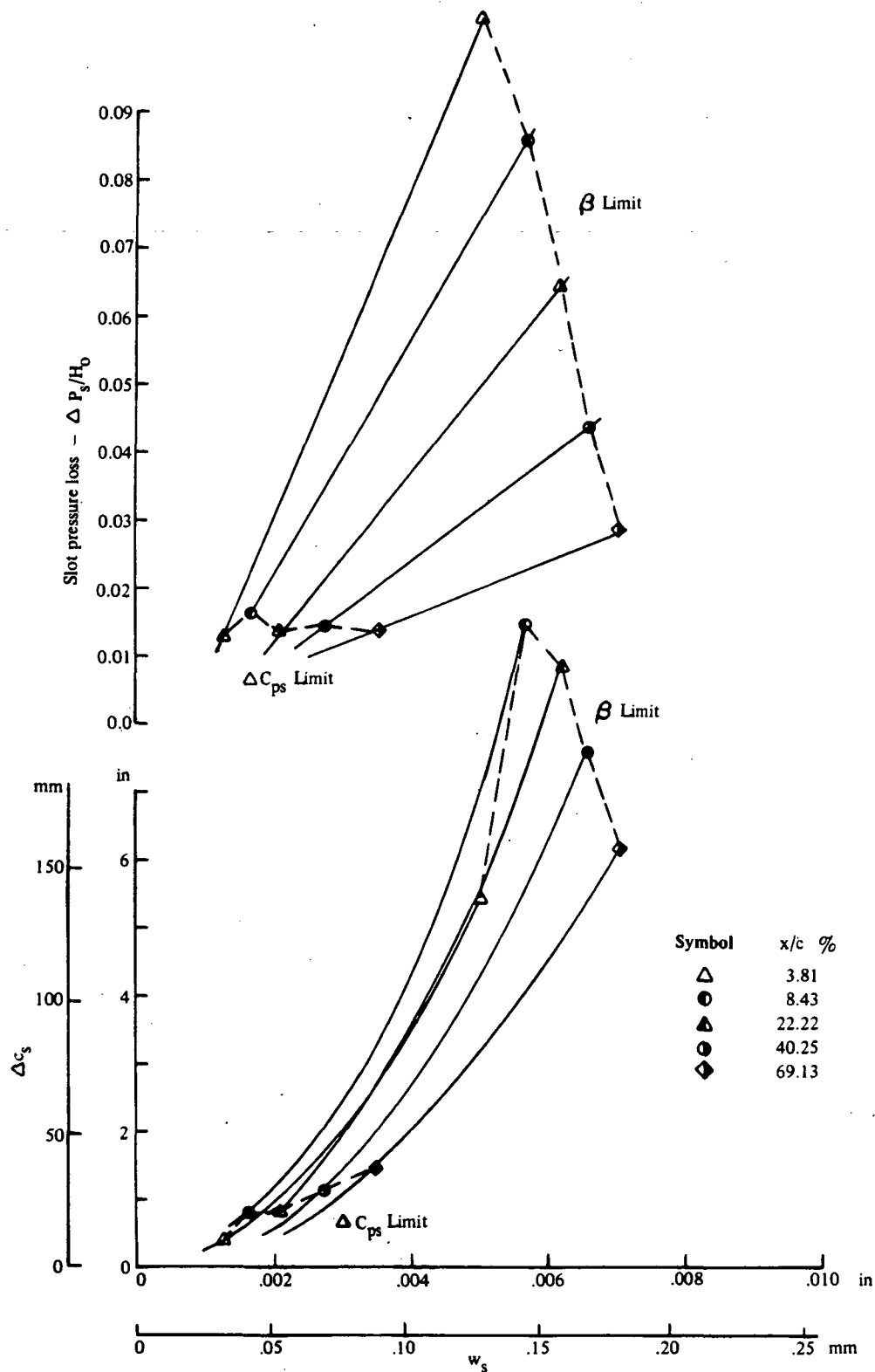


Figure 119. — Slot spacing and pressure loss vs. slot width, upper WS 1150, LFC-200-S

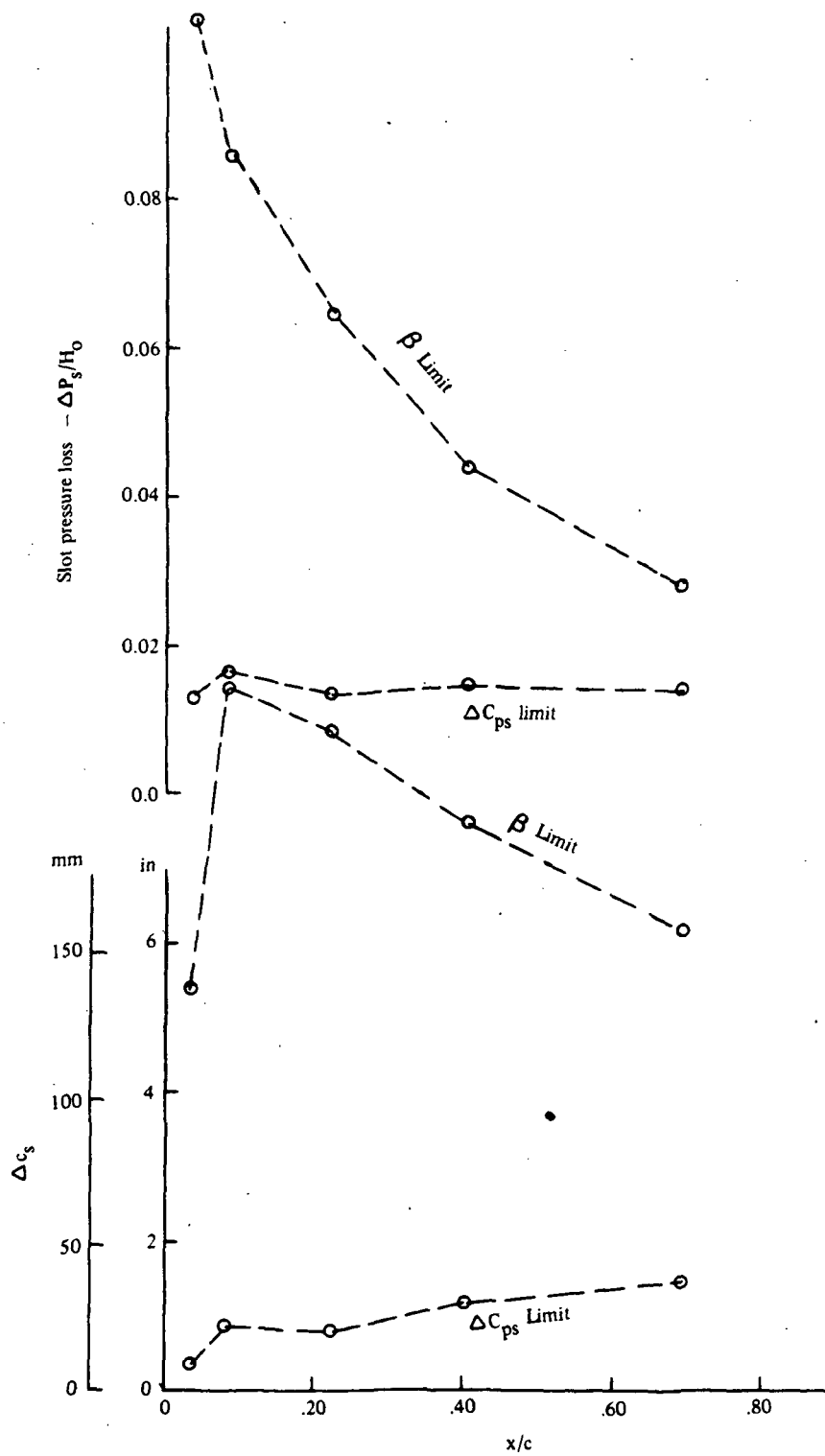


Figure 120. — Slot spacing and pressure loss vs. chord location, upper WS 1150, LFC-200-S

At chord locations greater than 10% in the wing-root region at WS 100, no values of w_s simultaneously satisfy the 0.03 lower limit for both ΔC_p and β for a t_s of 0.508 mm (0.020 in). This is a result of the large chord of the root station. Inspection of figure 115 reveals that the band of slot width values that satisfactorily meet the ΔC_p and β criteria narrows significantly at the higher chord locations.

As pointed out in section 6.3.1, two alternatives exist for coping with this problem. The leading edge of the slot may be rounded, thus providing relief from the lower limit of 0.03 for β , or t_s may be increased. Rounding the leading edge of the slot is extremely difficult to maintain in production on a quality control basis. Increasing t_s may be accomplished by either locally bonding material on the inner skin surface before the slot is cut or by chem-milling a thicker skin material to leave the desired thickness locally in the areas to be slotted.

Figure 121 presents slot spacing and pressure losses as a function of slot width and illustrates changes in these parameters with variations in t_s . At higher chord locations, increases in t_s are necessary. There are two possible values for t_s at most stations. This is shown more clearly in figure 122 in which slot spacing and pressure loss are plotted as a function of wing chord. In this figure, the increase in allowable slot spacing is clearly indicated. The pressure losses through the slot are affected to a minor extent. Slot pressure losses on the order of 1% are readily achievable.

The selection of slot spacing, slot width, and slot flow path over the surface of the wing is influenced by the design and production considerations of the wing panels. As described in section 6.2.3, the selected panel design provides slot ducts running in a spanwise direction at 0.051 m (2 in) chordwise intervals. It is desirable to hold this interval constant for the entire wing surface. The panels extend from $x/c = 0.05$ to 0.75 and are divided into spanwise segments to facilitate manufacture and maintenance. Eight panels are used on a semi-span surface. Figure 123 presents a scale planform of the wing upper surface for the LFC-200-S configuration illustrating the spanwise panel segments. Superimposed on this planform are lines of constant percent chord corresponding to those of the foregoing analysis.

On each cover panel, it is obviously beneficial to hold ΔC_p , w_s , and t_s constant for the span of the panel insofar as possible. The 0.051 m (2 in) intervals of the spanwise slot ducts dictates that the slots be cut in the surface in multiples of 0.051 m (2 in). It is apparent that to maintain this selection of slot spacing, the slot width must be adjusted for compatibility with the previously discussed criteria and requirements. A choice of constant slot spacing results in slot chordwise locations that are not constant from the inboard to outboard ends of a panel. Additionally, the slot spacing and width requirements vary as a function of spanwise location. It is, therefore, apparent that some compromises must be accepted in selection of the slot spacing and width from the inboard to the outboard ends of a panel. In addition, manufacturing cost dictates that maximum acceptable slot spacing be employed to the extent possible.

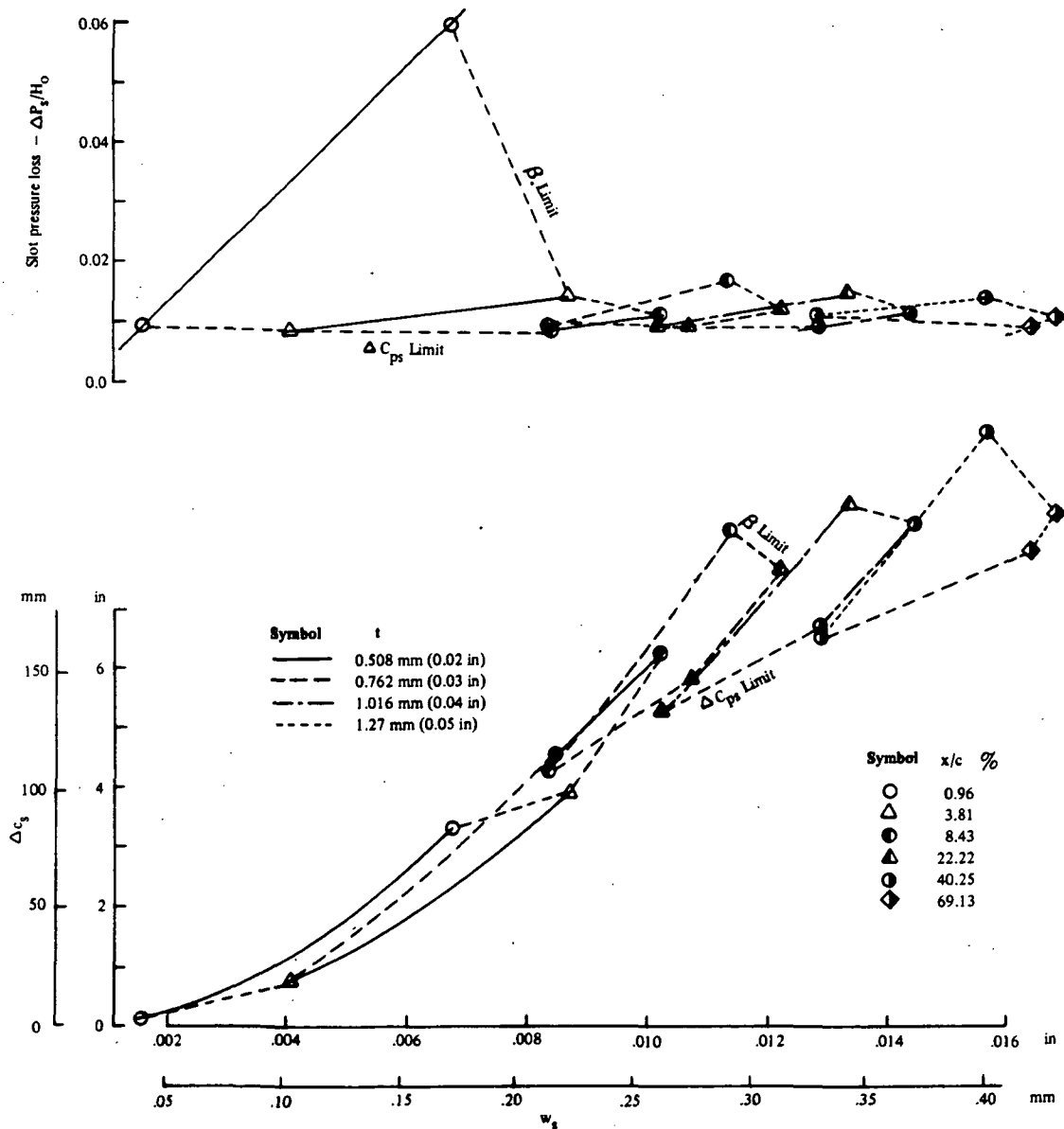


Figure 121. — Slot spacing and pressure loss vs. slot width, upper WS 100, LFC-200-S

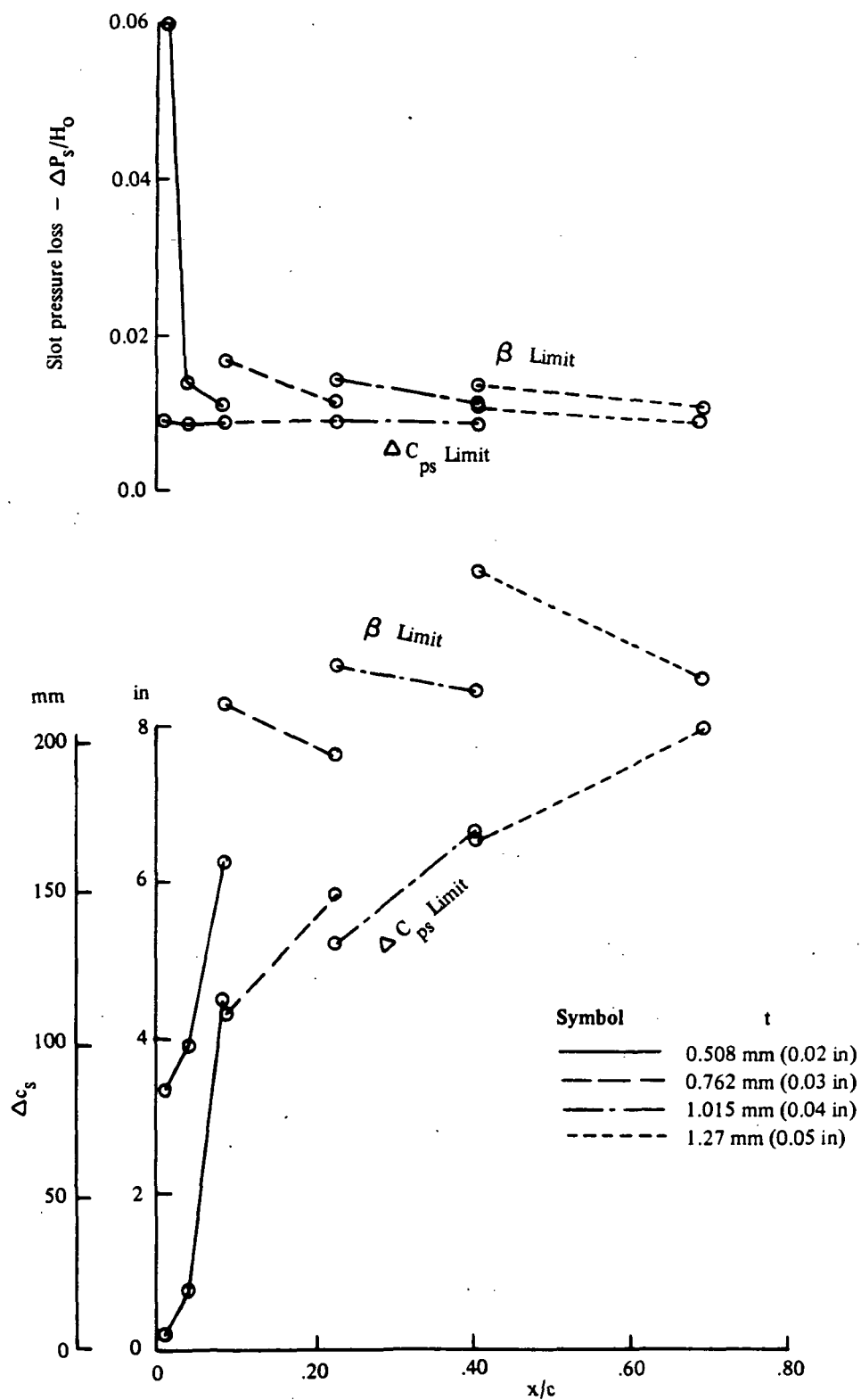


Figure 122. — Slot sizing and pressure loss vs. chord location, upper WS 100, LFC-200-S

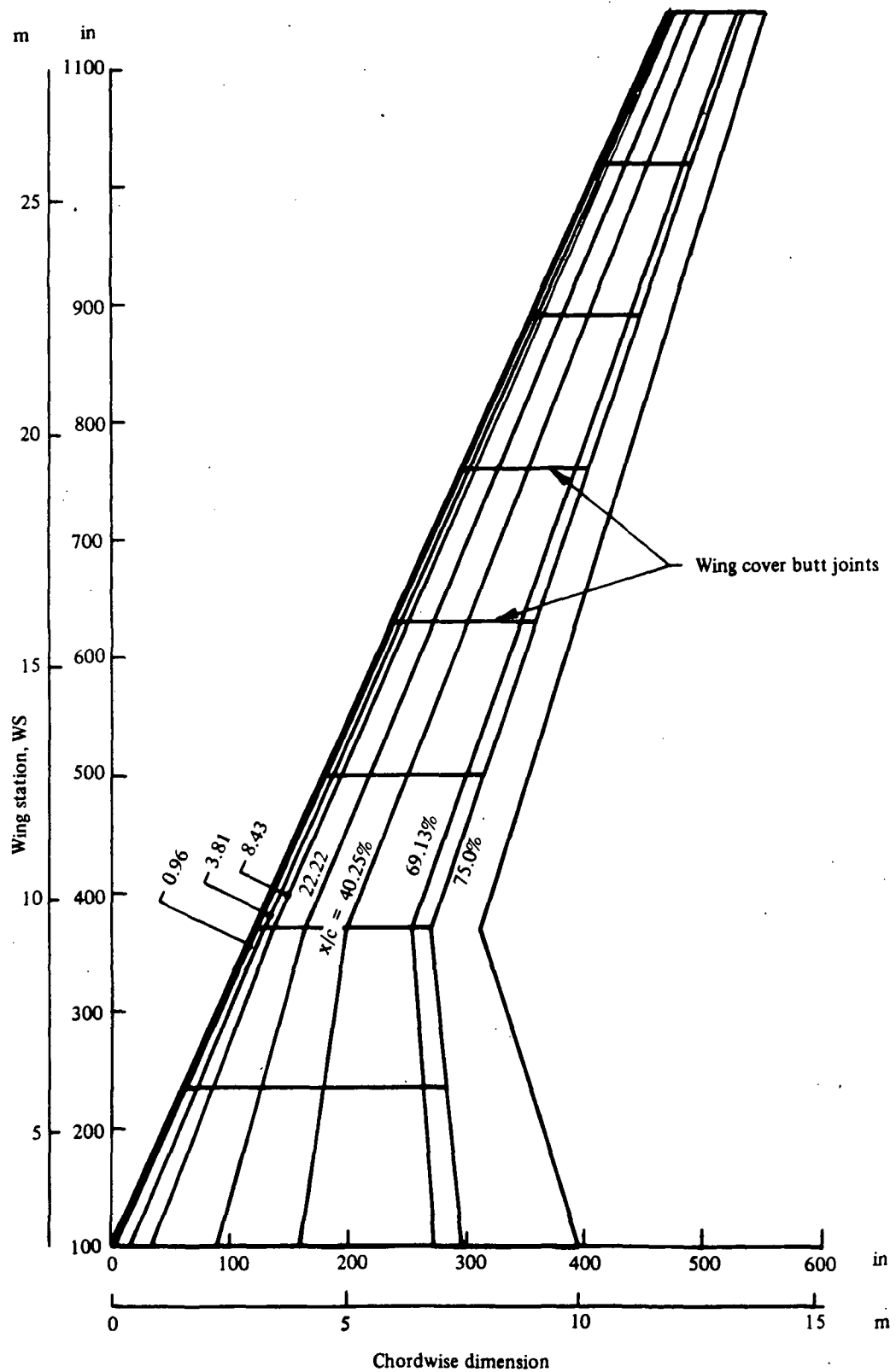


Figure 123. — Wing upper surface planform, LFC-200-S

With these considerations in mind, slot spacings were selected for each panel as illustrated in figure 124. It will be observed that 0.152 m (6 in) spacing is acceptable over the major part of the wing upper surface. The spacing shown for the leading edge is a nominal value. These slots may require cutting on wing elements rather than constant intervals. A portion of the wing root panel requires 0.051 m (2 in) spacing in the leading edge area while 0.203 m (8 in) spacing is required in the mid-chord area and aft.

Utilizing data represented by figures 116, 119, and 121, slot widths compatible with the figure 124 spacing pattern were selected for each cover panel. The associated slot pressure loss data are also available from figures 116, 119, and 121 and were assessed for compatibility with the requirements.

The selected slot widths are superimposed on the wing profile in figure 125. The effects of spanwise variations in spacing and slot width requirements on the constant spanwise slot width and spacing pattern is readily apparent. There is a relatively small step change in slot width of each panel joint in the wing surface outboard of station 370. These step changes are not serious, but slightly excessive suction flows result at the outboard ends of each panel. This may be overcome by locally reducing the size of the holes allowing the flow to pass from the spanwise slot ducts to the chordwise collector ducts. This entails some additional pressure drop as discussed in section 8.2.3.2, but is accepted as necessary for locally adjusting the suction flow through the skin.

The wing surface from WS 370 inboard presents a different pattern. This results from the rapid taper of the wing chord in this area. A constant slot width from the inboard to outboard ends of the panel does not produce a suitable match with the requirements, nor can the flow control holes from the slot ducts to the collector ducts satisfactorily correct the mismatch without excessive pressure losses. The slots in this region require tapering, which can be accomplished through manipulation of a laser from one end of the slot to another or in spanwise steps. If the slots are cut by saw, two cuts can be made employing a saw compatible with the slot width on the outboard end of the slot. The two cuts can be made by offsetting the inboard end between the first and second cuts, producing a uniformly tapering slot. In any case, the additional production cost for tapering these slots is not prohibitive.

In figure 125, it should be observed that the slots depicted represent bands in 0.025 mm (0.001 in) increments. The slot widths were defined more precisely than this, but manufacture to such tolerances is not practical. These step changes in slot width are compatible with aerodynamic requirements, since flexibility is provided through adjustment of the slot-duct to collector-duct holes.

The slot passage lengths in the wing section at the root required increases above the 0.508 mm (0.020 in) skin thickness to meet the ΔC_p and β criteria. These increases in slot passage length are presented in figure 126. Constant chordwise spacing for these variations was selected for ease of manufacture. These slot flow path lengths are compatible with the slot spacings and slot widths shown in figures 124 and 125, respectively.

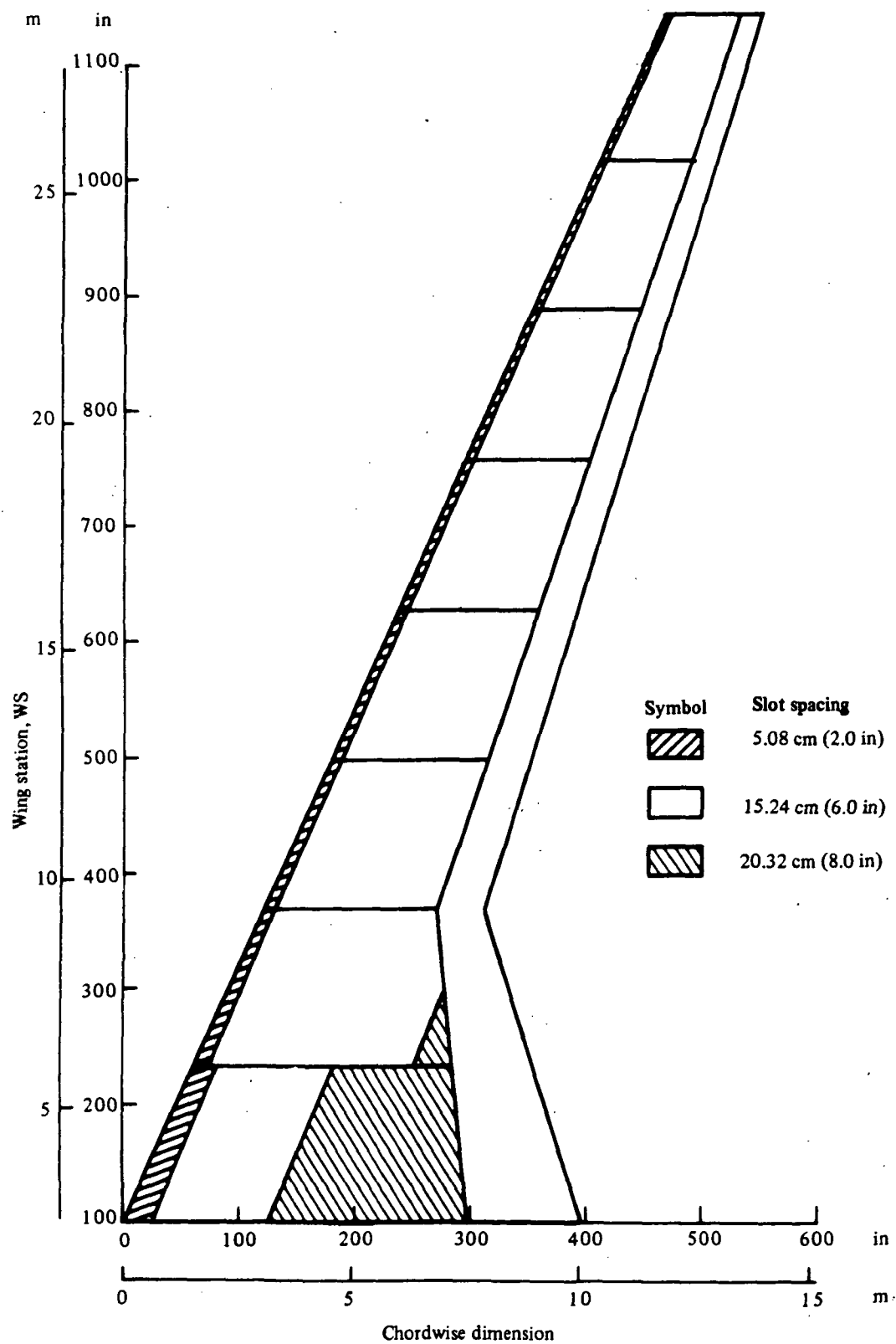


Figure 124. — Slot spacing planform, wing upper surface, LFC-200-S

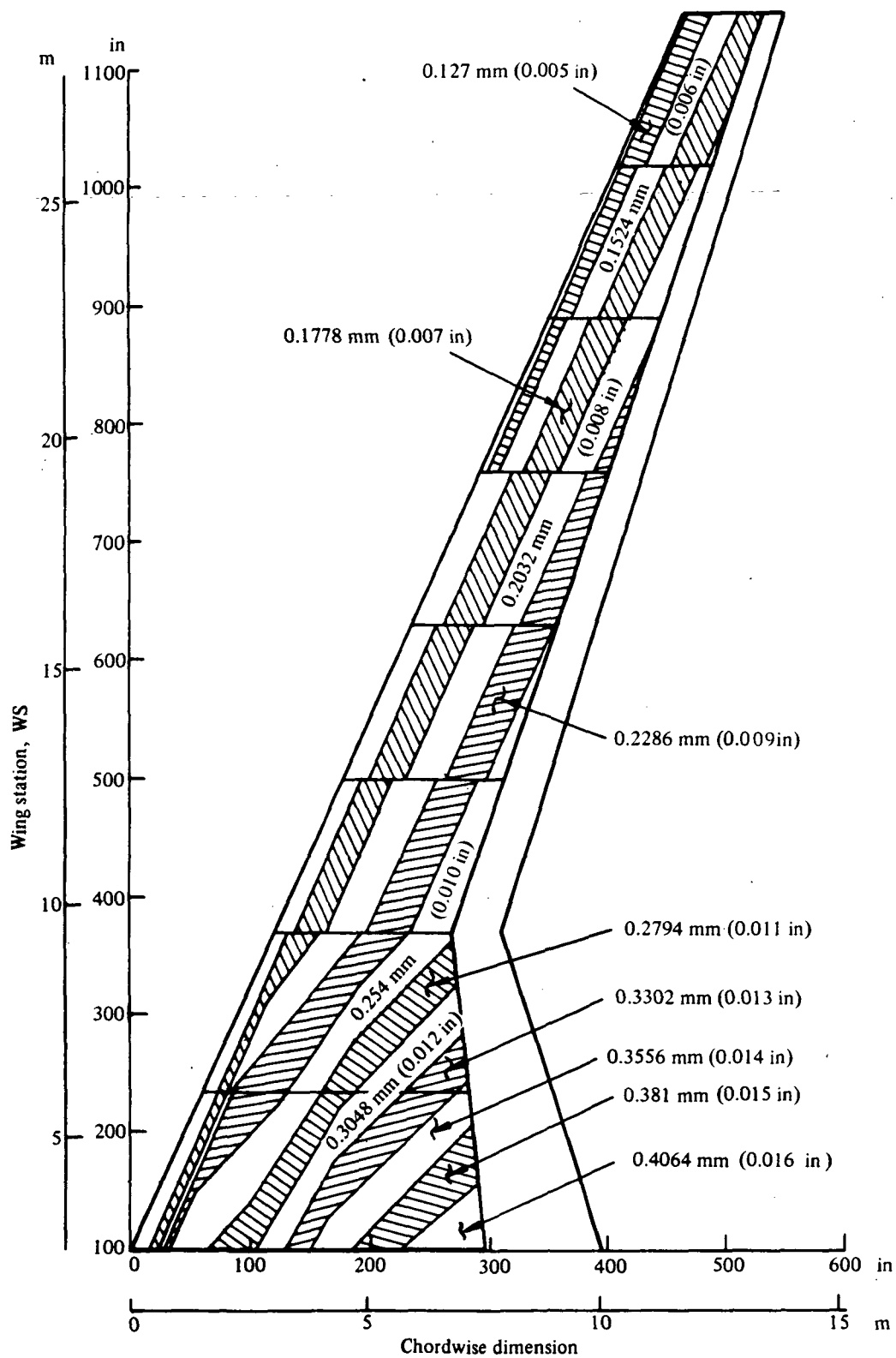


Figure 125. — Slot width, w_s , upper wing surface, LFC-200-S

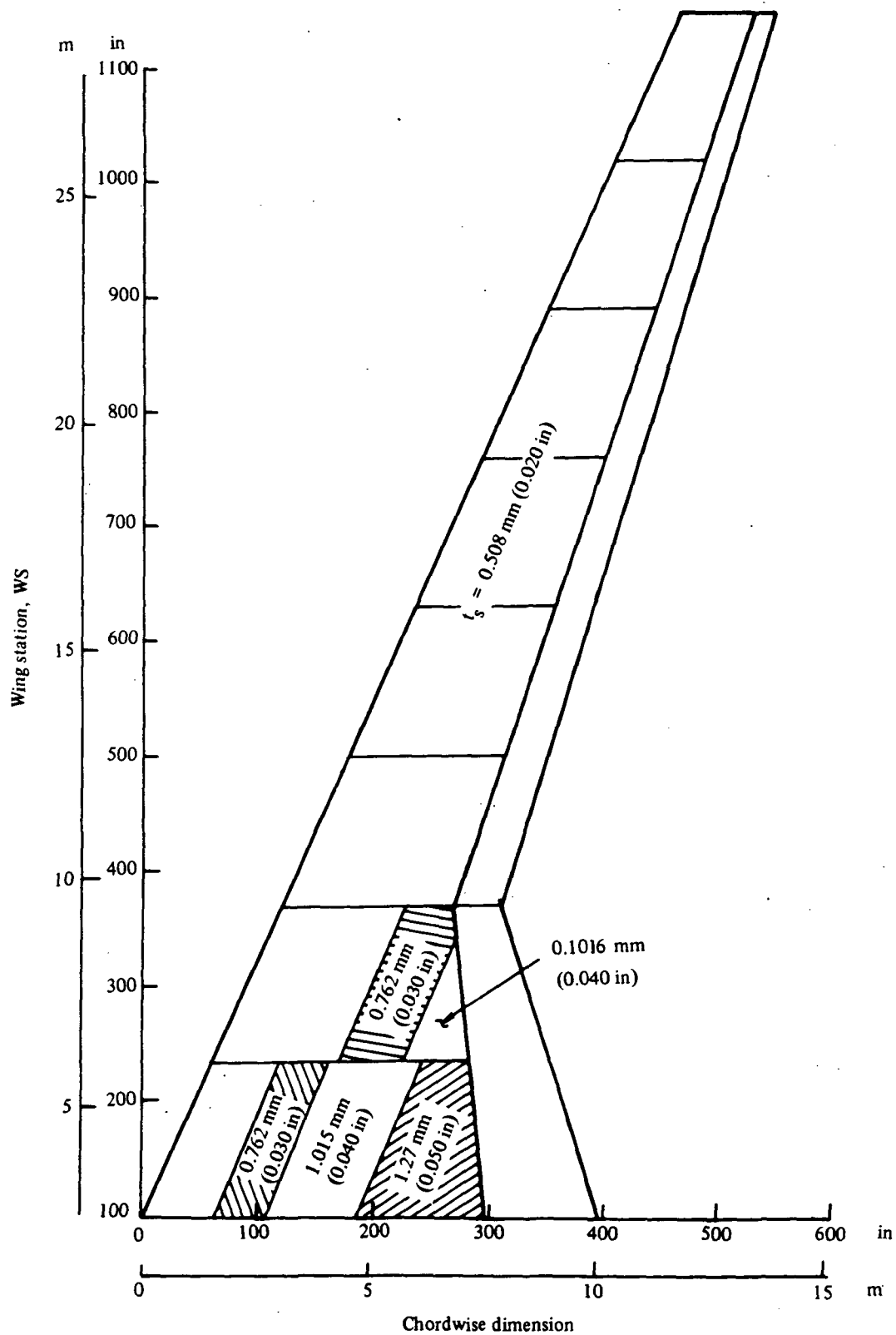


Figure 126. – Slot flowpath length, t_s , upper wing surface, LFC-200-S

The configuration selected for the LFC wing panels is entirely compatible with the LFC suction requirements and criteria.

The selected surface design does not present any insurmountable or costly production or maintenance problems. As for any system, a detailed design analysis is required to define the system to the level required for production. An extensive configuration-oriented test program is necessary to provide the required guidance for fine tuning the system before production is initiated.

Surface Panel Design – Continuing studies directed toward reducing weight and cost of LFC surface panels resulted in the selection of the configuration shown in figure 127 for the final LFC airplane series. LFC panels of identical construction and dimension are used for wing and empennage surfaces. The slotted outer skin is 0.508 mm (0.020 in) aluminum, the upper spacers are 0.254 mm (0.010 in) lightweight Kevlar, the drilled intermediate skin is 0.508 mm (0.020 in) Kevlar, the lower 1.015 mm (0.040 in) hat-shaped spacers are 0.508 mm (0.020 in) lightweight Kevlar, and the inner solid skin is 0.508 mm (0.020 in) Kevlar. Chordwise and spanwise edge members are lightweight Kevlar strips. Total panel thickness is 14.2 mm (0.56 in) thick. A typical surface panel segment construction is shown in figure 128.

The leading edge surface panels are identical dimensionally. They are constructed of aluminum in order to withstand the heat produced by electrical heating elements bonded into the panels to provide anti-icing capability. The leading edge panel segments extend from 4% upper surface chord to 4% lower surface chord. Typical wing section with panels installed is shown in figure 129. A weight summary for both the surface and leading-edge panels is presented in table 21.

Wing surface LFC panels are constructed in eight segments per upper surface and eight segments per lower surface on each wing. These panels, as described above, extend from 4% to 75% of the wing chord. Each panel segment is approximately 3.81 m (150 in) long spanwise, and vary in chordwise length from 1.52 m (60 in) for the outermost segment to 5.59 m (220 in) for the innermost segment.

Surface panels are installed on the basic wing with bolts and floating plate nuts on 0.152 m (6 in) centers around their periphery as shown in figure 128. Field bolts are installed on approximately 0.305 m (12 in) centers chordwise into wing rib caps which occur each 0.762 m (30 in) spanwise. The floating plate nuts and oversize holes in basic wing structure accommodate a predicted maximum differential movement of 2.03 mm (0.08 in) between skin panels and basic structure under 2.5g load conditions. To maintain smoothness and waviness tolerances, the surface panels are installed with the structural wing jigged to a 1g deflected position. Proper surface contour is achieved by use of liquid shims under the panels at each bolt location. After the panel segments are fastened in place, a putty-type sealer is used along each edge of a segment and at bolt locations. After setting, the putty is filed and sanded to meet prescribed smoothness criteria.

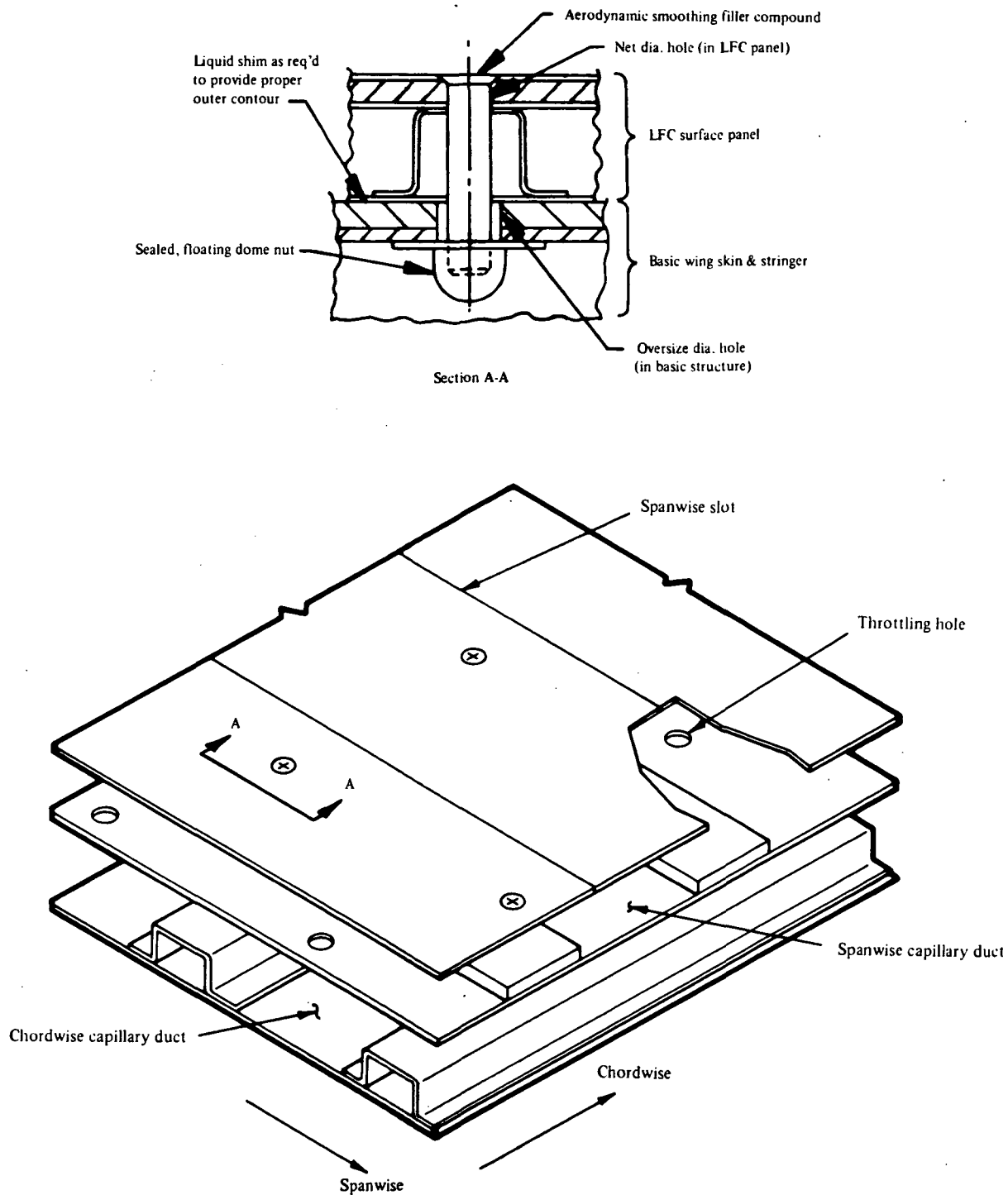


Figure 127. — Surface panel configuration, LFC-200-S

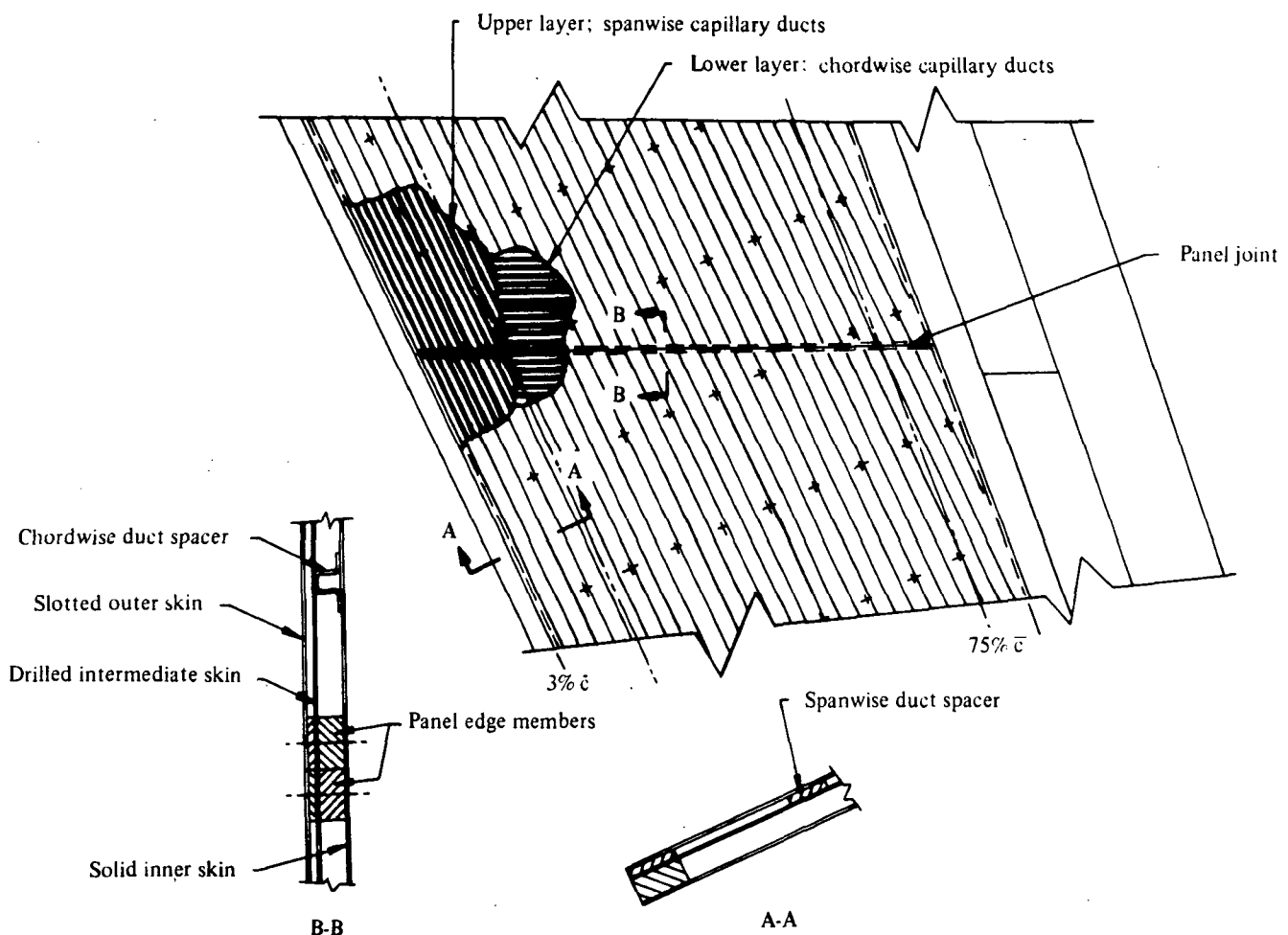


Figure 128. — Typical LFC surface panel

The requirement to allow for differential movement of the LFC surface panels under varying flight loads to prevent the imposition of structural loads precludes laminarization across panel joints. Consequently, although suction is maintained up to each attachment rib, it is probable that a .244 rad (14 deg) turbulent wedge will form at the leading edge of each joint. The resultant laminar areas for wing upper and lower surfaces are illustrated by figure 130. The wing regions of potential turbulent flow are utilized for the location of boost pumps, fuel probes, and fuel level control valves. Comparison of figures 130 and 106 illustrates this point.

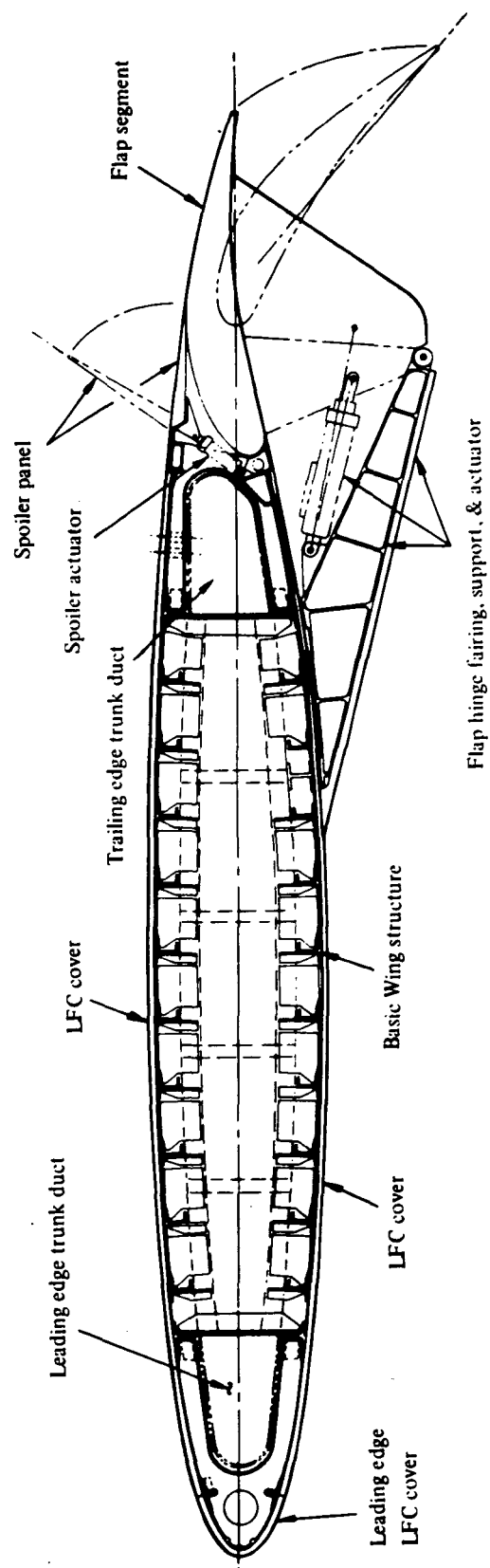


Figure 129. — Typical LFC wing section

TABLE 21. LFC SURFACE PANEL WEIGHT SUMMARY: LFC-200-S

<u>Main panel</u>	<u>kg/m²</u>	<u>lb/ft²</u>
Outer skin	1.406	.288
Intermediate skin	.703	.144
Inner skin	.703	.144
Chordwise edges	.074	.015
Spanwise edges	.097	.020
Upper spacer	.439	.090
Lower hat spacer	<u>.711</u>	<u>.146</u>
	4.135	.847
Miscellaneous - including liquid shims, adhesive, nuts and bolts, piccolos, and sealant	2.021	.414
	<u>6.156</u>	<u>1.261</u>
<u>Leading edge panels</u>		
Outer skin	1.406	.288
Intermediate skin	1.406	.288
Inner skin	1.406	.288
Chordwise edges	.293	.060
Spanwise edges	.386	.079
Upper spacer	3.500	.717
Lower hat spacer	<u>6.932</u>	<u>1.420</u>
	15.329	3.140
Normal skin (delete)	-3.662	-.75
Miscellaneous	<u>2.881</u>	<u>.59</u>
	14.548	2.98
Average weight - all panels	6.786	1.39

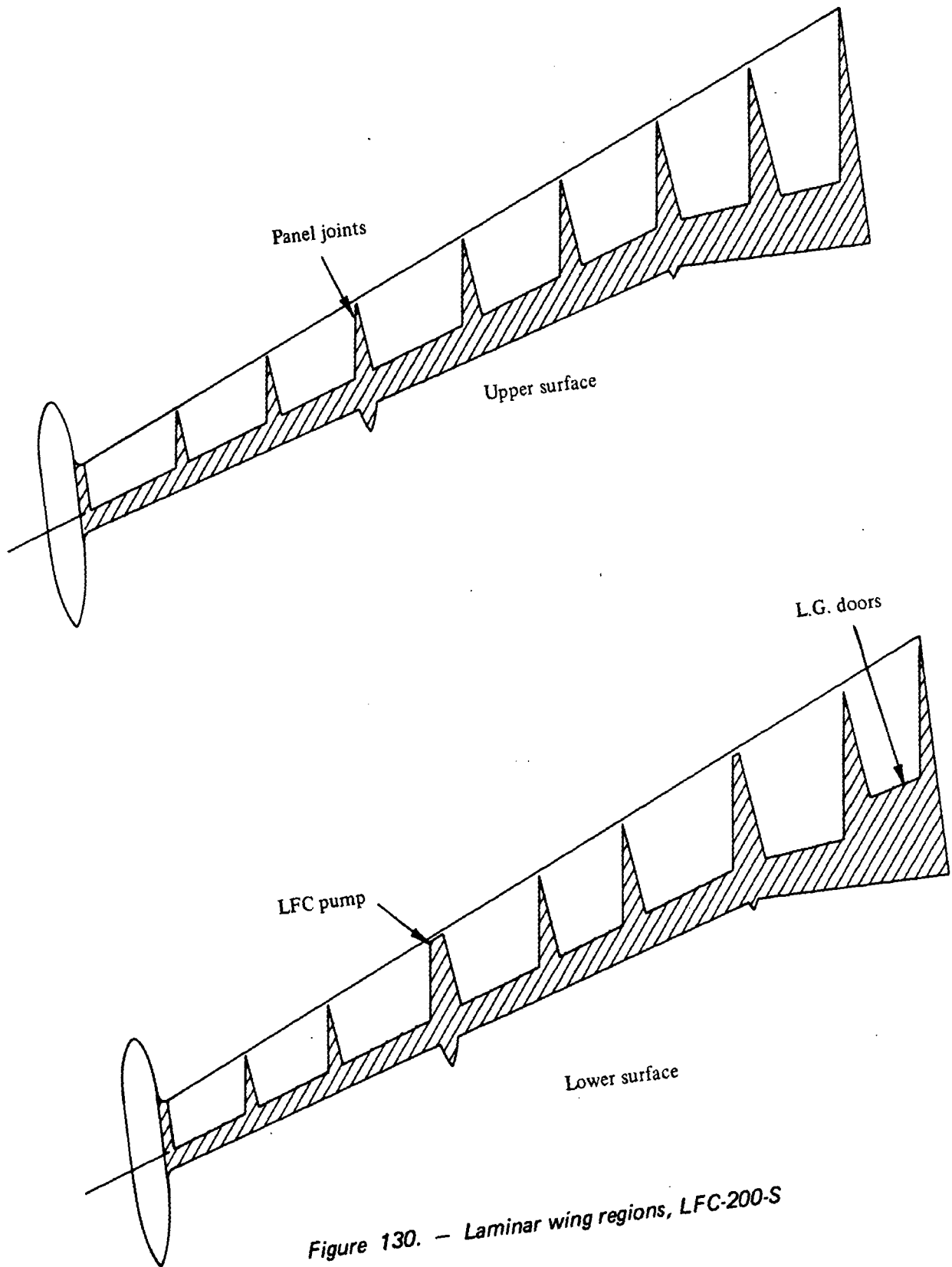


Figure 130. — Laminar wing regions, LFC-200-S

8.2.3.2 Ducting and Distribution

The basic criteria for the ducting and distribution system were discussed in section 6.3.1. In applying those criteria to the specific LFC suction requirements for the LFC-200-S airplane, the intent was to analyze the conceptual design in sufficient depth to validate the practicality and adequacy of the system and avoid any critical problems that would render the system unworkable. Conventional duct analysis procedures were employed throughout the evaluation and will not be discussed except as they relate directly to the LFC system.

Ducting System Analysis – A schematic diagram of the ducting system is presented in figure 131 which illustrates the general layout and nomenclature of the system. As shown, the slot ducts are 3.81 cm (1.5 in) wide by 2.54 mm (0.1 in) thick. These dimensions were selected for the entire suction surface skin and allow slot spacing in multiples of 5.08 cm (2 in). Although the schematic shows this spacing, every slot duct passage is not slotted nor are metering orifices cut between the slot duct and the collector duct. As described in section 8.2.3.1, the 15.2 cm (6 in) slot spacing used over most of the wing requires that only every third slot duct be used. Collector ducts are located on 5.08 cm (2 in) centers with the result that, after the slot flow has passed through the slot and entered the slot duct, it has less than 2.54 cm (1 in) of slot duct to traverse before reaching a metering hole. As described in the preceding section, the largest slots and slot spacing are located at the aft-most slot station on the surface. These aft-most slots thus have the highest flow in the slot ducts. Slot-duct flow was evaluated at the aft-most station on the wing upper surface and it was found that the maximum Mach numbers reached in the slot ducts were 0.0115 at the wing tip and 0.0154 at the wing root. This Mach number is of particular interest, since a high Mach number is indicative of spanwise pressure gradient and non-uniform spanwise distribution of slot flow. The very low Mach number of the flow in the slot duct also indicates that there is no acoustic interference on slot flow from this source. These flow characteristics were evaluated from the slot patterns and slot pressure loss data determined in the preceding section. The low Mach numbers in these ducts indicate that the slot duct width and height could be reduced. However, these dimensions were convenient for manufacturing, quality control, and weight, and there was no significant advantage in reducing these dimensions.

After the slot flow has traversed the slot duct, it passes through the metering orifice into the collector duct. The low Mach number of the flow in the slot duct indicates that no significant unintended pressure losses occur in the flow passing through the metering orifice. Collector duct flow on the upper wing surface is in the forward direction to the leading edge trunk duct located forward of the front wing spar. The flow from the aft-most slot incurs the largest pressure loss in the collector duct because of the longer flow path.

Figure 132 presents the collector duct local pressure loss $\Delta P/H_S$ and Mach number as a function of collector duct length. The aft-most slot in the root collector duct has the longest collector duct flow path. The ΔP value in the total system loss to the local point and includes slot pressure loss,

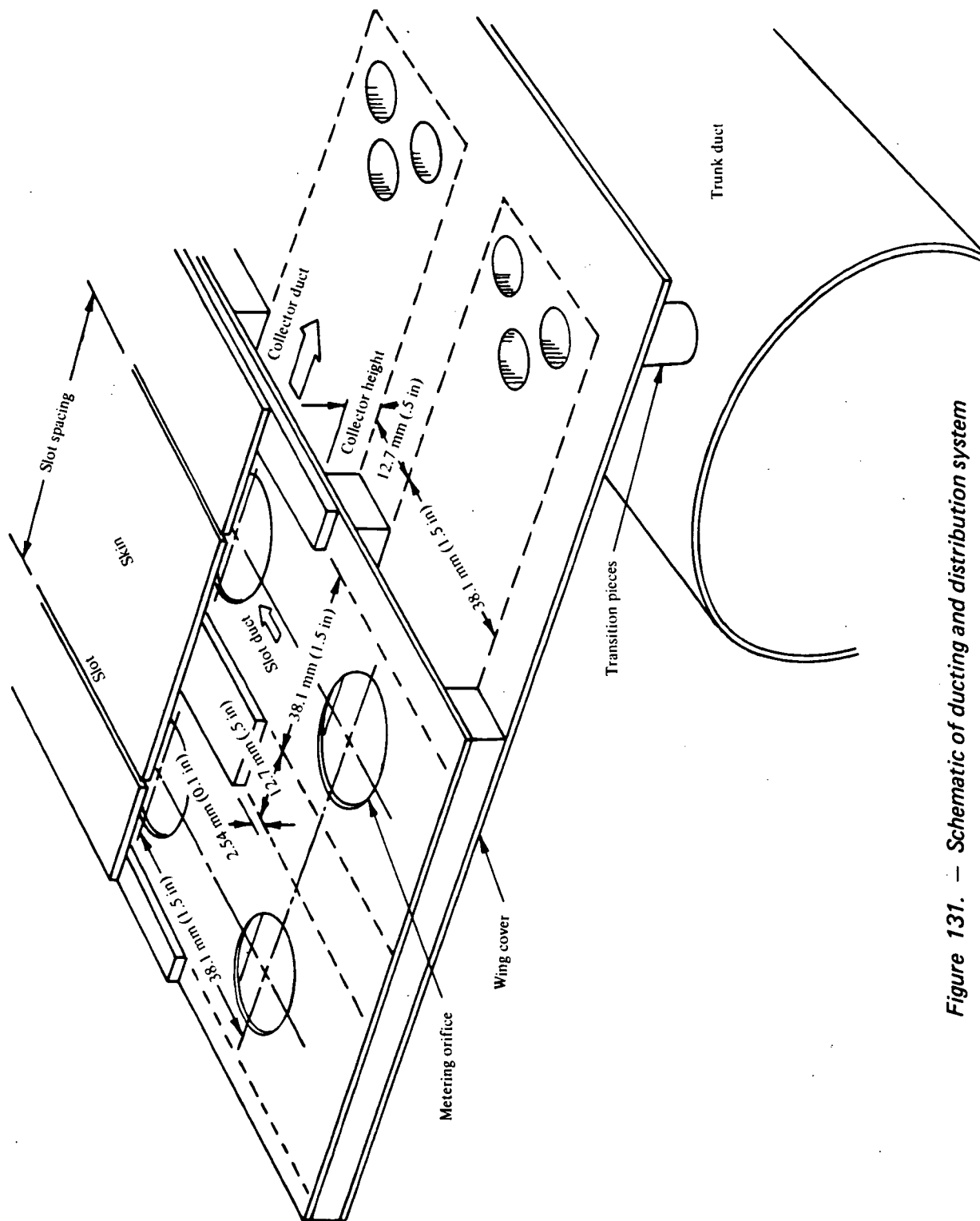


Figure 131. — Schematic of ducting and distribution system

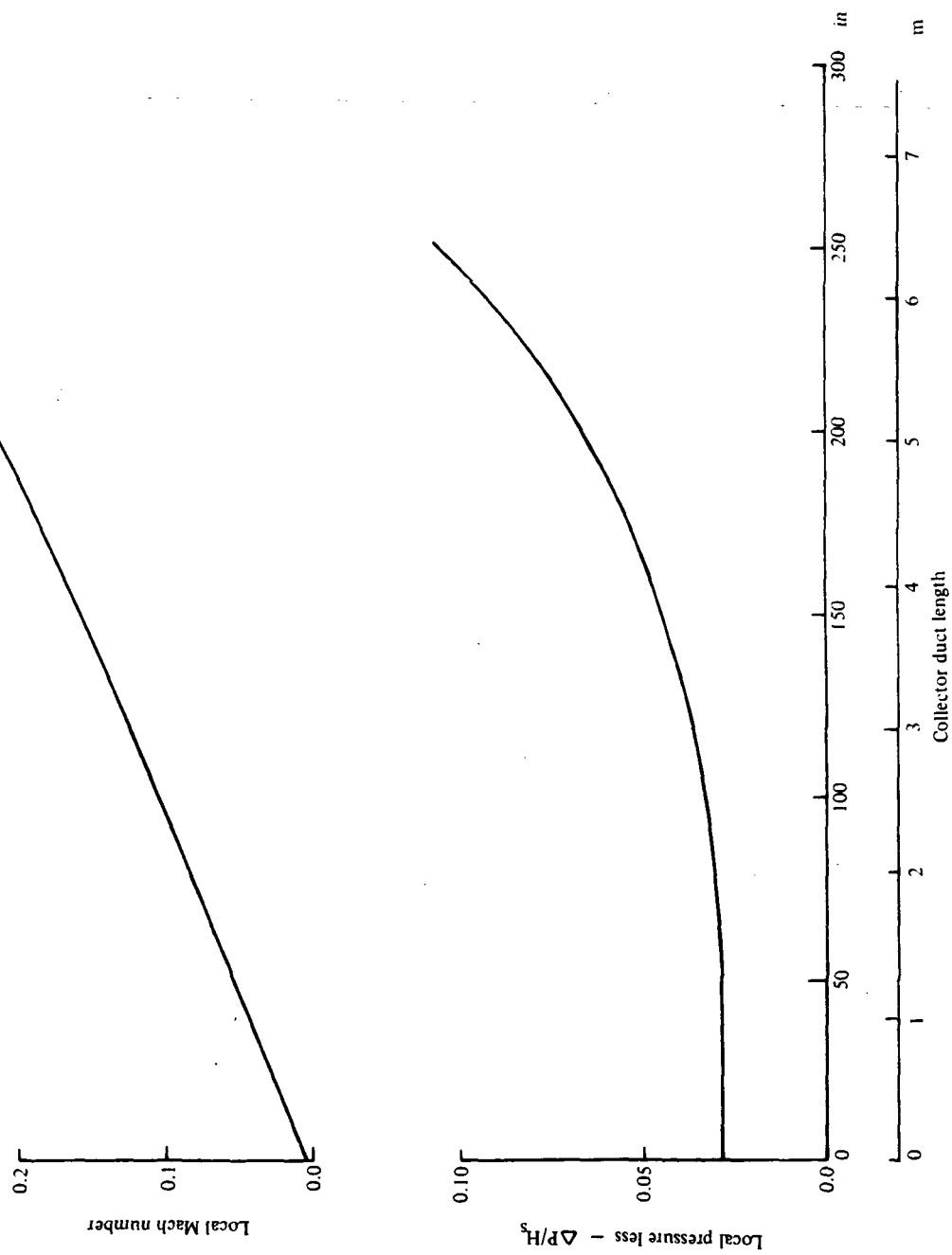


Figure 132. — Collector duct local characteristics, 1.016 cm (0.40 in) collector height, upper wing, LFC-200-S

slot duct loss, metering orifice loss and collector duct loss to the local point, and H_S is the local wing surface pressure. This figure illustrates the rapid rise in the collector duct Mach number and pressure loss as the flow passes through the duct. This rapid rise is the consequence of the continual introduction of additional flow as each metering orifice is passed. The flow from the aft-most slot is subjected to these Mach numbers and the consequent pressure losses. The pressure losses in the collector dictate the throttling necessary at each successive metering orifice in order to match the flow of the forward slots with those in the aft portion of the sucked area. If a forward slot is not adequately metered, i.e., the metering orifice does not have sufficient pressure drop, the forward slot flow will be higher than desired and the flow of the aft slots will be reduced by an approximately equivalent amount with the aft-most slot sustaining the greatest flow reduction.

The Mach numbers at the farthest run of the root collector indicate that the 0.2 Mach number target is exceeded for approximately 1.52 m (60 in) of the collector duct but the upper limit of 0.3 is not exceeded. An analysis of the effects of increasing the collector duct heights is shown in figure 133. This figure illustrates the accumulated pressure loss and Mach number at the collector duct exit as a function of collector height. The collector height of 1.02 cm (0.4 in) was selected as convenient to manufacture while resulting in a local peak collector Mach number less than 0.3. A decrease in this peak Mach number to 0.2 would require an increase in collector height of approximately 3.81 mm (0.15 in). Since it was desired to maintain a fixed collector height over the entire wing surface for manufacturing purposes, this represents a significant increase in cover weight with an even more significant impact on wing structural weight and fuel volume restrictions.

The accumulated pressure losses and Mach numbers were evaluated at the collector duct exit for a number of spanwise locations and are shown on figure 134 and 135, respectively as a function of wing station. It will be seen on figure 134 that the collector duct exit Mach number exceeds 0.2 from station 20 inboard, a spanwise distance of about 3.65 m (12 ft) and it exceeds Mach 0.25 for approximately half that distance. Collector exit Mach numbers over the remainder of the wing are quite low. The break in this curve occurs as a consequence of the wing bat, at which point the collector duct lengths increase rapidly closer to the fuselage.

Since the region of collector duct velocity in excess of 0.2 is quite small both spanwise and chordwise and the area above 0.25 Mach is substantially less, the selection of 1.01 cm (0.4 in) collector height was considered acceptable in light of the penalties associated with the alternatives.

An analysis was made of the forward trunk duct which carries the upper wing surface air to the suction pumps, assuming the maximum size for this duct is consistent with structural and fuel volume constraints. This duct exhibits some of the characteristics of the collector duct in that air is being added to the duct throughout its length. This effect is somewhat relieved by the fact that the trunk duct enlarges as it progresses toward the fuselage. The initial analysis was performed assuming all of the flow to enter a single suction unit in the fuselage or wing root area. In this configuration, the tip flow travels the greatest distance and is consequently subjected to the largest pressure losses. Therefore, the flow from the wing tip collector was analyzed starting at the

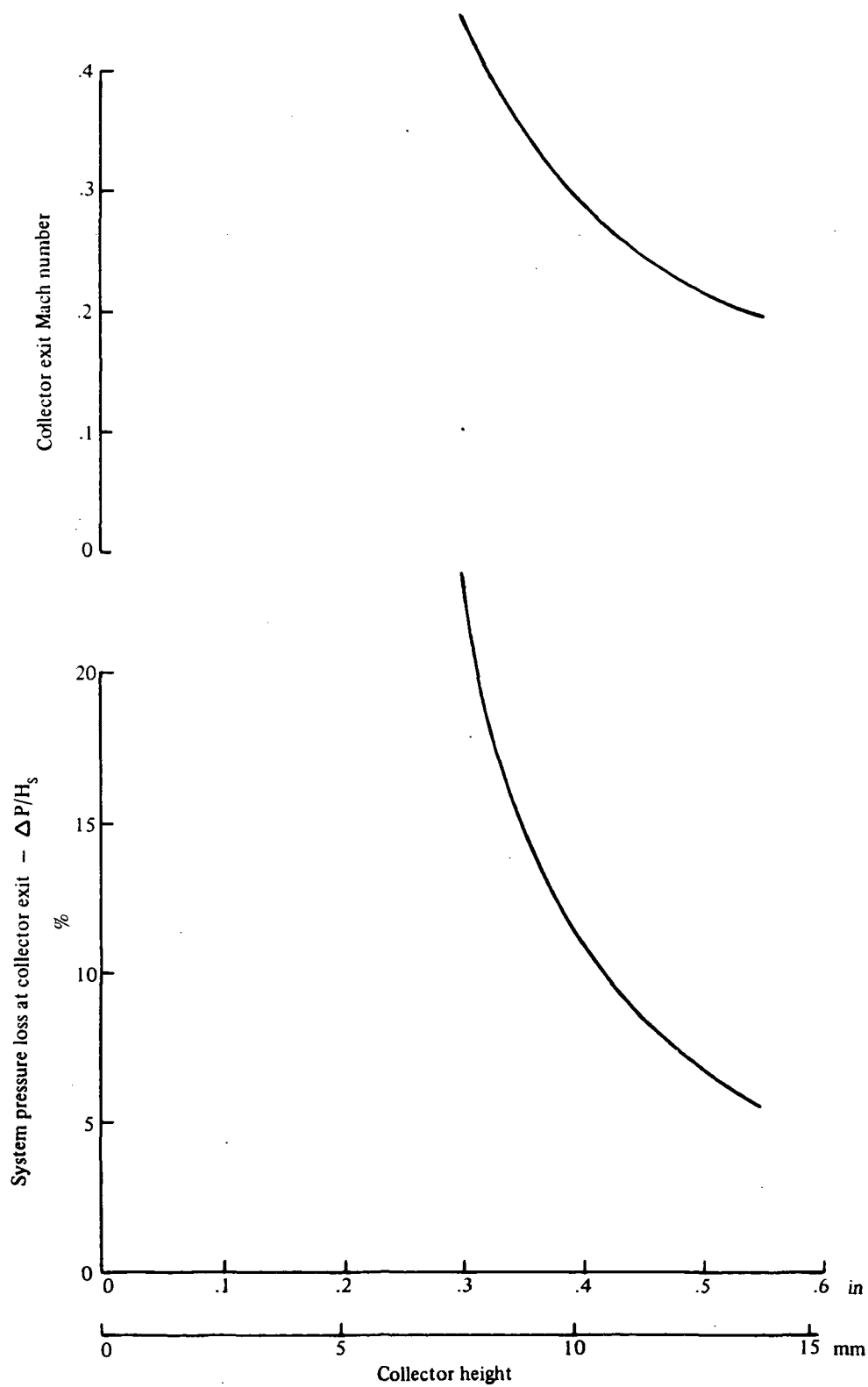


Figure 133. — Wing root collector duct characteristics, upper wing, LFC-200-S

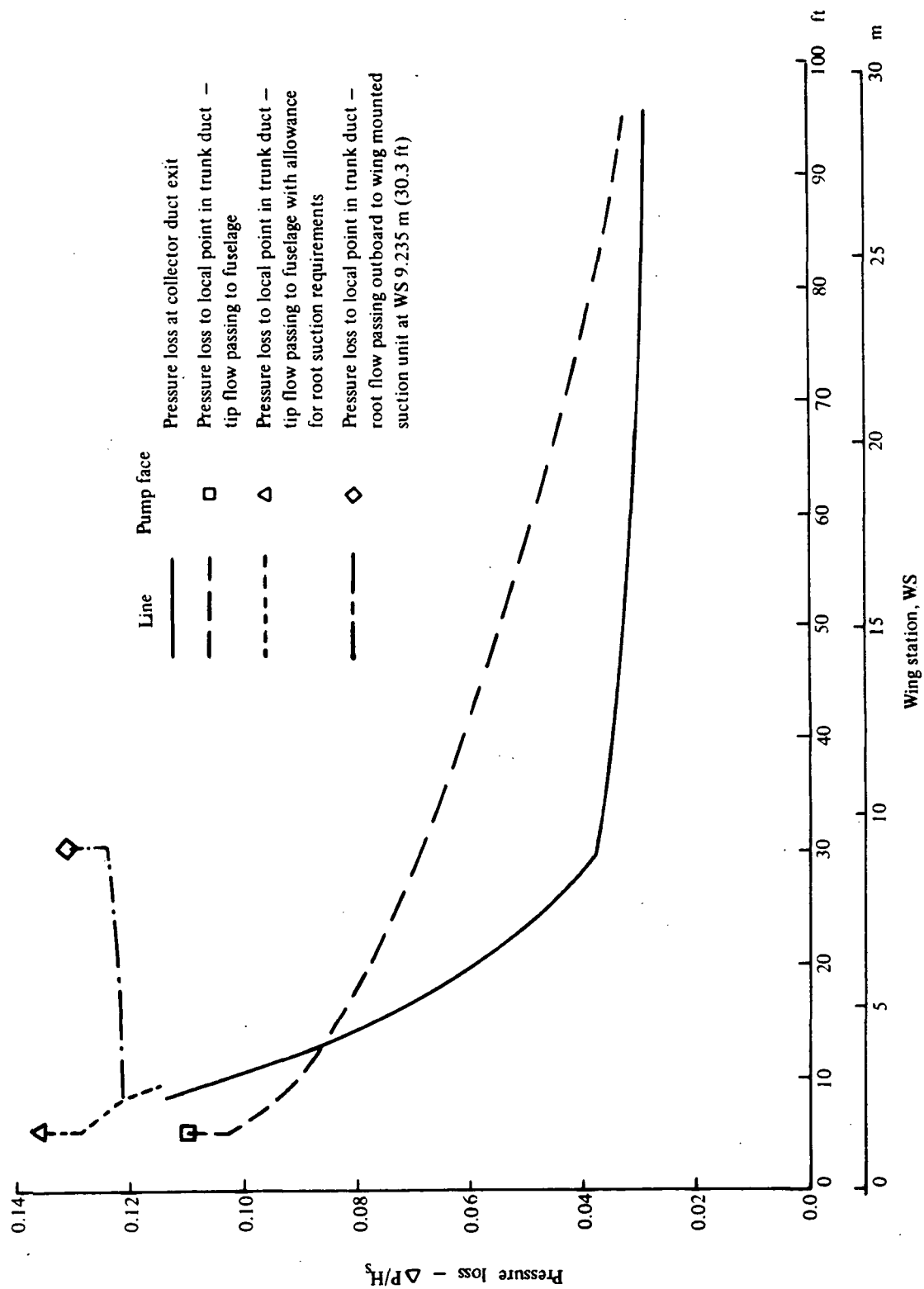


Figure 134. — Collector exit to trunk duct pressure matching, upper wing, LFC-200-S

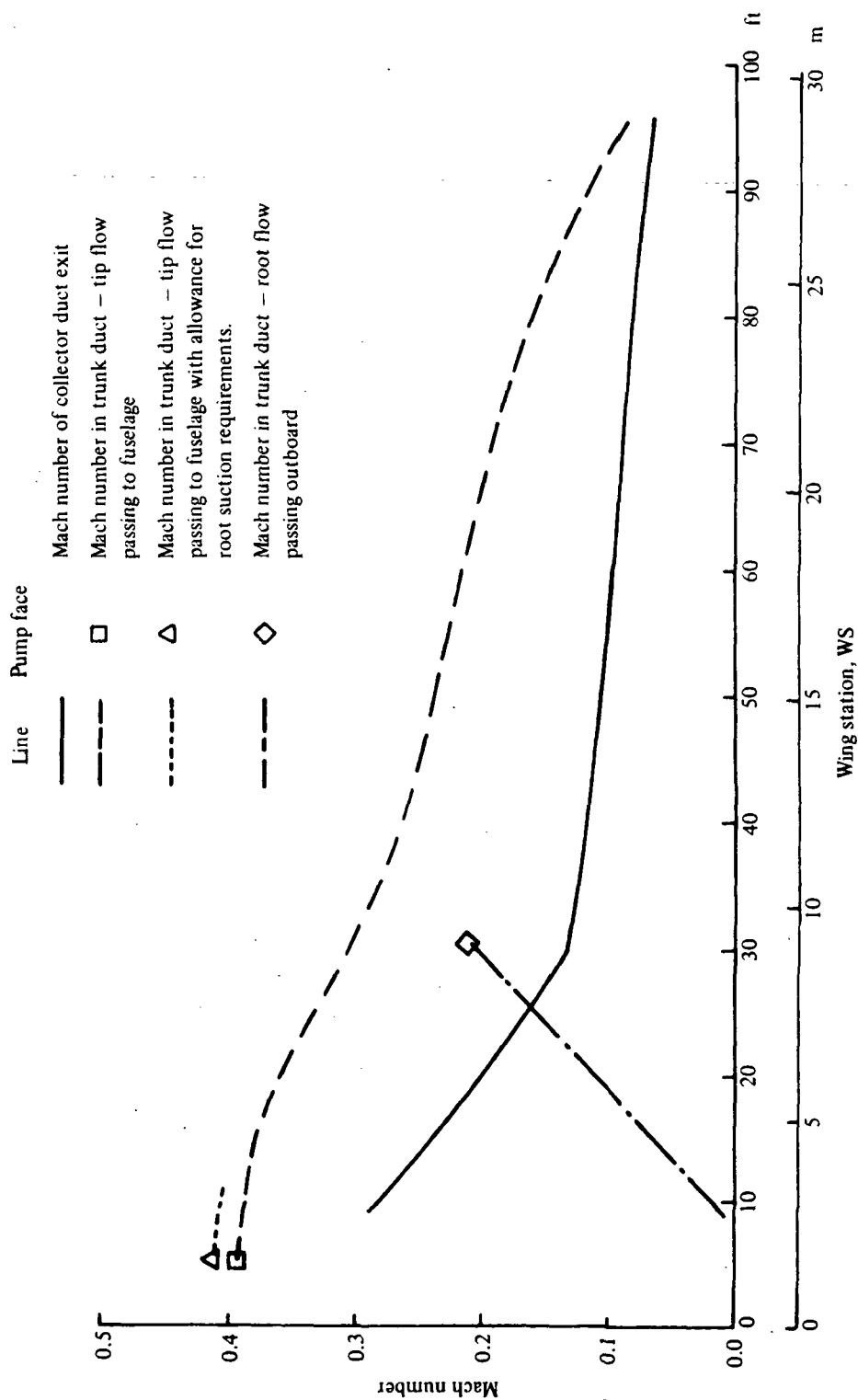


Figure 135. — Collector exit and trunk duct flow Mach number characteristics, upper wing, LFC-200-S

terminus of the collector. As in the case of the collector, the local pressure loss and duct Mach number were evaluated along the length of the trunk duct. In this case, the local pressure loss was evaluated including all losses to the terminus of the collector plus the losses in the transition from the collector to the trunk duct and the local trunk duct losses. The plots of these local pressure losses and Mach numbers are shown as the dashed lines on figures 134 and 135 and are superimposed on the plots of the collector exit loss and Mach numbers. The symbols at the inboard terminus of these curves represent the total system pressure loss at the suction pump compressor face and includes duct turning losses. This analysis revealed two unacceptable features. The trunk duct Mach numbers are excessive and the pressure loss characteristics do not match the collector characteristics in the wing root area.

Inspecting the Mach number characteristics of the trunk duct on figure 135 reveals that the trunk duct Mach number is in excess of 0.2 for nearly 60% of its length, exceeds 0.3 for over 25% of its length, and nearly reaches 0.4 at the point where it enters the fuselage. It would require a 25% increase in duct area at the wing root to reduce the duct Mach number to 0.3 and an 82% increase in duct area to reduce this Mach number to 0.2. Since the duct was selected at the maximum size compatible with wing volume constraints, this characteristic cannot be corrected by enlarging the duct.

The second problem results because the accumulated trunk duct pressure losses, shown as the dashed line on figure 134, are lower at the wing root than the corresponding collector duct losses. This indicates that the duct pressure is higher in the root area than the flow leaving the collectors. This is obviously unworkable and the root collector flow would reduce to a point where reduced collector losses would render the conditions compatible. This would result in inadequate suction flow in the root area. This could be readily solved by increasing the trunk duct losses leading up to this area, but would have the effect of increasing the trunk duct Mach number which is already excessive. The dotted line on figures 134 and 135 represent the trunk duct losses and Mach number in this immediate area required to solve the mismatch problem.

As a result of these analyses, it was necessary to utilize four wing-mounted suction units distributed along the wing span and a fifth tail-mounted unit to provide the empennage suction. In this five-pump configuration, one suction unit is located at the wing trailing edge break at WS 370. The root air is ducted outboard and the flow from WS 419 inboard is ducted inboard to this unit. WS 419 represents the wing location that splits the wing semi-span flow equally between inboard and outboard suction units. The pressure losses for the root collector duct flow passing outboard to WS 370 are shown as the broken line on figures 134 and 135 indicating a more than adequate accumulated pressure loss and therefore stream pressure between the collector exits and the trunk duct for all stations. Figure 135 indicates that the trunk duct Mach number, from the root collector flowing outboard, increases from a very low value at the root collector terminus to a value just over 0.2 at the location of the suction pump at WS 370.

The location for the outboard suction unit to divide the flow in the outboard section of the wing is at WS 718. Figure 135 shows that the trunk duct Mach number for the suction air flowing inboard from the wing tip collector reaches just over 0.2 and that locating the pump further outboard would further reduce this Mach number. Figure 134 illustrates that the trunk duct pressure losses at this station are quite acceptable in that there is an adequate difference between the collector exit $\Delta P/H_S$ and that of the trunk duct.

The remaining flow paths from the outer end of the inboard pump flow field (i.e., inboard of WS 419) to the inboard pump and from this station to the outboard pump for the outboard flow field are substantially less severe than those from the root and tip. The required metering of the suction airflow to provide the necessary match at the collector terminus between the collector exit pressures and the trunk duct may be readily provided by the collector to terminus transition pieces.

An analysis of the empennage ducting requirements revealed no significant problems in ducting this flow to a tall-mounted suction unit. The suction levels of the empennage are below those of the wing and there is ample room for internal ducting since there is no fuel volume constraint.

The foregoing analysis and selection of system represents a viable configuration with no critical problems. It is not considered to represent an optimum system, but existing alternatives can only be evaluated through an optimization trade study. A major consideration in determining the configuration was the limiting duct Mach numbers selected to minimize acoustic interference. These Mach number criteria were selected without test substantiation and could significantly alter the selected configuration.

Ducting System Design – Schematic illustrations of the ducting system for LFC-200-S are presented in figure 136 through 141. The boundary layer air is sucked through the slotted surface into the spanwise capillary ducts, through the metering orifices in the intermediate skin into chordwise collector ducts. From the collector ducts, the air moves through transfer ducts, shown in figure 136, into the trunk ducts in the wing leading and trailing edges, and finally into the LFC suction units as shown in figure 137.

The trunk ducts located in the leading and trailing edges increase in size as they progress spanwise toward the suction units. The shape and size of these ducts are constrained by wing depth, structural requirements, and the space required by controls and actuators. Examples of ducting constraints are shown schematically in figures 138 and 139.

Due to the odd shapes and tight bends and transitions in shape required within the trunk duct run, these ducts are fabricated from stiffened reinforced plastic. To conserve space within the limited volume of the leading and trailing edges, the faces of the wing spars are utilized as one wall of the duct. The ducts are made in short sections to facilitate removal and replacement for maintenance.

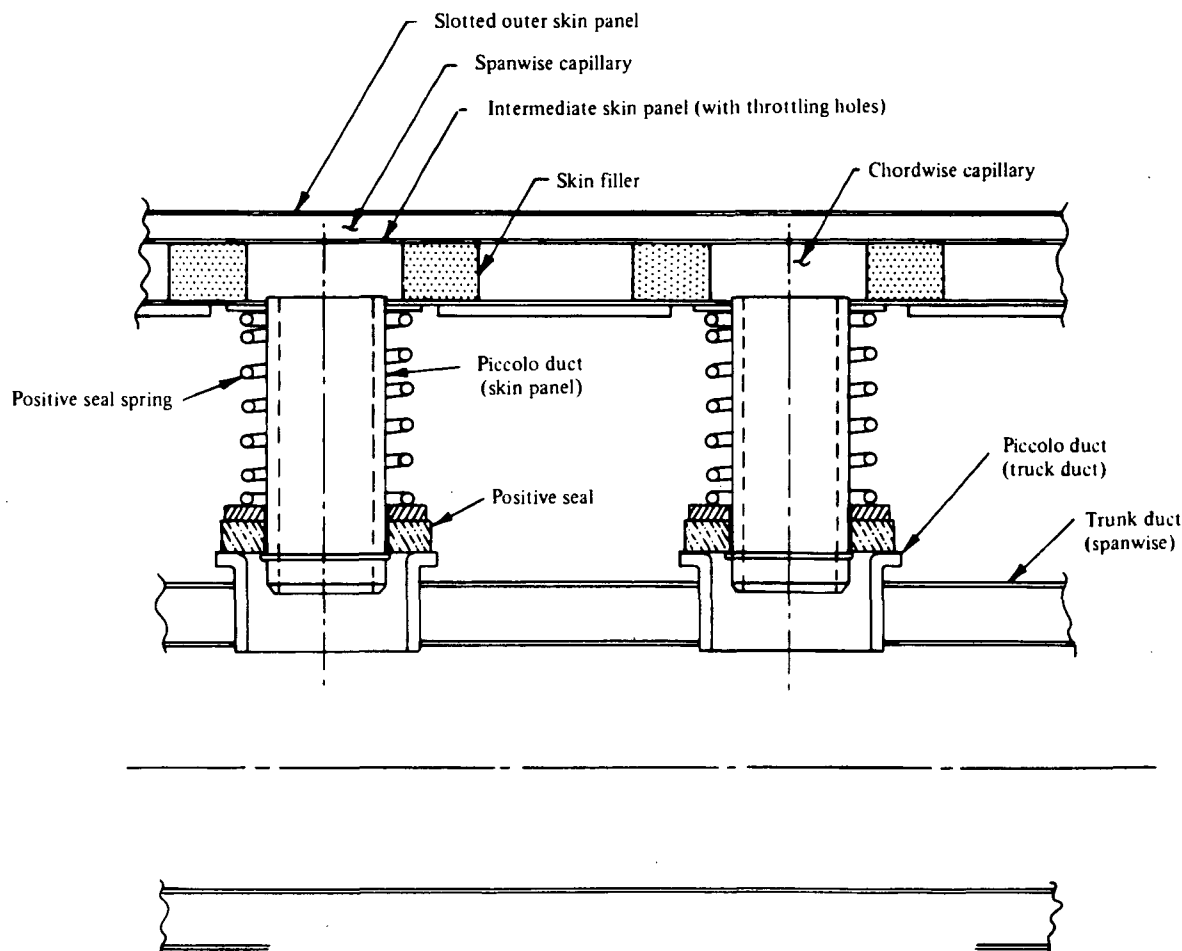


Figure 136. - LFC surface panel transfer ducting

Ducting within the horizontal tail is similar to that described above. Ducting in the vertical tail and to the aft-mounted suction unit is shown schematically in figures 140 and 141.

8.2.3.3 Suction Units

A general discussion of the suction unit criteria and requirements was presented in sections 6.4.1 and 6.4.2. The requirement for four wing-mounted suction units was established in the preceding section and the specific pumping requirements are those discussed in section 8.2.3. The four wing-mounted units are sized to accommodate one-fourth of the total wing suction flow requirement. Logistics, cost and maintenance dictate the requirement for a single suction unit configuration that is suitable for all locations. Since the flow from the wing surface has more than one source pressure level, each suction unit must be compatible with the same inlet flow conditions

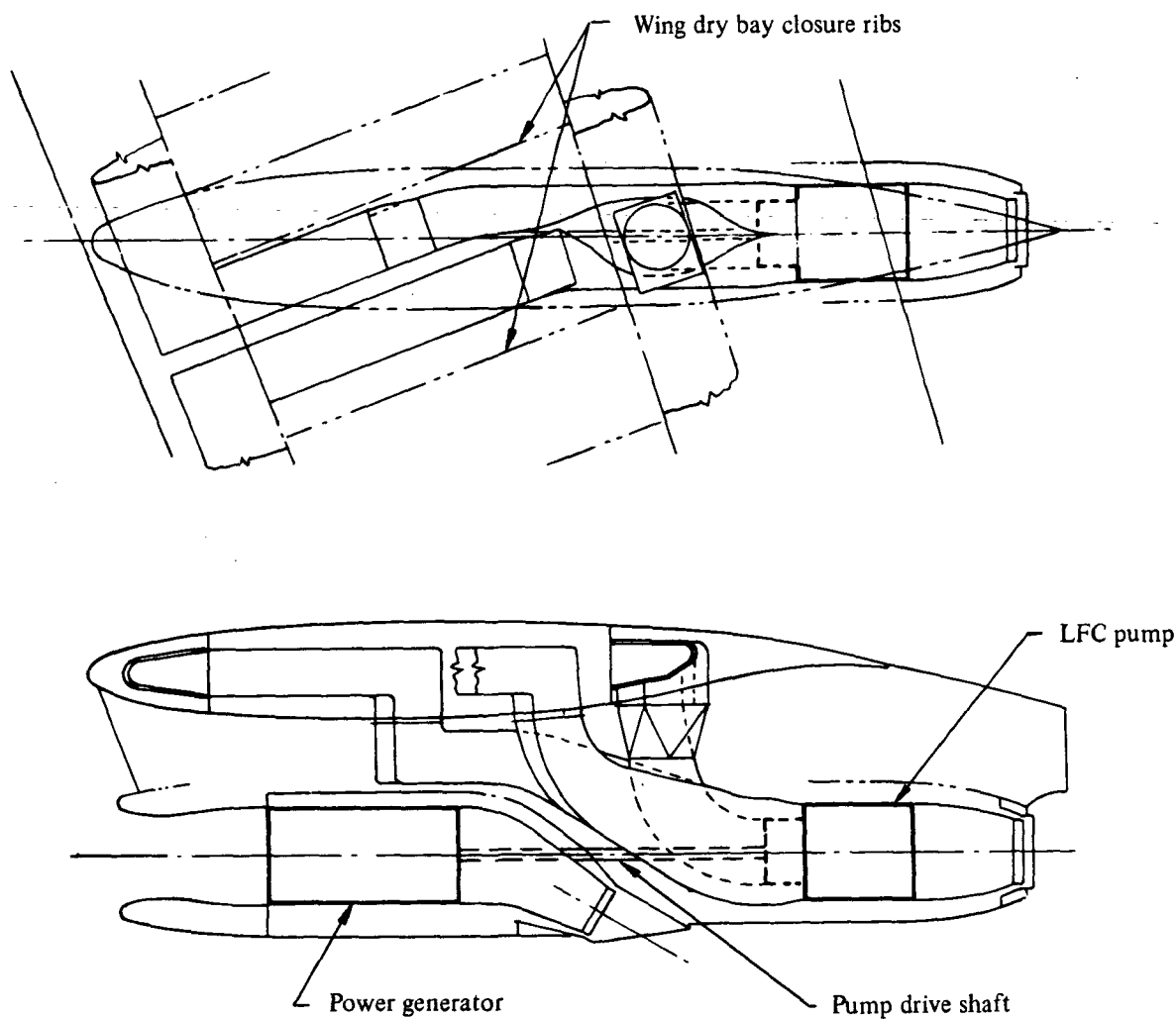


Figure 137. — Ducting arrangement for wing-mounted LFC suction units

and the same mix of airflow from the various source pressures. It is therefore necessary for each pump to be compatible with entering airflow at distinctly different pressure levels, since the differences in the source pressures are reflected throughout the ducting system. The lower source pressure air from the upper wing and leading edge is carried by the trunk duct in the wing leading edge while the higher source pressure air from the lower wing surface is carried by the trunk duct aft of the rear wing spar. Thus, each suction pump draws airflow in a fixed proportion from both the wing leading edge trunk duct and the aft trunk duct. This air reaches the suction unit at distinctly different pressure levels.

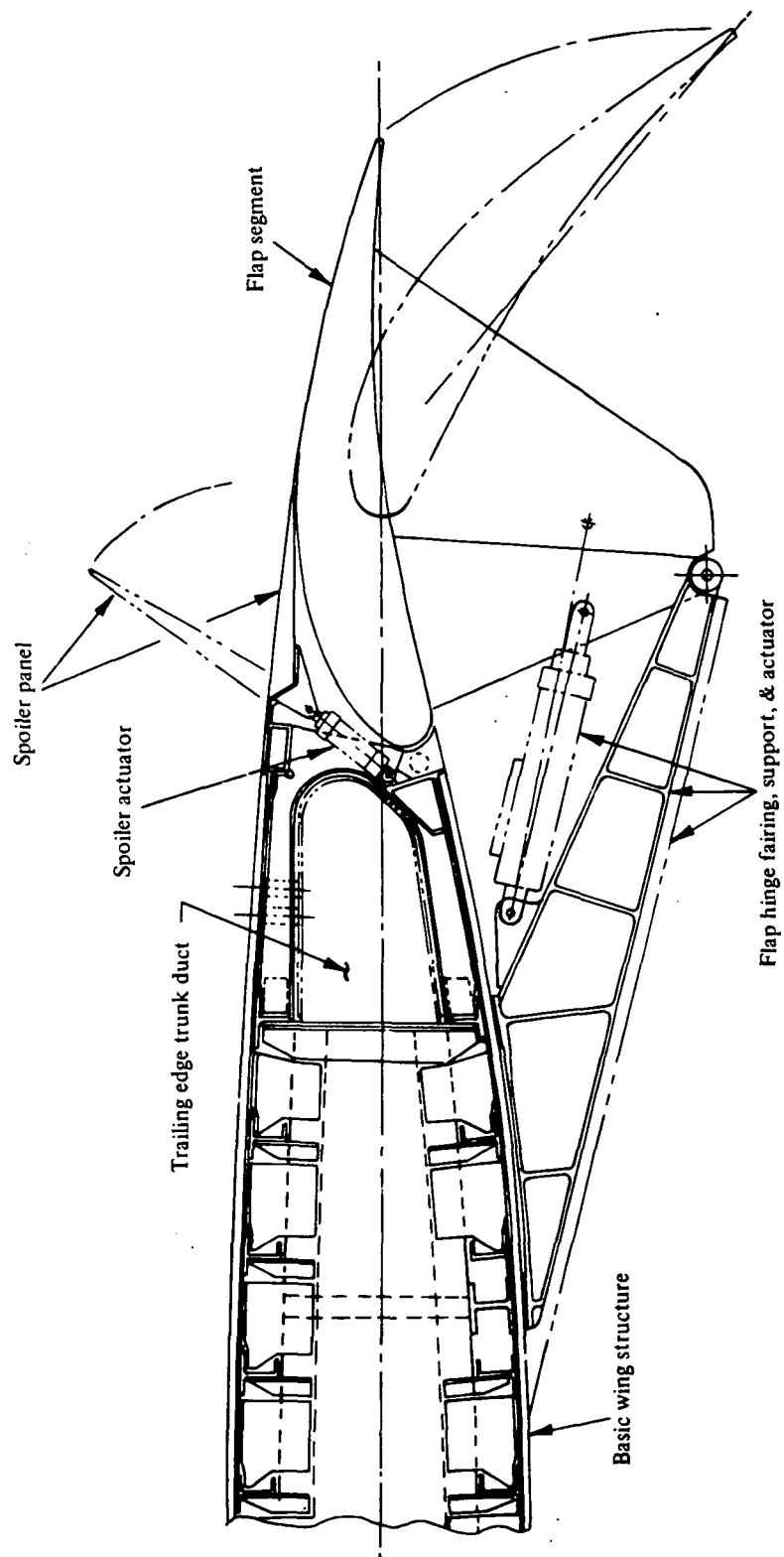


Figure 138. — Trailing-edge trunk duct, flap, and spoiler arrangement

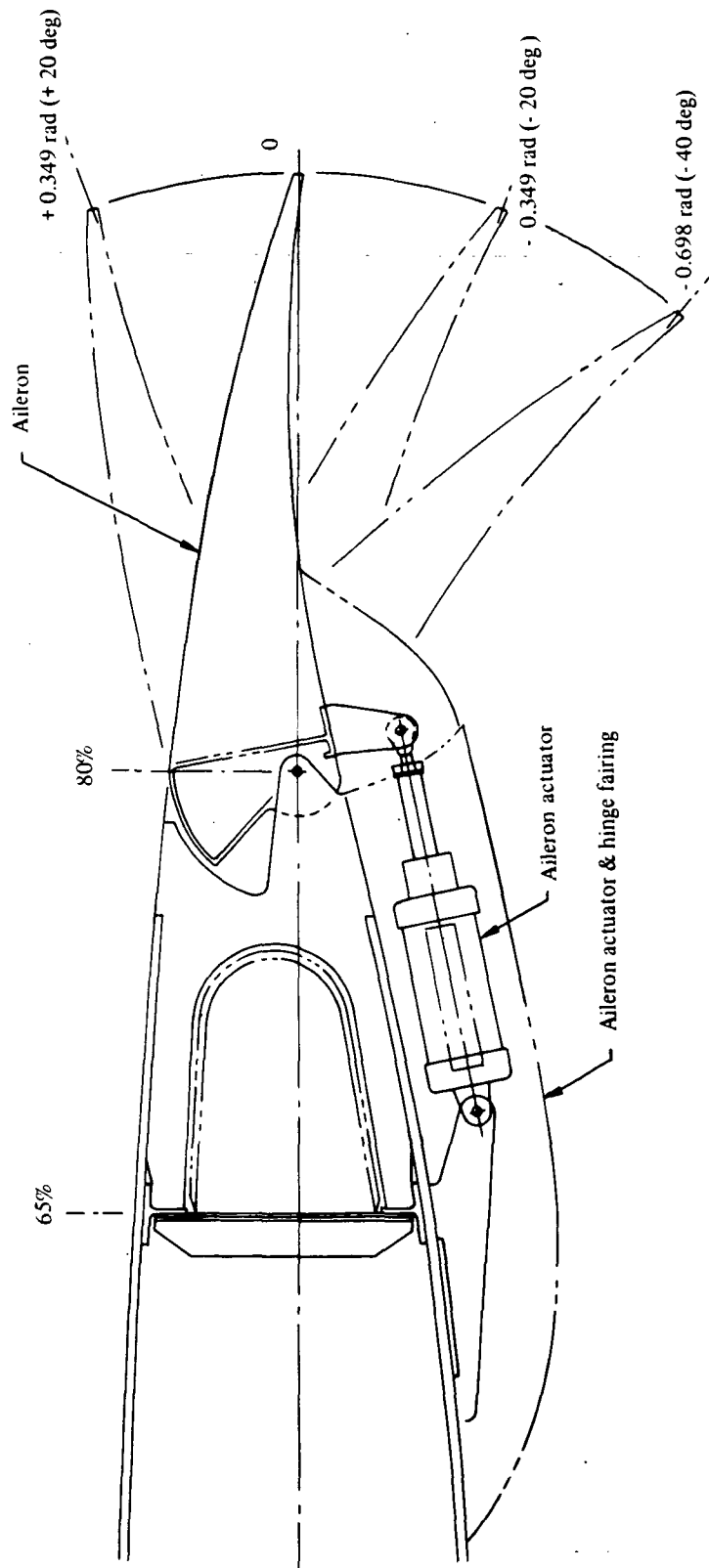


Figure 139. — Trailing-edge trunk duct and aileron arrangement

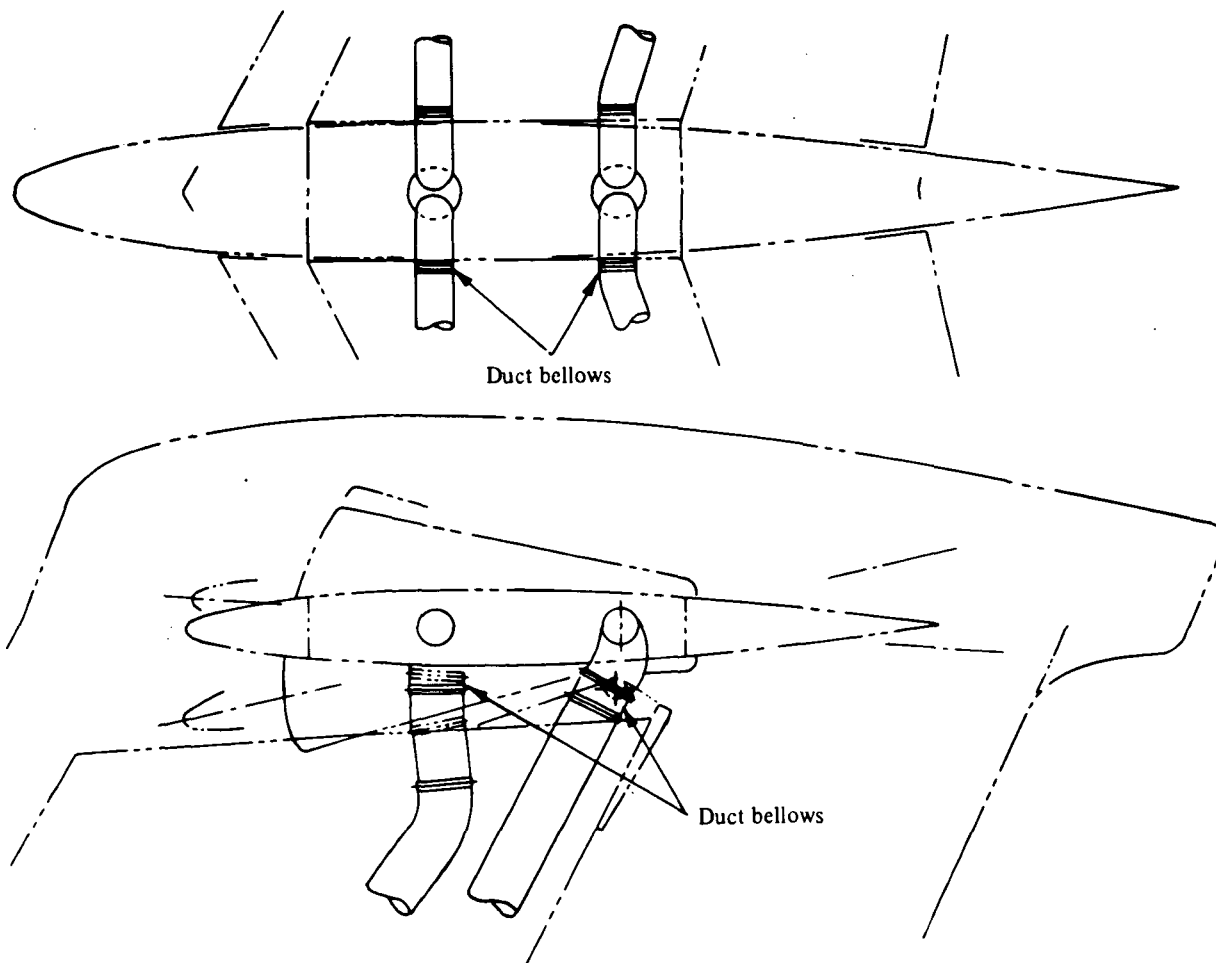


Figure 140. — Horizontal-to-vertical fin transfer ducting

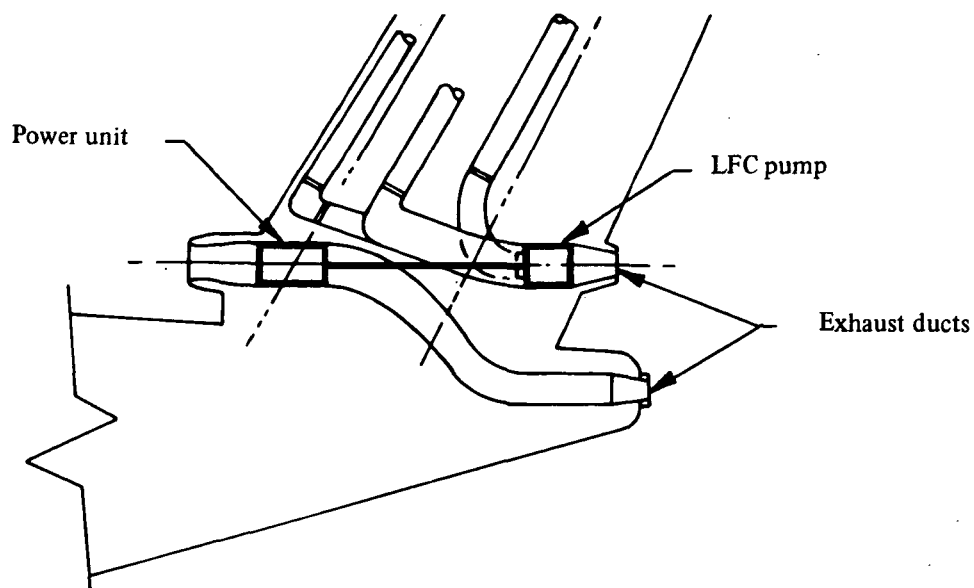


Figure 141. — Ducting arrangement for fin-mounted suction unit

The pump pressure ratio requirements are established by the pressure level of the entering air and the discharge pressure necessary for discharging this air from the unit at the selected exit velocity. Two suction pump exhaust velocities emerge as desirable choices. One choice is to discharge the air at the free stream velocity, in which case the gross thrust of the suction air exhaust just equals the drag of the wing surface friction, ram drag, and internal ducting losses of the suction airflow. Discharging at free stream velocity ideally produces 100 percent propulsive efficiency but since the gross thrust exactly equals the total drag for the sucked air, the net thrust is equal to zero. Since the penalties of taking this air aboard the airplane have already been paid, it is logical that a further increase in exhaust velocity should be imparted to this air to obtain a net thrust. This is a better expenditure of energy than taking additional air into a conventional engine and accelerating it to an elevated velocity, since the conventional engine must overcome the ram drag of additional ingested air. Elevating the exhaust velocity of the sucked air above that of free stream, however, produces diminishing returns as the velocity of the primary propulsion units is approached, assuming that the exhaust velocity of the primary propulsion unit is correct for the airplane. The second choice of discharge velocities requires elevating the discharge velocity to equal that of the primary propulsion system. In this case, the propulsive efficiencies of the suction system and primary propulsion system are equal. Elevating the air to velocities above that of the primary propulsion system is theoretically non-optimum since it results in poorer propulsive efficiency than that of the primary propulsion units. These choices of discharge velocity together with the temperature of the ingested air plus the temperature rise due to suction pump compression determine the required total pressure of the suction pump discharge. The discharge pressure so determined, ratioed to the pressures at the pump inlet define the pump pressure ratio.

If the suction unit could pump any combination of airflows and pressure ratios, the total airflow of the suction pump would be divided into a number of discrete airflows, each having a distinct pressure ratio depending on the source pressure at the surface of the wing and the slot and ducting system losses. However, the pump must have segmented flow paths for each discrete airflow/pressure ratio combination. The combinations of discrete airflow and pressure ratio defined by the suction requirements for the LFC-200-S wing are shown on figure 142, arranged in descending order of pressure ratio with the airflows normalized against the total wing suction pump airflow. The solid line on figure 142 indicates the pressure ratios required for the suction pump to discharge at free stream velocity, while the dashed line represents the pressure ratios required to discharge the airflow at the exhaust velocity of the primary propulsion units. The exhaust velocity of the primary propulsions was determined to be 408 m/sec (1340 ft/sec) for cruise conditions. For discharge at free stream velocity, 50.6 percent of the total airflow must be pumped through a ratio of 3.09, 58 percent of the airflow must be pumped through a pressure ratio of 2.31 or more, and 100 percent of the air must be pumped through a pressure ratio of 1.25 or more.

Figure 143 presents a similar plot of airflow/pressure ratio distribution for the empennage. In this plot, allowance was made for an increase in nominal suction of the vertical surfaces to counteract the high acoustic field from the primary propulsion units and the relaxed stability requirements relative to the horizontal surfaces.

Obviously, the requirements to meet the suction pressure ratios of both the wing in figure 142 and the empennage in figure 143 with a single pump configuration are somewhat incompatible. In

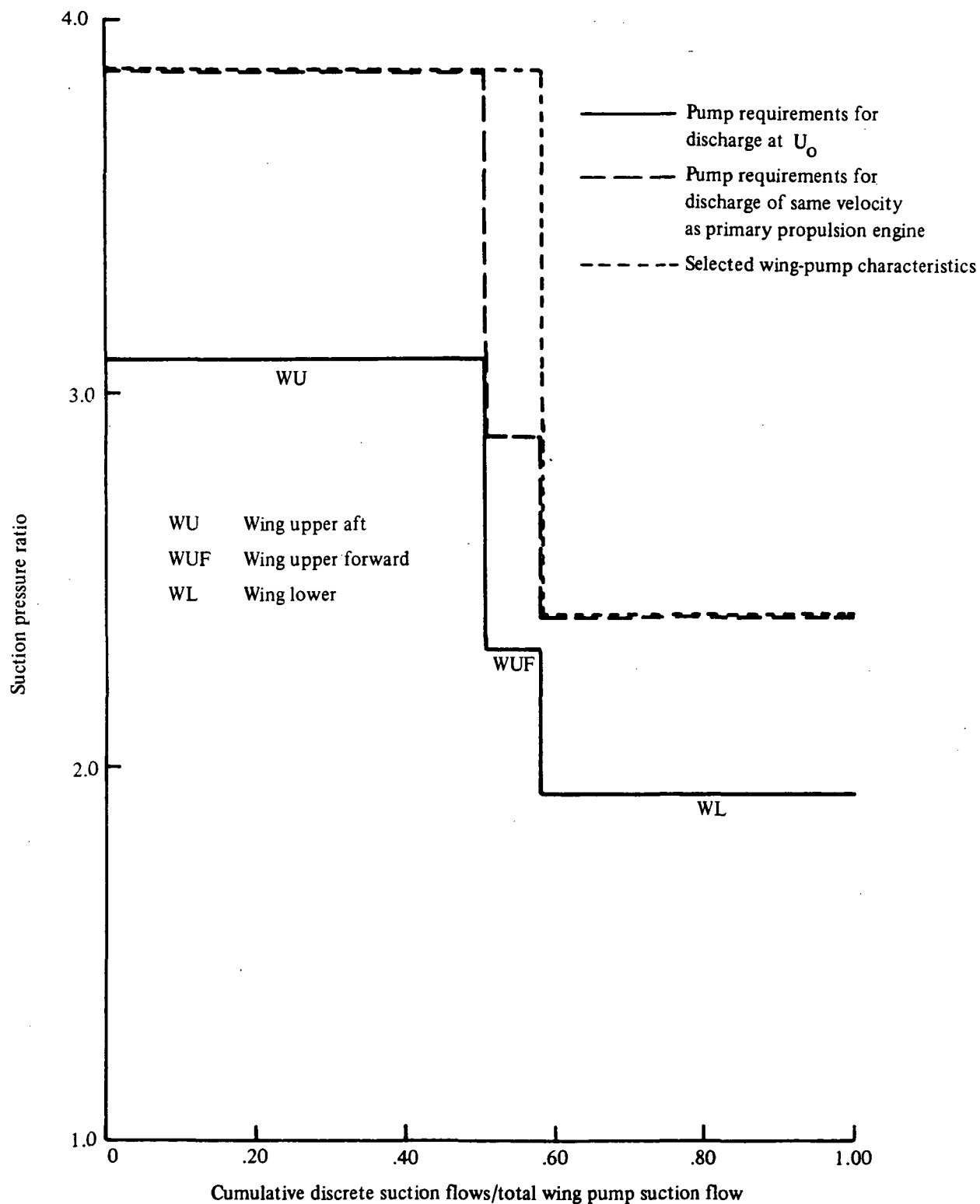


Figure 142. — Normalized wing suction characteristics, LFC-200-S

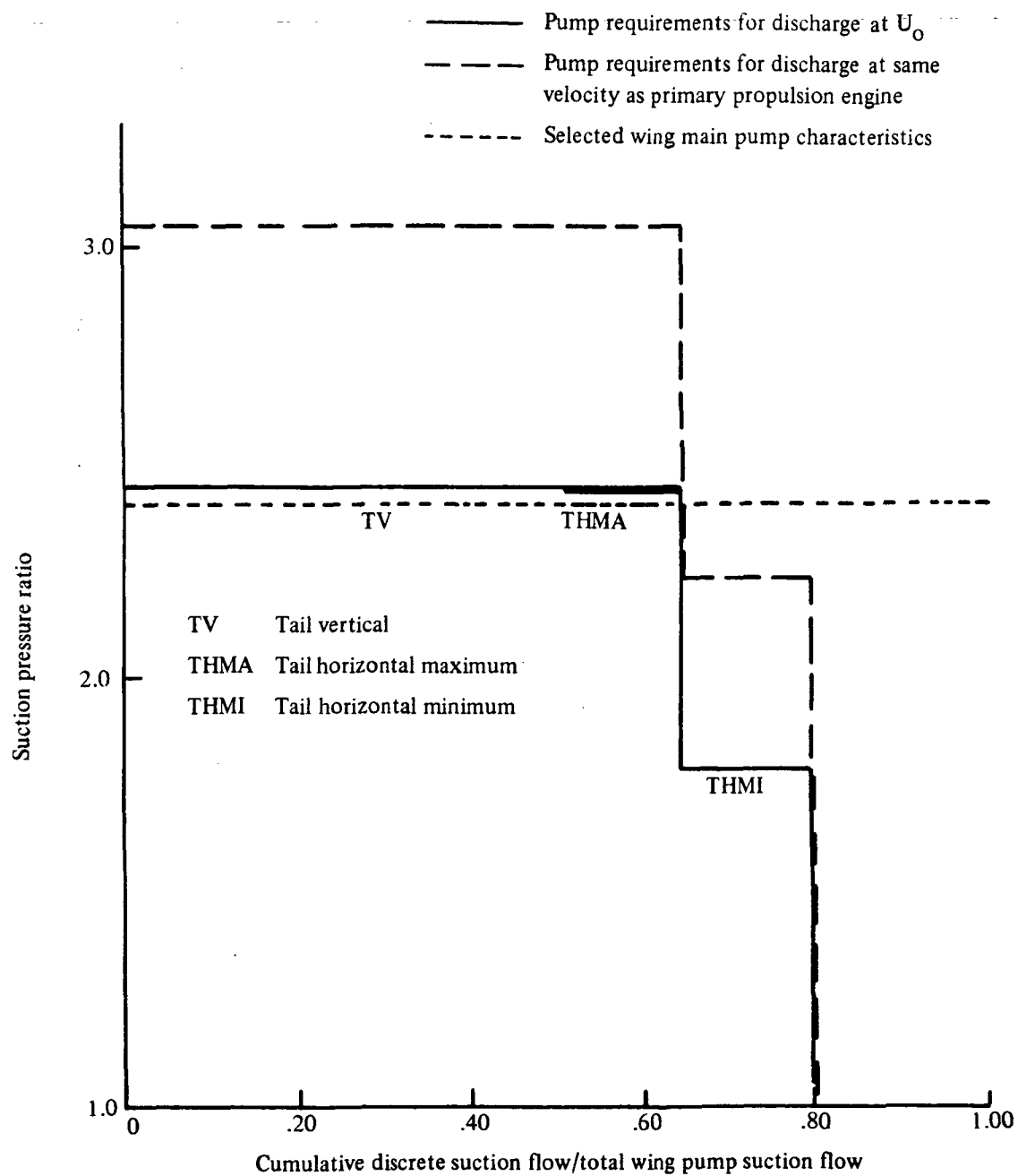


Figure 143. — Comparison of normalized wing and empennage suction characteristics, LFC-200-S

addition, configuring a suction pump to match the pressure ratios of some of the smaller increments of flow is unrealistic. Therefore, two levels of suction pump pressure ratio were selected to meet the wing pump requirements for the higher discharge velocity and are illustrated by the dotted line on figure 142. These pump ratios closely match the requirements for the wing with one relatively small area in which the pressure ratio is more than the required level.

The configuration of the pump compressor is dictated by these requirements. All of the suction airflow requires pumping through a pressure ratio of 2.40 or more while 58 percent of the flow requires an overall pressure ratio of 3.86. To meet these requirements, the pump concept includes a basic compressor with a pressure ratio of 2.40 with a pre-compression pump to compress 58 percent of the flow through a pressure ratio of 1.60 before it enters the main pump. The pre-compression pump is obviously of smaller diameter than the main compressor and may be mounted co-axially on the front of the main compressor. This configuration also provides a solution to the problem of commonality between the wing units and the empennage unit. The pre-compression unit is a modular unit which can be removed from the main compressor for empennage installations. The main compressor provides a single entry compressor for all of the empennage. There is still some minor incompatibility between the main compressor unit and the empennage requirements in that the flow is still 21 percent too high and 15 percent of the empennage air is subjected to more pressure ratio than is required. Compressor inlet conditions dictate that the flow enter the inlet without the distortion caused by the two pressure ratio levels of the empennage requirements. This may be eliminated by throttling the 15 percent of the flow from the vertical surfaces to bring it to the higher required pressure ratio or reducing the losses in the 64.5 percent of the flow from the horizontal surfaces requiring the ratio of 2.44. The reduction of losses is possible by greatly enlarging the ducting in the horizontal tail. Since the fuel volume constraints of the wing are not present in the empennage, it is possible to use very large ducting and a reduction of losses by 5 percent is possible. This reduces the higher empennage pressure ratio requirement to 2.32 which is well within the main suction pump capability. A combination of loss reduction in the horizontal and throttling in the vertical can bring the required pressure ratios to a level of 2.32 for the entire flow. Finally, the speed of the compressor may be reduced, thus reducing the main compressor ratio from 2.40 to 2.32 with an attendant reduction in airflow. Figure 144 illustrates the compatibility of this combination. The excess in potential suction flow may be utilized to apply suction to some additional surface area.

When the suction pump requirements established, the design of the compressor follows conventional procedures. A stage pressure ratio of 1.17 was selected for the pre-compressor unit. This is conservative by modern standards but the speed of this unit is dictated by the larger diameter of the main unit through which it is driven and is therefore lower than normal for a unit of this size. This results in a three stage unit. The main compressor has five stages with an average stage pressure ratio of 1.195. This average stage pressure ratio may be marginally high considering the adverse inlet distortions to which the unit may be subjected. However, in consideration of the relatively fixed operating conditions, it appears to be reasonable. The main suction pump housing includes mounting and splined drive adaptor on the front face for installation of the pre-compression unit. The weight and general envelope dimensions are shown schematically in figure 145.

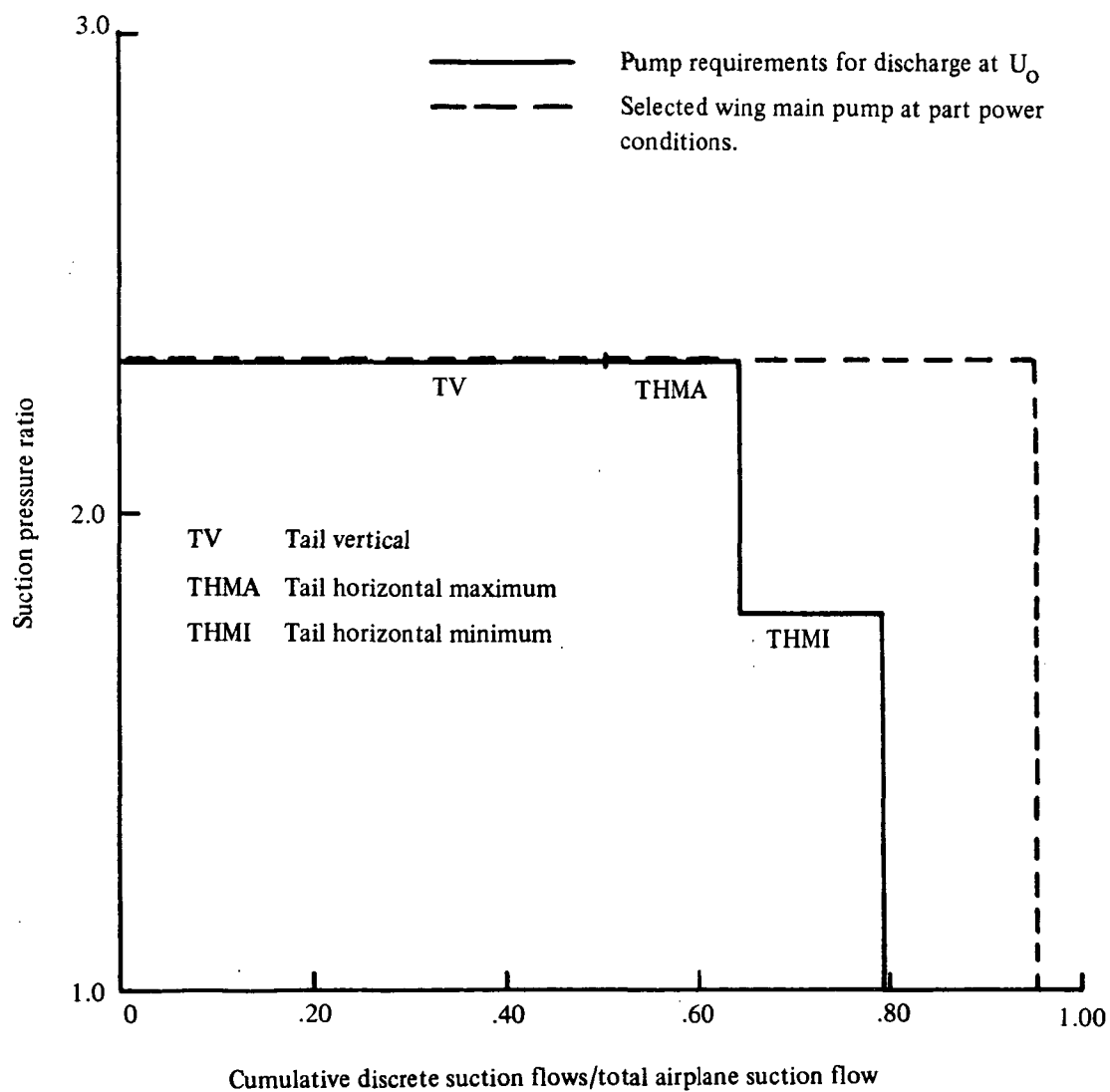


Figure 144. — Normalized empennage suction characteristics, LFC-200-S

The optimum method of powering the suction pump unit, as discussed in section 6.4.4, is a system integrated with the primary propulsion units. Obviously, a direct drive from the primary propulsion units is impractical with the aft-mounted primary engines. The second choice is a bleed and burn system utilizing bleed air from the primary units. Due to the long runs of high-pressure and high-temperature ducting required to reach the wing-mounted units, this method is also impractical. The ducting requires insulation throughout its length and the wing structure requires protection from potential leakage of high-temperature air. As a result of fuel volume and suction ducting requirements, there is inadequate wing volume for such additional ducting. Therefore, each suction pump is powered by an independent shaft engine. As discussed in section 6.4.3, the most efficient independent power unit utilizes ram air and compression independent of the suction units. The unit is representative of 1980-85 technology and was scaled from parametric data to provide the power to drive the suction pump. The envelope and weight of this unit is also shown schematically in figure 145. It will be noted that the power unit diameter and the main suction pump diameters are compatible for both units to be designed for operation at the same rotor speed. While this unit would not normally operate at sea level conditions, the unit is compatible for ground check out and test operations. The unit is naturally more than adequate for the reduced power requirements of the empennage but would readily meet the power requirements without significant performance penalty other than unit weight. The advantages of commonality with the wing units more than outweighs the weight penalty. The empennage suction unit is displayed schematically on figure 146.

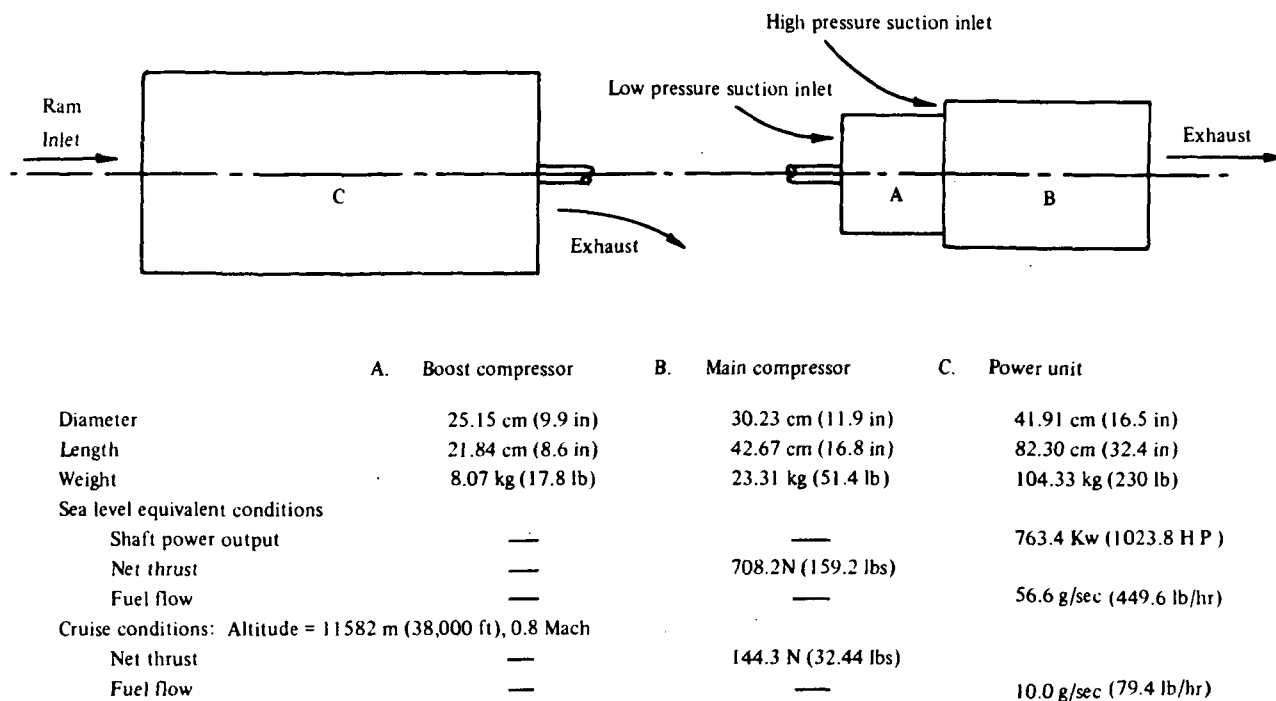
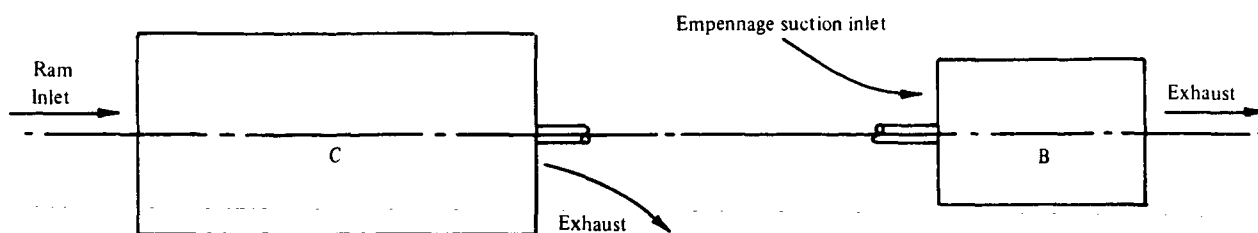


Figure 145. — Independently powered wing suction unit, LFC-200-S



	A. Boost compressor	B. Main compressor	C. Power unit
Diameter	—	30.23 cm (11.9 in)	41.91 cm (16.5 in)
Length	—	42.67 cm (16.8 in)	82.30 cm (32.4 in)
Weight	—	23.31 kg (51.4 lb)	104.33 kg (23.0 lb)
Sea level equivalent conditions			
Shaft power output	—	—	595.6 Kw (798.7 HP)
Net thrust	—	0	0
Fuel Flow	—	—	44.2 g/sec (350.8 lb/hr)
Cruise conditions: Altitude = 11582 m (38,000 ft), 0.8 Mach			
Net thrust	—	0	0
Fuel flow	—	—	7.79 g/sec (61.9 lb/hr)

Figure 146. — Independently powered empennage suction unit, LFC-200-S

The power unit is mounted forward of the suction unit so that ram air is taken directly into the power unit compressor. The power unit is attached to the forward frame of the main suction unit by a light weight truss structure. The suction unit is driven by a free turbine with the shaft exiting through a scroll vectoring the power unit exhaust aft and downward. The exhaust velocity of the unit is equal to free stream velocity to counteract the ram drag of the power unit.

The inlet to the wing suction units consists of a concentric bifurcated ducting system to introduce the low pressure air from the upper wing and leading edge into the pre-compression unit while the lower flow is introduced directly into the main suction compressor. Discharge from the suction unit is through a conventional conical nozzle oriented straight aft.

8.2.3.4 Controls

The nature of the LFC-200-S ducting system is such that each suction unit operates independently of all other units. The control system is self-contained for each unit. Since LFC operation is restricted to cruise or near cruise conditions, a high degree of control is not required by the pilot

other than essentially an on-off control. Unit operation is monitored by the flight engineer. A highly automated control system can be developed without requiring any significantly advanced technologies over those existing at the present.

The primary control of the suction unit is applied through a conventional governed speed control of the fuel flow to the shaft engine providing the independent drive for the suction compressor. The speed governing control requires appropriate biases for ram air inlet temperature and pressure, gas generator speed and/or burner discharge pressure.

The suction compressor is thus driven at essentially a governed speed. However, the lack of any direct feedback coupling between the suction compressor and the power generator does not provide assurance of the proper suction. This is accomplished by pressure sensors in the suction pre-compressor and main compressor inlets and the suction compressor discharge. Any adjustments between the pre-compressor and main compressor inlets must be dealt with either in the upstream ducting or in the compressor inlet. From a performance standpoint, variable inlet guide vanes for both suction compressor inlets are preferable and the selected unit includes an allowance for this arrangement. As the slot and ducting system becomes contaminated, reduced inlet pressures are required to maintain the desired suction flow. While suction compressor guide vane adjustments are suitable for maintaining the proper relative suction flows through the two inlets by an inlet pressure biased control, the proper absolute total flow can best be maintained by a control biased to maintain the proper exhaust nozzle pressure ratio, thus assuring the correct total suction airflow. This exhaust sensing is required to bias the shaft turbine speed governing to reduce the suction compressor speed if the suction flow is excessive or increase the speed if the flow is insufficient. Detailed dynamic analysis and experimentation is required for a definitive design but no significant technological problems are anticipated.

A potential problem exists in developing a procedure for starting the suction units. Unlike a propeller or helicopter shaft engine for which the propeller or rotor are put in flat pitch and starting is accomplished at zero aerodynamic load, the suction unit is required to start under a significant aerodynamic load. Reduced pressures exist in the ducting system even without suction because of the reduced pressures over the airfoil surfaces. The influence of ambient air on the exhaust system induces a significant pressure ratio and hence air load on the suction compressor even at very low speed and stall of the suction compressor may occur. Two means are available for countering this problem and include venting the suction unit inlets to ambient through a throttling system plus resetting the inlet guide vanes to a flat pitch to reduce the suction pump flow and pressure ratio to a minimum. The actual starting sequence of the shaft engine follows standard practice and is contained in the shaft engine control. The starting configuration of the suction pump inlet guide vanes and venting may be accomplished by a start selection switch and either switched to the controlled mode by the flight engineer or sequenced to suction compressor speed when the unit reaches sufficient speed for sustained stall-free operation.

Emergency control and automated shut-down procedures are provided for use in the event of suction slot blockage by ice or a failure in the system that prevents control of the system to nominal values. The flight engineer is responsible for monitoring proper operation of the system

and controls and detection of progressive system or suction unit deterioration.

The controls are somewhat more involved than conventional commercial installations, but do not present any problems from a technology, reliability, or operational standpoint.

8.3 CONFIGURATION LFC-200-R

8.3.1 GENERAL ARRANGEMENT

The LFC-200-R aircraft shown on figure 147 is very similar to the LFC-200-S vehicle described in section 8.2.1, differing only in aerodynamic surface areas. The most significant configuration difference is the use of two LFC suction units. The bleed-burn suction units are installed in wing root fairings, which also serve as main landing gear fairings, as shown in figure 148. LFC suction flow is ducted from each wing and the empennage surfaces into these pump units. Bleed air from the main propulsion engines is ducted forward beneath the cabin floor to the power generators. Cross-over ducting is included to permit reduced but symmetrical laminarization in the event of the failure of a single unit.

A weight statement for LFC-200-R is presented in table 22.

8.3.2 AIRCRAFT SYSTEMS

The aircraft systems for LFC-200-R are identical to those described in section 8.2.2 for the LFC-200-S airplane. Only minor differences resulting from size effect are apparent in the subsystems for LFC-200-R.

8.3.3 LFC SYSTEMS

The LFC-200-R configuration is based on the relaxed laminar boundary-layer criteria discussed in section 4.0. Evaluation of the required distributed suction velocity ratios required for meeting these criteria resulted in a reduction for v_s/U_o to 63.6 percent of those shown in figures 107, 108, and 109. The pressure coefficient values over the surface are assumed to be unaltered by the relaxation of the stability criteria and, therefore, the same as those presented in figures 110, 111, and 112. The laminarized-boundary layer velocity gradient for the relaxed boundary layer criteria was evaluated in the Laminar Boundary Layer Program and found to differ slightly from that for the stable boundary layer case. Although the differences were not significant, the relaxed criteria gradients were used in this evaluation and are presented in figure 149.

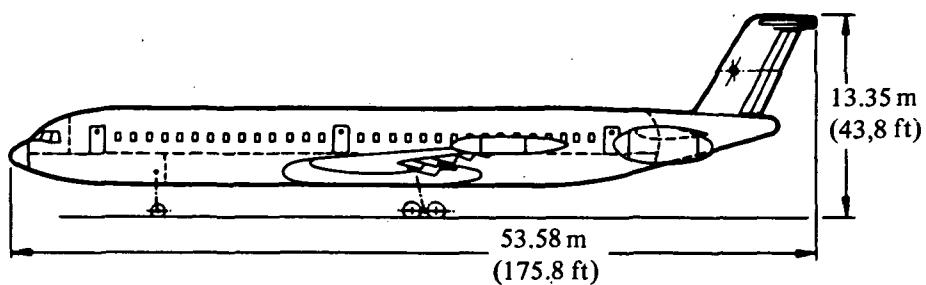
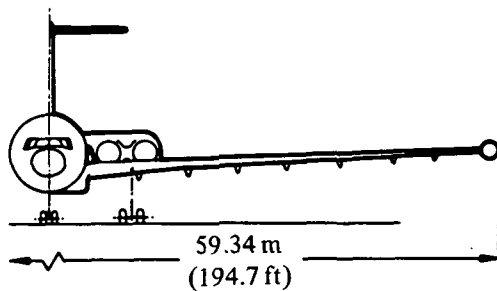
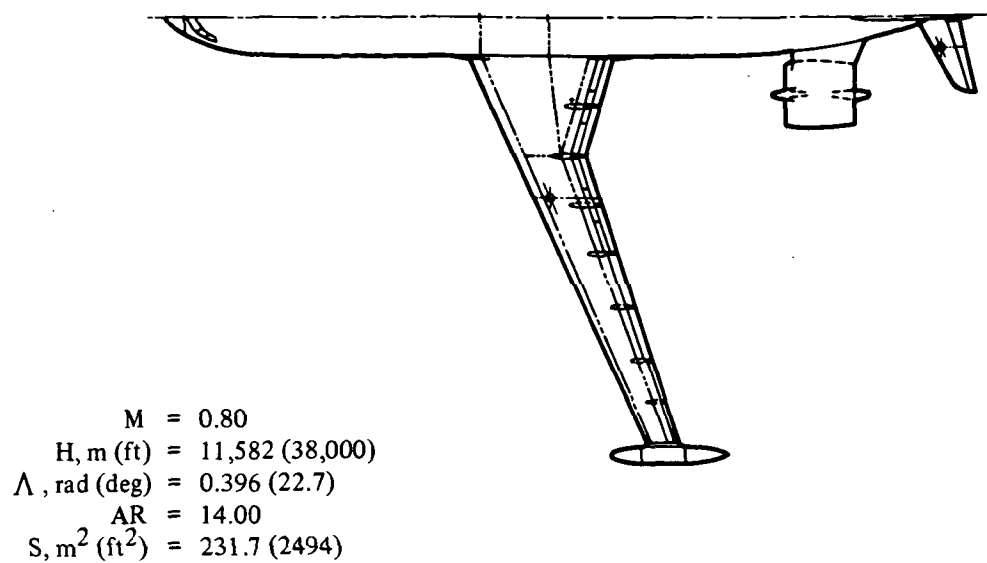


Figure 147. — General arrangement, LFC-200-R

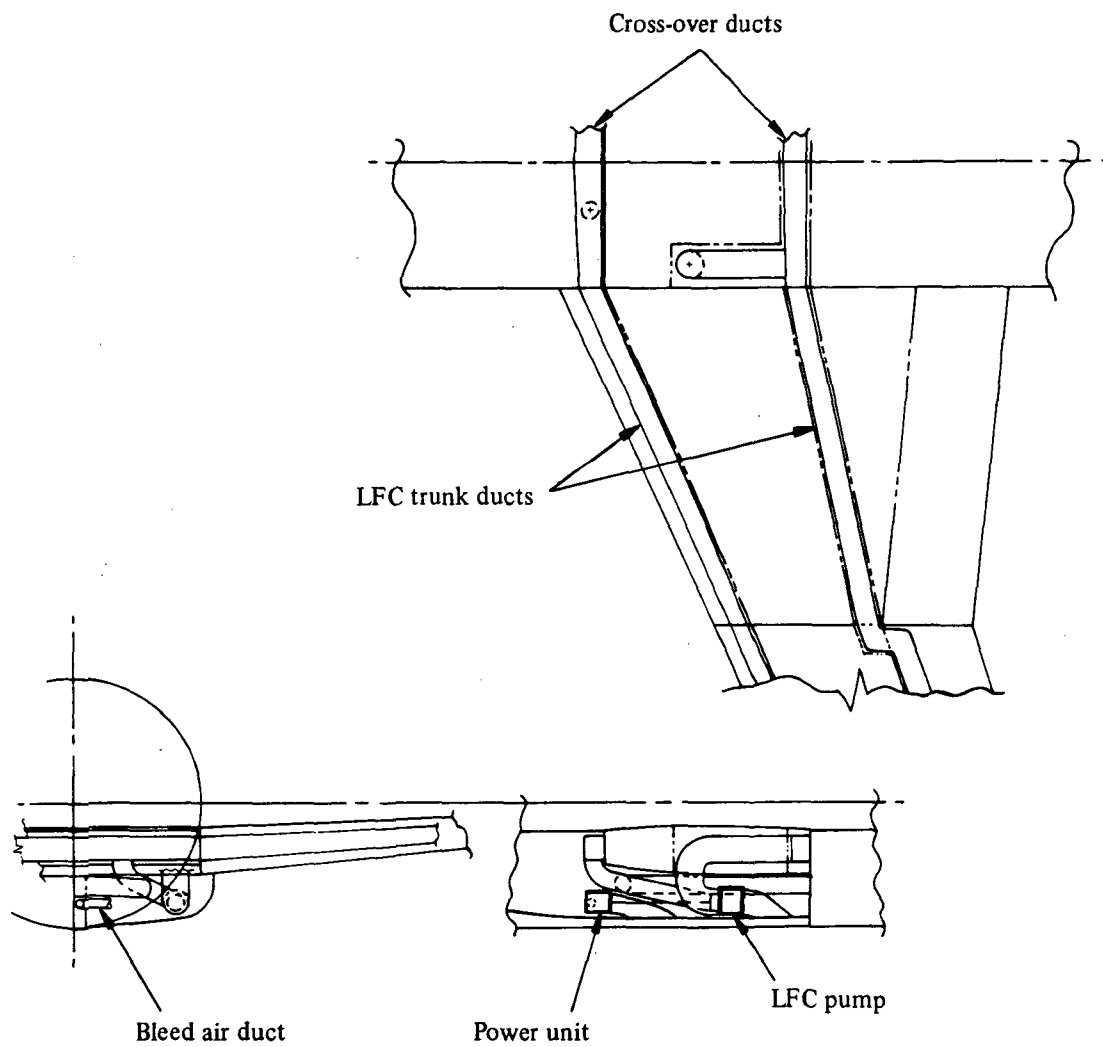


Figure 148. — LFC suction unit installation, LFC-200-R

TABLE 22. WEIGHT STATEMENT: LFC-200-R

Item	kg	lb
Structure	(46,863)	(103,313)
Wing	19,910	43,893
Wing LFC glove	1,859	4,098
Empennage	(1,941)	(4,279)
Horizontal tail	782	1,725
Horizontal LFC glove	145	320
Vertical tail	829	1,828
Vertical LFC glove	184	405
Fuselage	14,276	31,472
Landing gear	(6,734)	(14,846)
Nose	875	1,930
Main	5,859	12,916
Nacelle and pylon	(2,143)	(4,725)
Nacelle	897	1,977
Pylon	286	631
Noise treatment	960	2,117
Propulsion system	(10,322)	(22,756)
Engines	5,683	12,528
Fuel system	1,705	3,759
Thrust reversers	955	2,105
LFC engines	252	555
LFC installation	312	688
LFC ducts	508	1,121
Miscellaneous	907	2,000
Systems and equipment	(16,747)	(36,921)
Auxiliary power system	278	613
Surface controls	1,177	2,594
Instruments	587	1,295
Hydraulics and pneumatic	548	1,209
Electrical	2,212	4,876
Avionics	1,089	2,400
Furnishings	8,611	18,983
Airconditioning and AI	2,218	4,889
Auxiliary gear - equipment	28	62
Weight empty	(73,932)	(162,990)
Operating equipment	6,453	14,228
Operating weight	(80,384)	(177,217)
Payload - passenger	19,233	42,400
Cargo	4,536	10,000
Zero fuel weight	(104,153)	(229,617)
Fuel	48,534	106,995
Gross weight	(152,687)	(336,612)
AMPR weight	63,528	140,052

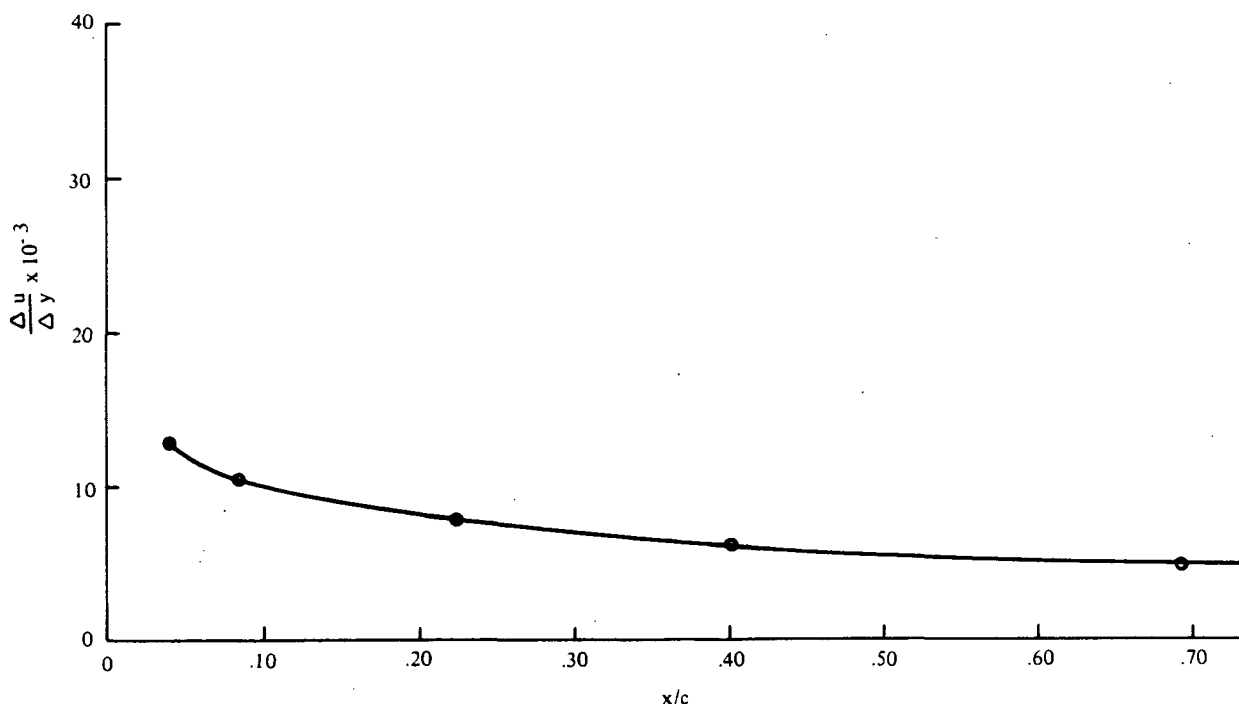


Figure 149. — Boundary layer velocity gradient, LFC-200-R

8.3.3.1 Surfaces

Slot Sizing and Spacing — An analysis of the upper wing suction surface requirements was conducted for this relaxed laminar stability case in accordance with the procedures discussed in section 8.2.3. For this analysis, the wing planform of the LFC-200-S configuration was used to facilitate the analysis and comparisons, although the LFC-200-R wing planform is slightly smaller. Figure 150 presents the resultant slot pressure loss $\Delta P/H_0$ and the slot spacing Δc_s as a function of the slot width for the upper wing surface at WS 370. This figure is directly comparable to figure 116 for the LFC-200-S configuration. For convenience, the same symbols for percent chord are used in both figures. It will be noted that the figures are quite similar except that the spacing levels of the LFC-200-R configuration are generally about 50 percent greater than those for the LFC-200-S configuration, while the slot widths are approximately 20 percent smaller for the same spacing. These trends are to be expected for the reduced suction flow case. The slot pressure losses are approximately the same for both configurations, with a one percent loss value possible at all wing chord locations. This might also be expected since the lower limit of the pressure loss is dictated by the ΔC_p slot lower limit criteria which was 0.03 in both cases. It was pointed out in section 4.0 that suction of the first 4.0 percent of the wing is not required for the LFC-200-R configuration. The 3.81 percent chordline is, therefore, representative of the forward extent of the suction surface.

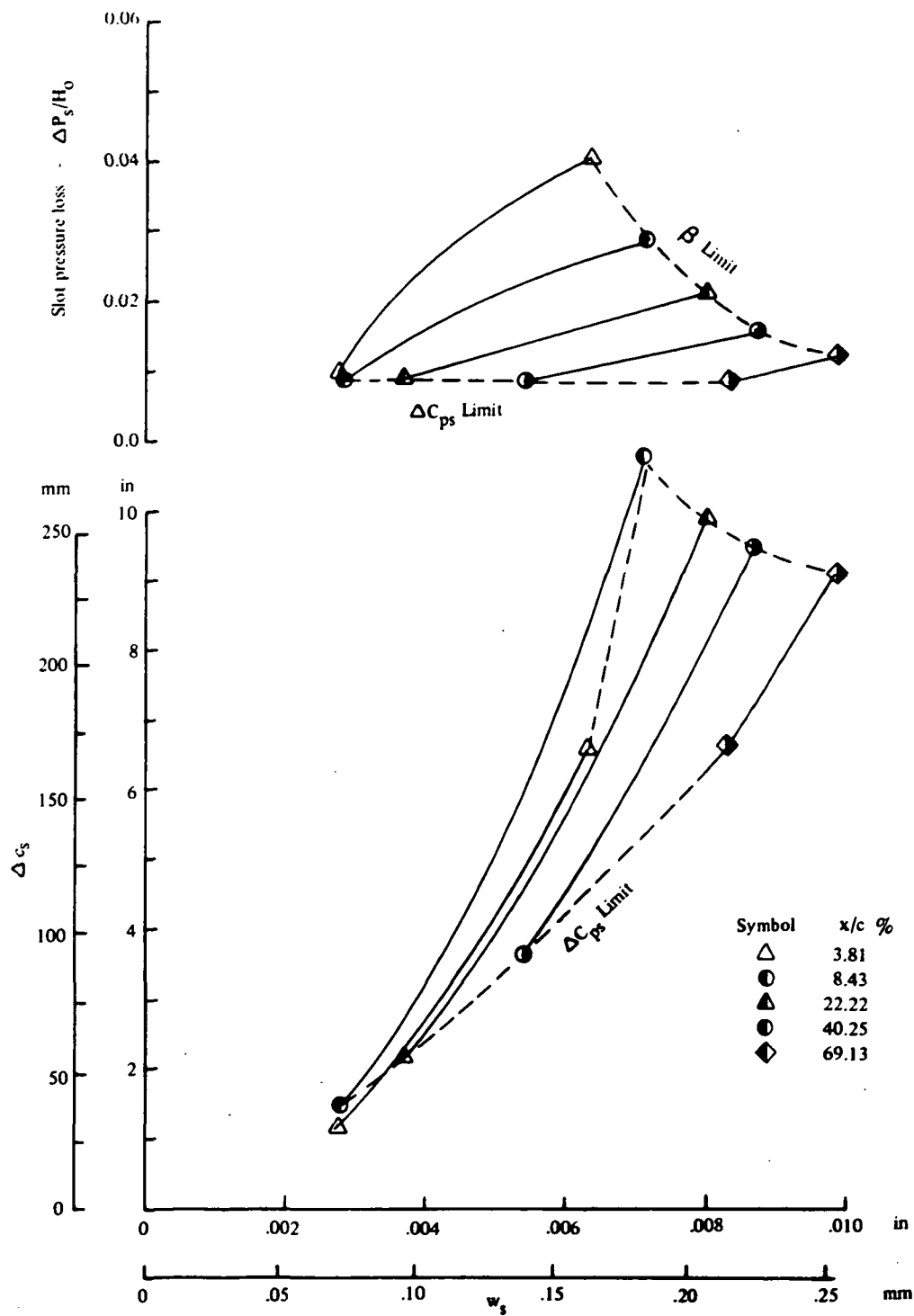


Figure 150. — Slot spacing and pressure loss vs. slot width, upper WS 370, LFC-200-R

Figure 151 presents the allowable limits for the slot spacing and the resultant pressure losses as a function of the percent chord. This figure is directly comparable to figure 117 for the LFC-200-S airplane configuration. The similarity of slot pressure loss characteristics is readily apparent as is the generally increased level of slot spacing for the LFC-200-R configuration.

These observations lead to a slot spacing planform for the LFC-200-R configuration that is basically similar to that depicted in figure 124 for the LFC-200-S configuration except that a 5.08 cm (2 in) larger spacing is used at all locations. Slots in the 4-percent chord leading edge region are eliminated on the LFC-200-R configuration. Employing this larger spacing necessitates a reduction in the slot widths that is generally represented by a .025 mm (.001 in) reduction to the planform schedule shown in figure 125 for the LFC-200-S configuration.

Comparison of the allowable slot width and slot spacing bands for the 69.13 percent chord stations in figure 116 and 150 reveals a slightly larger band for the LFC-200-R configuration. This indicates relaxation but not elimination of the requirement to increase the slot flow path lengths in the aft portion of the laminar region of the wing root. Therefore, the requirement for the 1.27 mm (0.050 in) flowpath length shown on figure 126 for the LFC-200-S configuration is eliminated for the LFC-200-R configurations and all other areas requiring increased flowpath length move aft.

No new problems are introduced in the slot design for the LFC-200-R configuration. In some respects the suction design becomes easier. The observations made in reference to porous and perforated surfaces for the LFC-200-S configuration are equally applicable to the LFC-200-R configuration.

Surface Design — LFC surface panels for LFC-200-R are identical in construction to the panels described in section 8.2.3.1. Dimensionally, the panels are thinner due to reduced flow required in the chordwise capillary ducts so that the lower hat-shaped spacers can be reduced to 6.35 mm (0.25 in). The overall surface panel thickness is 10.41 mm (0.41 in) thick. Table 23 presents a weight breakdown for this surface configuration.

TABLE 23. LFC SURFACE PANEL WEIGHT SUMMARY: LFC-200-R

Main panel	kg/m ²	lb/ft ²
Outer skin	1.406	.288
Intermediate skin	.703	.144
Inner skin	.703	.144
Chordwise edges	.054	.011
Spanwise edges	.068	.014
Upper spacer	.439	.090
Lower hat spacer	.605	.124
	<u>3.979</u>	<u>.815</u>
Miscellaneous	1.928	.395
	<u>5.907</u>	<u>1.210</u>

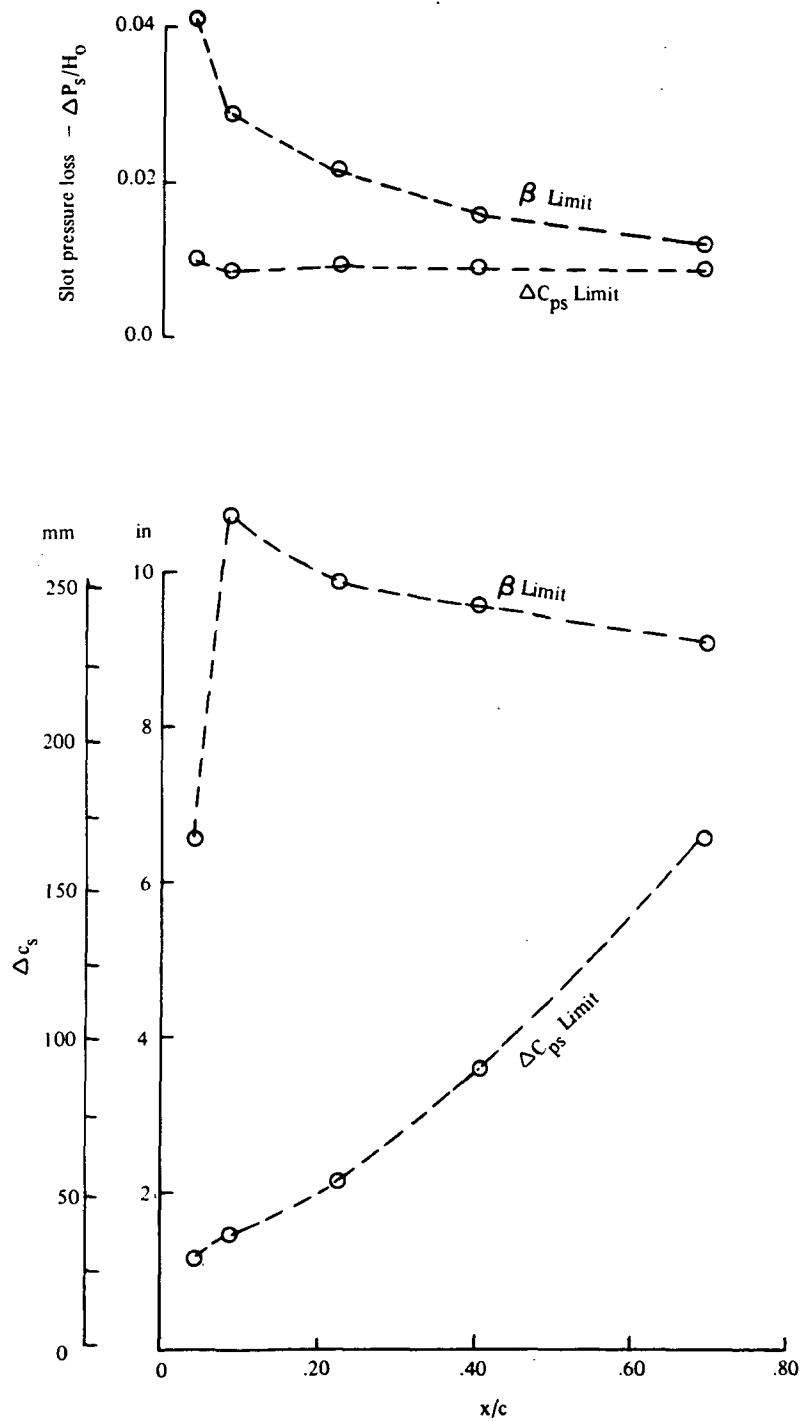


Figure 151. — Slot spacing and pressure loss vs. chord location, upper WS 370, LFC-200-R

Since leading edge suction is not required, no LFC surfaces are provided on the leading edge. Main surface panels extend from 3% to 75% chord on both upper and lower surfaces. A typical wing section with this surface panel segment construction is shown in figure 152. Empennage surfaces have LFC suction provided from 3% – 75% chord.

8.3.3.2 Ducting and Distribution

The basic ducting and distribution system criteria are those discussed in section 6.3.1. These criteria were applied to the specific LFC suction requirements for the LFC-200-R configuration in the same general manner as for the LFC-200-S configuration.

The schematic diagram of the system presented in figure 131 is equally applicable as are the general remarks concerning this configuration in section 8.2.3.2. In the case of the LFC-200-R configuration, the suction flows are reduced substantially from those of the LFC-200-S configuration resulting in different slot widths and spacings. The same slot duct configuration was retained for this configuration because it was originally selected primarily from the viewpoint of production and quality control. For LFC-200-R, this configuration results in maximum slot duct Mach numbers of 0.0097 and 0.008 for the wing root and wing tip, respectively. These are well below the selected criteria.

The collector ducts were evaluated in the same manner as discussed in section 8.2.3.2. A plot of the collector duct exit Mach number and accumulated system pressure loss are presented in figure 153 as a function of collector duct height for the longest collector duct at the wing root. A collector duct height of 6.35 mm (0.25 in) results in a 9.4 percent accumulated pressure loss at an exit Mach number of 0.26. These are considered acceptable, particularly in view of the earlier observation that these pressure losses and Mach numbers only occur in a small spanwise portion of the wing at the wing root. A 6.35 mm (0.25 in) collector height was therefore selected for this configuration since it results in the lightest cover weight and minimizes impact on wing structure and fuel volume.

Figure 154 presents the collector duct Mach numbers and accumulated local pressure loss as a function of collector length for the selected collector duct height. It will be noted that the values of these parameters are only slightly lower than for the LFC-200-S configuration. This is the result of the reduced collector height nearly offsetting the reduced suction flow. The pressure loss and Mach number at the exit of the collector duct are shown by the solid lines on figure 166 and 156, respectively. There is a short span for which collector duct exit Mach numbers are in excess of 0.2.

Superimposed on figures 155 and 156 are the trunk duct local pressure loss and Mach number values. The dashed line defines the values for the tip collector duct passing all the way to the fuselage. The peak Mach number in this duct is 0.225 in the root area and exceeds 0.2 Mach for about 20 percent of the semispan. It will be seen on figure 155 that, from the wing tip in to about the 9.14 m (30 ft) wing station, there is a favorable difference between the collector duct accumulated pressure losses and the trunk duct accumulated losses, indicating that the duct pressure is sufficiently below the collector exit pressure for the collector to exhaust into the trunk duct satisfactorily. Inboard of this station, however, the collector duct exit pressure losses rise

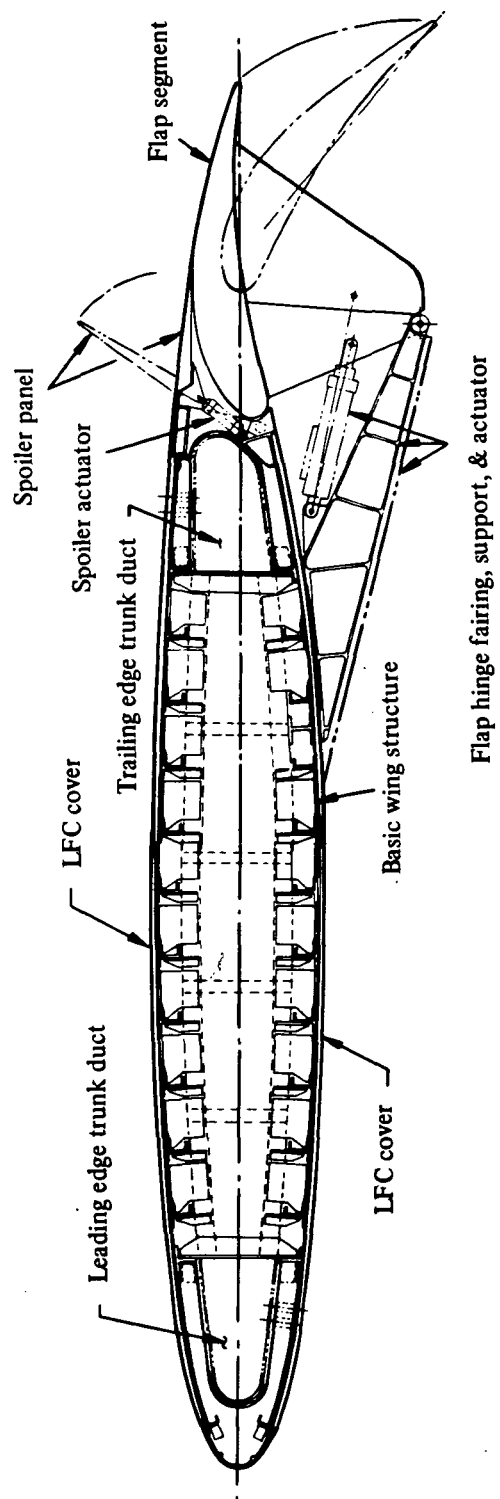


Figure 152. — Wing section, LFC-200-R

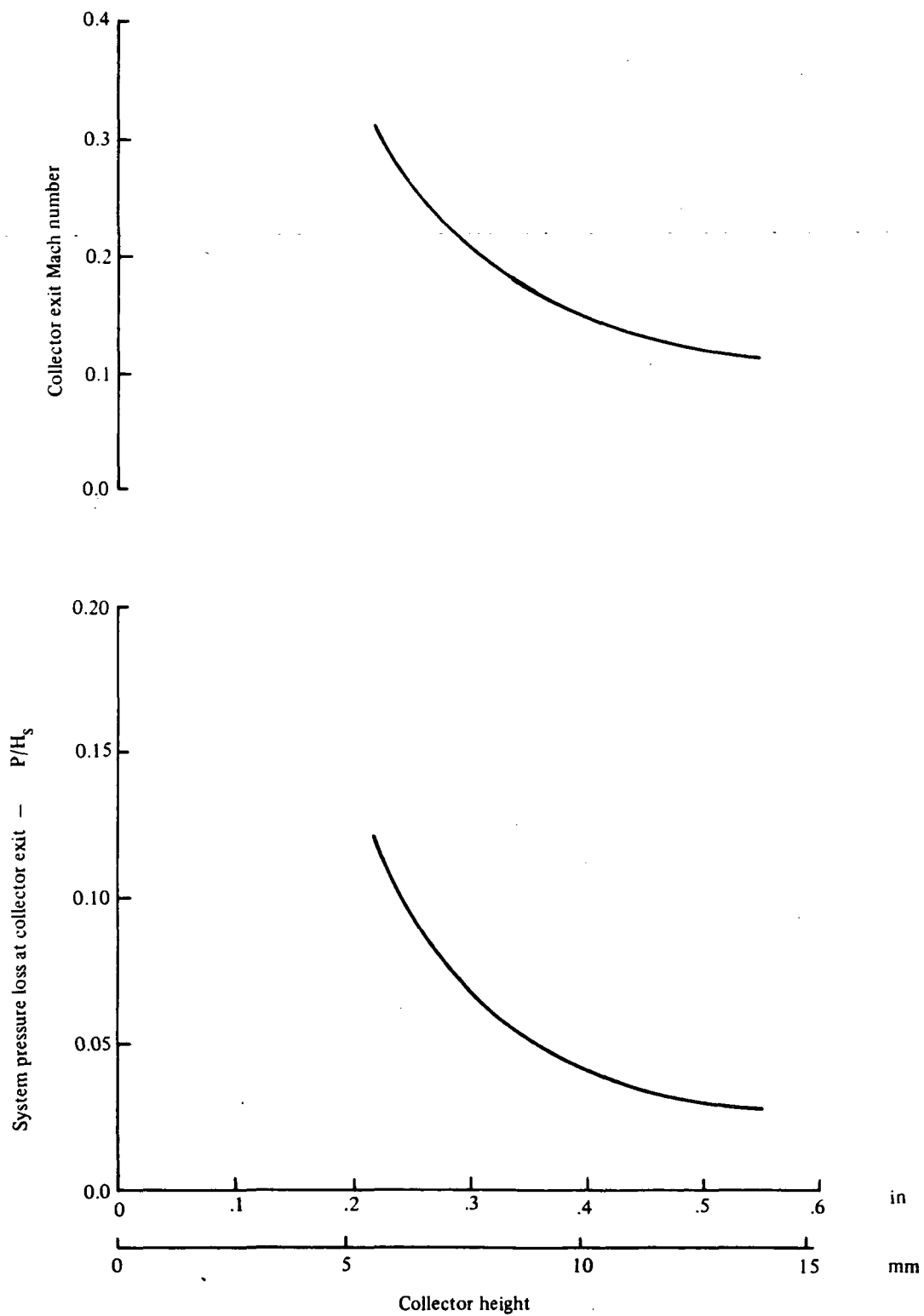


Figure 153. — Wing root collector duct characteristics, upper wing, LFC-200-R

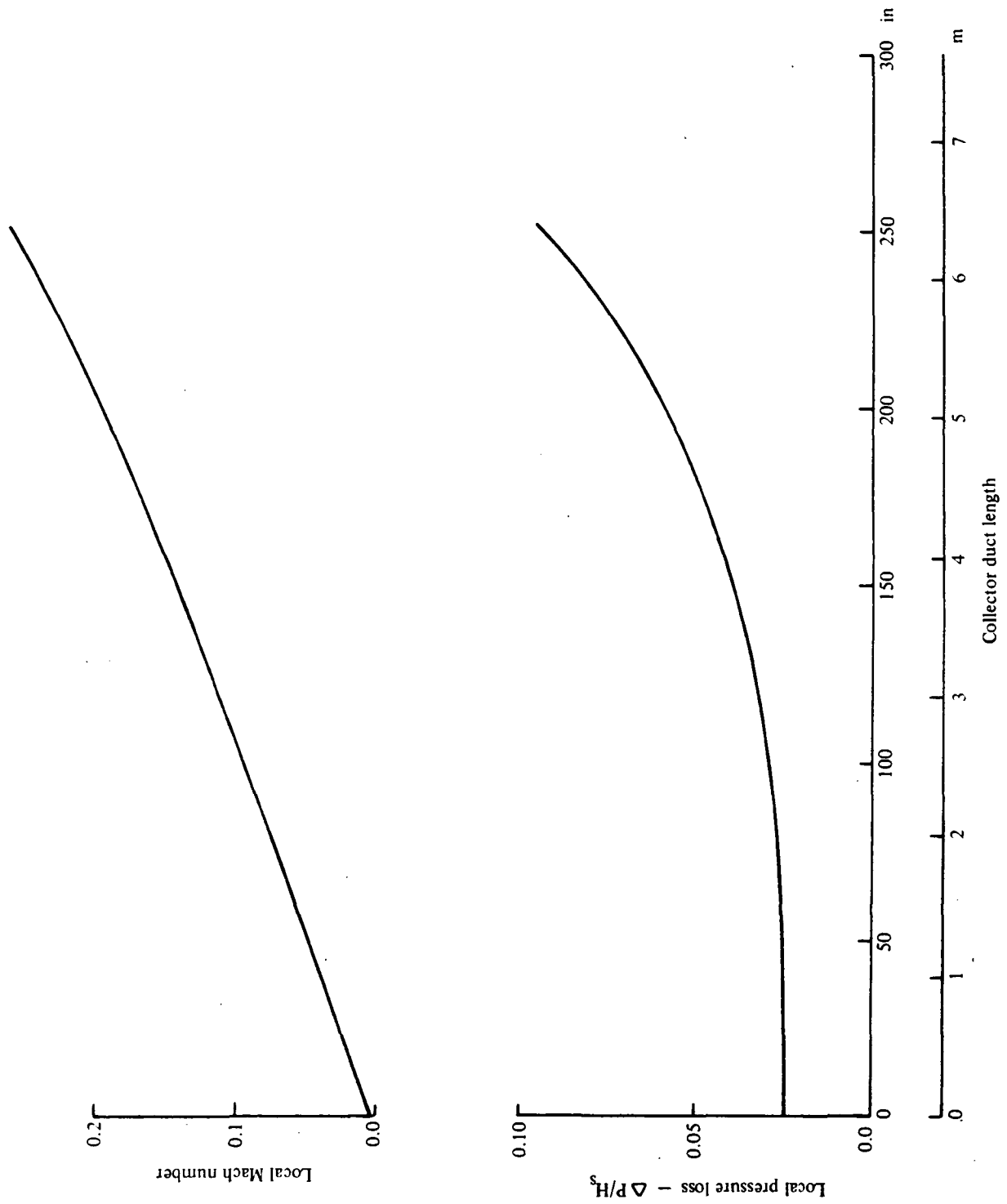


Figure 154. — Collector duct local characteristics, 0.635 cm (0.25 in) collector height, LFC-200-R

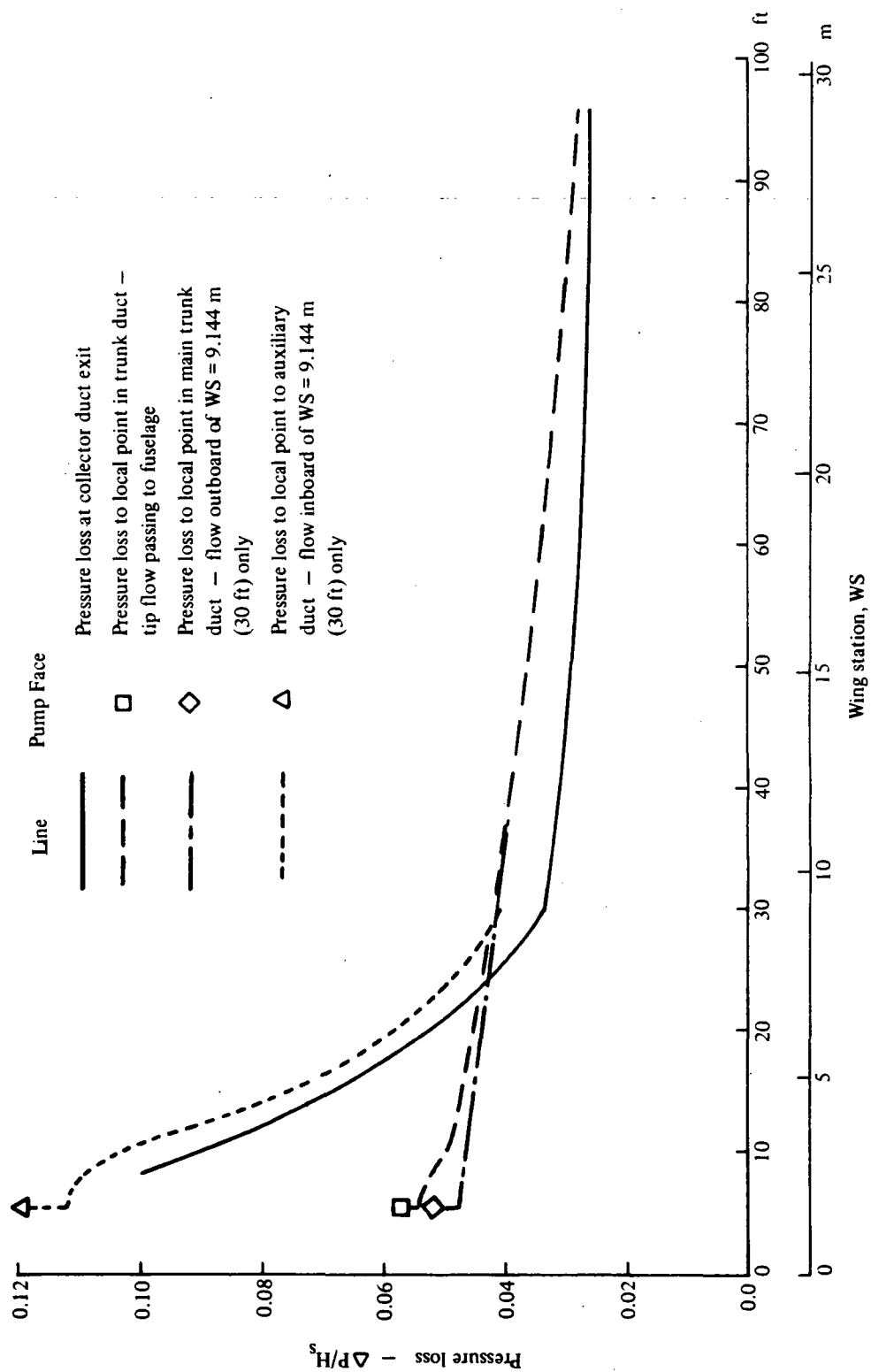


Figure 155. — Collector exit to trunk duct pressure matching, upper wing, LFC-200-R

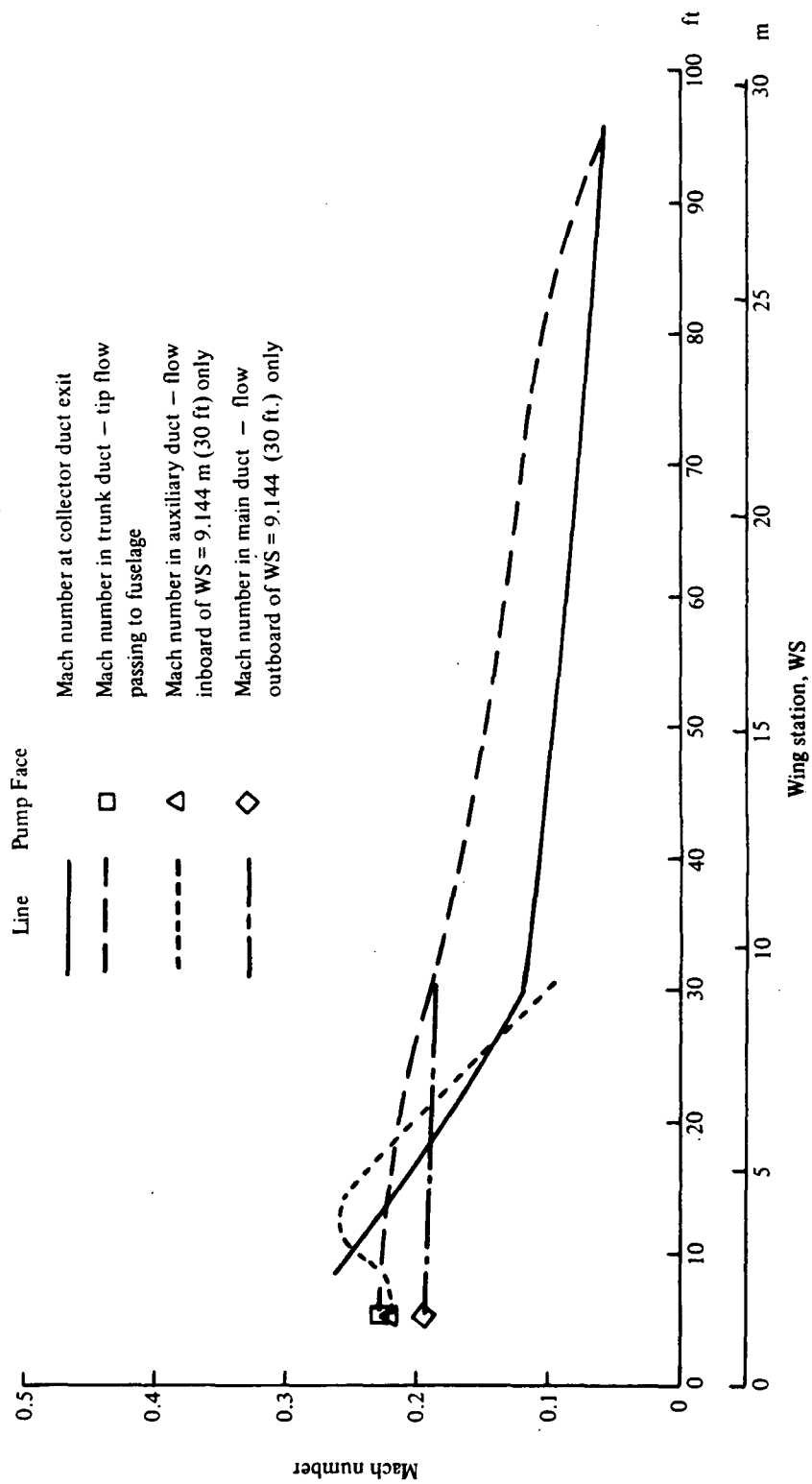


Figure 156. — Collector exit and trunk duct flow Mach number characteristics, upper wing, LFC-200-R

rapidly such that the collector exit pressure at the desired flow are below that of the trunk duct. Increasing the trunk duct pressure loss to accommodate these root collectors results in a rapid rise in duct Mach number in excess of 0.3.

By splitting the duct at the 9.14 m (30 ft) station, all of the flow from the wing surface outboard is ducted directly to the fuselage in a constant area duct with no further introduction of air from the root collectors. Characteristics of this flow are depicted on figures 155 and 156 by the broken line which shows a moderate increase in Mach number and pressure loss inboard. The remainder of the ducting space made available by the constant area main duct inboard is devoted to an auxiliary duct to collect only the high-pressure-loss root collector air. The characteristics of this duct flow are shown by the dotted line on figures 155 and 156. The duct pressures match the collector requirements and the duct Mach number reaches a maximum of 0.26 over a short span.

This solution was not available in the case of the LFC-200-S because the trunk duct Mach numbers in the root area were already excessive. This configuration only affords a means to provide a better pressure match between the collector and trunk but cannot provide any significant relief from high duct Mach numbers.

This ducting configuration permits the use of two suction units, one for each semispan, located in the fuselage near the wing root. The system has not been optimized and some further adjustment of the duct areas in the inboard 9.14 m (30 ft) of ducting could equalize the Mach numbers between the main trunk duct and the auxiliary duct. It also appears that an optimization is appropriate for the trade between the adverse effects of thicker collector ducts on wing-weight and fuel volume versus the increased duct losses of the thinner collectors. The conceptual design is found to be workable and provides for a satisfactory two suction unit system.

In this system, the empennage flows are ducted forward and equally divided between the two suction units. Duct space for the empennage does not present any problems since the volume constraints are not rigid. Two ducts of different pressure levels pass forward through the fuselage to the suction units at which point the flows are divided equally between the two suction units. Valves are provided at this point to shut off the suction from the empennage in the event of a suction unit failure. Similarly, valves are provided in the wing trunk ducts to shut off a portion of outboard wing area to permit continuation of as much symmetrical suction of the inboard wing as can be accommodated by the single operable pump.

8.3.3.3 Suction Units

The suction unit criteria and requirements discussed in sections 6.4.1 and 6.4.2 apply to the units for the LFC-200-R configuration. The specific suction requirements for these units were established in section 8.3.3.

In this configuration, each suction unit is sized to provide the total suction for one wing semispan plus half of the total empennage suction. This choice was made to permit operation of each unit with identical inlet conditions and therefore allow identical design for commonality.

The same general problems exist with the multi-pressure-levels at the inlet of the suction unit as discussed in connection with the LFC-200-S configuration. In addition, the problem is aggravated by the mix of both wing and empennage flows at the inlet of the LFC-200-R configuration. This is displayed by the solid line on figure 157 on which the various suction airflow sources are indicated. There is a mix of wing and empennage flows throughout the range of required pressure ratios with the absence of two clearly defined pressure ratios. A choice of three pressure ratios, 2.95, 2.33, and 1.84 appears to be logical. However, this entails two levels of pre-compression with three separate inlets to the suction unit. Three concentric inlet ducts would be required, two of which would involve a mix of wing and empennage flow. Such a configuration is quite complex and involves careful matching of the suction pump design with the flow requirements and ducting with associated weight increases. The alternative of two suction levels is more attractive because of the resulting simplification. Two choices are available for this type of system. One choice requires a pre-compression unit of 1.27 pressure ratio pumping 49 percent of the flow with the main compressor pumping 100 percent of the flow through a pressure ratio of 2.33. The other choice uses a pre-compression unit pumping 59.5 percent of the flow through a pressure ratio of 1.60 with the main compressor pumping 100 percent of the flow through a pressure ratio of 1.84. Both of these choices involve some inefficiency in that the suction unit is required to pump some portion of the airflow through a higher pressure ratio than is required by the source pressures and duct losses. However, the savings in complexity as compared to the three-pressure-ratio unit justifies this selection.

Of these two latter choices, the pre-compression unit pumping 59.5 percent of the flow through a pressure ratio of 1.60 is considerably more efficient and is shown by the dashed line on figure 157. It also affords a larger pre-compression unit and smaller main unit which is a less sensitive design configuration. Free stream velocity was assumed as the suction unit exhaust velocity in establishing the preceding suction unit pressure ratios.

The two-pump configuration allows installation of the suction units in the fuselage in the vicinity of the wing root. This location is awkward for a ram inlet for an independent power unit but is well suited for a bleed and burn system. In this installation, high-pressure compressor discharge air is bled from the primary propulsion units and ducted to the suction system power unit where it enters a combustor. Fuel is introduced and burned to achieve approximately the same burner exit temperature as that of the primary propulsion engines. This burner exhaust then passes through a turbine unit which includes air-cooled blading similar to that of the primary propulsion engines, utilizing a small portion of the bleed air for this cooling. More of the available energy is extracted from the combustion products than is the case for the primary engine turbine such that the exhaust of the suction unit power turbine is approximately free stream velocity. The turbine is directly coupled to the suction unit compressor.

Although some performance improvements were evidenced in the case of the LFC-200-S for exhausting the suction air at velocities equal to the exhaust velocity of the primary propulsion units, the same conclusion does not apply to the two-pump bleed and burn units. A higher suction compressor discharge pressure is required to exhaust at the higher velocity. This additional power requirement is ultimately reflected in a higher bleed flow from the primary propulsion engines with

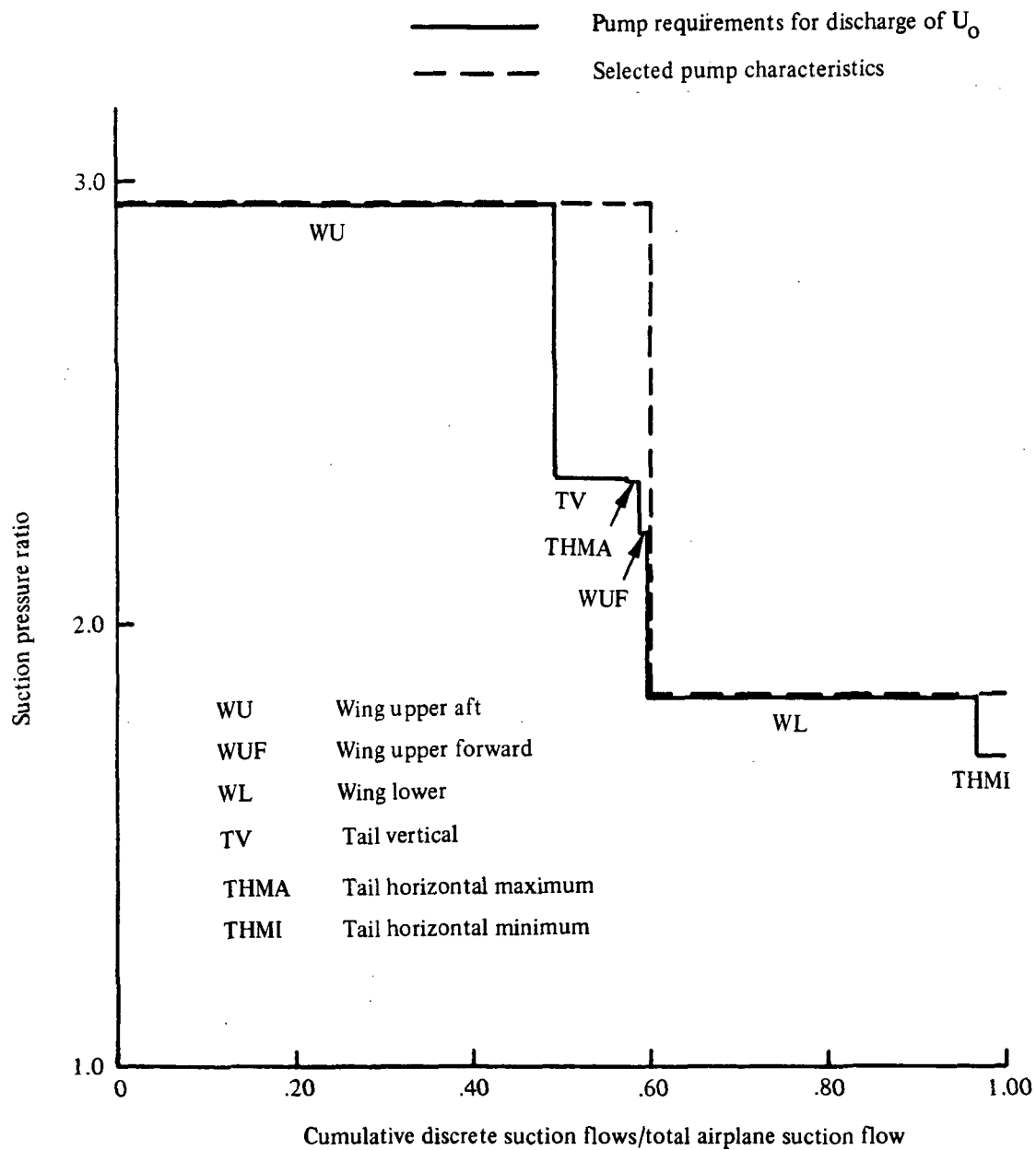
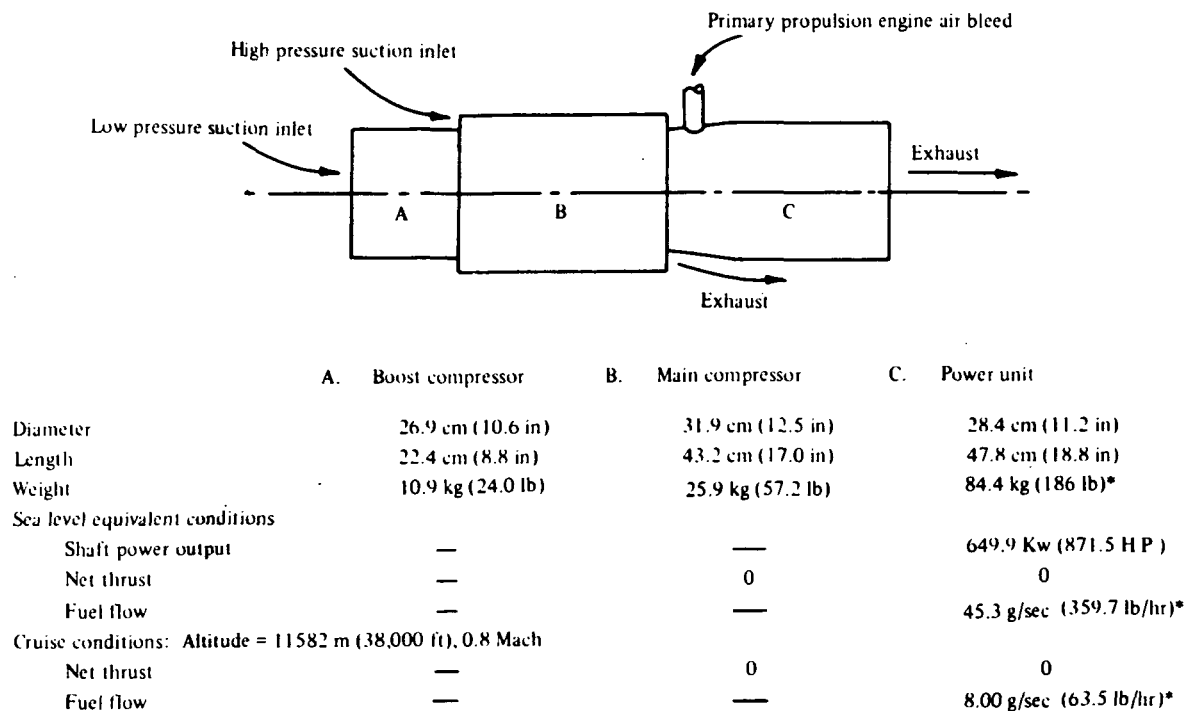


Figure 157. — Normalized airplane suction characteristics, LFC-200-R

an attendant increase in primary engine weight. Since the bleed-burn system entails losses in the bleed air, with lower turbine efficiencies, the tradeoffs for the elevated suction unit exhaust velocity are not as favorable as for the independently powered system. Free stream exhaust velocity was therefore selected for the two suction unit system. However, a more detailed tradeoff analysis would probably reveal an optimum exhaust velocity somewhat above free stream. In any case, the magnitude of the tradeoffs in an optimization would have an insignificant effect on the overall airplane performance.

A complete suction unit is shown schematically in figure 158. It is envisioned that these units may be assembled as a complete unit with the burner and turbine attached directly to the suction compressor unit at the discharge case hub in the manner of a core engine attachment to a fan. The compressor annulus is concentric with the burner and turbine. The compressor exhaust is either bifurcated around the burner and turbine exhausting downward and aft or the suction pump and turbine exhaust flows may be concentrically mixed and discharged through a common nozzle.

The suction pump technology selected for this unit was subject to the same considerations as for LFC-200-S suction pump. The pre-compression unit is a three-stage unit with a stage pressure ratio of 1.17. The main suction unit has four stages in contrast to five for the LFC-200-S with an average stage pressure ratio of 1.165. The reduction of main suction unit stages is largely the result of the choice of a lower discharge velocity for LFC-200-R.



* Includes penalties to primary propulsion engine weight and fuel flow resulting from bleed plus bleed ducting weight and pressure losses.

Figure 158. — Bleed-burn powered suction unit, LFC-200-R

The burner and turbine power unit have the same 1980-85 technology of the LFC-200-S independent power unit. The burner and turbine unit have the same weight and dimensional characteristics as those of a conventional shaft engine and are essentially scaled on the basis of output shaft power, recognizing that the full power developed by the turbine may be applied to the suction unit. A weight allowance was made for a bleed air distribution scroll into the burner.

The bleed air from the primary engines is ducted into a single manifold with a shut-off and check valve located at each primary engine. A single duct may convey this air to the burner units or dual ducts with shut-off valves may be provided from the manifold. If the single duct is employed, it is bifurcated in the vicinity of the burner with a shut-off valve provided for each burner. All of the high pressure bleed air ducting from the primary engines requires insulation throughout its length. Weight allowances were included for this ducting and insulation.

An essential of the bleed burn system is that the primary propulsion engines be designed for continuous bleed for the suction system. As was discussed in section 6.4.4, the SFC penalties to the conventional primary propulsion system for this bleed without proper design allowance outweigh many of the advantages that may otherwise be realized. Since the engines must be designed for essentially continuous bleed, a problem arises with the disposition of this bleed air when the suction system is not being operated. The obvious disposition of this bleed air is to discharge it through a nozzle to provide additional thrust. However, the noise generated by this extremely high pressure air would be prohibitive in the terminal area. Two alternatives emerge as possible solutions but the problem was not completely resolved in this study. The bleed may simply be shut-off at the primary engine, resulting in a mismatch in the primary engine between the core compressor and turbine. Whether the engine could tolerate this mismatch is not known since it would be in the direction to drive the core compressor toward stall. A reset of core compressor variable stators could possibly accommodate this mismatch with adverse effect but an in-depth engine analysis would be required to evaluate this modification. The second alternative is to direct this air through the suction unit burner and turbine without introducing fuel and burning. This would produce a relatively low level of suction unit turbine power, which could be absorbed by the suction unit compressor with the inlet vented to ambient through a throttling system and the suction ducting system shut-off. This system would introduce mis-match problems at the suction pump inlet which would require careful design of the ambient vents. The pressure ratio developed by the suction pump is such that the inlet would require considerable throttling of the ambient air to control the suction unit discharge pressure to a sufficiently low level that noise from this source would not be prohibitive.

8.3.3.4 Controls

The bleed-burn suction system controls are essentially quite similar to those described in section 8.2.3.4. The suction pump inlet vane controls for matching are identical as is the overall suction level control by the suction pump exhaust pressure bias. The basic speed governed control of the burner-turbine unit is somewhat different. The fuel flow to the burner is the primary speed governing control. However, since the burner air supply is independent of the turbine unit, proper biases and safeguards must be provided to prevent a flame-out of the burner or subjecting the

turbine to excessive temperatures. This is accomplished by sensing the burner inlet pressures as a bias and feedback to the fuel control. If fuel flows are reduced to a level approaching the lean blow-out limit, further fuel reductions are accompanied by a burner airflow reduction sensed by the burner inlet pressure. The upper limit of fuel flow is biased by the burner inlet pressure to prevent a high fuel flow and/or a low airflow from causing excessive turbine inlet temperatures. If the bleed airflow is reduced below the nominal level, as might occur in event of a primary engine failure, the burner fuel flow is automatically limited to a safe level.

Starting the bleed burn unit does not present any significant control problems. The suction compressor has the same stall protection as discussed in section 8.2.3.4. The power unit is started by introducing a limited amount of bleed air at which a controlled fuel flow is introduced and ignited. As the speed increases, the airflow and fuel flow are increased on a controlled schedule until the governed speed is reached. The aerodynamic starting load does not present any significant problem for the burner-turbine power unit.

8.4 CONFIGURATION LFC-400-S

8.4.1 GENERAL ARRANGEMENT

The LFC-400-S airplane is a wide body configuration designed to transport 400 passengers, their baggage, and 9072 kg (20,000 lb) of cargo over the intercontinental range of 10,186 km (5500 n mi) at a speed of Mach 0.80. The wide-body fuselage accommodates 80 first-class and 320 tourist-class passengers in a two-aisle cabin configuration.

The cabin provides the required entry/escape doors, lavatories and passenger service stations required for long-range operation. The flight deck has provisions for 3 crew members and controls and instrumentation compatible with international flight requirements.

As shown in figure 159, LFC-400-S is a low-wing T-tail monoplane with four aft-fuselage-mounted propulsion engines. Two bleed-burn LFC suction units are installed as shown in figure 148, one in each wing-root-fuselage fairing, which also houses the retracted main landing gear.

The wing is a moderately swept, high aspect ratio structure with outboard ailerons. Full-span flaps are provided to meet required field performance. Spoilers are located over the inboard flaps. Fuel is carried in the full span of the wing, including the cross fuselage wing box. LFC surface suction is provided from the leading edge to 75% on both upper and lower surfaces. Empennage LFC suction surfaces extend from the leading edge to 65% chord on all surfaces.

Table 24 presents a weight statement for LFC-400-S.

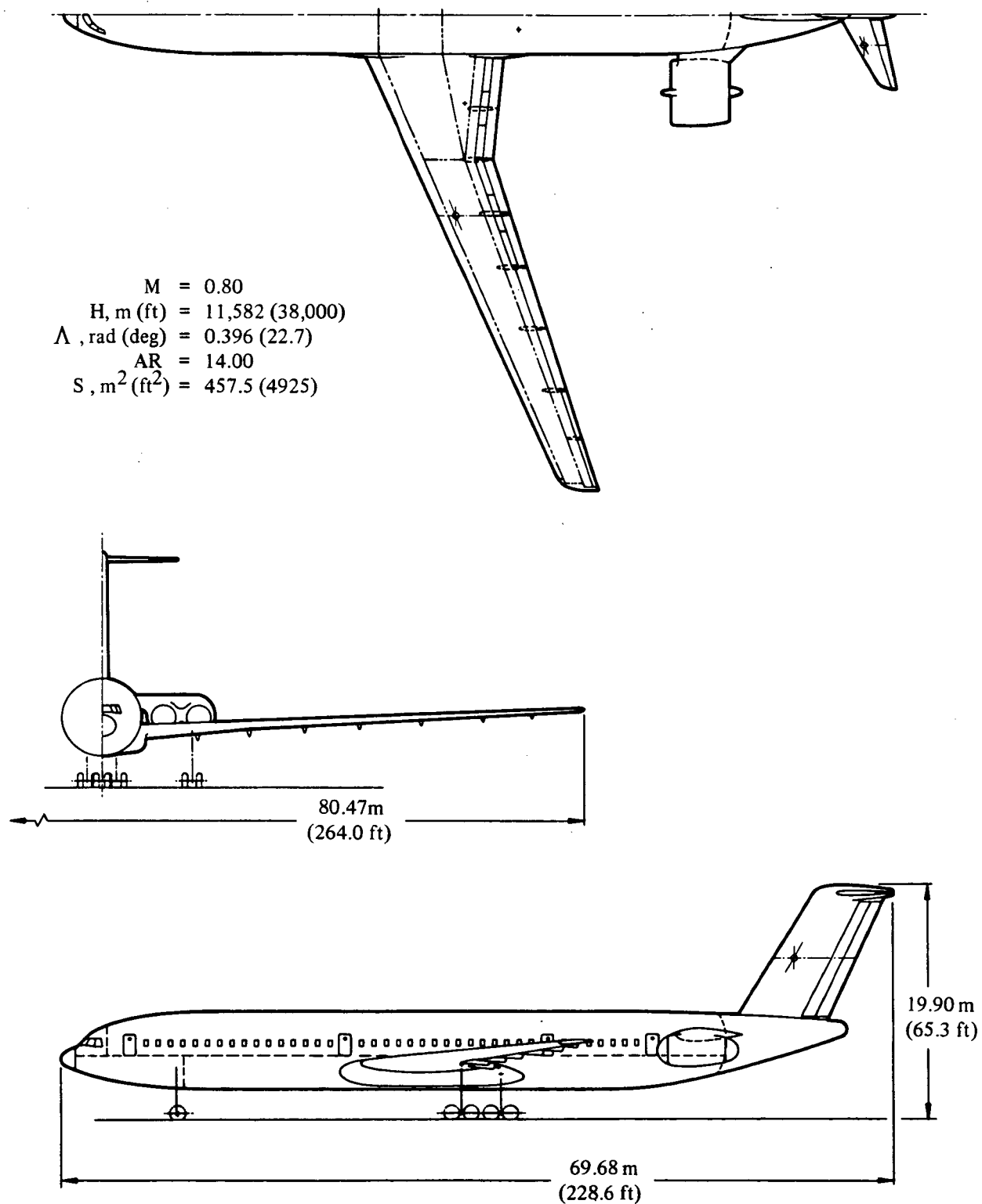


Figure 159. — General arrangement, LFC-400-S

TABLE 24. WEIGHT STATEMENT: LFC-400-S

Item	kg	lb
Structure	(111,544)	(245,908)
Wing	55,380	122,089
Wing LFC glove	5,171	11,401
Empennage	(4,532)	(9,991)
Horizontal tail	1,338	2,949
Horizontal LFC glove	323	713
Vertical tail	2,081	4,587
Vertical LFC glove	790	1,742
Fuselage	27,421	60,452
Landing gear	(14,317)	(31,563)
Nose	1,861	4,103
Main	12,456	27,460
Nacelle and pylon	(4,723)	(10,412)
Nacelle	1,886	4,158
Pylon	723	1,593
Noise treatment	2,114	4,661
Propulsion system	(21,358)	(47,086)
Engines	14,333	31,598
Fuel system	1,696	3,740
Thrust reversers	2,408	5,309
LFC engines	580	1,279
LFC installation	719	1,585
LFC ducts	715	1,576
Miscellaneous	907	2,000
Systems and equipment	(28,993)	(63,918)
Auxiliary power system	430	949
Surface controls	2,157	4,755
Instruments	684	1,507
Hydraulics and pneumatic	1,005	2,216
Electrical	2,967	6,542
Avionics	1,089	2,400
Furnishings	17,221	37,966
Airconditioning and AI	3,380	7,452
Auxiliary gear - equipment	59	131
Weight empty	(161,895)	(356,912)
Operating equipment	14,713	32,436
Operating weight	(176,608)	(389,348)
Payload - passenger	38,465	84,800
Cargo	9,072	20,000
Zero fuel weight	(224,145)	(494,148)
Fuel	97,750	215,498
Gross weight	(321,895)	(709,645)
AMPR weight	138,873	306,158

8.4.2 AIRCRAFT SYSTEMS

Except for the landing gear and size effects, the aircraft systems for LFC-400-S are identical to those described in section 8.2.2 for LFC-200-S. The LFC-400-S main landing gear is comprised of four struts. Two are wing-mounted and two are installed in the fuselage. Each strut carries a conventional four-wheel bogie. No form of MLG steering or swivelling is required. Hydraulically-powered nose gear steering is provided.

8.4.3 LFC SYSTEMS

The general discussion of the suction requirements presented in section 8.2.3 is equally applicable to the LFC-400-S configuration. The distributed suction velocity ratios v_s/U_o as shown in figures 107, 108, and 109 and the corresponding C_p characteristics presented in figures 110, 111, and 112 for the LFC-200-S configuration are applicable to LFC-400-S. The boundary layer velocity gradient of figure 113 is directly applicable to the LFC-400-S configuration. The significant differences between the LFC-200 and LFC-400 configurations lie in the larger chord and less constrained space for LFC ducting in the LFC-400 configuration.

8.4.3.1 Surfaces

Slot Sizing and Spacing – An analysis of the upper wing suction surface requirements was conducted for the LFC-400-S configuration in accordance with the procedures discussed in section 8.2.3. Figure 160 presents representative slot spacings and associated slot pressure losses as a function of slot width for the upper wing surface at WS 480. This wing station is analogous to WS 370 for the LFC-200-S configuration in that they both occur at the point where the wing trailing edge break occurs.

Figure 161 presents a scale planform of the LFC-400-S wing which may be compared to figure 123 for the LFC-200-S configuration. The companion plot to figure 160 is figure 162 which presents the slot spacing and slot pressure loss as a function of percent chord.

Comparison of figure 160 with figure 116 for the LFC-200-S configuration reveals that the band of allowable slot widths diminishes more rapidly for the LFC-400-S configuration than for the LFC-200-S configuration at increased percent chord. Maintaining a constant slot flow path length of 0.508 mm (0.020 in), does not produce a combination of spacing and lot width that will meet both the β and ΔC_p slot criteria aft of the 50 percent chord location on the LFC-400-S configuration. Increasing the slot flow path length to 0.762 mm (0.030 in) by the methods discussed in section 8.2.3.1 provides an adequate, although marginal solution to the 75% chord location. Figure 162 clearly illustrates the effect of this increase in slot flow path length.

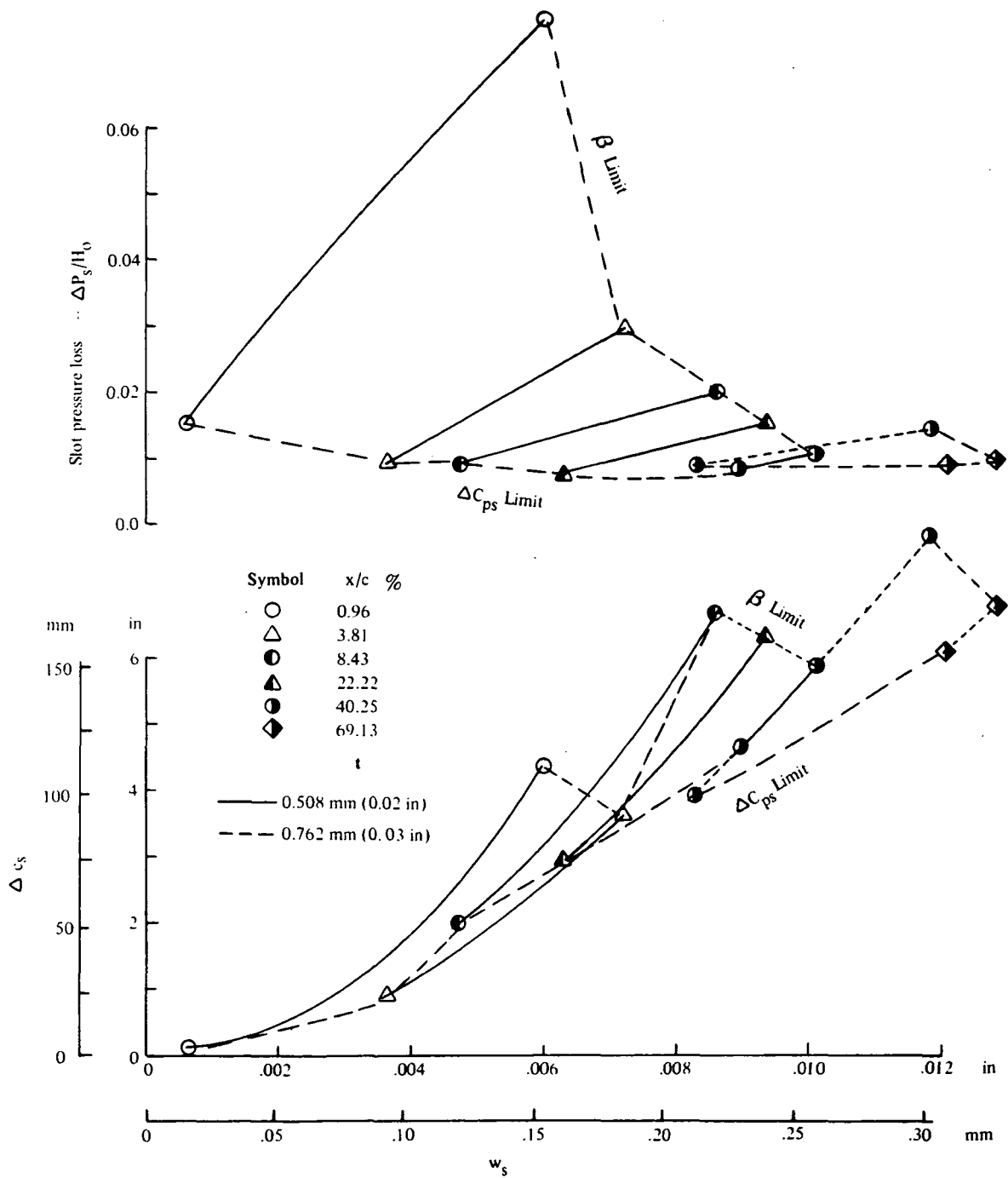


Figure 160. — Slot spacing and pressure loss vs. slot width, upper WS 480, LFC-400-S

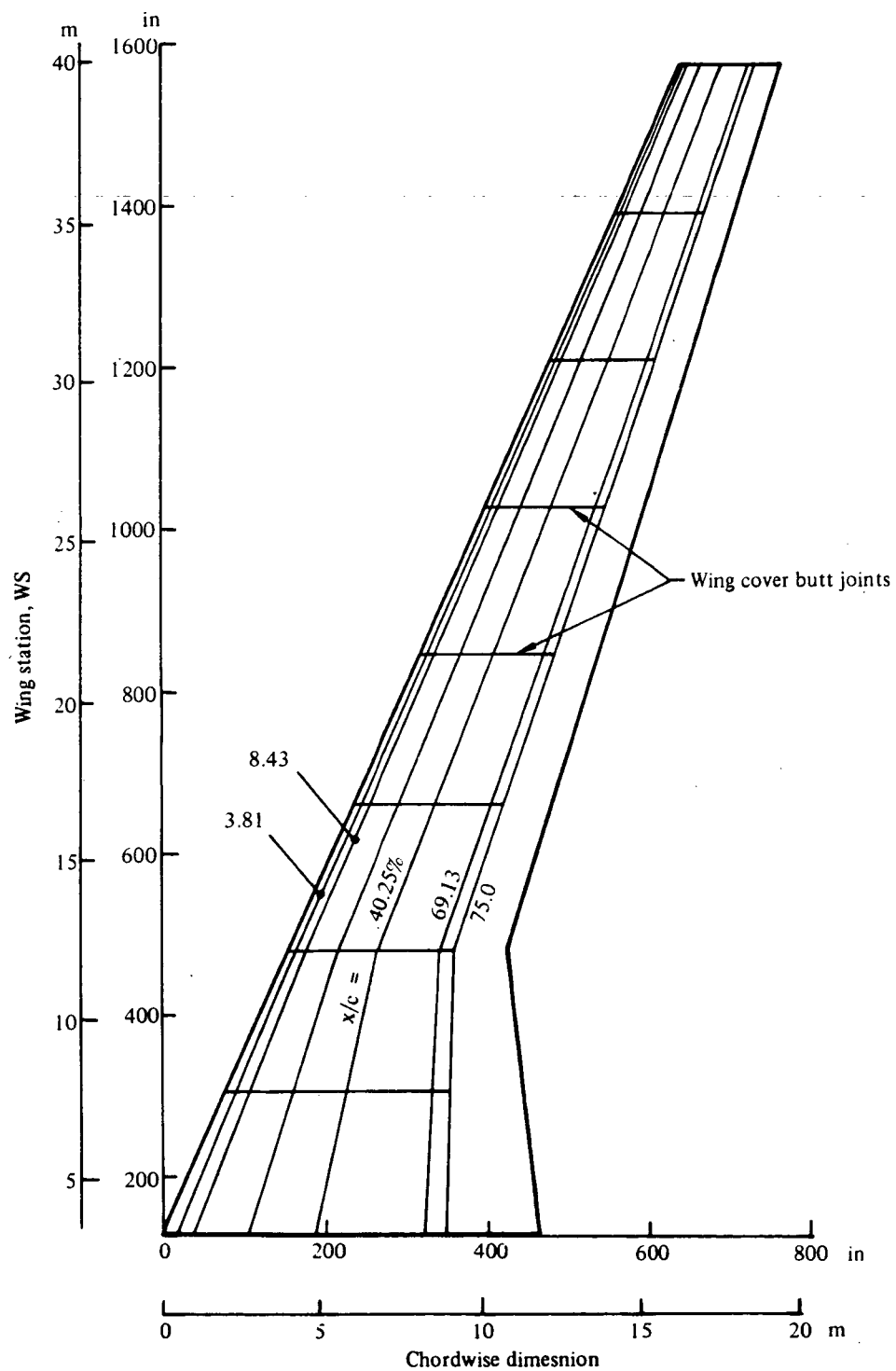


Figure 161. — Wing upper surface planform, LFC-400-S

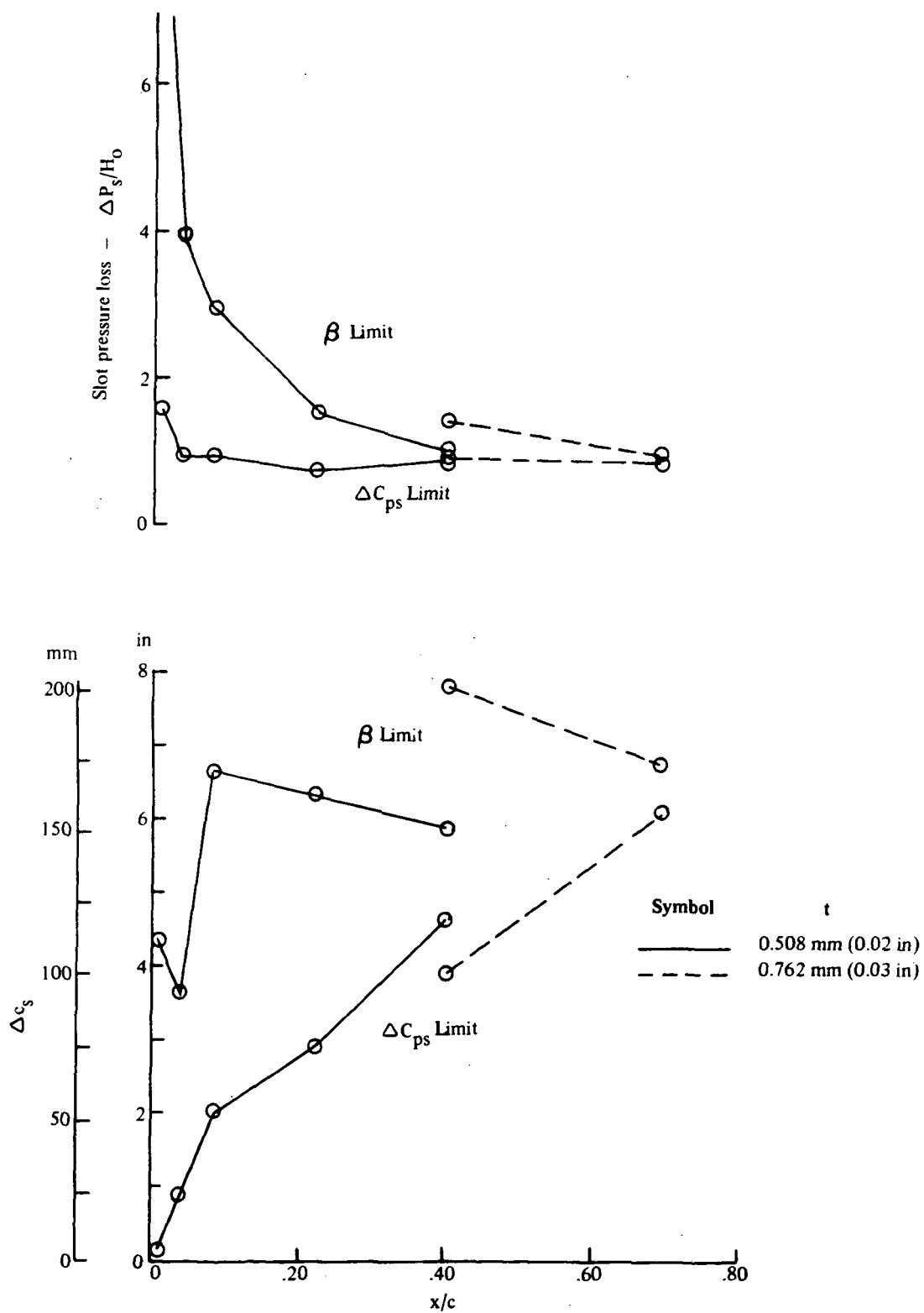


Figure 162. — Slot spacing and pressure loss vs. chord location, upper WS 480, LFC-400-S

This requirement for increasing the flow path length is the consequence of the relatively large chords of this wing station compared to the comparable wing station on the LFC-200-S configuration. This leads to the conclusion that the requirement to increase the slot flow path length may become a problem at the root section, since a considerable increase in slot flow path length was required at the aft root suction area for the LFC-200-S configuration. Comparison of figures 161 and 123 shows, however, that the bat in the wing root section is less severe on the LFC-400-S configuration. While the wing chord for the LFC-400-S configuration at WS 480 is 38 percent greater than that of the LFC-200-S at WS 370, the LFC-400-S wing chord is only 17 percent greater than the LFC-200-S at the wing root. While this does indicate that the LFC-400-S requires a substantial increase in suction slot flow path length toward the aft end of the wing root slotted area, it does not represent a problem. Although these increases in slot flow path length encroach on the spanwise slot ducts, ample flow area is available to maintain a low pressure loss in the system. The tip wing station of the LFC-400-S is representative of the characteristics of LFC-200-S configuration outboard of WS 370.

The slot spacing planform for the LFC-400-S is quite similar to that of the LFC-200-S shown in figure 124, and the slot width planform is quite similar to that shown in figure 125, except that comparison of figure 160 with figure 116 indicates that the slot widths for LFC-400-S are generally about 0.051 mm (0.002 in) larger than the corresponding location on the LFC-200-S wing. Both the relative area requiring increased slot flow path length and the maximum flow path length are significantly increased for the LFC-400-S by comparison with the LFC-200-S configurations shown in figure 126.

Surface Design – LFC surface panels for LFC-400-S are identical in construction to the panels described in section 8.2.3.1 for LFC-200-S. The panels are thicker to accommodate the increased suction requirements of the larger airplane. The difference lies in the lower hat-shaped spacers forming the chordwise capillary ducts. These spacers are 17.78 mm (0.70 in) thick, increasing the overall panel thickness to 21.84 mm (0.86 in).

Leading edge suction is required for LFC-400-S. These panels, except for thickness, are identical to the leading edge panels described in section 8.2.3.

A weight summary for the surface panels on this configuration is included as table 25.

8.4.3.2 Ducting and Distribution

The LFC suction system requirements defined for the LFC-400-S configuration were evaluated in accordance with the criteria established in section 6.3.1 by the methods described in section 8.2.3.2.

TABLE 25. LFC SURFACE PANEL WEIGHT SUMMARY: LFC-400-S

Panel t = 21.8 mm (0.86 in)		
<u>Main panel</u>	<u>kg/m²</u>	<u>lb/ft²</u>
Outer skin	1.406	.288
Intermediate skin	.703	.144
Inner skin	.703	.144
Chordwise edges	.117	.024
Spanwise edges	.156	.032
Upper spacer	.439	.090
Lower hat spacer	.918	.188
	4.442	.910
Miscellaneous	2.519	.516
	6.961	1.426
<u>Leading edge panel</u>		
Outer skin	1.406	.288
Intermediate skin	1.406	.288
Inner skin	1.406	.288
Chordwise edges	.474	.097
Spanwise edges	.620	.127
Upper spacer	3.500	.717
Lower hat spacer	12.137	2.486
	20.949	4.291
Normal skin (delete)	-3.662	-.75
Miscellaneous	3.662	.75
	20.949	4.291
Average weight - all panels	8.055	1.65

The system schematic in figure 131 is applicable to this configuration as are the general remarks in section 8.2.3.2. In the case of the LFC-400-S configuration, the levels of suction flow on a unit wing area basis are the same as those for the LFC-200-S configuration. However, the larger chords result in some changes to suction slot configuration as noted in section 8.4.3.1. These slot changes do not significantly alter the maximum slot duct Mach numbers from those of the LFC-200-S, so the same slot duct configuration is used for the LFC-400-S.

The longer chords of the collector ducts resulted in significantly increased flow at the collector duct exits. Figure 163 presents the Mach numbers and accumulated pressure losses at the exit of the wing root collector duct as a function of collector duct height. A collector duct height of 17.8 cm (0.7 in) was selected since it provides a peak Mach number of approximately 0.22 at the collector exit with an associated accumulated pressure loss of about 5 percent.

Figure 164 presents the local collector duct Mach number and accumulated pressure loss as a function of the collector duct length for the wing root collector duct. The larger collector duct height results in a lower duct loss characteristic which, combined with large area, results in a low loss over a large part of its length. These are considerably below the Mach number and loss characteristics of the LFC-200-S collectors shown on figure 132, which were severely influenced by the fuel volume and structural constraints.

The accumulated pressure losses and Mach numbers at the exits of the collectors are shown on figure 165 and 166, respectively. Comparison of the pressure losses of the LFC-400-S on figure 165 with those of the LFC-200-S on figure 134 shows that the LFC-400-S losses are about half those of the LFC-200-S from the wing tip inboard to the wing break. Inboard of the wing break, the LFC-200-S losses rise rapidly to about three times those of LFC-400-S at the wing root. This is a consequence of the relatively larger wing bat on LFC-200-S. A similar comparison of the Mach numbers on figures 166 and 134 reveals that the collector exit Mach numbers are almost identical from the wing tip inboard to the wing break, beyond which the LFC-200-S Mach numbers rise much more rapidly and are about 25 percent higher at the exit of the wing root collector.

The trunk duct local accumulated pressure losses and Mach numbers are shown as the dashed lines superimposed on figures 165 and 166. The characteristic of the trunk duct pressure loss is very similar to that for the LFC-200-S configuration but the level of loss is substantially lower for the LFC-400-S. This is largely due to the relatively increased space available for the trunk duct on the LFC-400-S configuration. The differential in pressure loss at the wing tip between the collector and trunk is greater than for LFC-200-S. This is a consequence of the longer tip collector with greater total flow but only about the same space for transition from the collector to the trunk in the case of the LFC-400-S configuration. The differential between the collector exit pressure loss and the trunk loss indicates that there is adequate differential in pressure for the flow to transition from the collector to the trunk across the entire span, unlike the LFC-200-S configuration. Figure 165 shows good compatibility between the collector exit pressure losses and the trunk losses throughout the wing span.

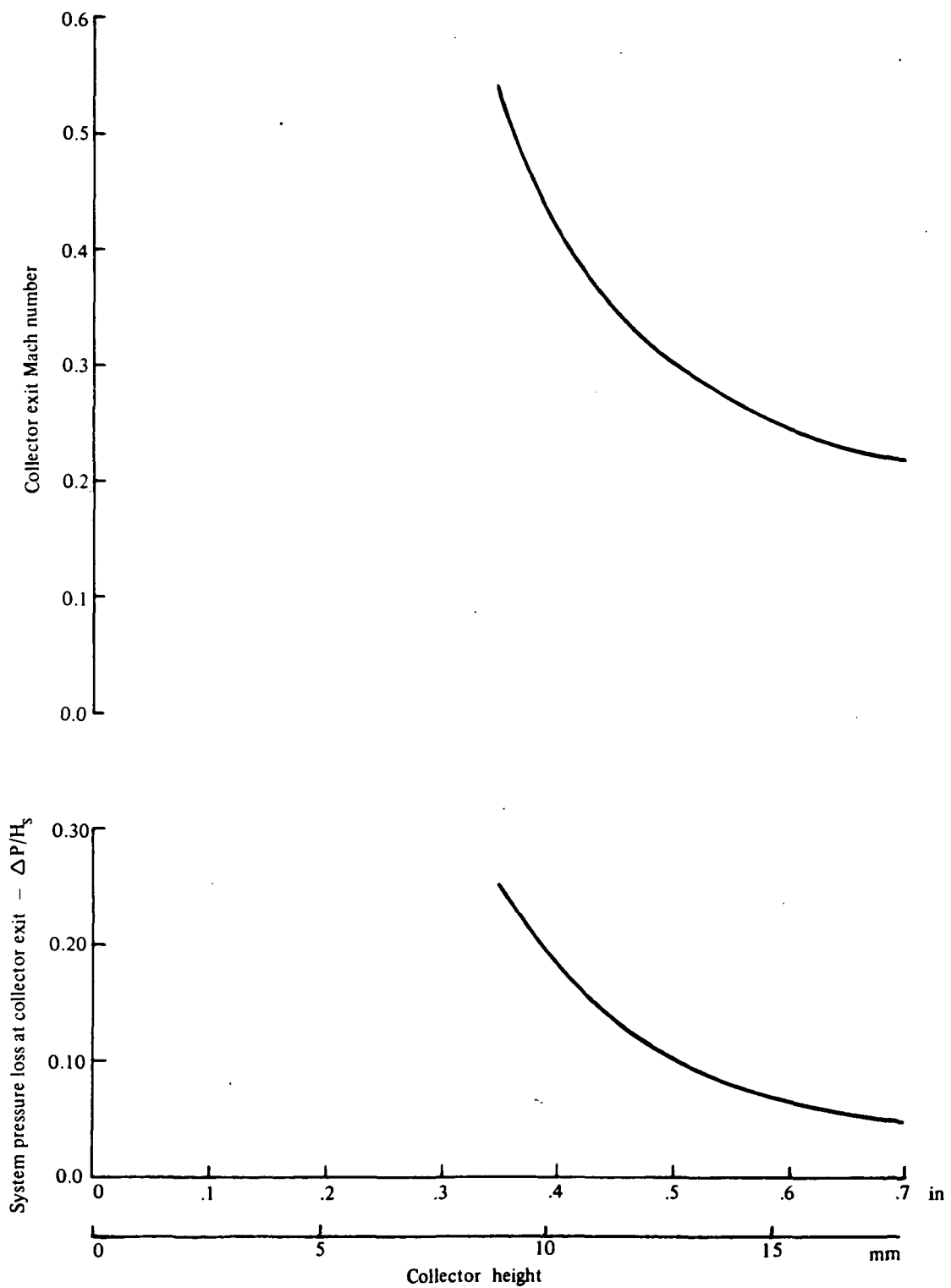


Figure 163. — Wing root collector duct characteristics, upper wing, LFC-400-S

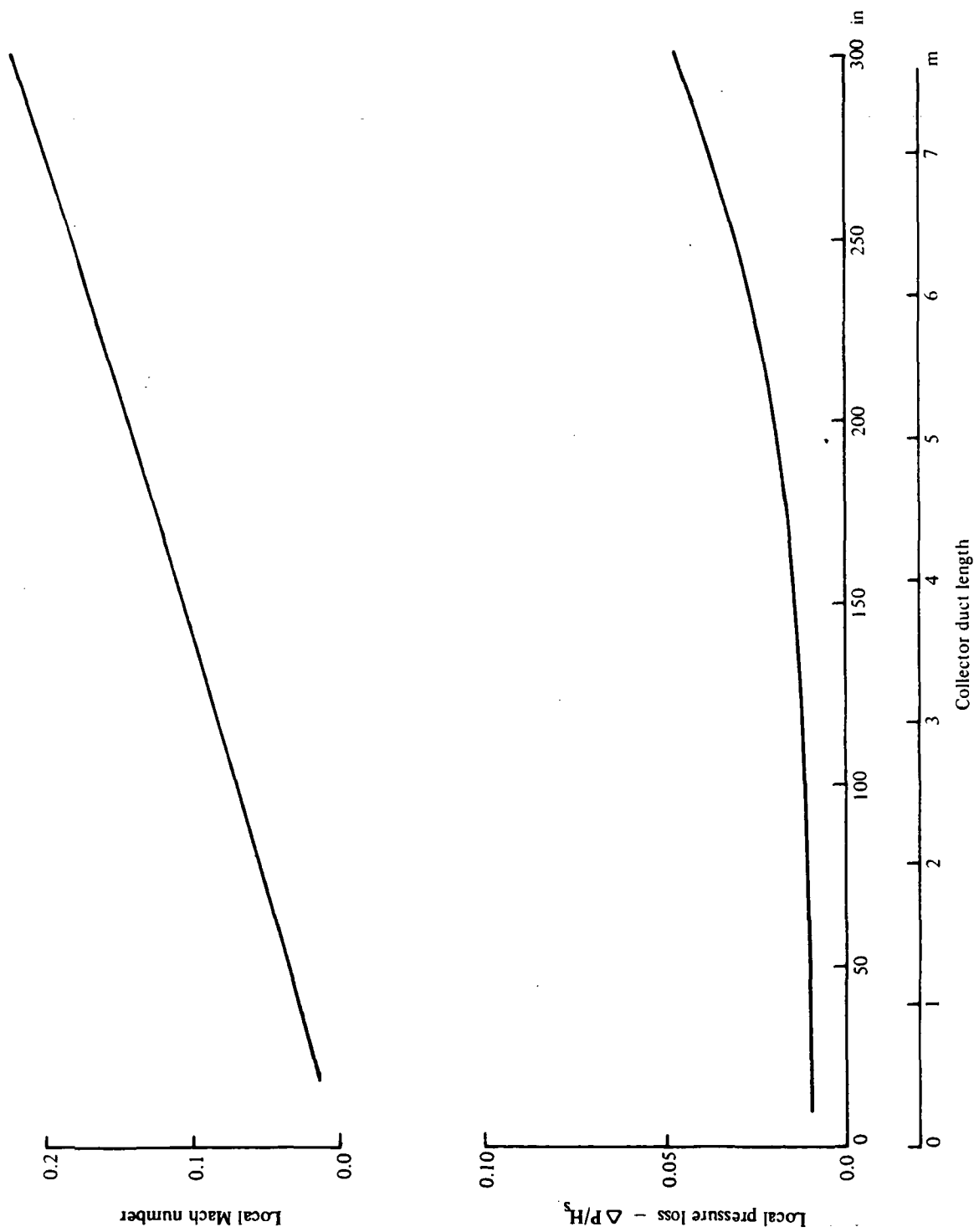


Figure 164. — Collector duct local characteristics, 1.778 cm (0.70 in) collector height, upper wing, LFC-400-S

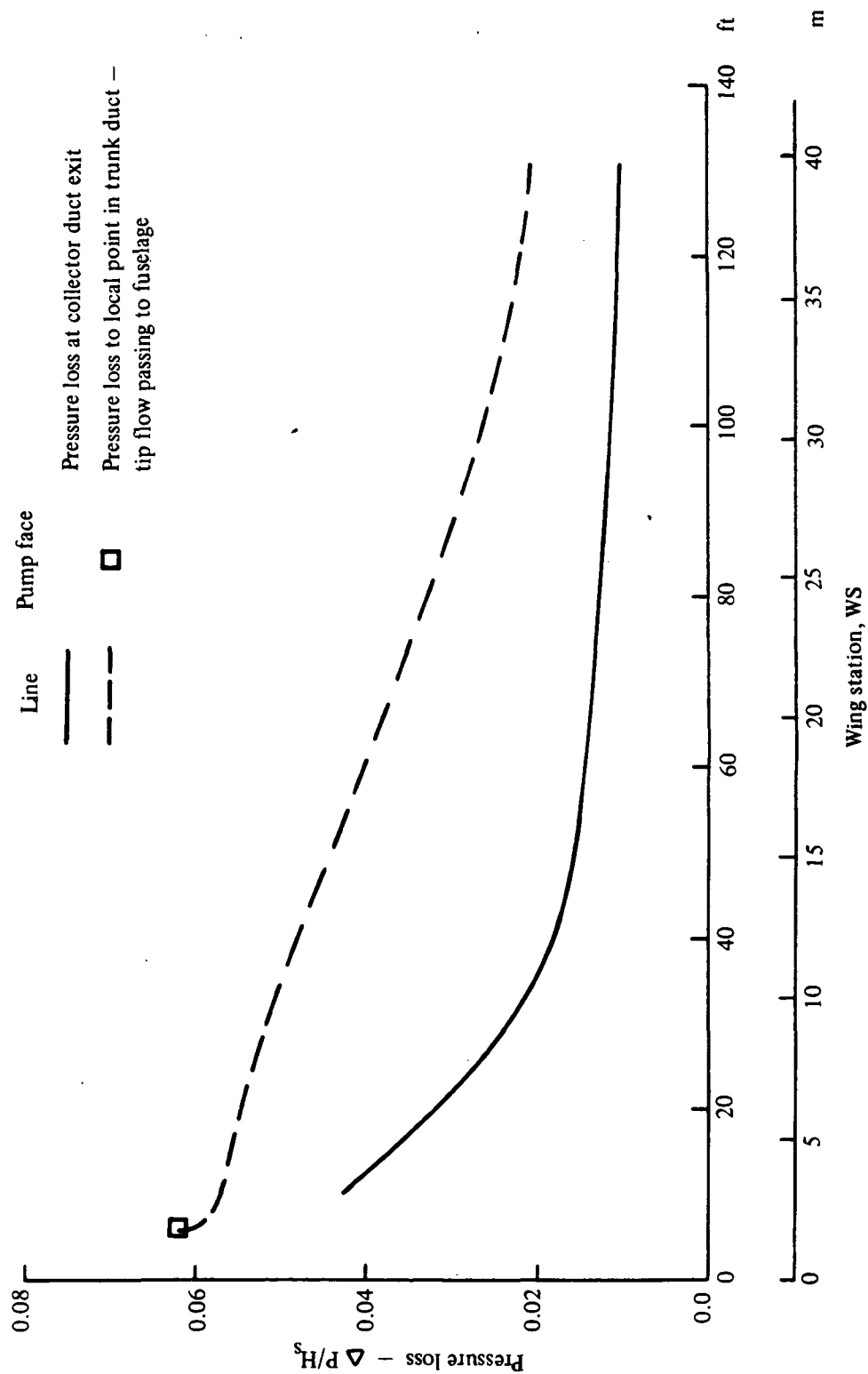


Figure 165. — Collector exit to trunk duct pressure matching, upper wing, LFC-400-S

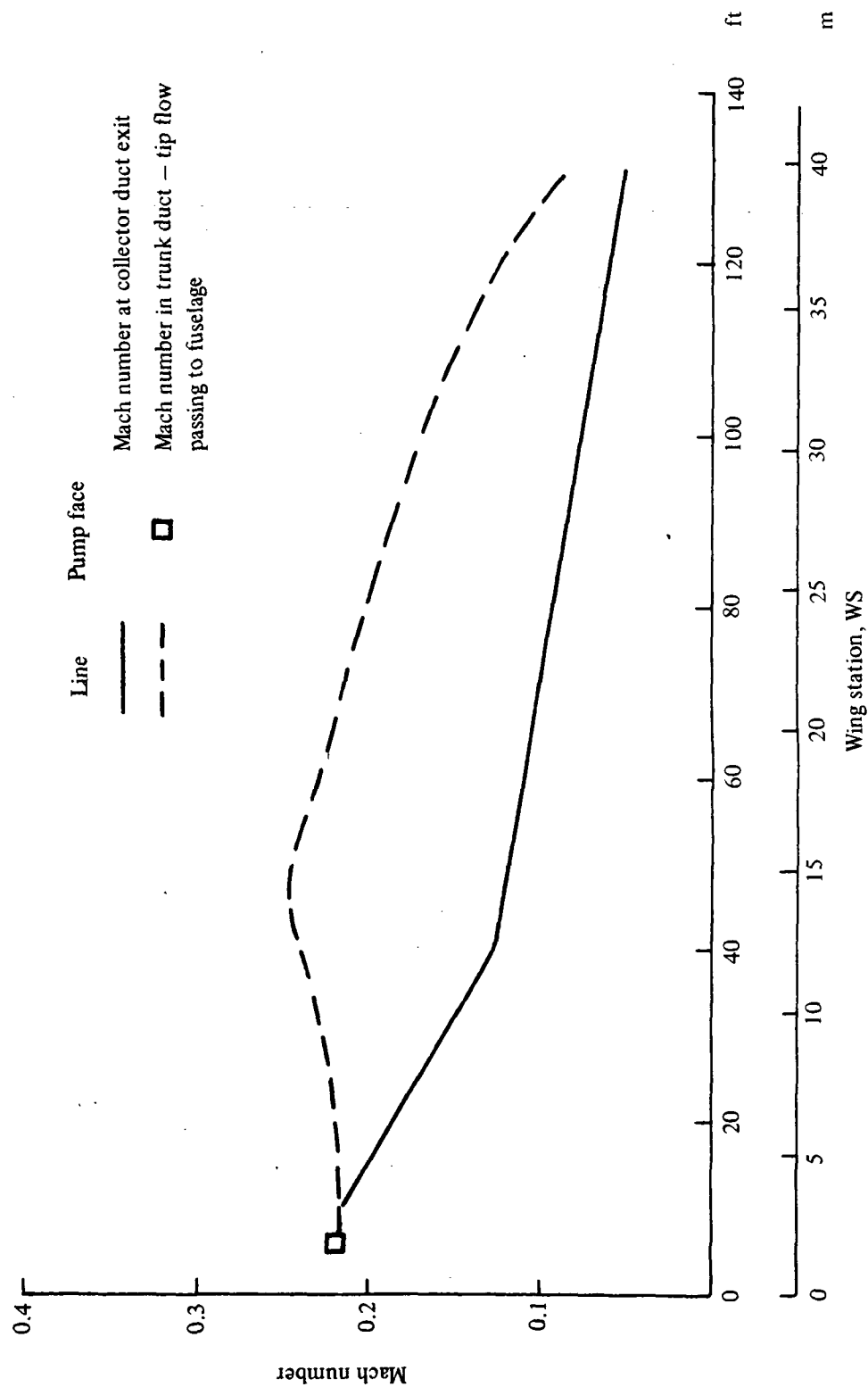


Figure 166. — Collector exit and trunk duct flow Mach number characteristics, upper wing, LFC-400-S

The trunk duct Mach numbers shown on figure 166 illustrate a short portion of the wing span near the wing break where the Mach numbers are higher than the 0.2 target but reach a peak of 0.245, well below the 0.3 limit. The Mach numbers fall off near the wing root, unlike the LFC-200-S Mach numbers of figure 135, because the duct area is increasing more rapidly than the smaller wing bat of the LFC-400-S configuration is adding collector flow to the trunk duct.

Although the ducting system was not optimized, the conceptual design is quite close to an optimum system and indicates complete compatibility with a two suction unit system. The selection of the two suction unit system entails ducting the empennage suction flows forward through the fuselage to the suction units located in the wing root as illustrated by figure 148.

8.4.3.3 Suction Units

The LFC-400-S suction units are subject to the same criteria and general requirements as described in sections 6.4.1 and 6.4.2. The specific suction requirements were discussed in section 8.4.3. As seen in the preceding section, the relaxation of the fuel volume and structural requirements relative to the available space for ducting permits ducting the entire flow from a wing semispan to the fuselage. This permits the integration of the wing and empennage suction requirements and the use of two suction units to provide the total airplane suction. As in the case of LFC-200-R, each unit provides the entire suction for one wing semispan and half of the empennage.

The similarities between the considerations and design features of the LFC-400-S suction units and those for the LFC-200-R are such that a detailed discussion of the LFC-400-S would be highly repetitious and the reader is therefore referred to section 8.3.3.3 for a more detailed discussion. Figure 167 presents the suction flow and pressure ratio relationship for LFC-400-S. The similarity with LFC-200-R shown in figure 157 is apparent. Although the percentage of flow that is pumped through a higher pressure ratio by the selected suction pump is greater than in the case of LFC-200-R, the discussion relative to the LFC-200-R is still applicable. Although the choice between a pre-compression unit pumping 42.5 percent of the flow and one pumping 62.5 percent of the flow is more marginal, the larger pre-compression unit is preferable.

Figure 168 presents a schematic of the LFC-400-S suction unit. The discussion of section 8.3.3.3 is applicable.

8.4.3.4 Controls

The bleed burn suction system controls for the LFC-400-R are the same as described in section 8.3.3.4 for the LFC-200-R. The basic differences between the units are only associated with size, which has no effect on the control concept.

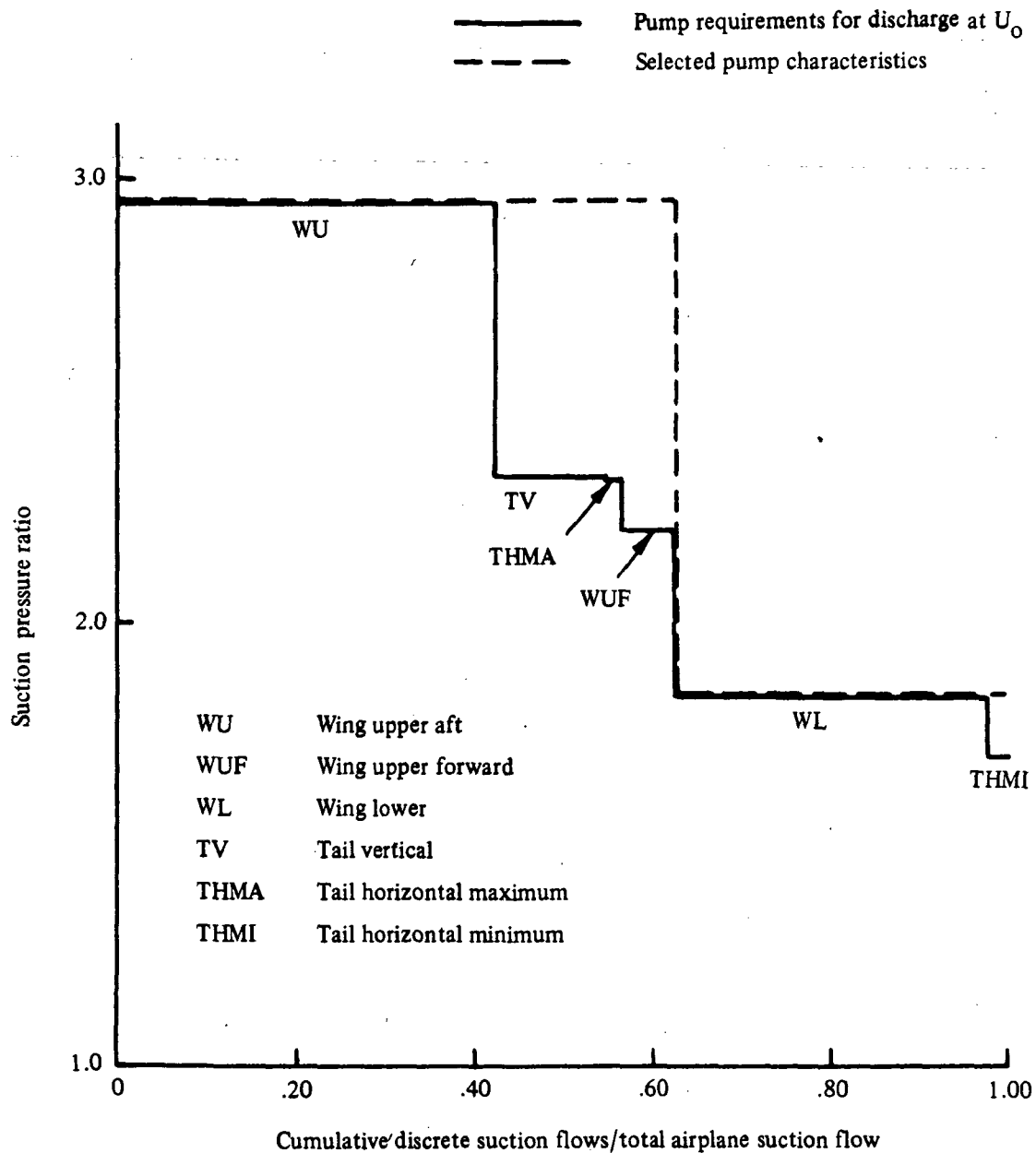
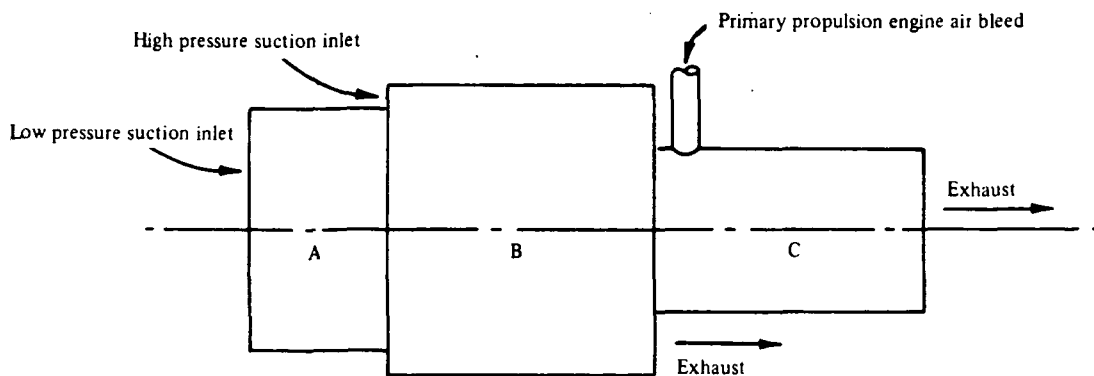


Figure 167. — Normalized airplane suction characteristics, LFC-400-S



	A. Boost compressor	B. Main compressor	C. Power unit
Diameter	51.3 cm (20.2 in)	60.7 cm (23.9 in)	33.5 cm (13.2 in)
Length	28.7 cm (11.3 in)	56.1 cm (22.1 in)	55.9 cm (22.0 in)
Weight	42.5 kg (93.7 lb)	103.5 kg (228.1 lb)	164.2 kg (362 lb)*
Sea level equivalent conditions			
Shaft power output	—	—	2324.7 Kw (3117.5 HP)
Net thrust	—	0	—
Fuel flow	—	—	159.9 g/sec (1268.7 lb/hr)*
Cruise conditions: Altitude = 11582 m (38,000 ft), 0.8 Mach			
Net thrust	—	0	—
Fuel flow	—	—	28.2 g/sec (224.0 lb/hr)*

* Includes penalties to primary propulsion engine weight and fuel flow resulting from bleed plus bleed ducting weight and pressure losses

Figure 168. — Bleed-burn powered suction unit, LFC-400-S

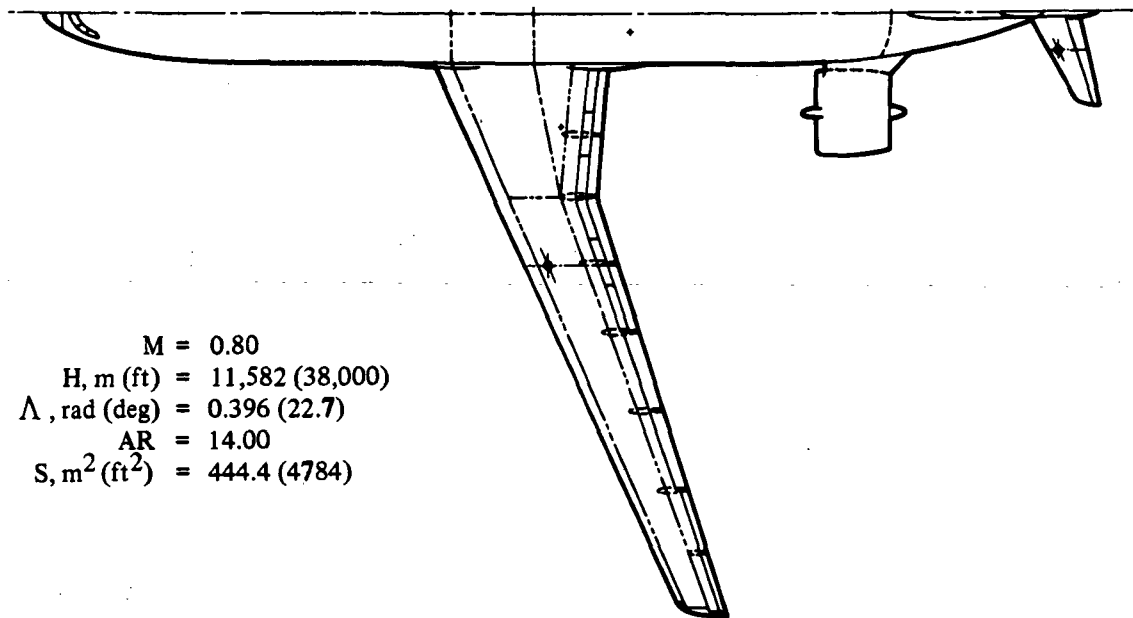
8.5 CONFIGURATION LFC-400-R

8.5.1 GENERAL ARRANGEMENT

The LFC-400-R airplane shown in figure 169 is identical to LFC-400-S described in section 8.4.1. Only the size of aerodynamic surfaces vary resulting from differences in LFC suction criteria. A weight statement for this configuration is presented in table 26.

8.5.2 AIRCRAFT SYSTEMS

The systems for LFC-400-R are identical to those described in section 8.4.2.



$M = 0.80$
 $H, \text{ m (ft)} = 11,582 (38,000)$
 $\Lambda, \text{ rad (deg)} = 0.396 (22.7)$
 $AR = 14.00$
 $S, \text{ m}^2 (\text{ft}^2) = 444.4 (4784)$

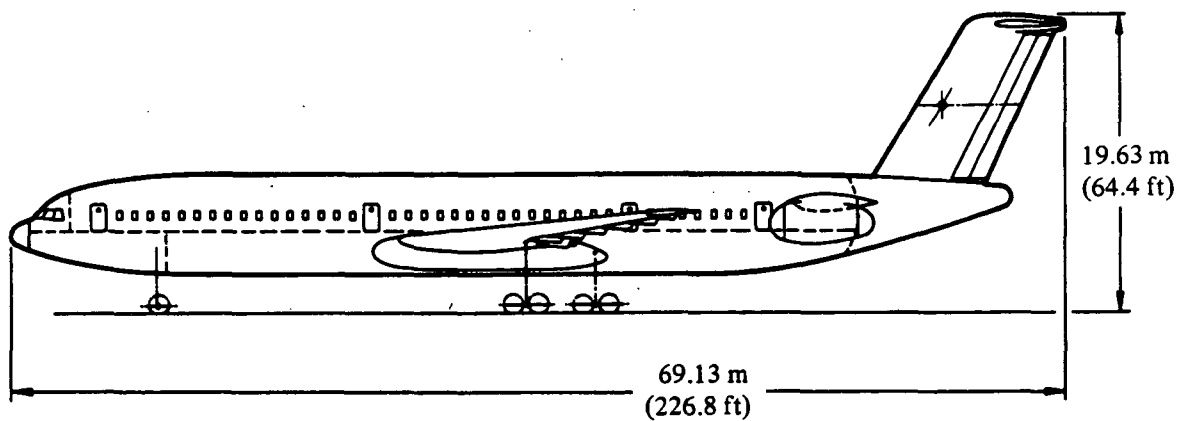
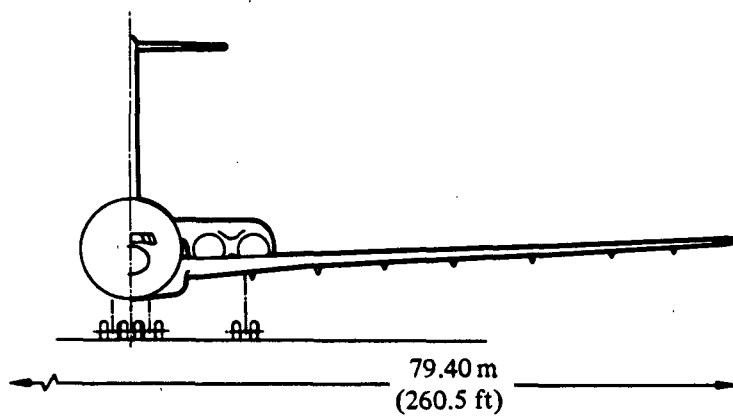


Figure 169. — General arrangement, LFC-400-R

TABLE 26. WEIGHT STATEMENT: LFC-400-R

Item	kg	lb
Structure	(106,388)	(234,542)
Wing	52,825	116,457
Wing LFC glove	3,665	8,079
Empennage	(4,072)	(8,978)
Horizontal tail	1,291	2,847
Horizontal LFC glove	227	500
Vertical tail	2,004	4,417
Vertical LFC glove	550	1,213
Fuselage	27,331	60,253
Landing gear	(13,908)	(30,662)
Nose	1,808	3,986
Main	12,100	26,676
Nacelle and pylon	(4,587)	(10,113)
Nacelle	1,835	4,045
Pylon	698	1,539
Noise treatment	2,054	4,528
Propulsion system	(20,332)	(44,824)
Engines	13,859	30,544
Fuel system	1,676	3,694
Thrust reversers	2,327	5,131
LFC engines	385	849
LFC installation	478	1,053
LFC ducts	704	1,553
Miscellaneous	907	2,000
Systems and equipment	(28,846)	(63,593)
Auxiliary power system	422	930
Surface controls	2,101	4,631
Instruments	681	1,501
Hydraulics and pneumatic	979	2,158
Electrical	2,933	6,467
Avionics	1,089	2,400
Furnishings	17,221	37,966
Airconditioning and AI	3,362	7,411
Auxiliary gear - equipment	58	128
Weight empty	(155,566)	(342,959)
Operating equipment	14,691	32,385
Operating weight	(170,257)	(375,344)
Payload - passenger	38,465	84,800
Cargo	9,072	20,000
Zero fuel weight	(217,794)	(480,144)
Fuel	94,861	209,128
Gross weight	(312,655)	(689,273)
AMPR weight	133,234	293,726

8.5.3 LFC SYSTEMS

The aerodynamic requirements for the LFC-400-R suction system are identical to those for the LFC-200-R configuration described in section 8.3.3. As in the case of the LFC-400-S configuration, the principal differences between the LFC-200 and LFC-400 configurations are due to the increased area and chord of the LFC-400 configurations. The combination of reduced suction flows in combination with the increased space for suction system ducting serve to make the LFC-400-R the least critical of the selected systems as far as the suction system design is concerned.

8.5.3.1 Surfaces

Slot Sizing and Spacing — The procedures of section 8.2.3 were employed to perform a limited analysis of the upper wing suction surface requirements. Although the relaxed laminar stability criteria resulted in a slight reduction in the wing area of the LFC-400-R configuration compared to that of the LFC-400-S configuration, the LFC-400-S planform was used to facilitate the analysis and comparisons. Figure 170 presents the resultant slot pressure loss and the slot spacing as a function of the slot width for the upper wing surface at WS 480. This figure is comparable to figure 160 for the LFC-400-S configuration and illustrates the increased spacing and slot width characteristic of the reduced suction flow configuration. The slot pressure losses remain approximately the same due to the lower limit constraint imposed by the ΔC_p slot criteria. Figure 171 presents the same parameters plotted as a function of percent wing chord. Comparison of these figures with figures 150 and 151 reflect the same differences that were observed in making a similar comparison of LFC-400-S and LFC-200-S.

From the foregoing comparisons, it is concluded that the LFC-400-R configuration presents no significant problems. As in the case of the LFC-200-R configuration, the slot spacing increases over those shown on figure 124 on the order of 5.08 cm (2 in). In the aft portion of the chord, it may be permissible to increase the spacing by as much as 10.16 cm (4 in) in some areas for the LFC-400-R configuration. Comparison of the slot widths indicates that the planform is approximately the same as for the LFC-400-S configuration or about 0.051 mm (0.002 in) larger than those shown on figure 125, but generally display the same planform characteristics.

As in the case of the LFC-400-S configuration, the slot flow path lengths required an increase over those shown on figure 126 for the LFC-200-S configuration. Comparison of figure 170 with 160 indicates that the necessity for increasing the slot flow path length on LFC-400-R is not as severe as in the case of LFC-400-S but the necessity for this increase does extend from the wing root outboard beyond WS 480. The planform pattern of this increased flow path length is similar to that shown on figure 124 but extends farther outboard. The methods of accomplishing this increase in flow path length are subject to the same considerations discussed in section 8.4.3.1 for the LFC-400-S configuration although the potential problems are significantly relieved.

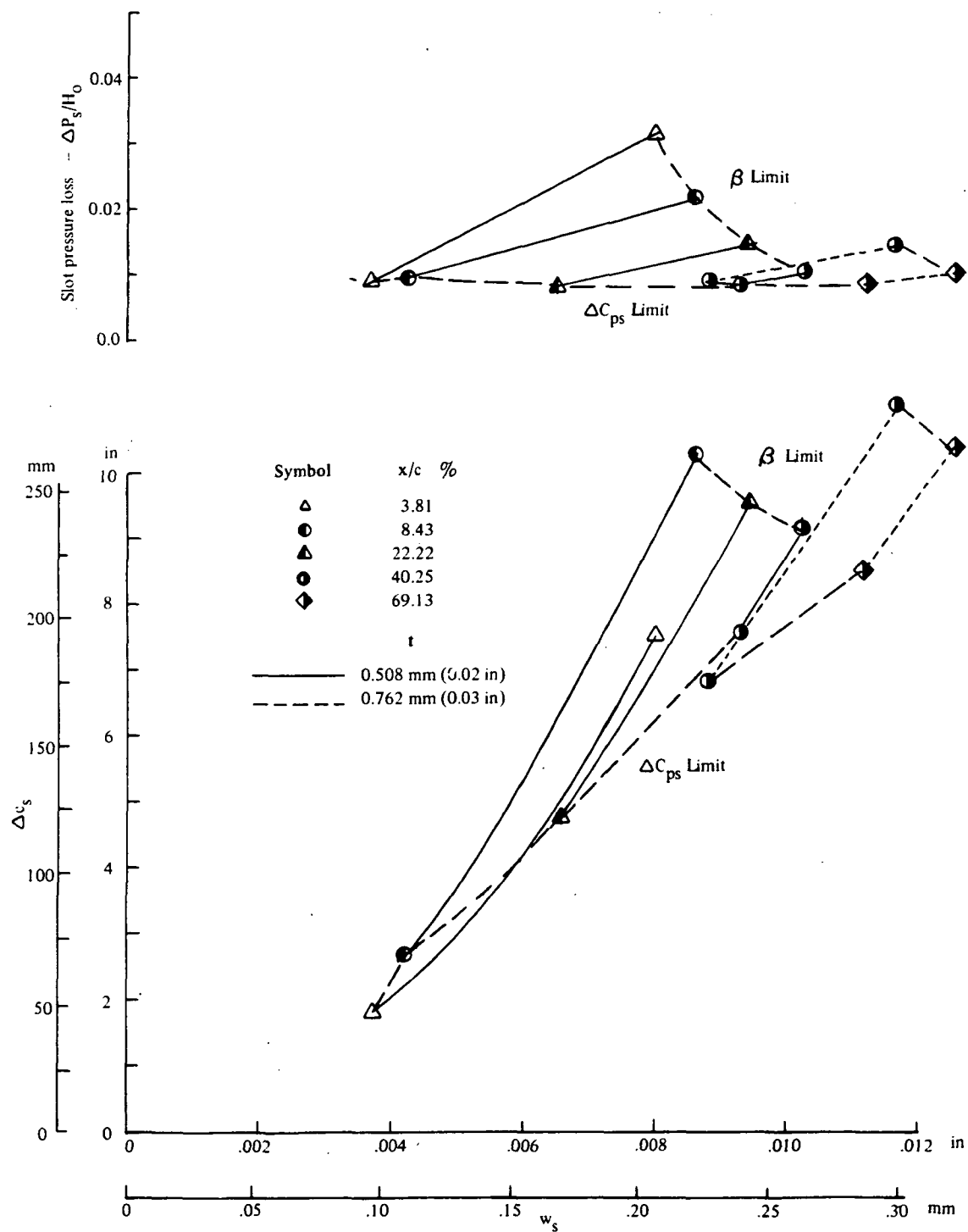


Figure 170. — Slot spacing and pressure loss vs. slot width,
upper WS 480, LFC-400-R

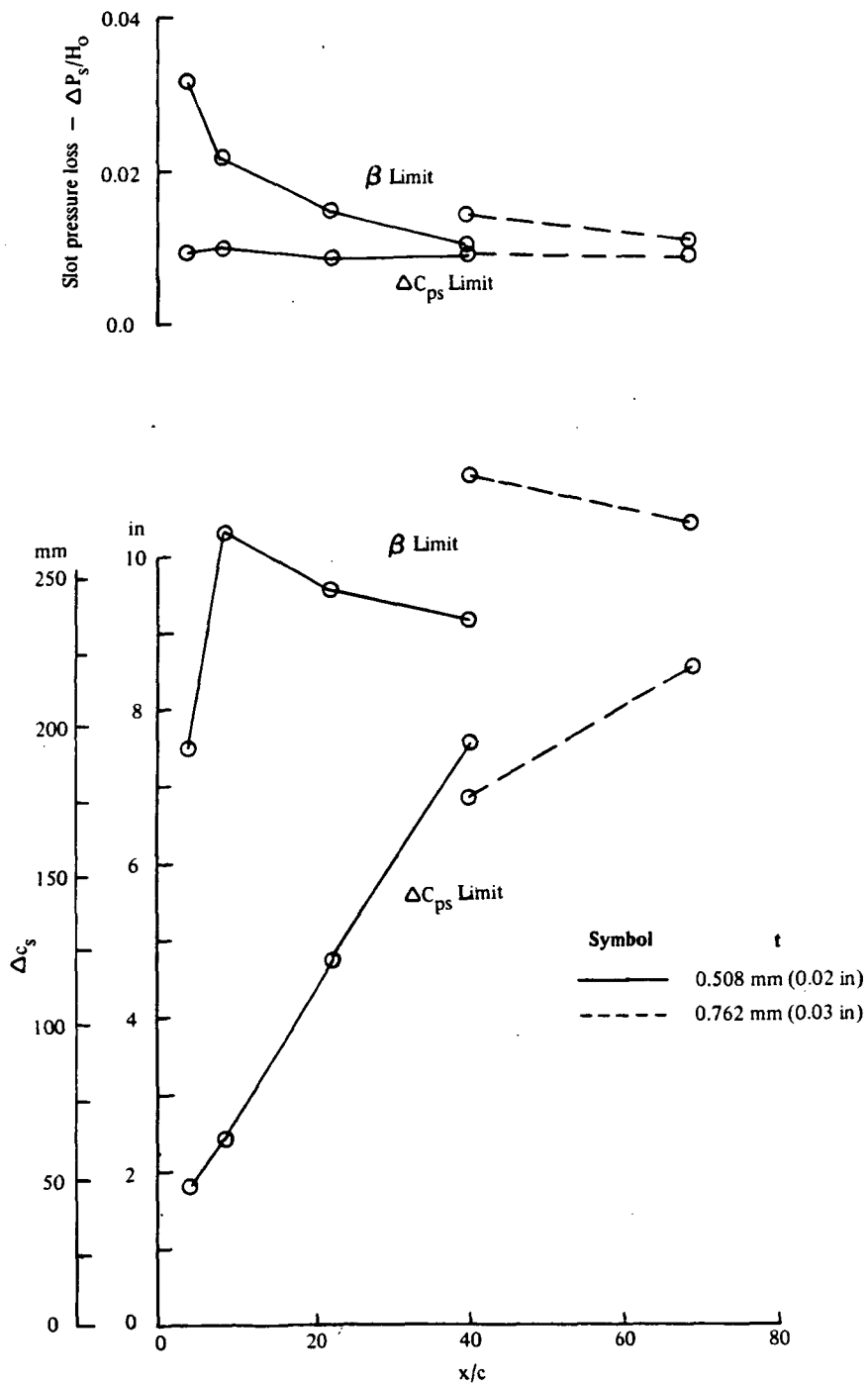


Figure 171. — Slot spacing and pressure loss vs. chord location, upper WS 480, LFC-400-R

The LFC-400-R conceptual design is acceptable from the above analysis and does not introduce any new problems. The the design is less critical than that for LFC-400-S. As a consequence of greater wing volume and a reduced requirement for suction flow, this configuration is the least critical design of either the LFC-200 or LFC-400 configurations.

Surface Design – LFC surface panels for LFC-400-R are identical in construction and thickness to those described in section 8.2.3.1. Since leading edge suction is not required for this airplane, surface panels are provided from 3% to 75% chord on upper and lower surfaces. Figure 152 shows a typical wing section with no leading edge suction.

8.5.3.2 Ducting and Distribution

The LFC suction requirements described earlier in section 8.5.3 were used in evaluating the ducting system for the LFC-400-R configuration within the constraints established in section 6.3.1. Methods described in section 8.2.3.2 were employed in this analysis.

The system schematic of figure 131 is applicable to the LFC-400-R configuration. The LFC-400-R suction flows based on unit wing area are the same as those for the LFC-200-R and are substantially below those of LFC-400-S of section 8.4.3. The wing plan view of LFC-400-S was assumed to be the same as that of LFC-400-S for comparative purposes. The larger wing chords of LFC-400-R compared to LFC-200-R result in significantly higher flows at the collector exit of LFC-400-R while the reduced unit flow levels compared to LFC-400-S result in lower flows than those of LFC-400-S. Thus, it was predictable that the characteristics of the collector duct requirements should fall between those of LFC-400-S and LFC-200-R. Similarly, the revised slot widths and spacings described in the previous section fell generally between these two configurations.

As discussed previously, the slot duct height of 2.54 mm (0.1 in) was selected for convenience of manufacture and quality control rather than aerodynamic necessity. The reduced flows of the LFC-400-R were entirely compatible with this configuration and the maximum slot duct Mach numbers were reduced from those of the LFC-400-S configuration.

The collector duct accumulated exit pressure losses and Mach numbers are presented in figure 172 as a function of collector duct height for the longest collector duct at the wing root. These characteristics predictably fall between those for the LFC-200-R shown on figure 153, and those for the LFC-400-S configuration in figure 163. Since figure 172 represents the longest collector, a Mach number slightly over the target of 0.2 was selected as acceptable since it occurs over a very small part of the span. This permits selection of a collector height of 1.016 cm (0.4 in) which results in a pressure loss of slightly over 6 percent of the wing root.

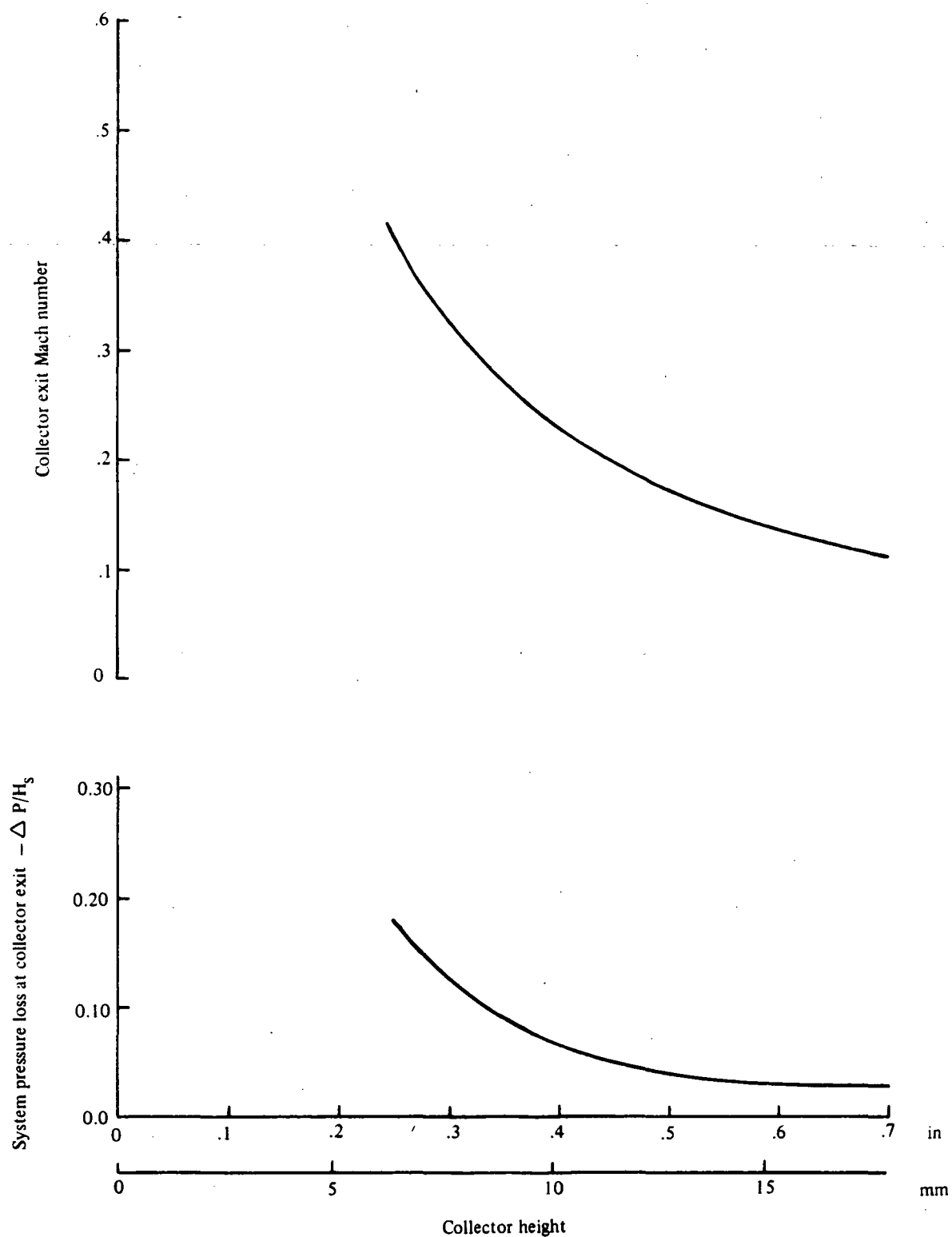


Figure 172. — Wing root collector duct characteristics, upper wing, LFC-400-R

The local accumulated pressure loss and Mach number for the wing root collector are shown on figure 173. This figure shows slightly higher Mach numbers and duct losses than for the LFC-400-S. This is a result of the selection of collector duct height. It was anticipated that the trunk duct for the LFC-400-R would be more than ample while the LFC-400-S trunk duct was found to have a relatively high Mach number. Consequently the collectors for the LFC-400-S were larger to reduce the collector duct pressure losses and relieve the trunk ducting requirements.

The accumulated pressure losses at the ends of the collector ducts are shown as the solid line on figure 174. As in the previous cases, there is a sharp rise in these pressure losses at the wing root. Over-plotted on this figure are the local accumulated pressure losses for the trunk duct. The dashed line illustrates the characteristics of the trunk duct losses for the maximum allowable trunk duct size within the general structural design constraints. This is the identical trunk duct size as that of LFC-400-S. The pressure losses associated with this trunk duct for the LFC-400-R are substantially less than for the LFC-400-S because of the reduced suction flow. This reduced loss presents a problem in that the trunk duct pressure losses from the wing station 9.144 m (30 ft) inboard fall below those of the collector exits. The consequence of this adverse pressure differential is a diminution of the suction flows to a level such that the collector losses decrease and the collector exit pressures rise to a level above that of the trunk. As a possible solution to this problem, the trunk duct is decreased in area by 38 percent throughout its length. The pressure loss characteristics of this duct are shown on the figure as the dotted line. This reduction in trunk duct size results in higher trunk duct losses and produces a favorable pressure differential between the collector duct exit and trunk duct for all wing stations.

The Mach numbers for the collector duct exits and the two trunk ducts described above are shown on figure 175. The highest Mach number for the maximum size trunk duct is only slightly over 0.15. The reduction of the trunk duct area results in a peak Mach number of nearly 0.26 over a short span.

Other alternatives exist to provide the compatibility between the collector duct exit and the trunk duct while avoiding the elevated trunk duct Mach numbers. A re-distribution of trunk duct area can reduce the peak Mach numbers while increasing the trunk duct pressure losses elsewhere in the duct. Another solution is to increase the collector heights, thereby reducing the accumulated pressure loss at the collector duct exit. This has the effect of increasing the cover weight while reducing the size of the suction units slightly. This type of optimization requires a lengthy evaluation to determine the overall impact on the airplane. In any case, the 38 percent reduction of trunk duct flow areas provides an acceptable solution and the alternatives become involved in an optimization which is well beyond the scope of the current effort.

The conceptual design for the LFC-400-R ducting system is acceptable within the criteria of section 6.3.1. Several alternatives exist for small potential improvements but involve careful optimization. The ducting permits a two suction unit system of the type illustrated in figure 148.

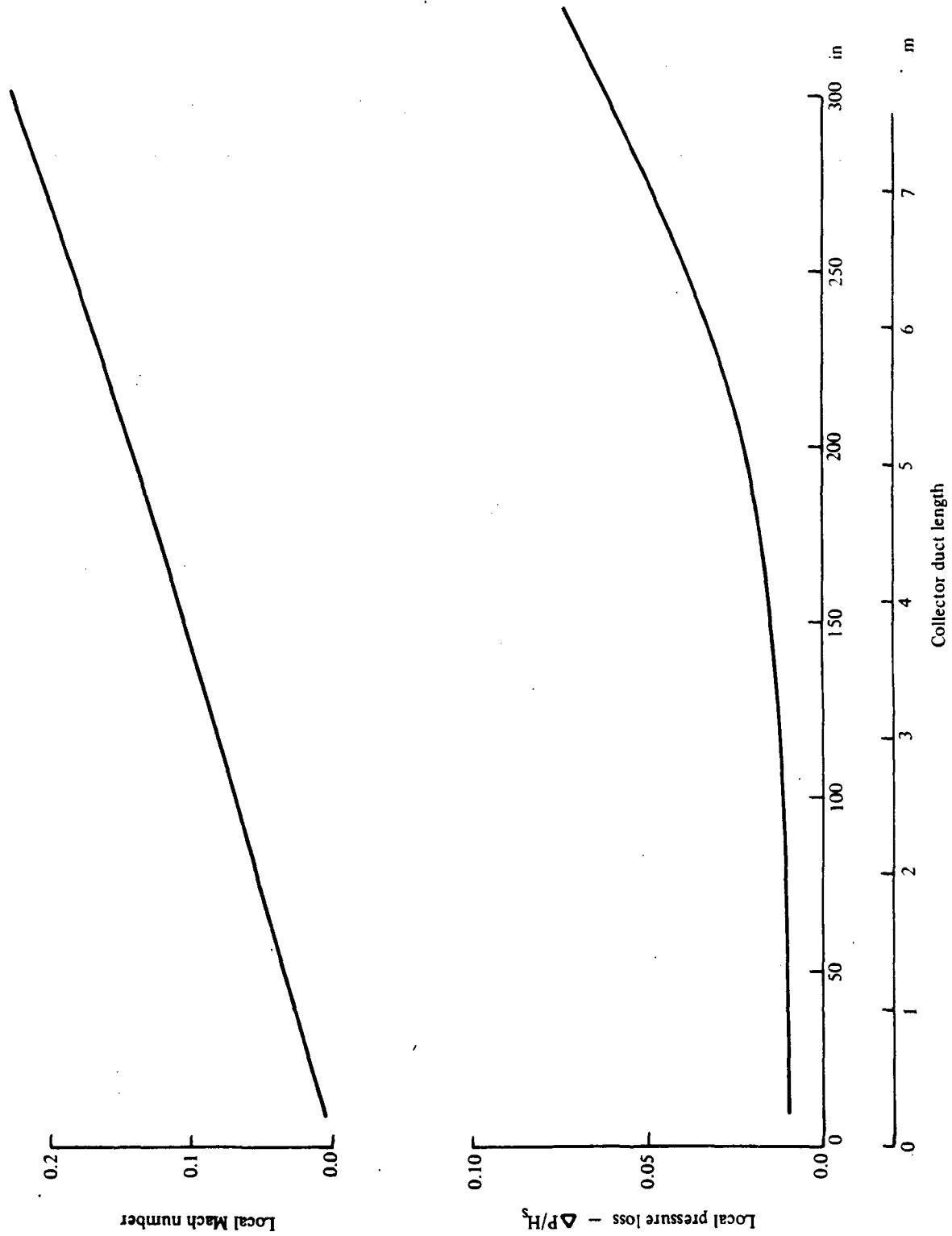


Figure 173. — Collector duct local characteristics, 1.016 cm (0.40 in) collector height, upper wing, LFC-400-R

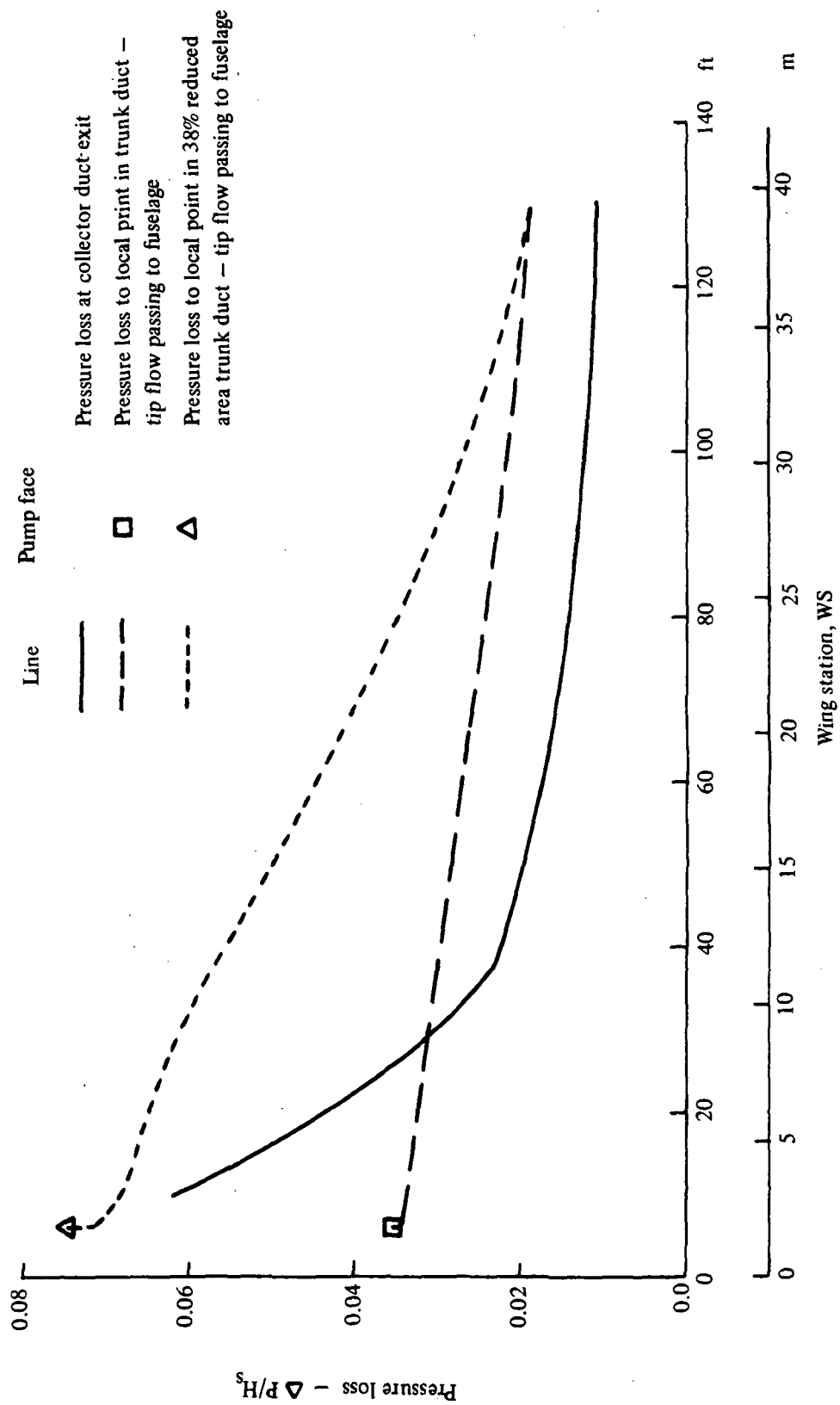


Figure 174. - Collector to trunk duct pressure matching, upper wing, LFC-400-R

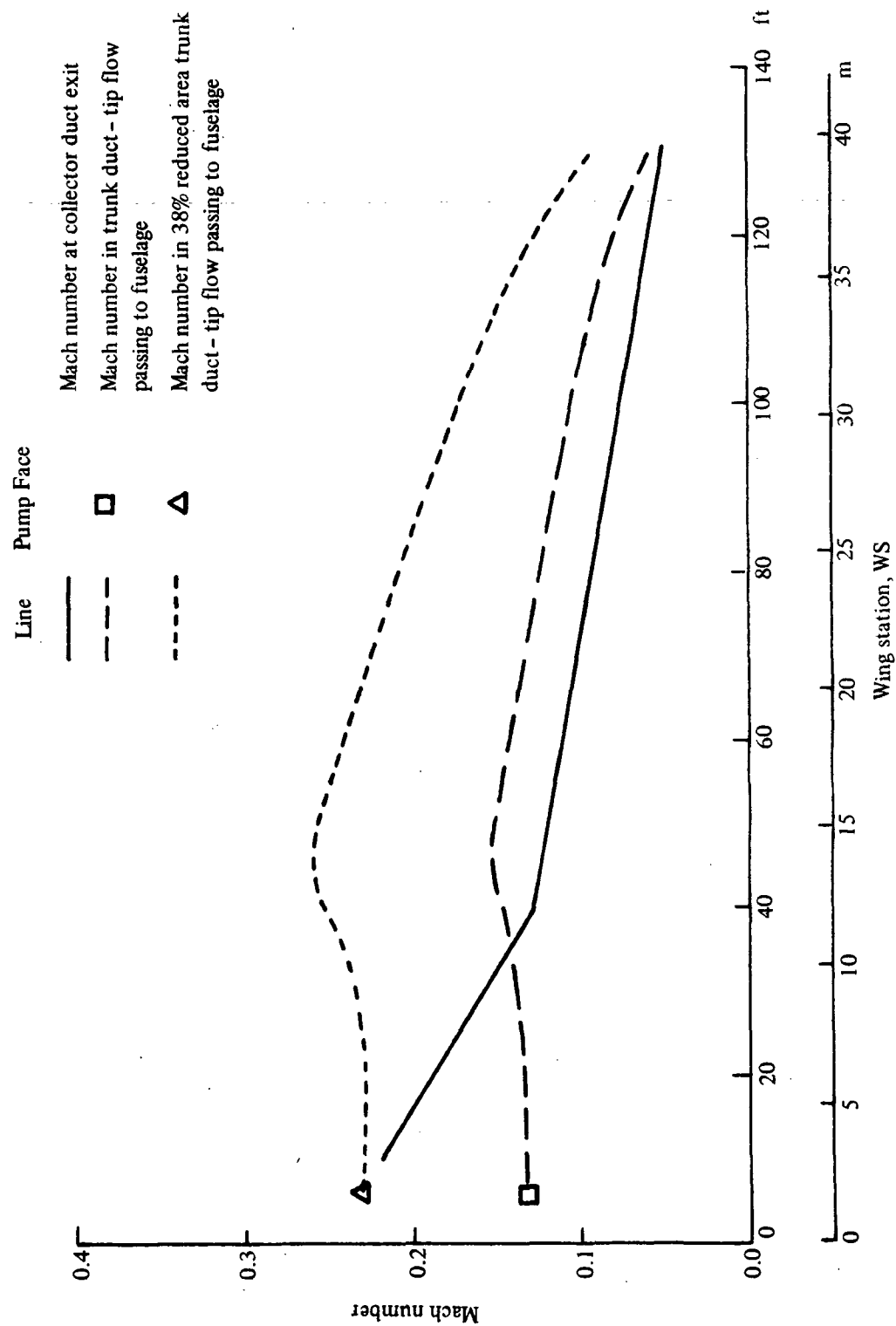


Figure 175. — Collector exit and trunk duct flow Mach number characteristics, upper wing LFC-400-R

8.5.3.3 Suction Units

The suction unit criteria and general requirements discussed in sections 6.4.1 and 6.4.2 are applicable to the LFC-400-R configuration. The specific suction requirements discussed in section 8.5.3 are reflected in figure 176. As in the case of LFC-400-S, the discussion of LFC-200-R suction units is also applicable to the LFC-400-R and the reader is therefore referred to section 8.3.3.3. A schematic of LFC-400-R suction unit is presented on figure 177. The discussion in section 8.3.3.3 is applicable.

8.5.3.4 Controls

The LFC-400-R bleed burn suction system is quite similar to the LFC-400-S and LFC-200-R systems except for unit size. The control concept for all three systems is identical and the reader is therefore referred to section 8.3.3.3 for a discussion of the control system of the LFC-200-R.

8.6 ACOUSTICS

It has been demonstrated in wind tunnel and flight tests of LFC airfoil sections that acoustic disturbances of various kinds can cause transition of an otherwise stable laminar boundary layer. A summary of the available data is presented in reference 15. The engineering analysis of the phenomena conducted for the LFC study aircraft includes the following:

- (1) Development of acoustically induced boundary layer transition criteria to determine allowable sound pressure levels at the wing surface as a function of chordwise Reynolds numbers and suction strength.
- (2) Prediction of acoustic environment over the LFC surfaces during cruise.
- (3) Identification of the LFC surface regions vulnerable to acoustically induced transition.
- (4) Minimization of acoustically induced transition:
 - o Impact on airplane configuration, including the location of power plants relative to LFC surfaces and nacelle treatment requirements.
 - o Local increase in suction requirements.

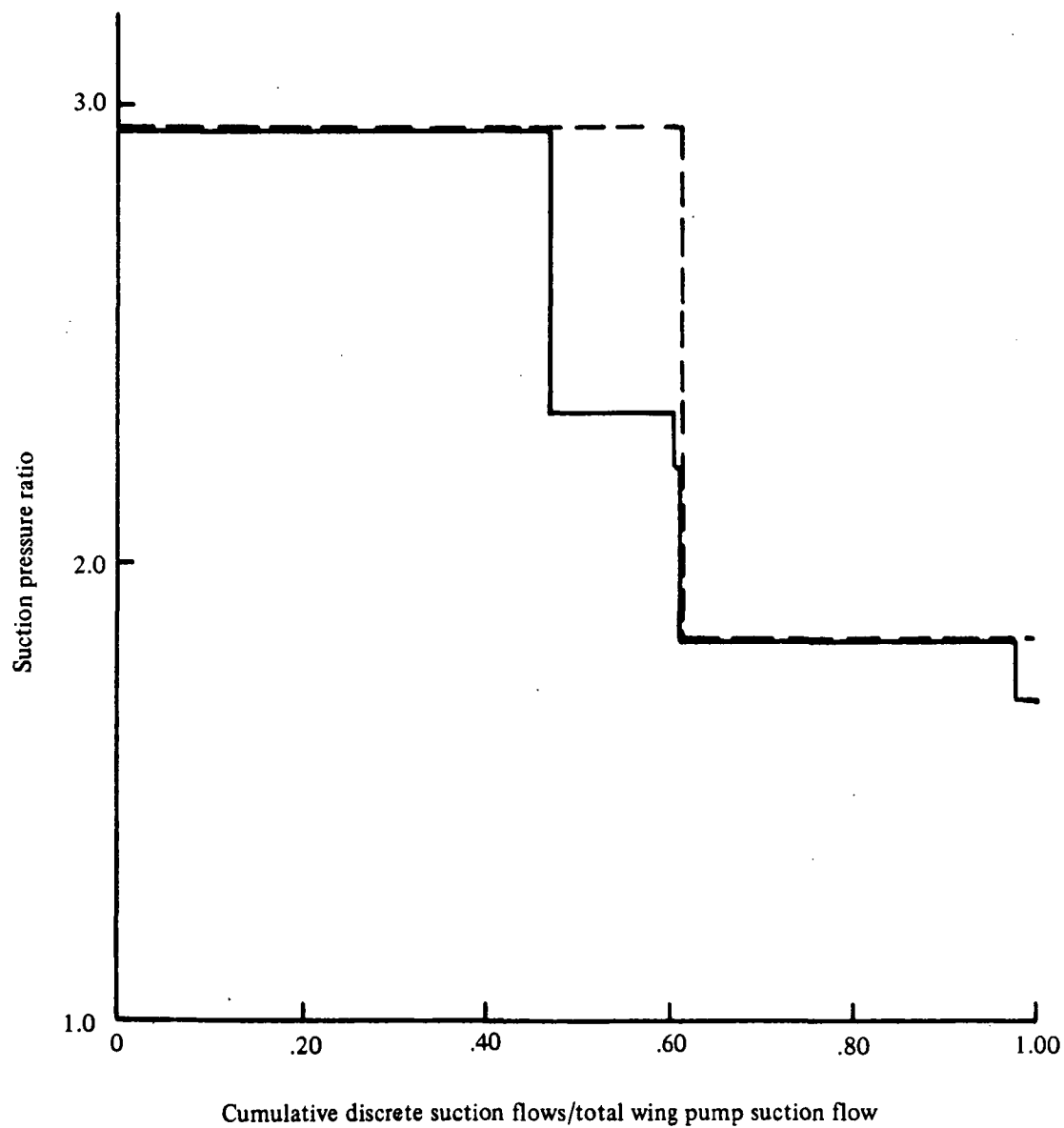
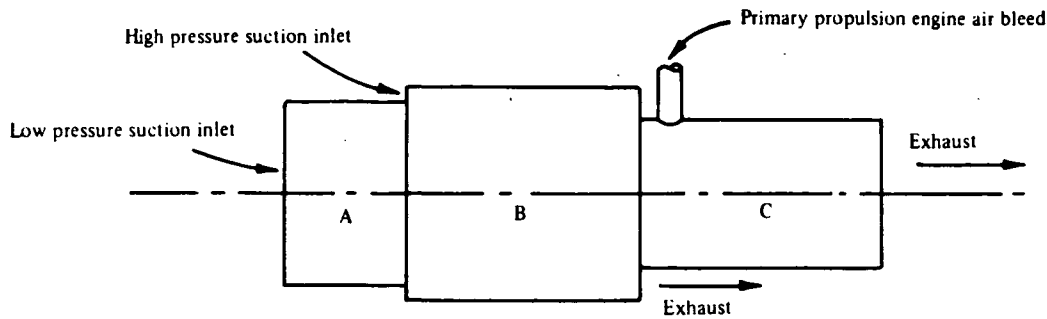


Figure 176. — Normalized airplane suction characteristics, LFC-400-R



	A. Boost compressor	B. Main compressor	C. Power unit
Diameter	38.1 cm (15.0 in)	44.5 cm (17.5 in)	31.0 cm (12.2 in)
Length	25.4 cm (10.0 in)	48.8 cm (19.2 in)	50.0 cm (19.7 in)
Weight	25.1 kg (55.4 lb)	57.9 kg (127.7 lb)	114.8 kg (253 lb)*
Sea level equivalent conditions			
Shaft power output	—	—	1282.9 Kw (1720.4 H P)
Net thrust	—	0	0
Fuel flow	—	—	89.0 g/sec (706.3 lb/hr)*
Cruise conditions: Altitude = 11582 m (38,000 ft), 0.8 Mach			
Net thrust	—	0	0
Fuel flow	—	—	15.7 g/sec (124.7 lb/hr)*

* Includes penalties to primary propulsion engine weight and fuel flow resulting from bleed plus bleed ducting weight and pressure losses

Figure 177. — Bleed-burn powered suction unit, LFC-400-R

8.6.1 ACOUSTIC DESIGN CRITERIA

Based on the collected experimental data presented in reference 15, the chordwise location, defined in terms of chordwise Reynolds number, at which acoustically induced transition occurs in the presence of basic suction is related to a velocity disturbance ratio, $\frac{\Delta U}{U_o}$, where ΔU is the disturbance velocity and U_o is the aircraft velocity. In this case ΔU is the acoustic particle peak velocity. The velocity disturbance ratio is related to the acoustic sound pressure level by the following:

$$\frac{\Delta U}{U_o} = \frac{10^{\left[\frac{\text{SPL (dB)}}{20} - 3.7 \right]}}{\gamma P M} \quad (1)$$

At the aircraft design cruise conditions of 11,582 m (38,000 ft) altitude and 0.8 Mach number this relationship becomes

$$\frac{\Delta U}{U_0} = 1.218 \times 10 \left[\frac{\text{SPL (dB)}}{20} - 10 \right] \quad (2)$$

where SPL (dB) is the overall sound pressure level in decibels referenced to 0.0002 dynes/cm².

Equation (2) is used with figure 5 of section 11 of reference 15 to derive an SPL versus transition Reynolds number relationship for the case of basic suction. Using a flat plate zero-pressure-gradient Reynolds number ($R = \frac{U}{\nu} s$) relationship, the transition distance from the leading edge is estimated. The final relationship between SPL and distance to transition from the leading edge, in the presence of basic suction is:

$$s = 10^{-0.04785 \text{ SPL (dB)} + 5.5850} \quad (3)$$

where s is in feet. This relationship is shown in figure 178, and it is the criteria which determines the location where acoustically induced separation is likely to occur. It is seen that the more intense the acoustic field the earlier acoustically induced separation occurs. Increasing suction strength has been shown to further delay acoustically induced separation.

It is known that the premature transition phenomena is frequency sensitive. Reference 27 indicates that the critical frequency range is approximately 500 to 5,000 Hz for both internal and external noise fields. The current analysis, however, is conducted in terms of overall sound pressure level. Extension to a frequency sensitive analysis is certainly required and is recommended as a further study.

8.6.2 AIRCRAFT CONFIGURATION CONSIDERATIONS

The LFC aircraft for which these analyses were conducted are described in section 8.2 – 8.5.

The engines are of the Pratt and Whitney STF 429 cycle, with a two-stage fan which has a takeoff pressure ratio of 1.88 and a bypass ratio of 6.0. The engine is adapted to all of the study aircraft. The engines and nacelles are acoustically designed such that the aircraft can comply with a nominal FAR 36-10 EPNdB. This was achieved through engine cycle selection to control jet noise levels and nacelle acoustic design to control fan noise. The extensive acoustic liner treatment includes wall and two flow splitters in the inlet, wall and two splitters in the fan discharge duct and wall treatment in the turbine. The nacelle is shown in figure 179.

8.6.3 LFC SURFACE ACOUSTIC ENVIRONMENT

The external acoustic environment over the LFC surfaces is created by noise radiated from:

- (1) The propulsion units which generate fan noise, compressor noise, turbine noise, jet

$M = 0.80$
 $H, m (ft) = 11,582 (38,000)$

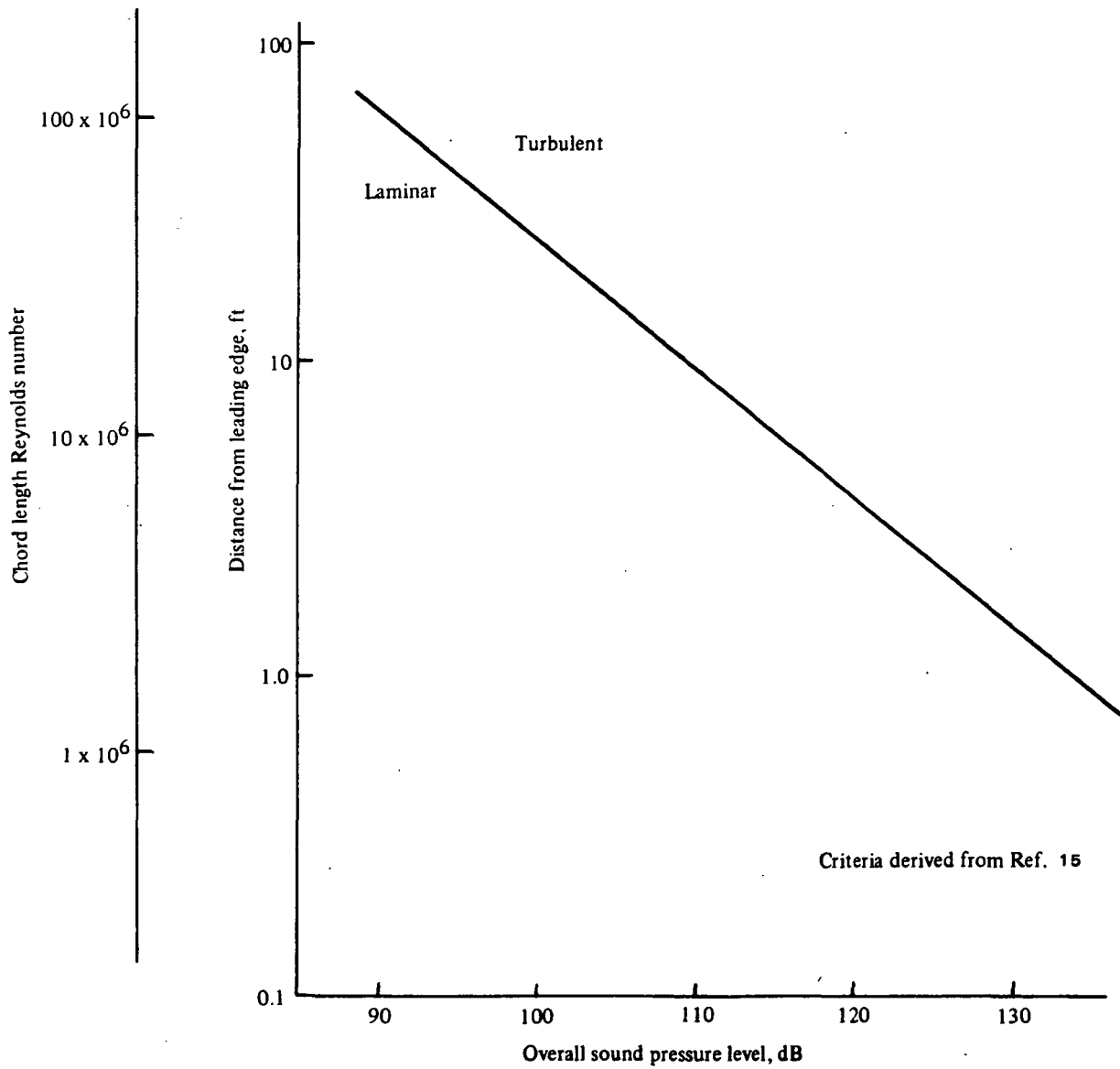


Figure 178. — Acoustically induced transition criteria

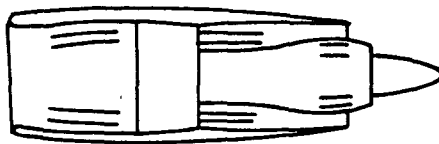


Figure 179. — Nacelle acoustic design for FAR 36 - 10 EPNdB

exhaust turbulent mixing noise, jet exhaust screech, and shock associated noise.

- (2) The suction units which generate compressor noise, turbine noise, jet exhaust noise, and jet exhaust shock cell noise.
- (3) Turbulent boundary layers in the vicinity of LFC surfaces.
- (4) Other unsteady aero-acoustic phenomena such as incident free stream turbulence, oscillating shock waves on and in the vicinity of the LFC surfaces, and locally separated flow areas.

The internal acoustic environment is created by:

- (1) Compressor noise from the suction unit propagating up the ducts to the LFC surface.
- (2) Noise generated by the "dirty flow" in the ducts.
- (3) Any resonance involving the duct volume and the suction slot (Helmholtz resonance) causing "chugging" at the slot.

Vibration of the surface, induced by structural response to aero-acoustic loading or from engine vibration transmission, creating disturbance ratios of the magnitude used in deriving figure 178 may also cause premature transition.

The above noise source acoustical characteristics are summarized in tables 27 and 28. The noise sources expected to dominate the environment, and which are therefore analyzed in detail, are the propulsion unit and the turbulent boundary layer noise. The shock cell screech and shock associated noise arising from the supercritical jet are described in references 28 and 29. Reference 28 shows how these noise sources, evident during cruise, were responsible for sonic fatigue failures on an aircraft empennage. This noise source is not further analyzed here, but it is highlighted as being a potential problem, requiring further investigation and analysis.

TABLE 27. EXTERNAL NOISE SOURCE CHARACTERISTICS

Source	Characteristics	Importance in creating transition
<u>Propulsion Units</u>		
Jet	Broad band, to 2,000 Hz	1
	Shock cell, discrete	1
	Shock associated noise	1
Fan	Discrete (MPT and tone), 500 to 5,000 Hz Inlet and discharge, with suppression	1
Turbine	Discrete and broad band, above 5,000 Hz Discharge, suppressed	2
<u>Suction Units</u>		
	Gas generator, compressor and turbine whines above 5,000 Hz	2
	Pump	
	Compressor whine above 5,000 Hz	2
	Possible shock noise in jet exhaust	2
<u>Boundary Layer</u>		
	Turbulent boundary layer over fuselage and adjacent to LFC areas. High OASPL's at surface (128 dB), but poor radiation.	1
	Upstream laminar boundary layer	3
<u>Other</u>		
Free stream incident turbulence	Broad band	3
Oscillating shocks on and in the vicinity of LFC surfaces	Discrete frequency	3
Local separated flow areas	Broad band	3

TABLE 28. INTERNAL NOISE SOURCE CHARACTERISTICS

Source	Characteristics	Importance in creating transition
Suction engine	Pump, compressor whine, transmitted through duct, about 5,000 Hz	2
Duct self noise	Flow noise in duct created by dirty flow, tortuous path, etc., broad band	2
Duct slot resonances	Could cause chugging at suction slot, discrete frequency	2

8.6.3.1 Propulsion Unit Noise

The aircraft propulsion units are designed to comply with the noise requirements of FAR 36 reduced by 10 EPNdB. The basic acoustic data used to predict the inflight noise levels were taken from reference 30, which reported static noise measurements from the recent quiet engine program. This report presents noise level data measured on a 45.7 m (150 ft) radius in overall and one-third octave bands for a heavily suppressed full-scale engine having a two-splitter inlet configuration whose thrust size and fan pressure ratio is very similar to that of the propulsion engines for the LFC-200-S and LFC-200-R configurations. The engines for the 400-passenger aircraft are about 3.2 dB noisier. These single engine sea-level-static acoustic data were used to predict the inflight propulsion noise environment at cruise for the study aircraft. The following procedure was used to accomplish this transformation:

- (1) Separating the static spectra into jet noise and fan noise components.
- (2) Applying relative velocity reduction to the jet noise.
- (3) Correcting the jet-noise levels for the effect of altitude and ambient conditions on jet acoustic power output.
- (4) Correcting the jet- and fan-noise levels for change in characteristic impedance effects.
- (5) Correcting the fan-noise levels for reduced mass flow at the right pressure ratio.
- (6) Correcting for static to inflight effect on directionality.
- (7) Correcting for the number of engines.
- (8) Surface pressure doubling.

This procedure produced the overall sound pressure noise level contours shown in figure 180 for the

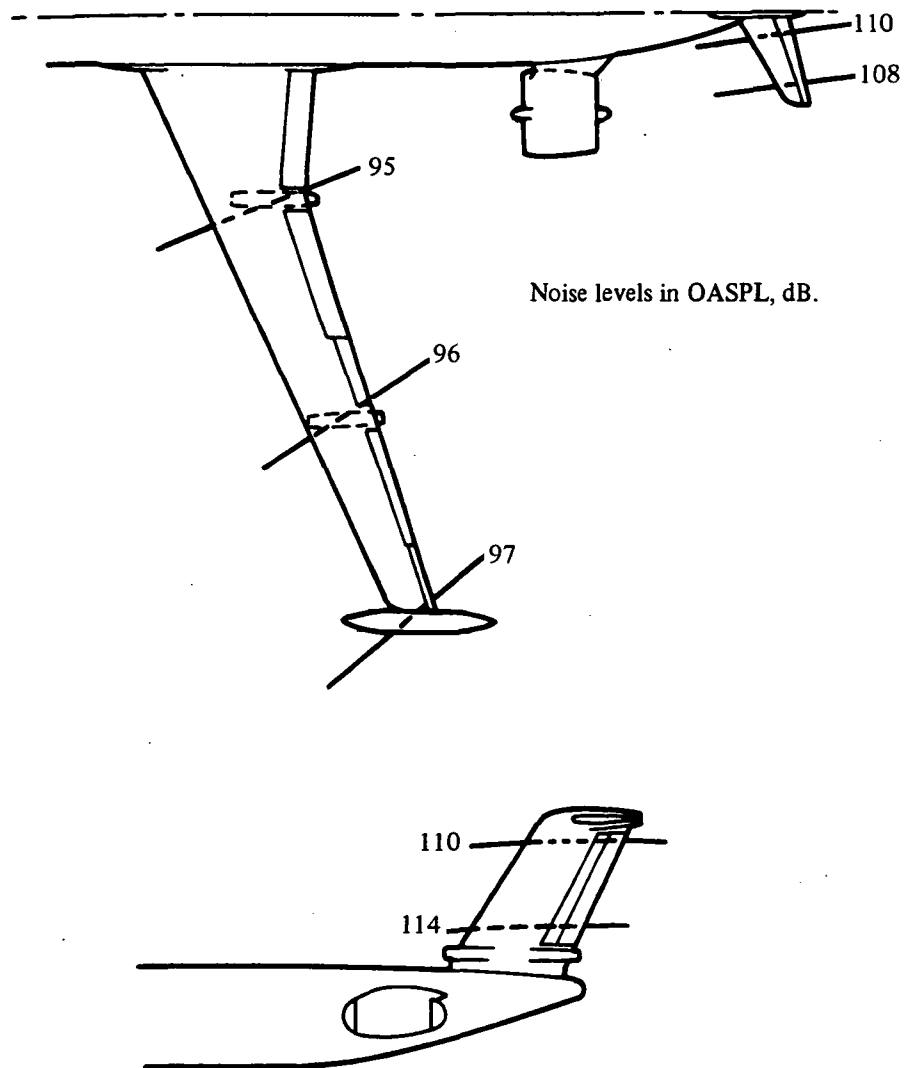


Figure 180. — Noise level contours, LFC-200-S and LFC-200-R

smaller aircraft and in figure 181 for the larger aircraft. At cruise, a shock wave on the upper surface aft of the LFC area prevents the propagation of the engine noise over that surface. The noise levels originating from the powerplant are considered to be the dominant noise source over the LFC surfaces.

8.6.3.2 Turbulent Boundary Layer Noise

During cruise, a microphone flush-mounted with the surface at locations where a normal turbulent boundary is developing indicates a fluctuating pressure level of 128 dB. Should local flow separation occur, this surface pressure could be higher. However, these high-level pressure

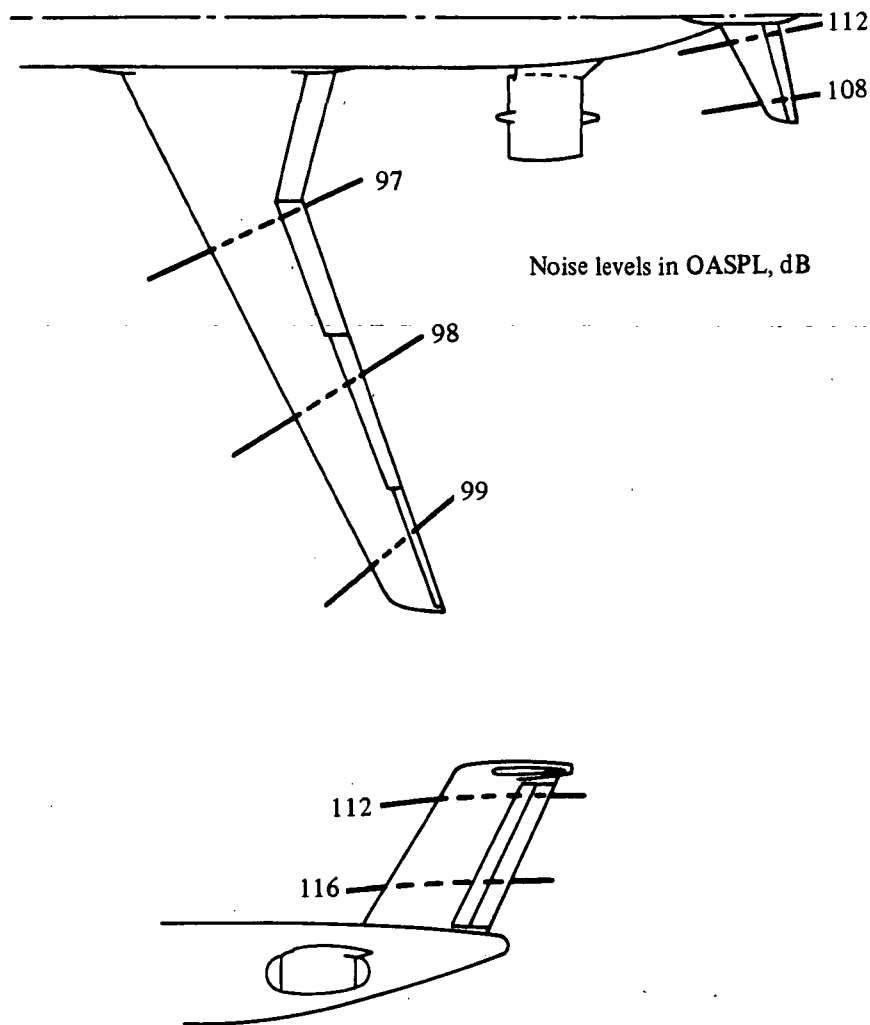


Figure 181. — Noise level contours, LFC-400-S and LFC-400-R

fluctuations within the turbulent boundary layer are very poor acoustic radiators. The noise level environment over the LFC surfaces generated by the turbulent flow over the fuselage and other areas is not considered to be as high as that originating from the propulsion system, except perhaps at the interface between the turbulent and LFC areas, i.e., wing root, vertical root, tip tank, and at suction unit mountings. Extra suction may be required at these interface locations. These aspects require further investigation.

8.6.3.3 Summary of Acoustic Environment

The predominant acoustic environment over the LFC surfaces during cruise is considered to be that generated by the power plants. The resulting overall sound pressure levels shown in figures 180 and 181 are summarized in table 29.

TABLE 29. MAXIMUM SOUND PRESSURE LEVELS ON LFC SURFACES

		Predicted maximum overall sound pressure levels, dB, over LFC surfaces		
<u>Configuration</u>	<u>Location of suction units</u>	<u>Lower wing surface</u>	<u>Vertical surface</u>	<u>Lower horizontal surface</u>
LFC-200-S	External, wing and vertical tail	97	114	110
LFC-200-R	Internal, fuselage	97	114	110
LFC-400-S	Internal, fuselage	99	116	112
LFC-400-R	Internal, fuselage	99	116	112

8.6.4 REGIONS SUBJECT TO ACOUSTICALLY INDUCED TRANSITION

The possibility of acoustically induced separation occurring is greatest in the vicinity of the trailing edge of the LFC surfaces. In figure 132, the predicted OASPLS and maximum LFC chordwise distance from the leading edge are shown for the wing lower surface, vertical surfaces, and horizontal upper and lower surfaces together with the transition criteria for the 200- and 400-passenger aircraft. Depending upon the LFC surface, laminar flow must be maintained in the presence of noise up to a Reynolds number of some 44×10^6 . However, it can be seen that the critical locations for both aircraft are on the vertical control surface closer to the engines where the higher sound pressure levels and higher Reynolds numbers exist. Here the overall sound pressure levels exceed the allowable level by up to 4 dB for the 200-passenger aircraft and 6 dB for the 400-passenger aircraft. These critical areas are shown hatched in figures 183 and 184. It is estimated that 20% to 65% of the exposed area on both sides of the vertical tail is subject to acoustically induced transition depending upon configuration. LFC-200-R has a critical area of 20%, compared to 35% for LFC-200-S, primarily because of the smaller dimensions of the empennage. The larger aircraft, LFC-400-S and LFC-400-R have 65% of the vertical LFC area vulnerable to acoustically induced transition, due to the higher Reynolds numbers and the higher noise level.

8.6.5 MINIMIZATION OF ACOUSTICALLY INDUCED TRANSITION

Control of acoustically induced laminar flow transition is obtained in the following ways:

- (1) Control of noise levels radiated by the sources.

M = 0.80
H, m (ft) = 11,582 (38,000)

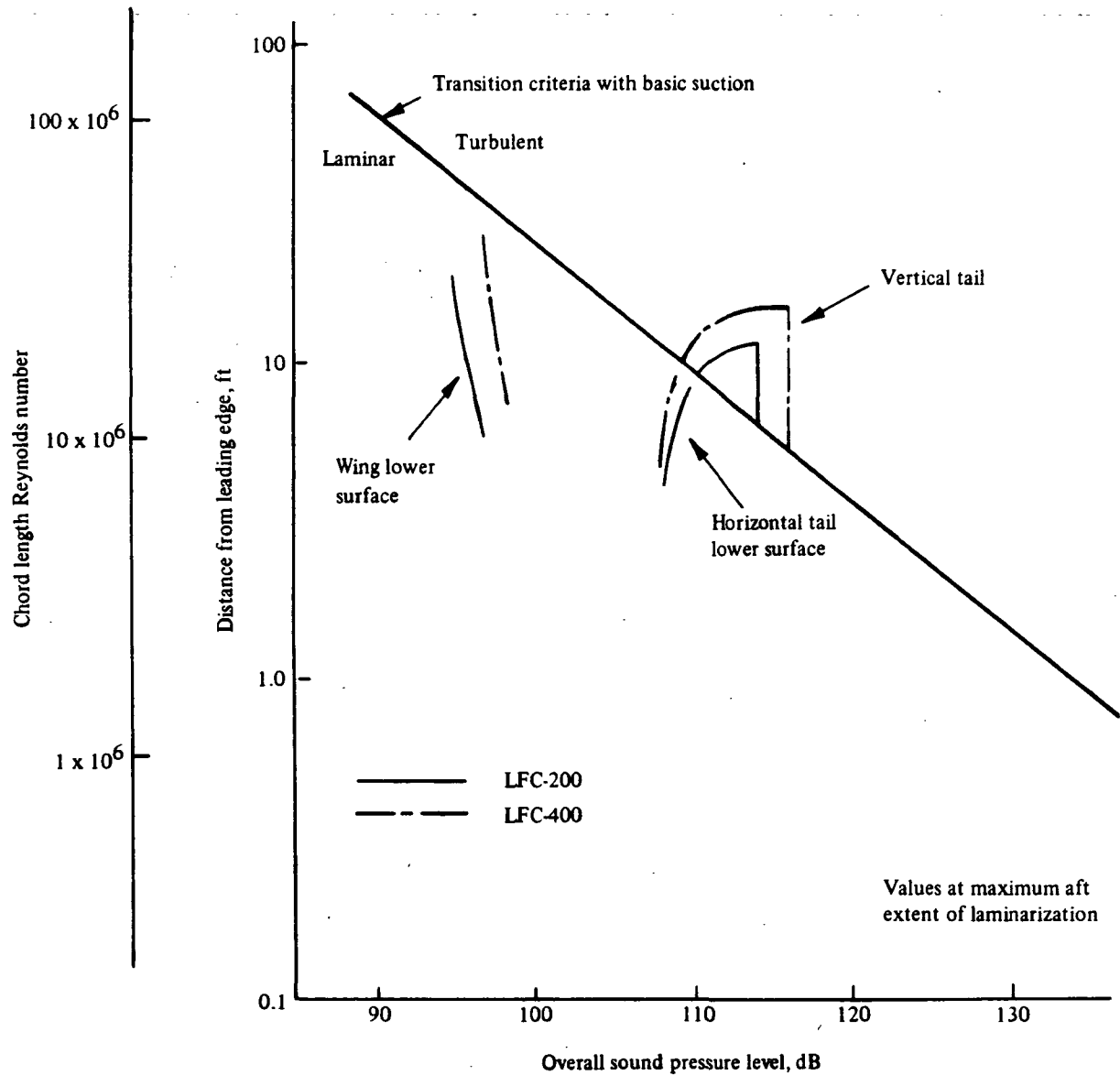


Figure 182. — Acoustically induced transition sensitivity

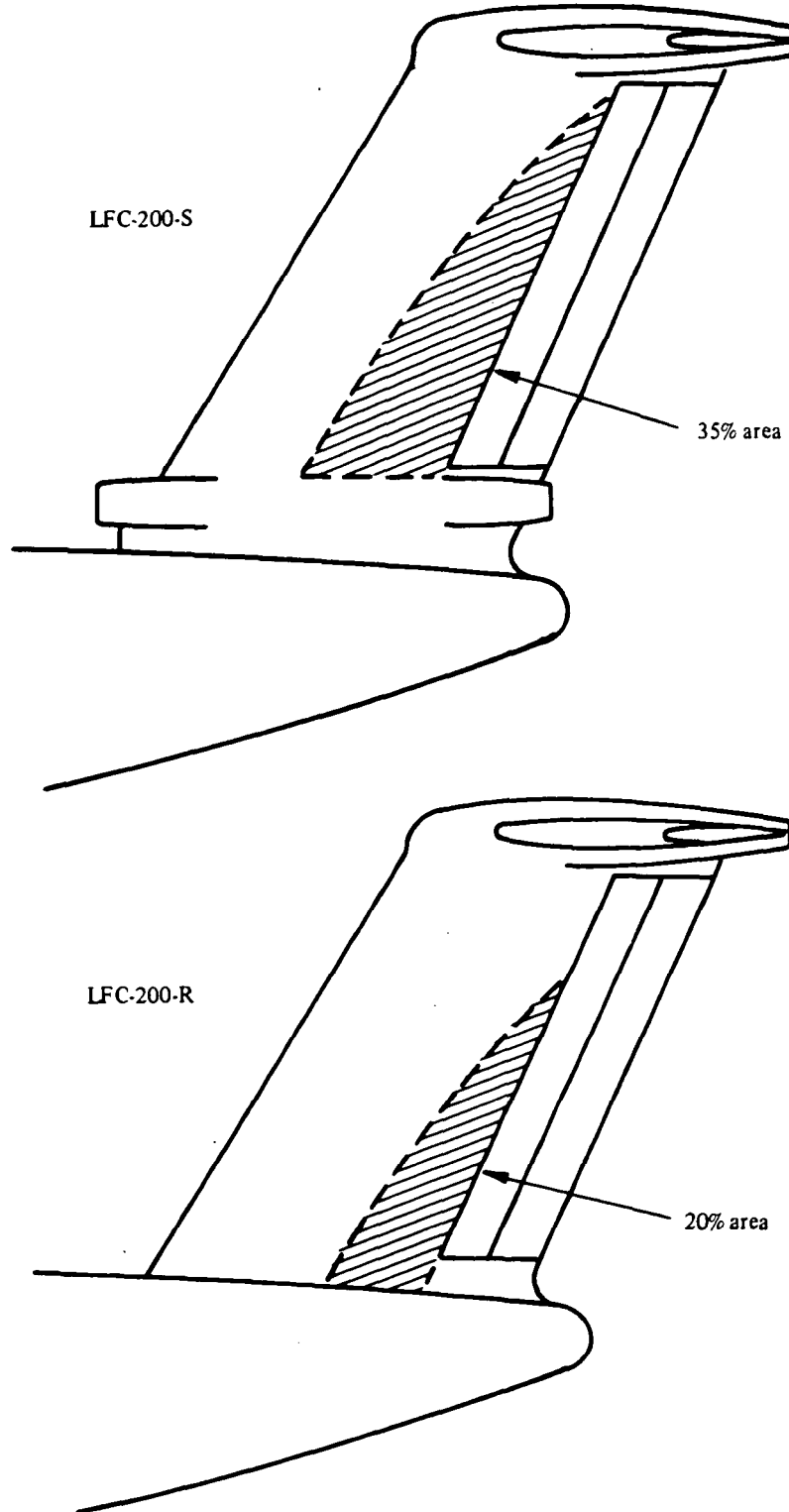


Figure 183. — LFC surfaces subject to acoustically induced transition, LFC-200-S and LFC-200-R

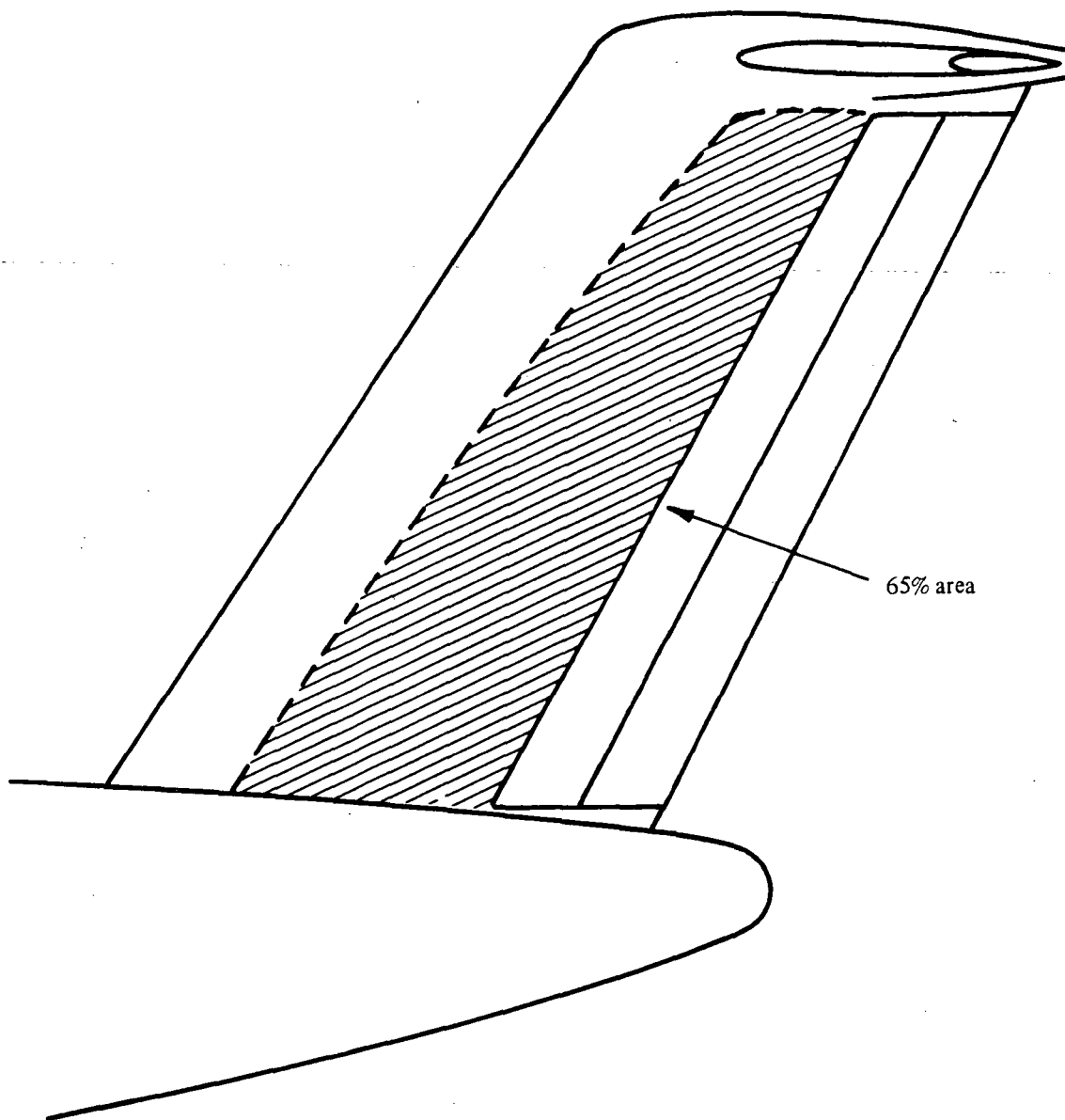


Figure 184. — LFC surfaces subject to acoustically induced transition, LFC-400-S and LFC-400-R

- (2) Placement of LFC surfaces in low-noise environments.
- (3) Placement of engine and suction units to minimize noise over the LFC surfaces.
- (4) Increase of suction as required.

The acoustic environment over the LFC surfaces in the study aircraft is minimized in the following ways:

- (1) Propulsion units are located on the fuselage in a rear position.
- (2) The aircraft are designed to comply with future stringent community noise requirements of FAR 36 minus 10 EPNdB. Thus, the engine incorporates an engine cycle for low jet noise and extensive nacelle acoustic absorption treatment for fan and turbine noise control. The acoustic nacelle reduces fan noise, in the critical transition frequency (500 to 6,000 Hz), by some 10 to 20 dB.
- (3) In most of the study aircraft, suction units are installed in fuselage fairings, thus providing cleaner wings and reducing local acoustic environment from suction unit inlet and discharge.

If the engines were not of FAR 36-10 design and were located on the wing, the acoustic environment would be much more severe, especially over the empennage.

Further maintenance of laminar flow is obtained by increasing the suction strength. The sensitivity of separation to suction in the presence of high noise is indicated in figure 185, taken from reference 15, which indicates that a modified suction distribution is more effective than the basic chordwise distribution in raising the sensitivity to acoustically induced transition. This is achieved by local chordwise increases to the suction distribution rather than an overall increase in suction. Reference 15 indicates that, for the configuration tested, this increase in suction should occur at the forward slots of the surface only. A 5 dB increase in sensitivity would require an increase in total suction quantity of about 10%, concentrated at the leading edge. For the study aircraft, maintenance of the laminar flow characteristics requires an increase of suction of the order of 10% to 20% on the vertical control surface. However, this transition sensitivity dependence upon suction quantity and chordwise suction distribution should be clearly defined for each configuration surface.

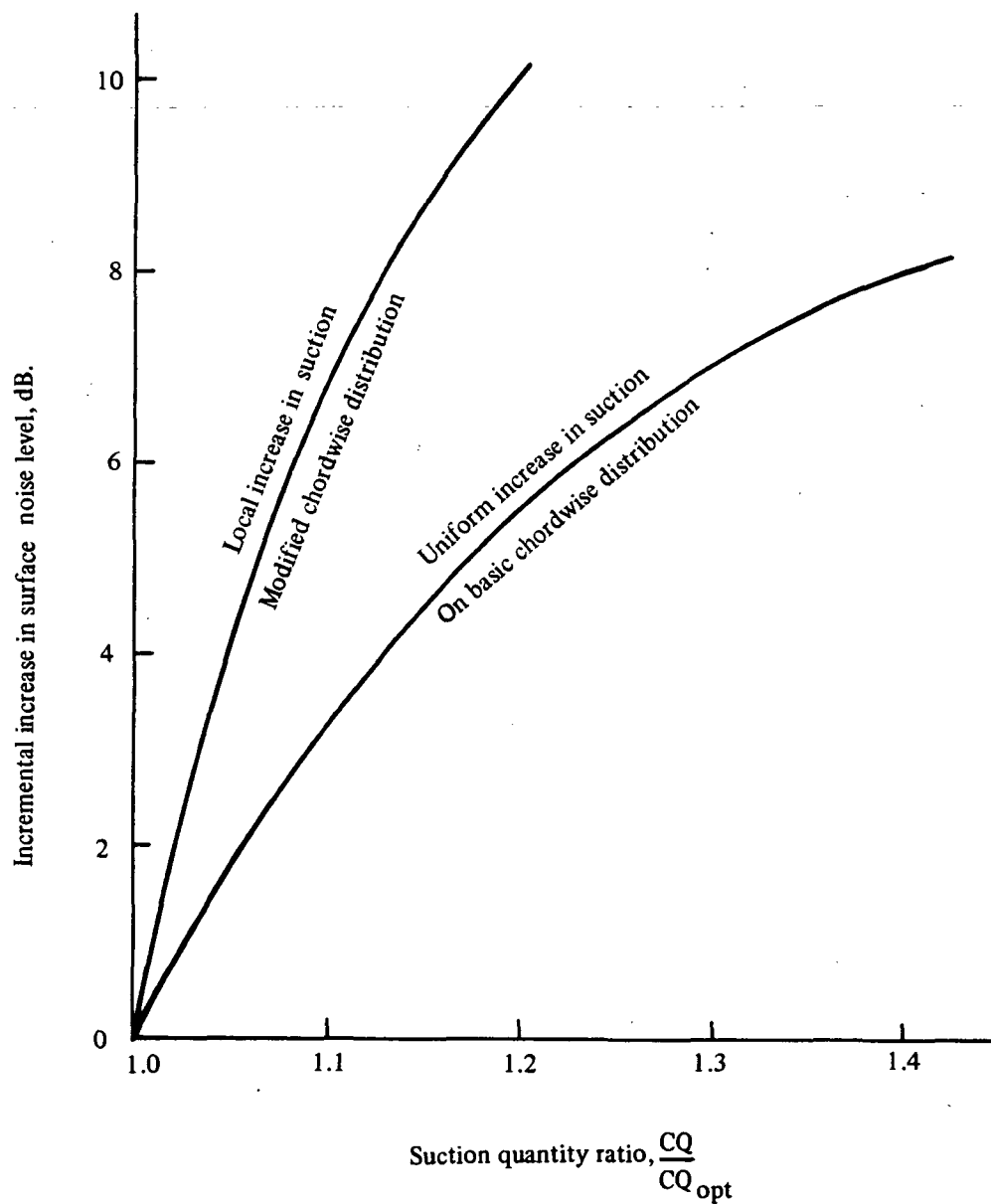


Figure 185. — Control of acoustically induced transition by increased suction

9.0 LFC MANUFACTURING, MAINTENANCE, AND OPERATION

9.1 INTRODUCTION

The LFC system elements which characterize the final configurations of the preceding section generate development, production, and operational requirements which are significantly different from those of conventional turbulent-flow transports. Consequently, this section is devoted to an analysis of the most important peculiarities of the four selected LFC study aircraft configurations. Procedures are outlined for manufacturing LFC system elements and the estimation of associated manufacturing costs. Considerations relevant to the routine maintenance of LFC aircraft are discussed, including an analysis of maintenance requirements for the study aircraft. In addition, an analysis of in-flight operational considerations is presented, including calculations of permissible surface roughness, sources of surface contamination, and the impact of in-flight LFC system loss on aircraft performance.

9.2 LFC MANUFACTURING CONCEPTS

In the definition of the final LFC aircraft configurations of the preceding section, it was assumed that both primary engines and LFC suction units were procured from a suitable engine manufacturer. All other LFC system elements, including the LFC surface panels, leading edge sections, and ducting, are fabricated by the airframe manufacturer. The procedures developed for the fabrication of these elements and the corresponding manufacturing costs are outlined in this section.

9.2.1 MANUFACTURING PROCEDURES

With the exception of differences in the dimensions of slots, slot spacing, chordwise collector ducts, and the trunk ducts, the LFC surface panels and ducting are the same for the four final LFC aircraft. While these differences cause variations in fabrication costs, the procedures employed are identical for all of the aircraft. The LFC surface and ducting configurations for which manufacturing procedures were developed are illustrated in section 8.

9.2.1.1 Surface Panel Fabrication

Fabrication of detailed parts for the LFC surface panels is illustrated schematically in figure 186.

OUTER SKIN

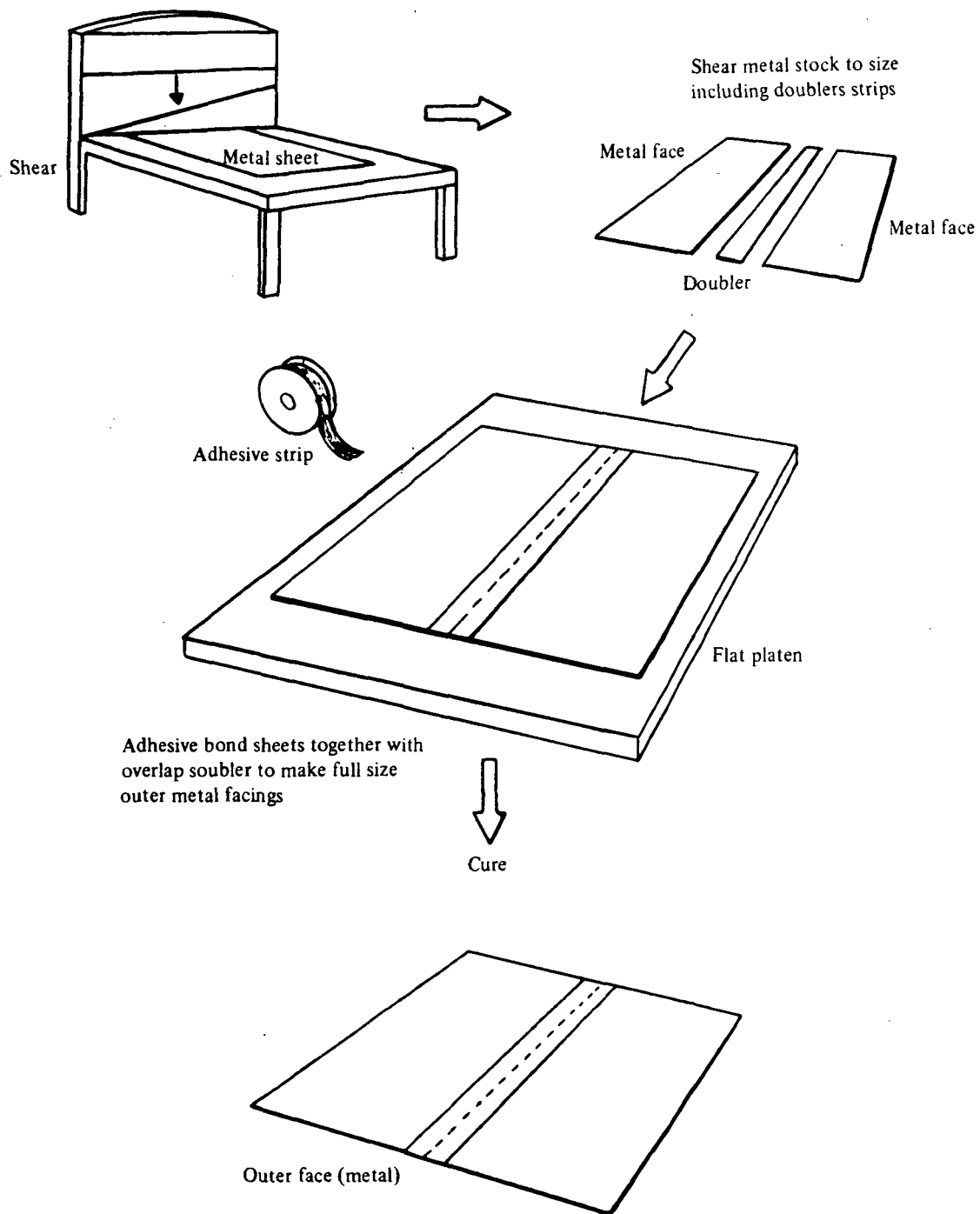
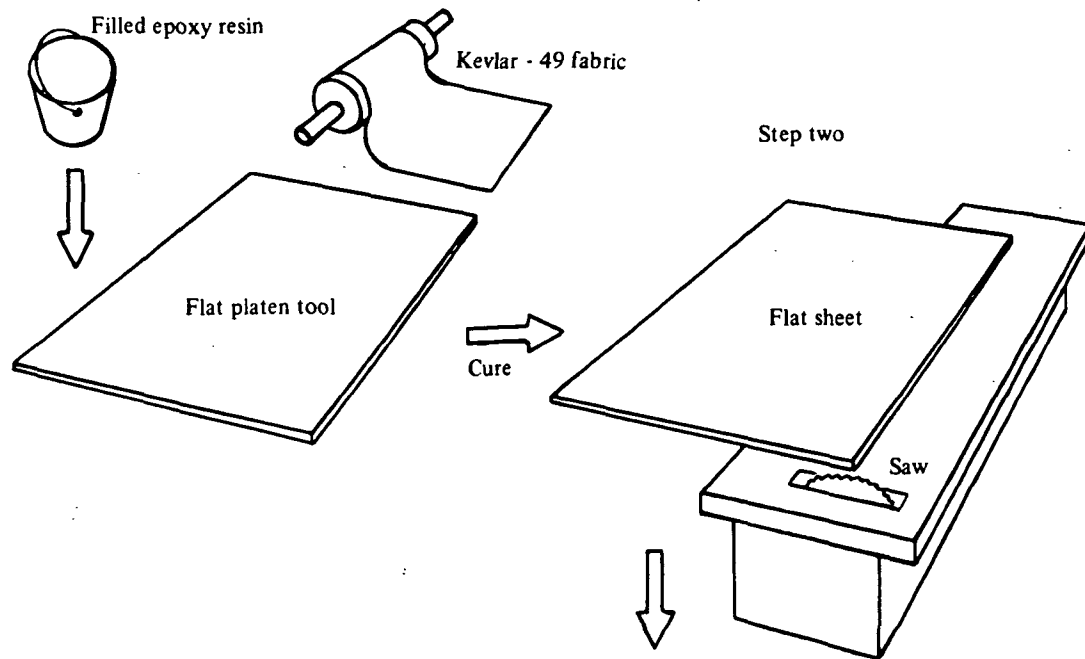
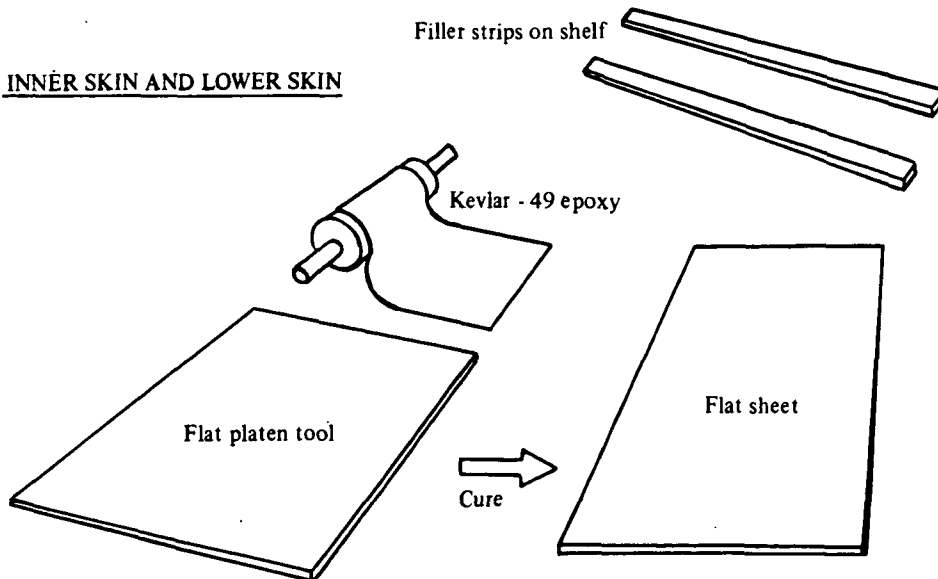


Figure 186. — Surface panel fabrication

FILLER STRIPS AND SPANWISE EDGE MEMBERS



INNER SKIN AND LOWER SKIN



CHORDWISE EDGE MEMBERS

(Same as filler strips except
contoured to fit wing contour)

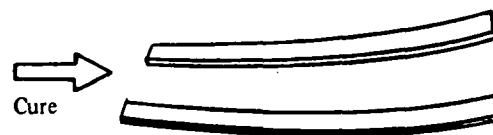
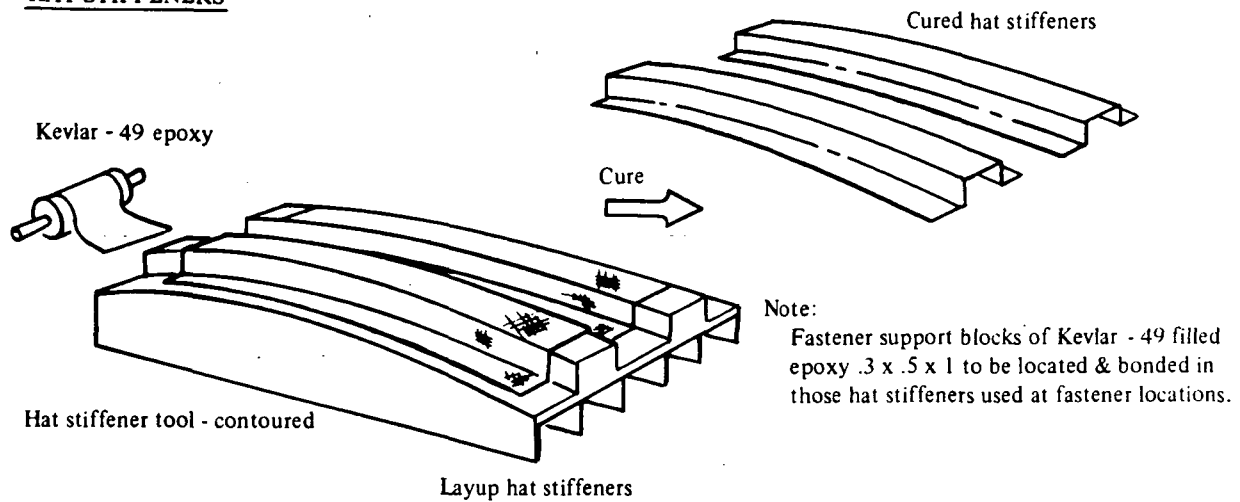


Figure 186. — Surface panel fabrication (continued)

HAT STIFFENERS



STIFFENED LOWER SKIN

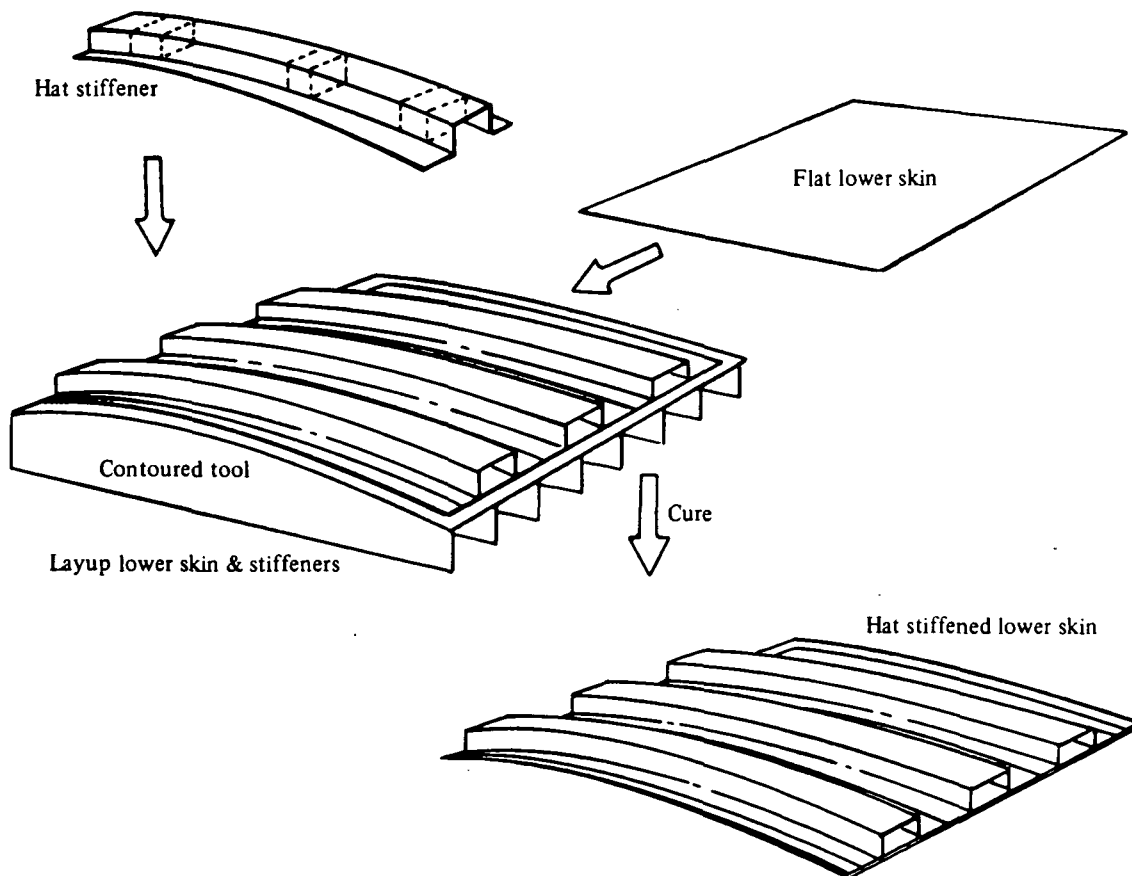


Figure 186. — Surface panel fabrication (continued)

Outer Skin – For each wing station location, the metal skins are cut to the appropriate size and shape in flat pattern form.

Due to the large size of each LFC panel, the skins are spliced with an equal thickness doubler and an appropriate overlap with splices running in the chordwise direction. The joining of the skin segments and the splice doublers is accomplished by structural adhesive bonding using a 120°C (250°F) curing modified epoxy in accordance with standard industry practice. The OML contour of the wing surface, having straight line segments, allows dropping of these skin segments and doublers into a female bonding fixture contoured to the wing OML during the fabrication of the skins, eliminating the need for any compound curvature forming. The surface preparation of these skins for adhesive bonding employs chromic acid anodizing, a standard practice used for adhesive bonding. The interior surface of these skins is primed with corrosion inhibiting adhesive primer which protects the prepared surface for subsequent bonding during LFC panel buildup.

Alternative Porous Composite Outer Skin – Using Kevlar-49/Polyimide pre-impregnated fabric of the fabric style to yield the proper skin thickness using one ply of material, the skins are laid-up on a flat platen tool with the appropriate bleeder and tool surface release systems. The lay-up is cured in accordance with the applicable industry standard polyimide resin cure procedures to achieve a porous laminate similar to those presently used in engine nacelle noise suppression applications. After removal of the cured, porous Kevlar-49/Polyimide face sheet from the flat platen, porosity is inspected for uniformity.

A layer of 5 mil thick, bondable-one-side, Tedlar^R (tradename of Dupont) or equivalent film, is positioned, treated-side-up, in a female bonding fixture, contoured to the wing surface OML. After applying a controlled coating of epoxy adhesive to one surface of the porous face sheet, it is positioned, adhesive side down, on the Tedlar film in the contoured tool, and cured in place to the Tedlar. The quantity of adhesive used is minimized to preclude blocking the face sheet porosity. The outer skin is now ready for joining with the remaining panel details.

Spanwise Filler Strips – Kevlar-49 fabric is combined with epoxy resin, to which glass micro-balloon spheres have been added for lower density, laid up, and cured in flat sheets of the appropriate finished thickness. The flat sheets are cut or machined into net-sized strips and stored until used. Kevlar 49 was selected for this application because it is the lowest density reinforcement with the lowest relative weight of candidate advanced composites. However due to its toughness, conventional cutting techniques tend to leave a “fuzz” of fibers at the cut edge. An alternative method should be considered wherein the Kevlar-49 and glass micro-balloon filled epoxy is formed into continuous net-sized strips by a process referred to as “pultrusion,” wherein the reinforcement and resin are pulled through a die with the resin cure occurring in the die. This process produces a net-sized strip with smooth surfaces without any exposed fiber for contact with environmental exposure.

Inner Skin – Kevlar-49 181 style fabric impregnated with epoxy resin is laid-up to the required thickness on flat platens and cured using industry standard curing procedures. The prepreg fabric is laid-up in standard widths, available up to 1.7 m (44 in) wide, with overlap splices running in the chordwise direction of the panels to make skins the full panel size. The splices are staggered such that no two overlap splices coincide, thereby reducing skin buildup due to overlap splices. After cure, the flat sheets are trimmed to flat pattern shapes.

Chordwise Edge Members – These members are made of Kevlar-49 and glass micro-balloon-filled epoxy using procedures the same as those for the spanwise filler strips, except that they are laid-up and cured in tools to a net molded shape to the contours applicable to the various wing station dimensions.

An alternative method to be considered is to produce these strips to net-shape from Kevlar-49 and glass micro-balloon filled polysulfone thermoplastic resin in continuous strips. By using automated progressive thermoplastic forming techniques, layers of net-width thermoplastic prepreg are fed through a series of progressive hot rolls to apply heat and pressure, compacting the layers to form the net-size strips. Using a heated, variable-shaped tool, the thermoplastic strips are thermo-formed to the required contour for each chordwise wing station location.

Lower Skin Hat Stiffeners – The hat stiffeners, to be joined with the lower skin, are fabricated of Kevlar-49 fabric, impregnated with epoxy resin. The prepreg is laid-up and cured in accordance with industry standard procedures on contoured tools with male corrugations to coincide with the contour at the respective wing station locations.

These hat stiffeners are trimmed to size and stored until later needed for bonding to the lower skins when spacers are used to locate the stiffeners.

Lower Skin – The lower skin is fabricated the same as the inner skin.

9.2.1.2 Surface Panel Assembly

Assembly of the LFC surface panel is illustrated by figure 187.

Outer Panel – The low density filler and edge member strips are coated with adhesive and positioned in the appropriate places on the outer skin in the contoured tool made to the LFC wing surface OML. The inner skin is then positioned over the filler strips. A metal caul plate is placed over the inner skin to serve as a pressure intensifier and to bridge the spanwise duct areas. The outer panel is cured in accordance with industry standard practice. throttling holes are drilled into the inner skin using an appropriately coordinated drill template. The Kevlar-49 laminate edges at

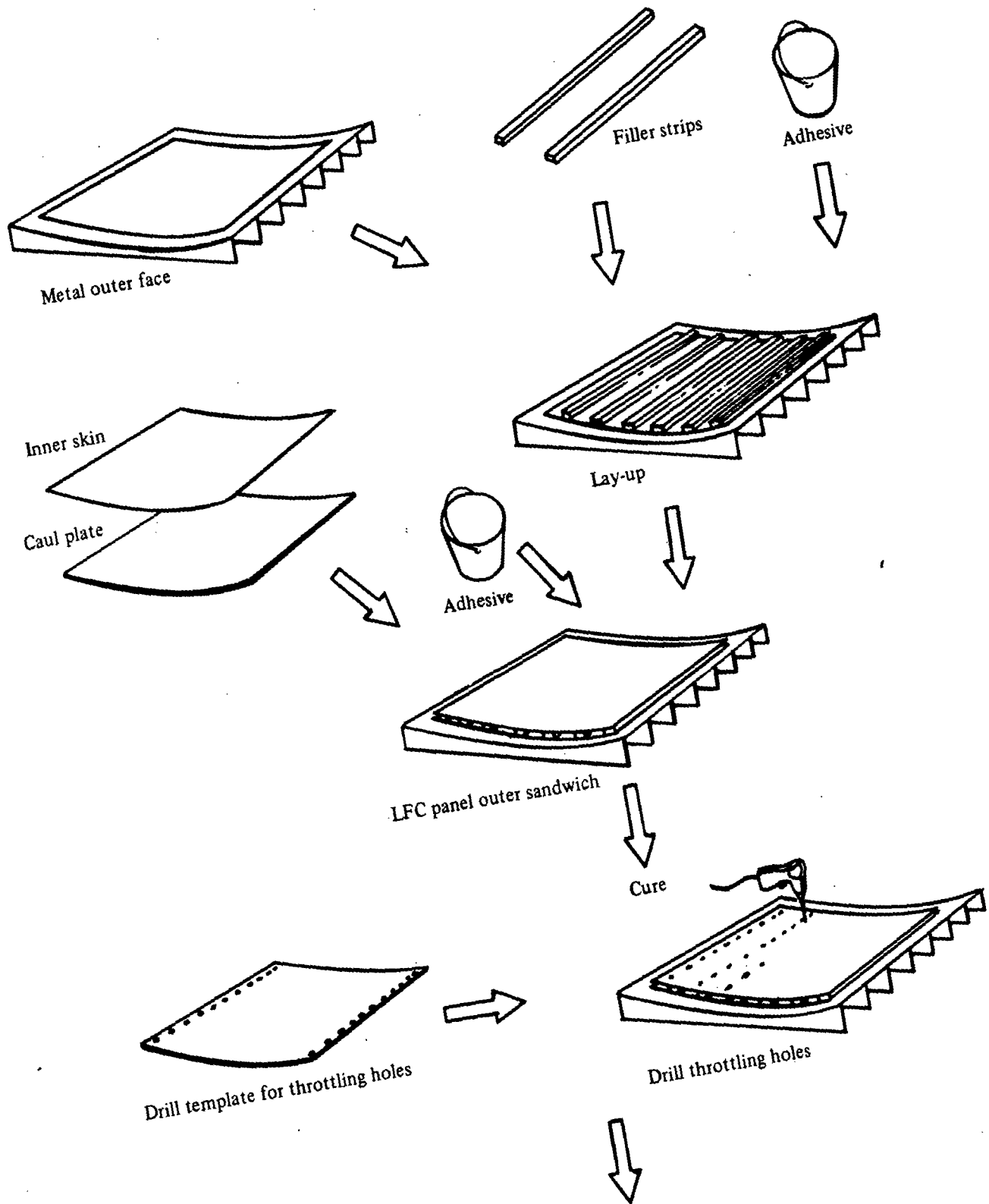


Figure 187. — Surface panel assembly

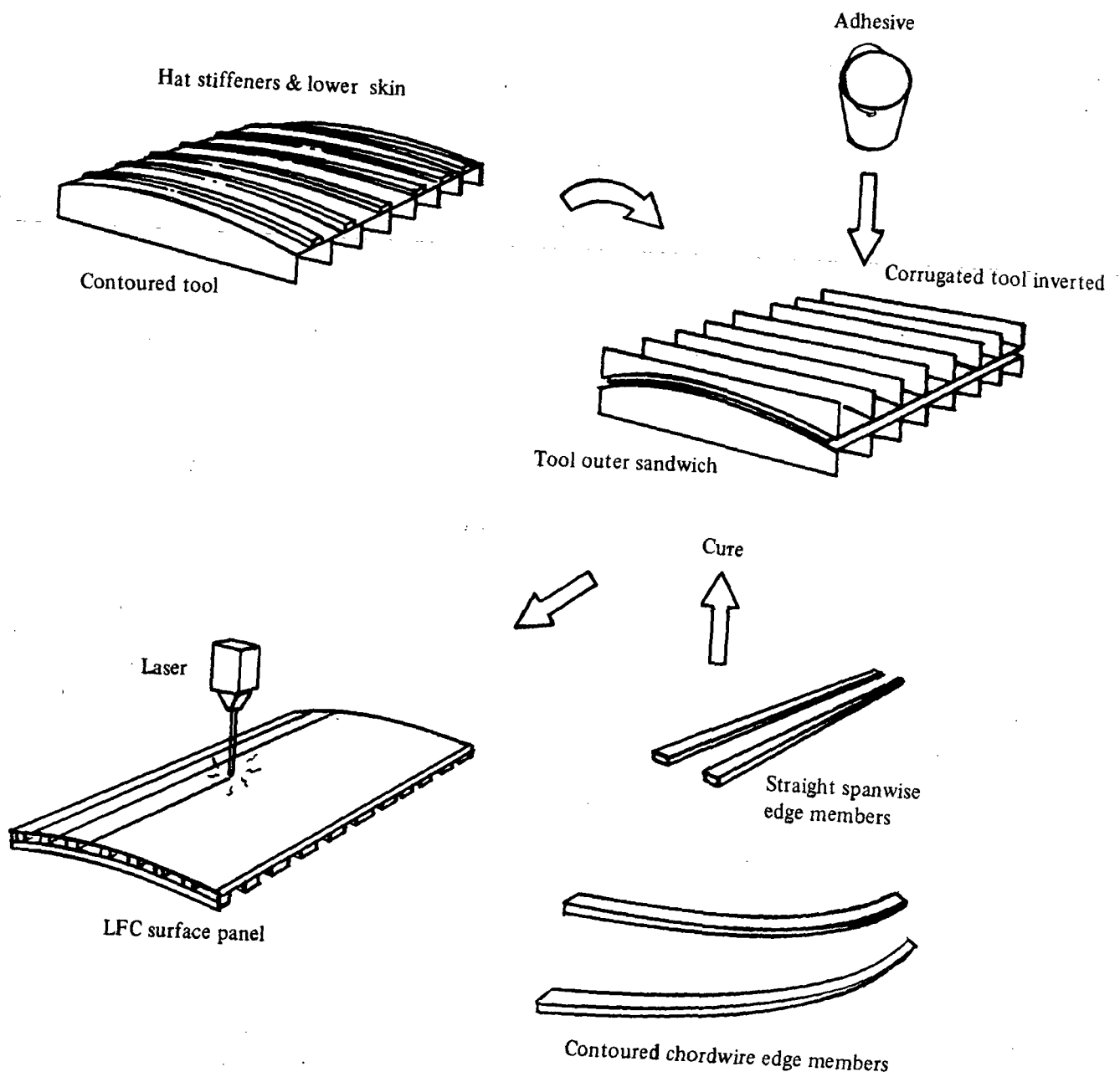


Figure 187. — Surface panel assembly (continued)

each hole are resin coated to seal the drilled laminate hole edges. Special drills and drilling techniques have been developed to minimize fiber "fuzzing" at cut edges of the Kevlar-49/epoxy laminate skin.

Complete LFC Panel – The stiffened lower skin, with epoxy adhesive applied to the hat stiffener crowns, is positioned on the inner skins. At the same time, the lower, contoured edge members with adhesive applied, are positioned and the lower panel is cured to the outer panel. Flexible mandrels are used inside the hat stiffeners to ensure firm contact and bond pressure, without distorting the hat stiffeners.

Panel Checkout and Slotting – The LFC panel is checked for aerodynamic smoothness and the slots are cut into the panels with the required dimensions and spacing using a numerically-controlled laser cutter.

9.2.1.3 Leading Edge Fabrication and Assembly

Figures 188 and 189 illustrate procedures for fabrication and assembly of LFC leading edge sections.

Skins – The outer, inner, and lower skins are fabricated from aluminum in flat patterns and taper roll formed to the wing leading edge contour. The skins are chromic acid anodized in preparation for adhesive bonding.

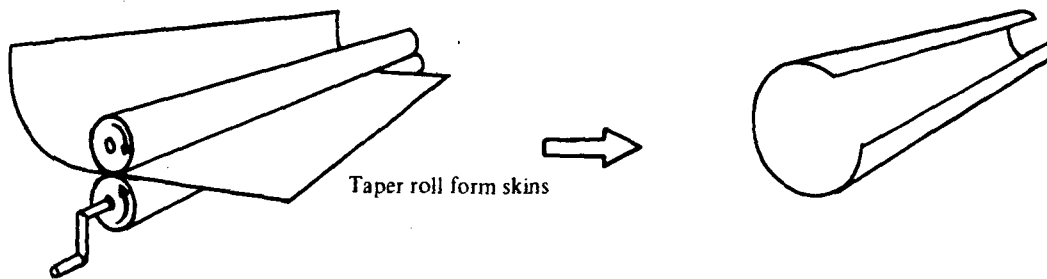
Spanwise Fillers – The spanwise fillers are made of a uniform rectangular cross section by shearing in full-length strips. The filler strips are chromic acid anodized in preparation for bonding.

Chordwise Fillers – The chordwise fillers between the inner and lower skin are made of rectangular aluminum bar of net-size cross section. Using a variable sized die, the aluminum bar is stretch formed to the appropriate contour depending upon wing station. The chordwise fillers are chromic acid anodized in preparation for bonding.

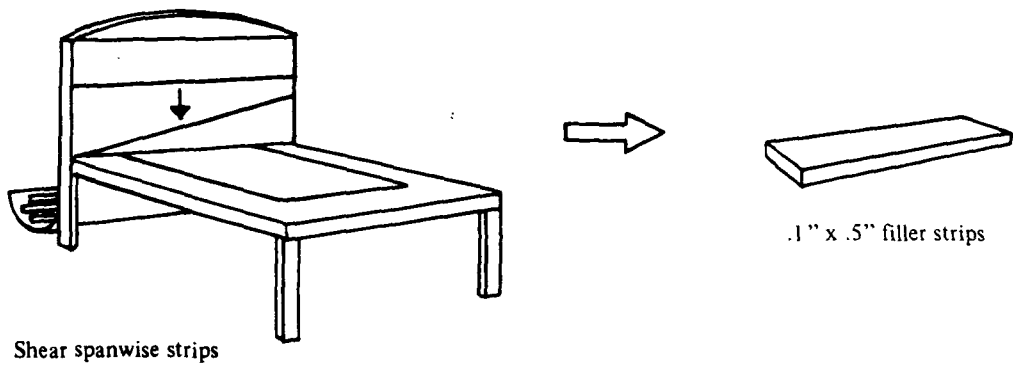
Anti-ice Heater Elements – Nichrome ribbon heater elements of the same width as the outer sandwich filler strips are used integrally in the high temperature bondline common to the outer skin. The elements are made in lengths to coincide with the spanwise fillers with electrical leads available for attachment to wire bundles leading to anti-icing controls.

Assembly – The outer skin, with a coating of corrosion inhibiting high-temperature adhesive over nichrome ribbon heater elements, is placed in a female bonding tool contoured to the leading edge OML. The spanwise fillers are positioned with adhesive over the heaters and covered by the inner

SKINS



SPANWISE FILLER STRIPS



CHORDWISE FILLER STRIPS

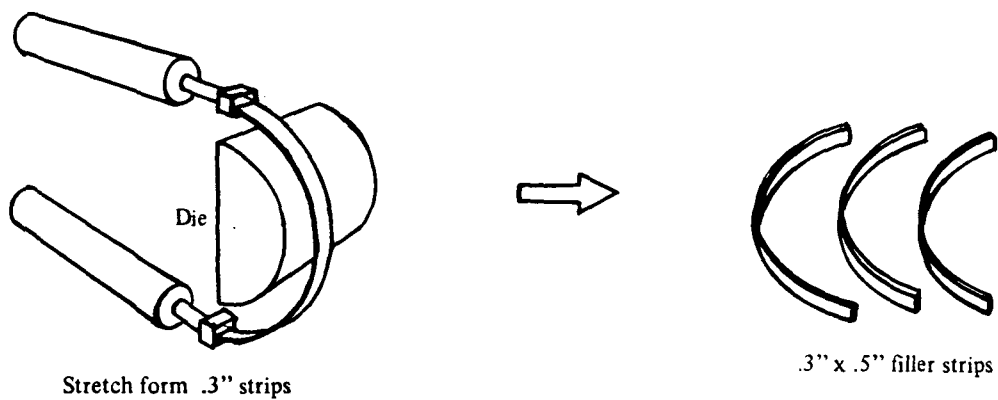


Figure 188. – Leading edge fabrication

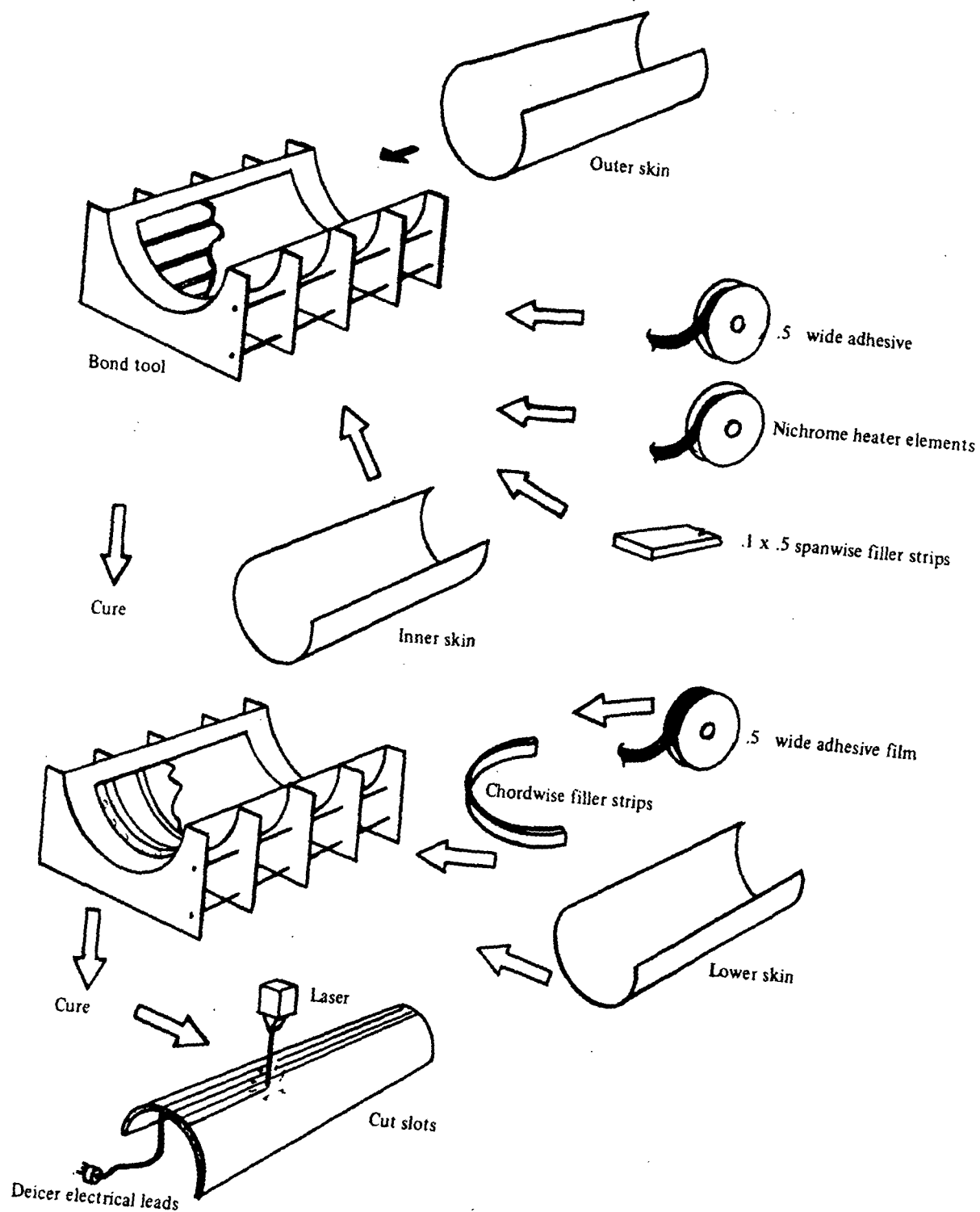


Figure 189. — Leading edge assembly

skin. Using industry standard procedures, the outer sandwich is cured. The adhesive-coated chordwise fillers are positioned and the lower skin is installed. The leading edge assembly is then cured. A temperature-resistant adhesive capable of withstanding temperatures of 177°C (350°F) during operation of the anti-icing system is used in the leading edge sections.

9.2.1.4 Ducting Fabrication and Assembly

Figures 190 and 191 illustrate fabrication and assembly of LFC ducting.

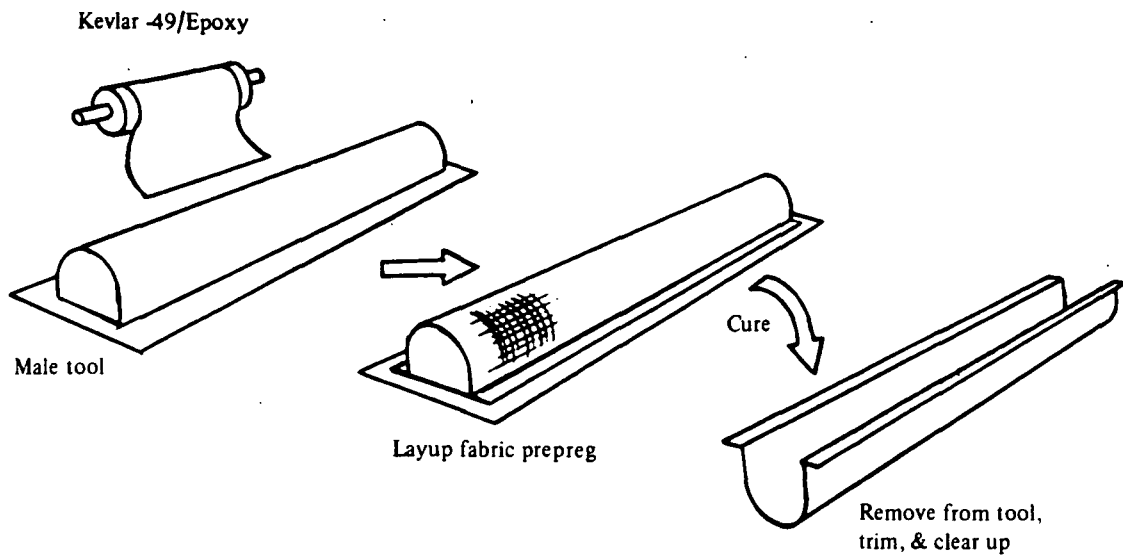
The forward and aft primary collection ducts have the forward face or aft face of the front and aft wing spars as one wall of the duct. The remaining portion of the primary ducts is fabricated by lay-up and curing of Kevlar-49/epoxy prepreg on male tools constructed to the inner mold line of the ducts to provide smooth surfaces for the air flow. These portions of the primary ducts are made with an outward facing flange for attachment to the spar web with fasteners. Where sections of the ducts meet, outward facing flanges are provided for joining duct ends with seal strips and mechanical fasteners. This provides duct section joining with no joint fasteners penetrating the smooth-walled air passage surface in the ducts.

Due to the irregular shape of these ducts, local stiffening is provided by secondary bonding of Kevlar-49/epoxy stiffeners as required, or by applying a layer of honeycomb core with an additional layup of Kevlar-49/epoxy prepreg to form an outer sandwich skin.

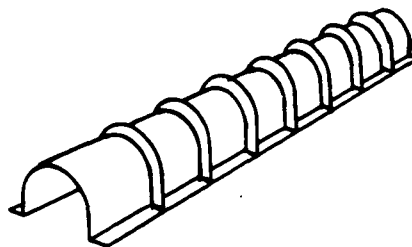
For the fabrication of secondary ducting, shown in figure 190, washout-type plaster mandrels are cast in female molds made to the inner mold line configuration of the primary trunk ducts. After curing of the cast mandrels and removal from the female molds, Kevlar-49/epoxy prepreg tape is wrapped over the mandrels, over-wrapped with heat-shrink tape, and cured. After curing the ducts, the mandrels are removed by washing out with high-pressure warm water. Finally, the cured ducts, after mandrel removal and cleanup, are sized by trimming to fit mating surfaces. This method was chosen because of the highly irregular duct shapes resulting from severe space limitations within the wing.

9.2.1.5 Installation

LFC surface panel installation is outlined in figure 192. Using coordinated drilling templates, fastener holes are drilled net size in the panels and pilot drilled in the wing cover structure. The holes in the wing cover structure are opened up and appropriate floating dome nuts installed. The panels are indexed in position on the wing structure and checked for aerodynamic contour. At each fastener location, any gaps between the panel and the wing structure are filled with a thixotropic epoxy castable shim. The shims are cured prior to fastener installation. A parting agent is applied to the wing surface to prevent the epoxy shims from bonding the panels to the wing structure.



Note:
Where stiffening is required, external stiffeners
can be added and cured with the basic port



or

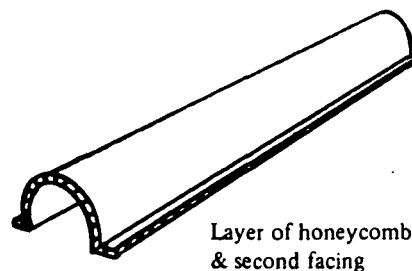


Figure 190. — Primary duct fabrication and assembly

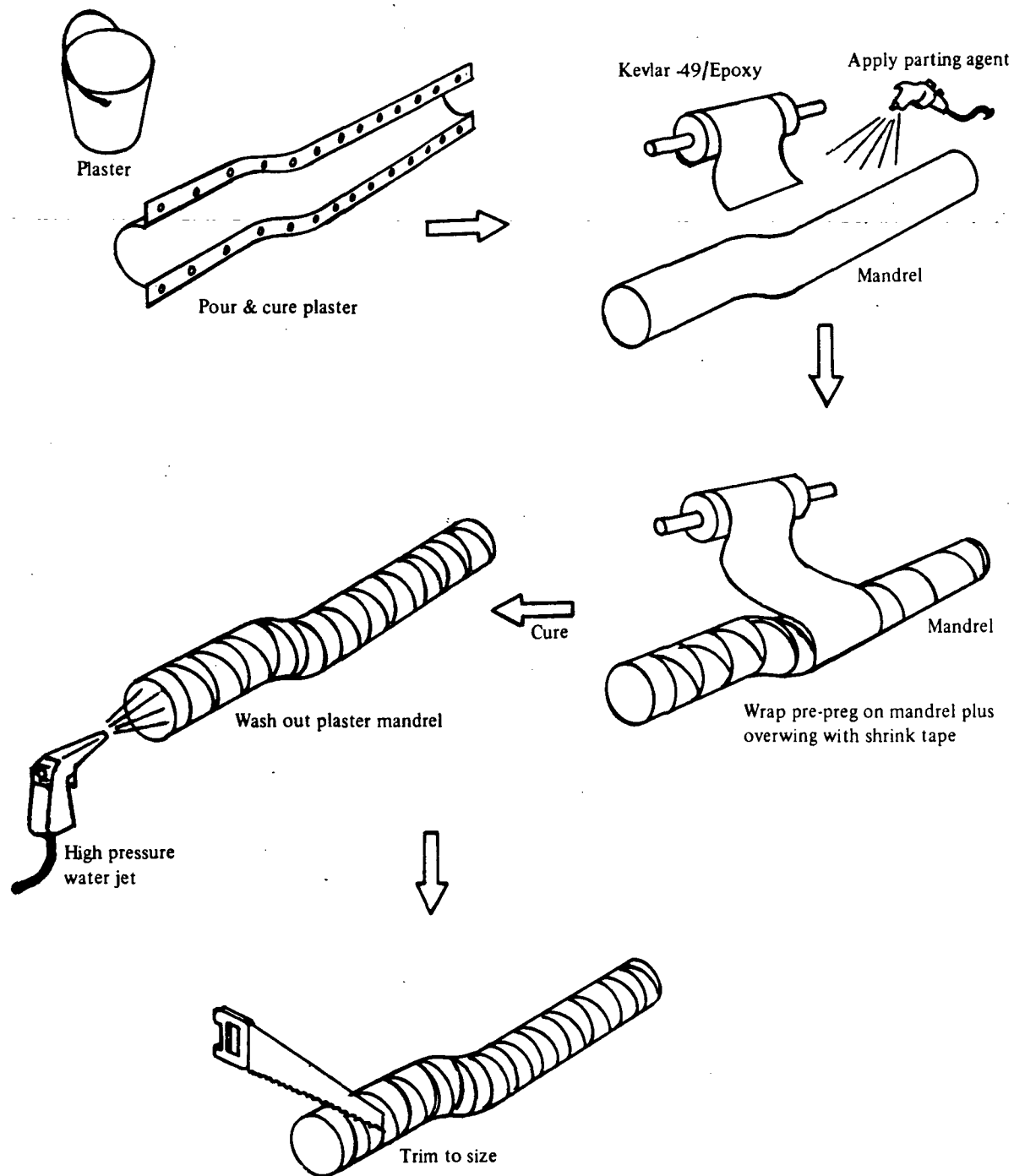


Figure 191. — Secondary duct fabrication and assembly

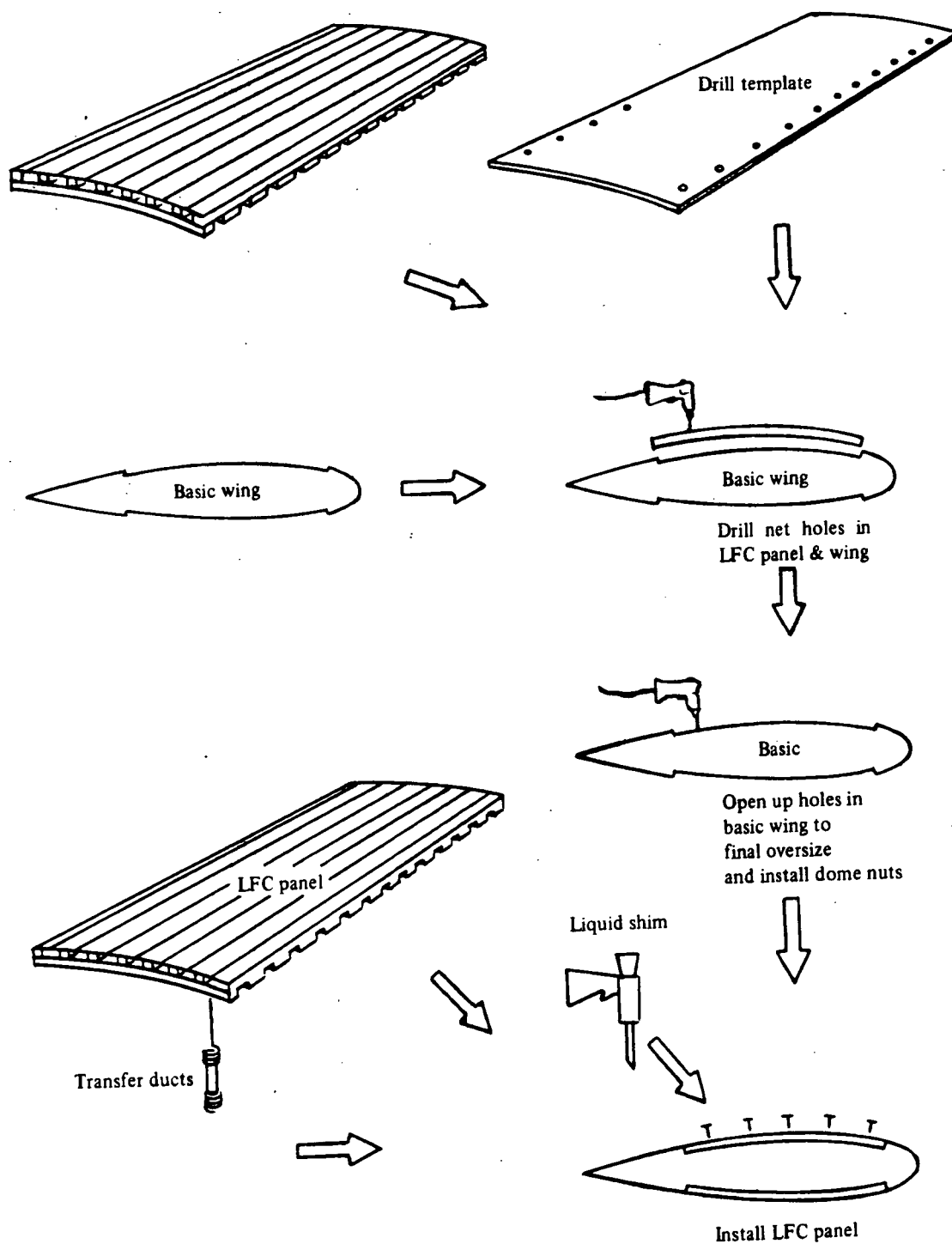


Figure 192. — Surface panel installation

During panel installation, blind "piccolo" tube connectors are snapped into place to connect the chordwise collection ducts in the panels to either the forward or rear primary collection ducts. Fasteners are installed through LFC panels into the floating dome nuts and tightened until the LFC panels and the cast shims fit snugly against the wing surface. Aerodynamic surface smoothing compound is applied around and over fastener heads for aerodynamic smoothness control. Gaps between panels and between panels and wing structure are filled with a highly elastomeric filling compound such as polysulfide sealant. During LFC panel installation, the wings are jacked-up into a 1 g upbending position to facilitate obtaining cruise position aerodynamic smoothness at all joints and fasteners.

The metallic leading edge sections are assembled to the wing structure with connectors to provide suction from the forward primary ducts. At the intersection of the metal leading edge and the LFC surface panels, a thermal insulation barrier is installed to isolate anti-icing heat.

After LFC panel installation and cleanup, the system is checked out for proper operation. At this point, the entire suction system, all duct interior surfaces, and external leading edge surfaces are coated with a long-life organosilicone rain-repellant coating (ref. 31) to form a hydrophobic surface. This minimizes the collection of water in the system and alleviates the problem of external organic contamination of the LFC surfaces.

The primary collection ducts are assembled in short sections to facilitate periodic removal for servicing needs. The ducts are attached to the forward face of the front spar or to the aft face of the rear spar using steel fasteners and sealing strips. Where sections meet, flanged joints are sealed with a seal strip and fastened mechanically. Similar flanged joints are used where secondary collection ducts connect the suction pumps to the primary ducts. Wherever ducts penetrate the wing structure, such as at the front spar and the lower wing cover, the ducts are secured in place using clips and brackets, attached to the duct by bonding and to the wing structure with fasteners.

9.2.2 MANUFACTURING COSTS

Cost estimates for the selected LFC surface panel and leading edge configurations were developed on the basis of a detailed assessment of the manufacturing and tooling plan outlined in the previous section. Based on similarity considerations and the existence of historical data, ducting was costed as aircraft secondary structure. All costs are calculated in 1975 dollars for 350 aircraft with an average lot size of 20 aircraft. Primary emphasis was placed on the development of production labor and material costs. Costs for recurring engineering, tooling, and quality assurance are typically calculated as a function of recurring production labor. The percentages used for these cost elements were 10, 20, and 15 percent, respectively.

9.2.2.1 Cost Estimation Procedures

In order to estimate costs which are sensitive to detail design concepts incorporating state-of-the-art advances, cost estimating methods with a high order of accuracy are required. This necessitates the use of the industrial engineering method and requires the application of time standard data and cost calculations for material. The output of this method provides standard hours for production labor and standard material costs. After the application of appropriate learning curve and material utilization factors, these data were exercised in the GASP to generate final cost data for the study aircraft.

9.2.2.2. Summary of Cost Estimates

Tables 30 through 33 summarize labor and material cost estimates for LFC surface panels and leading edge sections for the selected LFC aircraft. Surface panel estimates are based on a panel size of 2.54 m (100 in) by 3.81 m (150 in). Estimates for the leading edge sections are based on a section length of 3.81 m (150 in).

The data of these tables were converted to estimated actual labor hours and material costs through the application of learning curve and material utilization factors. These values were then converted to hour per pound and material dollar per point values and input to the GASP for aircraft cost determination.

In terms of standard hours per square foot of LFC surface, the panels for all of the final configurations require about 3.15 hr/ft². For purposes of comparison, a representative wing surface of machined skin construction requires 0.70 hr/ft² and a representative wing surface of skin and stringer construction requires 2.10 hr/ft². Since the LFC surface panels are non-structural, materials costs are somewhat less than for wing panels on a conventional aircraft. The data of table 31 indicate that the materials cost for a square foot of LFC surface panel is about \$18, compared to a cost of \$31 per square foot of skin and stringer wing surface.

9.3 LFC SYSTEM MAINTENANCE

Since the basic airframe and systems of LFC aircraft are similar to those of conventional transport aircraft in service today, the discussions of this section address only the aspects of the operational maintenance requirements which are peculiar to LFC aircraft. Investigations were limited to the maintenance significant areas of the LFC-peculiar systems which directly affect aircraft downtime and/or maintenance costs.

TABLE 30. STANDARD HOURS PER PANEL FOR LFC SURFACES

Operation	LFC-200-S	LFC-400-S	LFC-200-R	LFC-400-R
Fabricate Outer Skin	1.3635	1.3635	1.3635	1.3635
Fabricate Spacers Between Outer Skin and Inner Skin	44.7140	44.7140	44.7140	44.7140
Bond Outer Skin to Spacers	37.3500	37.3500	37.3500	37.3500
Fabricate Inner Skin, Drill Holes	43.0415	43.0415	43.0415	43.0415
Bond Inner Skin to Outer Skin Assembly	18.8000	18.8000	18.8000	18.8000
Fabricate Spacers Between Inner/Outer Skin Assembly and Lower Skin	3.7540	3.7540	3.7540	3.7540
Fabricate Stiffeners Between Inner and Lower Skin	52.2503	54.5555	51.0849	52.2573
Fabricate Lower Skin	36.8540	36.8540	36.8540	36.8540
Bond Spacers and Stiffeners to Lower Skin	37.3500	37.3500	37.3500	37.3500
Bond Lower Skin Assembly to Outer/Inner Skin Assembly	17.9820	17.9820	17.9820	17.9820
Machine Slots	17.8570	17.8570	17.8570	17.8570
Drill Holes for Piccolo Ducts	0.2772	0.2772	0.2772	0.2772
Drill Holes for Dome Nuts	0.6448	0.6448	0.6448	0.6448
Install Dome Nuts	8.9602	8.9602	8.9602	8.9602
Install Panel to Surface	<u>6.6170</u>	<u>6.6170</u>	<u>6.6170</u>	<u>6.6170</u>
Total	327.8155	330.1607	326.6501	327.8155

TABLE 31. MATERIAL COST PER PANEL FOR LFC SURFACES

Parts List	LFC-200-S	LFC-400-S	LFC-200-R	LFC-400-R
Outer Skin	\$ 104.83	\$ 104.83	\$ 104.83	\$ 104.83
Edge Members	39.00	39.00	39.00	39.00
Inner Skin	224.64	224.64	224.64	224.64
Filler Strips	140.40	140.40	140.40	140.40
Stiffeners	213.41	285.91	194.01	224.64
Lower Skin	224.64	224.64	224.64	224.64
Adhesive	31.20	31.20	31.20	31.20
Sealant	46.90	46.90	46.90	46.90
Bolts, Nuts	104.00	104.00	104.00	104.00
Dome Nuts/Fasteners	136.00	136.00	136.00	136.00
Liquid Shim	52.00	52.00	52.00	52.00
Piccolo Ducts	<u>500.00</u>	<u>500.00</u>	<u>500.00</u>	<u>500.00</u>
Total	\$1817.02	\$1889.52	\$1797.62	\$1828.25

9.3.1 MAINTENANCE REQUIREMENTS

Elements of the LFC system are logically categorized in the two major areas of LFC functional systems and LFC surfaces. Since the LFC functional systems, which include the suction units, valves, and controls, are similar to systems the commercial operators are currently maintaining, the majority of the discussions concern the LFC surfaces. The LFC functional systems present no maintenance requirements that are not being encountered on a day-to-day basis by commercial operators. However, the LFC surfaces present unique maintenance requirements which the

commercial operators have not previously encountered. These maintenance requirements result from the criticality of LFC surface smoothness and cleanliness. In operating the LFC aircraft, it is necessary to ensure that LFC surfaces are clean and that the spanwise slots are free from obstruction before each flight. Periodic cleaning of the surfaces and slots is fundamental to the consistent operation of the LFC system.

On-aircraft repair of LFC surfaces is limited because of the requirement to maintain continuity of the integral air passages within the surfaces. All surface repairs must be carefully controlled to maintain aerodynamic smoothness and conformity to surface contours.

TABLE 32. STANDARD HOURS PER SECTION FOR LFC LEADING EDGES

Operation	LFC-200-S LFC-400-S
Fabricate Outer Skin	1.8785
Fabricate Spacers Between Outer and Inner Skin	18.2900
Bond Outer Skin to Spacers	14.4700
Fabricate Inner Skin	1.8785
Bond Inner Skin to Outer Skin Assembly	7.2800
Fabricate Spacers Between Inner/Outer Skin Assembly and Lower Skin	18.2900
Fabricate Lower Skin	1.8785
Bond Spacers to Lower Skin	14.4700
Bond Lower Skin Assembly to Outer/Inner Skin Assembly	6.9600
Machine Slots	6.9200
Drill Holes for Piccolo Ducts	0.1074
Drill Holes for Dome Nuts	0.2496
Install Dome Nuts	3.4703
Install Panel to Surface	<u>2.5627</u>
Total	98.7055

Access to the LFC upper surfaces for maintenance must be obtained from maintenance stands to preclude damage resulting from maintenance personnel walking on the surfaces. This requires the use of special maintenance stands which span the upper surfaces in the chordwise direction.

Replacement of the LFC surface panels requires special skills and Ground Support Equipment (GSE) due to the stringent aerodynamic sealing requirements for all fasteners used to secure the surface to the basic wing structure. Special equipment is required to remove and replace the sealant and to check the surface for smoothness and contour after the installation.

Because of the skills and GSE involved in replacement of a panel, it is anticipated that the LFC surface panels will be replaced at an overhaul facility. Consequently, attention must be given to design detail to minimize the requirement to remove surface panels to permit maintenance on the aircraft fuel system.

TABLE 33. STANDARD HOURS PER SECTION FOR LFC LEADING EDGES

Parts List	LFC-200-S	LFC-400-S
Outer Skin	\$ 40.60	\$ 40.60
Edge Members/Spacers	203.14	292.44
Inner Skin	40.60	40.60
Lower Skin	40.60	40.60
Adhesive	12.08	12.08
Sealant	18.16	18.16
Bolts, Nuts	40.00	40.00
Dome Nuts/Fasteners	52.00	52.00
Liquid Shim	20.14	20.14
Piccolo Ducts	<u>195.00</u>	<u>195.00</u>
Total	\$662.32	\$751.62

Since the LFC surface slots are subject to clogging from contaminants in the atmosphere and permit water to enter the air passages, it is necessary to use LFC surface covers or park the aircraft in a hangar if it is to be on the ground for an extended period of time. Providing a method of pressurizing the LFC system during turn-arounds to preclude contamination of the slots and air passages is necessary to reduce requirements for cleaning the slots and extend system functional check intervals.

With proper maintenance manloading, turn-around of the LFC aircraft after a 10,186 km (5500 n mi) flight can be accomplished within the normal downtime scheduled by commercial operators for inter-continental flights. The LFC functional systems require no extraordinary turn-around maintenance. However, the LFC surfaces require detailed inspection and cleaning. It is assumed that LFC system functional capability is checked by the flight crew before landing and that no ground functional checking of the system is required. It is further assumed that the LFC systems are pressurized from a ground air source to preclude entry of contaminants into the system while the aircraft is on the ground being prepared for the next flight.

9.3.2 SCHEDULED MAINTENANCE CONCEPT

The projected scheduled maintenance for the LFC aircraft is based on the application of contemporary Airline/FAA Maintenance Steering Group (MSG) logic during the design phase. Scheduled maintenance requirements for the LFC functional systems are similar to those currently being performed on conventional commercial jet transport aircraft. However, the LFC surfaces require scheduled maintenance that is more comprehensive and critical than is currently being performed on a conventional wing and empennage.

The critical requirements for scheduled maintenance on the LFC surfaces include:

- o Determination of surface smoothness
- o Measurement of wing waviness
- o Measurement of system flow
- o Removal of LFC surfaces to permit inspection of basic wing surfaces
- o Cleaning surfaces, slots, and air passages
- o Correcting out-of-tolerance smoothness and waviness.

Operation of the LFC aircraft under present-day scheduled inspection concepts results in the following type inspections and intervals.

Type Inspection	Interval
Termination Check	After each flight
A Check	50 flight hours
C Check	1,000 flight hours
D Check	8,000 flight hours

A Check – The A check is considered to be the primary inspection. The inspection is generally preceded by other checks such as Preflight or In-transit checks. Portions of the A check may be delegated to one or more of the lesser checks. However, the A check items should not exceed 50 flight hours. The A check is approximately equivalent to a Home Station Check in the military environment.

C Check – The C check is a periodic check involving detailed inspections throughout the airplane to insure a continued condition of airworthiness. It involves system functional/operational checks and removal of access doors and panels to facilitate thorough inspection. The C check is approximately equivalent to a Major Isochronal Inspection in the military environment.

D Check – The D check requires a thorough and searching inspection of the airplane to insure a continued condition of airworthiness. The D check is intended to encompass the contents of the A and C checks plus detailed structural inspections and other specifically designated tasks. The D check is approximately equivalent to the PDM (Planned Depot Maintenance) in the military environment.

Basically, each of these inspections requires progressively more cleaning and checking of the LFC surfaces for flow and waviness, culminating in an 8,000 flying hour overhaul-type structural sampling program requiring removal of an LFC surface panel.

9.3.3 GROUND SUPPORT EQUIPMENT

Special GSE is required to support the LFC aircraft in operational service. The criticality of LFC surface smoothness, waviness, and cleanliness to proper LFC system operation presents unique GSE requirements.

Since commercial operators have extensive experience in maintaining similar systems, GSE for the LFC functional systems presents no unusual problems. However, GSE to support the LFC aircraft must include equipment to measure LFC surface waviness and complete LFC system flow. GSE is available to accomplish such measurements, but does not permit rapid accomplishment of these measurements on the extensive and complex surface areas on the LFC aircraft. Therefore,

development of appropriate GSE will facilitate completion of the required measurements with a minimum expenditure of aircraft downtime and manhours.

Other LFC-peculiar GSE includes wing and empennage covers. These covers must be used when the aircraft is parked outside for an extended period of time to prevent the accumulation of foreign particles in the surface slots with a resultant degradation of system performance.

Because of the criticality of LFC surface smoothness, it is necessary to use maintenance stands that span the surfaces chordwise when maintenance is required on the LFC upper surfaces. Surface smoothness requirements also dictate use of special slings and cradles for removal of installation, and transporting of LFC surface panels. Sealing and repair kits are required to facilitate removal, replacement, and resealing of LFC surface fasteners and to make minor repairs to the LFC surfaces.

Cleaning solvents and equipment are required to permit expeditious and thorough cleaning of clogged surface slots and air passages. Design considerations must include attention to eliminating areas in the air passages that trap water and cleaning solvents, and ultimately lead to corrosion problems.

9.3.4 MAINTENANCE COSTS

A comprehensive maintenance analysis was performed on the LFC peculiar systems to determine total labor and material costs required to maintain the LFC systems and to quantify the impact of the LFC systems on the maintenance costs of the basic aircraft.

Historical maintenance data for similar systems on conventional commercial and military jet aircraft formed the basis for the maintenance analysis. Factors were applied to account for differences in LFC aircraft systems and conventional aircraft systems. Data for the LFC functional systems were readily available, since these system components are in use on existing aircraft. However, with the exception of reference 14, maintenance data on LFC surfaces were not available. Therefore, data on conventional surfaces were used and adjusted to reflect the unique maintenance requirements of the LFC surfaces.

In conducting the maintenance cost analysis, both the labor and materials requirements for maintaining the following LFC system elements were evaluated:

- o Surfaces
- o Engines and controls
- o Suction pumps
- o Ducting and valves
- o Trim flap system
- o Anti-icing system

Requirements for the individual LFC system element were subsequently summed to obtain the total maintenance labor and material costs peculiar to the LFC aircraft. The maintenance costs for the LFC system were included with the maintenance costs for the basic airframe and aircraft systems, and exercised in the GASP to evaluate the impact of LFC system maintenance on the direct operating costs of LFC aircraft.

TABLE 34. MAINTENANCE LABOR REQUIREMENTS FOR LFC SYSTEMS, LFC-200-S

UNSCHEDULED MAINTENANCE			
<u>System</u>	<u>On Equipment (MMH/FH)</u>	<u>Component Repair/ Overhaul (MMH/FH)</u>	<u>Total Unscheduled Maintenance (MMH/FH)</u>
Surfaces			
Wing	.230		.230
Empennage	.112		.112
Engines and Controls	.248	.761	1.009
Suction Pumps	.062	.190	.252
Ducting and Valves	.012	.002	.014
Trim Flap System	.009	.003	.012
Anti-Icing System	.088	.006	.094
Totals	.761	.962	1.723
SCHEDULED MAINTENANCE			
<u>Inspection</u>	<u>Interval</u>	<u>MMH to Accomplish</u>	<u>MMH/FH</u>
Termination Check	After each flight	5.9	.480
A Check	50 FH	12.5	.250
C Check	1000 FH	150.0	.150
D Check (Airframe Overhaul)	8000 FH	1250.0	.156
Total			1.036
TOTAL MAINTENANCE			
<u>Type of Maintenance</u>		<u>MMH/FH</u>	
Unscheduled		1.723	
Scheduled		1.036	
Basic Fuel Cell Maintenance		0.310	
Total		3.069	

Tables 34 through 37 summarize maintenance labor requirements for the LFC systems of the LFC-200-S, LFC-200-R, LFC-400-S, and LFC-400-R configurations, respectively. Maintenance material requirements for the four aircraft are included in table 38. It will be observed that both the labor and material requirements of LFC-200-S are significantly greater than those of the other three configurations. This is a result of the use of five LFC suction units on LFC-200-S, as compared to two units on the LFC-200-R, LFC-400-S, and LFC-400-R configurations.

TABLE 35. MAINTENANCE LABOR REQUIREMENTS FOR LFC SYSTEMS, LFC-200-R

UNSCHEDULED MAINTENANCE			
<u>System</u>	<u>On Equipment (MMH/FH)</u>	<u>Component Repair/ Overhaul (MMH/FH)</u>	<u>Total Unscheduled Maintenance (MMH/FH)</u>
Surfaces			
Wing	.225		.225
Empennage	.110		.110
Engines and Controls	.084	.259	.343
Suction Pumps	.025	.076	.101
Ducting and Valves	.012	.002	.014
Trim Flap System	.009	.003	.012
Anti-Icing System	.088	.006	.094
Totals	.553	.346	.899
SCHEDULED MAINTENANCE			
<u>Inspection</u>	<u>Interval</u>	<u>MMH to Accomplish</u>	<u>MMH/FH</u>
Termination Check	After each flight	4.00	.325
A Check	50 FH	11.25	.225
C Check	1000 FH	142.00	.142
D Check (Airframe Overhaul)	8000 FH	1187.00	.148
Total			.840
TOTAL MAINTENANCE			
<u>Type of Maintenance</u>		<u>MMH/FH</u>	
Unscheduled		.899	
Scheduled		.840	
Basic Fuel Cell Maintenance		.310	
Total		2.049	

TABLE 36. MAINTENANCE LABOR REQUIREMENTS FOR LFC SYSTEMS, LFC-400-S

UNSCHEDULED MAINTENANCE			
<u>System</u>	<u>On Equipment (MMH/FH)</u>	<u>Component Repair/ Overhaul (MMH/FH)</u>	<u>Total Unscheduled Maintenance (MMH/FH)</u>
Surfaces			
Wing	.311		.311
Empennage	.152		.152
Engines and Controls	.099	.304	.403
Suction Pumps	.025	.076	.101
Ducting and Valves	.012	.002	.014
Trim Flap System	.011	.004	.015
Anti-Icing System	.117	.008	.125
Totals	.727	.394	1.121
SCHEDULED MAINTENANCE			
<u>Inspection</u>	<u>Interval</u>	<u>MMH to Accomplish</u>	<u>MMH/FH</u>
Termination Check	After each flight	7.3	.594
A Check	50 FH	16.9	.338
C Check	1000 FH	202.5	.203
D Check (Airframe Overhaul)	8000 FH	1687.5	.211
Total			1.346
TOTAL MAINTENANCE			
<u>Type of Maintenance</u>	<u>MMH/FH</u>		
Unscheduled	1.121		
Scheduled	1.346		
Basic Fuel Cell Maintenance	0.465		
Total	2.932		

TABLE 37. MAINTENANCE LABOR REQUIREMENTS FOR LFC SYSTEMS, LFC-400-R

UNSCHEDULED MAINTENANCE			
<u>System</u>	<u>On Equipment (MMH/FH)</u>	<u>Component Repair/ Overhaul (MMH/FH)</u>	<u>Total Unscheduled Maintenance (MMH/FH)</u>
Surfaces			
Wing	.305		.305
Empennage	.149		.149
Engines and Controls	.084	.259	.343
Suction Pumps	.025	.076	.101
Ducting and Valves	.012	.002	.014
Trim Flap System	.011	.004	.015
Anti-Icing System	.117	.008	.125
Totals	.703	.349	1.052
SCHEDULED MAINTENANCE			
<u>Inspection</u>	<u>Interval</u>	<u>MMH to Accomplish</u>	<u>MMH/FH</u>
Termination Check	After each flight	7.3	.594
A Check	50 FH	16.9	.338
C Check	1000 FH	202.5	.203
D Check (Airframe Overhaul)	8000 FH	1687.5	.211
Total			1.346
TOTAL MAINTENANCE			
<u>Type of Maintenance</u>		<u>MMH/FH</u>	
Unscheduled		1.052	
Scheduled		1.346	
Basic Fuel Cell Maintenance		0.465	
Total		2.863	

TABLE 38. MAINTENANCE MATERIAL REQUIREMENTS FOR LFC SYSTEMS

System	Maintenance Material Costs (\$/FH)			
	<u>LFC-200-S</u>	<u>LFC-400-S</u>	<u>LFC-200-R</u>	<u>LFC-400-R</u>
Surfaces				
Wing	1.118	1.509	1.097	1.479
Empennage	1.002	1.353	0.982	1.326
Engines and Controls	53.620	21.448	19.91	21.448
Suction Pumps	13.400	5.362	5.360	5.362
Ducting and Valves	0.869	0.348	0.860	0.348
Trim Flap System	0.270	0.338	0.270	0.338
Anti Icing System	1.560	2.106	1.560	2.106
Total	71.839	32.464	30.039	32.407

The following provides a comparison of the maintenance labor requirements in MMH/FH for the LFC system with those of other aircraft components and the total airplane:

	LFC-200-S	LFC-200-R	LFC-400-S	LFC-400-R
Airframe	5.41	5.27	7.47	7.29
Engines	3.31	3.30	3.66	3.64
LFC System	3.07	2.05	2.93	2.86
Total	11.79	10.62	14.06	13.79

Following are the corresponding comparative data for maintenance material costs in \$/FH:

	LFC-200-S	LFC-200-R	LFC-400-S	LFC-400-R
Airframe	57.31	53.95	88.34	85.83
Engines	84.96	82.60	165.26	161.11
LFC System	71.84	30.04	32.46	32.41
Total	214.11	166.59	286.06	279.35

As discussed in section 8.2.2, the consideration of maintenance requirements had a significant influence on the selection of design details for the final study aircraft. In addition to minimizing the number of LFC suction units and simplifying overall LFC system design, the final study aircraft are configured to facilitate maintenance of both the LFC system and basic aircraft system components. For example, the frequency of fuel system component maintenance makes it imperative that access provisions be provided for all fuel system components located in the wing. The final study aircraft provide such access. Removal of LFC surface panels is required only for major fuel cell maintenance and inspection of the basic wing structure.

The relatively low maintenance requirements of the LFC systems are a direct result of recognizing the maintenance peculiarities of LFC aircraft configurations.

9.4 OPERATIONAL CONSIDERATIONS

Essentially all potential in-flight problems attending the routine operation of LFC aircraft arise from the interaction of the LFC suction surfaces and the flight environment. While aerodynamic smoothness of the wing surface is necessary for the efficiency of any aircraft, it is of critical importance for aircraft with laminarized surfaces. Assuming that the smoothness criteria outlined in section 6.0 are satisfied during the production of the LFC surfaces, preventing surface contamination or the in-flight removal of such contamination becomes the primary operational consideration.

This section discusses allowable surface roughness for LFC aircraft, the source of surface contamination, potential solutions to contamination problems, and the penalty which results from in-flight LFC system loss.

9.4.1 PERMISSIBLE ROUGHNESS HEIGHT

The effect of surface roughness on boundary-layer behavior is the creation of vortex-like disturbances. Depending on the relation between the magnitude of the irregularity and the appropriate Reynolds number, these disturbances may be either damped or undamped. The undamped disturbances ultimately result in boundary-layer transition, with an accompanying increase in section drag.

Determination of the permissible roughness height as a function of flight and airfoil parameters was the subject of rather extensive investigations in the 1945-1965 period. However, very little effort has been expended in this area during the past decade. In the available literature, two different approaches are used in defining the allowable surface roughness. The procedure reported in references 15 and 32 expresses the permissible height of surface roughness elements in terms of the unit Reynolds number, R_N , and generally does not consider the influence of chordwise location of the element on permissible height. A more exact determination, reported in references 33 through 39, relates the permissible roughness height to a critical roughness Reynolds number,

$$R_k = \frac{u_k k}{\nu_k}$$

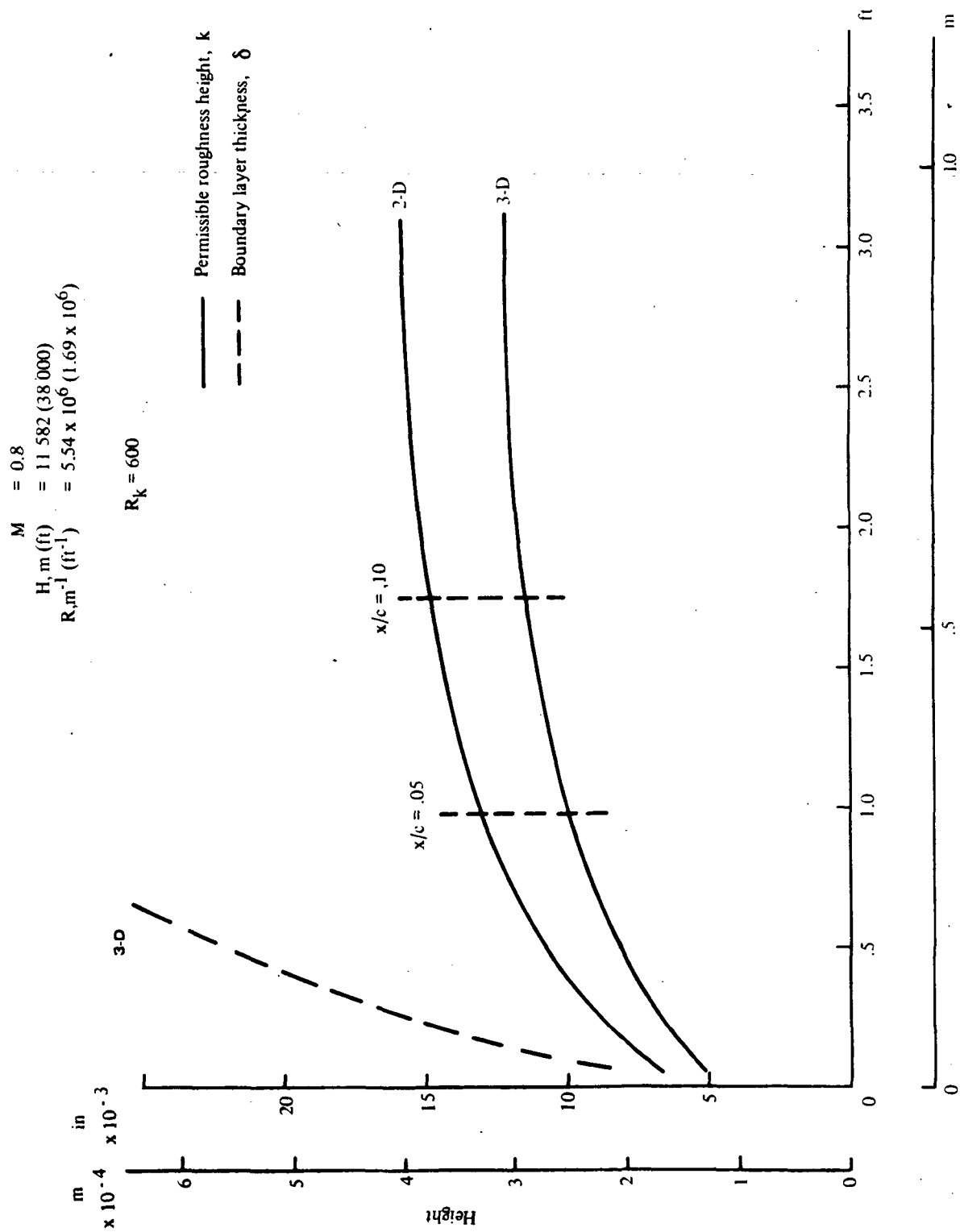
It is the consensus of these investigations that, if the roughness is sufficiently submerged in the boundary layer to permit substantially linear variation of the boundary-layer velocity up to the height of the roughness element, turbulent spots begin to appear immediately behind the element when R_k exceeds a critical value.

The variation of R_k with Reynolds number, airfoil section, and element fineness ratio was measured experimentally in references 34, 37, and 38. For a fineness ratio of one, values of R_k range from 250 to 680 for the airfoil sections investigated at high subsonic cruise speeds. These and other experimental data are summarized in references 35 and 36 and indicate that $R_k = 600$ is an appropriate value for the flight conditions of this study for isolated two- and three-dimensional roughness elements.

Based on the procedures outlined in reference 35, permissible roughness heights corresponding to the flight conditions for the study aircraft were calculated for a value of $R_k = 600$. These data, including an evaluation of the boundary-layer thickness, are presented in figure 193. For three-dimensional flow, permissible roughness heights range from about 1.27×10^{-4} m (0.005 in) at the stagnation point to about 3.05×10^{-4} m (0.012 in) at a point 0.61 m (2 ft) along the airfoil surface.

In reference 40, the effect of multiple roughness elements was investigated experimentally. It was found that multiple spanwise elements did not affect permissible roughness height if the spacing was greater than three element diameters. Multiple streamwise elements provided favorable interference when element spacing was less than four element diameters with a resultant increase of 20% in R_k . For spacing greater than four diameters, the unfavorable interference results in a 10% decrease in R_k .

Laminarization of the boundary-layer through the use of area suction appears to have little effect on permissible roughness height. As reported in reference 41, experiments conducted using area suction on a NACA 64A010 airfoil with a sintered bronze porous surface showed a relatively small increase in the size of the roughness element required to cause transition as compared to that of the airfoil without suction.



Surface distance to roughness element, s

Figure 193. — Permissible roughness height

9.4.2 SURFACE CONTAMINATION

While LFC surfaces are subject to contamination during both ground and flight operations, the procedures outlined in Section 9.3 are considered to be adequate for preventing or removing surface contamination encountered during airport operations. In-flight contamination, which includes natural roughness due to insects, moisture, and ice crystals, is addressed in the sections which follow.

9.4.2.1 Insects

There is great uncertainty in the magnitude of the problem presented by insects in the routine operation of LFC aircraft. While extensive data have been generated analytically and experimentally to illustrate the adverse effects of insect accumulation on laminar flow, little data are available which define the problems encountered in a realistic flight environment. In addition, the conclusions inferred by existing flight data are generally in poor agreement. For example, reference 42 reports the existence of a serious insect contamination problem and considers this to be one of the most difficult practical problems in employing laminar-flow wings. On the other hand, reference 9 minimizes the problems presented by insect accumulation in extensive flight testing of the X-21A.

A quantitative evaluation of the insect problem as it relates to the aircraft of this study will require extensive flight investigation and is thus well beyond the scope of the current effort. However, available data which are helpful in assessing the scope of potential problems are discussed below.

Nature of the Aerial Insect Population — In evaluating the probability of the formation of roughness due to insects, the primary considerations are the vertical dispersal of the insect population, the frequency with which insects of various sizes are encountered, and the probability that the insect will rupture upon encounter. Therefore, both entomological and meteorological factors must be considered.

The primary entomological factors influencing the accumulation of roughness are the size and rupture velocity of insects. Both of these characteristics obviously vary over a wide range as a function of the species considered. Figure 194 is a histogram of insect size in the aerial population near the ground. This figure and all other relevant data show that the great majority of insects are small. Experiments performed in both wind tunnels and the field have found insect rupture velocities ranging from 1.01 m/s (22.5 mi/hr) to 2.01 m/s (44.9 mi/hr) (ref. 43). The mean value of the minimum rupture velocity was found to be 1.09 m/s (24.3 mi/hr).

Rather extensive investigations of the impact of meteorological variables on the aerial insect population have yielded consistent correlations with regard to temperature, wind velocity, and altitude, (ref. 43, 44), but have not provided consistent data for variations in humidity, barometric pressure, light intensity, precipitation, or the electrical state of the atmosphere.

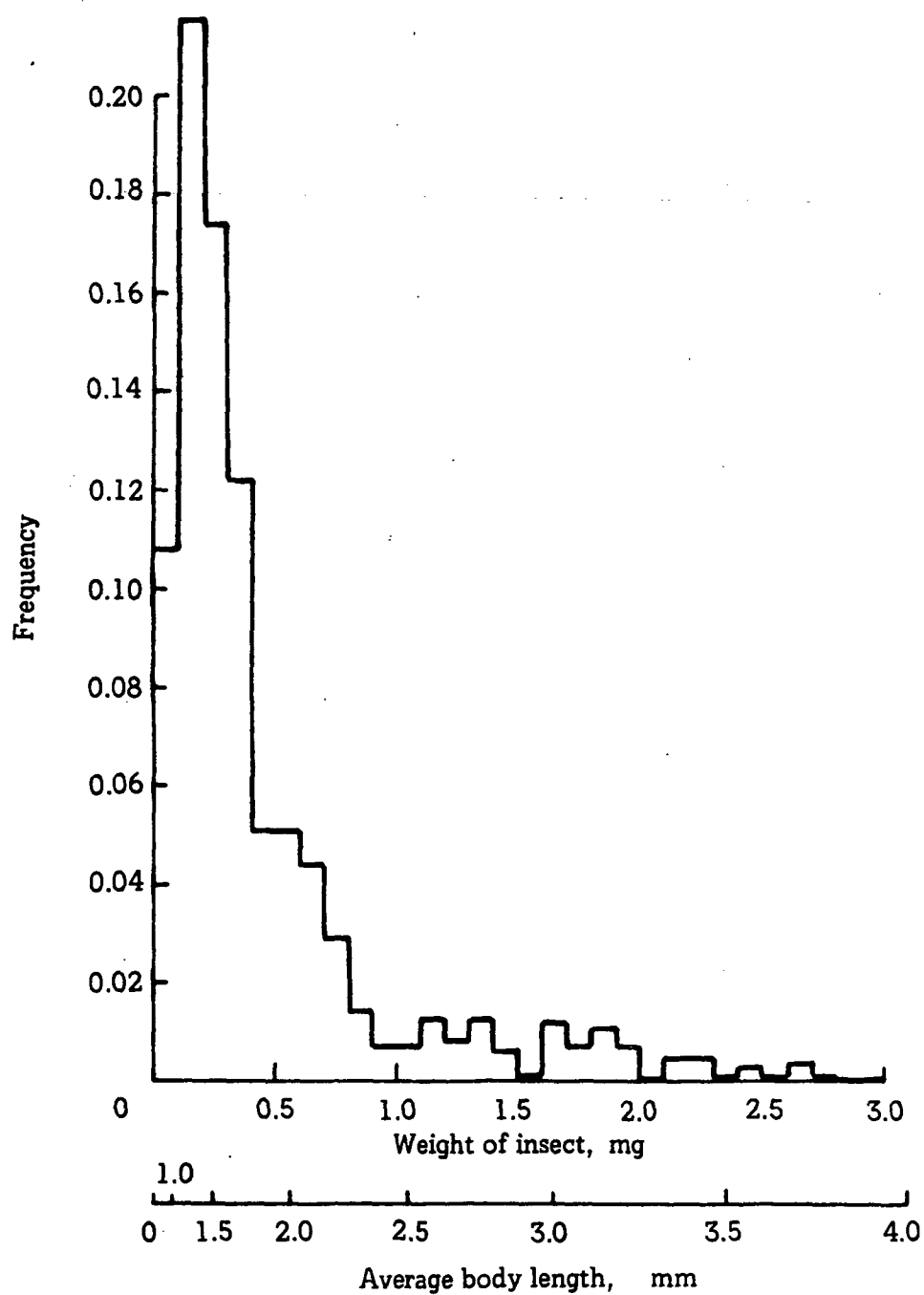


Figure 194. — Histogram of insect size in the aerial population near the ground

However, for selected geographical regions and climates, the available data provide an adequate definition of the characteristics of the airborne insect population. Figures 195, 196, and 197, illustrate effects of temperature, wind velocity, and altitude on the relative airborne insect population.(ref. 43).

Greater insight into the nature of the population density is provided by the data of table 39.

TABLE 39. MEAN INSECT SEPARATION DISTANCES

Altitude, m (ft)	Mean separation distance, m (ft)			
	Ref 45 Ref 46		Ref 47	
0	4.9	(16)	4.3	(14)
76.2 (250)	9.8	(32)	6.1	(20)
152.4 (500)	12.5	(41)	6.7	(22)
304.8 (1000)	14.9	(49)	7.6	(25)

Based on available data, the following is a summary of pertinent entomological and meteorological factors affecting the accumulation of roughness due to insects:

- (1) The great majority of the aerial insect population is very small, ranging in length from 1 to 3 mm (0.04 to 0.12 in).
- (2) The majority of the aerial insect population is relatively fragile, having a mean rupture velocity of 1.09 m/s (24.3 mi/hr).
- (3) The aerial insect population is greatest when the ground-level air temperature is about 25°C (77°F) and the wind velocity is from 0.27 to 0.54 m/s (6 - 12 mi/hr).
- (4) While there is a finite insect population at altitudes as great as 1524 m (5000 ft), approximately 90% of the insect encounters can be expected at altitudes below 304.8 m (1000 ft).

Geometrical Characteristics of Roughness Due to Insects – The primary geometrical considerations of interest in evaluating roughness resulting from insect accumulation are the chordwise extent of roughness and the roughness height.

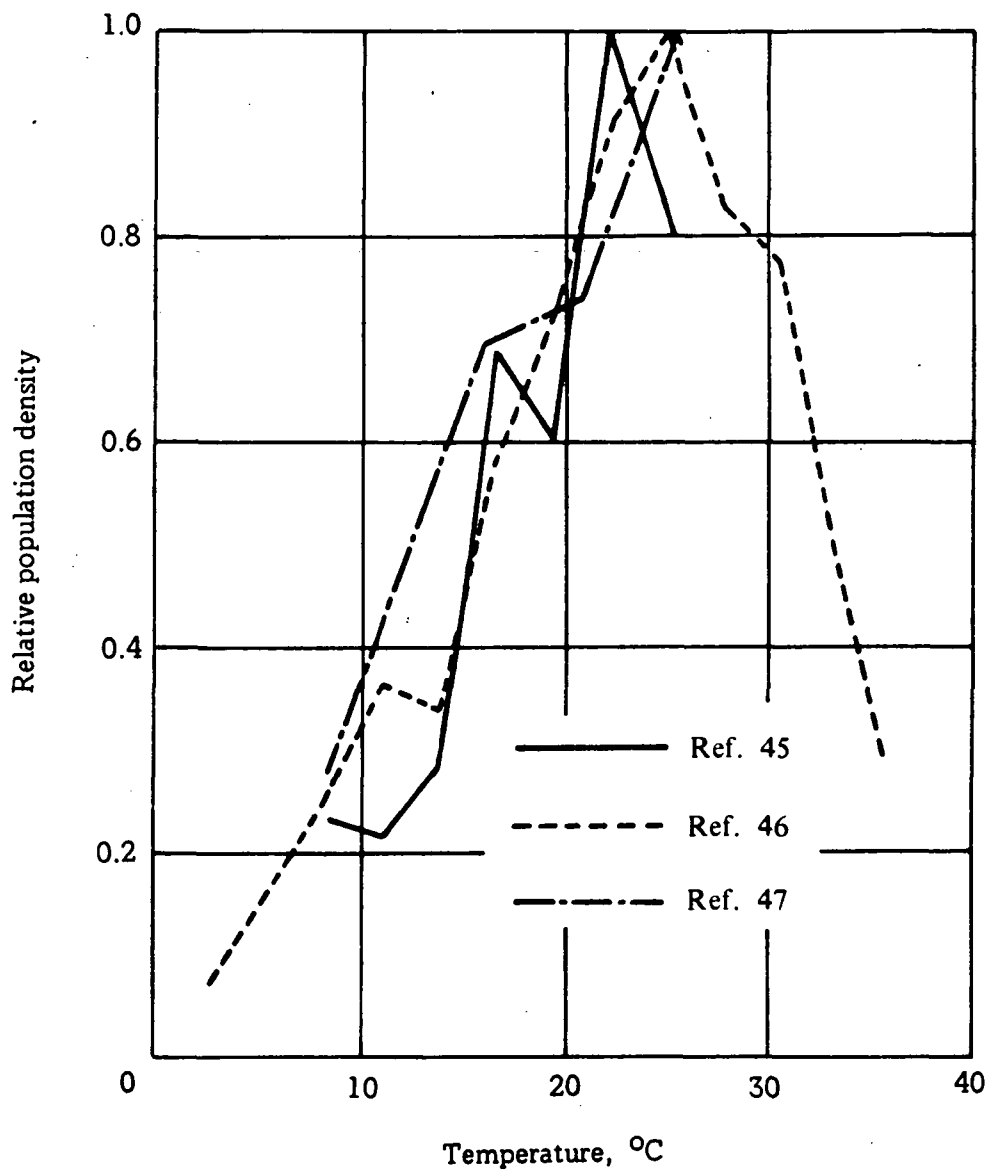


Figure 195. — Effect of air temperature on density of insect aerial population

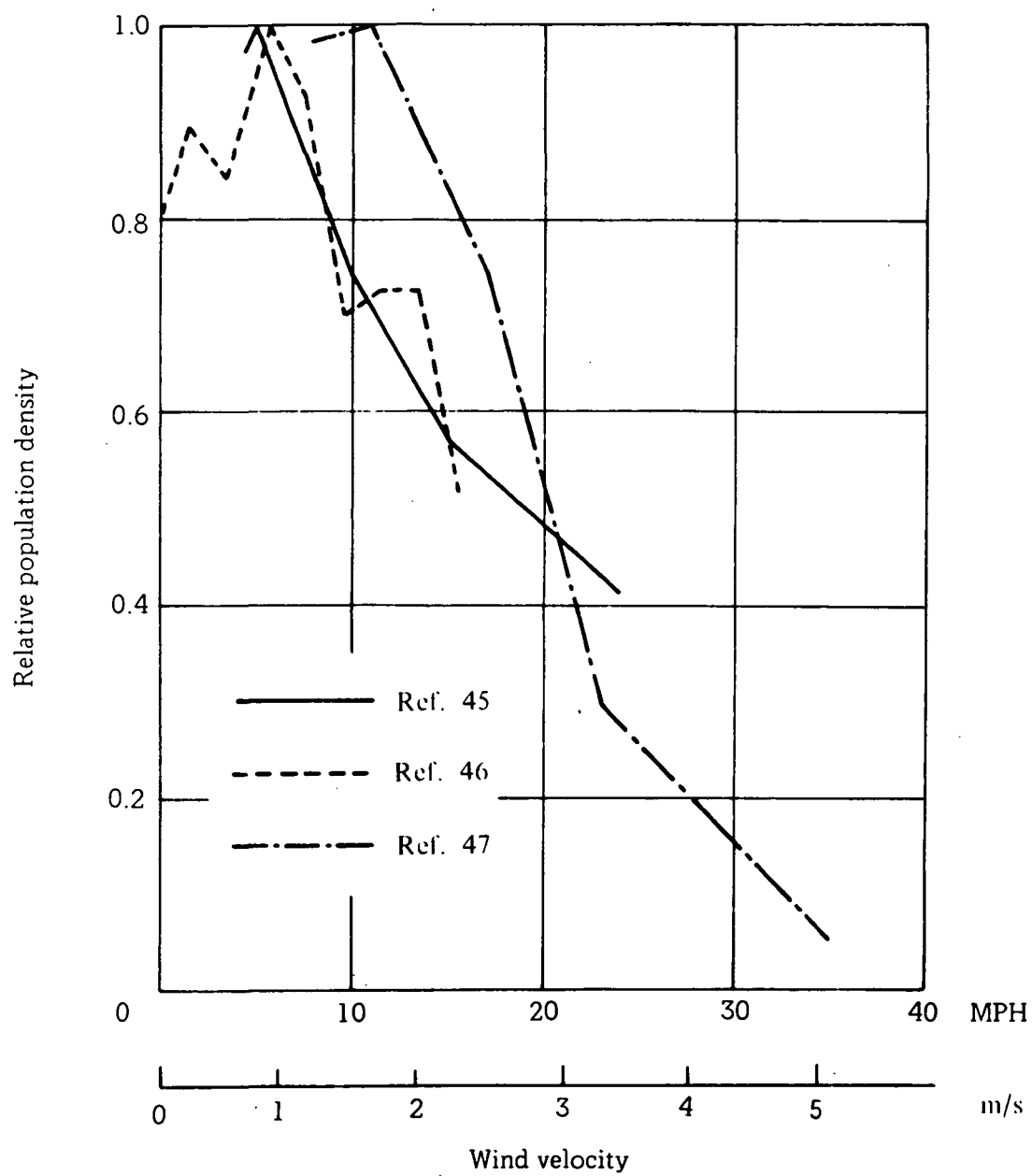


Figure 196. — Effect of wind velocity on density of insect aerial population

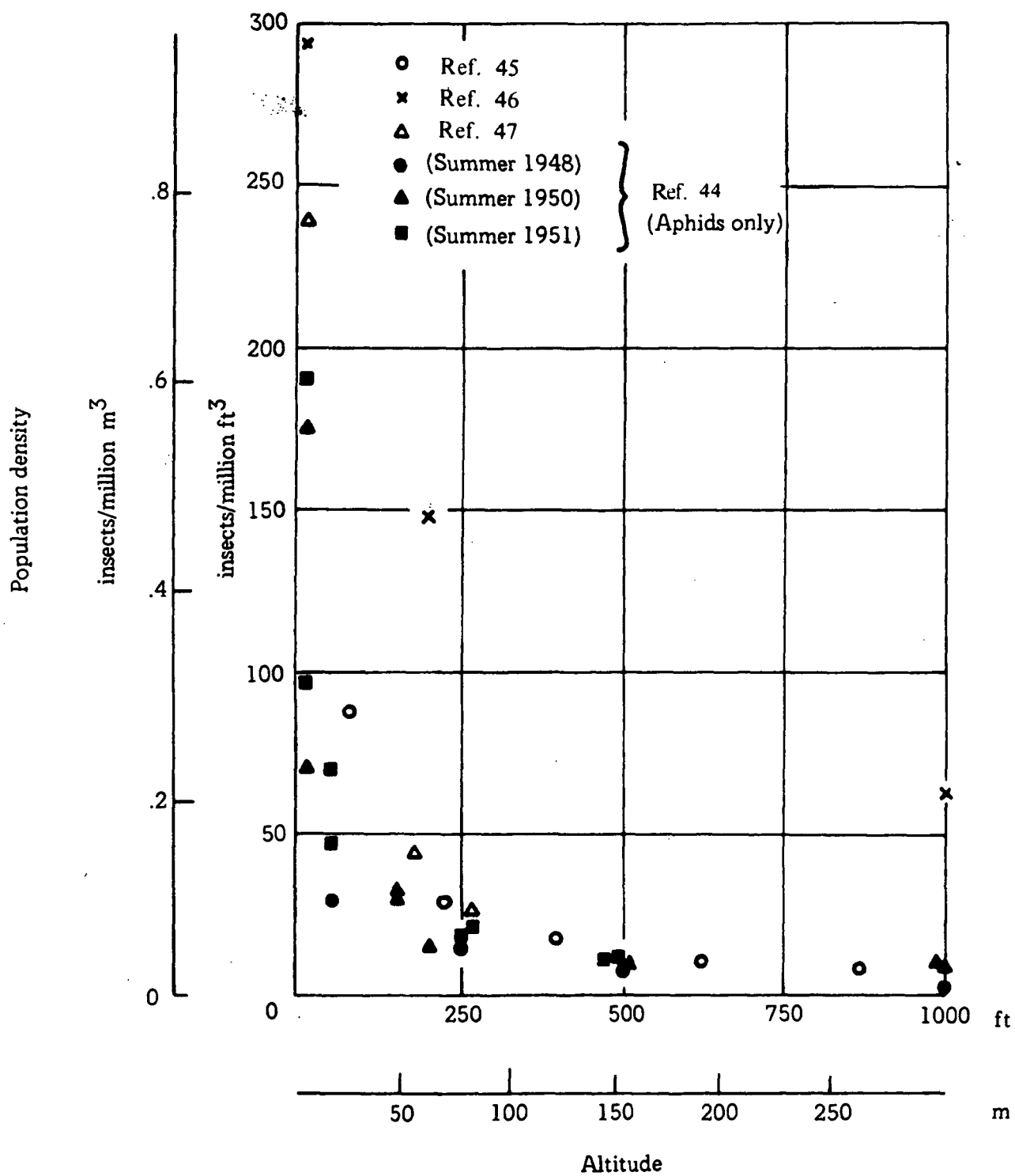


Figure 197. — Vertical distribution of insect aerial population density

Natural roughening is essentially a two-dimensional process (ref. 43). The maximum chordwise extent of roughness is a function of the airfoil geometry, the airfoil incidence angle, and the flight speed. While no applicable data exist for the modified supercritical airfoil section used in the current study, data from reference 48 are indicative of the chordwise accumulation of roughness for representative airfoil sections.

Figure 198 illustrates the chordwise extent of roughness for both upper and lower wing surfaces for varying wing incidence angles. For the range of wing incidence angles corresponding to the takeoff and initial climb phases of flight, this figure shows that the extent of roughness is limited to about $x/c = 0.05$ on the upper surface. However, roughness could extend well beyond $x/c = 0.30$ on the lower surface for high-performance aircraft.

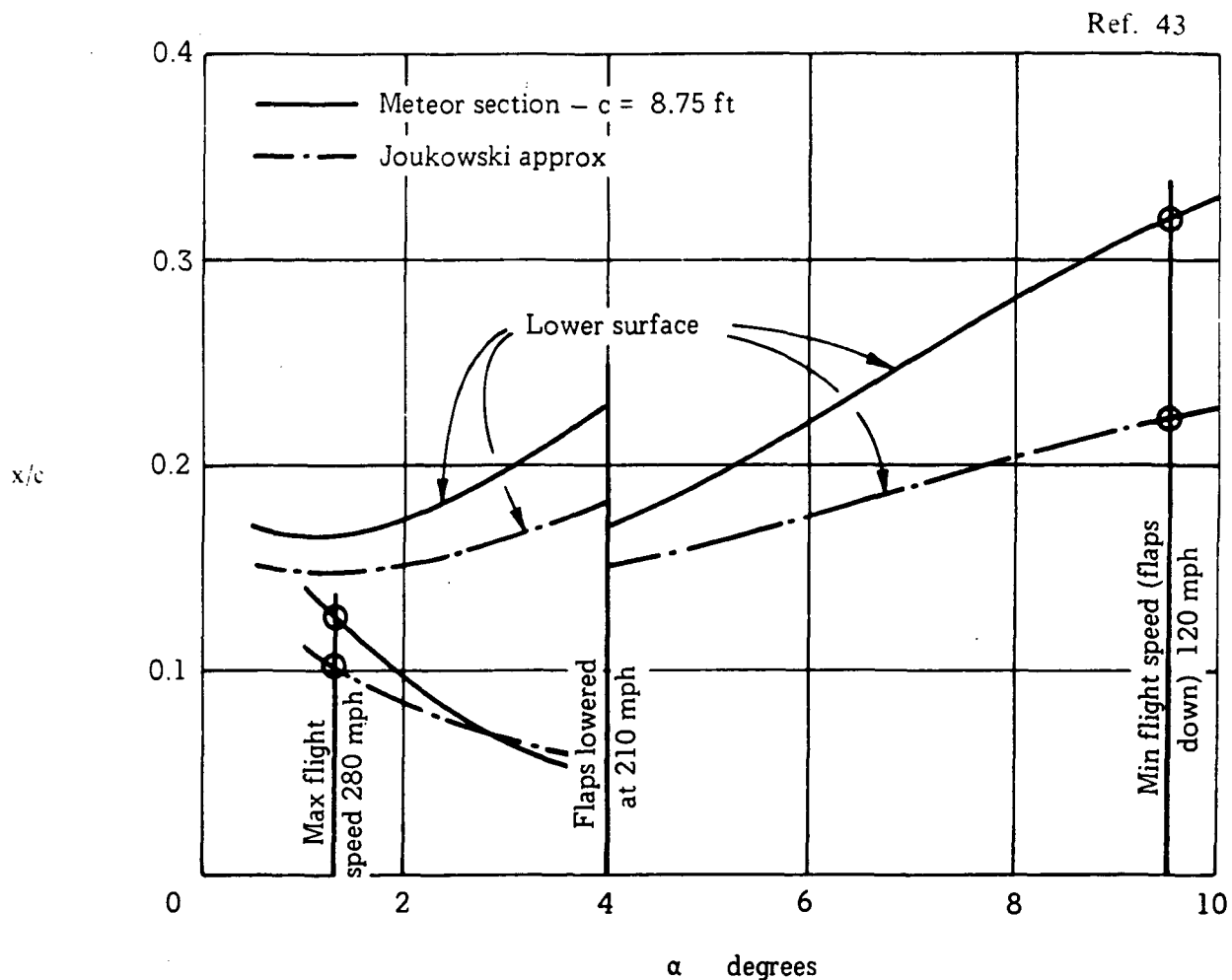


Figure 198. — Calculated chordwise variation of contamination over the normal range of incidence occurring in flight

C-5

Roughness height as a function of wing incidence angle is shown in figure 199 for a NACA 66-009 airfoil. This figure shows that greater incidence angles result in roughness extending to greater values of x/c and a decrease in the maximum roughness height. Figure 200 illustrates the effect of airfoil thickness on the accumulation of roughness. Generally, thinner airfoil sections are subject to a somewhat smaller accumulation of roughness in the leading-edge region, but accumulate roughness farther back on the wing. In all cases, the greatest accumulation of roughness is very near the forward stagnation point and decreases rapidly with increasing x/c .

Following is a summary of pertinent aspects of the geometrical characteristics of roughness due to insects:

- (1) The accumulation of roughness due to insects is essentially a two-dimensional process.
- (2) The greatest accumulation of roughness is near the forward stagnation point of the wing.
- (3) For practical flight conditions, the chordwise accumulation of roughness is limited to about $x/c = 0.05$ on the upper wing surface and $x/c = 0.40$ on the lower wing surface.

Relevance to the Study Aircraft – In applying the data of the preceding discussions to the aircraft configurations of this study, the following observations are pertinent:

- (1) The data defining the qualitative and quantitative characteristics of the aerial insect population are both limited and quite old. They are not considered to provide a comprehensive definition of the insect population as it exists in the vicinity of international airport facilities of 1985. For example, the influence of jet noise and jet exhaust on the insect population is not considered in the available data.
- (2) The airfoil sections for which data are available to define the influence of geometrical variables on insect accumulation are quite different from the modified supercritical section used on study aircraft. However, the general trends illustrated by these data are considered to be applicable.
- (3) The available insect accumulation data are primarily a result of an artificial wind-tunnel environment. Therefore, the qualitative aspects of these data are definitive, but the absolute magnitude of the accumulation problem is not representative of a realistic flight environment.

Assuming that the available data are generally valid, long-range, high-altitude aircraft of the type considered in this study are subject to insect accumulation only during operations below 304.8 m (1000 ft). Thus, only the takeoff, initial climb, terminal descent, and landing phases of the flight

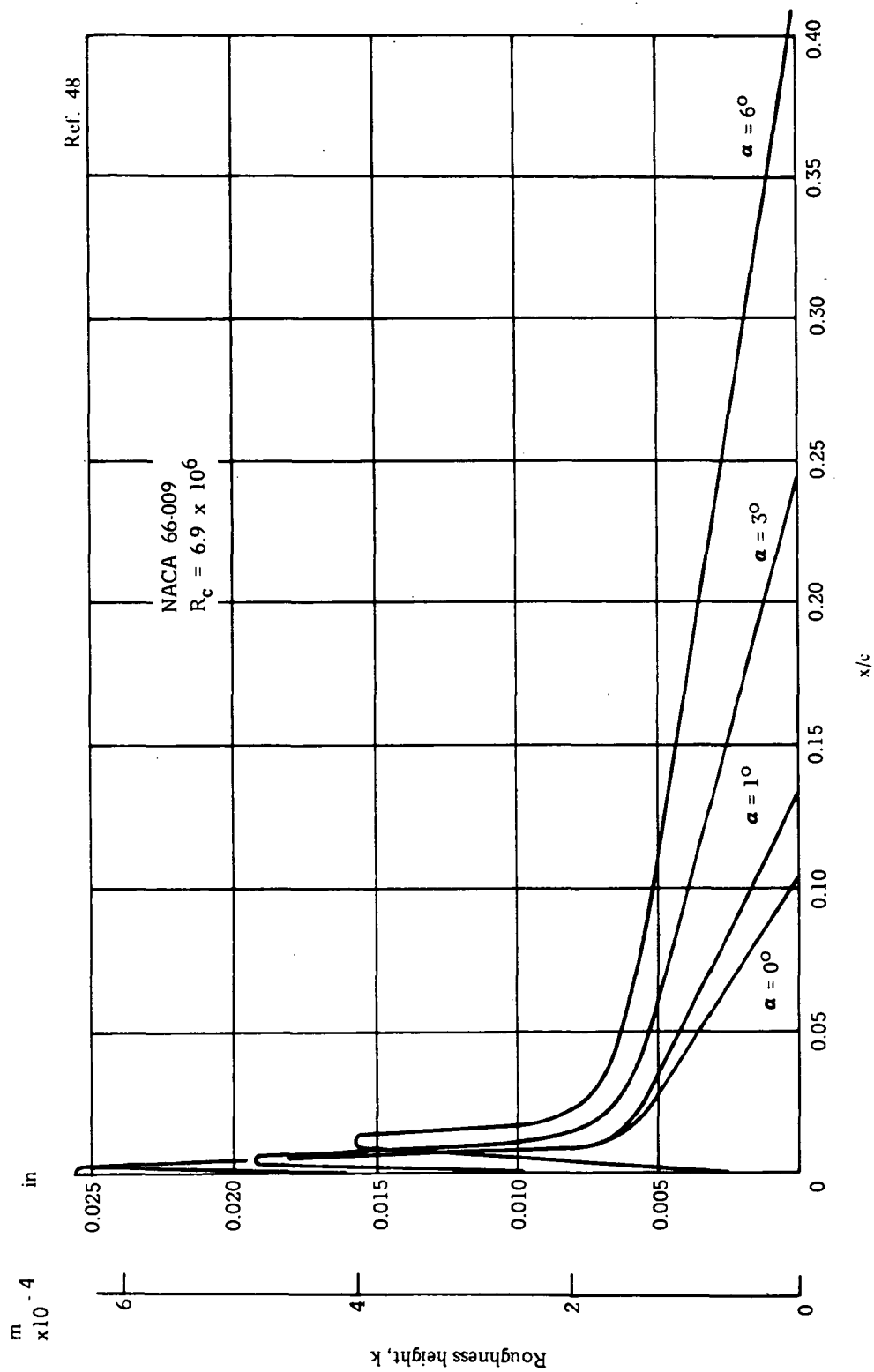


Figure 199. — Effect of incidence on lower surface roughness envelope

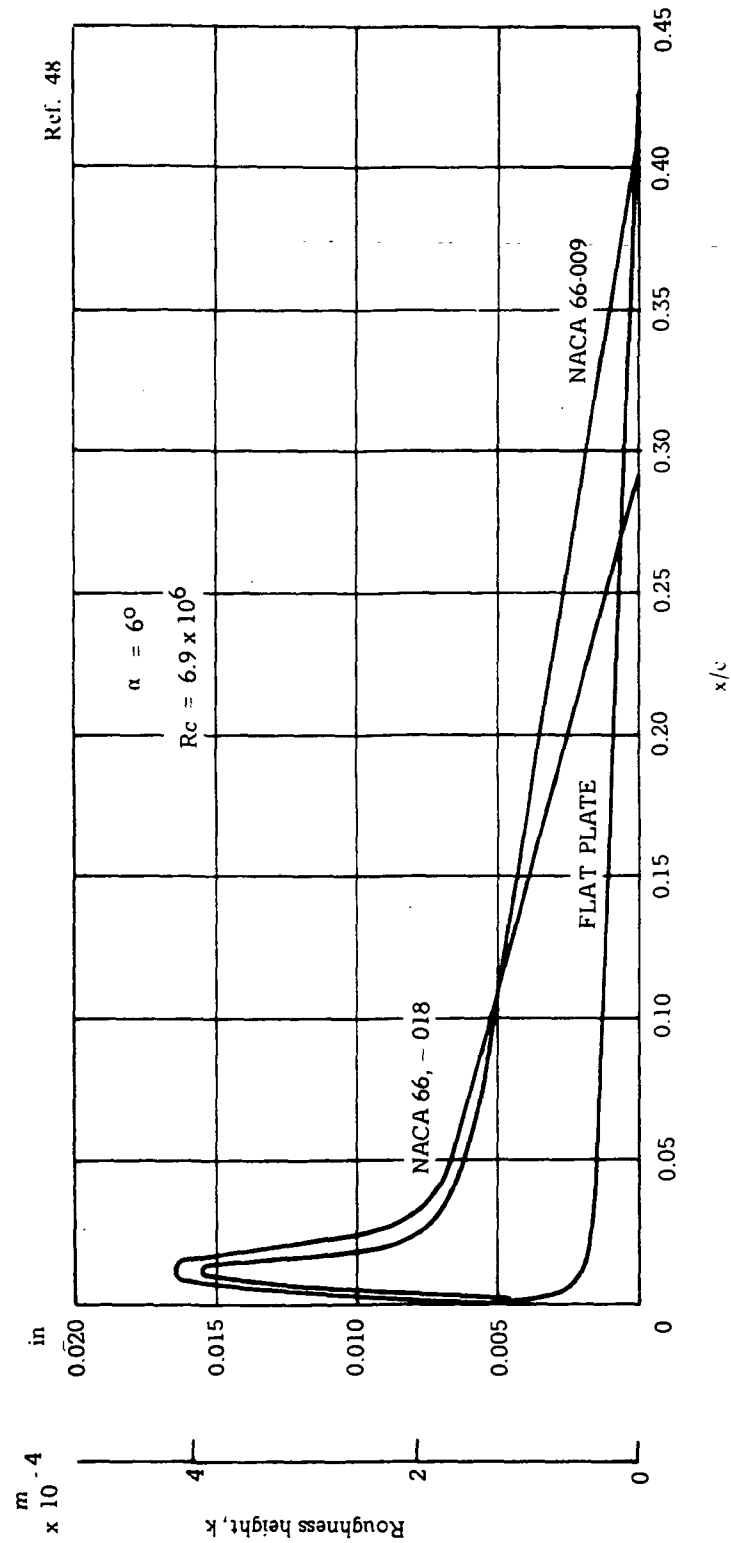


Figure 200. — Effect of wing profile on the lower surface roughness envelope

are subject to potential insect accumulation. Since cleaning the wing leading edge and LFC surfaces is considered to be a part of normal postflight operations, only the takeoff and initial climb portions of the flight result in insect accumulations with potential impact on aircraft flight performance.

The following outlines the performance of the 200-passenger LFC study aircraft during the normal takeoff and climb through the zone of potential insect contamination.

	Cumulative time, sec	Cumulative flight distance, m (ft)	
Ground roll	59.0	2700	(8861)
Climb to 10.6 m (35 ft)	64.8	2975	(9762)
Climb to 304.8 m (1000 ft)	108.3	6495	(21,308)

The LFC aircraft of this study are thus subject to insect contamination only during the first 108.3 sec or 6495 m (21,308 ft) of the flight.

Based on the data of figures 195 and 196, it is clear that a significant aerial insect population exists for a relatively small range of temperature and wind velocity. When meteorological conditions favoring a high-aerial insect population do exist, the above performance data in conjunction with the data of figure 197 permit estimation of the number of insect encounters per flight. The data of reference 47, representative of operations during daylight hours in summer in a temperate climate indicate that an aircraft of the size and performance considered in this study would be subject to 200 to 750 insect encounters per flight.

Figure 201, which combines the roughness height data of figures 199 and 196 with the permissible roughness height defined by figure 193, shows that the permissible roughness height may be exceeded forward of about $x/c = 0.03$. However, limited flight test data reported in reference 43 indicate that, for flight conditions similar to those of this study, the height of roughness due to insects may be more than halved near the leading edge and is completely removed aft of $x/c = 0.04$ through erosion of the contamination. Assuming the validity of these data, the resultant roughness height of about 1.73×10^{-4} m (0.007 in) at $x/c = 0.02$ shown in figure 201 for an incidence angle of 0.10 rad (6 deg) is very near the permissible roughness height at that location.

There is sufficient uncertainty in both the nature of the aerial insect population and the geometrical features of insect contamination on the airfoil of this study to preclude a definitive assessment of potential insect contamination problems. However, if the problem does exist, it appears to be minimal and is amenable to solution through the techniques discussed in succeeding sections.

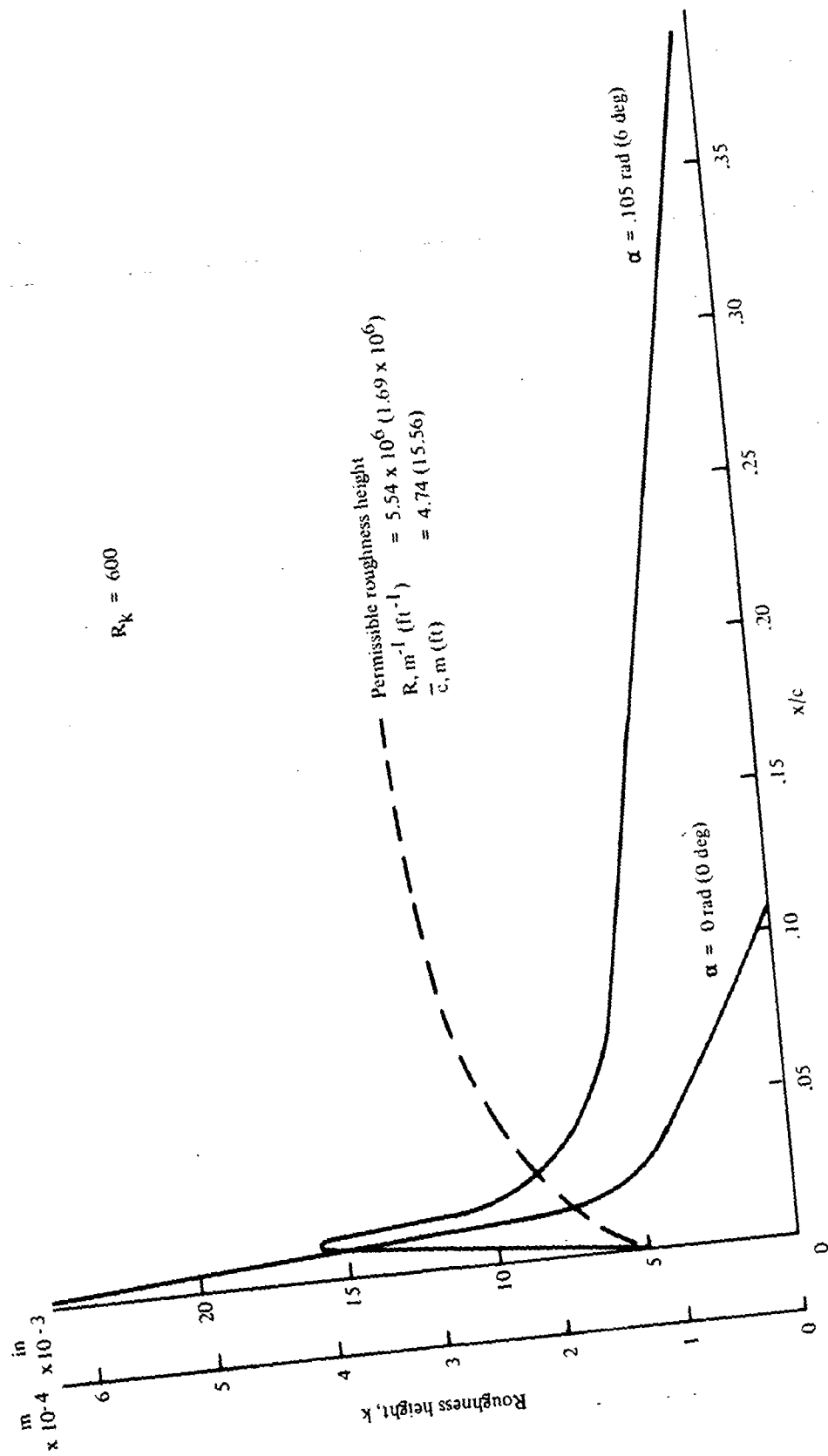


Figure 201. — Comparison of permissible and estimated roughness heights

Inflight Removal of Contamination – A variety of methods have been proposed for eliminating the roughness resulting from insect accumulation. Such methods, which are discussed extensively in reference 43, include the following:

- (1) Mechanical scrapers, which shear or scrape the deposits from the surface.
- (2) Deflectors shaped to act as traps to catch insects before they strike the surface or to deflect the insects away from the surface.
- (3) Leading-edge covers of paper, fabric, or other suitable material, which are attached to the surface before each flight and torn away after the aircraft is above the insect zone.
- (4) Leading-edge covers composed of substances which may be dissolved in flight by the discharge of a suitable solvent.
- (5) Leading-edge covers of materials which may be removed thermally, either by reduction to the molten state or by total combustion.
- (6) A layer of highly viscous fluid applied to the leading edge before flight in which insects are trapped and subsequently carried away under the shearing action of surface flow.
- (7) Liquids which are discharged over the surface continuously or intermittently to wash away the deposits as they form.
- (8) Removal of the turbulent boundary layer and the restoration of laminar flow by a suction slot located downstream of the critical region.

An additional scheme, proposed by Wortman in reference 49, employs a leading edge cover of elastic material to reflect insects upon impact and thereby prevent rupture and the attendant contamination. However, due to the erosion characteristics of suitably elastic materials, this method is not suitable for flight speeds above $M = 0.60$. In addition, the method is not adaptable to aircraft with highly-swept wings requiring suction near the stagnation point.

Fairly limited testing has been conducted for all of the methods outlined above, with the result that methods (7) and (8) appear to offer the greatest potential for a practical aircraft operating environment.

In method (7), water with about 5% by volume of detergent is discharged at a low rate of flow from small orifices in the leading edge of the wing while the aircraft is traversing the insect zone. Preliminary tests have shown that about 4.14 kg/m^2 (0.85 lb/ft^2) of water per minute is required to

keep the surface clean. For the 200-passenger study aircraft, to keep the region forward of $x/c = 0.03$ clean for the 1.8 minutes required to climb through the insect zone, the weight of water required is 451 kg (990 lb). Associated plumbing and storage tanks weigh about 45 kg (100 lb), for a total weight penalty of 496 kg (1090 lb). This represents less than one percent of the aircraft empty weight.

Method (8) involves the use of a suction slot immediately behind the roughened area to remove the turbulent boundary layer and thereby restore laminar flow. The limited experimental data available indicate that laminar flow can be restored if the surface is sufficiently smooth behind the suction slot. If the chordwise extent of roughness is greater than $x/c = 0.10$, the boundary layer thickness increases to the point that suction requirements become very large. For this condition, the associated suction system weight and fuel penalty may preclude the use of this method. However, if natural erosion is assumed to remove contamination behind the $x/c = 0.04$ position, this scheme may prove to be attractive in that it requires a relatively minor modification of the aircraft LFC system.

In addition to the methods outlined in the literature, two schemes for eliminating the insect contamination problem were developed as a part of the current study. Figure 202 illustrates two mechanical devices which remove accumulated surface roughness by rotating a clean leading edge into position after the aircraft traverses the insect zone. Manufacturing and maintaining these devices would be relatively costly due to the stringent smoothness requirements of the joints. These designs are further complicated by the limited volume available in the wing. However, it is anticipated that such problems are amenable to solution through the application of appropriate design efforts.

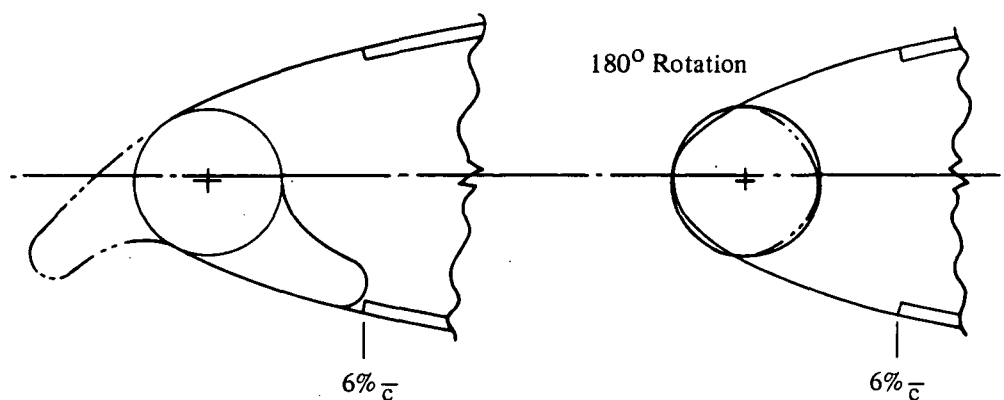


Figure 202. — Mechanical leading-edge devices for removal of insect contamination

Of all of the schemes devised for elimination of the insect contamination problem, perhaps those afforded by recent advances in materials technology offer the greatest promise. Recent advances in developing bonding techniques for Teflon and Tedlar films may permit the use of such materials as permanent leading-edge covers on LFC aircraft. Even greater potential lies in the application of hydrophobic compounds to LFC surfaces. The use of such surface conditions is supported by the requirement to reduce the exposed surface "wettability" or the tendency of foreign substances to adhere to the surfaces. The more wettable a surface, the lower the surface energy or adherence.

The duration of hydrophobic character of a water-repellent coating or film on a surface is measurable by the time that the coating or film will cause water or another liquid to form into separate small droplets on a coated surface rather than spreading in a continuous film over the coated surface. A qualitative measurement of the extent to which a solid surface is wetted by a liquid is provided by measuring the contact angle, which is the angle between the surface and the tangent to a drop of liquid where the drop intercepts with the surface.

A contact angle of 0 to 0.087 rad (5 deg) indicates that a surface is completely wettable by a liquid. Surfaces with a contact angle greater than 1.484 rad (85 deg) are generally referred to as being good water repellents, and surfaces with contact angles greater than 1.658 rad (95 deg) are considered to be excellent hydrophobes.

New long-life organosilicone rain-repellent coatings have been developed for use primarily on aircraft windshields and canopies (ref. 31). The synthesis of new rain-repellent compounds were based on current theories and mechanisms of compounds which are capable of forming a hydrophobic surface and of adhering satisfactorily to various substrates, particularly glass and plastics. The newly synthesized tin-silicone chelate type resins, alkyl-thiosilyl resins, and alkyl chlorosilanes partially hydrolized with isopropanol, exceed all presently known rain-repellent materials in hydrophobic properties and performance.

While an experimental investigation of these compounds for this application is necessary, current data indicate that these compounds may solve the insect contamination problem and facilitate general LFC surface maintenance simultaneously.

The following observations summarize the insect contamination problem as it applies to the LFC aircraft of this study.

- (1) It is not possible to state with certainty whether such a problem exists. Natural erosion of a accumulated insects may reduce roughness height to a level compatible with laminar flow.
- (2) If removal of insect contamination is required, any one of the following methods may be adapted to the requirements of the study aircraft:

- o Discharge of cleaning solution through orifices in the leading edge.
- o Restoration of laminar flow by a suction slot located downstream of the contamination.
- o Mechanical leading-edge devices.
- o Leading-edge coating of materials with very low surface adhesion.

9.4.2.2 Other Surface Contaminants

Since LFC aircraft are designed for cruise at relatively high altitudes and the LFC system is operated only during cruise conditions, the only surface contaminants likely to be encountered are clouds of ice crystals. Flight test data (ref. 7) show that if the particle size and density exceed critical limits in the case of water droplets in visible clouds or ice particles in high cirrus clouds, temporary partial or complete loss of laminar flow can occur. Laminar flow is regained immediately when the aircraft returns to clear air. Figure 203, taken from reference 50, illustrates the sensitivity of the laminar flow control system of the X-21A to size and density of suspended ice particles.

Studies conducted by the USAF and reported in reference 8 indicate that clouds of sufficient density to affect LFC operation exist a small fraction of the time at cruise altitudes appropriate for LFC aircraft. Figure 204 illustrates the percentage of flight time in clouds for routes representative of international commercial operations. For the majority of the flight routes, visible clouds exist for less than 6% of the flight time. On flights over tropical regions clouds exist for as much as 11% of the flight.

9.4.3 EFFECT OF IN-FLIGHT LFC SYSTEM LOSS

Figure 205 shows the decrease in the range capability of LFC-200-R as a function of the percent of total mission time for which the LFC system is ineffective. In generating the data for this curve, it was assumed that LFC system loss occurred at small intermittent intervals during the entire mission and that the LFC system remained in operation during the ineffective periods. Thus, fuel flow to the LFC suction units continued throughout the flight.

Existing data indicate that sufficient moisture exists at the flight altitude of interest to influence LFC system effectiveness 0.5% to 11% of the time, depending upon the season and the route flown. Thus, the maximum loss of range due to atmospheric moisture is about 222 km (120 n mi) for the study aircraft. Figure 205 also shows that, even if the LFC system is lost for 50% of the mission as a result of system failure, the loss of range capability is only 926 km (500 n mi).

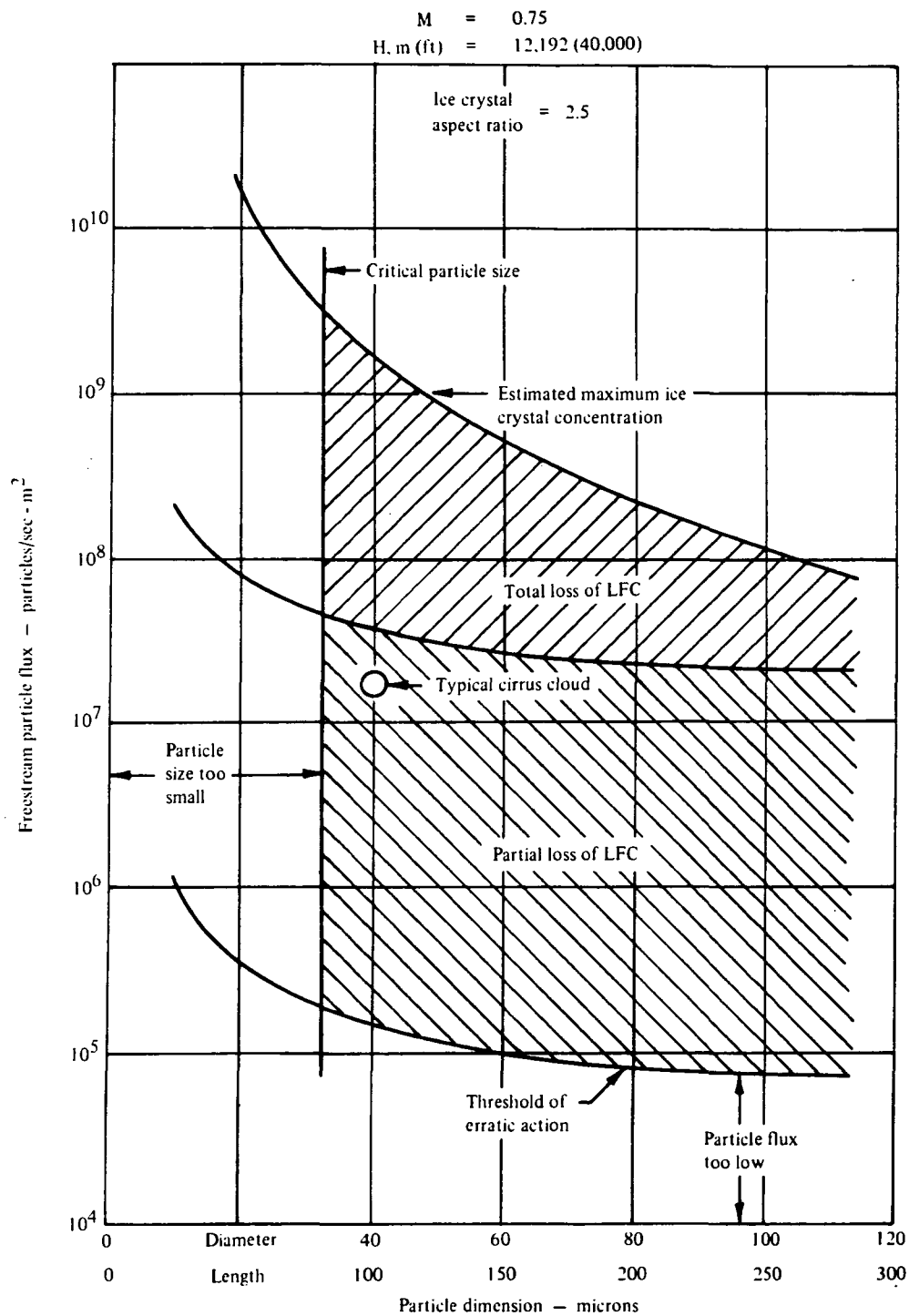


Figure 203. — Effect of ice crystals on LFC operation

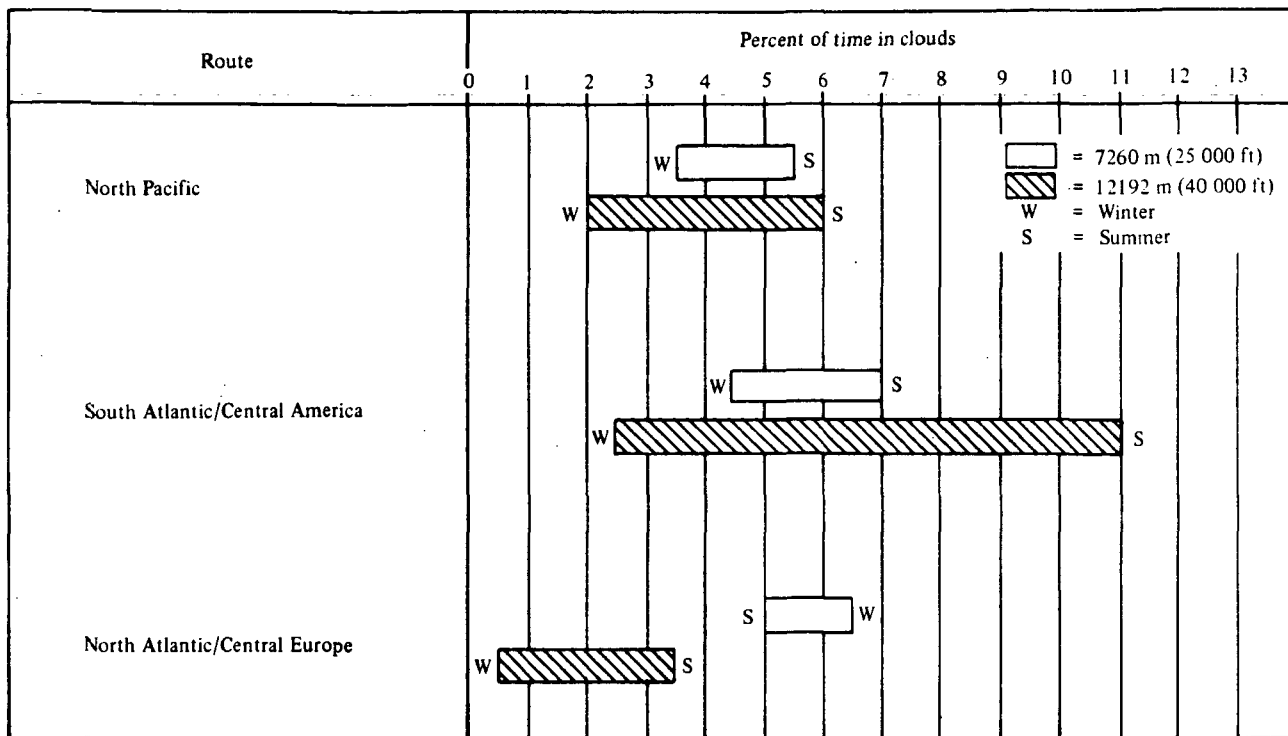


Figure 204. — Aircraft visible-cloud time

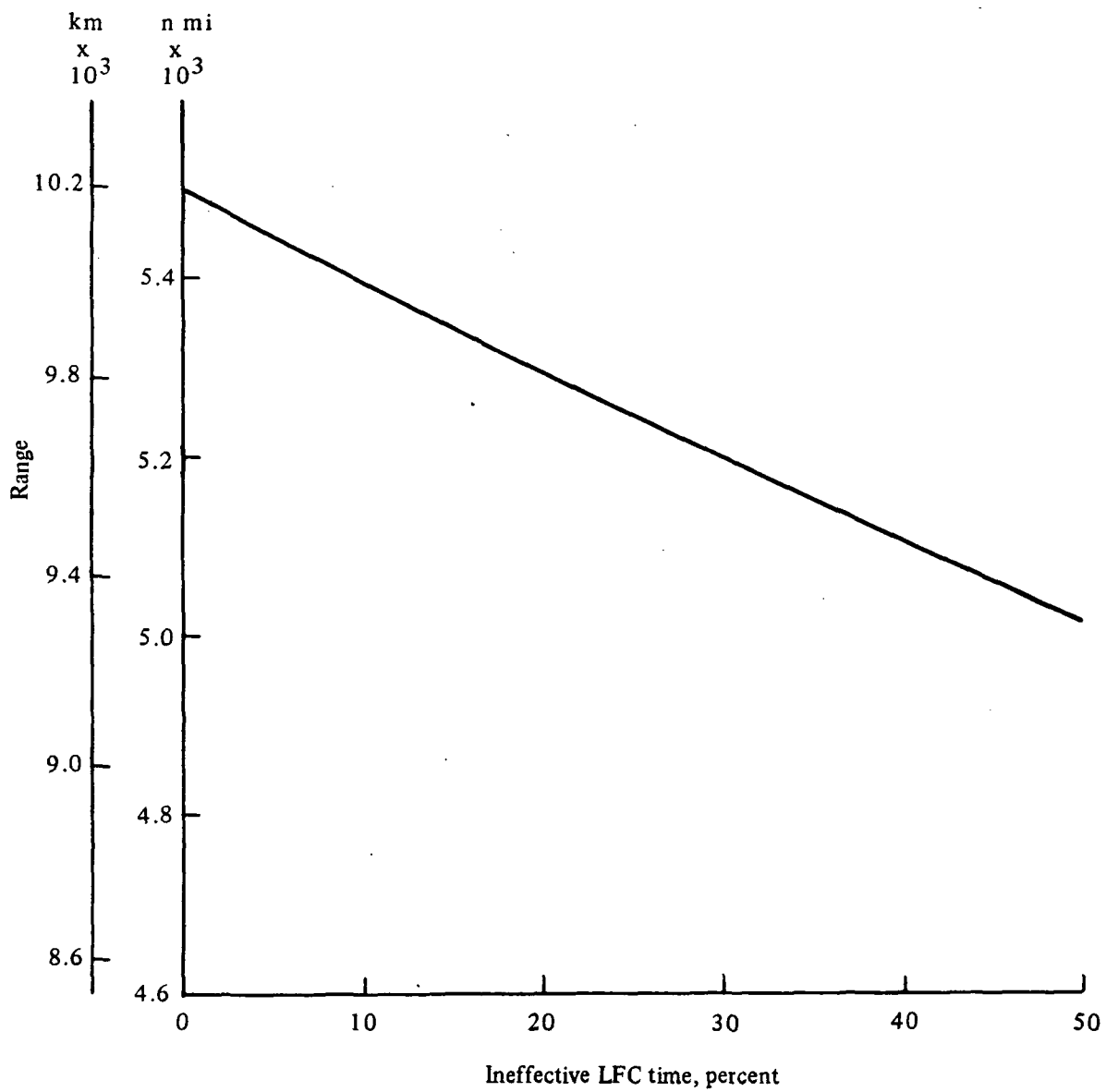


Figure 205. — Effect of LFC system loss on range capability, LFC-200-R

10.0 TF CONFIGURATION DEVELOPMENT

10.1 INTRODUCTION

Optimized advanced technology turbulent-flow aircraft were developed to establish reference levels of fuel and economic performance for use in evaluating the benefits of the final LFC aircraft described in section 8.0. Using the configuration parameters selected in section 5.3, optimized baseline aircraft were developed for both the 200- and 400-passenger missions. Based on the results of the configuration variations conducted for the LFC aircraft, applicable variations of the TF baselines were evaluated to ensure the selection of TF configurations demonstrating optimized fuel efficiency.

10.2 CONFIGURATION TF-200

10.2.1 CONFIGURATION VARIATIONS

The design constraints limiting the fuel efficiency of TF aircraft are generally the same as those of the LFC aircraft. Therefore, the results of the configuration variations conducted in section 7.5 to improve the performance of LFC aircraft are also applicable to the TF aircraft. The results of that section indicated that the addition of external fuel and relaxed static stability to the baseline configurations provided an improvement in fuel efficiency. Following the procedures used in selecting the final LFC configurations, these variations were evaluated individually and in combination through modification of the baseline TF configurations.

An additional variation of the TF-200 configuration was developed to evaluate the effect of including leading edge devices on the overall configuration performance.

Table 40 summarizes the characteristics and performance of the baseline TF-200 aircraft and the configuration variations evaluated. Both external fuel and RSS provide an improvement in fuel efficiency. The configuration with both external fuel and RSS demonstrates the lowest fuel consumption of those evaluated and was therefore selected for further development and subsequent comparison to the 200-passenger LFC aircraft.

Table 40 shows that the addition of leading edge devices to the TF-200 baseline permits the use of a much higher cruise power ratio with an attendant reduction in engine size. However, the loss of fuel volume, resulting from the relocation of the front spar to permit the installation of leading edge devices, requires a decrease in wing loading. This results in a configuration with higher fuel consumption than the configuration without leading edge devices.

TABLE 40. COMPARISON OF TF-200 CONFIGURATION VARIATIONS

Characteristic	Baseline	Variation			
		External Fuel	RSS	External Fuel RSS	External Fuel RSS Leading Edge Devices
Cruise M	0.80	0.80	0.80	0.80	0.80
Cruise altitude, m (ft)	10,973 (36,000)	10,973 (36,000)	10,973 (36,000)	10,973 (36,000)	10,973 (36,000)
Wing sweep, rad (deg)	0.436 (25.0)	0.436 (25.0)	0.436 (25.0)	0.436 (25.0)	0.436 (25.0)
Aspect ratio	12.50	12.50	12.50	12.50	12.50
Wing loading, kg/m ² (lb/ft ²)	596 (122.00)	636 (130.32)	609 (124.80)	652 (133.47)	628 (128.65)
Wing t/c ratio	.1140	.1093	.1124	0.1075	.1102
Wing area, m ² (ft ²)	294.6 (3172)	271.3 (2920)	279.6 (3010)	258.2 (2779)	271.1 (2918)
Cruise L/D	22.71	22.76	22.61	22.63	22.62
Engine thrust, N (lb)	112,637 (25,323)	115,786 (26,031)	111,142 (24,987)	114,936 (25,840)	104,452 (23,483)
Bypass ratio	6.00	6.00	6.00	6.00	6.00
Cruise power ratio	0.92	0.88	0.91	0.87	0.97
Gross weight, kg (lb)	181,045 (399,129)	177,931 (392,265)	175,717 (387,383)	173,434 (382,351)	175,550 (387,014)
Empty weight, kg (lb)	79,247 (174,706)	78,177 (172,349)	75,939 (167,413)	75,300 (166,006)	76,240 (168,078)
Block fuel, kg (lb)	61,776 (136,191)	60,155 (132,820)	60,064 (132,416)	58,788 (129,804)	59,755 (131,734)
Fuel efficiency, skm/kg fuel (ssm/lb fuel)	33.02 (9.30)	33.90 (9.55)	33.96 (9.56)	34.65 (9.77)	34.11 (9.61)
Flyaway cost, \$10 ⁶	24.063	23.802	23.382	23.218	23.192
DOC, \$/skm (\$/ssm)					
Fuel price, \$/l (\$/gal)					
0.066 (0.25)	0.829 (1.334)	0.819 (1.318)	0.810 (1.304)	0.804 (1.294)	0.803 (1.293)
0.132 (0.50)	1.084 (1.744)	1.068 (1.718)	1.058 (1.703)	1.046 (1.684)	1.050 (1.690)
0.264 (1.00)	1.594 (2.565)	1.564 (2.517)	1.554 (2.501)	1.532 (2.465)	1.543 (2.483)

Table 41 summarizes the reductions in fuel consumption provided by the TF-200 configuration variations.

**TABLE 41. REDUCTIONS IN FUEL CONSUMPTION FOR
TF-200 CONFIGURATION VARIATIONS**

	kg	lb	%
External fuel	1620	3571	2.6
RSS	1713	3775	2.8
External fuel and RSS	3989	6587	4.8

10.2.2 CONFIGURATION DESCRIPTION

10.2.2.1 General Arrangement

The general arrangement of the selected TF-200 configuration is shown in figure 206. A detailed weight statement for this aircraft is presented in table 42.

As illustrated by figure 206, the TF-200 configuration is very similar to the selected LFC-200 aircraft. The fuselages are identical and both configurations employ four aft-fuselage-mounted engines, a T-tail, tip-mounted external fuel tanks, and RSS. The major observable configurational differences in the selected LFC and TF aircraft is in the aspect ratio and wing sweep. LFC-200 configurations have an aspect ratio of 14.0 and a wing sweep of 0.396 rad (22.7 deg), while the corresponding values for TF-200 are 12.5 and 0.436 rad (25 deg).

10.2.2.2 Aircraft Systems

The aircraft systems for TF-200 are identical to those of the LFC-200 aircraft described in section 8.2.2.

10.3 CONFIGURATION TF-400

10.3.1 CONFIGURATION VARIATIONS

Development of the TF-400 configuration differed from that of the TF-200 aircraft in that the fuel volume constraint which influenced the design of the 200-passenger aircraft does not exist for the

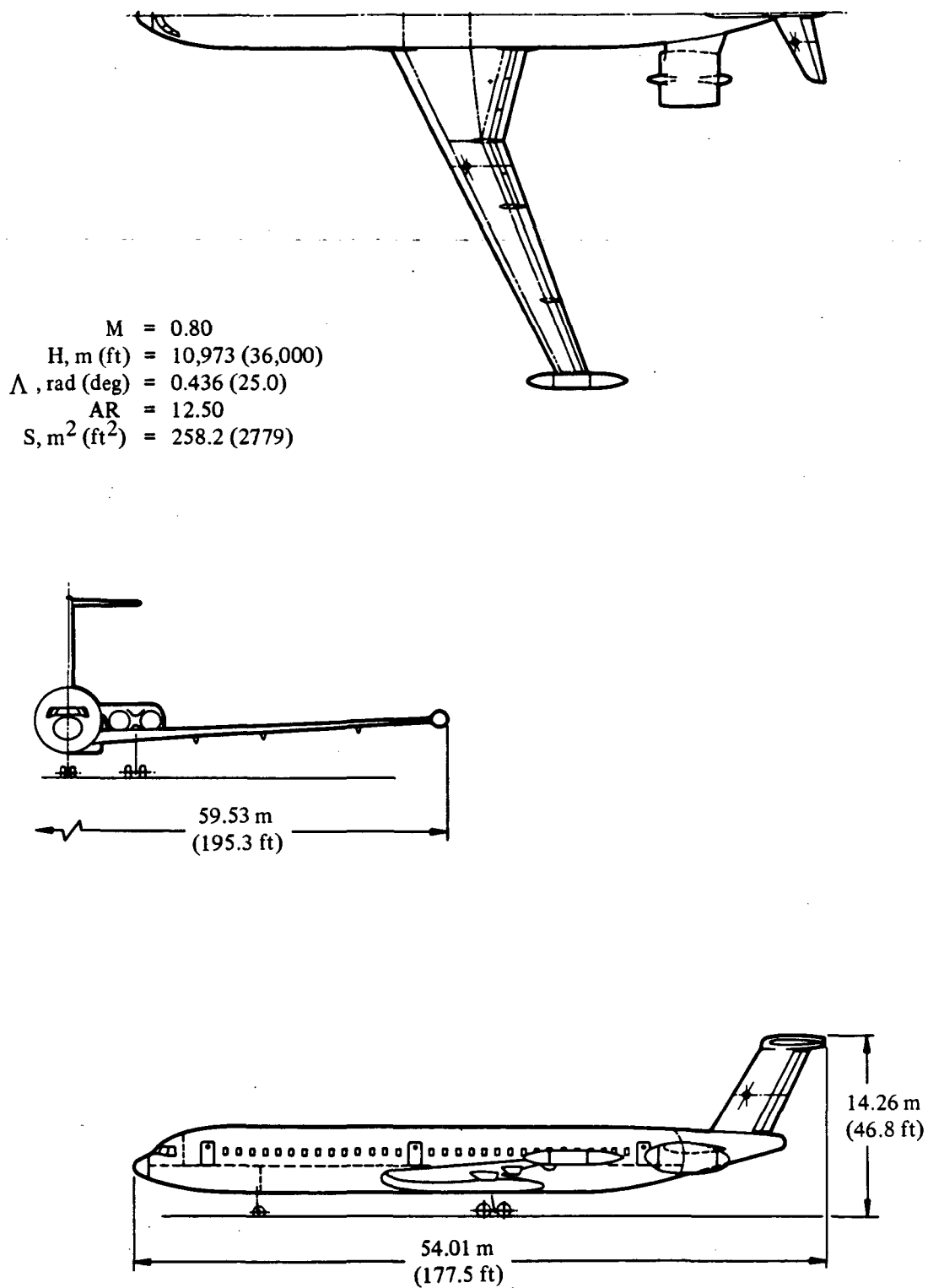


Figure 206. — General arrangement, TF-200

TABLE 42. WEIGHT STATEMENT: TF-200

Item	kg	lb
Structure	(47,203)	(104,062)
Wing	21,120	46,560
Wing LFC glove	0	0
Empennage	(1,832)	(4,039)
Horizontal tail	902	1,989
Horizontal LFC glove	0	0
Vertical tail	929	2,049
Vertical LFC glove	0	0
Fuselage	14,404	31,755
Landing gear	(7,318)	(16,134)
Nose	951	2,097
Main	6,367	14,036
Nacelle and pylon	(2,529)	(5,575)
Nacelle	1,047	2,308
Pylon	348	767
Noise treatment	1,134	2,499
Propulsion system	(10,901)	(24,032)
Engines	6,904	15,222
Fuel system	1,929	4,253
Thrust reversers	1,160	2,557
LFC engines	0	0
LFC installation	0	0
LFC ducts	0	0
Miscellaneous	907	2,000
Systems and equipment	(17,197)	(37,912)
Auxiliary power system	297	654
Surface controls	1,362	3,002
Instruments	587	1,294
Hydraulics and pneumatic	635	1,399
Electrical	2,326	5,127
Avionics	1,087	2,400
Furnishings	8,611	18,983
Airconditioning and AI	2,259	4,982
Auxiliary gear - equipment	32	71
Weight empty	(75,300)	(166,006)
Operating equipment	6,608	14,567
Operating weight	(81,908)	(180,573)
Payload - passenger	19,233	42,400
Cargo	4,536	10,000
Zero fuel weight	(105,677)	(232,973)
Fuel	67,757	149,378
Gross weight	(173,434)	(382,351)
AMPR weight	63,356	139,673

400-passenger aircraft. Removal of this constraint influences development of the 400-passenger aircraft as follows:

- (1) The internal fuel volume of the TF-400 aircraft is adequate to permit a wing loading greater than the 684 kg/m^2 (140 lb/ft^2) maximum considered for study aircraft. Therefore, the use of external fuel does not benefit the 400-passenger configurations.
- (2) As a result of the excess fuel volume available, it is possible to relocate the front spar of the wing as required to permit the installation of 0.12 c leading edge devices without a decrease in wing loading and the resultant adverse effect on fuel efficiency. Of the six final study aircraft, TF-400 is the only configuration which can utilize leading edge devices without penalizing fuel efficiency.

Since the use of external fuel was not necessary on the TF-400 aircraft, only one configuration variation was required to optimize the configuration. Table 43 outlines the characteristics and performance of the baseline TF-400 configuration and a variation of the baseline which incorporates relaxed static stability. Both configurations utilize leading edge devices. The addition of RSS reduces fuel consumption by 6428 kg (14,171 lb) or 5.4 percent. Therefore, the TF-400 configuration with RSS was selected for further development and comparison to the 400-passenger LFC aircraft.

10.3.2 CONFIGURATION DESCRIPTION

10.3.2.1 General Arrangement

The general arrangement of the selected TF-400 configuration is shown in figure 207. Table 44 outlines the corresponding weight statement.

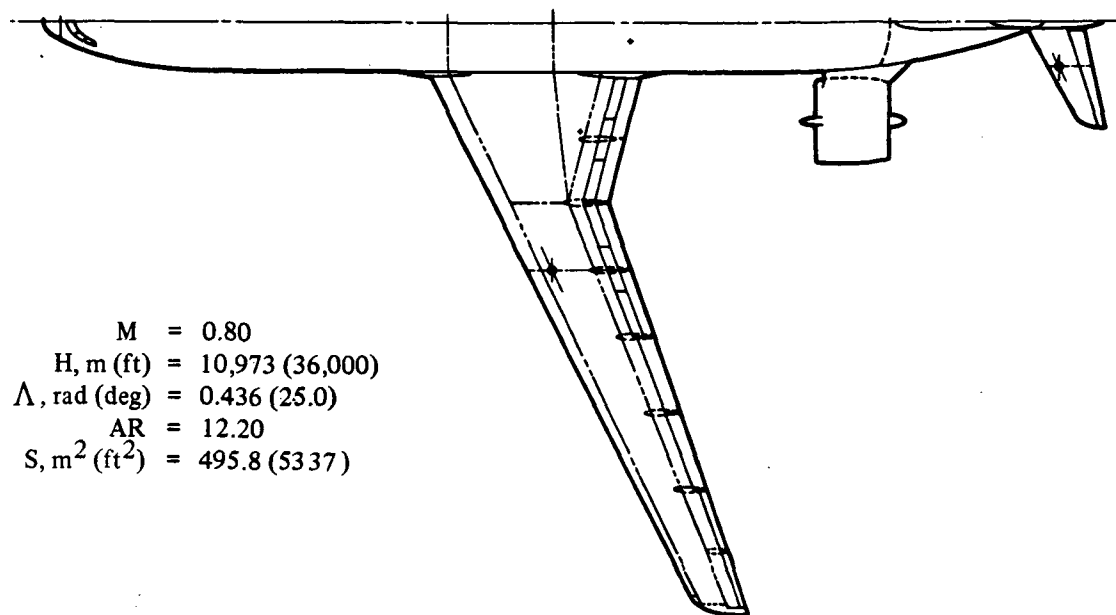
As in the case of the 200-passenger aircraft, the 400-passenger TF and LFC configurations are very similar. Fuselage, empennage, and engine arrangements are the same. The primary differences are in the use of 0.12 c leading edge devices on the TF-400 aircraft, aspect ratio, and wing sweep. The LFC-400 configurations have an aspect ratio of 14.0 and a wing sweep of 0.396 rad (22.7 deg). The TF-400 aircraft has an aspect ratio of 12.2 and a wing sweep of 0.436 rad (25 deg).

10.3.2.2 Aircraft Systems

The aircraft systems for TF-400 are identical to those of the LFC-400 aircraft described in section 8.4.2.

TABLE 43. COMPARISON OF TF-400 CONFIGURATION VARIATIONS

Characteristic	Baseline	RSS
Cruise M	0.80	0.80
Cruise altitude, m (ft)	10,973 (36,000)	10,973 (36,000)
Wing sweep, rad (deg)	0.436 (25.0)	0.436 (25.0)
Aspect ratio	12.20	12.20
Wing loading, kg/m ² (lb/ft ²)	684 (140.00)	684 (140.00)
Wing t/c ratio	.1037	.1037
Wing area, m ² (ft ²)	520.3 (5601)	495.8 (5337)
Cruise L/D	23.42	23.60
Engine thrust, N (lb)	231,060 (51,947)	220,269 (49,521)
Bypass ratio	6.00	6.00
Cruise power ratio	0.88	0.88
Gross weight, kg (lb)	366,276 (807,487)	348,982 (769,361)
Empty weight, kg (lb)	166,616 (367,320)	156,785 (345,645)
Block fuel, kg (lb)	119,127 (262,627)	112,700 (248,456)
Fuel efficiency, skm/kg fuel (ssm/lb fuel)	34.22 (9.65)	36.17 (10.20)
Flyaway cost, \$10 ⁶	38.873	37.208
DOC, ¢/skm (¢/ssm)		
Fuel price, \$/l (\$/gal)		
0.066 (0.25)	0.678 (1.091)	0.649 (1.045)
0.132 (0.50)	0.923 (1.486)	0.882 (1.419)
0.264 (1.00)	1.414 (2.276)	1.347 (2.167)



$M = 0.80$
 $H, \text{ m (ft)} = 10,973 (36,000)$
 $\Lambda, \text{ rad (deg)} = 0.436 (25.0)$
 $AR = 12.20$
 $S, \text{ m}^2 (\text{ft}^2) = 495.8 (5337)$

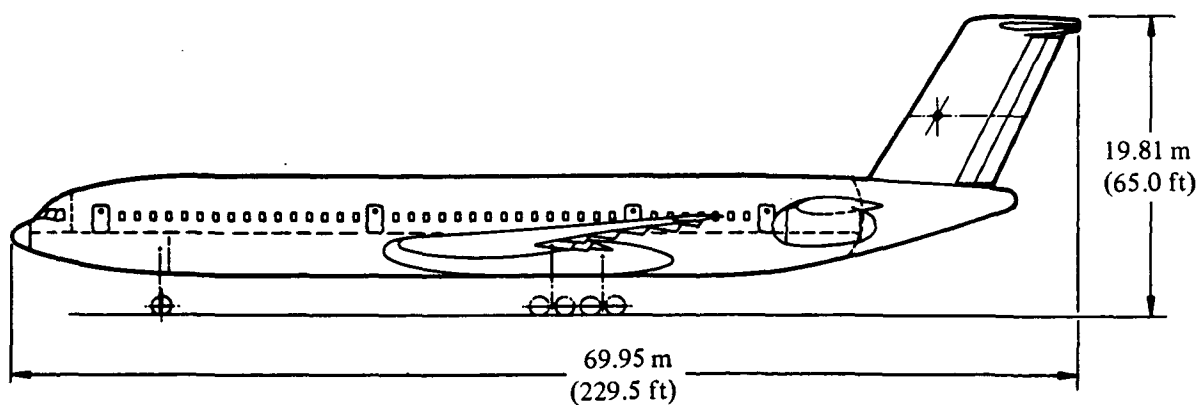
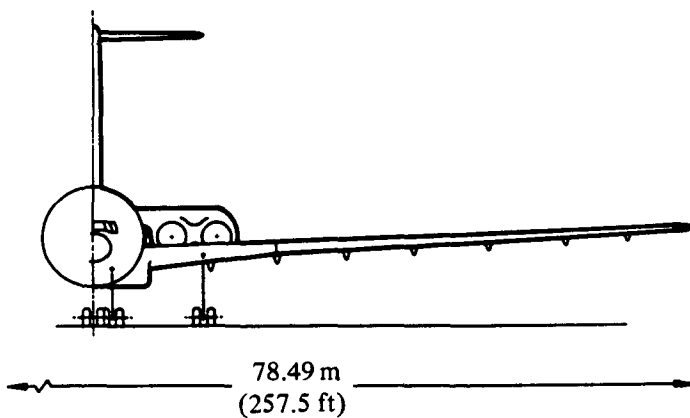


Figure 207. — General arrangement, TF-400

TABLE 44. WEIGHT STATEMENT: TF-400

Item	kg	lb
Structure	(106,730)	(235,295)
Wing	55,527	122,415
Wing LFC glove	0	0
Empennage	(3,979)	(8,772)
Horizontal tail	1,595	3,517
Horizontal LFC glove	0	0
Vertical tail	2,384	5,255
Vertical LFC glove	0	0
Fuselage	27,550	60,736
Landing gear	(14,900)	(32,848)
Nose	1,937	4,270
Main	12,963	28,578
Nacelle and pylon	(4,774)	(10,524)
Nacelle	1,905	4,200
Pylon	732	1,613
Noise treatment	2,137	4,711
Propulsion system	(19,766)	(43,576)
Engines	14,512	31,994
Fuel system	1,908	4,207
Thrust reversers	2,438	5,375
LFC engines	0	0
LFC installation	0	0
LFC ducts	0	0
Miscellaneous	907	2,000
Systems and equipment	(30,289)	(66,774)
Auxiliary power system	455	1,002
Surface controls	2,922	6,441
Instruments	679	1,496
Hydraulics and pneumatic	1,362	3,002
Electrical	3,064	6,754
Avionics	1,089	2,400
Furnishings	17,221	37,966
Airconditioning and AI	3,434	7,571
Auxiliary gear - equipment	64	142
Weight empty	(156,785)	(345,645)
Operating equipment	14,969	32,999
Operating weight	(171,754)	(378,645)
Payload - passenger	38,465	84,800
Cargo	9,072	20,000
Zero fuel weight	(219,291)	(483,445)
Fuel	129,691	285,916
Gross weight	(348,982)	(769,361)
AMPR weight	133,267	293,799

11.0 COMPARISON OF LFC AND TF AIRCRAFT

11.1 INTRODUCTION

The ultimate objective of the study reported herein is a comparison of the relative performance and economics of advanced technology laminar-flow-control and turbulent-flow transport aircraft optimized for the same mission. In section 8.0, optimized configurations are developed for both 200- and 400-passenger LFC transports based on two sets of laminar boundary layer criteria. Section 10.0 outlines the development of optimized TF transports which are directly comparable to the 200- and 400-passenger LFC aircraft in terms of technology level and productivity.

In this section, the LFC and TF aircraft are compared on the basis of weight, drag, fuel consumption, and cost. Production, research and development, and direct operating cost comparisons are included. For the LFC aircraft, the sensitivity of DOC to variations in the price of fuel, maintenance cost, production cost, and average stage length is evaluated. Summary comparisons are presented to illustrate the influence of configuration variations on LFC and TF aircraft, the relative fuel efficiency and DOC of 200- and 400-passenger transports, and the relative fuel efficiency of the study aircraft and current commercial transports.

11.2 COMPARISON OF 200-PASSENGER AIRCRAFT

Table 45 summarizes the geometry, weights, performance, fuel efficiency, and economics of the final 200-passenger TF and both 200-passenger LFC aircraft. With the same cruise Mach number and payload, all of these aircraft have the same productivity. The major geometrical difference is in the aspect ratio of 14.0 for the LFC aircraft and 12.5 for the TF configuration. As required by differences in gross weight and wing loading, there are also variations in the reference wing areas of the aircraft. It will be observed that the L/D of the LFC aircraft is about 28 percent greater than that of the TF aircraft.

Fuel consumption of LFC-200-S is 24.9% less than that of TF-200. The corresponding value for LFC-200-R is 28.2%. Compared to TF-200, the improvement in fuel efficiency for LFC-200-S and LFC-200-R is 33.2% and 39.4%, respectively.

Detailed comparisons of weight, drag, and cost are presented in the sections which follow.

TABLE 45. SUMMARY COMPARISON OF 200-PASSENGER TF AND LFC AIRCRAFT

Characteristic	TF-200	LFC-200-S	LFC-200-R
Cruise M	0.80	0.80	0.80
Cruise altitude, m (ft)	10,973 (36,000)	11,582 (38,000)	11,582 (38,000)
Wing sweep, rad (deg)	0.436 (25.0)	0.396 (22.7)	0.396 (22.7)
Aspect ratio	12.50	14.00	14.00
Wing loading, kg/m ² (lb/ft ²)	652 (133.47)	636 (130.33)	640 (131.00)
Wing t/c ratio	0.1075	0.1092	0.1088
Wing area, m ² (ft ²)	258.2 (2779)	241.4 (2599)	231.7 (2494)
Cruise L/D	22.63	29.00	28.76
Engine thrust, N (lb)	114,936 (25,840)	100,151 (22,516)	96,913 (21,788)
Bypass ratio	6.00	6.00	6.00
Cruise power ratio	0.87	0.78	0.78
Gross weight, kg (lb)	173,434 (382,351)	158,276 (348,934)	152,687 (336,612)
Empty weight, kg (lb)	75,300 (166,006)	77,271 (170,350)	73,932 (162,990)
Block fuel, kg (lb)	58,788 (129,604)	44,144 (97,320)	42,198 (93,028)
Fuel efficiency, skm/kg fuel (ssm/lb fuel)	34.65 (9.77)	46.15 (13.01)	48.29 (13.62)
Flyaway cost, \$10 ⁶	23.218	24.529	23.503
DOC, ¢/skm (¢/ssm)			
Fuel price, \$/l (\$/gal)			
0.066 (0.25)	0.804 (1.294)	0.819 (1.318)	0.761 (1.224)
0.132 (0.50)	1.046 (1.684)	1.002 (1.612)	0.935 (1.505)
0.264 (1.00)	1.532 (2.465)	1.366 (2.199)	1.284 (2.066)

11.2.1 WEIGHT

Table 46 presents a comparison of weight elements for the 200-passenger aircraft. The weight penalties of 4628 kg (10,201 lb) for the LFC system on LFC-200-S and 3260 kg (7187 lb) for the LFC system on LFC-200-R are almost balanced by the reduced weight of the airframe and propulsion systems for the smaller LFC aircraft, with the result that the empty weights of the three aircraft are approximately equal. The empty weight of LFC-200-S is 2.6% greater than that of TF-200, while the empty weight of LFC-200-R is 1.8% less than that of TF-200.

Due to the much lower fuel requirement of the LFC aircraft, the gross weights of the LFC-200-S and LFC-200-R aircraft are 8.7% and 12.0% less than that of TF-200.

11.2.2 DRAG

Drag coefficients based on the reference wing area are listed for the three 200-passenger aircraft in table 47. With the exception of the laminarized wing and empennage and a corresponding decrease in total interference and roughness drag, components of the TF and LFC aircraft have essentially equal drag. Relative to TF-200, the profile drag is reduced by 34.1% and 35.7%, for LFC-200-S and LFC-200-R, respectively. The total drag reduction is 24.7% for LFC-200-S and 23.5% for LFC-200-R.

11.2.3 COST

Production, research and development, and direct operating costs for the final 200-passenger TF and LFC aircraft are compared on tables 48, 49, and 50.

Since the LFC aircraft are somewhat smaller than the TF aircraft, the empty manufacturing cost of the basic airframe and engines is lower for these aircraft. However, addition of \$1.639 million for LFC system cost on LFC-200-S and \$1.049 million for LFC system costs on LFC-200-R results in a greater total flyaway cost for both LFC aircraft. The flyaway cost of LFC-200-S is 5.6% greater than that of TF-200. The flyaway cost of LFC-200-R is 1.2% greater than that of TF-200. It is interesting to note that the LFC system cost represents 8.7% of the total empty manufacturing cost for LFC-200-S. The corresponding value for LFC-200-R is 5.9%. Cost per pound for both airframe and LFC system elements may be calculated from the data of table 48 and the appropriate weight statement.

As discussed in section 3.4, R&D costs are largely dependent upon the aircraft production costs. The greater production cost of the LFC aircraft and the increase in flight test requirements for the

TABLE 46. COMPARISON OF WEIGHT ELEMENTS FOR 200-PASSENGER TF AND LFC AIRCRAFT

Item	TF-200		LFC-200-S		LFC-200-R	
	kg	lb	kg	lb	kg	lb
Wing	21,120	46,560	21,011	46,322	19,910	43,894
Horizontal Tail	902	1989	834	1838	782	1725
Vertical Tail	929	2049	899	1981	829	1828
Fuselage	14,404	31,755	14,327	31,586	14,276	31,472
Landing Gear	7318	16,134	6969	15,364	6734	14,846
Nacelle/Pylon	2529	5575	2213	4878	2143	4725
Propulsion System	10,901	24,032	9534	21,019	9250	20,392
Systems & Equipment	17,197	37,912	16,856	37,161	16,748	36,921
LFC System						
Surfaces			2766	6098	2188	4823
Engines			708	1560	252	555
Engine Installation			877	1933	312	688
Ducting			277	610	508	1121
Weight Empty	75,300	166,006	77,271	170,350	73,932	162,990
Operating Equipment	6608	14,567	6472	14,267	6453	14,227
Operating Weight	81,908	180,573	83,743	184,617	80,384	177,217
Payload	23,769	52,400	23,769	52,400	23,769	52,400
Zero Fuel Weight	105,677	232,973	107,512	237,017	104,153	229,617
Fuel	67,757	149,378	50,764	111,917	48,534	106,995
Gross Weight	173,434	382,351	158,276	348,934	152,687	336,612

TABLE 47. COMPARISON OF C_D COMPONENTS FOR 200-PASSENGER TF AND LFC AIRCRAFT

Item	<u>TF-200</u>	<u>LFC-200-S</u>	<u>LFC-200-R</u>
	$S_W = 258.2 \text{ m}^2 (2779 \text{ ft}^2)$	$S_W = 241.4 \text{ m}^2 (2599 \text{ ft}^2)$	$S_W = 231.7 \text{ m}^2 (2494 \text{ ft}^2)$
Wing	.0067	.0027	.0028
Fuselage	.0044	.0048	.0050
Upsweep	.0002	.0002	.0002
Pylon	.0001	.0001	.0001
Nacelle	.0013	.0013	.0013
Horizontal Tail	.0006	.00025	.0002
Vertical Tail	.0007	.00035	.0003
Compressibility	.0011	.0011	.0011
Interference	.0004	.0002	.0002
Roughness	<u>.0004</u>	<u>.0002</u>	<u>.0002</u>
Profile	.0159	.0112	.0114
Trim	.0012	.0012	.0012
Induced	<u>.0106</u>	<u>.0109</u>	<u>.0110</u>
Total	.0277	.0233	.0236

additional LFC systems is reflected in the R&D cost comparisons of table 49. Compared to TF-200, the R&D cost for LFC-200-S is greater by 2.3%. The R&D cost is essentially the same for TF-200 and LFC-200-R.

TABLE 48. COMPARISON OF PRODUCTION COSTS FOR 200-PASSENGER TF AND LFC AIRCRAFT

Cost Element	TF-200	LFC-200-S	LFC-200-R
Empty Mfg Cost	10.590	10.288	10.119
LFC System			
Surfaces		0.663	0.587
Ducting		0.046	0.085
Engines/Installation		<u>0.930</u>	<u>0.377</u>
Total Empty Mfg Cost	10.590	11.927	11.168
Sustaining Eng/Fee/Warranty	<u>6.536</u>	<u>6.833</u>	<u>6.709</u>
Airframe Cost	17.126	18.760	17.877
Engine Cost	3.365	2.991	2.909
Avionics Cost	.500	.500	.500
R&D Cost	<u>2.227</u>	<u>2.278</u>	<u>2.217</u>
Total Flyaway Cost	23.218	24.529	23.503
Millions of Dollars			

TABLE 49. COMPARISON OF R&D COSTS FOR 200-PASSENGER TF AND LFC AIRCRAFT

Cost Element	TF-200	LFC-200-S	LFC-200-R
Tech Data	15.987	16.281	15.817
Design Engineering	355.272	361.802	351.492
Development Tooling	214.291	214.246	207.873
Development Test Articles	99.757	104.316	102.432
Flight Test	34.033	39.540	38.419
Special Support Equipment	4.263	4.342	4.218
Development Spares	<u>55.808</u>	<u>56.796</u>	<u>55.687</u>
Total	779.411	797.323	775.938
Millions of Dollars			

Table 50 presents a breakdown of direct operating costs for the TF and LFC aircraft selected for the 200-passenger mission. At a fuel price of \$0.093/l (\$0.35/gal), the DOC of both of the LFC aircraft is lower than that of the TF aircraft. As a result of the additional maintenance required for LFC system elements, direct maintenance costs for LFC-200-S and LFC-200-R are greater than those of TF-200 by 40.5% and 17.0%, respectively. The difference in the maintenance costs of the LFC aircraft results from the use of five LFC suction units on LFC-200-S and two suction units on LFC-200-R.

The combination of reduced maintenance costs for the smaller main propulsion engines and the lower fuel consumption of LFC aircraft compensates for the additional LFC system maintenance. Fuel costs for LFC-200-S and LFC-200-R are lower than those for TF-200 by 24.8% and 28.1%, respectively.

An evaluation of the sensitivity of DOC to variations in fuel price, LFC maintenance costs and LFC production costs for 200-passenger aircraft is presented in section 11.4.

TABLE 50. COMPARISON OF DOC ELEMENTS FOR 200-PASSENGER TF AND LFC AIRCRAFT

Cost Element	TF-200		LFC-200-S		LFC-200-R	
	\$	%	\$	%	\$	%
Flying Operations	10,153	55.3	8419	46.3	8138	48.1
Flight Crew	2548	13.9	2494	13.7	2472	14.6
Fuel and Oil	6926	37.7	5207	28.6	4977	29.4
Hull Insurance	679	3.7	719	4.0	689	4.1
Direct Maintenance	3220	17.5	4524	24.9	3766	22.2
Airplane						
Labor	409	2.2	419	2.3	408	2.4
Materials	618	3.4	672	3.7	642	3.8
Engine						
Labor	262	1.4	259	1.4	258	1.5
Materials	1151	6.3	1023	5.6	995	5.8
LFC System						
Labor			245	1.3	164	1.0
Materials			883	5.0	369	2.2
Maintenance Burden	780	4.2	1023	5.6	930	5.5
Depreciation	4993	27.2	5245	28.8	5028	29.7
Total DOC per Flight	18,366	100.0	18,188	100.0	16,932	100.0
Fuel Price = \$0.093/l (\$0.35/gal)						

11.3 COMPARISON OF 400-PASSENGER AIRCRAFT

Characteristics of the final 400-passenger TF and LFC aircraft are summarized in table 51. As in the case of the 200-passenger aircraft, all of the 400-passenger aircraft provide the same productivity and therefore are directly comparable in terms of fuel efficiency and cost. The geometry of the TF and LFC aircraft differs primarily in the selection of aspect ratio. The TF aircraft has an aspect ratio of 12.2, while both of the LFC aircraft have an aspect ratio of 14.0. All of the 400-passenger aircraft have a wing loading of 684 kg/m^2 (140 lb/ft^2). Differences in wing area are consistent with gross weight variations among the aircraft. L/D of the LFC aircraft is about 27% greater than that of the TF configuration.

Fuel consumption for LFC-400-S and LFC-400-R is 24.4% and 26.7% less than that of TF-400. Compared to TF-400, the improvement in fuel efficiency for LFC-400-S and LFC-400-R is 32.4% and 36.4%, respectively.

Detailed comparisons of weight, drag, and cost for the 400-passenger aircraft are presented in the sections which follow.

11.3.1 WEIGHT

A comparison of weight elements for the 400-passenger aircraft is provided by table 52. The LFC system weight penalty is 8299 kg (18,295 lb), or 5.1% of the empty weight for LFC-400-S. For LFC-400-R, the corresponding weight is 6009 kg (13,247 lb), or 3.9%. The empty weight of LFC-400-S is 3.3% greater than that of TF-400, while LFC-400-R has an empty weight which is about 1% lower than that of TF-400.

The reduced fuel requirement of the LFC aircraft results in gross weights for LFC-400-S and LFC-400-R which are 7.8% and 10.4% less than that of TF-400.

11.3.2 DRAG

Drag coefficients for the 400-passenger TF and LFC aircraft are listed in table 53. The distribution of drag is generally similar to that described for the 200-passenger aircraft. Laminarization of the wings and empennage provides a reduction of 35.3% and 36.5% in profile drag for the LFC-400-S and LFC-400-R aircraft. Based on total drag, the corresponding values are 20.3% and 22.2% less than for the TF aircraft.

TABLE 51. SUMMARY COMPARISON OF 400-PASSENGER TF AND LFC AIRCRAFT

Characteristic	TF-400	LFC-400-S	LFC-400-R
Cruise M	0.80	0.80	0.80
Cruise altitude, m (ft)	10,973 (36,000)	11,582 (38,000)	11,582 (38,000)
Wing sweep, rad (deg)	0.436 (25.0)	0.396 (22.7)	0.396 (22.7)
Aspect ratio	12.20	14.00	14.00
Wing loading, kg/m ² (lb/ft ²)	684 (140.00)	684 (140.00)	684 (140.00)
Wing t/c ratio	0.1037	0.1033	0.1033
Wing area, m ² (ft ²)	495.8 (5337)	457.5 (4925)	444.4 (4784)
Cruise L/D	23.60	30.05	29.90
Engine thrust, N (lb)	220,269 (49,521)	217,881 (48,984)	211,502 (47,550)
Bypass ratio	6.00	6.00	6.00
Cruise power ratio	0.88	0.70	0.71
Gross weight, kg (lb)	348,982 (769,361)	321,895 (709,645)	312,654 (689,273)
Empty weight, kg (lb)	156,785 (345,645)	161,895 (356,912)	155,556 (342,959)
Block fuel, kg (lb)	112,700 (248,456)	85,123 (187,661)	82,599 (182,096)
Fuel efficiency, skm/kg fuel (ssm/lb fuel)	36.17 (10.20)	47.88 (13.50)	49.35 (13.91)
Flyaway cost, \$10 ⁶	37.208	39.435	38.343
DOC, \$/skm (\$/ssm)			
Fuel price, \$/l (\$/gal)			
0.066 (0.25)	0.649 (1.045)	0.627 (1.009)	0.612 (0.985)
0.132 (0.50)	0.882 (1.419)	0.803 (1.292)	0.782 (1.259)
0.264 (1.00)	1.347 (2.167)	1.154 (1.857)	1.123 (1.808)

TABLE 52. COMPARISON OF WEIGHT ELEMENTS FOR 400-PASSENGER TF AND LFC AIRCRAFT

Item	TF-400		LFC-400-S		LFC-400-R	
	kg	lb	kg	lb	kg	lb
Wing	55,527	122,415	55,380	122,089	52,825	116,457
Horizontal Tail	1595	3517	1338	2949	1291	2847
Vertical Tail	2384	5255	2081	4587	2004	4417
Fuselage	27,550	60,736	27,421	60,452	27,331	60,253
Landing Gear	14,900	32,848	14,317	31,563	13,908	30,662
Nacelle/Pylon	4774	10,524	4723	10,412	4588	10,114
Propulsion System	19,766	43,576	19,344	42,646	18,765	41,369
Systems & Equipment	30,289	66,774	28,992	63,918	28,845	63,593
LFC System						
Surfaces			6285	13,856	4442	9792
Engines			580	1279	385	849
Engine Installation			719	1585	478	1053
Ducting			715	1576	704	1553
Weight Empty	156,785	345,645	161,895	356,912	155,566	342,959
Operating Equipment	14,969	33,000	14,713	32,436	14,691	32,385
Operating Weight	171,754	378,645	176,608	389,348	170,257	375,344
Payload	47,537	104,800	47,537	104,800	47,537	104,800
Zero Fuel Weight	219,291	483,445	224,145	494,148	217,794	480,144
Fuel	129,691	285,916	97,750	215,497	94,861	209,129
Gross Weight	348,982	769,361	321,895	709,645	312,655	689,273

TABLE 53. COMPARISON OF C_D COMPONENTS FOR 400-PASSENGER TF AND LFC AIRCRAFT

Item	TF-400	LFC-400-S	LFC-400-R
	$S_W = 495.8 \text{ m}^2 (5337 \text{ ft}^2)$	$S_W = 457.5 \text{ m}^2 (4925 \text{ ft}^2)$	$S_W = 444.4 \text{ m}^2 (4784 \text{ ft}^2)$
Wing	.0062	.0025	.0026
Fuselage	.0037	.0042	.0042
Upsweep	.0001	.0001	.0001
Pylon	.0001	.0001	.0001
Nacelle	.0012	.0013	.0013
Horizontal Tail	.0005	.0002	.0002
Vertical Tail	.0010	.0004	.0004
Compressibility	.0011	.0011	.0011
Interference	.0004	.0002	.0002
Roughness	<u>.0004</u>	<u>.0002</u>	<u>.0002</u>
Profile	.0147	.0103	.0104
Trim	.0012	.0012	.0012
Induced	<u>.0120</u>	<u>.0126</u>	<u>.0126</u>
Total	.0279	.0241	.0242

11.3.3 COST

Production, research and development, and direct operating costs for the 400-passenger aircraft are listed on tables 54, 55, and 56.

As shown in table 54, the LFC system cost of \$1.887 million accounts for 10.1% of the total empty manufacturing cost for LFC-400-S. For LFC-400-R, the corresponding values are \$1.539 million and 8.5%. Total flyaway cost of the LFC-400-S and LFC-400-R aircraft are 6.9% and 3.1% greater than that of TF-400.

R&D costs for the final study aircraft aircraft are compared in table 55. As in the case of the 200-passenger comparisons, the higher production costs of the LFC aircraft and the additional flight test requirements imposed by the LFC systems results in somewhat higher R&D costs for the LFC aircraft.

TABLE 54. COMPARISON OF PRODUCTION COSTS FOR 400-PASSENGER TF AND LFC AIRCRAFT

Cost Element	TF-400	LFC-400-S	LFC-400-R
Empty Mfg Cost	17.241	16.794	16.524
LFC System			
Surfaces		1.056	.892
Ducting		.110	.109
Engines/Installation		.721	.538
Total Empty Mfg Cost	17.241	18.681	18.063
Sustaining Eng/Fee/Warranty	9.752	10.259	10.035
Airframe Cost	26.993	28.940	28.098
Engine Cost	5.873	5.819	5.673
Avionics Cost	.500	.500	.500
R&D Cost	3.842	4.176	4.073
Total Flyaway Cost	37.208	39.435	38.344
Millions of Dollars			

TABLE 55. COMPARISON OF R&D COSTS FOR 400-PASSENGER TF AND LFC AIRCRAFT

Cost Element	TF-400	LFC-400-S	LFC-400-R
Tech Data	28.338	32.265	31.433
Design Engineering	629.734	717.009	698.511
Development Tooling	385.553	388.941	379.540
Development Test Articles	148.314	156.078	152.673
Flight Test	59.543	69.771	68.164
Special Support Equipment	7.557	8.604	8.382
Development Spares	<u>85.475</u>	<u>88.876</u>	<u>86.883</u>
Total	1,344.514	1,461.544	1,425.586
Millions of Dollars			

A comparison of direct operating cost elements for the 400-passenger TF and LFC aircraft is presented in table 56. For the selected fuel price of \$0.093/l (\$0.35/gal), the DOC for LFC-400-S is 6.9% less than that of TF-400. The decrease in DOC for LFC-400-R is 8.4%. The addition to direct maintenance costs due to the LFC system is approximately the same for both LFC configurations. Total direct maintenance relative to TF-400 is 19.2% greater for LFC-400-S and 16.8% greater for LFC-400-R.

Fuel costs for LFC-400-S and LFC-400-R are reduced by 24.4% and 26.7%, respectively, relative to TF-400.

The sensitivity of DOC to variations in fuel price, LFC maintenance costs and LFC production costs for 400-passenger aircraft is evaluated in section 11.4.

TABLE 56. COMPARISON OF DOC ELEMENTS FOR 400-PASSENGER TF AND LFC AIRCRAFT

Cost Element	TF-400		LFC-400-S		LFC-400-R	
	\$	%	\$	%	\$	%
Flying Operations	17,372	57.4	14,138	49.7	13,788	49.7
Flight Crew	3023	10.0	2964	10.4	2942	10.6
Fuel and Oil	13,261	43.8	10,020	35.2	9724	35.1
Hull Insurance	1088	3.6	1154	4.1	1122	4.0
Direct Maintenance	4870	16.1	5806	20.4	5690	20.5
Airplane						
Labor	570	1.9	578	2.0	569	2.1
Materials	983	3.2	1055	3.7	1025	3.7
Engine						
Labor	287	1.0	287	1.0	285	1.0
Materials	2008	6.6	1990	7.1	1940	7.0
LFC System						
Labor			234	0.8	228	0.8
Materials			399	1.4	398	1.4
Maintenance Burden	1022	3.4	1263	4.4	1243	4.5
Depreciation	8028	26.5	8489	29.9	8255	29.8
Total DOC per Flight	30,270	100.0	28,433	100.0	27,733	100.0
Fuel Price = \$0.093/l (\$0.35/gal)						

11.4 EVALUATION OF DOC SENSITIVITY

11.4.1 FUEL PRICE, LFC MAINTENANCE COST, AND LFC PRODUCTION COST

From May 1973 to July 1975, a period of slightly more than two years, the average price paid by international carriers for a gallon of jet fuel increased from \$0.029/l (\$0.11/gal) to \$0.093/l (\$0.35/gal), an increase of 218%. Current indications are that the price of fuel will continue to increase for the foreseeable future. Therefore, it is reasonable and informative to examine the influence of increases in fuel price above the current level on the relative DOC of turbulent-flow and laminar-flow-control transport aircraft.

Figures 208 through 211 illustrate the variation of DOC with fuel price for the six final study aircraft. In these figures, the DOC for each of the final LFC aircraft and the corresponding TF aircraft is shown as a function of fuel price. The point of intersection of the LFC and TF curves defines the fuel price above which the LFC aircraft provides lower DOC than the TF aircraft. Following are the fuel prices at which the LFC and TF aircraft have equal DOC:

	Fuel price	
	\$/l	\$/gal
LFC-200-S	0.082	0.31
LFC-200-R	0.029	0.11
LFC-400-S	0.042	0.16
LFC-400-R	0.026	0.10

Figures 208 through 211 also illustrate the impact of variations in the cost of maintaining LFC systems on DOC. In generating these data, the maintenance costs peculiar to the LFC system, as described in section 9.3, were varied by a factor of ± 0.5 . This variation of 50% about the nominal LFC system maintenance cost changes the fuel price at which LFC and TF aircraft have equal DOC by about $\pm \$0.034/l$ (\$0.13/gal) for LFC-200-S and $\pm \$0.016/l$ (\$0.06/gal) for LFC-200-R, LFC-400-S, and LFC-400-R. As discussed in section 11.2.3, the impact of such a variation is much greater on LFC-200-S than on the other three configurations because of the number of LFC suction units. The maintenance requirements of the five LFC suction units employed on LFC-200-S are appreciably greater than those attending the two units used on all of the other LFC configurations.

A similar sensitivity study was conducted to evaluate the influence of variations in the production cost of LFC system elements on DOC. As shown by figures 212 through 215, a variation of $\pm 20\%$

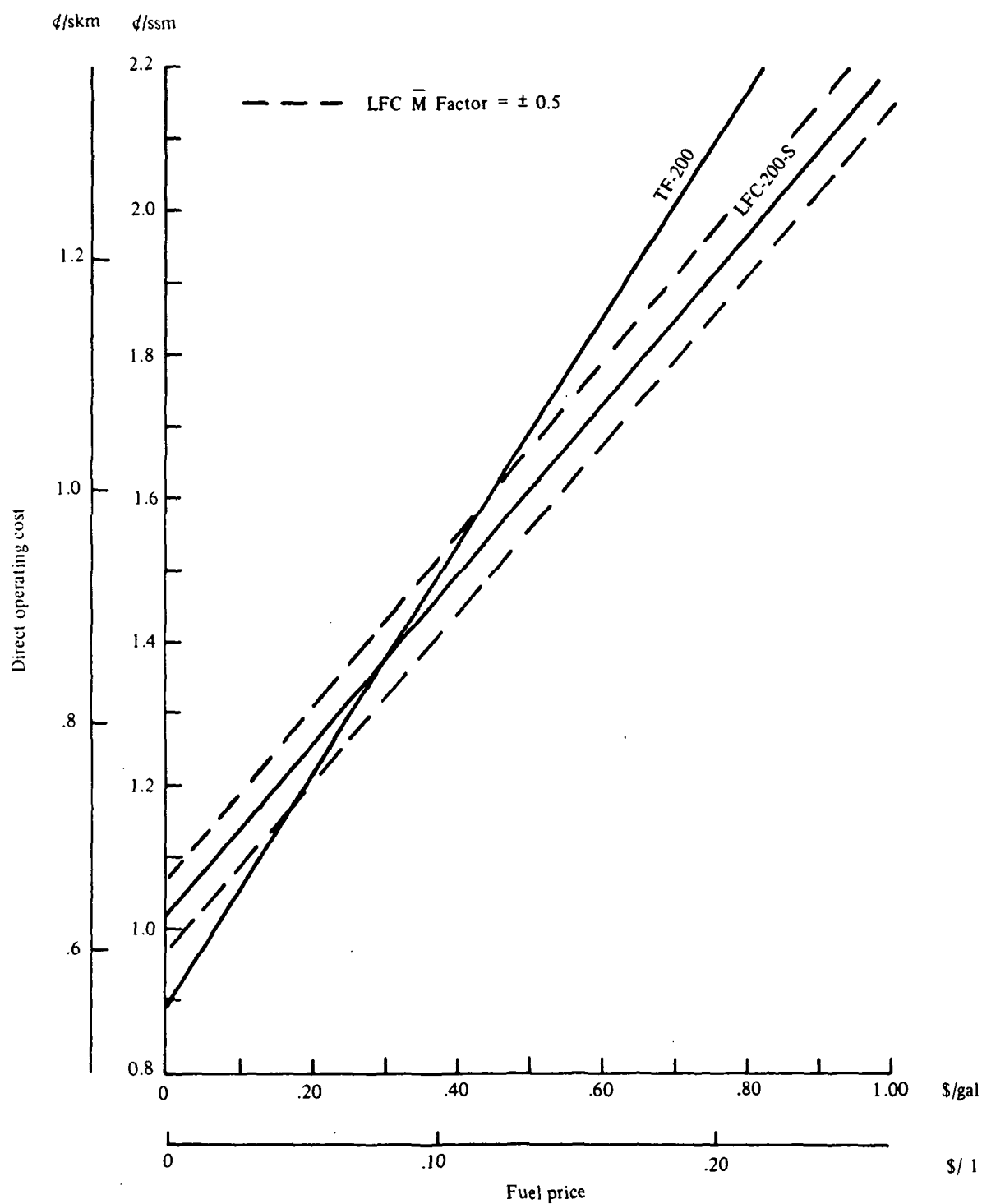


Figure 208. — Sensitivity of DOC to fuel price and LFC maintenance cost, TF-200 and LFC-200-S

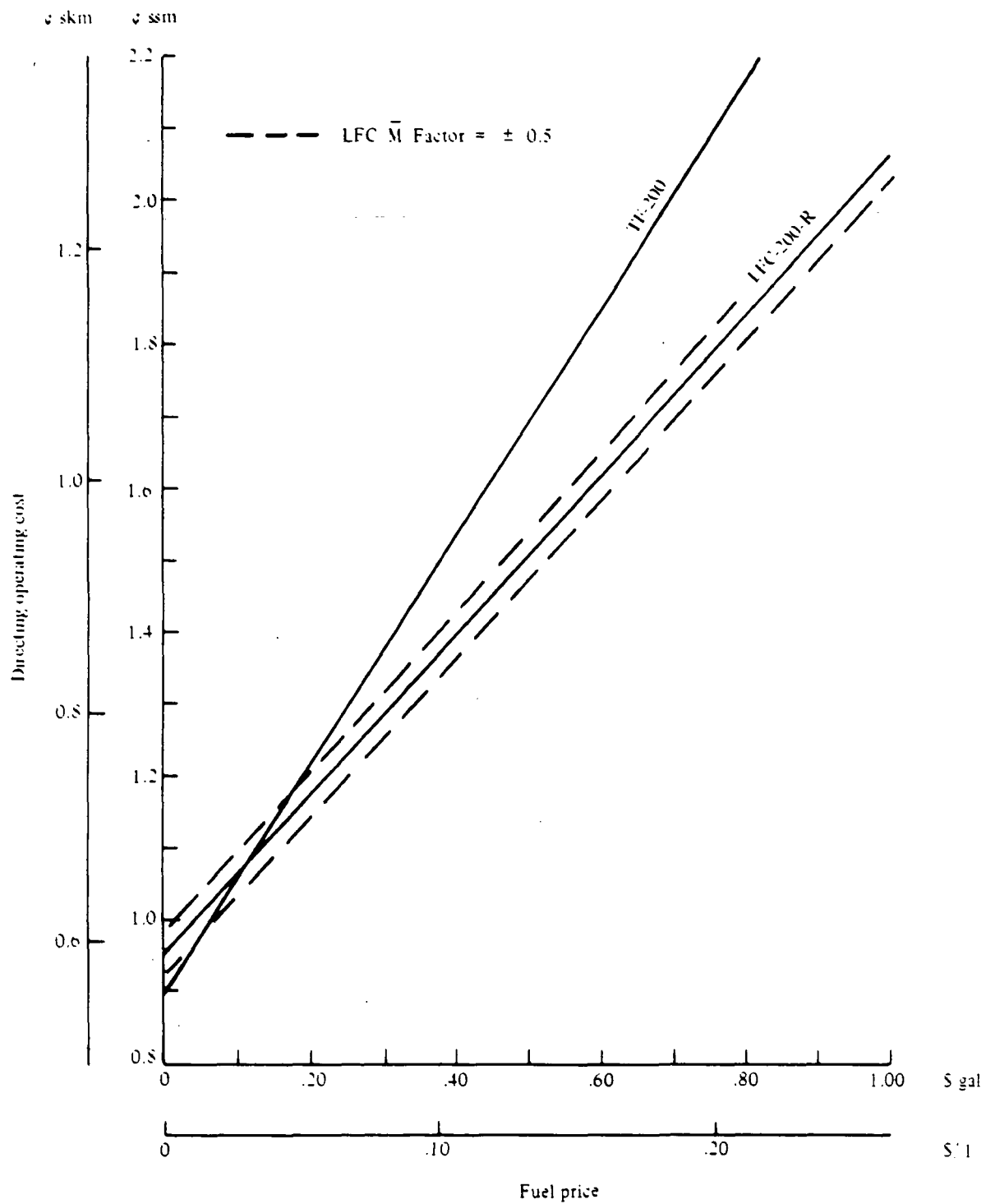


Figure 209. — Sensitivity of DOC to fuel price and LFC maintenance cost, TF-200 and LFC-200-R

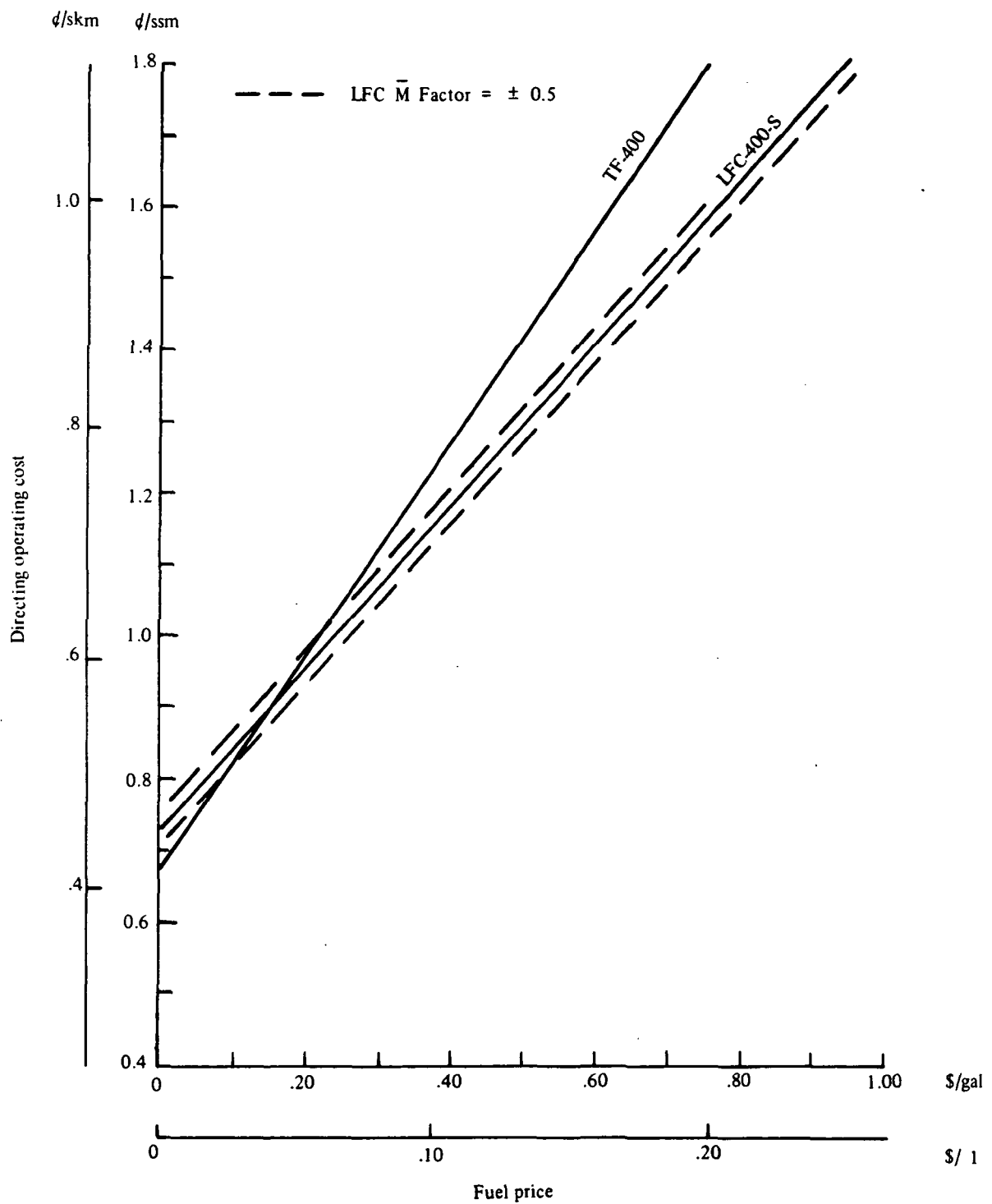


Figure 210. — Sensitivity of DOC to fuel price and LFC maintenance cost, TF-400 and LFC-400-S

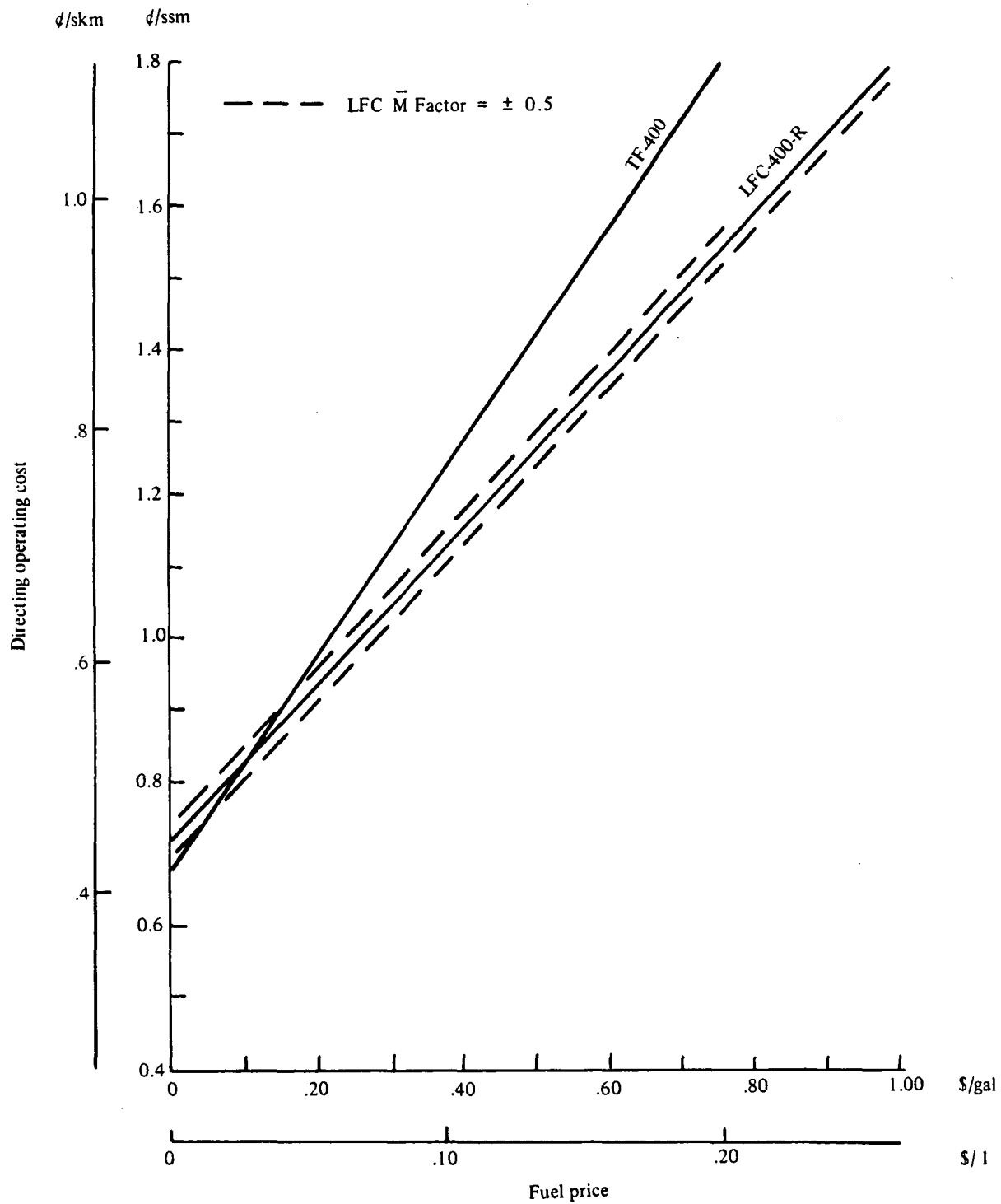


Figure 211. — Sensitivity of DOC to fuel price and LFC maintenance cost, TF-400 and LFC-400-R

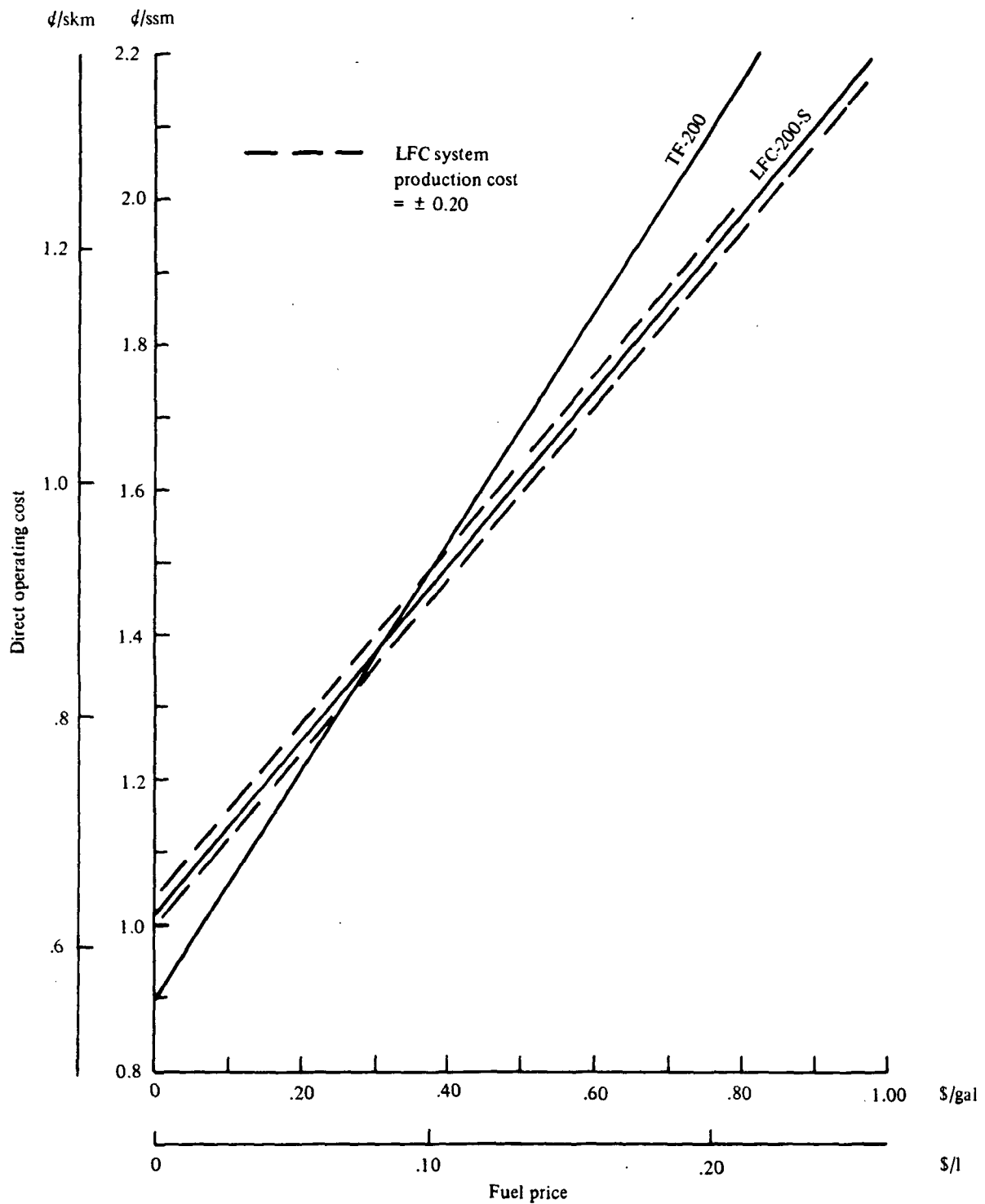


Figure 212. — Sensitivity of DOC to fuel price and LFC production cost, TF-200 and LFC-200-S

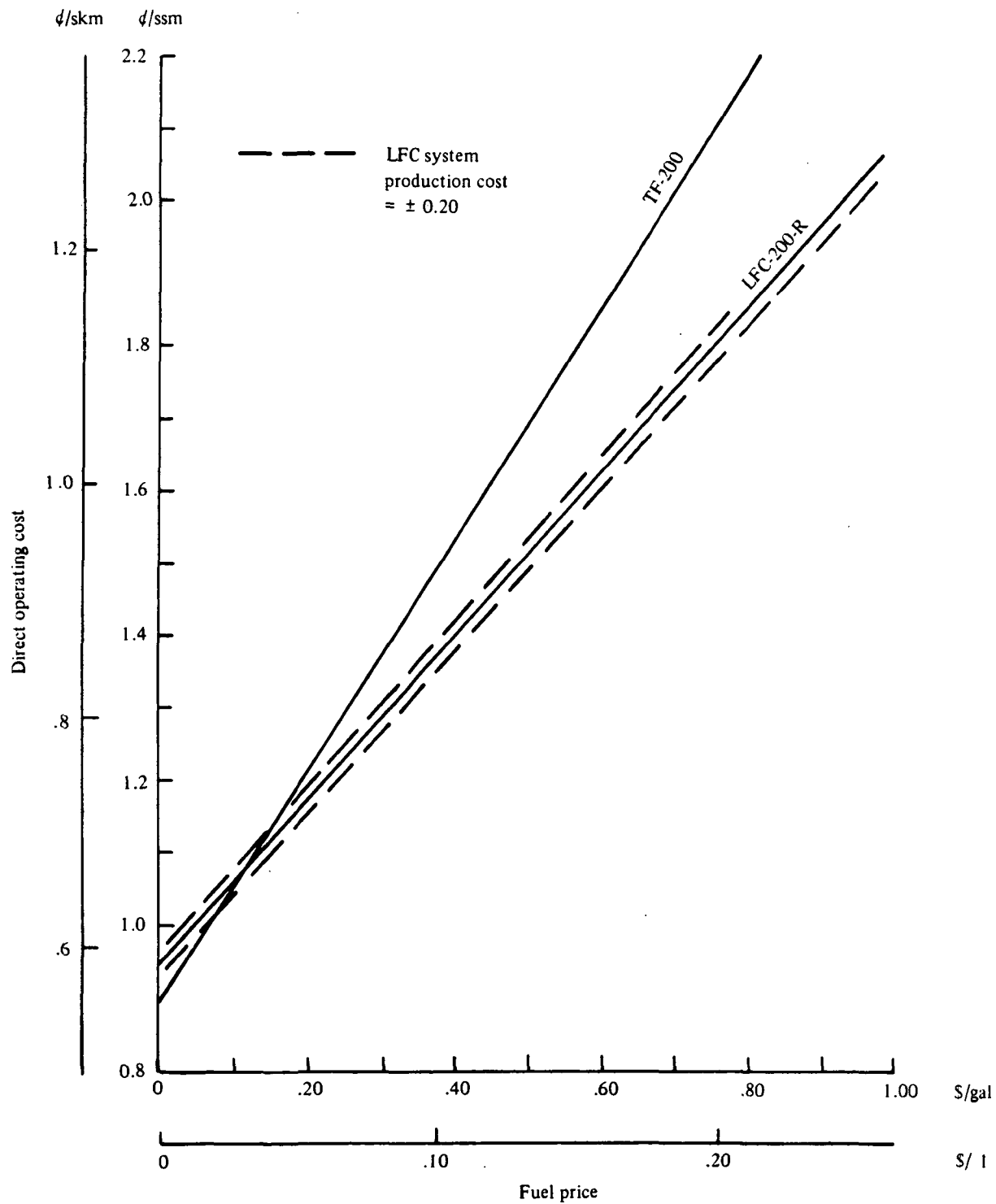


Figure 213. — Sensitivity of DOC to fuel price and LFC production cost, TF-200 and LFC-200-R

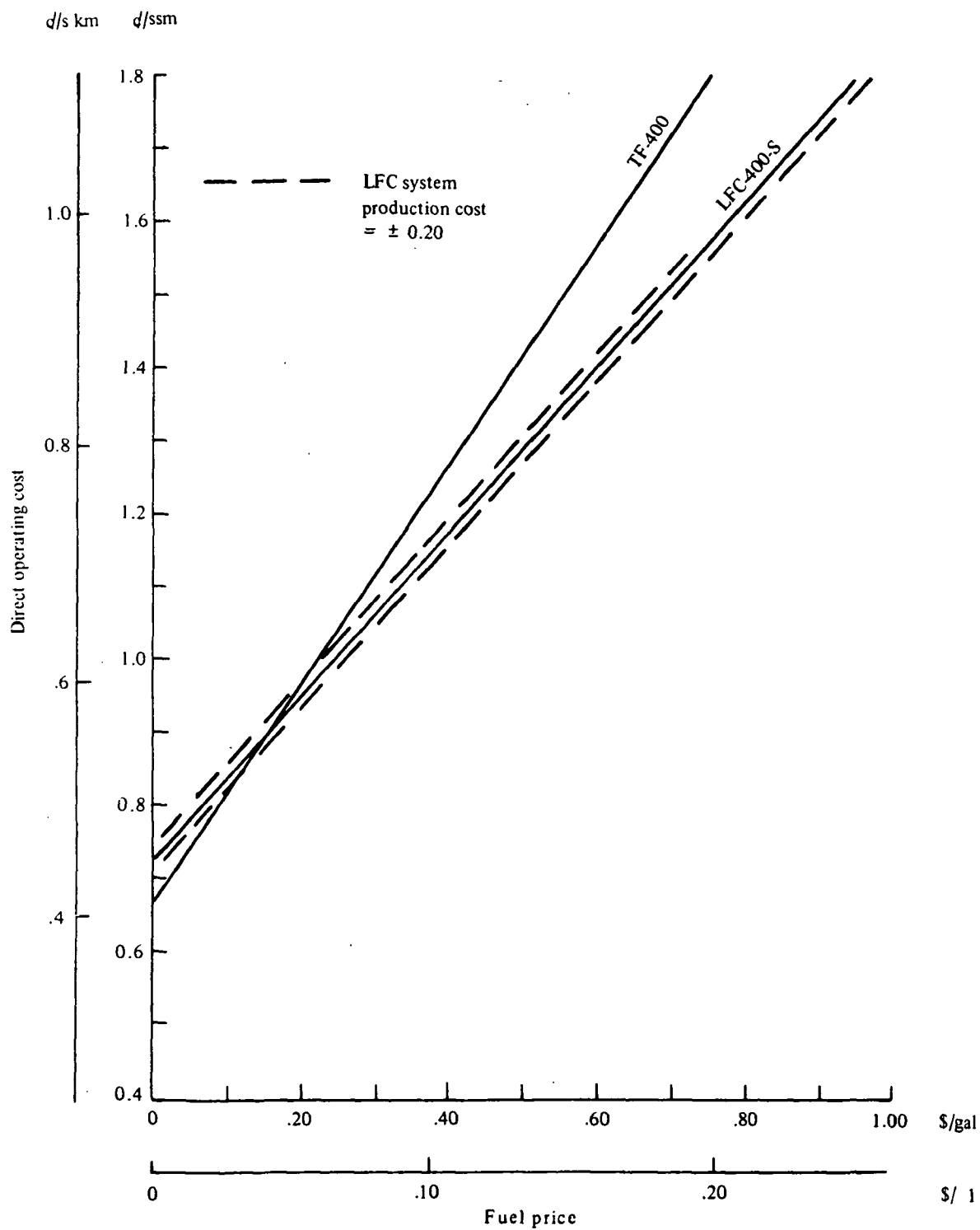


Figure 214. — Sensitivity of DOC to fuel price and LFC production cost, TF-400 and LFC-400-S

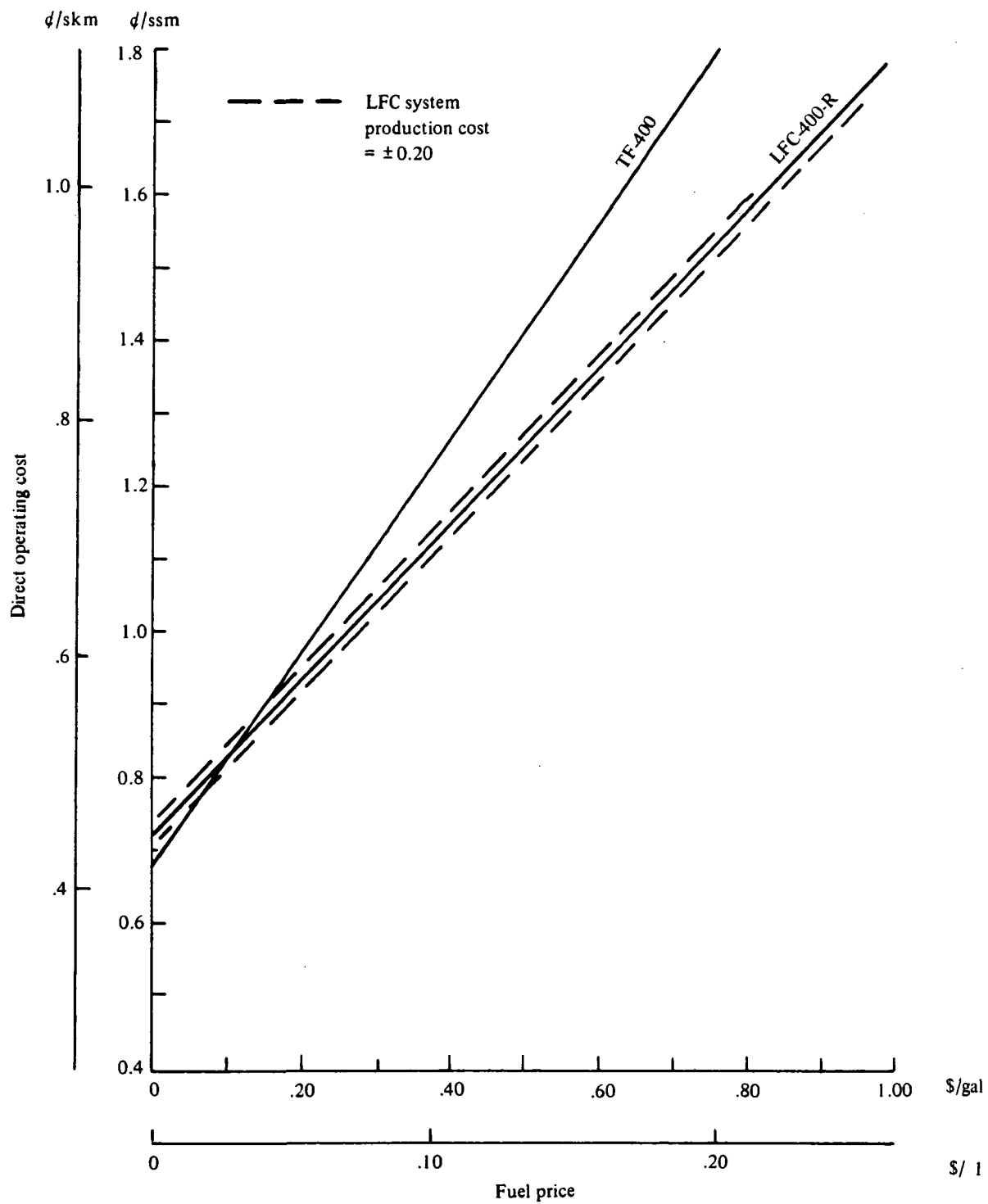


Figure 215. — Sensitivity of DOC to fuel price and LFC production cost, TF-400 and LFC-400-R

in the production cost of the LFC system has a relatively small impact on the relative DOC of TF and LFC aircraft. This variation changes the fuel price at which LFC and TF aircraft have equal DOC by about $\pm \$0.016/1$ (\$0.06/gal) for LFC-200-S and $\$0.011/1$ (\$0.04/gal) for LFC-200-R, LFC-400-S, and LFC-400-R.

11.4.2 STAGE LENGTH

All of the preceding comparisons of fuel efficiency and DOC were based on an assumed average stage length equal to the design range of 10,186 km (5500 n mi). To gain insight into the relative performance of LFC and TF transports under varying operating conditions, a study was conducted to evaluate the influence of average stage length on DOC. This analysis was completed for the LFC-200-R and the TF-200 configurations.

In calculating DOC for the reduced stage lengths, only the fuel required for the mission was included in the aircraft gross weight at the beginning of the flight. Consequently, the takeoff gross weight decreases progressively as stage length is reduced. The variations of takeoff gross weight, block time, mission fuel, and block fuel are shown as a function of stage length in figures 216, and 217 for the TF-200 and LFC-200-R aircraft. Based on the data of these figures, the resultant DOC for TF-200 and LFC-200-R are shown as a function of stage length in figure 218.

The DOC for both the TF and LFC aircraft are observed to follow the anticipated trend in that DOC increases as stage length is reduced below the design range. However, due to the additional system elements on the LFC aircraft which have maintenance requirements sensitive to the number of operating cycles, the DOC of LFC-200-R increases at a faster rate than that of TF-200. At the design range of 10,186 km (5500 n mi), the DOC of LFC-200-R is 7.9% less than that of TF-200. This value decreases to 6.2% at 5556 km (3000 n mi) and 3.5% at 2778 km (1500 n mi).

11.5 SUMMARY COMPARISONS

To establish a reference frame for the evaluation of study results, this section compares the relative impact of configuration variations on TF and LFC aircraft, summarizes the fuel efficiency and DOC of 200- and 400-passenger aircraft, and relates the fuel efficiency of study aircraft to that of current commercial transports.

11.5.1 CONFIGURATION VARIATIONS

In the development of final LFC and TF configurations, a number of configuration variations were evaluated to ensure the selection of optimum aircraft for final comparisons. As a result of the

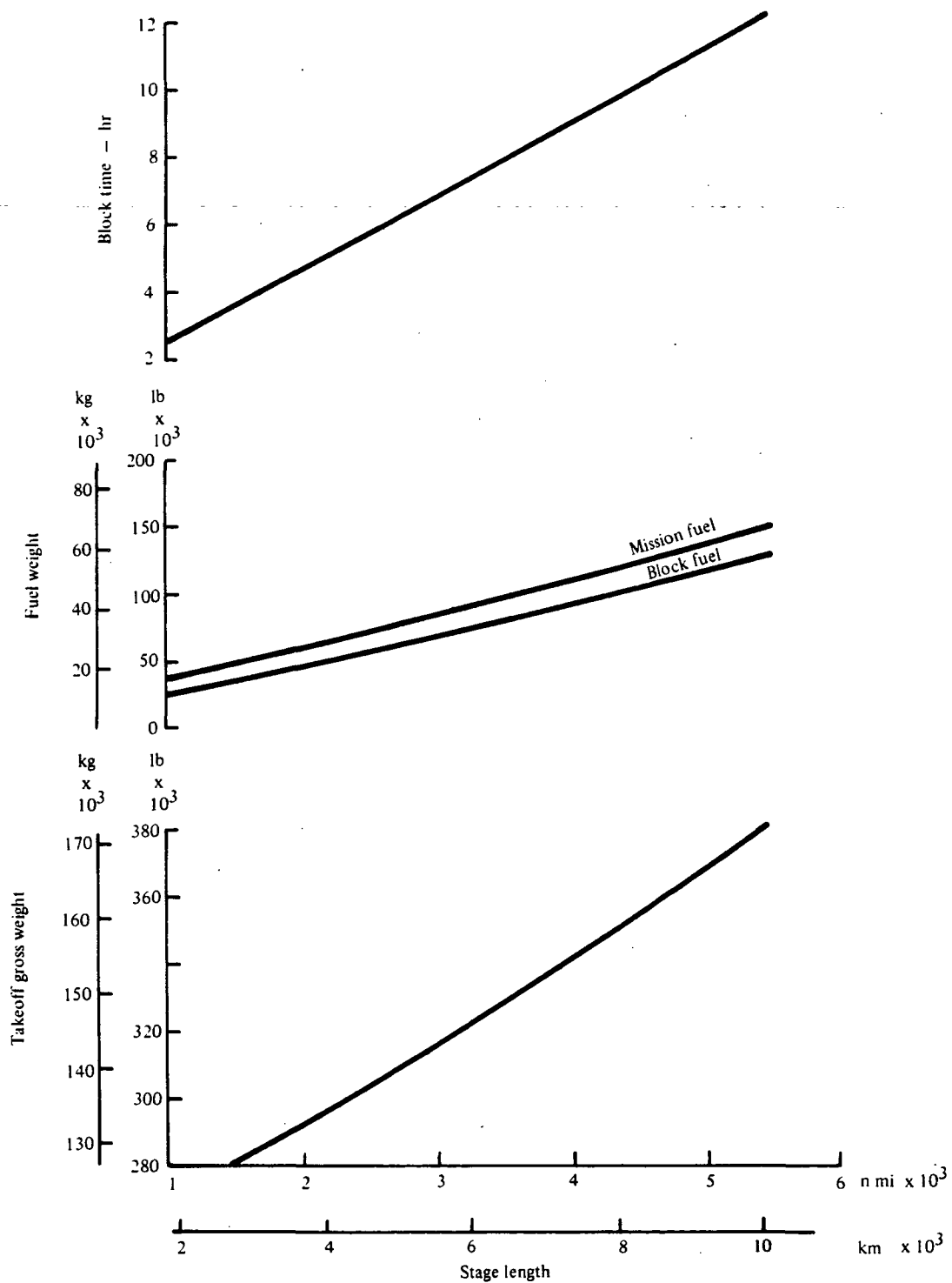


Figure 216. — Variation of aircraft and mission parameters with stage length, TF-200

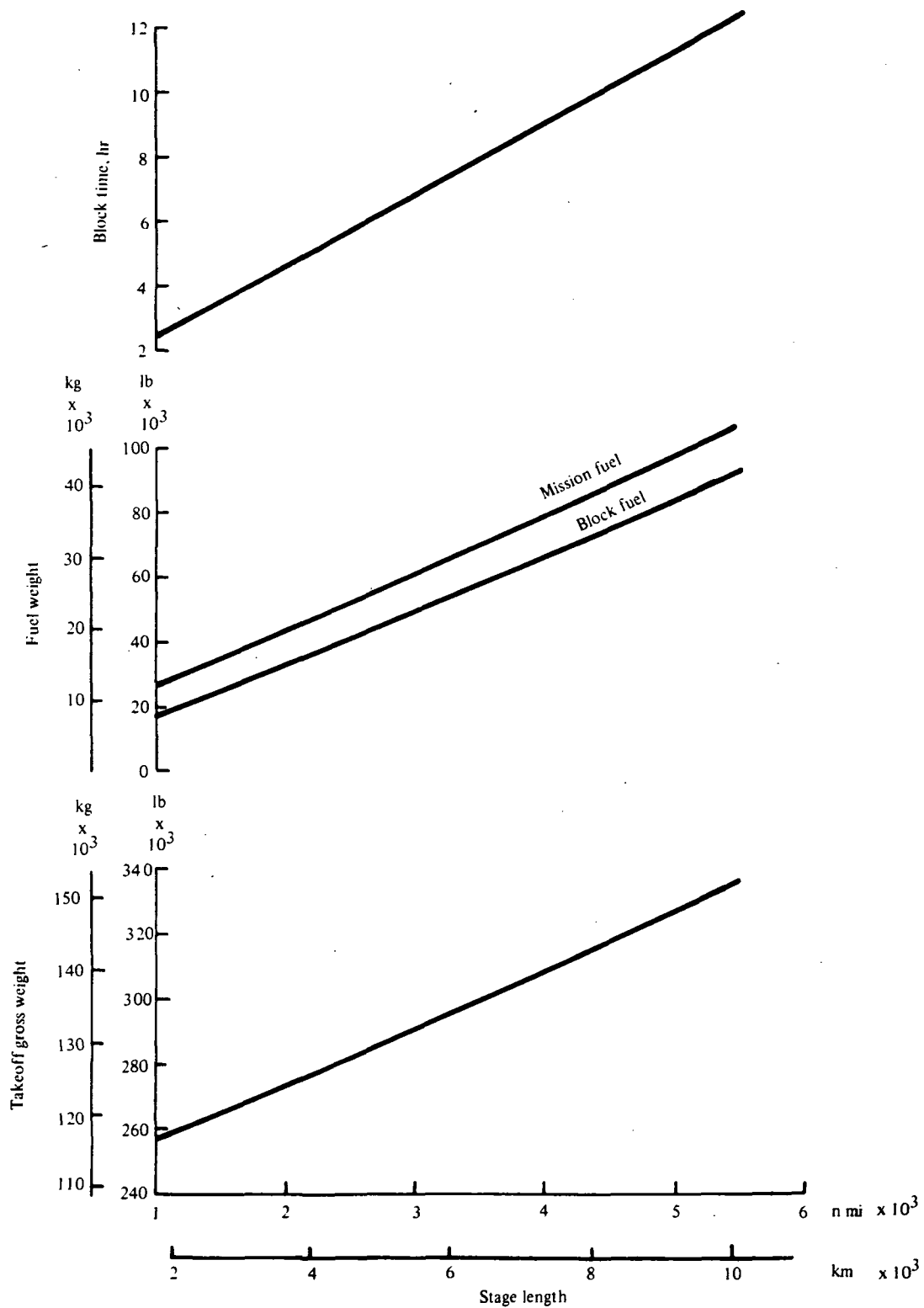


Figure 217. — Variation of aircraft and mission parameters with stage length, LFC-200-R

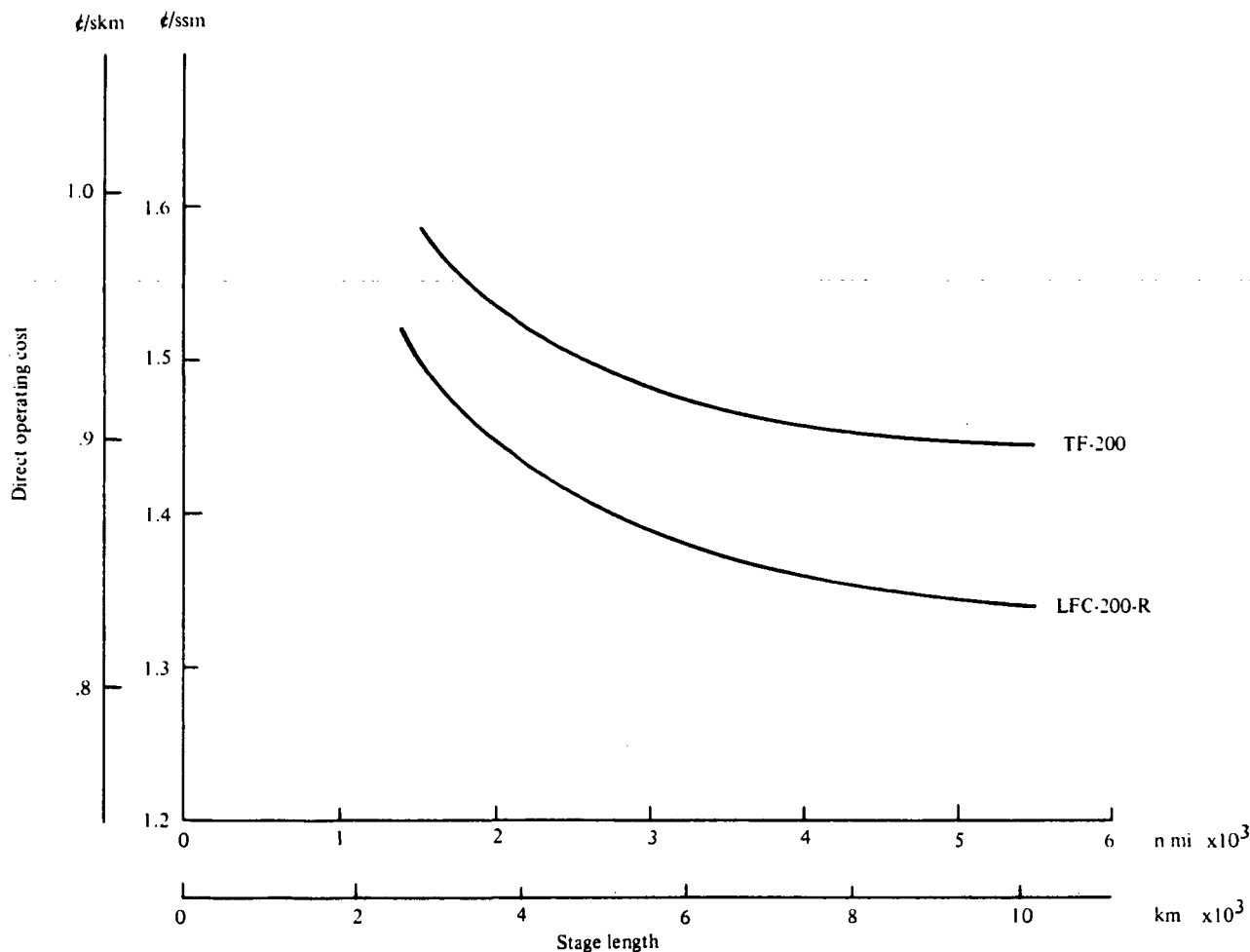


Figure 218. — Sensitivity of DOC to stage length, TF-200 and LFC-200-R

configuration evaluations described in section 7.5, it was established that fuel efficiency was improved by adding external fuel tanks and relaxed static stability to all of the 200-passenger configurations and by adding relaxed static stability to the 400-passenger configurations. The relative benefits of such variations for TF and LFC 200- and 400-passenger aircraft are summarized in table 57.

It is important to observe that all of the configuration variations result in a greater reduction in fuel consumption for both the 200- and 400-passenger TF aircraft than for the corresponding LFC configurations. For example, the addition of external fuel and RSS to TF-200 results in a 4.8% reduction in fuel consumption while the benefit for LFC-200-S is 2.1%. Similarly, the use of RSS on TF-400 provides a 5.4% reduction in fuel consumption. The corresponding LFC configurations benefit by a maximum of 3.7%.

TABLE 57. REDUCTIONS IN FUEL CONSUMPTION FOR LFC AND TF CONFIGURATION VARIATIONS

Configuration	Variation								
	External fuel			RSS			External fuel RSS		
	kg	lb	%	kg	lb	%	kg	lb	%
TF-200	1620	3571	2.6	1713	3775	2.8	2989	6587	4.8
LFC-200-S	407	897	0.9	635	1400	1.4	924	2038	2.1
LFC-200-R	156	345	0.4	418	921	0.9	601	1326	1.4
TF-400				6428	14171	5.4			
LFC-400-S				3299	7272	3.7			
LFC-400-R				2758	6081	3.2			

These results are to be expected, since any decrease in the size of the wing and empennage, which results from the addition of both external fuel and RSS, provides a greater benefit to TF aircraft than LFC aircraft. Performance of the TF aircraft is improved by reduction in both weight and drag. Since the drag of the wings and empennage of the LFC aircraft is only 35% of that of the TF aircraft, the drag reduction afforded by resizing is of little significance, and the LFC aircraft benefits primarily through the weight reduction.

11.5.2 FUEL EFFICIENCY

A summary comparison of the fuel consumption, the fuel savings afforded by the addition of LFC, and the fuel efficiency of the six final study aircraft is outlined in table 58. Depending on the boundary layer stability assumed, reductions in fuel consumption range from 24.9% to 28.2% for the 200-passenger LFC aircraft and 24.5% to 26.7% for the 400-passenger configurations. Improvement of fuel efficiency ranges from 32.4% for LFC-400-S to 39.4% for LFC-200-R.

The greater fuel savings and improvement in fuel efficiency of the 200-passenger LFC aircraft as compared to the 400-passenger LFC aircraft is a result of the relative performance of the TF configurations used for comparison. Of all of the final study aircraft, only the TF-400 configuration has adequate wing volume to permit the use of leading edge devices. As a result, the takeoff performance of this configuration permits a better match of cruise and takeoff thrust requirements, with an attendant improvement in fuel efficiency relative to the TF-200 configuration.

TABLE 58. SUMMARY COMPARISON OF FUEL EFFICIENCY

Configuration	Block fuel			Fuel efficiency		
	kg	lb	%	s km/kg	ssm/lb	%
TF-200	58,788	129,604		34.65	9.77	
LFC-200-S	44,144	97,320	-24.9	46.15	13.01	33.2
LFC-200-R	42,198	93,028	-28.2	48.29	13.62	39.4
TF-400	112,700	248,456		36.17	10.20	
LFC-400-S	85,123	187,661	-24.5	47.88	13.50	32.4
LFC-400-R	82,599	182,096	-26.7	49.35	13.91	36.4

11.5.3 DIRECT OPERATING COST

Tables 59 and 60 summarize comparisons of DOC and the influence of DOC variations for the six final study aircraft. Table 59 lists DOC for the study aircraft based on the current fuel price of \$0.093/l (\$0.35/gal) for international carriers. At this fuel price, the DOC of the 200-passenger LFC aircraft is 1% to 7.8% below that of the TF-200 configuration. The DOC reduction for LFC-200-S and LFC-400-R is 6.1% and 8.4%, respectively, as compared to TF-400.

Table 60 summarizes the fuel prices which result in equal DOC for TF and LFC aircraft and illustrates the effect of variations in both LFC maintenance cost and LFC production cost.

11.5.4 COMPARISON WITH CURRENT TRANSPORTS

The comparisons of section 11.5.2 showed that the fuel efficiency of the LFC study aircraft is 32.4% to 39.4% greater than that of the comparable TF study aircraft. However, a realistic evaluation of the study aircraft requires consideration of the performance of the advanced technology TF transports which were developed for comparison with the LFC study aircraft. Based on the data of reference 5, figure 219 shows the fuel efficiency of representative current commercial transports as a function of stage length. The corresponding curves for the 200-passenger study aircraft are included for comparison. At a stage length of 5631 km (3500 s mi), the TF and LFC transports demonstrate improvements in fuel efficiency of 9.7% and 50%, respectively, when compared to the best of the current transports. At the design range of 10,186 km (6333 s mi) for the study aircraft, the fuel efficiency of TF-200 is 63.8% greater than that of current transports. Compared to the same transport at this range, the fuel efficiency of LFC-200-R is greater by 130.8%.

TABLE 59. SUMMARY COMPARISON OF DOC

Configuration	DOC	
	<u>¢/s km</u>	<u>¢/ssm</u>
TF-200	.901	1.450
LFC-200-S	.892	1.436
LFC-200-R	.831	1.337
TF-400	.743	1.195
LFC-400-S	.697	1.122
LFC-400-R	.681	1.095
Fuel price = \$0.093/l (\$0.35/gal)		

TABLE 60. SUMMARY COMPARISON OF DOC VARIATIONS

Configuration	Fuel price for equal TF and LFC DOC					
	$\bar{M} = 0.5$		$\bar{M} = 1.0$		$\bar{M} = 1.5$	
	\$/l	\$/gal	\$/l	\$/gal	\$/l	\$/gal
LFC-200-S	.047	.18	.082	.31	.116	.44
LFC-200-R	.013	.05	.029	.11	.045	.17
LFC-400-S	.021	.08	.042	.16	.058	.22
LFC-400-R	.011	.04	.026	.10	.042	.16
	$\bar{P} = 0.8$		$\bar{P} = 1.0$		$\bar{P} = 1.2$	
LFC-200-S	.066	.25	.082	.31	.098	.37
LFC-200-R	.018	.07	.029	.11	.040	.15
LFC-400-S	.032	.12	.042	.16	.053	.20
LFC-400-R	.016	.06	.026	.10	.037	.14
\bar{M} = LFC maintenance cost factor \bar{P} = LFC production cost factor						

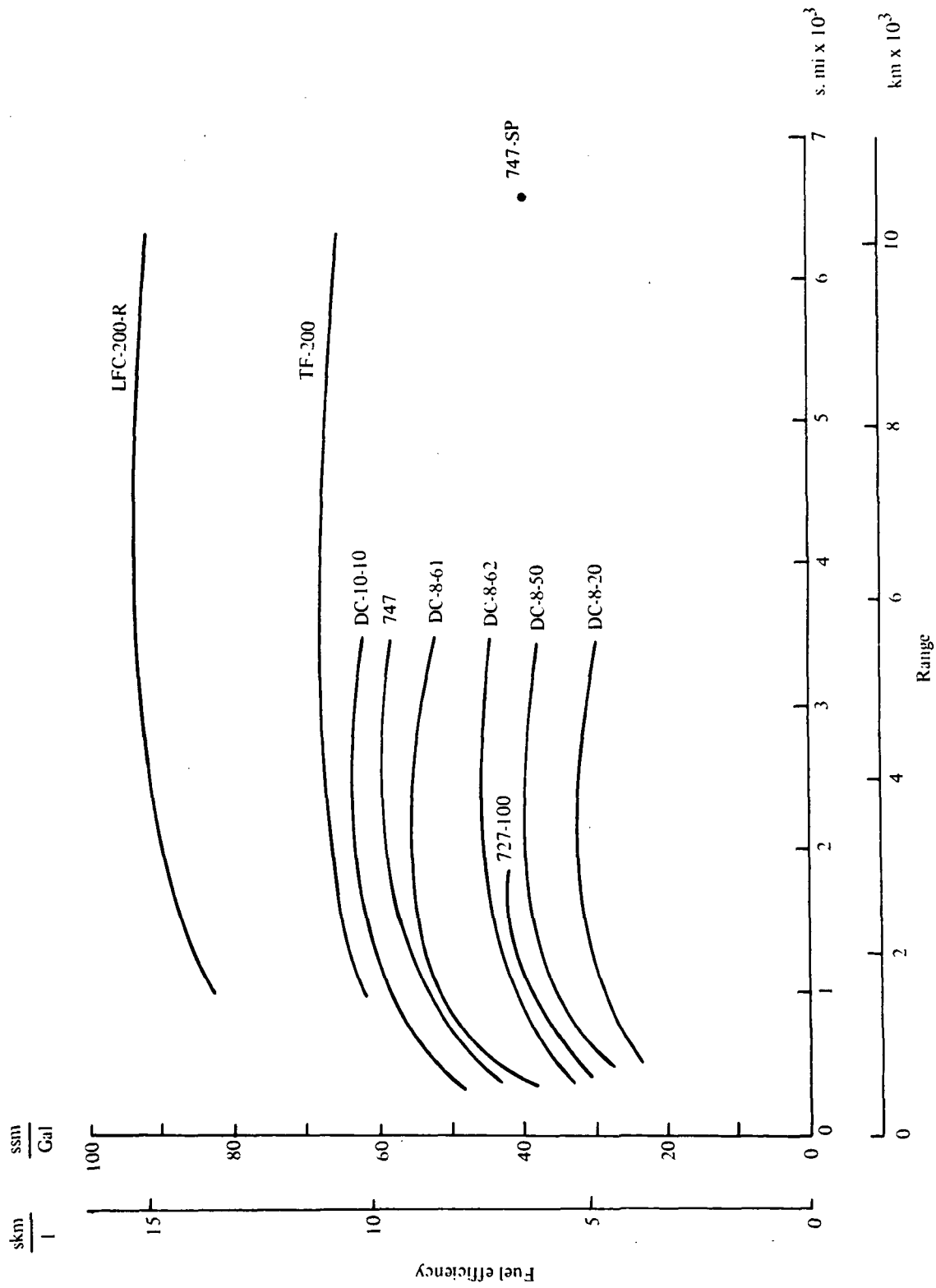


Figure 219. — Fuel efficiency comparisons

12.0 RESEARCH AND TECHNOLOGY REQUIREMENTS

12.1 INTRODUCTION

The technical feasibility of laminar flow control was demonstrated over a decade ago by the X-21A program described in detail by reference 15 and the economic advantages of LFC transports were quantified in the comparisons of LFC and TF aircraft in the preceding section. As evidenced by the analyses described in sections 4 through 10 of this report, the economic comparisons are based on a realistic assessment of the penalties attending the incorporation of LFC on a transport aircraft.

Although the technical feasibility has been established and a realistic assessment of economic feasibility has been conducted, it is anticipated that two basic requirements must be satisfied before LFC is employed on an operational commercial transport:

- (1) Aircraft manufacturers must be convinced that the technology is available to develop and build LFC aircraft without assuming unreasonable levels of risk in satisfying performance guarantees.
- (2) The commercial airlines must be convinced of both the economic advantages and the reliability of LFC transports in the airline operating environment.

It is anticipated that these requirements can be satisfied only through a flight validation program which duplicates or closely approximates the airline operating environment. A properly coordinated flight validation program is required to establish the viability of LFC in the profit-oriented commercial airline environment characterized by high utilization rates and stringent schedule requirements. Such a program can provide the data necessary to perform economic evaluations based on observed performance, reliability, and maintainability factors and will permit a convincing comparison of the economic advantages of LFC as compared to alternative fuel-conservation techniques.

As evidenced by the X-21A program, the technology requisite to the demonstration of the technical feasibility of LFC was available in 1960. However, the technology necessary for the development of an LFC aircraft compatible with routine operation in the airline environment is not available. Consequently, this section is devoted to a discussion of the research and technology programs necessary for the development of such an LFC demonstrator aircraft.

12.2 LFC AIRFOIL DEVELOPMENT

During the study, several problem areas in aerodynamics were identified for the LFC configurations representative of future production aircraft. A problem fundamental to the development of future LFC aircraft is that of defining analytically, at an early stage in the aircraft optimization process, the level of suction required to laminarize the boundary layer.

The basic difficulty results from the lack of a set of boundary layer stability criteria integrated into the overall flow field solution, and the relation of these criteria to the actual occurrence of transition.

A second requirement is that of providing an LFC airfoil "data bank" at an early stage in the design optimization process to facilitate the economical selection of optimum airfoils for specific mission requirements. A part of this task is the identification of the required surface smoothness to permit design of practical and economical suction surfaces. In order to keep LFC suction levels as low as possible, the use of a trailing-edge trimming device appears to be necessary. The methodology for incorporating such a device has not been developed and tested.

These requirements are discussed in the sections which follow, along with the approach to solution of the problems, and recommended funding and schedules.

12.2.1 LAMINAR BOUNDARY LAYER STABILITY CRITERIA

The first task encountered in the design of an LFC wing is an evaluation of the stability of the laminar boundary layer and a determination of the level of stability required to avoid transition. Reference 15 discusses the criteria used for defining stability limits during the X-21 program. In this reference it is stated that, "In general, the experimental crossflow Reynolds numbers are of the order of eighty percent higher than the theoretical minimum limiting values." Unfortunately, some of the theoretical programs in use at the time of the X-21 study are not available, and the full implications of this mismatch between theory and experiment cannot be evaluated on a consistent basis for advanced supercritical airfoils. In addition, acoustic effects on boundary layer stability and the incremental suction requirements, as outlined in section 11 of reference 15, were not well quantified theoretically. Most of the X-21 acoustic criteria were established on an experimental basis. While this technical approach is acceptable after baseline configuration has been selected, it cannot be used economically in conducting the optimization studies which are a desirable prelude to the design of a production configuration.

An integrated theoretical flow solution is required which:

- (1) Calculates the laminar boundary layer for a compressible, three-dimensional flow over a lifting surface shape.
- (2) Determines the character of the laminar boundary layer with regard to its stability or instability for a given level of suction.
- (3) If the boundary layer is found to be unstable, either
 - (a) increases suction to produce stability
 - (b) calculates the amplification of disturbances in the region of unstable laminar boundary layer
 - (c) increases suction as required to prevent transition, or
 - (d) permits transition and merges the upstream boundary layer calculation with a turbulent boundary layer calculation downstream
- (4) Integrates boundary layer calculations into the total flow picture in a manner similar to that outlined in reference 51.

In order to produce such a computational method, the following tasks are required:

- (1) Establish a modular concept for the theoretical methodology and complete the following major component modules of an integrated computational program:
 - (a) Module for calculating the characteristics of a laminar boundary layer with suction.
 - (b) Module for evaluating stability of a given laminar boundary layer, including the effects of variations in both suction and acoustic disturbance levels.
 - (c) Module for predicting rate of growth of disturbances in an unstable laminar boundary layer.
 - (d) Module for merging the "transitional" laminar boundary layer calculation into a turbulent boundary layer calculation.
 - (e) Module for estimating the pressure distribution around an arbitrarily shaped lifting surface of finite thickness at high subsonic speed.
 - (f) A control module for integrating functions of modules (a) through (e) into the desired computational program.

A modular approach is preferred, since this allows a choice of alternative partial solution methods and subsequent insertion and trial within the overall solution framework as a means of facilitating continuous improvement of the methodology or expediting availability.

- (2) With use of the integrated computational program, design, fabricate, and test an LFC wing to verify overall program validity and define areas of required improvement.
- (3) Incorporate identified program improvements.
- (4) Design and test a second, significantly different LFC wing to verify improvements in methodology.

This research and technology item is considered to be fundamental to a significantly improved understanding of the LFC wing optimization problem.

Cost/Schedule – The following time spans and funding levels indicate the scope of the program:

Task	Time Span	Cost
(1) (a)	15 months	\$ 50,000
(b)	10 months	40,000
(c)	6 months	30,000
(d)	3 months	15,000
(e)	11 months	100,000
(f)	6 months	45,000
(2)	9 months	200,000
(3)	6 months	50,000
(4)	8 months	150,000

The anticipated total cost of such a program is approximately \$680,000. The total time span of the program depends on specific scheduling of the activities, allocation of manpower, and availability of the interfacing methodologies. A minimum achievable time span is about 44 months, assuming that work on the interlocking modules of Task (1) can be judiciously scheduled. Excluding Tasks (3) and (4), the initial version of the methodology can be obtained and verified in approximately 30 months at a cost of approximately \$480,000.

12.2.2 AIRFOIL DESIGN DATA BANK

In the 1930-1940 period, significant effort was expended by NACA and others on the development of families of low-drag airfoils utilizing part-chord laminar flow. Most of the airfoils subsequently adopted by NACA for continued development became known as the NACA 6-series airfoil family. As early as 1947, as evidenced by reference 52, NACA investigators attempted to further improve high-speed lift/drag performance of those sections by use of aft-loading. During the 1950's, English investigators expended effort in developing the "peaky" airfoil concept, which further extended general airfoil performance possibilities. Since 1960, Whitcomb of NASA and others have continued the evolution of the basic high-speed airfoil shape to combine high aft loading with a large upper surface region of almost constant velocity supercritical flow. This "supercritical airfoil" concept has resulted in definition and testing of numerous airfoils which can be characterized as members of a supercritical airfoil family.

Subsequent to 1960, aerodynamicists devoted considerable effort to design of "shock-free" airfoils, which are special cases of the airfoil with a supercritical upper surface flow region. For this type of airfoil, the maximum supercritical velocity is reached near the airfoil leading edge. The flow is then gradually decelerated supersonically without significant shocks down to subsonic values at chordwise positions usually greater than 50 percent. The pressure rise to the required trailing edge pressure is accomplished rapidly over the aft end of the airfoil downstream of the supercritical region. Some recent examples of such "shock-free" airfoils are given in reference 52.

A common feature of the more recent airfoil developments has been the concentration on turbulent-flow airfoils. The last concentrated effort on laminar flow airfoils was the X-21 program, in which a NASA 6-series type airfoil was employed. For the 6-series type airfoil, effort has been concentrated primarily on achievement of natural laminar flow without the aid of a powered suction system. There is little airfoil data which can be used in early design stages to establish a preferred LFC airfoil section for specific aircraft design mission requirements.

Based on the results of this study, the supercritical airfoil has features which make it a good choice as an LFC airfoil. However, one liability is the possibility of high-shock wave drag which may partially cancel the drag saved through the use of LFC. The shock-free airfoil versions of supercritical airfoils avoid this problem but may suffer losses of lift capability and sustain additional suction flow requirements when compared with the supercritical airfoil. Basic LFC airfoil design studies, with the purpose of identifying the optimum level and chordwise distribution of upper surface supercritical lift, are therefore required to ensure that the proper active LFC airfoil family is identified. After a preferred concept is properly identified, work should proceed in establishing the proper airfoil data base, both experimentally and theoretically, for use in subsequent aircraft design. To achieve these objectives, the following tasks are necessary:

- (1) Using available design and analysis tools, design in detail three families of airfoils for the anticipated LFC commercial mission requirements. These families are:
 - (a) A high aft-loaded rooftop airfoil with shapes similar to those in reference 52.
 - (b) A supercritical airfoil.
 - (c) A “shock-free” supercritical airfoil.

The following represent a minimum of nominal design Mach numbers, lift coefficients and sweep angles necessary for each airfoil concept:

Mach No.	Lift Coefficient*	Sweep Angle*
.8	.48	18 ⁰
.8	.48	22 ⁰
.8	.48	26 ⁰
.8	.60	18 ⁰
.8	.60	22 ⁰
.8	.60	26 ⁰
.8	.72	18 ⁰
.8	.72	22 ⁰
.8	.72	26 ⁰

***For Whitcomb supercritical airfoils**

- (2) Using the total data base from (1) above, conduct a brief aircraft design trade study to identify the most likely candidate airfoil sections for initial LFC flight demonstration work.
- (3) Redesign one baseline airfoil of each family as required for compatibility with LFC flight demonstration work.
- (4) Fabricate low-speed and high-speed wind tunnel models with LFC for each of the concepts from (3). These models should have the capability for test at both the nominal sweep angle and at zero sweep. In this way, tangential and crossflow Reynolds number theoretical criteria can both be correlated with experimental results. If possible, these models should also have the capability for either slot or porous area suction. Whether this is possible strongly depends on the model sizes and wind tunnels to be utilized.

- (5) Conduct both low-speed and high-speed tests with the above models to verify or determine suction requirements for the three airfoil concepts. If possible during these tests, evaluate alternative suction surface schemes (slot versus area or combined slot/area). In addition, simulate the effects of surface smoothness and production steps and gaps and determine revised suction requirements.

Noise data should be taken during the tests and acoustic disturbances should be introduced during one phase of testing to determine the effect on suction requirements.

- (6) Based on analysis of preceding results; design, fabricate, and test a three-dimensional wing for verifying choice of a preferred airfoil concept and its required suction. This activity should be an integral part of Task (2) in section 12.2.1, and could be expanded to include the total wing design and test program outlined in section 12.5.2.

Cost/Schedule — The following time spans and funding levels define the scope of the program required for establishing a fixed geometry airfoil design data bank:

Task	Time Span	Cost
(1)	9 months	\$135,000
(2)	2 months	35,000
(3)	2 months	15,000
(4)	8 months	180,000
(5)	6 months	65,000
(6)*	9 months	200,000

* The cost of this task depends upon the extent of integration with the programs of sections 12.2.1 and 12.5.2

The anticipated total cost of tasks under section 12.2.2 is \$430,000 if proper phasing of work in sections 12.2.1 and 12.2.2 is accomplished. The minimum possible total time span required is about 38 months. These programs are complemented by the program suggested in section 12.3.

12.2.3 TRAILING-EDGE TRIMMING DEVICES

To stabilize the shock location on LFC airfoils at varying Mach numbers and lift conditions, this study has established a requirement for introducing a trailing edge trimming device. Experimental exploration of this device on laminar-flow airfoils was conducted by Wortmann (ref. 54) and Pfenninger (ref. 55). Wortmann's investigations were at low Mach number and Reynolds number

and did not include the effects of LFC. Pfenninger's work did include exploration of LFC, but was done at low Mach number and low Reynolds number. Therefore, a requirement exists for extending the data base to include the advanced airfoils delineated in section 12.2.2 at higher Reynolds numbers and at high subsonic Mach number, and defining the methodology for translating predictable sectional airfoil results into three-dimensional wing designs.

Cost/Schedule — The above objectives can be accomplished by integrating investigations of variable geometry airfoils into the program described in section 12.2.2. Each of the tasks described in that section would have additional related work on airfoils with trailing-edge flaps. The required incremental costs and time spans are as follows:

Task	Incremental Time Span	Incremental Cost
(1)	2 months	\$ 60,000
(2)	—	10,000
(3)	—	10,000
(4)*	6 months	150,000
(5)*	5 months	60,000
(6)**	2 months	40,000
(7)	—	—

* Cost and time could be reduced if the flap provisions are integrated into models used in section 12.2.2.

** Time span and costs are quoted assuming integration of this task into work described in section 12.2.2.

The anticipated total cost of the above tasks is not more than \$330,000 if integrated into the program described in section 12.2.2. The corresponding incremental time involved should not exceed 9 months.

12.3 LFC SYSTEM DEVELOPMENT

An area of significant risk in the design of an operational LFC aircraft is the tolerance of the LFC aerodynamic performance to variations in LFC system performance. Previous efforts in the area of achieving and demonstrating the performance advantage of LFC, culminating in the X-21A flight test program, were largely oriented to construction and testing in a research atmosphere with careful hand-tuning to achieve the desired level and distribution of suction to optimize LFC performance. The X-21A design included a large number of orifices and adjustable valves so that the suction flow profiles over the aerodynamic surfaces could be adjusted to achieve satisfactory LFC performance.

For an operational commercial airplane, economical production must be achieved through the adoption of a simplified system, compatible with large-scale production techniques and tolerances. Little or no adjustment of the suction system will be acceptable on individual airplanes. As a consequence of these restrictions, suction flow profiles on new operational aircraft will reflect local chordwise and spanwise variations in suction flow from the optimum suction flows desired. These flow variations will influence the actual level of performance improvement available from LFC. It is therefore necessary to recognize the influence of these tolerances on LFC in the initial airplane suction system design.

The programs required to eliminate the risks associated with suction flow variations fall naturally into the following four categories:

- (1) Definition of LFC suction level limits and aerodynamic performance variations between these limits.
- (2) Surface design techniques and sensitivities of surface configurations to tolerances and deterioration.
- (3) Duct design concepts and techniques to reduce variations in suction flow levels and distributions.
- (4) Suction pump concepts and control systems to provide minimum variations in suction flow levels.

These requirements may be met by independent efforts or integrated with other R&T programs in some cases. The specific programs are outlined below.

12.3.1 SUCTION TOLERANCES

A program to provide the design guidance on suction flow limits and the effects of flow variations on LFC performance can be accomplished by augmenting the tasks outlined in section 12.2.

Analysis – An initial analytical evaluation of tolerance characteristics can be performed through follow-on efforts associated with the integrated computational program discussed in section 12.2.1. Using this program, the nature of aerodynamic influences governing the suction tolerance effects on LFC performance may be determined and the effects on a range of airfoil shapes compatible with the LFC airplane may be quantified. This analysis should first be oriented toward exploration of overall suction levels having an otherwise ideal distribution. Following this, both spanwise and chordwise suction flow variations should be evaluated as a function of x/c for various levels of overall suction. From these analyses, both maximum and minimum suction flow profiles can be produced for a range of airfoils.

Test Evaluation – Following the above analysis, selected specific suction flow variations may be applied to the verification wing testing of section 12.2.1 or some other compatible LFC wing to verify the analytical evaluation. These tests should include an evaluation of suction requirements to maintain LFC in the presence of both internally and externally generated noise. In the event that verification is inadequate, these data may be used to provide an update to the integrated computational program and conduct a limited analytical re-evaluation.

Interim Design Guidance – From this limited general testing, the magnitude of problems associated with non-optimum suction flow may be assessed and interim limiting suction flow level and distribution design criteria may be established for use in further analytical studies of the entire suction system and LFC airplane system studies. These same criteria may be used to establish production tolerance goals.

As progress is made toward the actual fabrication of an LFC demonstrator airplane and wing geometry is defined, a more detailed test evaluation of suction level and distribution characteristics will be required to provide more pertinent and specific suction system design guidance.

Cost/Schedule – The following funding and time spans cover the initial analytical and test effort required to establish interim design guidance required to provide low risk in system studies and design analyses. Further efforts at a later point in the program are not reflected below but are largely dependent on the outcome of these initial efforts and are anticipated to be of significantly larger magnitude.

	Time Span	Cost
Analysis	3 - 6 months	\$ 40,000
Testing	3 months	100,000
Interim Design Guidance	4 months	20,000

12.3.2 SURFACE DESIGN

The suction surface design criteria readily available in the literature are somewhat limited and are primarily oriented to slot configurations. The scope of this study did not permit an elaborate analytical evaluation of either the existing criteria or techniques. The only consistent description of suction surface design techniques is found in reference 15, which deals exclusively with slotted surface configurations, and provides inadequate recognition of production tolerances, deterioration, or trades between slot spacing and slot width.

While the three basic LFC surface concepts (slots, porous surfaces, and perforated surfaces) are quite different in character, they have distinctly similar requirements and potential aerodynamic problems in application. The best approach for meeting the chordwise suction flow distribution

requirements over the surface appears to be through spanwise ducting under the surface with chordwise distribution of suction flow controlled by metering this flow as it leaves the ducts. Thus, the imposed suction is segmented chordwise. In order to maintain uniform spanwise distribution of suction flow into these ducts, a carefully selected minimum pressure drop must exist across the surface in order to eliminate local spanwise suction flow perturbations. Analysis in this study indicated that this may be reasonably accomplished by selection of slot width and spacing but cannot be controlled by porosity without creating excessive sensitivity to dirt. Similarly, the minimum hole sizes suitable for manufacturing perforated surfaces are too large for adequate control and too sensitive to contamination. LFC is not likely to be satisfactory if control is achieved by decreasing hole density. It is therefore probable that both the porous and perforated surfaces will require the use of spanwise strips of porous or perforated surface interspersed chordwise with smooth impervious surfaces. Thus, for all three surface concepts, there is a non-suction surface over which boundary layer build-up occurs. The boundary layer is subsequently removed by applied suction through a slot, porous strip, or perforated strip.

The slot criteria and design techniques available in the literature are largely oriented toward the definition of the unique local slot configuration required to maintain the boundary layer within an allowable range of thickness. At low values of x/c , a broad range of spacing and slot width combinations are suitable, while at high x/c a small band of combinations are available. No consideration is given to the dependence of LFC performance or sensitivity on the slot width/spacing combination. Given the option, large slots and large spacing should invariably be chosen to reduce production costs and increase allowable production tolerances. However, these choices may degrade performance and increase system sensitivity to production tolerances and deterioration.

A program is required to provide the suction surface design criteria and techniques and must include sufficient data to permit a selection among slotted, porous, and perforated surfaces. The large number of required surface configurations and aerodynamic simulations dictate that test panels of fairly large size be employed for these evaluations and tested in a wind tunnel facility to adequately simulate flight conditions. The test panels must be configured to simulate the leading edge and an airfoil surface chord of relatively large scale due to limitations in the scaling of slots, holes, and porosity. The test panel configurations require capability for variations in suction concept, spacing, suction level, and suction distribution with discrete variations in slot cutting methods, porosities, and hole sizes and densities. Concurrently with the basic program, the effects of internal and external noise on suction requirements should be evaluated and the minimum level of suction to maintain LFC should be determined. A requirement for approximately ten to fifteen test panels is anticipated, with the suction distribution controlled by the basic test section on which the surface panels are mounted.

Cost/Schedule – The time spans and funding levels anticipated for this program are as follows:

	Time Span	Cost
Test Hardware	6 months	\$150,000
Test	3 months	100,000
Analysis	4 months	25,000

12.3.3 DUCTING DESIGN

Techniques for ducting design are well documented and are relatively straightforward. However, the suction system requirements impose unique constraints on the ducting system. The system must establish and maintain the requisite suction levels while maintaining a low pressure loss and low sensitivity to production tolerance and deterioration. The system must be free of undesirable resonance characteristics. In the interest of initial cost, reliability, and maintenance, these objectives should be accomplished in the basic design without the use of controllable valving or individual adjustments.

The program should consist of an analytical study of alternative ducting concepts and combinations in which various controlling devices, such as orifices and venturis, are simulated. Deteriorations are simulated by introducing various pressure losses for the suction surface and the ducting by assuming various ducting surface roughness characteristics.

This may be accomplished by creating a computer program to perform these analyses and should include evaluations of resonance characteristics. Analysis of combinations of these simulations will establish the ducting configurations which minimize variations in suction distribution, complexity, and pressure loss.

At the conclusion of the analytical program, the analysis should be confirmed by a test simulation of one or more configurations in which a test panel is constructed and tested in the "new" condition, subsequently subjected to simulated deterioration, and re-tested.

Cost/Schedule – The time span and funding for this program are estimated as follows:

	Time Span	Cost
Computer Program	8 months	\$ 50,000
System Analysis	8 months	50,000
Test Confirmation	8 months	100,000

12.3.4 SUCTION UNITS

The basic technology for design of the LFC suction units is available or will be provided by other propulsion development programs in the intervening period. The selection of specific suction units should, however, be assessed in greater depth than was possible in this study. Some of the required

technology and design guidance should be provided by other system studies, but the types of suction power systems and suction unit controls should be specifically investigated. These investigations could be performed independently.

The power systems can be investigated at any point in the effort and should consist of a purely analytical effort oriented to a few selected typical LFC airplane configurations. The analysis should be oriented toward a detailed comparison of all the primary concepts with complete weight, drag and fuel consumption definitions to provide trade-off data for use in design selections in subsequent system studies.

The suction unit control systems investigation should specifically explore the problem areas associated with matching low- and high-pressure suction airflows to the various suction pressure and flow levels associated with variations in flight conditions and levels of suction system deterioration. This investigation should also consider potential problems in starting the suction units at altitude. The initial studies should be oriented to identifying any technology areas requiring further effort in order to provide a low level of risk.

Cost/Schedule – The estimated time spans and funding of these programs are as follows:

	Time Span	Cost
Power Unit Analysis	8 months	\$40,000
Suction Unit Control Analysis	8 months	40,000

It should be noted that further technology requirements may result from the control system analysis. A relatively large suction unit development program will ultimately be required, but his program does not represent an R&T requirement.

12.4 MATERIALS

As outlined in section 6, a rather extensive program is required in the evaluation and selection of materials for LFC surfaces. Many of the criteria for LFC surface materials are dependent upon the results of the analyses described in sections 12.2 and 12.3, which establish the relative merits of slotted, perforated, and porous surfaces. However, prior to the selection of an optimum LFC surface configuration and the definition of surface criteria, materials investigations are required to provide a background for ultimate materials selection.

Since the characteristics of materials adaptable to slotted and perforated LFC surfaces are reasonably well known, most of the tasks in this area relate to porous materials. In the following

sections, materials programs are categorized in the areas of analysis and laboratory tests and flight test investigations.

12.4.1 ANALYSIS AND LABORATORY TESTING

The materials investigations outlined below, requiring analytical studies and laboratory testing, are required.

- (1) *Air Flow/Porosity Measurements* – Analytical predictions have established equivalent sea level air flow and ΔP requirements for porous LFC surfaces. The porosity of available porous materials has not been correlated to mass air flow and ΔP . Static air flow tests are required for a range of facing thickness and porosity to permit the correlation of ΔP , thickness, and porosity.
- (2) *Surface Micro-Smoothness* – The effect of surface micro-smoothness on both the maintenance of the laminar boundary layer and the efficiency of the LFC system has not been established. Economic considerations may establish practical limits to the smoothness of porous LFC surface materials. For example, purchased aluminum sheet has a RHR of about 80 while molded fiber reinforced plastics have a RHR of 64. Wind tunnel tests are required to evaluate surfaces of several RHR values and porosities while maintaining laminar flow. This will permit the development of relationships between surface smoothness, ΔP , and suction required for laminarization of the boundary layer.
- (3) *Surface Contamination* – Porous LFC surfaces are effective only to the extent that the surface can be maintained free of contamination. Methods for cleaning or decontaminating clogged surfaces must be provided. Tests are required in which LFC surface panels are contaminated with various foreign materials. Cleaning solutions such as approved solvents, alkaline solutions, and water may be used to remove the contamination both by scrubbing and by backflushing. Mass air flow and pressure drop should be measured for quantitative evaluation of the decontamination effectiveness.
- (4) *Environmental Evaluations* – Unsealed resin matrix composites have shown some degree of structural degradation when exposed to flight environments. In general, a greater degree of voids content results in greater degradation. LFC porous surfaces are intentionally made porous and, as a result, environmental degradation may represent a serious problem. Porous composite LFC panel surfaces should be fabricated and exposed to accelerated environmental cycling to evaluate the compatibility of such materials with the anticipated flight environment.

- (5) *Hydrophobic Coatings* – Control of contamination in LFC systems is critical to efficient LFC operation. Besides providing smooth surfaces throughout the LFC system, improved efficiency may be possible through the use of improved rain repellent (hydrophobic) organosilicone coatings. Contamination/decontamination tests of LFC panels operated in simulated flight regimes are required. These tests will compare untreated panels to panels treated with improved hydrophobic coatings.

Cost/Schedule – Following are the estimated costs and time span for the tasks outlined in this section:

Task	Time Span	Cost
1	6 months	\$ 60,000
2	9 months	200,000
3	6 months	60,000
4	12 months	100,000
5	9 months	75,000

12.4.2 FLIGHT TESTING

In order to minimize the risks associated with in-service deterioration of the suction surface, a program should be initiated at an early date to evaluate surface concepts in a realistic environment. Such an evaluation could be accomplished through a program similar to that employed for evaluating engine inlet duct acoustic paneling. In that program, small test panels were installed in the inlets of nacelles in active service with the airlines and were subjected to a realistic flight environment for extended periods of time. A similar program could be employed for evaluation of suction surfaces.

A realistic evaluation of suction surfaces requires that suction flow of a realistic level be applied to the surface. For a relatively small panel, this may be achieved by utilizing natural pressure differentials existing on the airplane to create the desired suction flow with an insignificant adverse effect on airplane performance. Such a condition may be achieved by locating the panel on the inner surface of the nacelle inlet where an appreciable pressure differential exists relative to the outer surface of the inlet at cruise. The panel is vented to the outside of the nacelle with throttling devices to achieve the desired flow at cruise. While on the ground, the pressure differentials across such a panel are reversed and controlled by a check valve that opens when the airplane achieves sufficient speed to prevent reversed flow. Panel and vent locations can probably be determined which closely simulate the actual desired LFC flight suction spectrum.

The panels may be removed periodically for a laboratory test in which the pressure drop across the panel is evaluated. As appropriate, the panel may be cleaned by techniques applicable to service LFC airplanes.

Cost/Schedule – Such a program can be conducted at a relatively modest cost and should provide a major reduction in risk relative to suction surface deterioration from erosion, contamination, and cleaning procedures. This is particularly important with respect to contamination and cleaning techniques for a porous surface.

The funding and time span for this program are estimated below for the testing of 20 panels. The estimates of cost are rather nebulous because of the required airline participation.

	Time Span	Cost
Flight installation	48 months	\$150,000
Laboratory evaluation	8 months	50,000

12.5 DESIGN

The objective of minimum energy consumption for LFC aircraft results in a configuration which employs a high aspect ratio wing. Such a configuration is further enhanced through the employment of an advanced technology airfoil, active controls for relaxed static stability and load alleviation, and advanced composite structure. To develop such an advanced configuration will require a significant amount of design study, much of which has been initiated by NASA, both in-house and under contract. Additional design studies requisite to the development of practical LFC aircraft are outlined in this section.

12.5.1 HIGH-ASPECT-RATIO WINGS

The problems involved in evaluating the effects of high-aspect ratio wings during advanced design are compounded because such configurations are outside the bounds of experience with previously built aircraft. An analytical evaluation of high aspect ratio effects requires the following:

- (1) Evaluate variations in wing weight by identifying a contemporary medium-aspect-ratio configuration as a baseline and conducting geometric parameter variations in aspect ratio and sweep angle.
- (2) Evaluate the effect of the variations in (1) on the weight and characteristics of the fuselage, landing gear, empennage, control systems, and other airplane components using design data and analytical/statistical weight estimation methods.

The study of wing geometric parameters described above is used to produce weight relationships for geometric and design parameter variations. These relationships are then used to derive

mission-oriented configuration parameters which, in turn, yield a selected mission configuration. The selected configurations are then assessed using analytical procedures to confirm the weight relationship results.

Following are some of the design considerations to be evaluated in a wing aspect ratio study for a laminar flow control aircraft:

- o Aeroelastic stiffness and fatigue constraints.
- o Effect of aeroelastic deformation on slot widths.
- o Geometric constraints, including taper, sweep, thickness, and planform configuration.
- o LFC constraints, such as duct location and flexibility effects.
- o Aircraft stability constraints.
- o Gust and dynamic load effects.
- o Body flexibility/stability constraints.
- o Type of construction, material utilization, and producibility constraints.
- o Airfoil technology.
- o Design cruise speed and wing loading.
- o Available fuel volume.
- o Engine location and pylon stiffness.

Cost/Schedule – It is estimated that the analytical investigations of this task would require a funding level of \$100,000 to \$200,000 over a period of six to twelve months.

12.5.2 LFC WING DESIGN

In any study aimed at the application of LFC to a production airplane, the selection of LFC surface configuration must be made early in the program. As discussed in section 6 of this report, non-structural LFC surface panels were selected for the airplanes considered in the current study. However, it is recognized that the potential for weight savings may accrue through the use of structural or integrated LFC surface designs. Structural LFC surfaces present an array of problems requiring solution prior to incorporation on a production airplane. Brief discussions of significant considerations in surface design are given below.

Selection of Surface Materials – The surface materials available include metals and filamentary materials such as graphite and boron. Metals are most compatible with slotted surfaces because uniform slots are easily attained. Boron and graphite are generally limited to porous surface configurations. Prior to the selection of filamentary materials for use in combination with structural LFC surfaces, the adequacy of such advanced materials in basic wing structure applications must be determined.

Joining – Subsequent to the choice of basic wing materials, the methods of joining elements of the wing must be selected. Mechanical fasteners and bonding each offer distinct advantages in an LFC wing. However, in evaluating bonding as a joining method, the inspection and maintenance of LFC system and wing components must be considered.

Panel Sizing – The ideal LFC wing would employ a single-piece LFC surface and thus eliminate surface joints. In the time frame of interest, a single-piece LFC wing is impractical for an operational aircraft in the airline operating environment. Therefore, the sizing of LFC surface panels must be evaluated on the basis of both manufacturing and operational criteria.

Inspection and Maintenance – A structural or integrated LFC surface creates problems in gaining access to fuel cells and other systems normally located within the wing, including LFC ducting and flight controls. An integrated LFC surface presents peculiar design problems when considering maintenance and repair. Access for periodic scheduled and unscheduled maintenance must be provided by the basic design.

Leading-Edge Devices – While the need for insect contamination removal is still a matter of conjecture, further study should be accomplished to identify several valid designs for such devices. Such devices may involve mechanical wipers, liquid washers, or integrated devices for the removal of contamination and low-speed lift augmentation.

The installation of any mechanical device in the leading edge creates a potential LFC suction discontinuity, increases airframe weight, and complicates manufacturing and maintenance. Such a leading edge device must accommodate the deflections inherent in a swept, high-aspect-ratio wing, and must be reliable and easy to maintain in airline service. A design study on a finite wing configuration is required to produce a viable configuration for such a device.

Trailing-Edge Integration – Depending on the design requirements of an LFC airplane and the airfoil section employed, extending LFC suction into the trailing-edge region normally occupied by ailerons and flaps may become desirable. Problems associated with providing suction on these control surfaces include carrying ducting across movable joints and wing slots and providing adequate space within the wing to accommodate the additional duct area along with necessary fuel volume and space for hinges, actuators, wiring, and control cabling.

A detail design study on a base-point wing with a finite airfoil shape is required to arrive at one or more reasonable configurations to be used as a basis for future aircraft designs.

Cost/Schedule – An integrated approach to the development of an LFC wing requires the design, fabrication, and ground testing of a high-aspect-ratio swept wing complete with all required operational systems. Testing must include loading cycles with systems operating to the extent necessary to secure data in all of the potential problem areas.

Following are the approximate costs and time spans associated with this program:

	Time Span	Cost
Design Analysis	1 1/2 years	\$2,500,000
Fabrication	1 year	2,000,000
Static and Functional Testing	2 years	5,000,000

12.6 MANUFACTURING AND QUALITY CONTROL PROCEDURES

The procedures outlined in section 9.2 for the manufacturing of LFC surface panels are considered to be within the technological capabilities of major airframe manufacturers in the 1980-1985 period. However, the relative complexity of LFC surfaces and the stringent surface smoothness and waviness criteria establish the requirement for an extensive program to validate manufacturing and quality control procedures. The nature of such a program is outlined below.

Development of Representative Tooling – Large area tooling required for the manufacture of LFC surface panels must provide aerodynamic smoothness and waviness control while being lightweight and thermally stable. Concepts for such shell-type tools have been used for relatively small assemblies but must be scaled up in size to demonstrate applicability for LFC panel manufacture. This development includes not only the tooling face materials but tool face supporting structure and support equipment and facilities required for heat-up and cool-down during the cure cycles.

Concepts for manufacturing ducting have been used on relatively small ducts having smooth interior surfaces. These concepts must also be scaled up to assure economical application to ducting of the size required for LFC systems.

Typical LFC panels should be manufactured using full-size tooling scaled up from existing concepts. These panels should be made using materials and sub-structural elements fabricated using the latest tooling technology.

Methods for producing porous or slotted surfaces require validation as economical and practical procedures for manufacturing LFC panels. Typical LFC panels should be manufactured using faces made of reinforced composite materials in which inherent porosity techniques, such as the use of fugitive materials, have been incorporated. In the case of metal facings having slots, techniques employing electron beams and lasers should be compared to jewelers saws for the fabrication of slots.

Validation of Costs – A major obstacle to the application of LFC to aircraft has been the projected high cost of manufacturing LFC surfaces. The low-cost manufacturing concepts outlined in section 9 may eliminate this obstacle, but cost validation is required.

Typical manufacturing operations necessary to produce LFC surfaces and ducting systems should be performed with simultaneous detailed cost tracking and analysis. Detailed cost predictions and validation should be conducted using these cost tracking data and the advanced cost estimating methods currently under development.

Quality Control Procedures – The surface smoothness and waviness criteria of LFC surfaces make quality control extremely important in this application. It is anticipated that a high degree of in-process quality checks would be utilized in the manufacturing phase. The latest quality control practices must be utilized in establishing a complete quality control plan along with the pre-plan functions in an effort to identify critical areas. Methods for mechanizing the quality checks should be evaluated and included in the cost validation effort. This effort must specifically address the problem of economically and accurately assessing the surface smoothness and waviness conditions.

Cost/Schedule – The program outlined in this section would involve funding of about 2.5 million dollars over a 3 year period.

12.7 OPERATIONAL EVALUATIONS

As discussed in section 9, there is great uncertainty in the magnitude of the problem presented by contamination of the LFC surfaces due to both insects and atmospheric contaminants. Existing data relevant to this potential problem were collected prior to 1966 and are applicable to airfoil sections, aircraft performance characteristics, and flight environments quite different from those of current aircraft. Therefore, the applicability of these data to an advanced LFC transport aircraft is questionable. Consequently, it is necessary that a flight investigation be conducted to evaluate the nature of this well-publicized potential problem area and permit the development of practical surface maintenance procedures. Such a program should satisfy the following criteria:

- (1) Utilization of an airfoil section, wing geometry, suction system, and aircraft performance characteristics representative of the probable operational aircraft.
- (2) Operation of the aircraft in the commercial airline flight environment to include the flight routes and terminal areas of representative geographical regions.
- (3) Consideration of seasonal variations in the insect population and atmospheric contaminants.

The data resulting from these flight investigations are necessary to establish both the existence and magnitude of the LFC surface contamination problem, facilitate the development of surface maintenance procedures, and quantify the cost of surface maintenance.

Cost/Schedule — it is obvious that a comprehensive evaluation of the contamination problem, as provided by the program outlined above, would be rather costly and time-consuming. While it would be difficult to justify the expense of such an effort alone, this program is a logical application of the flight validation vehicle.

As an alternative to the comprehensive program described above, worthwhile data may be collected through the use of a representative LFC glove section on an existing research aircraft or RPV. While the data collected in this way are somewhat less definitive, it should be possible to extrapolate such data with reasonable accuracy. A program of this type could be conducted for less than \$500,000 over a period of two years.

REFERENCES

- 1 McLaughlin, J.: *Technological Development for Fuel Conservation in Aircraft and in the Prospective Use of Hydrogen as an Aviation Fuel*. SAWE Journal, Vol 34, No. 1, January 1975.
- 2 Clay, C. W. and Sigalla, A.: *The Shape of the Future Long-Haul Transport Airplane*. AIAA Paper 75-305, February 1975.
- 3 Black, R. E. and Stern, J. A.: *Advanced Subsonic Transports — A Challenge for the 1990's*. AIAA Paper 75-304, February 1975.
- 4 Nagel, A. L., Alford, W. J., and Duggan, J. F.: *Future Long-Range Transports: Prospects for Improved Fuel Efficiency*. NASA TM-X-72659, February 1975.
- 5 Shevell, R. S.: *Technology, Efficiency, and Future Transport Aircraft*. Astronautics and Aeronautics, September 1975.
- 6 Antonatos, P. P.: *Laminar Flow Control Concepts*. Astronautics and Aeronautics, July 1966.
- 7 Whites, R. C., Sudderth, R. W., and Wheldon, W. G.: *Flight Test Results of the Laminar Flow Control X-21 Airplane*. Astronautics and Aeronautics, July 1966.
- 8 Anon.: *Division Advisory Group Review — X-21A Program Summary*. DAG 65-1-0, Northrop Corporation, Norair Division, 1965.
- 9 Anon.: *Report of Review Group on X-21A Laminar Flow Control Program*. USAF Aeronautical Systems Division, November 1965.
- 10 Lange, R. H., et al: *Study of the Application of Advanced Technologies to Long-Range Transport Aircraft*. Vol. I, NASA CR-112088, prepared by the Lockheed-Georgia Company under Contract NAS1-10701, May 1972. CONFIDENTIAL
- 11 Levenson, G. S., and Barro, S.M.: *Cost-Estimating Relationships for Aircraft Airframes*. RM-4845-PR. Rand Corporation, Santa Monica, Calif., February 1966.
- 12 Sallee, G. P.: *Economic Effects of Propulsion System Technology on Existing and Future Transport Aircraft*. NASA CR-134645, July 1974.
- 13 Anderson, J. L.: *A Parametric Determination of Transport Aircraft Price*. SAWE Paper 10 71, May 1975.

References (Continued)

- 14 Staff, LFC Engineering Section: *Laminar Flow Control Demonstration Program Final Report, LFC Maintenance, Operation, and Cost Analysis*. NOR-61-143, Northrop Corporation, Norair Division, 1964.
- 15 Staff, LFC Engineering Section: *Laminar Flow Control Demonstration Program Final Report, LFC Design Data*. NOR-61-141, Northrop Corporation, Norair Division, April 1964.
- 16 Boundary Layer Research Section: *Summary of Laminar Boundary Layer Control Research*. ASD-TDR-63-554, Northrop Corporation, Norair Division, March 1964.
- 17 Anon.: *STOL Aircraft Quiet Clean Propulsion System Study, Parametric Engine Data*. NASA CR-135015 and NASA CR-135016, May 1972.
- 18 Anon.: *Preliminary Performance and Installation Data for Several ATT Engines*. NASA CR-12D950, July 1972.
- 19 Edwards, J. B.: *Fundamental Aspects of Propulsion for Laminar Flow Aircraft*. Boundary Layer and Flow Control, Vol. 2, G. V. Lachman, ed., Pergamon Press, 1961, pp. 1077-1122.
- 20 Lachman, G. V.: *Aspects of Design, Engineering and Operational Economy of Low Drag Aircraft*. Boundary Layer and Flow Control, Vol. 2, G. V. Lachman, ed., Pergamon Press, 1961, pp 123-1165.
- 21 Bauer, F., Garabedian, P., and Korn, D.: *Supercritical Wing Sections*, Lecture Notes in Economics and Mathematical Systems, Vol. 66, Springer-Verlag, New York, 1972.
- 22 Bennett, J. A., Hicks, K., Wall, R. L., and Smathers, G. H.: *LGX-124, LGX-125 High Speed Wind-Tunnel Tests of 0.21 Scale Models of an Advanced Logistic Cargo Aircraft with Two Basic Wing Designs*. Lockheed-Georgia Company ER-9992, May, 1969.
- 23 Pfenninger, W. and Bacon, J. W.: *About the Development of Swept Laminar Suction Wings with Full-Chord Laminar Flow*. Report NOR 60-299, Northrop Corp., 1960.
- 24 Anon: *Final Report on LFC Aircraft Design Data, Laminar Flow Control Demonstration Program*, NOR 67-136, Northrop Corporation, Norair Division, June 1967.
- 25 Rosenhead, L.: *Laminar Boundary Layers*, Oxford University Press, 1966.

References (Continued)

- 26 Staff, LFC Manufacturing Engineering Section: *Laminar Flow Control Demonstration Program Final Report, LFC Manufacturing Techniques*. NOR 61-142 Northrop Corporation, Norair Division, March 1964.
- 27 Pfenninger, W., and Reed, V. D.: *Laminar-Flow Research and Experiments*. Astronautics and Aeronautics, July 1966.
- 28 Hay, J. A. and Rose, E. G.: *In-Flight Shock Cell Noise*. British Aircraft Corp. Ltd., December 1968.
- 29 Fisher, M. J., Harper Bourne, M., and Lush, P.A.: *Shock Associated Noise*. Institute of Sound and Vibration Research, University of Southampton
- 30 Cornell, W. G.: *Experimental Quiet Engine Program – Summary Report*. NASA CR-2519, March 1975.
- 31 Maltenieks, O. J.: *Transparent Rain-repellent Polymer Coatings*. Modern Plastics, February 1971.
- 32 Lachman, G. V.: *Laminar Flow to Date*. Handley Page Bulletin, Vol. 24, No. 231, Winter 1958.
- 33 Nenni, J. P., and Gluyas, B. L.: *Laminar Flow Control Aerodynamic Analysis Procedures*. Astronautics and Aeronautics, July 1966.
- 34 Gregory, N. and Walker, W. S.: *The Effect on Transition of Isolated Surface Excrescences in the Boundary Layer*. R & M No. 2779, Her Majesty's Stationery Office, 1956.
- 35 Braslow, A. L. and Knox, E. C.: *Simplified Method for Determination of Critical Height of Distributed Roughness Particles for Boundary-Layer Transition at Mach Numbers from 0 to 5*. NACA TN 4363, September 1958.
- 36 Braslow, A. L. and von Doenhoff, A. E.: *The Effect of Distributed Surface Roughness on Laminar Flow*. Boundary Layer and Flow Control, Vol. 2, G. V. Lachman, ed., Pergamon Press, 1961, pp. 657-681.
- 37 Loftin, L. K., Jr.: *Effects of Specific Types of Surface Roughness on Boundary-Layer Transition*. NACA WR L-48, 1946.

References (Continued)

- 38 Von Doenhoff, A. E. and Horton, E. A.: *A Low-Speed Experimental Investigation of the Effect of a Sandpaper Type of Roughness on Boundary-Layer Transition*. NACA TN 3858, October 1956.
- 39 Tani, I.: *Effect of Two-Dimensional and Isolated Roughness on Laminar Flow*. Boundary Layer and Flow Control, Vol. 2, G V. Lachman, ed., Pergamon Press, 1961, pp 637-655.
- 40 Carmichael, B. H.: *Critical Reynolds Numbers for Multiple Three Dimensional Roughness Elements*. NAI-58-589, Northrop Aircraft, Incorporated, July 1958.
- 41 Braslow, A. L. and Schwartzberg, M. A.: *Experimental Study of the Effects of Finite Surface Disturbances and Angle of Attack on the Laminar Boundary Layer of an NACA 64 A 010 Airfoil with Area Suction*. NACA TN 2796, October 1952.
- 42 Davies, H.: *Drag Analysis: Achievement of Laminar Flow*. Flight, February 1951, pp. 212-214.
- 43 Coleman, W. S.: *Roughness due to Insects*. Boundary Layer and Flow Control, Vol. 2, G. V. Lachman, ed., Pergamon Press, 1961, pp. 682-747.
- 44 Johnson, C. G.: *The Distribution of Insects in the Air and the Empirical Relation of Density to Height*. J. An. Ecol., Vol. 26, 1957, pp. 479-494.
- 45 Hardy, A. C. and Milne, P. S.: *Studies in the Distribution of Insects by Aerial Currents*. J. An. Ecol. Vol. 7, 1938, pp. 199-229.
- 46 Glick, P. A.: *The Distribution of Insects, Spiders, and Mites in the Air*. Tech. Bull. No. 673, U. S. Dept. Agriculture, 1939.
- 47 Freeman, J. A.: *Studies of the Distribution of Insects by Aerial Currents*. J. An. Ecol. Vol. 14, 1945, pp. 128-154.
- 48 Coleman, W. S.: *The Characteristics of Roughness from Insects as Observed for Two-Dimensional Incompressible Flow Past Airfoils*. J. Aerosp. Sci., Vol. 26, No. 5, May 1959, pp. 264-286.
- 49 Wortman, F. X.: *A Method for Avoiding Insect Roughness on Aircraft*. NASA TT F-15, 454, April 1974.

References (Continued)

- 50. Pfenninger, W.: *Flow Problems of Swept Low Drag Suction Wings of Practical Construction at High Reynolds Numbers*. Norair Division, Northrop Corporation, March 1967.
- 51. Stevens, W. A., Goradia, S. H., and Braden, J. A.: *Mathematical Model for Two-Dimensional Multi-Component Airfoils in Viscous Flow*. NASA CR-1843, July 1971.
- 52. Graham, D. J.: *High-Speed Tests of an Airfoil Section Cambered to Have Critical Mach Numbers Higher than Those Attainable with a Uniform-Load Mean Line*. NACA TN No. 1396, 1947.
- 53. Boerstoeel, J. W. and Huizing, G. H.: *Transonic Shock-Free Airfoil Design by an Analytic Hodograph Method*. J. Aerosp. Sci., Vol. 12, No. 9, September 1975, pp. 730-736.
- 54. Wortmann, F. X.: *On the Optimization of Airfoils with Flaps*. Soaring, May 1970, pp. 23-27.
- 55. Pfenninger, W.: *Experiments on a Laminar Suction Airfoil of 17 Percent Thickness*. Journal of the Aeronautical Sciences, April 1949, pp. 227-236.

NTIS does not permit return of items for credit or refund. A replacement will be provided if an error is made in filling your order, if the item was received in damaged condition, or if the item is defective.

Reproduced by NTIS
National Technical Information Service
U.S. Department of Commerce
Springfield, VA 22161

This report was printed specifically for your order from our collection of more than 2 million technical reports.

For economy and efficiency, NTIS does not maintain stock of its vast collection of technical reports. Rather, most documents are printed for each order. Your copy is the best possible reproduction available from our master archive. If you have any questions concerning this document or any order you placed with NTIS, please call our Customer Services Department at (703)487-4660.

Always think of NTIS when you want:

- Access to the technical, scientific, and engineering results generated by the ongoing multibillion dollar R&D program of the U.S. Government.
- R&D results from Japan, West Germany, Great Britain, and some 20 other countries, most of it reported in English.

NTIS also operates two centers that can provide you with valuable information:

- The Federal Computer Products Center - offers software and datafiles produced by Federal agencies.
- The Center for the Utilization of Federal Technology - gives you access to the best of Federal technologies and laboratory resources.

For more information about NTIS, send for our *FREE NTIS Products and Services Catalog* which describes how you can access this U.S. and foreign Government technology. Call (703)487-4650 or send this sheet to NTIS, U.S. Department of Commerce, Springfield, VA 22161. Ask for catalog, PR-827.

Name _____
Address _____

Telephone _____

**- Your Source to U.S. and Foreign Government
Research and Technology.**